Wastewater Reuse and Watershed Management

Engineering Implications for Agriculture, Industry, and the Environment



Ajai Singh
Editor

APPLE ACADEMIC PRESS
CRC Press
Taylor & Francis Group

WASTEWATER REUSE AND WATERSHED MANAGEMENT

Engineering Implications for Agriculture, Industry, and the Environment

WASTEWATER REUSE AND WATERSHED MANAGEMENT

Engineering Implications for Agriculture, Industry, and the Environment

Edited by
Ajai Singh, PhD, FIE

APPLE ACADEMIC PRESS

Apple Academic Press Inc.
3333 Mistwell Crescent
Oakville, ON L6L 0A2
Canada

Apple Academic Press Inc.
1265 Goldenrod Circle NE
Palm Bay, Florida 32905
USA

Exclusive worldwide distribution by CRC Press, a member of Taylor & Francis Group

International Standard Book Number-13: 978-1-77188-746-5 (Hardcover)
International Standard Book Number-13: 978-0-42943-398-6 (eBook)

Library and Archives Canada Cataloguing in Publication

Title: Wastewater reuse and watershed management : engineering implications for agriculture, industry, and the environment / edited by Ajai Singh, PhD, FIE.

Names: Singh, Ajai, 1970- editor.

Description: Includes bibliographical references and index.

Identifiers: Canadiana (print) 20190071753 | Canadiana (ebook) 2019007177X | ISBN 9781771887465 (hardcover) | ISBN 9780429433986 (PDF)

Subjects: LCSH: Water reuse. | LCSH: Watershed management.

Classification: LCC TD429 .W37 2019 | DDC 628.1/62—dc23

Library of Congress Cataloging-in-Publication Data

Names: Singh, Ajai, 1970- editor.

Title: Wastewater reuse and watershed management : engineering implications for agriculture, industry, and the environment / editor: Ajai Singh.

Description: Palm Bay, Florida : Apple Academic Press, 2019. | Includes bibliographical references and index.

Identifiers: LCCN 2019006910 (print) | LCCN 2019008242 (ebook) | ISBN 9780429433986 (ebook) | ISBN 9781771887465 (hardcover : alk. paper)

Subjects: LCSH: Water reuse. | Watershed management.

Classification: LCC TD429 (ebook) | LCC TD429 .W353 2019 (print) | DDC 628.1/62--dc23

LC record available at https://lccn.loc.gov/2019006910

Apple Academic Press also publishes its books in a variety of electronic formats. Some content that appears in print may not be available in electronic format. For information about Apple Academic Press products, visit our website at **www.appleacademicpress.com** and the CRC Press website at **www.crcpress.com**

ABOUT THE EDITOR

Ajai Singh, PhD, FIE

Ajai Singh, PhD, FIE, is an Associate Professor in the Department of Water Engineering and Management at the Central University of Jharkhand, Ranchi, India. He has more than 18 years of experience in teaching, research, and extension. He is a Fellow of the Institution of Engineers (India) and a life member of various societies. He has more than 30 research papers published in national and international journals of repute. Dr. Singh has authored one textbook, *Introduction to Drip Irrigation Systems*, which has proved to be very useful for graduate and postgraduate students of agricultural/civil engineering. He has been conferred the Distinguished Services Certificate (2012) by the Indian Society of Agricultural Engineers, New Delhi. He teaches subjects such as finite element methods, groundwater hydrology, micro irrigation, watershed management, and numerical methods.

CONTENTS

CONTRIBUTORS

Niva Bara
Head, Department of Agricultural Extension, Birsa Agricultural University, Kanke, Ranchi, Jharkhand, 834006, India

Amartya Kumar Bhattacharya
Chairman and Managing Director, MultiSpectra Consultants, 23, Biplabi Ambika Chakraborty Sarani, Kolkata – 700029, West Bengal, India, E-mail: dramartyakumar@gmail.com

Sabinaya Biswal
AGFE Department, Indian Institute of Technology, Kharagpur – 721302, West Bengal, India, E-mail: sabin9937@gmail.com

Nupur Bose
Associate Professor, Department of Geography, A.N. College, Patna – 23, Bihar, India

Anita Chakraborty
Senior Technical Officer, Centre for Environmental Management and Participatory Development, Salt Lake, Kolkata – 700106. E-mail: anitagcenator@gmail.com

Saswati Chakraborty
Department of Civil Engineering, Indian Institute of Technology Guwahati, Guwahati – 781039, India

Surendra Chandniha
Research Associate, National Institute of Technology, Roorkee, Uttrakhand, India

Ravish Chandra
Central Agricultural University, Pusa, Samastipur (Bihar), India, E-mail: ravish.cae@gmail.com

Suman Kumar Dey
Professor, Department of Geography, Ramsaday College, Amta, Howrah, West Bengal, India

Ashok Ghosh
Professor & Head, Research Section, Mahavir Cancer Sansthan & Research Centre, Patna – 801505, Bihar, India

Pranab Kumar Ghosh
Department of Civil Engineering, IIT Guwahati – 781039, India

A. K. Gosain
Professor, Indian Institute of Technology Delhi, Hauz Khas, New Delhi – 110016, India

S. Goswami
Professor, Department of Earth Science, Sambalpur University, Sambalpur, Odisha

Saurabh Kumar Gupta
Research Scholar, School of Natural Resource Management, Centre for Land Resource Management, Central University of Jharkhand, Brambe, Jharkhand, India

Subrata Halder
Executive Engineer (A-I), State Water Investigation Directorate, Government of West Bengal, India

V. K. Jain
Subject Matter Specialist, KVK, RVSKVV, Ashok Nagar, Madhya Pradesh, India

Kiran Jalem
Assistant Professor, Centre for Land Resource Management, Central University of Jharkhand, Ranchi, India, E-mail: jalemkiran@gmail.com

Madan Kumar Jha
Professor, AGFE Department, Indian Institute of Technology, Kharagpur – 721302, West Bengal, India

Garima Jhariya
Institute of Agricultural Sciences, Banaras Hindu University, Varanasi (U.P.) 221005, India, E-mail: garima2304@gmail.com

Mintu Job
Assistant Professor, Department of Agricultural Engineering, Birsa Agricultural University, Kanke, Ranchi, Jharkhand, 834006, India, E-mail: mintujob@rediffmail.com

D. R. Kaushal
Professor, Indian Institute of Technology Delhi, Hauz Khas, New Delhi – 110016, India

Anil Kumar
Associate Director, Water Business Group, CH2M HILL (India) Pvt. Ltd, Noida – 201301, India, E-mail: anil.kumar2@ch2m.com

Chandrajeet Kumar
Research Scholar, UGC-RGNF-SRF, Department of EWM, A.N. College, Patna 23, Bihar, India, E-mail: mail4chandrajeet@yahoo.com

Nishant Kumar
Technical Specialist, Drinking Water and Sanitation Department, Government of Jharkhand, Ranchi, India

Randhir Kumar
Research Scholar (PhD), Center for Water Engineering and Management, Central University of Jharkhand, Ranchi, India

Satish Kumar
PhD Scholar, Indian Institute of Technology Delhi, Hauz Khas, New Delhi, India – 110016, E-mail: satish.kumar140@gmail.com

Neeta Kumari
Department of Civil and Environmental Engineering, B. I. T. Mesra, Ranchi – 835215, India, E-mails: neetak@bitmesra.ac.in, neeta.sinha2k7@gmail.com

Priti Kumari
Assistant Professor, Department of Civil Engineering, GGSESTC, Bokaro, Jharkhnad. E-mail: priti.9407@gmail.com

A. K. Lohani
Scientist G, National Institute of Hydrology, Roorkee, Uttrakhand, India

B. K. Mandal
Meteorological Centre Ranchi, India Meteorological Department, B. M. Airport Road, Hinoo, Ranchi – 834002, India

Swati Maurya
Institute of Environment and Sustainable Development, Banaras Hindu University, Varanasi – 221005, India, E-mail: mauryaswati35@gmail.com

Brijesh Kumar Mishra
Department of Environmental Science and Engineering, Indian Institute of Technology (Indian School of Mines), Dhanbad – 826004, India, E-mail: bkmishra3@rediffmail.com

K. L. Mishra
College of Agricultural Engineering, Jawaharlal Nehru Krishi Vishva Vidhyala Jabalpur (M.P.) – 480661, India

D. Nandi
Assistant Professor, Department of RS & GIS, North Orissa University, Baripada, Odisha, India, E-mail: debabrata.gis@gmail.com

Ipsita Nandi
Institute of Environment and Sustainable Development, Banaras Hindu University, Varanasi – 221005, India, E-mail: ipsitabhu@gmail.com

Sadaf Nazneen
School of Environmental Sciences, Jawaharlal Nehru University, New Delhi – 110067, India, E-mail: sadafnazneen01@gmail.com

Arvind Chandra Pandey
Professor, Centre for Land Resource Management, School of Natural Resource Management, Central University of Jharkhand, Brambe, Jharkhand, India, E-mail: arvindchandrap@yahoo.com

H. K. Pandey
Department of Civil Engineering, MNNIT Allahabad, India

Varsha Pandey
Institute of Environment and Sustainable Development, Banaras Hindu University, Varanasi – 221005, India, E-mail: varshu.pandey07@gmail.com

Prabeer Kumar Parhi
Assistant Professor, Centre for Water Engineering and Management, Central University of Jharkhand, Brambe, Ranchi, India, E-mail: prabeer11@yahoo.co.in

Gopal Pathak
Department of Civil and Environmental Engineering, B.I.T. Mesra, Ranchi – 835215, India

Rajani K. Pradhan
Institute of Environment and Sustainable Development, Banaras Hindu University, Varanasi – 221005, India, E-mail: rkpradhan462@gmail.com

N. Janardhana Raju
School of Environmental Sciences, Jawaharlal Nehru University, New Delhi – 110067, India

Rajeev Ranjan
Collage of Agricultural Engineering, Jawaharlal Nehru Krishi Vishva Vidhyala Jabalpur (M.P.) – 480661, India

Priti Sagar
Research Scholar, Centre for Water Engineering and Management, Central University of Jharkhand, Brambe, 835205, Jharkhand, India, Email: sagarpriti68@gmail.com

P. C. Sahu
Reader, Department of Geology, MPC Autonomous Colleges, Baripada, Odisha

Abhisek Santra
Department of Civil Engineering, Haldia Institute of Technology, Haldia, West Bengal

Kavita Shah
Institute of Environment and Sustainable Development, Banaras Hindu University, Varanasi, 221005, India

Arvind Kumar Shakya
Research Scholar, Department of Civil Engineering, IIT Guwahati, India – 781039,
E-mail: a.shakya@iitg.ernet.in

R. S. Sharma
Meteorological Centre Ranchi, India Meteorological Department, B. M. Airport Road, Hinoo,
Ranchi – 834002, India, E-mail: radheshyam84@rediffmail.com

Astha Singh
Department of Environmental Science and Engineering, Indian Institute of Technology
(Indian School of Mines), Dhanbad – 826004, India

C. S. Singh
Assistant Professor, Department of Agronomy, Birsa Agricultural University, Kanke, Ranchi,
Jharkhand, 834006, India

P. K. Singh
Professor, Department of Irrigation & Drainage Engineering, College of Technology,
G. B. Pant University of Agriculture and Technology, Pantnagar – 363145, Uttarakhand,
E-mail: singhpk68@gmail.com

Prashant K. Srivastava
Institute of Environment and Sustainable Development, Banaras Hindu University, Varanasi – 221005, India

Stuti
Research Scholar, School of Natural Resource Management, Centre for Land Resource Management,
Central University of Jharkhand, Brambe, Jharkhand, India, E-mail: stuti@cuj.ac.in

Sarika Suman
Banaras Hindu University, Varanasi, India

Sushmita
Research Scholar, Department of EWM, A.N. College, Patna 23, Bihar, India

Nity Tirkey
Research Scholar, Centre for Water Engineering and Management, Central University of Jharkhand,
Ranchi, India, E-mail: nitytirkey@gmail.com

A. K. Tiwari
Assistant Professor, Department of Horticulture, Birsa Agricultural University, Kanke, Ranchi,
Jharkhand, 834006, India

Vivek Tiwari
Banaras Hindu University, Varanasi, India, E-mail: viveektiwary@gmail.com

Sachin Kumar Tomar
Department of Civil Engineering, Indian Institute of Technology (Guwahati), Guwahati – 781039, India,
E-mail: sachintomar306@gmail.com

Vinod Kumar Tripathi
Department of Farm Engineering, Institute of Agricultural Sciences, Banaras Hindu University,
Varanasi, U.P., 221005, India, E-mail: tripathiwtcer@gmail.com

Utkarsh Upadhayay
Research Scholar, Centre for Water Engineering and Management, Central University of Jharkhand,
Jharkhand, Ranchi, India, E-mail: utkarsh.wem.cuj@gmail.com

Devendra Warwade
Assistant Professor, Department of Physics, Government College Sehore, Barktulla University, Bhopal, M.P., India

Pratibha Warwade
Assistant Professor, Center for Water Engineering and Management, Central University of Jharkhand, Brambe, Ranchi – 835205, India, E-mail: pratibhawarwade@gmail.com

Naval Kishor Yadav
Department of Civil Engineering, Haldia Institute of Technology, Haldia, West Bengal

ABBREVIATIONS

AC	activated carbon
AGR	aerobic granular reactor
AHP	analytical hierarchy process
ANN	artificial neural network
AOI	area of interest
APHA	American Public Health Association
ASCII	American Standard Code for Information Interchange
BC	biochar
BHPV	Bharat Heavy Plates & Vessels
BOD	biochemical oxygen demand
BSIL	Beekay Steel Industries Ltd.
BWDB	Bangladesh Water Development Board
CCI	climate change initiative
C_{eff}	coefficient of efficiency
CGWB	Central Ground Water Board
CNTS	carbon nanotubes
COD	chemical oxygen demand
CSI	cumulative score index
CVD	chemical vapor deposition
DAS	days after sowing
DDW	doubled distilled water
DEM	digital elevation model
DIC	dissolved inorganic carbon
DMICDC	Delhi Mumbai Industrial Corridor Development Corporation
DOC	dissolved organic carbon
DS NVPH	double span naturally ventilated polyhouse
DSSAT	decision support system for agrotechnology transfer
DVC	Damodar Valley Corporation
DW	dug well
EC	electrical conductivity
ECs	emerging contaminants
EDC	endocrine disrupting chemicals
EDS	environmental design solutions
EKW	East Kolkata Wetlands

EPA	Environmental Protection Agency
E_R	effective rainfall
ET_O	reference evapotranspiration
FESEM	field emission scanning electron microscope
gcm^{-3}	gram per centimeter cube
gl^{-1}	gram per liter
GLOF	glacial lake outburst floods
GPS	global positioning system
GSA	grain-size analysis
GSDC	grain-size distribution curves
GSV	granule settling velocity
ha	hectare
HMI	human-machine interface
HP	hand pump
HRT	hydraulic retention time
HSZ	hydrological sensitive zones
ICAR	Indian Council of Agricultural Research
ICASA	International Consortium for Agricultural Systems Applications
IMDMCC	Inter-Ministerial Disaster Management Co-Ordination Council
IPCC	Intergovernmental Panel on Climate Change
IR	net depth of irrigation
IWMED	Institute of Wetland Management and Ecological Design
IWRM	integrated water resource management
KRB	Kosi River Basin
LAI	leaf area index
LDR	linear decision rule
LST	land surface temperature
MBC	modified biochar
MBIR	Manesar Bawal Investment Region
MCDM	multi-criteria decision-making
MCL	maximum contaminant level
mgl^{-1}	milligram per liter
mh^{-1}	meter per hour
MIF	multi-influencing factor
MLD	million liter per day
MLVSS	mixed liquor volatile suspended solids
$mmday^{-1}$	millimeter per day
NASA	National Aeronautics and Space Administration
NDMC	National Disaster Management Council
NDVI	normalized difference vegetation index

NEO	NASA Earth Observation
NGA	National Geospatial-Intelligence Agency
NOAA	National Oceanic and Atmospheric Administration
OECD	Organization for Economic Co-Operation and Development
PCA	principal component analysis
POWER	prediction of worldwide energy resources
qha^{-1}	quintal per hectare
RIMCS	remote irrigation monitoring and control system
RLD	root length density
RMSE	root mean square error
RWSP	Rural Water Supply Scheme of Panchayati Raj
SBC	single board computer
SBR	sequencing batch reactor
SMC	soil moisture content
SMD	soil moisture deficit
SOP	standard operating policy
SRTM	shuttle radar topographic mission
SWMM	stormwater management model
TDS	total dissolved solids
TDSS	total dissolved and suspended solids
TEAP	terminal electron accepting processes
TSS	total suspended solids
TWI	topographic wetness index
UHI	urban heat island
VES	vertical electrical soundings
VSA	variable source area
VSS	volatile suspended solids
WHO	World Health Organization
WRC	water retention curve
WT NVPH	walking tunnel naturally ventilated polyhouse
WUE	water use efficiency

PREFACE

The Centre for Water Engineering and Management came into existence in July 2010 and is presently offering five-year integrated MTech, two-year MTech degrees, and a separate PhD program in Water Engineering and Management. With a mission to encourage innovative approaches of thinking, the center is in the process of developing highly skilled manpower in the field of water engineering. Water is at the core of sustainable development and is critical for socioeconomic development, healthy ecosystems, and for human survival itself.

The world's population is increasing and concentrating more and more in urban areas. This trend is particularly intense in developing countries, where an additional 2.1 billion people are expected to be living in cities by 2030. These cities produce billions of tons of waste every year, including sludge and wastewater. In India, the estimated sewage generation from Class I cities and Class II towns (representing 72% of urban population) is 38,524 million liters/day (MLD), of which there exists a treatment capacity of only 11,787 MLD (about 30%). How the treated wastewater is being used is something that needs to be looked into. India needs a national wastewater reuse policy to help address the urban and rural water demand by quantifying the targets and laying out legislative, regulatory, and financial measures to achieve those targets. It is a matter of great pride that the Government of Jharkhand has devised a Jharkhand Waste Water Policy 2017 to ensure increased use of recycled water for other purposes apart from drinking, through the provision of appropriate technologies for water recycling and protection of the environment.

The International Conference on Water and Wastewater Management and Modelling was held January 16–17, 2018 at Ranchi, India. The conference received a good number of research papers and review articles. The research papers were reviewed critically, and we are happy to have them collected in this volume. This will ensure larger distribution and circulation of the edited book in the research and teaching community across the world. The book is organized in chapters covering major themes of the conference; the chapters are divided into sections, and the sections into topical subsections.

The authors want to record their gratitude to all the contributing authors who participated in the conference. We take this opportunity to express our

gratitude towards our Honorable Vice Chancellor, Prof. Nand Kumar Yadav 'Indu,' for his constant encouragement and support. I would like to thank the editorial staff, Sandy Jones Sickels, Vice President, and the production team at Apple Academic Press, Inc., for considering this book to publish when reuse of wastewater needs to be encouraged and streamlined in developing nations. Special thanks are due to the AAP production staff for bringing the quality production.

I request readers to offer their valuable and constructive suggestions that may help to improve future endeavors.

I express my deep admiration to my wife, Punam, and daughter Anushka, for their unconditional support and cooperation during the preparation of this book.

—**Ajai Singh, PhD, FIE**

PART I
Wastewater Management

CHAPTER 1

VERMIFILTRATION OF ARSENIC CONTAMINATED WATER USING VERMIFILTRATION TECHNOLOGY: A NOVEL BIO-FILTER MODEL

CHANDRAJEET KUMAR[1], SUSHMITA[2], NUPUR BOSE[3], and ASHOK GHOSH[4]

[1]*PhD Scholar, UGC-RGNF-SRF, Department of EWM, A.N. College, Patna 23, Bihar, India, E-mail: mail4chandrajeet@yahoo.com*

[2]*PhD Scholar, Department of EWM, A.N. College, Patna 23, Bihar, India*

[3]*Associate Professor, Department of Geography, A.N. College, Patna–23, Bihar, India*

[4]*Professor and Head, Research Section, Mahavir Cancer Sansthan and Research Centre, Patna 801505, Bihar, India*

ABSTRACT

Arsenic toxicity has become a global concern owing to the increasing contamination of soil, groundwater, and crops in many regions of the world, and Bihar is one of the worst affected states of India where Arsenic concentration has been found up to 1861 ppb in groundwater. As Arsenic has a high magnitude of solubility, its removal from contaminated water and soil is very difficult. Vermifiltration of Chemically contaminated and sewage water using earthworms is a newly conceived novel technology with several advantages over the conventional water filtration systems. Certain species of earthworms (*Eisenia fetida* and *Eudrillus euginae*) have been found to purify the contaminated wastewater. Their bodywork as a 'bio-filter' having the capacity to bio-accumulate high concentrations of toxic chemicals in their tissues and the resulting purified water (termed as Vermiaqua) becomes almost chemical and pathogen-free. To make vermifiltration unit,

a vermifilter bed was prepared using plastic drum which was in depth filled with a large, medium, small size stone chips followed by sand and humid soil at the top layer and 5000 earthworms were released in the moist soil top layer. Water controller knob was attached with a sample container which allows 50–60 drops per minute water input into the top layer of vermifilter bed which was also attached with Filtrate collector container through pipe for filtrate collection. Prepared arsenic trioxide solutions of 10,000 μgl^{-1} and 20,000 μgl^{-1} were poured in separate sample collection container and allowed to pass through layers of vermifilter bed for continuous three days and on the fourth day purified water was collected in nitric acid washed filtrate collection container and analyzed by atomic absorption spectrophotometer (AAS). According to the AAS analysis, the arsenic concentration of 10,000 μgl^{-1} and 20,000 μgl^{-1} values were decreased to 7.716 μgl^{-1} and 6.186 μgl^{-1}, respectively and accordingly in the body tissue of earthworms, 127.9 μgl^{-1} and 63.81 μgl^{-1} arsenic were found, respectively.

1.1 INTRODUCTION

Arsenic is a known carcinogen and a mutagen. Since the arsenic contaminated groundwater is leading to a host of health problems, often culminating in diseases with high fatality rates, like cancer. Tragically, most of the worst geogenic arsenic affected areas are located in developing economies of the world, and there is an ever-increasing demand for arsenic-free water in these heavily populated areas. The fluvial plains of South Asia have borne the brunt of incidences of arsenicosis, or chronic diseases due to arsenic poisoning, across countries of Bangladesh, India, Nepal, and Pakistan. This global health issue can be best controlled by halting direct and indirect ingestion of arsenic that is taking place through contaminated drinking water and arsenic contaminated agricultural produce, and simultaneously supplying clean water for drinking and irrigation purposes. Several proven filtration technologies are now globally in place, broadly categorized in Mandal et al. (2002). Earthworms have over 600 million years of history in waste and environmental management. Charles Darwin called them as the 'unheralded soldiers of mankind,' and the Greek philosopher Aristotle called them as the 'intestine of earth,' meaning digesting a wide variety of organic materials including the waste organics from earth (Darwin and Seward, 1903). Earthworms harbor millions of 'nitrogen-fixing' and 'decomposer microbes' in their gut. The distribution of earthworms in soil depends on factors like soil moisture, availability of organic matter, and pH of the soil. They occur

in diverse habitats especially those which are dark and moist. Earthworms are generally absent or rare in soil with a very coarse texture and high clay content or soil with pH 4 (Gunathilagraj, 1996). In a study made by Kerr and Stewart (2006), it was opined that fetida can tolerate soils nearly half as salty as seawater. Earthworms can also tolerate toxic chemicals in the environment. *E. fetida* also survived 1.5% crude oil containing several toxic organic pollutants (OECD, 2000). Some species have been found to bio-accumulate up to 7600 mg of lead (Pb) per gm of the dry weight of their tissues (Ireland, 1983). They can tolerate a temperature range of 5 to 29°C. A temperature of 20–25ºC and moisture of 60–75% are optimum for good worm function (Hand, 1988).

Vermifiltration of wastewater using waste eater earthworms is a newly conceived novel; an innovative technology developed by our research collaborator. Earthworms bodywork as a 'biofilter' and they have been found to remove the 5 days BOD by over 90%, COD by 80–90%, total dissolved solids (TDS) by 90–92% and the total suspended solids (TSS) by 90–95% from wastewater by the general mechanism of 'ingestion' and biodegradation of organic wastes, heavy metals and solids from wastewater and also by their 'absorption' through body walls (Sinha et al., 2015). Most successful species are the Tiger Worms (*Eisenia fetida*). Vermifiltration system is low energy dependent and has a distinct advantage over all the conventional biological wastewater treatment systems—the 'activated sludge process,' 'trickling filters,' and 'rotating biological contractor' which are highly energy intensive, costly to install and operate, and do not generate any income. This is also an odor free process. The most significant advantage is that there is 'no sludge formation' in the process as the earthworms eat the solids simultaneously and excrete them as vermicast. This plagues most municipal council in the world as the sludge being a biohazard requires additional expenditure on safe disposal in secured landfills. In the vermifilter process, there is 100% capture of organic & inorganic materials and any pathogen, and capital and operating costs are much lesser. Earthworm's bio-accumulate all toxic chemicals including the 'endocrine disrupting chemicals' (EDCs) from sewage which cannot be removed by the conventional systems. A pilot study on vermifiltration of sewage was made by Xing et al. (2005) at Shanghai Quyang Wastewater Treatment Facility in China. Taylor (2003) studied the treatment of domestic wastewater using vermifilter beds and concluded that worms could reduce BOD and COD loads as well as the TDSS (total dissolved and suspended solids) significantly by more than 70–80%. Hartenstein and Bisesi (1989) studied the use of earthworms for the management of effluents from intensively housed livestock which contains

very heavy loads of BOD, TDSS, nutrients nitrogen (N) and phosphorus (P). The worms produced clean effluents and also nutrient-rich vermicompost. Bajsa et al. (2003) also studied the Vermifiltration of domestic wastewater using vermicomposting worms with significant results.

1.2 EXPERIMENTAL DESIGN

1.2.1 CONSTRUCTION AND INSTALLATION OF THE VERMIFILTRATION UNIT

To make vermifiltration unit, three plastic drums of 80-liter capacity were taken. Out of these three drums, two of them were prepared as vermifilter unit for arsenic filtration and remaining one was prepared as control (Figure 1.1). In the control unit, all other materials were organized in the same way as in vermifilter unit except earthworms. All three plastic drums were filled with different layers consisting of large size pebbles with 10" height, medium size pebbles (10"), small size pebbles (10") followed by sand (6–7"), and humid soil (20") at the top layer to prepare filter (Figure 1.2). Finally, 5000 number of earthworms (*Eisenia fetida*) weighing approximately 5 kg were released in the moist soil layer of two filter unit to prepare vermifiltration unit.

FIGURE 1.1 Construction and installation of the vermifiltration unit.

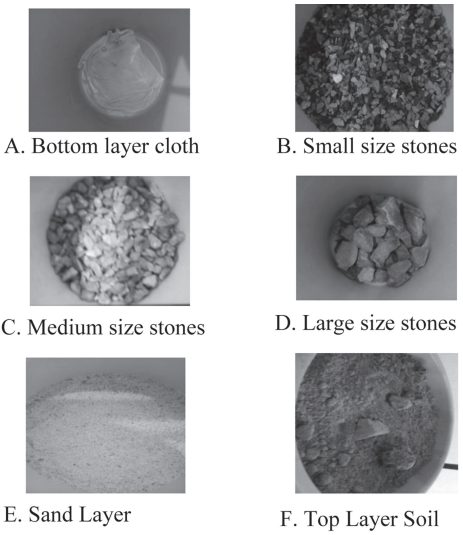

FIGURE 1.2 Different layers of vermifiltration unit.

A movable iron stand of approximately 150 kg was prepared to have 4 columns and 3 rows to keep 3–4 filtration unit, sample containers, and filtrate collector containers. Upper row carries the sample container, middle row carries the plastic drum (vermifilter bed), and the lower row carries the filtrate collector container. Water controller knob was attached with a sample container which allows 50–60 drops per minute water input into the top layer of vermifilter bed (Figure 1.3). A base of plastic drums were joined with filtrate collector container through the pipe for filtrate collection. Filtrate collection containers were rinsed with nitric acid and tightly packed for prevention of arsenic oxidation.

FIGURE 1.3 Top layer of the vermifiltration Unit.

1.3 METHODOLOGY

1.3.1 PREPARATION OF DIFFERENT CONCENTRATION OF ARSENIC Trioxide Sample

About 1.320 gm of arsenic trioxide and 4.0 gm of NaOH were weighed and dissolved completely in a round bottom volumetric flask containing 100 ml distilled water and a total volume of 1 liter was maintained for preparing a stock solution of 1000 μgl^{-1}. From this stock, different concentrations of 10,000 μgl^{-1} and 20,000 μgl^{-1} were prepared.

1.3.2 FILTRATION OF ARSENIC THROUGH VERMIFILTRATION PROCESS

Prepared arsenic trioxide solutions of 10,000 μgl^{-1} and 20,000 μgl^{-1} were poured in separate sample collection container and allowed to pass through controlled water knob 50–60 drops per minute into top layer (soil + earthworm) of vermifiltration bed for continuous three days and on fourth day, vermifiltered water was collected in nitric acid washed filtrate collection container. In control unit (without earthworms), 10,000 μgl^{-1} arsenic trioxide solution was allowed to pass through controlled water knob 50–60 drops per minute into soil layer and the remaining process was the same.

1.3.3 ANALYSIS OF VERMIFILTERED ARSENIC TRIOXIDE SAMPLE BY ATOMIC ABSORPTION SPECTROPHOTOMETER (AAS)

About 50 ml of vermifiltered water was mixed with concentrated HNO_3 in Griffin beaker and covered with watch glass then placed on hotplate (90–120°C) to evaporate continuously till getting the final volume up to 5 ml. Again 5 ml concentrated HNO_3 was added in cooled 5 ml remaining sample and placed on hotplate (90–120°C) to evaporate continuously till getting the final volume to 3 ml. Griffin beaker wall and watch glass were washed with distilled water or 1% HNO_3. Finally, digested samples were filtered through What's Mann Filter Paper No. 1 to remove silicate, and other insoluble impurity and volume were adjusted to 50 ml with 1% HNO_3 and analyzed by AAS.

1.3.4 ANALYSIS OF EARTHWORMS' BODY TISSUE BY AAS

About 0.5 mg earthworms were weighed and washed with 1% HNO_3 for cleaning and treated with 5 ml concentrated HNO_3 and kept for overnight for digestion, then placed on hotplate (90–120°C) to evaporate continuously till getting the final volume 1 ml. Now, nitric acid and perchloric acid were added in the digested sample in the 6:1 ratio. Again, this was placed on hotplate (90–120°C) to evaporate continuously till getting the final volume to 1 ml. Finally, the digested sample was filtered through What's Mann Filter Paper No. 1 to remove silicate, and other insoluble impurity and volume were adjusted to 50 ml with 1% HNO_3 and analyzed by AAS.

1.4 RESULTS AND DISCUSSION

According to the AAS analysis, the arsenic concentration of 10,000 μgl^{-1} and 20,000 μgl^{-1} value were decreased to 7.716 μgl^{-1} and 6.186 μgl^{-1}, respectively, but the control value decreased only to 80.780 μgl^{-1} (Table 1.1). Accordingly, in the earthworm's body tissue, 127.9 μgl^{-1} and 63.81 μgl^{-1} arsenic were found in Test 1 and Test 2, respectively. In control, soil absorbs only 19.58 µg/l arsenic because of normal arsenic holding capacity and due to long exposure of air, oxidation, and precipitation of Arsenic.

TABLE 1.1 Arsenic Levels in Vermifiltered Solutions

	Control 10,000 μgl^{-1}	**Test 1 10,000 μgl^{-1}**	**Test 2 20,000 μgl^{-1}**
Vermifiltered Arsenic Water	80.780 μgl^{-1}	7.716 μgl^{-1}	6.186 μgl^{-1}
Earthworms' Body Tissue (0.5 mg)	No Earthworms were used	127.9 μgl^{-1}	63.81 μgl^{-1}
Soil Testing (0.5 mg)	19.58 μgl^{-1}	144.7 μgl^{-1}	92.37 μgl^{-1}

In Test 1, because of Earthworm's high arsenic holding capacity along with soil, 144.7 μgl^{-1} Arsenic was absorbed. However, in Test 2, under twice the amount of arsenic concentration in the input solution, earthworms were found to absorb less arsenic in their body in comparison to those of Test 1. Likewise, the soil also held 92.37 μgl^{-1} of arsenic which is comparatively lesser from the soil of Test 1.

1.5 CONCLUSIONS

Although this is indicative that Earthworms are highly tolerable to arsenic assimilation because of high absorbance capacity and thereby they are able to minimize the concentration of arsenic, certain research questions have been generated by this experiment:

1. The pathway of arsenic through the soil-earthworm-sand-small stone chips-medium stone chips large stone chips in both Test 1 and Test 2 environments need to be studied.
2. Reduced arsenic concentration levels in Test 2 phases need immediate research interventions. The results imply that with increasing doses of arsenic, the threshold values of arsenic uptake by soils and earthworms of filter beds decline significantly. If this be nature's behavior in limiting arsenic uptake by soil microbes and earthworms, this has tremendous potential in scientifically identifying the gene's responsible for this.
3. To identify the role of microbes, present in the gut of earthworms in arsenic conversion.

KEYWORDS

- **arsenic**
- **bio-filter**
- **earthworms**
- **vermiaqua**
- **vermifiltration technology**

REFERENCES

Bajsa, O., Nair, J., Mathew, K., & Ho, G. E., (2003). Vermiculture as a tool for domestic wastewater management, *Water Science and Technology*, IWA Publishing, *48*(11/12), 125–132.

Darwin, F., & Seward, A. C., (1903). *More Letters of Charles Darwin*. A record of his work in series of hitherto unpublished letters, John Murray, London, *2*, 508.

Gunathilagraj, K., (1996). *Earthworm: An Introduction*. Indian Council of Agricultural Research Training Program, Tamil Nadu Agriculture University, Coimbatore.

Hand, P., (1988). Earthworm biotechnology. In: *Green Shields Resources and Application of Biotechnology: The New Wave*. MacMillan Press Ltd., US.

Hartenstein, R., & Bisesi, M. S., (1989). Use of earthworm biotechnology for the management of effluents from intensively housed livestock, *Outlook Agriculture*, *18*(2), 72–76.

Ireland, M. P., (1983). *Heavy Metals Uptake in Earthworms, Earthworm Ecology* (pp. 247–265). Chapman & Hall, London.

Kerr, M., & Stewart, A. J., (2006). Tolerance test of *Eisenia fetida* for sodium chloride, US Department of Energy, *Journal of Undergraduate Research.* doi: https://www.osti.gov/servlets/purl/1051306.

Mandal, B. K., & Suzuki, K. T., (2002). Arsenic round the world: A review. *Talanta*., *58*, 201–235.

OECD, (2000). Guidelines for testing organic chemicals. Proposal for new guidelines earthworms' reproduction tests (*E. fetida andrei*). *Organization for Economic Co-Operation and Development*. https://www.oecd.org/env/ehs/testing/Draft-Updated-Test-Guildeline-222-Earthworm-Reproduction-Test.pdf.

Sinha, R. K., Kumar, C., Hahn, G., Patel, U., & Soni, B. K., (2015). Embarking on second green revolution by vermiculture for production of chemical-free organic foods, production of crops and farm soils and elimination of deadly agrochemicals from earth: Meeting the challenges of food security of 21st century by earthworms. Nova Science Publishers, Inc. *Sir Charles Darwin's "Friend of Farmers" Agricultural Research Update*, *10*, 1–47.

Sinha, R. K., Misra, N. K., Singh, P. K., Ghosh, A., Patel, U., Kumar, J., et al., (2015). Vermiculture technology for recycling of solid wastes and wastewater by earthworms into valuable resources for their reuse in agriculture (organic farming) while saving water and fertilizer, In: Rajeev, P. S., & Abhijit, S., (eds.), *Waste Management: Challenges, Threats and Opportunities*, Nova Science Publications, USA. pp. 233–256, ISBN: 978-1-63482-150-6.

Taylor, (2003). The treatment of domestic wastewater using small-scale vermicompost filter beds. *Ecol. Eng*., *21*, 197–203.

Xing, M., Yang, J., & Lu, Z., (2005). *Microorganism-Earthworm Integrated Biological Treatment Process: A Sewage Treatment Option for Rural Settlements*. ICID 21st European Regional Conference. http://www.zalf.de/icid/ICID_ERC2005/HTML/ERC2005PDF/Topic_1/Xing.pdf.

CHAPTER 2

PERFORMANCE OF AN AEROBIC GRANULAR REACTOR TREATING ORGANICS AND AMMONIA NITROGEN WITH TIME

SACHIN KUMAR TOMAR and SASWATI CHAKRABORTY

Department of Civil Engineering, Indian Institute of Technology (Guwahati), Guwahati – 781039, India,
E-mail: sachintomar306@gmail.com

ABSTRACT

Aerobic granules were developed in a sequencing batch reactor (SBR) for treating phenol (400 mgl^{-1}), thiocyanate (SCN^-) (100 mgl^{-1}) and ammonia-nitrogen (NH_4^+-N) (100 mgl^{-1}). Reactor performance was analyzed in terms of pollutant degradation profile in one cycle of 6 h with respect to time. Mean biomass size and volatile suspended solids (VSS) were 1334.24 ± 30.56 µm and 4.90±0.40 gl^{-1} in the reactor, respectively. Within initial 30 min, effluent phenol, SCN^-, and COD (chemical oxygen demand) decreased to 1.93, 6.64 and 145.81 mgl^{-1} from initial values of 400, 100 and 1015.71 ± 33.83 mgl^{-1}, respectively. Complete phenol and SCN^- degradations required almost 120 min. Maximum COD removal achieved was 90.37%. NH_4^+-N removal required a longer time than other pollutants. Kinetic analysis showed that 180 min was adequate for the degradation of all pollutants and to achieve nitrification by aerobic granules.

2.1 INTRODUCTION

The economic and efficient treatment of industrial wastewaters is a great challenge since they comprise of complex matter consists of several

organic compounds (like aromatic compounds), inorganic compounds, and ammonia (Kim and Kim, 2003). Usually, physicochemical processes are practiced to treat industrial wastewaters in spite of having serious drawbacks such as high operational cost, incomplete degradation of aromatic compounds and production of other hazardous byproducts (Kim and Ihm, 2011). The drawbacks of physicochemical processes can be overcome by biological processes. However, the aromatic compounds can cause inhibition to the biological processes (Khalid and Naas, 2012). Phenol with a concentration of 110–487 mgl^{-1} is found with other inhibitory and toxic compounds like thiocyanate (SCN^-) and ammonia-nitrogen (NH_4^+-N) in wastewaters from coal liquefaction, coal gasification and synthetic fuel processing, etc. (Li et al., 2011; Zheng and Li, 2009). When phenol and (SCN^-) are present with ammonia, these compounds inhibit nitrification; therefore require to be removed before nitrification (Jeong and Chung, 2006; Kim et al., 2008). The rate-limiting step in wastewater treatment is the removal of ammonia by nitrification because of the very slow growth rate of nitrifying bacteria and susceptibility to environmental factors as well as other factors like inhibition by aromatic compounds. Therefore, growth and maintenance of sufficient nitrifying bacteria are very difficult in wastewater treatment systems based on suspended or fixed culture (Ochoa et al., 2002; Ramos et al., 2016).

Aerobic granule based biological treatment systems serve as an alternative approach for treating the complex industrial wastewaters (Gao et al., 2011). Aerobic granules are the microbial aggregates contain millions of organisms per gram of biomass with a regular round shape, a distinct outline and a compact structure formed via self-immobilization of microorganisms without any support/carrier under aerobic condition by applying controlled loading and operating conditions (Beun et al., 1999; Liu and Tay, 2007). Aerobic granulation has become an efficient and promising technology in biological wastewater treatment systems because of several advantages over conventional treatment systems such as excellent settling behavior, a compact structure, high metabolic activity, tolerance towards higher and shock loadings and ability to degrade toxic compounds like phenol (Adav et al., 2008; Corsino et al., 2015). That's why it has been extensively used in treating various wastewaters including industrial, nutrient-rich, and toxic wastewaters (Kishida et al., 2009; Val del Rio et al., 2012; Zhao et al., 2015). Aerobic granulation has a great potency for removing both organic and ammonium pollutants simultaneously in an economic manner (Singh and Srivastava, 2011). The works of literature are very limited for removing both phenols

with ammonia nitrogen simultaneously by aerobic granular reactor (AGR) (Liu et al., 2005; Ramos et al., 2016). The limitation in the efficient operation of AGR for nitrification can be overcome by providing a selective approach to improve nitrifying granulation for effective ammonia conversion (Wu et al., 2017). Aerobic granule can tolerate the toxic effect of high concentration of toxic compounds due to a mass transfer shield of embedded cells provided by them (Ho et al., 2010). AGR is largely operated as a sequencing batch reactor (SBR). SBR is having a unique feature to be operated in a cyclic mode comprising of filling, aeration, settling, and withdrawal as compared to a continuous culture. To the best of authors' knowledge, the very limited study addressed the kinetic behavior of toxic pollutants like phenol and (SCN^-) along with nitrification in one cycle. The present study aims to investigate the performance of AGR in removing toxic pollutants like phenol, (SCN^-), and to achieve nitrification with time in one cycle.

2.2 MATERIALS AND METHODS

2.2.1 EXPERIMENTAL SET-UP

The present study was carried out in a laboratory scale reactor operated in sequential batch mode. The reactor had a working volume of 6 l. The working height, and an inner diameter (ID) of the reactor was 212 and 6 cm, respectively (H/D ratio of 35). Aeration was provided by an oil-free compressor at a rate of 2 l min^{-1} by air stone kept at the bottom in the reactor. The influent synthetic wastewater was introduced from the bottom of the reactor with the help of a peristaltic pump. The up-flow liquid velocity in the reactor was maintained at a rate of 2 mh^{-1}. The reactor was maintained at room temperature (25–30°C).

2.2.2 CHARACTERISTICS OF SEED

The inoculum was collected from activated sludge unit of wastewater treatment plant of Indian Oil Corporation Limited (IOCL), Noonmati, Guwahati, Assam. The suspended and volatile solids in IOCL sludge were 2.42 ± 0.16 and 1.72 ± 0.15 gl^{-1}, respectively. The particle size of sludge was of 32.78 ± 0.01 µm. The sludge volume index (SVI_{30}) was 50.13 mlg^{-1}. In the reactor, 3 L sludge was used for working volume of 6 L.

2.2.3 FEED CHARACTERISTICS

The influent synthetic wastewater consisted of phenol of 400 mgl^{-1}; ammonia nitrogen (NH_4^+–N as NH_4Cl) of 100 mgl^{-1} and thiocyanate (SCN^- as KSCN) of 100 mgl^{-1}. Feed pH was maintained between 7.5–8 by using sodium hydrogen carbonate and phosphate buffer (using 72.3 gl^{-1} of KH_2PO_4 and 104.5gl^{-1} of K_2HPO_4). This phosphate buffer also worked as a phosphorus source for microorganisms. Phosphate buffer of 1 mll^{-1} and trace metals solution of 1 mll^{-1} was added in the synthetic feed in the reactor. The stock trace metal composition was taken from previous literature (Sahariah and Chakraborty, 2011). The composition of stock trace metal solution was: $MgSO_4.7H_2O$: 10,000 mgl^{-1}, $CaCl_2.2H_2O$: 10,000 mgl^{-1}, $FeCl_3.6H_2O$: 5000 mgl^{-1}, $CuCl_2$: 1000 mgl^{-1}, $ZnCl_2$: 1000 mgl^{-1}, $NiCl_2.6H_2O$: 500 mgl^{-1}, $CoCl_2$: 500 mgl^{-1}.

2.2.4 OPERATIONAL STRATEGY

The operational schedule of the reactor is given in Table 2.1. The reactor was operated in the sequential batch mode with a volume exchange ratio of 50%; i.e., 50% of reactor working volume was decanted in each cycle, and the similar amount of fresh feed was added to the reactor. Settling time was kept constant for 5 min in the reactor throughout the study, except for the initial 15 days, when it was 15 min to prevent severe washout of biomass from the reactor. The reactor was operated at a cycle time of 6 h. Hydraulic retention time (HRT) was calculated using Eq. (1) and HRT value is given in Table 2.1.

$$\text{HRT (day)} = \frac{\text{Reactor volume (L)}}{\text{Volume decanted per cycle (L)} \times \text{No. of cycles per day}} \quad (1)$$

Reactor was acclimatized for concentrations of phenol, (SCN^-), and ammonia up to 400, 100 and 100 mgl^{-1}, respectively. After 45 days of acclimatization period, the desired concentrations of pollutants were obtained. Then the reactor was operated for another 27 days with same feed and the same operating condition for steady state.

2.2.5 ANALYTICAL METHODS

The granule size was measured by a laser particle size analyzer (Mastersizer 2000, Malvern Instruments) and occasionally by field emission scanning electron microscope (FESEM) (Sigma, Zeiss). For FESEM analysis the

TABLE 2.1 Operational Schedule of Reactor

Operational time (day)	No of cycles/d	Cycle time (h)	Distribution of cycle time (min)				HRT (h)	OLR*	NLR**	ULV***
			Feeding	Reaction	Settling	Withdrawal				
1–75	4	6	30	320	5	5	12	2.13	0.20	2

*Organic loading rate (kg COD/m^3.day);

**Nitrogen loading rate (kg NH_4^+-N/m^3.day);

***Up flow liquid velocity (mh^{-1}).

granules were fixed with 2% glutaraldehyde overnight at 4°C after washing with phosphate buffer (pH 7.0) and then was dehydrated with ethyl alcohol and dried (Wang et al., 2007). Granule settling velocity (GSV) (mh^{-1}) was determined by the free settling test as described by Yu et al. (2009). Analysis for phenol, ammonia nitrogen, nitrite, (SCN^-), chemical oxygen demand (COD), suspended solids, volatile suspended solids (VSS), SVI_{30} was carried out according to standard methods (APHA, 2005). Nitrate was analyzed by ion chromatograph (792 Basic IC, Metrohm) using anion column (Metrosep ASupp 5–250/4.0) and carbonate fluent.

2.3 POLLUTANTS DEGRADATION IN ONE CYCLE IN THE REACTOR

An analysis was carried out during a steady-state condition of the reactor (70^{th}–72^{nd} day). At steady state VSS, average size and SVI_{30} were 4.90±0.40 gl^{-1}, 1334.24 ± 30.56 µm and 67.69±7.13 mlg^{-1}, respectively. GSV was 35.79 ± 2.20 m/h. FESEM images of granule are given in Figure 2.1.

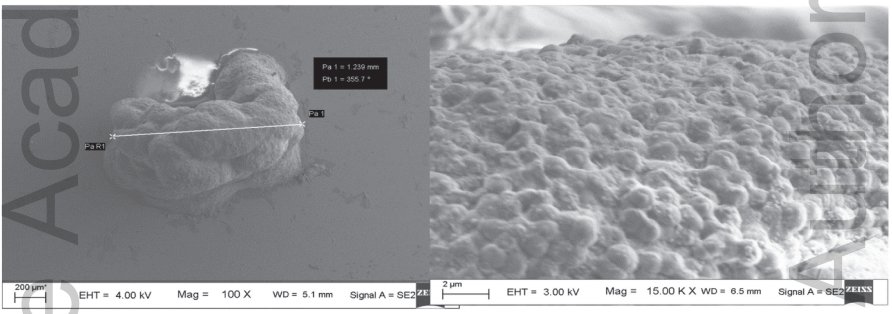

(a) (b)

FIGURE 2.1 FESEM images of the granule.

In the present study, organic loading rate and nitrogen loading rate in the reactor were 2.13 kg COD/m^3.day and 0.20 kg NH_4^+-N/m^3.day, respectively with influent COD: NH4$^+$-N ratio of 10.65. From Figure 2.2, it can be observed that within the initial 30 min, effluent phenol and COD decreased to 1.93 and 145.81 mgl^{-1} from initial values of 400 and 1015.71 mgl^{-1}, respectively. Complete phenol degradation required almost 120 min and maximum COD removal achieved was 90.37% (effluent 111.97 mgl^{-1}) after 240 min. 93.36% SCN^- (concentration of 6.64 mgl^{-1}) was removed in initial 30 min and required almost 120 min to degrade completely (Figure 2.3).

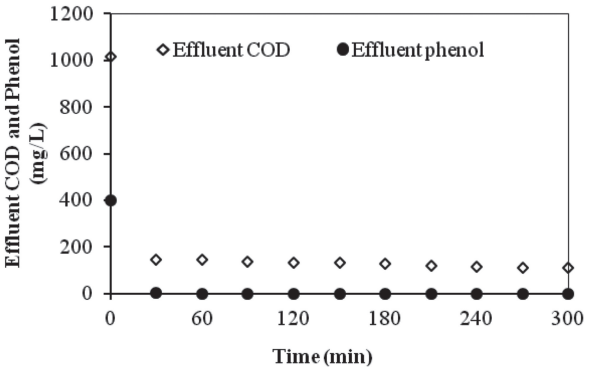

FIGURE 2.2 Effluent concentration profile of COD and phenol (mgl^{-1}) with time.

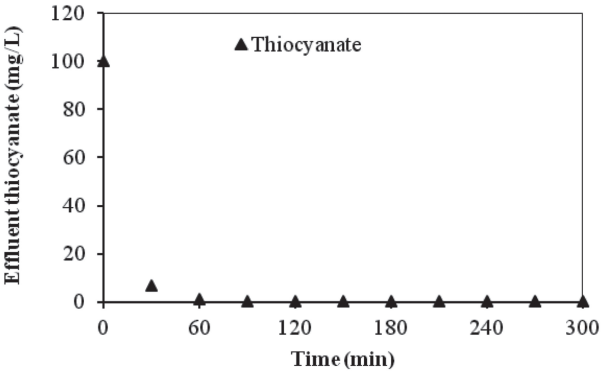

FIGURE 2.3 Effluent concentration profile of thiocyanate (mgl^{-1}) with time.

NH_4^+-N removal though started along with other pollutants, required a longer time than other pollutants. Only 40% removal was achieved in initial 30 min and complete removal required 180 min from an initial concentration of 100 mgl^{-1} and 24 mgl^{-1} NH_4^+-N generated from complete degradation of 100 mgl^{-1} SCN^- (Figure 2.4). NO_3^--N profile (Figure 2.5) shows that at the initial time almost 70 mgl^{-1} of NO_3^--N was already present in the reactor due to accumulation from the previous cycle. The concentration of NO_3^--N increased with time. At 300 min, NO_3^--N concentration was 128.79 mgl^{-1} from the total initial NH_4^+-N of 124 mgl^{-1} (Figure 2.5). From Figure 2.5, it was observed that during the first 150 min, NO_2^--N concentration increased up to 98.15 mgl^{-1} and afterward it started to reduce. At 300 min, it was almost negligible, indicating the complete nitrification process. Deng et al. (2016) reported 93% COD and 41% nitrogen removals within the initial 30 min in

acetate fed AGR from initial values of 700 and 37 mgl^{-1}, respectively. In the present study, COD removal was a little bit slower than this reported value. However, NH_4^+-N removal was faster. Wu et al., (2017) observed relatively long time period (>15 h) for achieving complete nitrification during the study of the impact of exogenous addition of nitrifying granular sludge cellular extract on nitrification efficiency, which was much higher as compared to the present study (6 h).

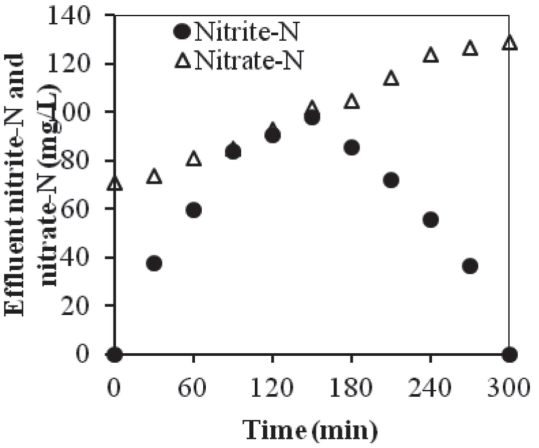

FIGURE 2.4 Effluent concentration profile of ammonia-N (mgl^{-1}) with time.

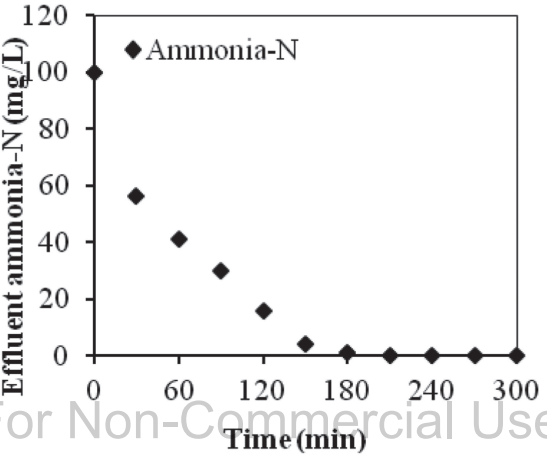

FIGURE 2.5 Effluent concentration profile of nitrite-N and nitrate-N (mgl^{-1}) with time.

2.4 CONCLUSIONS

Aerobic granules were successfully cultivated with phenol, (SCN^-), and ammonia nitrogen at a cycle time of 6 h and kinetic analysis in one cycle was observed. Complete degradation of phenol and (SCN^-) (99%) required 120 min. Maximum COD removal was observed after 240 min, and it was around 90%. Complete nitrification required a longer time than other pollutants and was achieved after 180 min. Kinetic analysis showed that 180 min was sufficient for removal of all pollutants, indicating that cycle time of 6 h can be decreased further to 3 h for better utilization of the reactor.

ACKNOWLEDGMENT

Authors would like to acknowledge their Institute providing instrument facility for FESEM images and to Indian Oil Corporation Limited (IOCL), Noonmati, Guwahati for providing sludge.

KEYWORDS

- **aerobic granules**
- **chemical oxygen demand**
- **nitrification**
- **sequencing batch reactor**
- **volatile suspended solids**

REFERENCES

Adav, S. S., Lee, D. J., Show, K. Y., & Tay, J. H., (2008). Aerobic granular sludge: Recent advances. *Biotechnology Advances*, *26*(5), 411–423.

Al Khalid, T., & El Naas, M. H., (2012). Aerobic biodegradation of phenols: A comprehensive review. *Critical Reviews in Environmental Science and Technology*, *42*(16), 1631–1690.

APHA, (2005). *Standard Methods for the Examination of Water and Wastewater* (21st edn.). APHA, AWWA, WPCF, American Public Health Association, Washington, DC, USA.

Beun, J. J., Hendriks, A., Van Loosdrecht, M. C. M., Morgenroth, E., Wilderer, P. A., & Heijnen, J. J., (1999). Aerobic granulation in a sequencing batch reactor. *Water Research*, *33*(10), 2283–2290.

Corsino, S. F., Campo, R., Di Bella, G., Torregrossa, M., & Viviani, G., (2015). Cultivation of granular sludge with hypersaline oily wastewater. *International Biodeterioration and Biodegradation*, *105*, 192–202.

Deng, S., Wang, L., & Su, H., (2016). Role and influence of extracellular polymeric substances on the preparation of aerobic granular sludge. *Journal of Environmental Management*, *173*, 49–54.

Gao, D., Liu, L., Liang, H., & Wu, W. M., (2011). Aerobic granular sludge: Characterization, mechanism of granulation and application to wastewater treatment. *Critical Reviews in Biotechnology*, *31*(2), 137–152.

Ho, K. L., Chen, Y. Y., Lin, B., & Lee, D. J., (2010). Degrading high-strength phenol using aerobic granular sludge. *Applied Microbiology and Biotechnology*, *85*(6), 2009–2015.

Jeong, Y. S., & Chung, J. S., (2006). Simultaneous removal of COD, thiocyanate, cyanide, and nitrogen from coal process wastewater using fluidized biofilm process. *Process Biochemistry*, *41*(5), 1141–1147.

Kim, K. H., & Ihm, S. K., (2011). Heterogeneous catalytic wet air oxidation of refractory organic pollutants in industrial wastewaters: A review. *Journal of Hazardous Materials*, *186*(1), 16–34.

Kim, S. S., & Kim, H. J., (2003). Impact and threshold concentration of toxic materials in the stripped gas liquor on nitrification. *Korean Journal of Chemical Engineering*, *20*(6), 1103–1110.

Kim, Y. M., Park, D., Jeon, C. O., Lee, D. S., & Park, J. M., (2008). Effect of HRT on the biological pre-denitrification process for the simultaneous removal of toxic pollutants from cokes wastewater. *Bioresource Technology*, *99*(18), 8824–8832.

Kishida, N., Tsuneda, S., Kim, J., & Sudo, R., (2009). Simultaneous nitrogen and phosphorus removal from high-strength industrial wastewater using aerobic granular sludge. *Journal of Environmental Engineering*, *135*(3), 153–158.

Li, H. Q., Han, H. J., Du, M. A., & Wang, W., (2011). Removal of phenols, thiocyanate, and ammonium from coal gasification wastewater using moving bed biofilm reactor. *Bioresource Technology*, *102*(7), 4667–4673.

Liu, Y. Q., & Tay, J. H., (2007). Influence of cycle time on kinetic behaviors of steady-state aerobic granules in sequencing batch reactors. *Enzyme and Microbial Technology*, *41*(4), 516–522.

Liu, Y. Q., Tay, J. H., Ivanov, V., Moy, B. Y. P., Yu, L., & Tay, S. T. L., (2005). Influence of phenol on nitrification by microbial granules. *Process Biochemistry*, *40*(10), 3285–3289.

Ochoa, J., Colprim, J., Palacios, B., Paul, E., & Chatellier, P., (2002). Active heterotrophic and autotrophic biomass distribution between fixed and suspended systems in a hybrid biological reactor. *Water Science and Technology*, *46*(1/2), 397–404.

Ramos, C., Suárez-Ojeda, M. E., & Carrera, J., (2016). Biodegradation of high-strength wastewater containing a mixture of ammonium, aromatic compounds, and salts with simultaneous nitritation in an aerobic granular reactor. *Process Biochemistry*, *51*(3), 399–407.

Sahariah, B. P., & Chakraborty, S., (2011). Kinetic analysis of phenol, thiocyanate and ammonia-nitrogen removals in an anaerobic–anoxic–aerobic moving bed bioreactor system. *Journal of Hazardous Materials*, *190*(1), 260–267.

Singh, M., & Srivastava, R., (2011). Sequencing batch reactor technology for biological wastewater treatment: A review. *Asia-Pacific Journal of Chemical Engineering*, *6*(1), 3–13.

Val del Rio, A., Figueroa, M., Arrojo, B., Mosquera-Corral, A., Campos, J., García-Torriello, G., & Méndez, R., (2012). Aerobic granular SBR systems applied to the treatment of industrial effluents. *Journal of Environmental Management*, *95*, S88–S92.

Wang, S. G., Liu, X. W., Gong, W. X., Gao, B. Y., Zhang, D. H., & Yu, H. Q., (2007). Aerobic granulation with brewery wastewater in a sequencing batch reactor. *Bioresource Technology*, *98*(11), 2142–2147.

Wu, L. J., Li, A. J., Hou, B. L., & Li, M. X., (2017). Exogenous addition of cellular extract N-acyl-homoserine-lactones accelerated the granulation of autotrophic nitrifying sludge. *International Biodeterioration and Biodegradation*, *118*, 119–125.

Yu, G. H., Juang, Y. C., Lee, D. J., He, P. J., & Shao, L. M., (2009). Enhanced aerobic granulation with extracellular polymeric substances (EPS)-free pellets. *Bioresource Technology*, *100*(20), 4611–4615.

Zhao, X., Chen, Z., Wang, X., Li, J., Shen, J., & Xu, H., (2015). Remediation of pharmaceuticals and personal care products using an aerobic granular sludge sequencing bioreactor and microbial community profiling using Solexa sequencing technology analysis. *Bioresource Technology*, *179*, 104–112.

Zheng, S., & Li, W., (2009). Effects of hydraulic loading and room temperature on the performance of the anaerobic/anoxic/aerobic system for ammonia-ridden and phenol-rich coking effluents. *Desalination*, *247*(1–3), 362–369.

CHAPTER 3

EAST KOLKATA WETLANDS (EKW), INDIA: A UNIQUE EXAMPLE OF RESOURCE RECOVERY

ANITA CHAKRABORTY[1], SUBRATA HALDER[2], SADAF NAZNEEN[3], and SUMAN KUMAR DEY[4]

[1]*Senior Technical Officer, Centre for Environmental Management and Participatory Development, Salt Lake, Kolkata – 700106, India, E-mail: anitagcenator@gmail.com*

[2]*Executive Engineer (A-I), State Water Investigation Directorate, Government of West Bengal, India*

[3]*School of Environmental Sciences, Jawaharlal Nehru University, New Delhi – 110067, India*

[4]*Professor, Department of Geography, Ramsaday College, Amta, Howrah, West Bengal, India*

ABSTRACT

The age-old practice of utilizing wastewater into fishpond in the East Kolkata Wetlands (EKW), India is a unique example of resource recovery. The wetlands, providing a range of ecosystem services, form the base of ecological security of the entire region and livelihoods of the dependent communities. Being a dynamic ecosystem, the wetland is subject to influence from various natural as well as human factors. Integrated management of this ecosystem is crucial for maintaining the rich productivity of the wetland ecosystem as well as achieving the wise use of resources. The resources recovered from city sewage are used in three kinds of economic activities, i.e., wastewater fisheries, vegetable farming on a garbage substrate and paddy cultivation using pond effluent. In the entire recovery operation, the

fishponds play a crucial and central role in the waste recycling process. The wetlands act as 'sink' for sewage and waste material from Kolkata that lacks any substitutable sewage treatment facility for its 4.5 million residents. About 3500 tons of municipal waste and 68 million liters of raw sewage drain into the wetland system on a daily basis. Sewage-fed fisheries that utilize such large volumes of sewage generated by the city started functioning as early as 1883. In 1940, about 4,682.22 ha of wetland area produced 0.14 t of fish per ha utilizing the municipal sewage. The profit-generating potential of the wetlands in terms of aquaculture aroused interest in local farmers as well as local landlords who leased out most of the ponds to commercial managers. The conspicuous result was employment generation through the production of fish and vegetables as well as a steady supply of food materials to the urban markets. There are 264 fish farms operating on a commercial basis. They cover a total area of about 2858.65 ha. The fish farms consist of units of various sizes from large holdings locally called bheries and relatively smaller ones called jheels due to their trench-like elongated shapes. But all these fish farms generally have similar types of produce, farming practice and distribution system. However, inappropriate understanding of the significance of these wetland practices has led to the gradual loss of system efficiency.

3.1 INTRODUCTION

The East Kolkata Wetland (EKW) sustains the World's largest and perhaps, the oldest integrated resource recovery (Figure 3.1) and practice based on a combination of agriculture and aquaculture, and provide livelihood support to a large, economically underprivileged population of around 20,000 families which depend upon the various wetland products, primarily fish and vegetables for sustenance. The wetland complex is located on the eastern fringes of Kolkata city as is one of the largest sewage fed fish ponds spread over an area of 12,500 ha. The Wetland Complex forms a part of the extensive inter-distributaries wetlands regimes formed by the Gangetic detla.

Based on its immense ecological and socio-cultural importance, the Government of India declared EKW as a wetland of International Importance under the Ramsar convention in the year 2003. At present wetland system produces over 15,000 MT per annum fish from its 264 functioning aquaculture pond, locally called *bheries*. Additionally, about 150 MT of vegetables are produced daily. Thus it is prudent to say that EKW servers as the backbone of food security of the Kolkata City (Figure 3.2).

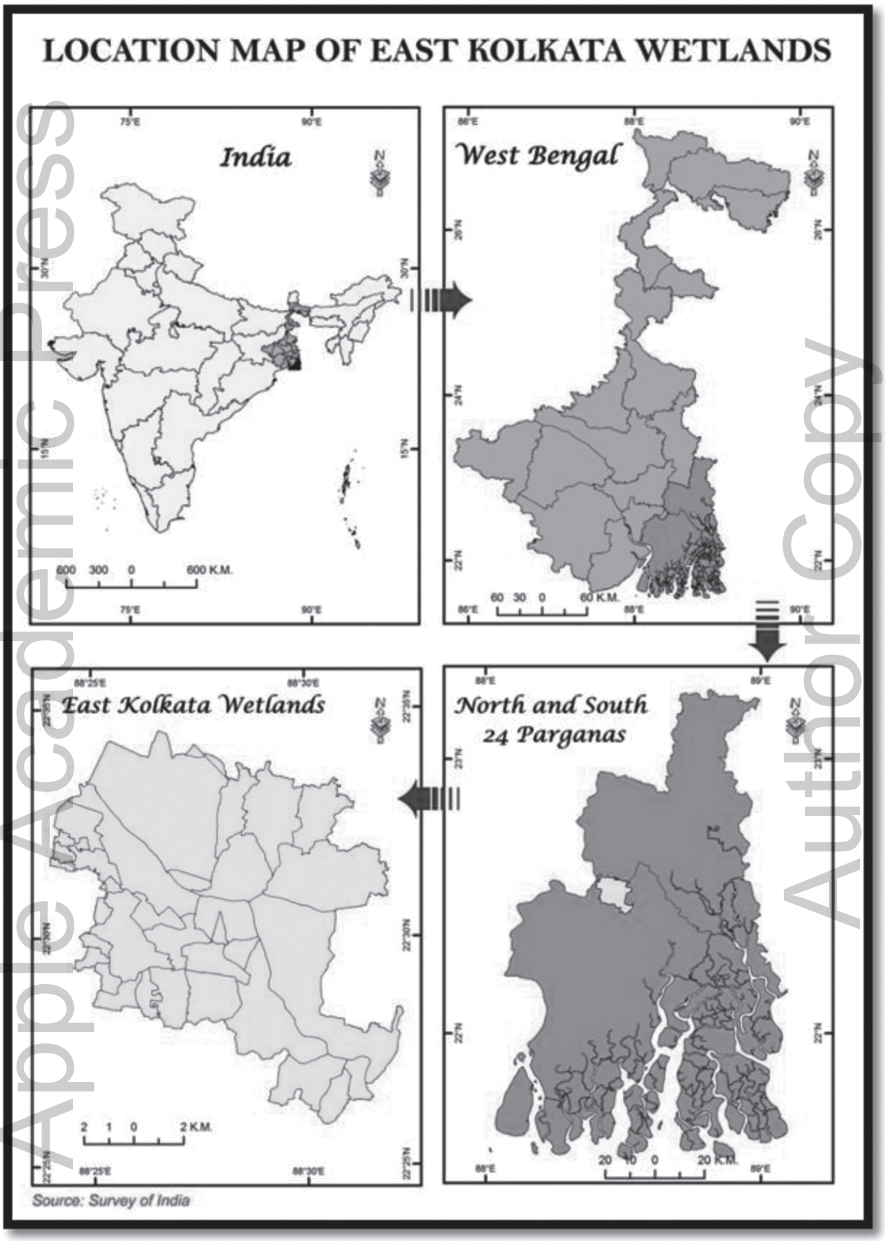

FIGURE 3.1 **(See color insert.)** Location map of EKW, Kolkata.

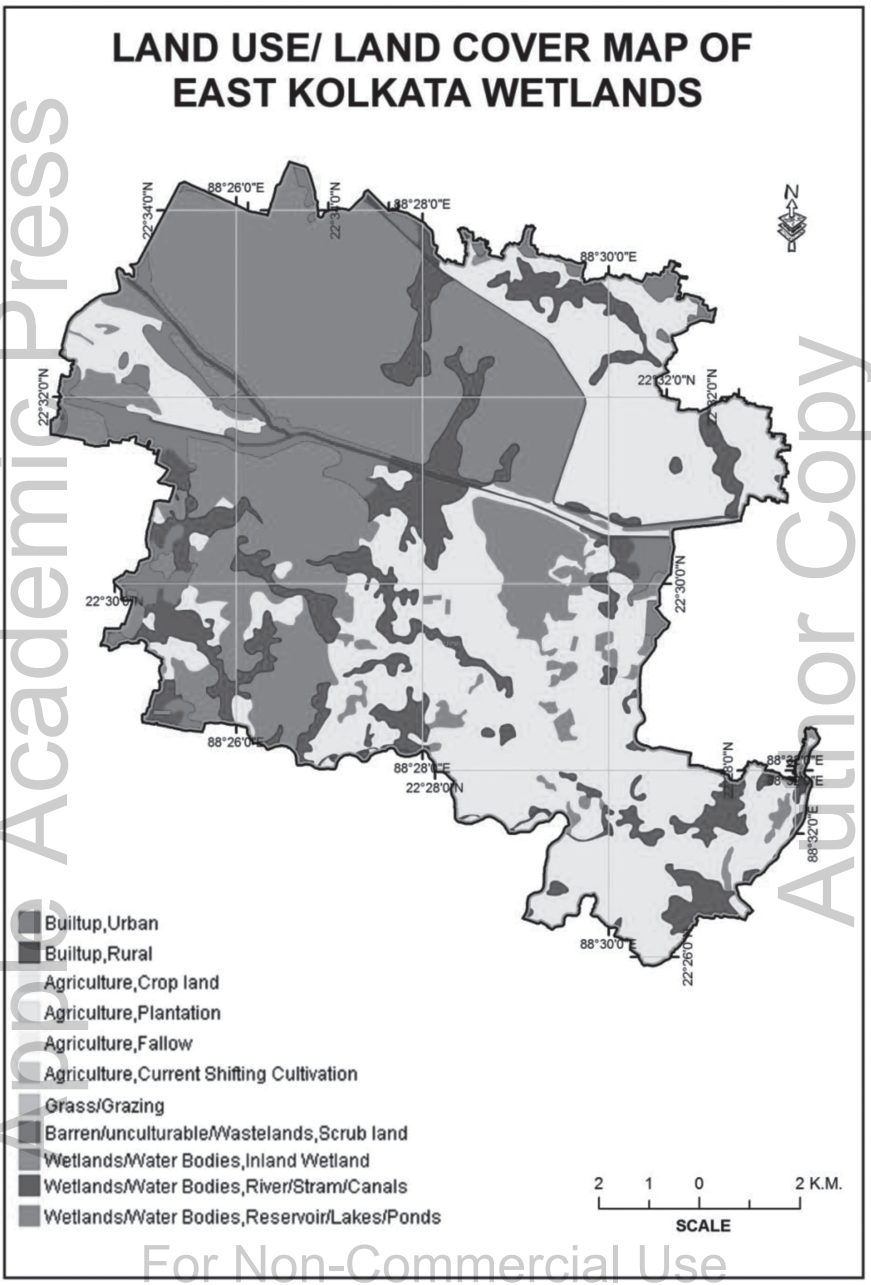

FIGURE 3.2 **(See color insert.)** Current land use and land cover of EKW.

EKW sets a conventional example of harnessing natural resource of wetland ecosystem for aquaculture and agriculture (including horticulture) ensuring community participation and their traditional knowledge. This wetland system also gives the best practice of augmentation of local communities into conservation and management practices. Thus this makes the wetland complex stands amongst one of the 17 case studies of wise use of wetlands by the Ramsar Convention (Bunting et al., 2011).

3.1.1 GENESIS OF EKW

The genesis of the East Kolkata Wetlands is strongly connected with the development of the city, changing courses of the River and waste management system of Kolkata. The city is located right on top of the mature Sundarbandelta which exceeds up to the northern fringe. Historically it was a part of mangrove and forestland of delta system. The Rivers in this deltaic region was characterized by improper drainage pattern and massive swamp formation with numerous wetlands (locally called as *bheries*). This complex network of river and its floodplain wetlands attract the East India Company as a navigational path to reach the hinterland of Bengal. Thus the city was established by Job Charnock in the year 1690 on the bank of River Hugli with a view to promote trade of goods. During this period the wetland complex boarding the eastern fringes of the city was nothing but was an insignificant jungle. These wetlands were called the salt lake. Presently this wetland complex is a part of EKW which also represents the remnant beds of mighty tidal River Bidyadhari and its spill areas. Initially brackish in character the wetlands were turned into freshwaters after the death of River Bidyadhari and subsequent loss of the connection with the other river system both upstream and downstream (Kundu and Chakraborty, 2017).

During the period of late eighteen century, a sudden annihilation in Rajmahal results in the shift of the Ganga to the Padma (Sengupta, 1980). This results in the disruption and gradually death of the connecting rivers, tributaries, estuaries, and network of channels between the Bidyadhari. River Damodar which principally contribute to the upland discharge to the Jamuna-Bidyadhari also changes its course in the due process. Thus in the absence of the upland water and sudden clogging of the interconnected channels, the Bidyadhari become depended solely on rainfall in its drainage basin. The situation further aggravated with an increase in tidal silt ingress and at the face of improper upland discharge to flush it down. Construction of bridges and channels further deep-rooted the situation and finally sealed

the fate of the whole region. This event was perhaps marked as the landmark in the transformation of the ecosystem. Gradually the region converted into a large number of marsh and swamp area of varying size which later converted in ponds for both fish and paddy cultivation (Kundu and Chakraborty, 2017).

Gradually Kolkata also grew up into a large urban and trade center without any proper sewerage and solid management systems in place. The expansion of the city since its inception shows an adhocism rather than following a planned approach with respect to its spatial dimension and extension of the infrastructure, keeping its topology in mind. This unplanned approach often results in drainage congestion resulting in health impacts. The entire waste was initially dumped into the River Hugli, a practice which abandoned due to the frequent outbreak of malaria in the year 1757, 1762, 1770 affecting more than 76, 000 lives in Kolkata (Kundu et al., 2012). The practice was abandoned, and a committee was established to look for an alternate solution of the drainage problem. The committee recommended the transfer of all waste to salt lakes, as the city has a natural eastward slope. The wetlands were nearly 8.5 feet below the highest point of the city and thus recommendation strongly suggested for the construction of a series of sewers and pumping stations towards the salt lake. In 1864, a portion of the salt lakes was acquired for the dumping of solid waste. Though the first attempt of freshwater aquaculture was opted much later in 1918 (Kundu and Chakraborty, 2017).

Subsequent development of the wastewater channel in the city itself and the rapid growth in the settlements ensure more sewerage directly promoting and adoption of the waste fed aquaculture in the lakes. The wetland system presently has 264 functioning ponds (*bheries*). The solid waste dumping areas on the western fringe of the wetland complex were fully conversed to horticulture since 1876. Application of sewage was sequenced skillfully on the basis of detention time needed to improve the water quality appropriate for aquaculture activity.

The wetlands act as 'sink' for sewage and waste material from Kolkata that lacks any substitutable sewage treatment facility for its 4.5 million residents (Census of India, 2011). About 3500 tons of municipal waste and 68 million liters of raw sewage drain into the wetland system on a daily basis. Sewage-fed fisheries that utilize such large volumes of sewage generated by the city started functioning as early as 1883. In 1940, about 4,682.22 ha of wetland area produced 0.14 ton of fish per ha utilizing the municipal sewage. The profit-generating potential of the wetlands in terms of aquaculture aroused interest in local farmers as well as local landlords who leased out most of the ponds to commercial managers. The conspicuous result was employment

generation through the production of fish and vegetables as well as a steady supply of food materials to the urban markets. The present manuscript is an effort to broadly represent the ecology-economic interface of wetland uses with special emphasis on the aquaculture practices in the wetland complex.

3.2 MATERIALS AND METHODS

Strategically observation and discussion were compiled on the data provided by the State Government Authorities of West Bengal responsible for the Conservation of EKW (Figure 3.3). Personal interviews with the stakeholders and the concerned authority depended on EKW was done to underpin the key issues faced by them. Also, a review on secondary literature for the survey authentication and ground proofing were done.

FIGURE 3.3 East Kolkata Wetlands, India.

3.3 OBSERVATION AND DISCUSSIONS

East Kolkata Wetland is the best existing example which provides a range of goods and services (Table 3.1) that contribute to human well-being and poverty alleviation. Communities living near wetlands are highly dependent on these services and are directly harmed by their degradation.

TABLE 3.1 Wetland Goods and Services Provided by the EKW

Goods		Services
• Fishery through aquaculture		• Flood control
• Agriculture	→	• Navigational path
• Horticulture		• Sewarage channels
• Animal husbandary		• Sewage treatment
• Water supply	←	• Garbage dumpyard
• Rugs from waste		• Nutrient and pesticides removal
• Recreation and scientific interest		• Heavy metal removal
		• Biodiversity

The economic activities that have mushroomed all over the have literally converted urban waste into wealth. Hence, this vast wetland has earned the title of Waste Recycling Region (WRR). These economic activities, of which agriculture, horticulture, and fisheries are the most important ones, have provided employment to thousands of people who dwell in the East Kolkata Wetland region and its outskirts.

The sewage of the entire Kolkata city enters the wetlands through a network of drainage channels which flows into the canal and ultimately falls in the fish ponds. During the entire process, the fishers believe the sunlight trigger the biochemical process/reaction which ultimately purifies the water entering the fish pond. For example, BOD (biochemical oxygen demand) is believed to be reduced through a symbiotic bio-chemical process between the algae and the bacteria present inside the sewage, where energy is drawn from algal photosynthesis. Each hectare of a shallow water body is capable of removing about 237 kg of BOD per day. This helps in the reduction of coliform bacteria prone to be pathogenic in nature, which even in a conventional mechanical sewage treatment plants may not be able to eliminate fully.

The effluents from the fish ponds are channelized to the southeastern region where abundant of paddy field was located. At present and still in the record there are 264 fish farms operating on a commercial basis. They cover a total area of about 2858.65 ha. The fish farms consist of units of various sizes from large holdings locally called *bheries* and relatively smaller ones called *jheels* due to their trench-like elongated shapes. But all these fish farms generally have similar types of produce, farming practice and distribution system.

A variety of sweet water fishes were cultured in the *bheries*. The main varieties in the existing practice of polyculture practice include:

1. Indian Major Carp – Rahu (*Labeo rohita*), Catla (*Catla catla*), Mrigal (*Cirrihinus mrigala*).
2. Indian Minor Carp – Bata – (*Labeo bata*).
3. Exotic Variety – Silver Carp (*Hypophthalmichthys molitrix*), Common Carp (*Cyprinuscarpio*), Grass Carp (*Tenopharyngodon idella*).
4. Tilapia–Nilotica (*Oreochromisnilotica*), Mosambica (*Tilapia mosambica*).

Apart from these cultured varieties (except Tilapia), some other varieties including forage fishes are also occasionally available in the *bheries*. These varieties are Punti (*Puntius japonica*), Sole (*Channa striatus*), Lata (*Channa punctatus*), Chyang (*Channa gachua*), Singi (*Heteropneustes fossillis*), Magur (*Clarias batrachus*), Fouli (*Notopterus notopterus*), Pungus (*Pangasius pangasius*), etc.

Despite of such a promising overview of fishery it has been observed that the average sizes of marketable fishes are not of the optimum weight (in grams). The prime reason behind the scenario is being that the fishes are normally netted/harvested much before they attain mature marketable growth and sizes. The main reasons for this are that the management/owners are compelled to create the maximum number of man-days possible in a year to provide employment to direct laborers viz. harvesters, carriers, etc. and the impending threat of poaching. Production and yield per hectare of fish varies among the *bheries* depending upon the conditions of production. Till today it has not been possible to study all possible variables that affect the production and yield of fish in this region. However, data which are available to give a reasonably sensible indication in this context require reconfirmation and updating.

The maximum numbers of *bheries* (125) fall within the area range of above two and below 10 hectares, followed by 76 *bheries* within the range up to two hectares, and 34 *bheries* fall within the range above 10 hectares to 20 hectares. More than 89% of *bheries* fall within the area range of up to 30 hectares. The maximum average yield (i.e., 6.48 $MTha^{-1}$) has been achieved in the *bheries* of more than 70 hectares in size. The yield is recorded to be increased with an increase in the size of *bheries*; thereafter, it tends to decrease as the size gets bigger and is lowest (i.e., 2.89 MT where *bheri* size is between 30 and 40 hectares). Yield per hectare again increases steadily with the increase in the *bheri* size and is the highest at 6.48 MT in fish farms where the effective area of the water body is above 70 hectares. Larger size *bheries*, though few, are more organized in terms of operations, planning through efficient management of production schedules, utilization of

manpower, sewage, better procurement planning, monitoring water quality and fish health and efficient personnel management, etc. All these combine to provide the right synergy for achieving better production performance and per hectare yield.

In terms of annual production, 45 operating *bheries* reported 'increasing trend,' 61 *bheries* reported 'decreasing trend,' while in 76 *bheries* production was reported to be at an even level during the past three years. No proper indication of production trend was available in the remaining 82 *bheries*.

For a *bheri* to be operated efficiently, the following conditions are critical:

a) Maintenance of the required depth of water at all the three stages of the production process, e.g., at nursery pond, rearing pond and stocking pond with proper inlet-outlet management of sewage.
b) Availability of quality spawn/fry/fingerlings at required time and quantity.
c) Proper and efficient deployment of working personnel, ensuring satisfactory labor productivity and congenial labor relations.
d) Monitoring fish health.

The most important requisite to run a fishpond efficiently is an adequate and safe supply of wastewater. This is related to a number of other factors and deserves more elaborate discussion and research. Poor quality of sewage brings in lower quantity of nutrients and higher toxic load for the fish to feed upon. Low quality of sewage-borne nutrients requires supplementing with nutrients from outside. This entails more expenditure and increased operational costs that affect viability. In such situations, the *bheri* owners, with additional input costs, seek to add value to their produce (fish) to get higher returns and recover the additional expenditure incurred on fish nutrients/feed.

One way of countering this situation is by allowing the fishes to grow bigger. As this means lesser number of netting (harvesting) days resulting in the loss of man-days, the workers' union does not allow this to happen (Figure 3.4). This, in turn, gives birth to a situation of conflicting interests.

The following three types of ponds are required according to the stage of culture operation and ultimately production.

1. Nursery pond;
2. Rearing pond; and
3. Stocking pond.

Each of them is facilitate with proper inlet-outlet for the management of sewage inflow and waste outflow.

FIGURE 3.4 Fishponds of EKW.

Introduced stocks were raised in five major phases:

1. Pond preparation (mostly done in winters);
2. Primary fertilization (initial introductions of wastewater into the pond and allow to undergo natural purification, and stirring of the pond in order to reduce anaerobic conditions in the sediments);
3. Stocking of fish (initially stock a small number of fish for the test of acclimatization, growth, and water quality and subsequently introduction of seed in measured number);
4. Secondary fertilization (periodic introductions of wastewater into the ponds throughout the culture period), and finally; and
5. Fish harvesting (taken at different times according to species, growth, and market demand).

A flow diagram of pond preparation to harvesting of fish is shown in Figure 3.5.

During the entire operation, silt traps are pits at the edges of *bheries*, which trap the silt buildup in the ponds. Traps were periodically dredged, and the residues were used to strengthen dikes. Dredging and draining out of ponds were periodically done before the monsoons to release the nutrient locked in the bottom as well as deseeding of unwanted fish species and macrophytes. Farmers also believe that this step helps to kill the pathogenic parasites affecting the fish in culture period.

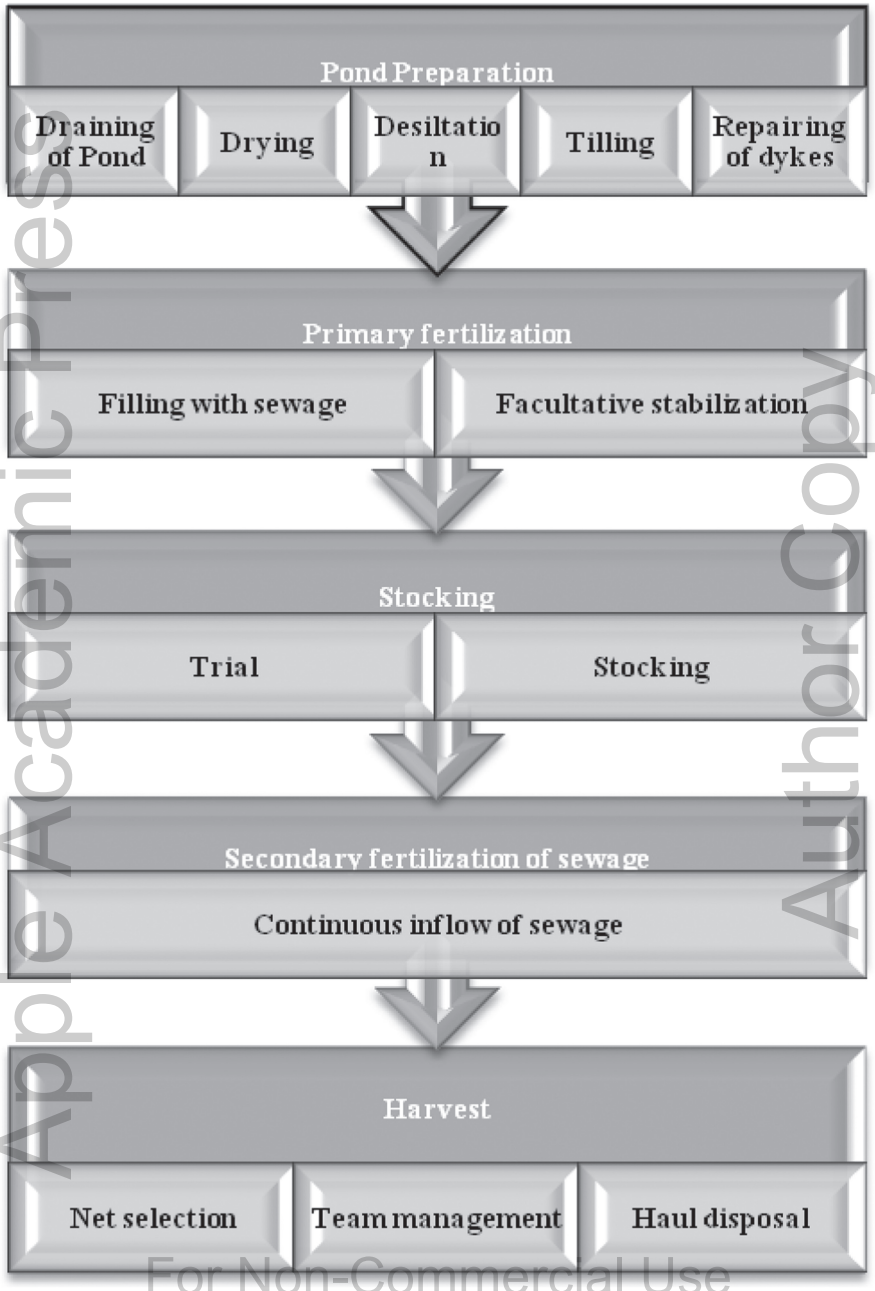

FIGURE 3.5 Flow diagram of pond preparation to harvest.

The stakeholders specifically involved for their livelihood in the wetland migrate at various part of the wetland complex with respect to the seasonal need. Usually, they get engaged in agriculture farming, garbage sorting, and aquaculture activities like trading, auctioneering, selling, making nets, maintaining drainage, and reinforcing banks. Apart from livelihood the stakeholders fully depend on the wetland for the fishes and vegetables required for their daily consumption need. During the entire process of self-purification of sewage, one macrophyte species (*Eichhornia crassipes*) commonly known as water hyacinth, play a role in the system's function. Some of the major supports it provides were:

1. Breaks the surface waves.
2. Stabilizes the bank erosion.
3. Used as replacement of expensive like stone or concrete to strengthen the banks.
4. Provide shade to fish during the month of summer.
5. The roots, well known to absorb metal ions, help to leach heavy metals out of the water.
6. Used as feed for cattle like buffalo usually decomposed and fed to carp.

Land Ownership: There are various types of land ownership of fishponds in EKW (Ghosh and Sen, 1987):

1. Owner-managed: but this is disappearing because of uncertainties of the wetlands' future.
2. Cooperatives: 13 Cooperatives with 300 fishers are present, these function well without any external assistance.
3. State Government Corporation: only two ponds are presently operational.

3.3.1 INCOME AND EXPENDITURE

This has not been studied extensively in any scientific study and approaches thus reliability on the presently available data is questionable (Ghosh, 1985a, 1985b; IWMED, 1986). Private fishers and farmers were also reluctant share to share the financial nitty-gritty, and thus relying on the State-managed fishponds is too few to represent the entire area fully.

3.4 CONCLUSIONS

Despite of the potential to provide multiple natural and social services, the cultural practice in the wetlands are still operated an informal way. As such, they need further study, effective maintenance, monitoring, and upgrading. Fast urban development and encroachment on eastward of the city is one of the major threats to the systems. Waste from the tanneries releasing untreated effluent directly into the wetlands, further threatening the water quality. Siltation of the ponds is a common phenomenon affecting the water depth in culture operation.

The presence of the Mafia in the control of fishponds had impacted the overall operation of the wetland complex. Impact of sewage and the threshold limit of nutrient (macro and micro) for the sustainable culture operation required to be scientifically established. Although researches confirmed the production of fish was not affected even by levels of ammonia-nitrogen concentration of 5.13 mgl^{-1} (the maximum limit is 0.1 mg^{-1}). But there still lies the possibility of transfer of the fatal micronutrient and heavy metals in the higher food chain.

Indian municipalities rely on the informal sector to supplement over-burdened waste management services; there remain questions about the system's effectiveness and more importantly, the environmental and moral issues of relying on so-called "ragpickers" to sort municipal garbage. First, these are the poorest members of society, typically women and children. The work is filthy and dangerous as it puts workers most of whom do not wear protective clothing or gloves into contact with broken glass and medical and other hazardous wastes. Many suffer from injuries and chronic skin diseases. Secondly, only garbage which can be sold is removed, which also means that some non-biodegradable wastes which have no commercial value, such as plastic and foil wrappings, remain in the soil where vegetables are grown. Third, the composting plants are taking biodegradable garbage (which is sold to tea gardens) from the vegetable farmers, is presently, adversely impacting the soil quality drastically. As a result, vegetable farmers have begun using chemical fertilizers to enhance soil fertility.

There is an absence of policies and strategies to guide coordinated actions within river basin linking coastal processes. Full ranges of ecosystem services of EKW were not integrated into the developmental plan. Water allocations are biased towards human uses ignoring ecological aspects. There is a huge lack of involvement of stakeholders, particularly marginalized communities. Lack of baseline information for planning and decision making is a major hindrance for the sustainable management of this wetland. Absence of

effective institutional mechanisms is also a noteworthy issue to be tackled in the present and future. Management Planning Framework which is required for the sustainable conservation and wise use of wetland complex can be summarized as:

1. Management zoning identifying entire wetland area as core zone accommodating the ongoing practices and rationalizing proposed land use planning and direct basin as buffer zone.
2. Establishing a hierarchical and multi-scalar inventory of hydrological, ecological, socioeconomic, and institutional features to support management planning and decision making.
3. Ensuring hydrological connectivity of EKW with freshwater and coastal processes at basin level.
4. Environmental flows as a basis for water allocation for conservation and developmental activities.
5. Biodiversity conservation through habitat improvement of endangered and indigenous species.
6. Ecotourism development for enhancing awareness income generation and livelihood diversification.
7. Poverty reduction through sustainable use of land and other resource development and utilization.
8. Formation of multi-stakeholder groups for planning, implementation, and monitoring of MAP.
9. Strengthening EKWMA with adequate legal and administrative powers.
10. Capacity building at all levels for technical and managerial skills.
11. Result oriented monitoring and evaluation at activity, outcome, and impact levels.
12. Integrated management planning for EKW to achieve conservation and wise use of wetlands.
13. The Ramsar framework for wetland inventory assessment and monitoring which is a multi-scalar approach has been adopted for the purpose.
14. Interconnectivity in management planning.

ACKNOWLEDGMENT

The authors are thankful to East Kolkata Wetland Authority for providing all available information pertaining to East Kolkata Wetland. They are also

thankful to Dr. Nitai Kundu, Senior Scientist, IESWM, Kolkata for helping in developing the manuscript.

KEYWORDS

- **bheries**
- **East Kolkata Wetlands**
- **fish farms**
- **jheels**
- **sewage**

REFERENCES

Bunting, S. W., Edward, P., & Kundu, N., (2011). *Environmental Management Manual: East Kolkata Wetlands*. CEMPD and Manak Publishers, New Delhi, pp. 1–156.

Ghosh, D., & Sen, S., (1987). Ecological history of Calcutta's wetland conversion. *Environmental Conservation*, *14*(3), 219–226.

Ghosh, D., (1985). *Cleaner Rivers: The Least Cost Approach*. A village linked programme to recycle municipal sewage in fisheries and agriculture for food, employment, and sanitation. Government of West Bengal, India, 32.

Gosh, D., (1985). *Dhapa Report, From Disposal Ground to WAR (Waste-as-Resource) field*. Submitted to Calcutta Municipal Corporation (Preliminary Draft). Government of West Bengal, India, 32.

IWMED, (1986). *Growing Vegetables on Garbage*, *A Village Based Experience of City Waste Recycling*. Institute of Wetland Management and Ecological Design, Calcutta, India, 33.

Kundu, N., & Chakraborty, A., (2017). East Kolkata Wetlands: Dependence for ecosystem goods and services, In: Anjan Kumar Prusty, B., Rachna Chandra, & Azeez, P. A., (eds.), *Wetland Science*, *Perspective from South Asia* (pp. 381–406).

Kundu, N., Pal, M., & Saha, A., (2012). *East Kolkata Wetlands – Demographic & Livelihood Profile*, Manak Publishers, New Delhi.

Sengupta, B. K., (1980). *Kalikatar Pasei Laban Radh: Mahanagarer Sathi Ebom Bandhu Harader Cromo Bibartener Etihas Matsa Chasi Diibas Palan-o Seminar* (A salt marsh near Kolkata: a companion and friend, Fish farmers day celebration cum seminar).

PART II
Integrated Water Resources Management

CHAPTER 4

INTEGRATED WATER RESOURCE MANAGEMENT PLAN

ANIL KUMAR

Associate Director, Water Business Group, CH2M HILL (India) Pvt. Ltd, Noida – 201301, India, E-mail: anil.kumar2@ch2m.com

ABSTRACT

The freshwater shall be recycled and reused for the nonpotable and industrial process, as fresh water is a finite and vulnerable natural resource. Unique and innovative solutions are the demand for newly developed Indian cities to meet their water demands and thus looking at future water challenges, there is a need to search for alternate potential sources of water. For long-term development of a region, it is necessary to plan sustainable future water resource programme to meet demand during peak summers, which can be a potential concern for the industrial growth of the region. An IWRM plan involves across the board usage of available water resources in several combinations and manages sources in such a way that they are reliable and sustainable throughout the planning horizon. IWRM modeling together with detailed cost-benefit analysis was found to be economical than the traditional schemes to meet the demand of the MBIR region.

4.1 INTRODUCTION

Freshwater is a finite and vulnerable resource essential to sustain life, development, and the environment. With the continued growth of Indian cities and its periphery areas, the population is continuously increasing and thus the demand for water. Competing demands for water within the context of climate uncertainty and a growing population require unique and innovative solutions. Failure to recognize the economic value of water has led to

wasteful and environmentally damaging uses of resources. Looking at the future water challenges, there is a need for an approach that leads to the development of potential alternative potential sources of water to minimize the overexploitation of freshwater sources.

Integrated water resource management (IWRM) plan is a systematic process for the sustainable development, allocation, and monitoring of water resource use in the context of social, economic, and environmental objectives to ensure effective, equitable, and sustainable water management. In simple terms, all the different uses of water resources are considered together for the sustainable water management approach to meet potable and non-potable demands of water. IWRM plan promotes development that coordinates management of water, land, and related resources so as to maximize the resultant economic and social welfare. One of the major aspects considered in the development of this approach includes the identification and development of an optimized solution that is based on a techno-economic evaluation of various available water sources or combinations thereof.

4.2 IWRM MODEL

It is observed that many water utilities around the world find it difficult to maintain desired water supply levels during the peak summer months and dry spells especially when only one source of water, which can be a potential concern for the industrial growth of the region. Several water utilities have implemented water reclamation (wastewater recycle and reuse) to augment the water supplies, especially for non-potable applications to meet the water scarcity where potable water demands are the demands that require drinking water quality for end-users that involve direct consumption or a high likelihood of direct consumption of the water by people. These demands include water for sinks, showers, and dishwashers and non-potable water demands are the demands for end-users that do not involve direct consumption by people can be met with non-potable water. For long-term development of a region, it is necessary to plan future water resource programmes in a rational and integrated for all users.

The above schematic diagram include potential system components such as rainfall, rivers, external supply and groundwater under water supply; residential, institutional, horticultural, and fire fighting under water demand; drinking water treatment plant, reuse/recycle treatment plant, and wastewater treatment plant for the complete water demand cycle of a region (Figure 4.1). Capital and operating costs for each step in the cycle are factored into the

optimization analysis and balanced with other essential criteria to arrive at optimal decisions. The complete model can be developed to work with multiple data sets to reflect a range of future conditions. This allows a region to evaluate changes in system operations in response to climate change effects, or deviation from planning scenarios resulting in changes to supply and/or demand projections.

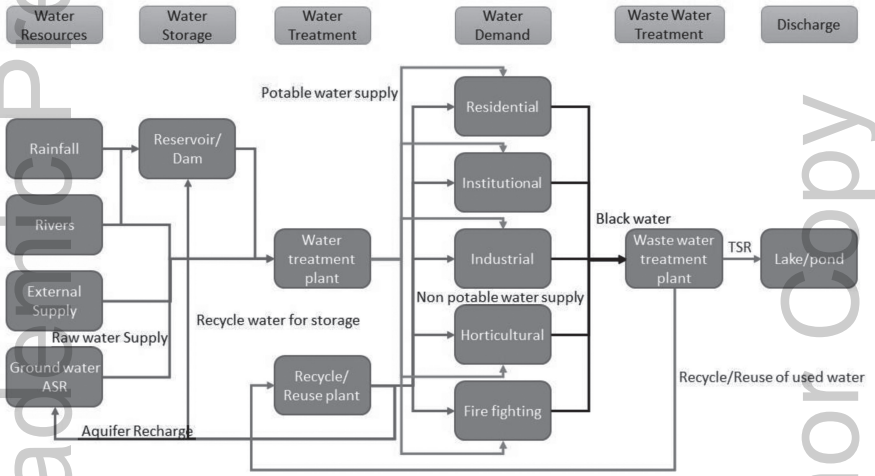

FIGURE 4.1 Schematic diagram of water resources and demand.

4.3 KEY COMPONENTS AND INTERRELATIONSHIP OF INTEGRATED WATER MANAGEMENT

IWRM can be developed by relating components of a region such as water supply, wastewater, water, etc. Figure 4.2 shows the interrelationship of all the key components of IWRM. The planning cycle of IWRM is given in Figure 4.3.

4.4 PLANNING OF IWRM

Typical issues that are considered and addressed while developing an IWRM Plan includes:

- Developing interfaces between macroeconomic and water resource decision making.

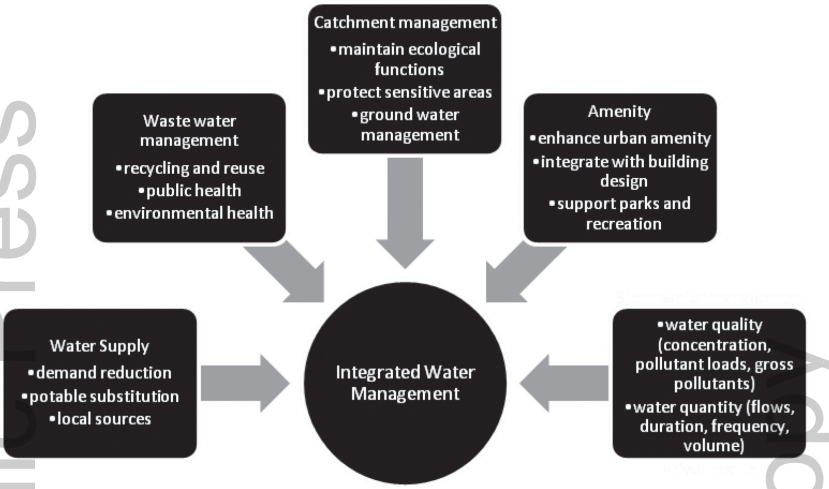

FIGURE 4.2 Interrelationship of key components of IWRM.

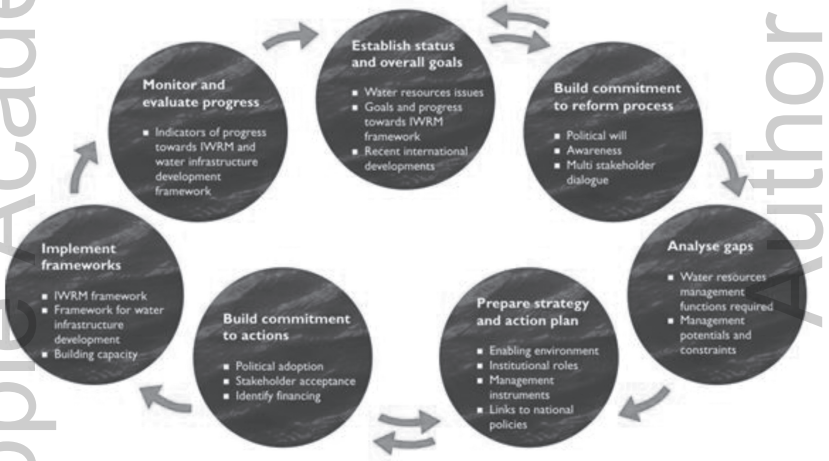

FIGURE 4.3 **(See color insert.)** IWRM planning cycle.

- Assessment of the efficiency of existing water infrastructure such as water and wastewater treatment plant, water supply infrastructure, stormwater drainage system, sewerage network system.
- Availability of non-conventional water resources and conservation technologies in the region, including an assessment of potential options for the development of these resources.

- Water quality and broader environmental issues related with existing conventional and nonconventional sources of water.
- Existing data collection system and access to information by users.
- Policy instruments and the legal and regulatory framework governing water resource management in the region.
- The role of the state in managing water resources in the region and potential for public-private partnership in any water resource development program.
- Processes for reconciling water quantity and quality needs of all water users.
- Mechanisms for consultation and public participation.
- Water allocation systems.
- Capacity building.
- Management agencies.
- Mechanisms to achieve financial sustainability.

4.5 RELIABILITY OF SOURCES IDENTIFIED IN THE IWRM PLAN

Reliability of sources is a very important aspect for the overall success of an IWRM plan. An IWRM plan involves across the board usage of available water resources in several combinations, apart from identifying the new and sustainable water sources such as the use of recycled water. While prioritizing the identification of existing or derived water source, such as recycled water, it is imperative that a comprehensive and detailed reliability analysis for a given source should be performed. It should be aligned with the national water policies, statutes governing the usage of water resources, and any proposed water infrastructure development project.

Overall feasibility of an identified option in an IWRM plan largely depends on its life cycle cost, which includes operational, maintenance, and any associated cost related with technology up gradation. While prioritizing the implementation plan, it should be kept in mind that resources optimizing the life cycle cost of the identified option are selected. The ultimate objectives of an IWRM plan are to develop and implement national/regional strategies, plans, and programs with regard to IWRM, and introduce measures to improve the efficiency of water infrastructure to reduce losses and increase recycling of water. A successful IWRM plan employs the full range of policy instruments, including regulation, monitoring, voluntary measures, market, and information-based tools, land-use management and cost recovery of water services.

4.6 DEMAND MANAGEMENT

Demand management should be a critical part of any IWRM Plan. As opposed to the supply side solutions, the cost for implementing demand management measures is modest to relatively low. In the long term, effective demand management would enable best practice management of overall water supply and infrastructure. There is sufficient scope to suggest ways to reduce the actual water consumption rate by using the world's best management water practices such as:

- Water-saving fixtures/devices.
- Behavior change and social awareness/education programmes.
- Leakage detection and repair.
- Minimization of non-revenue water losses.

The 150 lpcd is a guideline or aspirational design figure. In actual practice, water usage can be made significantly less and therefore reduce the amount of water resources to find, minimize the size of water infrastructure and reduce the capital cost and operating costs. It is likely that any new Indian city could realistically achieve a domestic water demand of at least 135 lpcd and may be able to achieve 120 lpcd with a little more effort aggressively and implementing the following measures:

- Higher plumbing and piping standards to prevent leaks.
- Strict construction standards, contract supervision, and leak testing.
- Leakage and non-revenue water monitoring and correction.
- Pricing signals to deter the waste of water and leakages.
- Strict controls and enforcement of water use rules.
- High levels of public awareness campaigns and education.

4.7 CASE STUDY

DMICDC is developing Manesar Bawal Investment Region (MBIR) in Haryana state as one of the industrial cities proposed to be developed in Phase 1 and CH_2M HILL International has developed IWRM plan for the region.

- The development of MBIR is projected to transform the land uses from predominately agriculture-based production to one that is dominated by residential, industrial, and open space land use with

a projected population of 3.2 billion and estimated water demand of 1060 MLD for the year 2040.

- MBIR is located in within a water-stressed area of Haryana state that does not have any perennial river, and the state receives surface water from Yamuna, Sutlej, Ravi, and Beas Rivers under various interstate water-sharing agreements and Water to MBIR is provided under a Canal Rotation Program and Water to these canals is supplied in rotation, for an average of 15 days in a month.
- The area falls under the overexploited category for extraction of Groundwater and extensive over-exploration of shallow aquifer, and often uncontrolled groundwater extraction has been done at such a high rate that it has exceeded the rate of groundwater recharge.
- MBIR has limited availability of existing wastewater treatment infrastructure, and most of the sewage that is currently being generated is unutilized.

The recommended IWRM Plan requires the development of a range of surface water and recycled water resources. Surface water resources are predominately from the JLN Canal System. Recycled water is produced from the wastewater or sewage generated within the MBIR development area. Rainwater harvesting by the collection of water from rooftops is also recommended. The alternatives were subjected to a high-level screening exercise to shortlist potential alternatives. The primary criterion's adopted for recommending potential alternatives are:

- **Economic Criteria (35%)** is a "relative cost" to provide a high-level indication of the cost of the option.
- **Environmental Criteria (20%)** is dominated by residuals generation since this is expected to have the largest environmental impact.
- **Social Criteria (20%)** prioritized by health and safety risks along with the impact on users. Slightly less weight was given to organizational benefits and community acceptance.
- **Technical Criteria (25%)** all factors are equally weighted since each of these factors is essential in integrated water management.

IWRM modeling together with detailed cost-benefit analysis identified following combination to satisfy the requirements for robustness, reliability, and resilience as well as deliver the most optimal balance of environmental, social, and financial outcomes for the proposed MBIR development.

- JLN canal water freed up from agriculture.
- Use of water savings from WJC system relining and/or de-silting (between Munak to Khubru Head).
- Use of water savings from WJC system relining and/or de-silting (between Khubru and Loharu Head).
- Use water savings from WJC system relining and/or de-silting (between Loharu and JC III Pump House).
- Recycled water generated within MBIR (internal water recycling).
- Local rainwater harvesting (rooftop).

Thus, a combination of the option of only the relining and desilting of existing canals is able to save such a large amount of water and meet most of the demand of the MBIR region. Economically, IWRM scheme was found to be more economical as compared with the traditional schemes of meeting demands of MBIR region. For meeting the demand of 1060 MLD in MBIR region, master plan was developed presenting the block cost estimate to be 11,436 crores which included development of reservoir, irrigation canals, underground transmission and conveyance system for potable water only and no scheme for management of wastewater whereas IWRM plan of MBIR for meeting the same demand estimated the cost to be 4,998 crores including treatment plants, water distribution system, sewage collection system, sewage treatment plants and rising mains for potable and non potable water supplies.

From the above comparison, it can be concluded that IWRM projects can be implemented for prestigious regions like MBIR to meet potable and nonpotable water demands utilizing even the used water for nonpotable requirements.

KEYWORDS

- **demand management**
- **IWRM model**
- **IWRM plan**

CHAPTER 5

EVALUATION OF GRAVITY-BASED DRIP IRRIGATION WITH PLASTIC MULCH ON RAISED BED CULTIVATION OF SUMMER OKRA AT FARMERS FIELD IN RANCHI DISTRICT

MINTU JOB[1], NIVA BARA[2], A. K. TIWARI[3], and C. S. SINGH[4]

[1]*Assistant Professor, Department of Agricultural Engineering, Birsa Agricultural University, Kanke, Ranchi, Jharkhand, 834006, India, E-mail: mintujob@rediffmail.com*

[2]*Head, Department of Agricultural Extension, Birsa Agricultural University, Kanke, Ranchi, Jharkhand, 834006, India*

[3]*Assistant Professor, Department of Horticulture, Birsa Agricultural University, Kanke, Ranchi, Jharkhand, 834006, India*

[4]*Assistant Professor, Department of Agronomy, Birsa Agricultural University, Kanke, Ranchi, Jharkhand, 834006, India*

ABSTRACT

Tank-based drip irrigation with plastic mulch is a viable option for farmers with small and fragmented land holdings and in places where the power supply is interrupted. Based on the survey in Chipra village, Nagri Block of Ranchi, a gravity-based low-pressure drip irrigation system was designed so that the system can be operated in low holding areas. Tank placed at a temporary platform of 2 to 3 meters was found to be sufficient for obtaining an acceptable uniformity of water distribution for a bed length of 15 meters with a water application rate of 1.2 lh^{-1}. Based on the field study with ten farmers on a unit size on 500 m^2 area, Okra production was successful with

this system which enabled each farmer to get an average profit of Rs. 7209 from each plot for summer season okra. An average yield of 144 qha^{-1} was obtained with this system of cultivation which was 56% more compared to the conventional method of cultivation. In addition, there was a water saving of 37% through this method. Use of Silver-black polyethylene mulch beside moderating the microclimate inside the bed also restricted weed growth with weed dry mass of 8 g/m^2 and 12 g/m^2 after 30 and 60 days after sowing. All other growth parameters of okra under drip irrigation and plastic mulch were superior to the conventional method of cultivation which resulted in increased yield, water use efficiency and economic benefits.

5.1 INTRODUCTION

"Don't earn enough to adopt TECHNOLOGY-Don't have the technology to earn ENOUGH." Farmers in Jharkhand are caught up in this vicious cycle for years. It is generally believed that the benefits of modern farm technology have been availed of only by large farmers. However, the fact is that even small farmers can utilize selected farm technologies for efficient farm operations. Drip irrigation along with a mulching system of cultivation is among one of the combinations which is technically feasible and economically viable for almost all orchards and vegetable crops. Cultivation of off seasonal crop using a method like drip irrigation, mulching, can give a higher income to the farmers which otherwise is not possible through conventional method. Okra is one of the most remunerative crops grown in this region and cultivated mostly in as a rainy season crop. Although some pockets of Ranchi district where there are perennial sources of water it is also grown as summer crops. Due to inclement climatic conditions like severe cold in January, its cultivation is delayed till the start of the early summer season; as a result, the available water sources get dried up and coupled with inefficient irrigation system the yield is much lower than its potential. Many researchers have reported higher application efficiency of drip irrigation system over the conventional irrigation methods. Sivanappan and Padmakumari (1980) compared drip and furrow irrigation systems and found that about 1/3rd to 1/5th of the normal quantity of water was enough for the drip-irrigated plots compared to the normal quantity of water applied to plots under surface irrigation in vegetable crops. Sivanappan et al. (1987) recommended drip system of irrigation in place of conventional furrow irrigation due to the economy in water utilization to the extent of 84.7% without any loss of yield. The response of okra to drip irrigation in terms of yield

improvement was found to be different in different agroclimatic and soil conditions in India. The increase in the yield of okra to the tune of 40% was reported under drip irrigation (Patil, 1982). In another study, the yield was reported to be slightly lower to that of conventional furrow irrigation (Patil et al., 1993). Based on the study conducted at Rahuri, India, Khade (1987) reported 60.1% higher yield of okra with water saving of 39.5% under drip irrigation as compared to conventional furrow irrigation.

A gravity fed drip irrigation system is a cheap and effective way to apply water for a smaller sized crop area. This system does not require any electricity for pumps as the system uses the force of gravity to push water through the drip line. Most of the smallholder farmers in India rely on rainfed agriculture and frequently face dry spells and droughts that affect agricultural productivity. The gravity fed drip irrigation technologies are the solution to them as it bridges dry spells, mitigate against droughts and ensure food security. Thus, appropriate, affordable, accessible, gravity fed drip irrigation system can be the better alternative for small landholders. Thus a technically proven system consisting of raised bed cultivation of okra under plastic mulch and gravity based drip irrigation system was evaluated for small farm holding for its technical feasibility and economic viability.

5.2 MATERIALS AND METHODS

An effort was made in this direction through Farmers First Programme Under Directorate of Extension, Birsa Agricultural University, which worked with around 1000 farm families in villages Chipra and Kudlong under Nagri Block Ranchi. These farm families were marginalized by remoteness, inaccessibility, very small landholding, and traditional farming methods. Cash income was very low, and in many households, the main problem was still to achieve basic food security. The income was so poor that they had to struggle to make both ends meet. Out of compulsion most of the families including women were forced to work in a brick kiln as seasonal workers to bring cash flow. They had literally abandoned farming for quite some time as traditional farming with conventional crops in mostly rain-fed uplands gave very less dividends.

With the belief that technology interventions, which address land productivity of marginalized farmers, hold the key to usher effective means of addressing the issue of rural poverty alleviation. New interventions were pondered to bring back these families into cultivation for making a living. Now the first and the most difficult step was to bring back the confidence in

these farmers who have left farming for quite some time and had adjusted themselves with being kiln workers. Initial Survey was conducted in Chipra and Kudlong villages by Farmer FIRST team of BAU. It was felt that intervention which is tangible and effect of which can be seen in a short time would be best to bring back the confidence in these farm families. After doing much exercise, plasticulture intervention was found most suited to start with. The difficulty was, as it always happens with new technologies, was to convince farmers about the concept. On the principle of seeing is believing, the group of farmers were given exposure visit to Birsa Agricultural University and ICAR for Eastern region where cultivation under drip irrigation (both pressurized and gravity fed). Vegetable crops under mulching in raided bed, cultivation, and nursery growing under low-cost polyhouse were shown. The same group was imparted multiple training at Birsa Agricultural University on different plasticulture application. Scientist from Birsa Agricultural University also imparted training though guest lecturer in multiple trainings organized by Farmers FIRST programme during Mahila Saptaah organized from March 6–12, 2017. After these training and seeing into the ground reality of their situation, farmers were inclined towards gravity based drip irrigation and black polyethylene mulching. 10 Farmers five each from Chipra and Kudlong were selected for this intervention.

Ten Farmers were chosen for this intervention and crop selected based on a survey done and seeing the seasonality and market condition okra (var-Osaka, F1 hybrid) was selected and planted in 500 m^2 area under gravity drip irrigation and mulching. Pressure for irrigation was made through an overhead tank placed at the height of 1.5 to 2 m. All technical aspects were looked into while designing the system and all agronomic measures followed.

5.2.1 LOCATION AND LAYOUT OF FIELD PLOT

The field experiment was conducted during February to May in 2017 at the Chipra and Kudlong villages of Nagri Block, Ranchi. The soil at the farmers' field were mostly sandy loam (18.4% clay, 22.6% silt, and 59.0% sand) having a bulk density of 1.39 g/cm^3 with a basic infiltration rate of 1.8 cmh^{-1}. A field plot measuring 1000 m^2 was vertically divided into three equal parts (i.e., T1, T2 and T3) and 10 farmers from two villages viz. chipra and kudlong were the replications. The layout of the field with drip irrigation network is shown in Figure 5.1. Osaka-Eastern seeds (F_1 hybrid) variety of okra was selected and the seeds were sown at a spacing of 30 cm in the third week of Feb. Paired row planting was adopted with one lateral catering to the

water needs of two rows of okra in raised bed plantation spaced at 0.5m in a bed with a top width of 80 cm. Standard agronomic practices such as fertilization and plant protection measures were applied during the crop period. The fertilizer doses of 100 kg N, 50 kg each of P and K along with 20 t of farmyard manure per hectare were applied to meet nutritional requirement of crop. In order to prevent fungal infection and attack of insects, Carbendazim with Dethane M 45 and Emida Cloropid were applied. The lateral lines were laid parallel to the crop rows and each lateral served two rows of crop. The laterals were provided with 'online' emitters of 2 lph discharge capacity at 0.6 m interval. In this arrangement there may be a possibility of overlapping of moisture front in the longitudinal direction under mulched condition partly due to lateral spread of moisture regime and mainly due to condensation of water vapor underneath the much so as it act as line source of irrigation. The treatments followed for the study were as stated below:

T_1 Control-farmers practice (Flood irrigation with 3 cm of water in furrows);

T_2 100% of irrigation requirement met through drip only;

T_3 100% of irrigation requirement met through drip with black plastic mulch.

Ten farmers were chosen for this intervention and crop selected based on a survey done and seeing the seasonality and market condition okra (var-Osaka, F1 hybrid) was selected and planted in 500 sq.m area under gravity drip irrigation and mulching. Pressure for irrigation was made through an overhead tank placed at the height of 1.5 to 2 m. All technical aspects were looked into while designing the system and all agronomic measures followed.

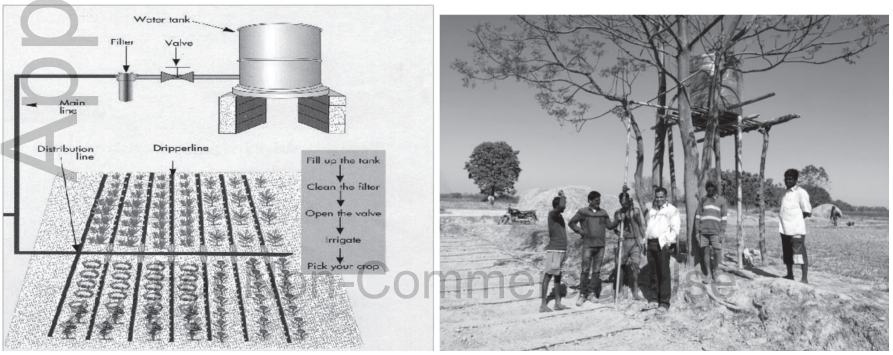

FIGURE 5.1 Drip layout with the overhead tank at farmers field.

5.2.2 ESTIMATION OF IRRIGATION WATER REQUIREMENT

The daily irrigation water requirement for the okra crop was estimated using the following relationship

$$IR = ETo \times Kc - ER \quad (1)$$

where,

IR is net depth of irrigation (mmday^{-1});
ETo is the reference evapotranspiration (mmday^{-1});
Kc is the crop coefficient;
ER is the effective rainfall (mmday^{-1}).

The net volume of water required by the plant can be calculated by the relationship

$$V = IR \times \hat{A} \quad (2)$$

where,

V is the net volume of water required by a plant (l day^{-1}).
$\hat{A}$ is the area under each plant (m^2).

That is, the spacing between rows (m) and spacing between plants (m). Since there was no effective rainfall during the crop growth period conducted at farmers field at Nagri, Block of Ranchi, rainfall occurring during these months can be taken as effective rainfall (Michael, 1981). In control plots, furrow irrigation was given at an interval of 10 days. The depth of irrigation water required for all the plants was roughly given up to 3 cm depth. Biometric observations were taken from selected plants in each treatment at 30 days interval. The operational and fixed costs of cultivation of were factored in a while calculating the cost of cultivation. The income from produce was estimated using the prevailing average market price @ Rs 18–20 per kg of produce. The net seasonal income from produce was estimated by subtracting the total seasonal cost from the income of the produce. The benefit-cost ratio, net income, and water-use efficiency were determined.

5.3 RESULTS AND DISCUSSION

The number of irrigation were divided into the four distinct crop growth stages, and the amount of irrigation was determined by climatological

parameters based on the average monthly evapotranspiration of the area obtained from the Meteorological Department of the Birsa Agricultural University Ranchi. The number of irrigation at various stages of growth were 5, 21, 16 and 4 at an interval of 1 day for drip irrigation only and in the treatment drip irrigation with plastic mulching the number of irrigation provided at an interval of 2 days were 3, 14, 7, 7 at germination, vegetative, flowering, and harvest stages. In control (furrow irrigation) irrigation to the depth 3 cm was provided at an interval of 10 days. Total irrigation for furrow method of irrigation (control) was 27 cm while through drip irrigation without plastic mulch was 15.6 cm and for the treatment drip irrigation with plastic mulch was around 9 cm (Tables 5.1 and 5.2). Thus, it could be easily said that there is water saving of more than 80% through drip irrigation alone and if it is used in combination with plastic mulch, then there is further saving of water and irrigation frequency can also be reduced. Apart from this mulch also helps to arrest weed growth and moderate the soil temperature. This facilitates better growth and development of the crop.

The effect of drip irrigation on biometric parameters such as plant height, plant girth, fruits per plant, fruit length and fruit yield was compared with that of furrow irrigation treatments. The experimental results of these biometric observations for the year under consideration are presented in Table 5.3.

The results have shown increased yield attributing characters like plant height (56, 96 and 176 cm), plant girth (9.4, 13.9 and 21.0 mm) at 30, 60 and 90 DAS, respectively were highest for treatment T3 (Drip irrigation + mulching). Fruit per plant (15–23), fruit length (13.5 cm), fruit diameter (25.2 cm) and fruit yield (142.6 qha^{-1}) under plastic mulch and drip irrigation were also higher as compared to other treatments. The results corroborated the findings of Sivanappan and Padmakumari (1980) and Khade (1987). It can be seen that the plant growth and yield were greater in drip with mulch as compared to drip alone.

5.4 CONCLUSIONS

The drip irrigation is economical and cost-effective when compared with furrow irrigation. The use of drip either alone or in combination with mulch can increase the okra crop yield significantly over furrow irrigation to the tune of 35.5 to 51.2%. To irrigate 1 ha of okra crop with drip irrigation 150 l/m^2 water will be needed for this agroclimatic condition. The maximum duration of operation of drip irrigation is 42.3 min during peak demand of the crop with the emitter capacity of 2 lph. The net income could be increased

TABLE 5.1 Total Water Applied in Okra Crop During Entire Cropping Season (February 26, 2012 to June 10, 2012) Under Drip Irrigation

Month	Number of irrigations	Crop Stage	Frequency	Water/irrigation (l/m^2)	Liters/ plant	Time/ irrigation (h-minutes)	Monthly water application
February	2	Germination	Daily	1.16	0.17	10.53	2.32
March	14	Germination(3)	Daily	1.29	0.19	11.61	3.87
		Vegetative(11)	Alternate day	1.80	0.27	16.20	19.8
April	15	Vegetative (10)	Alternate day	2.66	0.40	24	26.6
		Flowering(5)	Alternate day	3.64	0.55	32.82	18.2
May	15	Flowering (11)	Alternate day	4.70	0.70	42.30	51.7
		Harvesting(4)	Alternate	4.48	0.67	40.32	17.92
June	3	Harvesting	Alternate	3.40	0.51	30.60	10.2
Total	50						150.61

TABLE 5.2 Total Water Applied in Okra Crop During Entire Cropping Season (February 26, 2012 to June 10, 2012) Under Drip Irrigation and Plastic Mulch

Month	Number of irrigations	Crop Stage	Frequency	Water/irrigation (l/m^2)	Liters/ plant	Time/ irrigation (h-minutes)	Monthly water application
February	1	Germination	Alternate days	1.16	0.17	10.53	1.16
March	10	Germination(2)	Alternate	1.29	0.19	11.61	2.58
		Vegetative(8)	3 days	1.80	0.27	16.20	14.4
April	9	Vegetative (6)	3 days	2.66	0.40	24	15.96
		Flowering(3)	3 days	3.64	0.55	32.82	10.92
May	10	Flowering (4)	3 days	4.70	0.70	42.30	14.1
		Harvesting(6)	3 days	4.48	0.67	40.32	26.88
June	1	Harvesting	3 days	3.40	0.51	30.60	3.4
Total	31					Total 89.4	

TABLE 5.3 Growth and Yield as Influenced by Different Treatments

Treatment	Plant Height (cm)			Plant girth (mm)			Fruits per plant	Fruit length (mm)	Fruit dia (mm)	Fruit yield qha^{-1}
	30	60	90	30	60	90				
Control (Flood Irrigation)	33	70	112	6.7	10.4	16.3	11–16	10.5	23.0	94.4
Irrigation with Drip System	49	88	148	8.1	12.6	19.2	14–21	12.8	24.5	128.2
Drip Irrigation + Plastic Mulch	59	96	176	9.4	13.9	21.0	15–23	13.5	25.2	142.6

by about 47.74% by adopting drip with plastic mulch and 29.21 for drip over furrow irrigation The benefit-cost ratio was found to be highest (1.64) for treatment under drip irrigation with mulch followed by (1.44) for drip without mulch (Table 5.4). The water use efficiency for the treatment drip with mulch was found out to be 1620 Kg/ha-cm, and that of treatment with only drip irrigation was 1440 kg/ha-cm while in farmers practice (control) it was 350 kg/ha-cm.

TABLE 5.4 Calculation of Benefit-Cost Ratio of Onion for First Year Under Different Treatments (Prices are Given in Indian Rupees)

S. No	Cost Economics	Treatments		
		T_0	T_1	T_2
1	Fixed cost	-	195000	244,049
	a) Depreciation	-	8404	10,532
	b) Interest	-	19500	12,202
	c) Repair and maintenance	-	1950	2,640
	Total (a+b+c)	-	25374	25374
2	Fixed cost total		207304	269423
3	Annual fixed cost (considering life of 10 years)	-	20730	20730
2	Cost of cultivation	72000	92730	92730
3	Fertilizer cost (Rs/ha)	3650	3650	3650
4	Mulch material (Rs/ha) (life 3 season)	-	-	9500
4	Irrigation charges	4896	3480	2088
5	Seasonal total cost (Rs/ha)	80546	99860	107968
6	Yield of produce (Kg/ha)	9440	12820	14260
7	Selling price (Rs/kg)	18	19	20
8	Income from produce (6x7), (Rs/ha)	169920	243580	285200
9	Net seasonal income (8–5), (Rs/ha)	89374	143720	177232
10	Benefit-Cost ratio (9/5)	1.11	1.44	1.64

ACKNOWLEDGMENT

Authors are thankful to Farmers First Programme of ICAR and Department of Extension Education, BAU, Ranchi for providing the financial assistance for conducting this work and for providing necessary facilities to carry out the programmes at farmers field.

KEYWORDS

- **drip irrigation**
- **plastics mulch**
- **uniformity**
- **water use efficiency**

REFERENCES

Khade, K. K., (1987). *Highlights of Research on Drip Irrigation* (pp. 20–21). Mahatma Phule Agricultural University. India, Pub. No. 55.

Michael, A. M., (1981). *Irrigation Theory and Practice* (Reprint 1st edn., pp. 539–542), Vikas Publishing House, New Delhi, India.

Sivanappan, R. K., & Padmakumari, O., (1980). *Drip Irrigation* (p. 15). Tamil Nadu Agricultural University, Coimbatore, India, SVNP Report.

Sivanappan, R. K., Padmakumari, O., & Kumar, V., (1987). *Drip Irrigation* (1st edn., pp. 75–80). Keerthi Publishing House, Coimbatore, India.

CHAPTER 6

ASSESSMENT OF AGRICULTURAL DROUGHT USING A CLIMATE CHANGE INITIATIVE (CCI) SOIL MOISTURE DERIVED/SOIL MOISTURE DEFICIT: CASE STUDY FROM BUNDELKHAND

VARSHA PANDEY, SWATI MAURYA, and PRASHANT K. SRIVASTAVA

Institute of Environment and Sustainable Development, Banaras Hindu University, Varanasi – 221005, India,
E-mail: varshu.pandey07@gmail.com

ABSTRACT

Soil moisture information is very important for agricultural drought monitoring, which is now possible to be measured using the Earth observation datasets. Drought conditions can be directly related to the Soil Moisture Deficit (SMD) variable by using the soil moisture data and soil physical properties. In this chapter, we have used Climate Change Initiative (CCI) Soil Moisture data in integration with soil hydraulic parameters for the derivation of SMD. The field capacity estimated from the simulated Water Retention Curve (WRC) through ROSETTA, which can be used for the transformation of CCI soil moisture data into SMD over Bundelkhand region. The analysis of results indicates that a large part of the Bundelkhand region is facing moderate to severe drought conditions derived from the SMD model developed in this study.

6.1 INTRODUCTION

Drought is more damaging and diverse in nature in comparison to other hazard types such as floods, tsunamis, etc. It emerges gradually over a large

area and generally lasts for the long time span. Monitoring of drought is complex as it varies both spatially and temporally; therefore, it requires state-of-the-art tools and techniques. The extremity of agricultural drought can be best estimated by the soil moisture levels. The deficit in soil moisture due to rainfall shortage is highly correlated with drought phenomenon. Soil moisture is a key variable in hydrological modeling, meteorological modeling (Nandintsetseg and Shinoda, 2011) hazard event estimation such as flood and drought, as well as plant growth vegetation health monitoring. Therefore, precise monitoring and spatiotemporal estimation of soil moisture are important. Now, under the climate change initiative (CCI), a long-term record of soil moisture is available for hydrological modeling. On the other hand, the Soil Moisture Deficit/Depletion (SMD) is the important variable for flood and drought forecasting. The SMD provides an estimation of agricultural drought by representing the amount of water requirement to raise the soil moisture content of the plant root zone to field capacity (FC) (Srivastava, 2014). The prolonged condition of SMD in the soil may lead to drought, if the same situation persists for a long period (Srivastava, 2013). Therefore, in the purview of the above, the main focus of our study is to use CCI soil moisture for SMD evaluation during the Kharif season.

6.2 MATERIALS AND METHODOLOGY

6.2.1 STUDY AREA

The Bundelkhand region lies at the heart of India located below the Indo-Gangetic plain to the north with the undulating Vindhyan mountain range spread across the northwest to the south. The Uttar Pradesh region of Bundelkhand has worst affected drought area, lies between $24^{0}00'$ and $26^{0}05'$ N latitudes and $78^{0}00'$ and $82^{0}05'$ E longitudes (Figure 6.1). The main rivers are the Sindh, Betwa, Ken, Bagahin, Tons, Pahuj, Dhasan, and Chambal, and constitute the part of Ganga basin. The topography of the region is highly undulating, with rocky outcrops and boulder-strewn plains in a rugged landscape. The major soils include alluvial, medium black, and mixed red and black soil (Singh and Phadke, 2006).

6.2.2 DATASETS

The ESA's remote sensing CCI soil moisture (CCI-SM) combined product used in this study for the estimation of agricultural/soil moisture drought.

The CCI-SM combined product has a 25 km spatial and daily temporal resolution with its reference time at 0:00 UTC, having product version 02.2 in NetCDF–4 classic file format over a global scale. CCI-SM represents the values from the upper few millimeters to centimeters from the soil surface to estimation of the influence of soil depth on drought phenomenon. In this study, the blended product made by fusing active and passive is used (Nicolai, 2017). Soil maps can provide soil inputs such as soil texture, bulk density, organic carbon, infiltration, soil depth, and water holding capacity, etc., to models for predicting hydrological and climatic conditions. The Digital Soil Map of World (DSMW) used in this study and prepared by the Food and Agriculture Organization (FAO) of the United Nations is in vector form, at 1: 5,000,000 scale, in the geographic projection (Latitude-Longitude) (https://searchworks.stanford.edu/view/4059679). The main types of soil in this region are Chromic Luvisols (Sandy Clay loam soil), Eutric Cambisols (Loam soil), Orthic Luvisols (Sandy Loam soil), and Chromic Vertisols (Clay soil). In the study area, the dominant soil types that exist are sandy clay loam and sandy loam soil. These types of soils show very poor water holding capacity and high infiltration rate, which cause SMD in the area.

6.2.3 ROSETTA MODEL

There are number of PTFs based on linear and non-linear regression, and Artificial Neural Network (ANN) is used in the scientific study that relates the descriptive equations such as (Van Genuchten, 1980) with calculated soil properties. In this paper, Rosetta Lite (version 1.1) inbuilt in HYDRUS 1D (version 4.16.0110) model, based on ANN analysis is used for predicting soil hydraulic properties. The ROSETTA model executes five hierarchical input parameters for WRC prediction. WRC is the curve which represents the relationship between the soil moisture content and the soil water potential. In this study, for WRC estimation percentage of sand, silt, and clay + bulk density have been taken into account. The soil moisture content at different potential using Rosetta is based on algorithms described by Van Genuchten (1980) and Schaap (2001) represented in the following equation:

$$\theta(h) = \theta_r + \frac{\theta_s - \theta_r}{[1+(\alpha h)^n]^m} \tag{1}$$

where *θ(h)* represents the WRC in terms of soil moisture content, θ(cm^3cm^{-3}) as a function of the soil water potential *h* (cm), θ*r* and θ*s* (cm^3cm^{-3}) are the residual and saturated soil water contents respectively, *n*, and α (1/cm) are

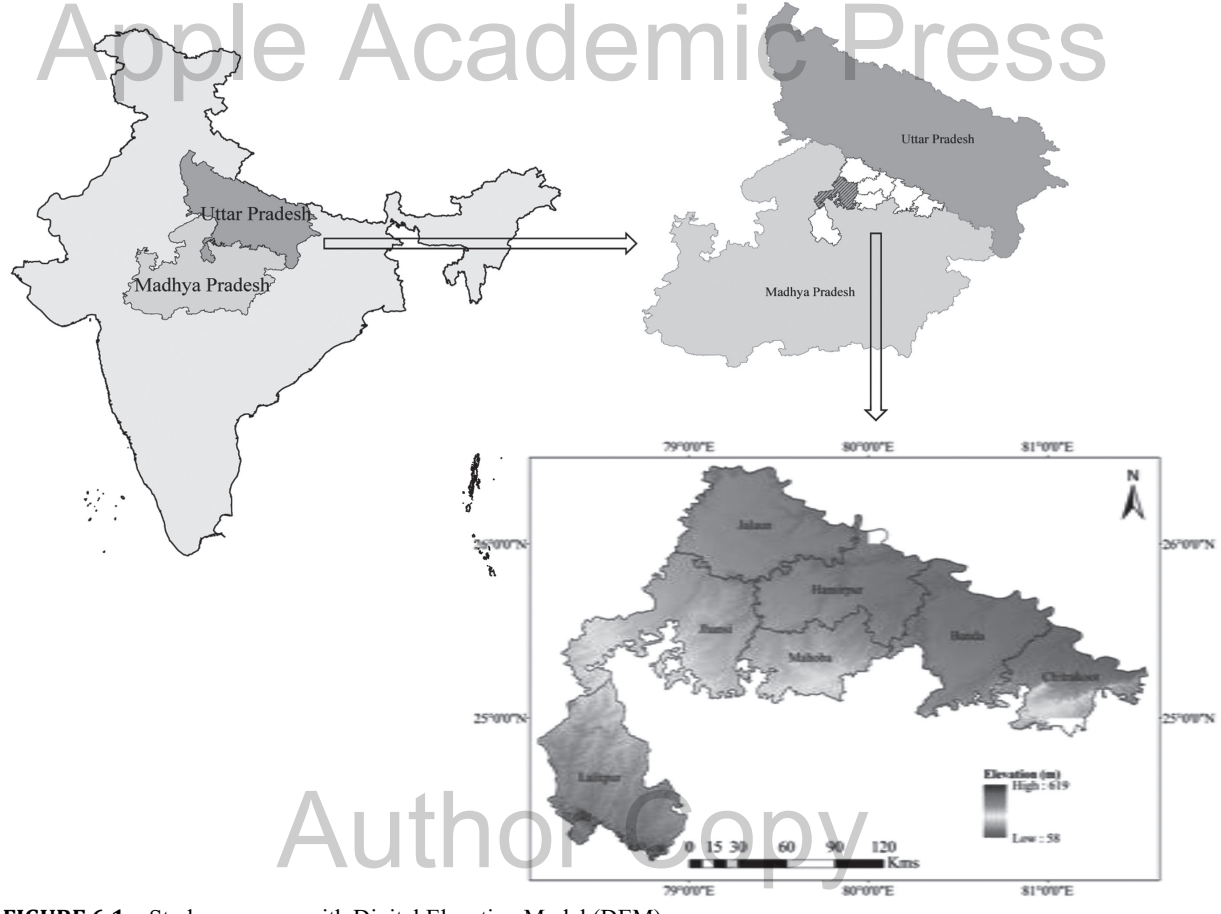

FIGURE 6.1 Study area map with Digital Elevation Model (DEM).

the curve shape parameters and *m* is empirical constant, which can be related to the *n* as:

$$m = 1 - 1/n, \text{ For } n > 1 \quad (2)$$

6.2.4 SOIL MOISTURE DEFICIT (SMD)

SMD is calculated based on soil moisture content and FC. It is the difference between the moisture content available in the plant root zone and the amount of moisture content that the soil can hold against gravity. The primary thematic layers for SMD estimation were prepared using software Arc GIS (version 10.1) for SMD estimation. All the soil datasets were georeferenced to the World Geographic System 84 (WGS84) coordinate system and then reclassified by assigning FC values estimated from the ROSETTA model. Then FC map is prepared by importing FC values generated by WRC (Figure 6.2), and soil moisture climatology map is also generated by CCI-SM datasets from 2002 to 2014 using Cell Statistic tool. The obtained layer was resampled for any geographical mismatch. The difference between FC and SMC (Soil Moisture Content) gives SMD. In hydrological modeling, FC is considered as the upper limit for soil moisture because extra water above FC cannot be held in the soil and will be drained away very quickly either as surface runoff or groundwater runoff. The SMD is calculated using a different hydrological model such as PDM by the following equation.

$$SMD = FC - SMC \quad (3)$$

6.3 RESULTS AND DISCUSSION

6.3.1 HYDRAULIC SOIL PARAMETERS

Despite soil hydraulic properties are typically measured in laboratories by in-situ soil samples, we used the Rosetta model, which is well tested at many locations, because of practical and economic constraints. The basic soil information (such as soil type, percents of sand, silt, and clay, bulk density) along with FC is shown in Table 6.1. Using the basic soil information, Rosetta depending upon Pedotransfer functions, measured soil hydraulic parameters for the formulation of water retention curve (WRC). WRC is defined as the amount of water retained in soil under a definite matric potential. It is based

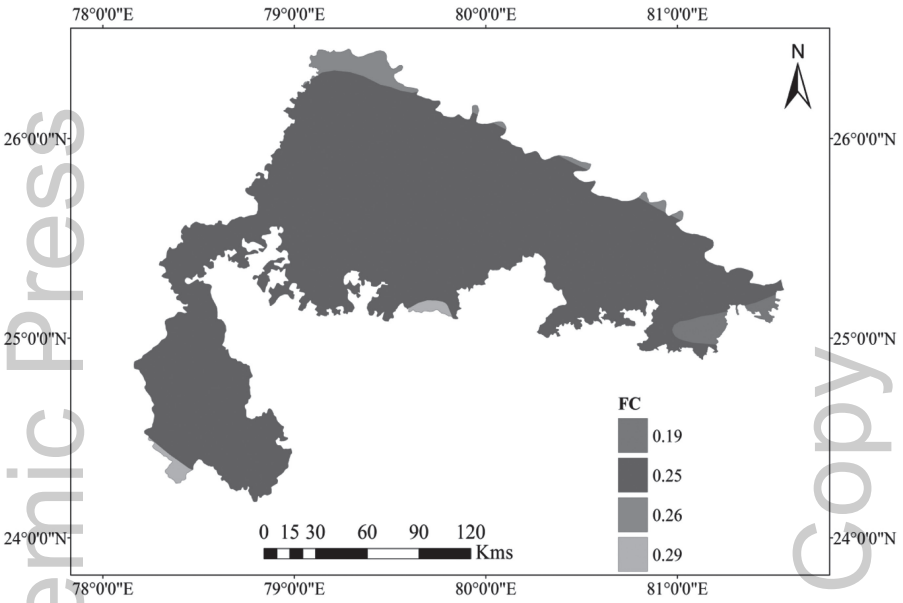

FIGURE 6.2 **(See color insert.)** Field capacity map of study area.

on soil texture, bulk density, organic matter, etc. and can be used for FC and Permanent Wilting Point (PWP) estimation of the soil.

TABLE 6.1 Soil Properties Derived From FAO-UNESCO for Bundelkhand-UP Region

Soil Type	% of Sand	% of Silt	% of Clay	Bulk Density (gcm^{-3})	Field Capacity (at 33 Kpa)
Sandy Clay Loam	59	11.2	29.8	1.6	0.25
Clay	20.8	23.5	55.7	1.7	0.29
Sandy Loam	71.9	8.9	19.2	1.5	0.19
Loamy	41.7	32.1	26.2	1.3	0.26

In the Bundelkhand-UP region, the dominant soil type is sandy clay loam and sandy loam as compared to the clay and loamy soil type. As the variation in soil types determines soil moisture retention capacity of the soil, ROSETTA based on soil type is used for estimation of the FC. The estimated WRCs for four soil type of the region is shown in Figure 6.3. After perusal of obtained result, we find that the FC of sandy loam (0.18 m^3m^{-3}) is found lower than among four soil type. Sandy clay loam (0.24 m^3m^{-3}), the dominant soil type of

the area having moderate FC which indicates the poor water holding capacity and consequently fast infiltration the region. Therefore, soil water drained into the lower surface of soil layers and occurrence of SMD. Hence the region tends to drain out soil water and causes a higher chance of drought condition.

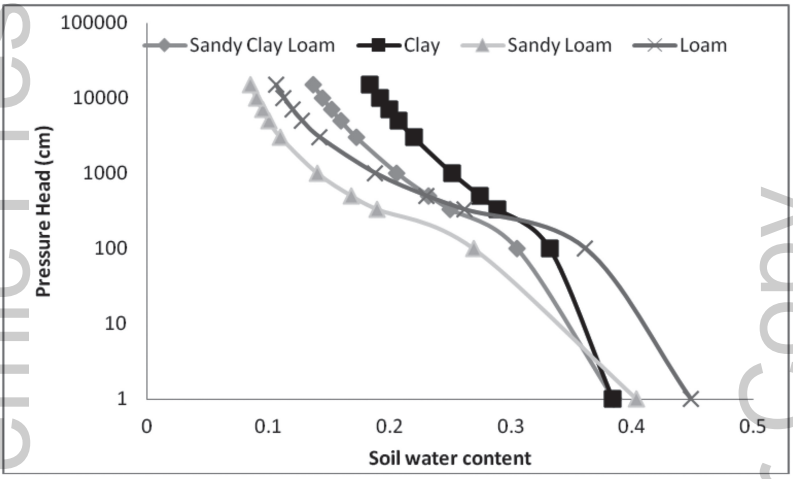

FIGURE 6.3 Water retention curve for different soils in Bundelkhand-up region.

6.3.2 SOIL MOISTURE DEFICIT (SMD)

The SMD is an important indicator for representing the degree of soil saturation; it is inversely related to the soil moisture in the soil layer. Therefore, a low (or negative) SMD indicates water surplus or little capacity for infiltration whereas, a high SMD (or positive) values means below FC and rain can infiltrate to the capacity of the SMD amount. In saturated soil, all of the available soil pores are full of water, but water will drain out of large pores under the force of gravity. The SMD represents the degree of soil saturation and is inversely proportional to the soil moisture content. The estimated SMD of the study area ranges from –0.04 to 0.07 m as shown in Figure 6.4. Negative SMD values observed less than 5% of the total study area indicating water surplus or lower infiltration capacity mostly seen in the parts of Lalitpur and Banda districts. Whereas, positive SMD values observed the rest of the area (>95%) found in all the districts indicating moisture content below FC or higher infiltration rate (Figure 6.4). We observed negative SMD in the southern regions at the high altitudes and positive values in the northern region at low altitudes.

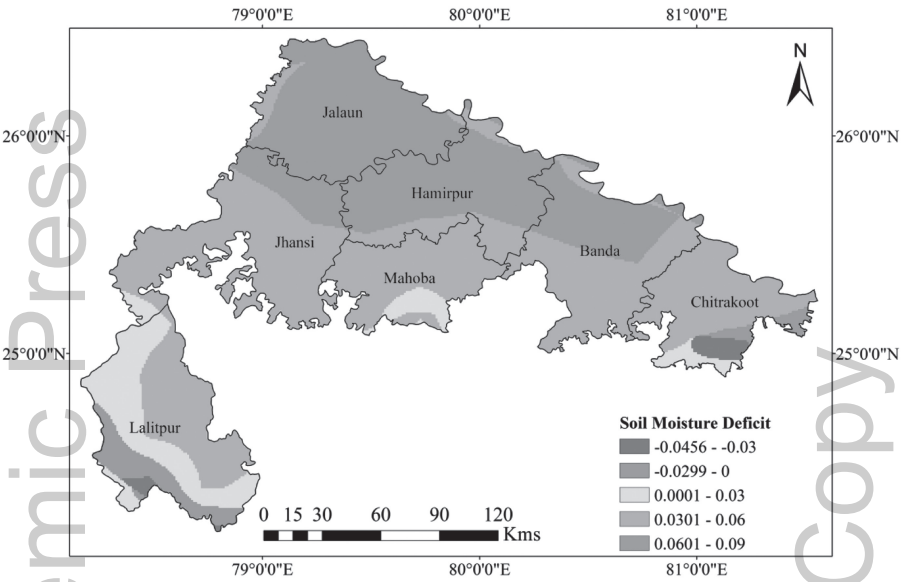

FIGURE 6.4 (See color insert.) Soil moisture deficit (SMD) of the study area.

6.4 CONCLUSIONS

Agricultural drought is one of the major natural hazards due to its impact at large spatial scale, gradually emergence over a long period, and long-lasting behavior. Agricultural drought management in the past is based on meteorological observations and water supply, but decision-makers have required drought response operations that should be available and accessible for use in a short period of time and need to be updated on the latest drought situation, especially soil moisture conditions. This study explores the satellite-based CCI soil moisture derived SMD for monitoring agricultural drought spatially. The development of a spatial map of SMD is based on soil moisture content and FC of the soil. The results depicted that more than 90% area is prone to the drought with 0.09 to 0.03 SMD value. These regions namely Jalaun, Hamirpur, and Jhansi are situated in the middle of the study region and require better irrigation scheduling for crop production. Further study will be continued to consider information from other sources to improve the spatial resolution of soil moisture estimation and better algorithms to utilize CCI-SM products as well as derivation of agricultural drought.

KEYWORDS

- **agricultural drought**
- **CCI soil moisture**
- **field capacity**
- **soil moisture deficit**

REFERENCES

Digital soil map of the world and derived soil properties. https://searchworks.stanford.edu/view/4059679 (accessed on 10/12/2018).

Nandintsetseg, B., & Shinoda, M., (2011). Seasonal change of soil moisture in Mongolia: Its climatology and modeling, *International Journal of Climatology*, *31*, 1143–1152.

Nicolai-Shaw, N., Zscheischler, J., Hirschi, M., Gudmundsson, L., & Seneviratne, S. I., (2017). A drought event composite analysis using satellite remote-sensing based soil moisture. *Remote Sensing of Environment. 203*, 216–225.

Schaap, M. G., Leij, F. J., & Van Genuchten, M. T., (2001). ROSETTA: A computer program for estimating soil hydraulic parameters with hierarchical pedotransfer functions. *Journal of Hydrology, 251*, 163–176.

Singh, S., & Phadke, V., (2006). Assessing soil loss by water erosion in Jamni River Basin, Bundelkhand region, India adopting Universal Soil Loss Equation using GIS. *Current Science,* 1431–1435.

Srivastava, P. K., Han, D., Ramirez, M. A. R., & Islam, T., (2013). Appraisal of SMOS soil moisture at a catchment scale in a temperate maritime climate. *Journal of Hydrology, 498*, 292–304.

Srivastava, P. K., Han, D., Rico-Ramirez, M. A., O'Neill, P., Islam, T., & Gupta, M., (2014). Assessment of SMOS soil moisture retrieval parameters using tau–omega algorithms for soil moisture deficit estimation. *Journal of Hydrology, 519*, 574–587.

Van Genuchten, M. T., (1980). A closed-form equation for predicting the hydraulic conductivity of unsaturated soils. *Soil Science Society of America Journal, 44*, 892–898.

CHAPTER 7

EVALUATING THE USE OF "GOODNESS-OF-FIT" MEASURES IN A WATER MOVEMENT MODEL

VINOD KUMAR TRIPATHI

Department of Farm Engineering, Institute of Agricultural Sciences, Banaras Hindu University, Varanasi, U.P.–221005, India, Email: tripathiwtcer@gmail.com

ABSTRACT

To reduce hunger and eradicate poverty, then not only is achieving security for water, energy, and food for people critical, but also in doing so a far more integrated and cross-sector planning framework will be needed. The demand of wastewater (WW) for irrigation is gradually increasing due to escalating competition for freshwater by urban, industrial, and agricultural users. To sustain or increase agricultural production, there is a need to adopt highly efficient irrigation technologies such as surface or subsurface drip irrigation (SDI) systems. Studies related to water distribution under any irrigation system and water quality are important for efficient water and nutrients application. In the present study, the water dynamics under surface and subsurface drip irrigation was evaluated by taking cauliflower as a test crop on sandy loam soil. The calibrated model predicted all the parameters close to observed values with RMSE values ranging from 0.05 to 0.92. HYDRUS-2D model has the ability to predict water distribution with reasonably good accuracy in present crop and soil condition.

7.1 INTRODUCTION

Sources of freshwater at places in Africa, Asia, and South America are fast running out owing to accelerated net extraction for human use. Freshwater

availability for irrigation in arid and semi-arid regions is a major concern around the World (Sikdar, 2007; Tripathi et al., 2016a). In the Millennium Development Goal formulated at the UN Millennium Development Summit in the year 2000, lack of access to safe water by the world's poor was pledged to be cut into half by 2015. There is plenty of water around us in the oceans, in terrestrial water bodies such as rivers and lakes, as ice and snow in the Polar Regions, on mountain tops, and in subsurface aquifers. But easily accessible fresh water is dwindling because of extensive agriculture, enhanced industrial activities and increasing domestic use. By all these anthropogenic activities polluted water is generated as byproduct called as wastewater (WW). Potentially the most efficient irrigation systems over traditional systems are often recommended to overcome this problem. Sustainability of water resources depends upon the magnitude of the overall productivity gain following the shift from traditional irrigation method to micro-irrigation system, the pattern of use of the saved water, and the type and a potential number of adopters (Namara et al., 2007).

To obtain the best possible delivery of water and solute under drip irrigation (DI) system decision for the optimum distance between emitters and depth of placement of lateral tube play an important role. It depends upon the dimensions of the wetted volume and the distribution of water and solute within the wetted volume. To control the groundwater contamination, subsurface drip irrigation (SDI) is the safest way of WW application (WHO, 2006; Tripathi et al., 2016b). It also leads to the reduction of weeds, evaporation from the soil surface and consequently to an increase in the availability of water for transpiration and overall water use efficiency in comparison to surface DI system (Romero et al., 2004). Uniform distribution of WW and nutrients in the crop root zone increases the efficacy of fertilizers and to maintain a dry soil surface to reduce water losses due to evaporation in case of SDI. Irrigation with WW through a subsurface drip system alleviates health hazards, odor, and runoff into surface water bodies due to no aerosol formation and produce does not come into direct contact with poor quality water. Longevity of emitters with a lateral tube also increases by subsurface placement. SDI has a special advantage of securing system safety against pilferage and damage by animals and during intercultural operations (Tripathi et al., 2014). Several empirical, analytical, and numerical models have been developed to simulate soil water content and wetting front dimensions for surface and SDI systems (Angelakis et al., 1993; Cook et al., 2003). Due to advances in computer speed, and the public availability of numerical models simulating water flow in soils, many researchers have become interested

in using such models for evaluating water flow in soils with DI systems (Lazarovitch et al., 2007; Provenzano, 2007).

HYDRUS–2D (Simunek et al., 1999) is a well-known Windows-based computer software package used for simulating water, heat, and/or solute movement in two-dimensional, variably saturated porous media. This model's ability to simulate water movement for DI conditions has been assessed by many researchers (Simunek et al., 2008). Cote et al. (2003) used the HYDRUS–2D model to simulate soil water transport under SDI. They discussed that soil water and soil profile characteristics were often not adequately incorporated in the design and management of drip systems. Results obtained from simulation studies indicated that in highly permeable coarse-textured soils, water moved quickly downwards from the dripper.

Skaggs et al. (2004) compared HYDRUS–2D simulations of flow from an SDI line source with observed field data involving a sandy loam soil and an SDI system with a 6 cm installation depth of drip lateral and 3 discharge rates. They found very good agreement between simulated and observed soil moisture data. Ben-Gal et al. (2004) explained that one of the main problems with SDI systems is soil saturation near the emitter and its effects on emitter discharge resulting from the net pressure on the emitter outlet. To solve this problem, they installed the drip tube in a trench, and filled it with gravel to eliminate saturation, and net pressure around the emitter then simulated their conditions using HYDRUS–2D, and found good agreement between observed and simulated data. Lazarovitch et al. (2007) modified HYDRUS–2D further so that it could account for the effects of backpressure on the discharge reduction using the characteristic dripper function. Provenzano (2007) assessed the accuracy of HYDRUS–2D by comparing simulation results and experimental observations of matric potential for SDI systems in a sandy loam soil with a 10 cm installation depth in thoroughly mixed or repacked soils, and also found satisfactory agreement. However, our study was performed under field condition on undisturbed soil profiles.

Studies on the effect of depths of placement of drip laterals with WW do not appear to have caught researchers' attention so far. No measured data of soil water distribution in the root zone of drip irrigated with WW for cauliflower crop are available. Rahil and Antonopoulos (2007) using WANISIM, a 1-D model investigated the effects of irrigation on soil water and nitrogen dynamics with reclaimed WW using DI and application of nitrogen fertilizer for plant growth. The model simulated the temporal variation of soil water content with reasonable accuracy. However, an overestimation of the measured data was observed during the simulation period. Therefore, the

present study was undertaken to understand the dynamics of municipal WW for simulating the water transport processes in the soil under the surface and SDI system. Such an understanding can help in identifying the best irrigation strategy for efficient use of WW. The simulation model Hydrus–2D (Simunek et al., 1999) was selected for the current study for simulation and modeling of soil water content under DI system for cauliflower crop. The simulated results were compared with field data involving placement of emitter lateral at surface and subsurface (15 cm depth).

7.2 MATERIALS AND METHODS

7.2.1 LOCATION AND SOIL OF EXPERIMENTAL SITE

The present study was conducted at Research Farm of Indian Agricultural Research Institute, New Delhi, India The soil of the experimental area was deep, well-drained sandy loam soil comprising 61% sand, 18% silt, and 21% clay. The bulk density of soil was 1.56 gcm^{-3}, field capacity was 0.16 percent, and saturated hydraulic conductivity was 1.13 cmh^{-1}.

7.2.2 CROP PRACTICE AND DESCRIPTION OF IRRIGATION SYSTEM

The cauliflower (cv: *Indame 9803*) seeds were sown in the seed tray (plug tray) under the poly house in the third week of September 2008 and 2009. Twenty-five days old cauliflower seedlings were transplanted at a plant to plant and row to row spacing of 40 cm x 100 cm, respectively. Daily irrigation was applied following the methodology formulated by Allen et al. (1998).

A DI system was designed for cauliflower crop in sandy loam soil using the standard design procedures. The control head of the system consisted of sand media filter, disk filter, flow control valve, pressure gauges, etc. Drip emitters with rated discharge 1.0×10^{-6} m^3s^{-1} at a pressure of 100 k Pa were placed on the lateral line at a spacing of 40 cm. The best treatment, i.e., WW filtered by the combination of gravel media and disk filter with the placement of lateral at surface and subsurface (15cm) was considered for the simulation study. The crop water demand for irrigation was estimated on the basis of Penman-Monteith's semi-empirical formula. The actual evapotranspiration was estimated by multiplying reference evapotranspiration with crop coefficient ($ET = ET_0 \times K_C$) for different crop growth stages. The crop coefficient during the crop season 2008–2009, and 2009–2010 was adopted as 0.70,

0.70, 1.05 and 0.95 at initial, developmental, middle, and maturity stages, respectively (Allen et al., 1998).

7.2.3 SOIL WATER CONTENT

The soil water contents were collected from the crop root zone along and across the DI lateral tube. It was collected from the surface (top visible layer within 2 cm), 2–15, 15–30, 30–45 cm layers of soil for the placement of lateral at surface and subsurface at 15 cm depth. Frequency Domain Reflectometry (FDR) was used for the determination of soil water content.

7.2.4 DESCRIPTION OF MODEL

HYDRUS–2D (Simunek et al., 1999) is a finite element model, which solves Richard's equation for variably saturated water flow and convection-dispersion type equations for heat transport. The flow equation includes a sink term to account for water uptake by plant roots. The model uses the convective-dispersive equation in the liquid phase and the diffusion equation in the gaseous phase to solve the solute transport problems. It can also handle nonlinear non-equilibrium reactions between the solid and liquid phases, linear equilibrium reactions between the liquid and gaseous phases, zero-order production, and two first-order degradation reactions: one which is independent of other solutes, and one which provides the coupling between solutes involved in sequential first-order decay reactions. The model can deal with prescribed head and flux boundaries, controlled by atmospheric conditions, as well as free drainage boundary conditions. The governing flow and transport equations are solved numerically using Galerkin-type linear finite element schemes.

7.2.5 ROOT WATER UPTAKE

The root uptake model (Feddes et al., 1978) assigns plant water uptake at each point in the root zone according to soil moisture potential. The total volume of the root distribution is responsible for 100% of the soil water extraction by the plant, as regulated by its transpiration demand. The maximum root water uptake distribution reflects the distribution in the root zone having roots that are actively involved in water uptake. The root zone

having maximum root density was assigned the value of 1. Root distribution was assumed to be constant throughout the growing season. Maximum depth for simulation was taken as 60 cm.

7.2.6 INPUT PARAMETERS

There are two commonly used models describing soil moisture behavior, the Brooks-Corey model and the van Genuchten model. The van Genuchten model is most appropriate for soils near saturation (Smith et al., 2002). Soils within the root zone under DI system remains at near saturation throughout the crop season. Therefore, van Genuchten analytical model without hysteresis was used to represent the soil hydraulic properties. Sand, silt, and clay content of soil were taken as input and by Artificial Neural Network (ANN) prediction; the soil hydraulic parameters were obtained and are given in Table 7.1. A simulation was carried out applying irrigation from a line source as in the real case for each individual dripper.

TABLE 7.1 Estimated Soil Hydraulic Parameters

Soil layer	Soil depth (cm)	Qr (θ_r)	Qs(θ_s)	Alpha(α) (cm^{-1})	η	Ks (cmh^{-1})
1	0–15	0.0403	0.3740	0.0079	1.4203	1.09
2	15–30	0.0396	0.3748	0.0059	1.4737	0.7
3	30–45	0.0338	0.3607	0.0048	1.5253	1.39
4	45–60	0.0261	0.3682	0.0142	1.3875	1.22

Where θ_r and θ_s are the residual and saturated water contents, respectively; α is a constant related to the soil sorptive properties; η is a dimensionless parameter related to the shape of water retention curve, and K_s represent the saturated hydraulic conductivity.

7.2.7 INITIAL AND BOUNDARY CONDITIONS

Observed soil water in the soil profile was taken as initial water content. For all simulated scenarios, the bottom boundary was defined by a unit vertical hydraulic gradient, simulating free drainage from a relatively deep soil profile (Rassam and Littleboy, 2003). The no-flux boundary was used on the vertical side boundaries of the soil profile because the soil water movement will be symmetrical along these boundaries. The system was divided into four layers depending on the variability of the soil physical properties. To

account the dripper discharge during irrigation, a flux type boundary condition with a constant volumetric application rate of dripper for irrigation duration was considered. During no irrigation period, flux was kept as zero. Time variable boundary condition was used in HYDRUS–2D simulations to manage the flux boundary depending on irrigation water requirement during irrigation and no irrigation period. In surface placement of drip lateral, the top boundary was considered as at atmospheric condition but a small part of the top boundary, around the dripper from where the water is applied to crop, was taken as time variable boundary condition. Under subsurface placement of drip lateral at 15 cm depth, the topsoil surface was considered at an atmospheric boundary condition. The atmospheric boundary is usually placed along the top of the soil surface to allow for interactions between the soil and the atmosphere. These interactions include rainfall, evaporation, and transpiration (root uptake) given in the time variable boundary conditions. The flux radius and subsequently fluxes per unit area, resulting from one meter of drip lateral was determined. No-flux boundary is impermeable and does not allow water into or out of the soil profile through it.

7.2.8 MODEL VALIDATION BY COMPARISON BETWEEN THE SIMULATED AND OBSERVED VALUES

To quantitatively compare the results of the simulations, observed and simulated values for water content was compared. The coefficient of efficiency (C_{eff}) and the root mean square error (RMSE) were the two statistical indices used to evaluate the predictions of the model quantitatively. The RMSE has also been widely used to evaluate the models (Skaggs et al., 2004).

7.3 RESULTS AND DISCUSSION

Distribution of water in the root zone soil profile with filtered WW is influenced by soil type, dripper discharge, depth of placement of drip lateral, quality of irrigation water and extraction of water by crop.

7.3.1 CALIBRATION OF MODEL

The HYDRUS–2D model was calibrated mainly for hydraulic conductivity values of the sandy loam soil. The model worked well with the measured

hydraulic conductivity values. The model gives the spatial and temporal distribution of water content in simulated layers at pre-decided time steps. Field observations for water content in the soil were taken at 4 and 24 h after irrigation. Simulated and observed values of water at 4 and 24 h after irrigation were used to evaluate the performance of the model. RMSE values varied from 0.013 to 0.015. This indicates that Hydrus–2D can be used to simulate the water distribution with very good accuracy.

7.3.2 SOIL WATER DISTRIBUTION

Soil water content was determined using FDR by placing three access tubes at a distance of 0,15, and 30 cm away from lateral pipe up to a depth of 1.0 m. Observed soil water distribution at the initial, development, middle, and maturity stages are presented in Figure 7.1. During the initial growth stage (after 25 days of transplanting), when root length density (RLD) and leaf area index (LAI) was less than 1.0, 23% water content was observed within 10 cm of the radius. The downward movement of water was more than its lateral movement at all growth stages of crop due to gravity force playing a predominant role in comparison to the capillary force in an experimental plot. The higher values of water content near the drip lateral confirming the result obtained by Souza et al., (2003). Soil water content just below the dripper, i.e., 0.0 cm away from the lateral pipe was more throughout the crop season, almost at the level of field capacity, in all depths of placement of laterals. Soil water content at the surface at initial, developmental, middle, and maturity stages of the cauliflower was found to be 23.5, 24.1, 25.0, and 26.1%, respectively.

The soil surface appeared moist under subsurface placement of drip lateral at 15 cm depth in all growth stages of cauliflower. Soil water content above the dripper (at the surface) at initial, developmental, middle, and maturity stage of the cauliflower were found to be 17.1, 16.8, 16.3, and 15.6%, respectively under subsurface drip by placement of drip lateral at 15 cm depth (Figure 7.1). A significant difference ($P<0.01$) was observed in soil water contents of surface soil between placement of lateral at the surface and 15 cm depth.

Wetted soil bulb of 30 cm in width and 50 cm depth had more than 17% soil water content, which was very conducive for good growth of crop during development stage resulting in higher cauliflower yields at subsurface placed drip lateral (placement of drip lateral at 15 cm depth). At the initial and developmental stage of the crop, the active root was confined up to 15 cm soil depth. However, the placement of drip lateral at 15 cm soil depth, adequate soil water was found at 30, 45 and 60 cm soil depths (Figure 7.1).

Water that moved beyond the 40 cm soil depth was not available for plants at any stage.

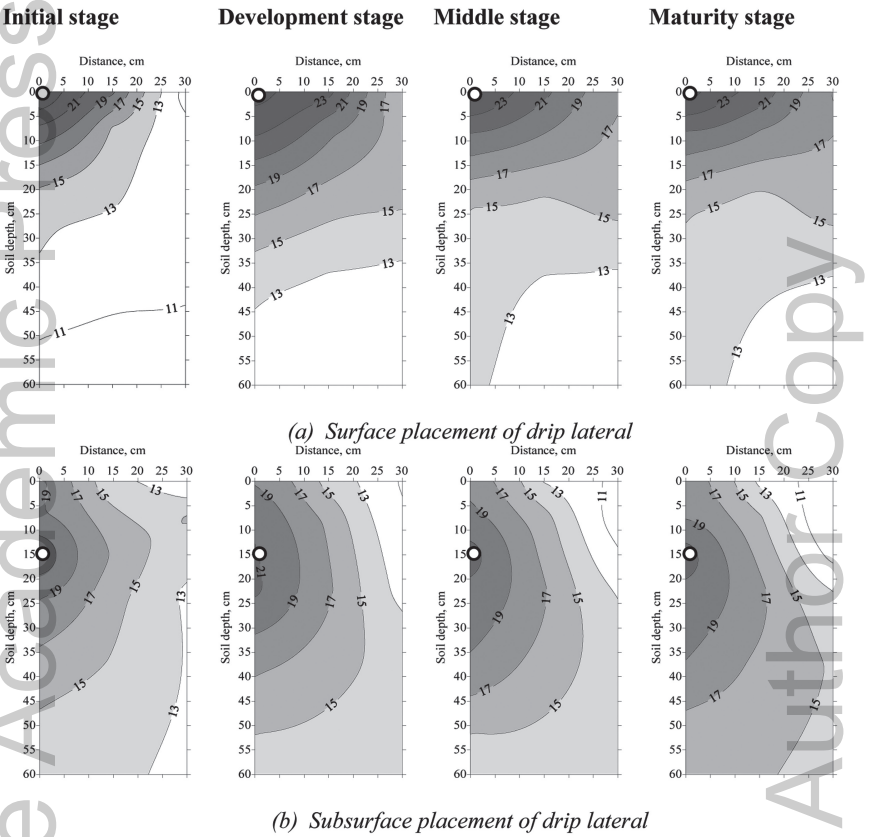

FIGURE 7.1 **(See color insert.)** Observed soil water (volumetric in percent) distribution in the field.

Higher yield was achieved by maintaining relatively high water content in root zone conducive to good plant growth by placement of lateral at 15 cm depth under successive irrigation event. The high water content of the soil around the drippers facilitates better water transmission to the surrounding soil and keeps on replenishing the crop root zone (Segal et al., 2000). Therefore, keeping the drip lateral within the crop root zone and sufficiently below the soil surface replenishes the root zone effectively due to gravity flow in light soils and simultaneously reduces evaporation losses due to restricted upward capillary flow.

7.3.3 SIMULATION OF SOIL WATER DISTRIBUTION

The soil water content distribution from the model-simulated values are presented in Figure 7.2, and after comparison from observed values, statistical parameters are presented in Table 7.2. It shows good agreement between predicted and measured soil water content. The simulated values of water content at soil surface under surface placement of drip lateral were 24.2, 25.1, 25.8, and 25.9% at initial, developmental, middle, and maturity stage of the crop. Simulated soil water content above the dripper on soil surface at initial, developmental, middle, and maturity stage of the cauliflower were found 20.3, 18.6, 18.5, and 18.2%, respectively, under subsurface placement of drip lateral at 15 cm depth (Figure 7.2). The lower coefficient of efficiency and RMSE values were observed by subsurface placement of drip lateral at 15 cm depth.

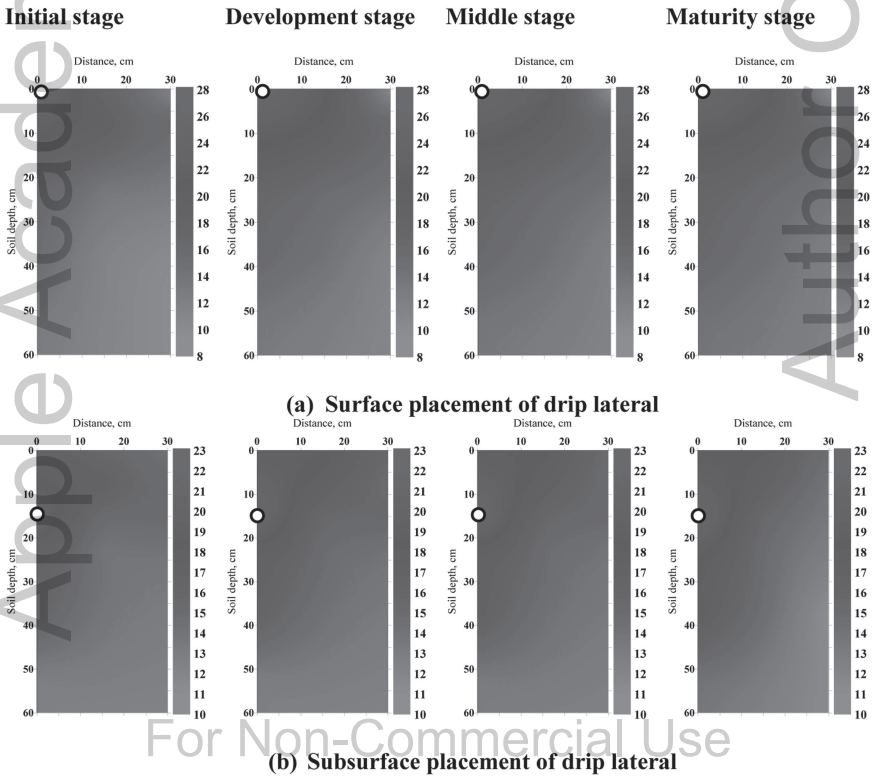

FIGURE 7.2 (See color insert.) Simulated soil water (volumetric in percent) distribution with the model.

TABLE 7.2 Statistical Parameters Indicative of Performance of Model for Water Content

Depth of placement of lateral	Statistical parameters	Crop growth stages			
		Initial	Developmental	Middle	Maturity
Surface	RMSE	0.05	0.87	0.68	0.92
	$C_{eff.}$	–0.41	–0.01	–1.29	–2.25
Subsurface	RMSE	0.06	0.23	0.52	0.39
	$C_{eff.}$	–2.36	–2.59	–1.98	–3.51

The input parameters for the simulation of HYDRUS–2D model were determined by detailed field experimentation. However, a few were taken from published literature matching to our soil and similar crop condition. It was found that the wetting patterns obtained during application of water generally consist of two zones, a saturated zone close to the dripper (5 cm around the dripper). The wetting pattern of elliptical shape was found under subsurface placement of drip lateral at 15 cm depth. Wetted depth was found larger than the surface-wetting radius resulting in more water below dripper under subsurface placement of drip lateral at 15 cm depth because of dominant nature of gravity force in comparison to capillary forces. The saturated radius was taken constantly throughout the crop season, from where flux entered.

The current version of Hydrus–2D has the limitation and does not calculate the time variable saturated radius. The difference observed between experimental and simulated soil water distribution may be attributed to the differences in saturated hydraulic conductivity of soil (observed and simulated by the model as an intermediate step). The root water uptake model was taken from the literature. Many researchers have tried this software and reported its usefulness for simulation and modeling of water distribution (Mailhol et al., 2001; Cote et al., 2003; Gardenas et al., 2005).

7.4 CONCLUSIONS

In this chapter, the software Hydrus–2D predicted the soil water content with high accuracy under DI. Adequate distribution of water content in the root zone of cauliflower is possible with the placement of drip lateral at 15 cm depth from the soil surface. The requirement of a large number of accurate parameters matching with the field condition is important for the simulation of soil water content in the root zone of the crop. Subsurface application of water increases water availability in the root zone of cauliflower crop

enhanced the crop yield. The results of this study will be supportive for prediction of water availability in the root zone as well as a selection of irrigation method for different crops.

KEYWORDS

- **HYDRUS–2D**
- **root zone**
- **simulation**
- **wastewater**
- **water content**

REFERENCES

Allen, R. G., Pereira, L. S., Raes, D., & Smith, M., (1998). *Crop Evapotranspiration-Guidelines for Computing Crop Water Requirements* (p. 300). FAO Irrigation and Drainage Paper No., 56, FAO, Rome, Italy.

Angelakis, A. N., Rolston, D. E., Kadir, T. N., & Scott, V. N., (1993). Soil-water distribution under trickle source. *J. Irrig. Drain. Eng. ASCE*, *119*, 484–500.

Ben-Gal Alon Lazorovitch, N., & Shani, U., (2004). Subsurface drip irrigation in gravel-filled cavities. *Vadose Zone Journal*, *3*, 1407–1413.

Cook, F. J., Thorburn, P. J., Fitch, P., & Bristow, K. L., (2003). Wet Up: A software tool to display approximate wetting pattern from drippers. *Irrigation Science*, *22*, 129–134.

Cote, C. M., Bristow, K. L., Charlesworth, P. B., Cook, F. J., & Thorburn, P. J., (2003). Analysis of soil wetting and solute transport in subsurface trickle irrigation. *Irrigation Science, 22*, 143–156.

Dukes, M. D., & Scholberg, J. M., (2005). Soil moisture controlled subsurface drip irrigation on sandy soils. *Applied Engineering Agriculture, 21*(1), 89–101.

Feddes, R. A., Kowalik, P. J., & Zaradny, H., (1978). *Simulation of Field Water Use and Crop Yield* (pp. 189). John Wiley and Sons, New York.

Lazarovitch, N., Warrick, A. W., Furman, A., & Simunek, J., (2007). Subsurface water distribution from drip irrigation described by moment analyses. *Vadose Zone J., 6*(1), 116–123.

Mailhol, J. C., Ruelle, P., & Nemeth, I., (2001). Impact of fertilization practices on nitrogen leaching under irrigation. *Irrig. Sci., 20,* 139–147.

Namara, R. E., Nagar, R. K., & Upadhyay, B., (2007). Economics, adoption determinants, and impact of micro-irrigation technologies: Empirical results from India. *Irrigation Science, 25*, 283–297.

Provenzano, G., (2007). Using HYDRUS–2D simulation model to evaluate wetted soil volume in subsurface drip irrigation systems. *J. Irrig. Drain. Engg., 133*(4), 342–349.

Rahil, M. H., & Antonopoulos, V. Z., (2007). Simulating soil water flow and nitrogen dynamics in a sunflower field irrigated with reclaimed wastewater. *Agricultural Water Management, 92*, 142–150.

Rassam, L., & Littleboy, M., (2003). Identifying vertical and lateral components of drainage flux in hill slopes. In: *Proceeding of MODSIM 2003*. Townsville, Queensland, Modeling and Simulation Society of Australia and New Zealand.

Romero, P., Botia, P., & Garcia, F., (2004). Effects regulated deficit irrigation under subsurface drip irrigation conditions on water relations of mature almond trees. *Plant Soil, 260*, 155–168.

Segal, E., Ben-Gal, A., & Shani, U., (2000). Water availability and yield response to high-frequency micro-irrigation in sunflowers. *Proceedings of the 6th Int. Micro-Irrigation Congress, Int. Council Irrigation Drainage*. Cape Town, South Africa.

Sikdar, S. K., (2007). Water; water everywhere, not a drop to drink? *Clean Technology Environmental Policy, 9*, 1–2.

Simunek, J., Sejna, M., & Van Genuchten, M. T. H., (1999). The HYDRUS–2D software package for simulating the two-dimensional movement of water, heat and multiple solutes in variably saturated media, version 2.0. *Rep. IGCWMC-TPS-53, Int. Ground Water Model. Cent., Colo. Sch. of Mines, Golden, CO*, 251.

Simunek, J., Van Genuchten, M. T. H., & Sejna, M., (2008). Development and applications of the HYDRUS and STANMOD software packages, and related codes. *Vadose Zone J., 7*(2), 587–600.

Skaggs, T. H., Trout, T. J., Simunek, J., & Shouse, P. J., (2004). Comparison of HYDRUS–2D simulations of drip irrigation with experimental observations. *Journal of Irrigation Drainage Engineering, 130*(4), 304–310.

Smith, R., Smettem, K. R. J., Broadbridge, P., & Woolhiser, D.A. (2002). *Infiltration Theory for Hydrologic Applications. American Geophysical Union Water Resources Monograph* Series, Vol. 15, 210 p.

Smith, R., Smettem, K. R. J., & Broadbridge, P., (2002). *Theory for Hydrological Applications*. American Geographical Union, USA.

Souza, C. F., & Matsura, E. E., (2003). Multi-wire time domain reflectometry (TDR) probe with electrical impedance discontinuities for measuring water content distribution. *Agricultural Water Management*, *59*, 205–216.

Tripathi, V. K., Rajput, T. B. S., & Patel, N., (2014). Performance of different filter combinations with surface and subsurface drip irrigation systems for utilizing municipal wastewater. *Irrigation Science*, *32*(5), 379–391.

Tripathi, V. K., Rajput, T. B. S., & Patel, N., (2016b). Biometric properties and selected chemical concentration of cauliflower influenced by wastewater applied through surface and subsurface drip irrigation system. *Journal of Cleaner Production, 139*, 396–406.

Tripathi, V. K., Rajput, T. B. S., Patel, N., & Kumar, P., (2016a). Effects on growth and yield of eggplant (*Solanumm elongema L.*) under placement of drip laterals and using municipal wastewater. *Irrigation and Drainage*, *65*, 480–490.

WHO, (2006). *Guidelines for the Safe Use of Wastewater, Excreta, and Greywater* (Vol. II & IV), WHO Press, Geneva, Switzerland.

CHAPTER 8

MOLLUSCS AS A TOOL FOR RIVER HEALTH ASSESSMENT: A CASE STUDY OF RIVER GANGA AT VARANASI

IPSITA NANDI and KAVITA SHAH

Institute of Environment and Sustainable Development, Banaras Hindu University, Varanasi, 221005, India, Email: ipsitabhu@gmail.com

ABSTRACT

Rivers are the main source of fresh water. Recent scenarios of anthropogenic activities are degrading the health of the river. Any river conservation or restoration programs require a proper insight into the extent of degradation towards the health of the river. Monitoring only the physicochemical properties does not give a proper picture of the health of the river. It requires a holistic approach wherein the health is assessed on certain well-defined parameters. This further requires some simple and robust tools for easy monitoring of river health. Bio-indicator serves as one such tool since their diversity changes with changing characteristics of river water quality. River Ganga at Varanasi is also home to a large variety of aquatic fauna. This paper utilizes this species richness for designing a tool taking mollusks as bio-indicator for health assessment of River Ganga at Varanasi. It also tries to define the reliability and accuracy for using mollusks as a robust and easy tool for river health assessment.

8.1 INTRODUCTION

Rivers in the current scenario are under permanent pressure of various forms of pollution causing anthropogenic activities. River ecosystems act as a sink

for various kinds of toxicants emerging from different sources of pollution (Salánki et al., 2003). These toxic pollutants are severely degrading the health of the rivers (Cairns et al., 1993). Riverine biodiversity act as an indicator of the health of the river system (Boulton, 1999). Altered flow regimes and pollution are adversely affecting the biotic makeup of the river (Bunn and Arthington, 2002; Strayer and Dudgeon, 2010). Evaluating biotic components using bioindicator can reveal the real scenario of river health (Nandi et al., 2016). A bioindicator is an organism (or a part or community of an organism) that provides information about the quality of environment making changes in the morphological, histological or cellular structures, their metabolic processes, their population structure or in their behavioral pattern (Markert et al., 2003). Bioindicator response to the aquatic pollutants in two ways, i.e., either by accumulating the pollutants or by showing visible specific changes in the characteristics or population structure (Markert et al., 2003). Bioindicator are selected for pollution monitoring based on certain specific characteristics (Füreder and Reynolds, 2003) which includes: (1) clear taxonomy; (2) wide distribution; (3) occurrence in large numbers with appropriate visible body size; (4) restricted mobility; (5) site specificity; (6) narrow specific ecological demands and tolerance; (7) clear feeding structure; (8) long lifespan and generation time; (9) sensitivity to specific pollutants; (10) low genetic and ecological variability; (11) response to specific pollutant/substance should be representative to other taxas or even ecosystem; and (12) easy to sample, store, recognition, and robust during handling.

Degrading water quality in this era demands shift in the management strategies for pollution abatement towards a proper understanding of the extent of pollution. Simply measuring the physicochemical characteristics of water does not reveal the real scenario of river health (Nandi et al., 2016). Furthermore, these techniques are tedious and time-consuming as well as need expertise. The recent time now demands a shift in river health assessment program from traditional water quality monitoring towards assessment health using bioindicators. Mollusk belongs to the highly diverse group of macroinvertebrate (Patil, 2013). With a species diversity of 2,00,000, the mollusk stands second in species richness after arthropods (Patil, 2013; Strong et al., 2008). They also have diverse forms of ecological habitats with a long and sedentary form of living (Grabarkiewicz and Davis, 2008; Patil, 2013). Slight changes in the physicochemical characteristics of the river water adversely affect species characteristics, richness, and species diversity of the mollusk (Pérez-Quintero, 2011; 2012). These features make mollusk a potent indicator for assessing water quality thereby health status of rivers.

In a preview of the above, the study is focused upon identifying certain species of mollusk from aquatic biodiversity which can be used as a tool for river health assessment studies.

8.2 MATERIALS AND METHOD

8.2.1 STUDY AREA

Varanasi located at 25.28° N latitude and 82.96° E longitude is the oldest living city in the world (Singh, 2011). Being situated at the bank of holy River Ganga, it is also considered as the spiritual capital of India (Singh, 2011). The city is situated in the eastern part of Uttar Pradesh along the left crescent-shaped bank of River Ganga (Mohanty, 1993). River Ganga of Varanasi serves as a home to a wide variety of aquatic biodiversity (Sarkar et al., 2012). The right bank usually consists of large stretches of sand bed (Nandi et al., 2017). These stretches of sand bed form the home to various types of macroinvertebrates (Sinha et al., 2007). Massive changes have been observed in the water quality of Varanasi which continues to degrade each day. Literature reveals the deterioration of water of Varanasi and thus is unfit for human consumption (Mishra et al., 2009; Namrata, 2010). These changes are also affecting the general characteristics of benthic macroinvertebrates (Sinha et al., 2007). This forms the aquatic biodiversity which can serve the role of bioindicator for easy monitoring of the health of River Ganga at Varanasi. The right bank from beyond Asi River to Teliyanala ghat (Figure 8.1) was selected as a study site for studying the mollusk species specific to this stretch which can be used as a bioindicator for river health.

8.2.2 COLLECTION OF SAMPLE

The mollusk was collected along the respective Ghats using handpick method (Fuller, 1978). Proper photographs were taken, and the collected mollusk was kept in a glass bottle in 10% formalin. Photographs of the natural site containing the mollusk are shown in Figure 8.2. Water samples were collected in polyethylene bottles and borosil bottles and taken to a lab for further analysis using the APHA method.

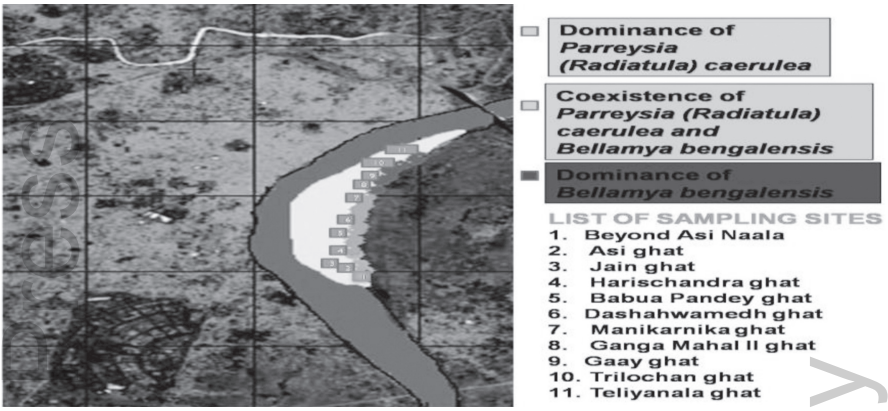

FIGURE 8.1 Study site.

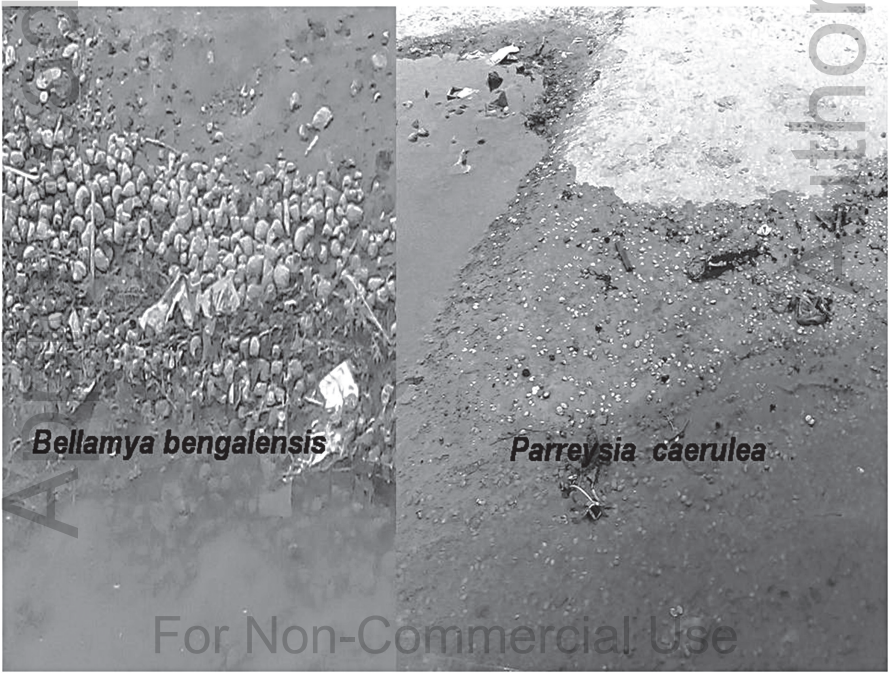

FIGURE 8.2 Molluscs species at their natural habitat

8.2.3 METHODOLOGY

The collected mollusk species were identified from Zoological Survey of India, Pune. The nomenclatures of these species are detailed in Table 8.1. Numbers of Mollusk obtained are listed in Table 8.2. The water samples were analyzed for various physicochemical parameters and heavy metals and the value of analysis thus obtained are listed in Table 8.3. A correlation matrix was also computed between water quality parameters and a number of individuals of mollusk obtained at each site using IBM SPSS statistical 20 software Table 8.4.

TABLE 8.1 Nomenclature of the Species Observed Along the Right Bank of River Ganga at Varanasi

Species Name	**1. *Parreysia (Radiatula) caerulea***	**Species 2. *Bellamya bengalensis***
Picture		
Phylum	Mollusca	Mollusca
Class	Bivalvia	Gastropods
Order	Trigoinoida	Mesogastropoda
Family	Unionidae	Viviparidae
Genus	*Parreysia (Radiatula)*	*Bellamya*
Species	*caerulea*	*bengalensis*

TABLE 8.2 Number of Mollusk Obtained in Each Representative Ghat

Sites	**Gastropods (Bellamya)**	**Bivalvia (Parreysia)**
R1	0	10
R2	0	10
R3	2	12
R4	2	10
R5	3	12
R6	11	2
R7	8	9
R8	10	6
R9	7	8
R10	11	0
R11	11	0

TABLE 8.3 Water Quality Analysis at the Representative Sites at the Right Bank of River Ganga

Sites	Calcium (mgl^{-1})	COD (mgl^{-1})	Nitrate (mgl^{-1})	Dissolved Oxygen (mgl^{-1})	Chloride (mgl^{-1})	As (mgl^{-1})	Fe (mgl^{-1})	Ni (mgl^{-1})
R1	30.602	30	3.057	9	34.253	0.2975	1.494	0.0291
R2	29.98	35	3.419	8	35.228	0.1102	1.143	0.0034
R3	30.247	37	3.753	8	35.264	0.0638	1.38	0.0018
R4	30.12	25	2.314	7.4	35.804	0.0469	0.561	0.0017
R5	30.31	37	3.311	7.4	35.708	0.0368	0.843	0.0077
R6	31.123	101	1.949	6.4	36.687	0.0341	0.905	0.0012
R7	27.314	85	1.867	6.8	37.425	0.0334	1.901	0.0014
R8	26.709	105	1.82	6.4	37.655	0.0295	0.575	0.0009
R9	26.79	117	1.365	6	37.783	0.0262	2.085	0.0018
R10	27.674	110	1.361	6	37.977	0.0331	0.488	0.0007
R11	23.769	135	1.307	6	38.992	0.0345	0.734	0.0008

8.3 RESULTS AND DISCUSSION

A change in dominance trend was observed along the entire stretch of the river bank. The dominance of *Parreysia (Radiatula) caerulea* (bivalvia) was observed in the stretch of R1 (beyond Asi River)-R5 (Babua Pandey ghat) after which there appeared a change in trend with rising in *Bellamya bengalensis* (gastropod) population. Codominance of the two species was observed in the stretch of R6 (Dashashwamedh ghat)-R9 (Gaay ghat). R10 (Trilochan ghat)-R11 (Teliyanala ghat) observed the dominance of *Bellamya bengalensis*. This change in dominance trend of the two species can be attributed to the topology of the river bank. The sites which are located on the extreme sides of the meander observe the dominance of a particular species while at the meander bend there is codominance of both the species (Figure 8.1). The correlation matrix reveals that both the species showed a significant correlation with dissolved oxygen, calcium, nitrate, and COD. *Parreysia* (bivalvia) showed positive correlation with DO, nitrate while negative correlation with COD and chloride. On the other hand, *Bellamya* (gastropod) showed negative correlation with dissolved oxygen, nitrate, and calcium but positive correlation with COD and chloride. Apart from these Bellamya showed negative correlation with arsenic (Table 8.4). The observation from correlation matrix highlights that *Parreysia* species are more adapted to cleaner environment

TABLE 8.4 Correlation Matrix of Mollusk Species and Water Quality

		Calcium	COD (mgl^{-1})	Nitrate	Dissolved Oxygen	Chloride	As	Fe	Ni	Bellamya
Calcium	Pearson Correlation	1	–0.786**	0.725*	0.683*	–0.871**	0.396	0.006	0.380	–0.630*
	Sig0. (2–tailed)		0.004	0.012	0.021	0.000	0.228	0.987	0.248	0.038
	N	11	11	11	11	11	11	11	11	11
COD (mg/l)	Pearson Correlation	–0.786**	1	–0.882**	–0.901**	0.935**	–0.512	–0.036	–0.470	0.928**
	Sig0. (2–tailed)	0.004		0.000	0.000	0.000	0.108	0.917	0.145	0.000
	N	11	11	11	11	11	11	11	11	11
Nitrate	Pearson Correlation	0.725*	–0.882**	1	0.872**	–0.891**	0.460	0.095	0.403	–0.850**
	Sig0. (2–tailed)	0.012	0.000		0.000	0.000	0.154	0.780	0.219	0.001
	N	11	11	11	11	11	11	11	11	11
Dissolved Oxygen	Pearson Correlation	0.683*	–0.901**	0.872**	1	–0.946**	0.795**	0.192	0.720*	–0.906**
	Sig0. (2–tailed)	0.021	0.000	0.000		0.000	0.003	0.573	0.012	0.000
	N	11	11	11	11	11	11	11	11	11
Chloride	Pearson Correlation	–0.871**	0.935**	–0.891**	–0.946**	1	–0.681*	–0.144	–0.630*	0.895**
	Sig0. (2–tailed)	0.000	0.000	0.000	0.000		0.021	0.672	0.038	0.000
	N	11	11	11	11	11	11	11	11	11
As	Pearson Correlation	0.396	–0.512	0.460	0.795**	–0.681*	1	0.232	0.942**	–0.606*
	Sig0. (2–tailed)	0.228	0.108	0.154	0.003	0.021		0.492	0.000	0.048
	N	11	11	11	11	11	11	11	11	11
Fe	Pearson Correlation	0.006	–0.036	0.095	0.192	–0.144	0.232	1	0.231	–0.246
	Sig0. (2–tailed)	0.987	0.917	0.780	0.573	0.672	0.492		0.494	0.465
	N	11	11	11	11	11	11	11	11	11

TABLE 8.4 *(Continued)*

		Calcium	COD (mgl^{-1})	Nitrate	Dissolved Oxygen	Chloride	As	Fe	Ni	Bellamya
Ni	Pearson Correlation	0.380	–0.470	0.403	0.720*	–0.630*	0.942**	0.231	1	–0.538
	Sig0. (2–tailed)	0.248	0.145	0.219	0.012	0.038	0.000	0.494		0.088
	N	11	11	11	11	11	11	11	11	11
Bellamya	Pearson Correlation	–0.630*	0.928**	–0.850**	–0.906**	0.895**	–0.606*	–0.246	–0.538	1
	Sig0. (2–tailed)	0.038	0.000	0.001	0.000	0.000	0.048	0.465	0.088	
	N	11	11	11	11	11	11	11	11	11
Parreysia	Pearson Correlation	0.543	–0.821**	0.775**	0.733*	–0.750**	0.318	0.431	0.338	–0.853**
	Sig0. (2–tailed)	0.084	0.002	0.005	0.010	0.008	0.341	0.186	0.310	0.001
	N	11	11	11	11	11	11	11	11	11

*Correlation is significant at the 0.05 level (2-tailed).

**Correlation is significant at the 0.01 level (2-tailed).

with higher DO content and less COD (Subba Rao, 1989; Patil, 2011). High chloride content indicate water polluted with human urine and feces (Piocos and de La Cruz, 2000). A positive correlation of *Bellamya* with chloride shows that they are more adapted in water contaminated with human urine and feces. Nitrate is known to cause oxidative stress in species of *Bellamya* hence there exist a negative correlation between *Bellamya* and nitrate concentration (Chinchore and Mahajan, 2013). Calcium plays a significant role in the growth and shell formation of *Bellamya* species (Baby et al., 2010) and hence it could be the reason for a strong negative correlation between population of *Bellamya* species and calcium content. Studies have reported sensitivity of *Bellamya bengalensis* towards arsenic (Ray, 2016; Ray et al., 2013); hence, this could probably be the reason for a negative correlation between arsenic concentration and population density of *Bellamya bengalensis*. These results highlights the role of *Bellamya* and *Parreysia* as bioindicator for water quality and pollution wherein *Parreysia* preferred more or less polluted habitat while *Bellamya* sustained better in polluted habitat. These species can be used as tool for assessing health of River Ganga at Varanasi.

8.4 CONCLUSIONS

Traditional monitoring of physicochemical properties of river water does not provide a real idea about the status of the health of the river. The time now demands a change towards a holistic approach involving biomonitoring of riverine diversity. The macroinvertebrate population provides the real scenario of the river health. Mollusc has highly rich diversity, and hence they provide the scope for application as bioindicator. The study focused on identifying mollusk diversity along the river stretch. Two mollusk varieties, i.e., *Parreysia (Radiatula) caerulea* (bivalvia) and *Bellamya bengalensis* (gastropod) were observed along the stretch with a change in dominance along the stretch. River water quality assessment conducted in parallel and the correlation matrix thus obtained reveals that *Parreysia* shows a positive correlation with DO while the negative correlation with COD and chloride whereas *Bellamya bengalensis* shows a negative correlation with DO and positive correlation with COD suggesting *Parreysia* as a better indicator of good water quality. Furthermore, *Bellamya* shows a positive correlation with chloride which substantiates the fact that it can be used as an indicator of human feces polluted water. *Bellamya* also showed significant correlation with heavy metals which further highlight its role as a bioindicator. These aspects of the study highlight the role of *Bellamya* and *Parreysia* as an indicator of water quality. These mollusk

species can be used as bioindicator as simple tools for assessing river health. Further studies can be conducted in these lines to further strengthen the role of mollusk species as bioindicators for river health assessment.

KEYWORDS

- **bioindicator**
- **mollusk**
- **River Ganga**
- **river health assessment**
- **Varanasi**

REFERENCES

Baby, R., Hasan, I., Kabir, K., & Naser, M., (2010). Nutrient analysis of some commercially important mollusks of Bangladesh. *Journal of Scientific Research*, *2*(2), 390–396.

Boulton, A. J., (1999). An overview of river health assessment: Philosophies, practice, problems, and prognosis. *Freshwater Biology*, *41*(2), 469–479.

Bunn, S. E., & Arthington, A. H., (2002). Basic principles and ecological consequences of altered flow regimes for aquatic biodiversity. *Environmental Management*, *30*(4), 492–507.

Cairns, J., McCormick, P. V., & Niederlehner, B., (1993). A proposed framework for developing indicators of ecosystem health. *Hydrobiologia*, *263*(1), 1–44.

Chinchore, S., & Mahajan, P., (2013). Protective role of Coriandrum sativum (coriander) extracts on lead-induced alterations in the oxygen consumption of freshwater gastropod snail, Bellamya Bengalensis (Lamarck). *International Journal of Pharmaceutical Sciences and Research*, *4*(7), 2789.

Fuller, S. L. (1978). *Fresh-Water Mussels (Mollusca: Bivalvia: Unionidae) of the Upper Mississippi River: Observations at Selected Sites within the 9-Foot Channel Navigation Project on Behalf of the US Army* (No. 78-33). Academy of Natural Sciences of Philadelphia PA Div of Limnology and Ecology.

Füreder, L., & Reynolds, J., (2003). Is Austropotamobius pallipes a good bioindicator? *Bulletin Français de la Pêche et de la Pisciculture*, *370/371*, 157–163.

Grabarkiewicz, J., & Davis, W. (2008). *An Introduction to Freshwater Mussels as Biological Indicators (Including Accounts of Interior Basin,* Cumberlandian and Atlantic Slope Species) EPA-260-R-08-015. US Environmental Protection Agency, Office of Environment.

Markert, B. A., Breure, A. M., & Zechmeister, H. G., (2003). Definitions, strategies, and principles for bioindication/biomonitoring of the environment. *Trace Metals and Other Contaminants in the Environment, 6*, 3–39.

Mishra, A., Mukherjee, A., & Tripathi, B., (2009). Seasonal and temporal variations in physicochemical and bacteriological characteristics of River Ganga in Varanasi. *Int. J. Environ. Res*, *3*(3), 395–402.

Mohanty, B., (1993). *Urbanization in Developing Countries: Basic Services and Community Participation.* Concept Publishing Company.

Namrata, S., (2010). Physicochemical properties of polluted water of river Ganga at Varanasi. *International Journal of Energy and Environment*, *1*(5), 823–832.

Nandi, I., Srivastava, P. K., & Shah, K., (2017). Floodplain mapping through support vector machine and optical/infrared images from land sat 8 OLI/TIRS sensors: Case study from Varanasi. *Water Resources Management*, *31*(4), 1157–1171.

Nandi, I., Tewari, A., & Shah, K., (2016). Evolving human dimensions and the need for continuous health assessment of Indian rivers. *Curr. Sci., 111*, 263–271.

Patil, J. V., (2011). *Study of Selected Faunal Biodiversity of Toranmal Area.* Toranmal Reserve Forest.

Patil, S. R., (2013). A preliminary study of molluscan fauna of singhori wildlife sanctuary, raisen, Madhya Pradesh, India. *Indian Forester*, *139*(10), 932–935.

Pérez-Quintero, J. C., (2011). Freshwater mollusk biodiversity and conservation in two stressed Mediterranean basins. *Limnologica-Ecology and Management of Inland Waters*, *41*(3), 201–212.

Pérez-Quintero, J. C., (2012). Environmental determinants of freshwater mollusk biodiversity and identification of priority areas for conservation in Mediterranean watercourses. *Biodiversity and Conservation*, *21*(12), 3001–3016.

Piocos, E.A., & De la Cruz, A. A., (2000) *Solid Phase Extraction and High Performance Liquid Chromatography With Photodiode Array Detection of chemical indicators of Human Faecal contamination in water*, 23:8,1281-1291, DOI: 10.1081/JLC-100100414

Ray, M., Bhunia, A. S., Bhunia, N. S., & Ray, S., (2013). Density shift, morphological damage, lysosomal fragility and apoptosis of hemocytes of Indian mollusks exposed to pyrethroid pesticides. *Fish & Shellfish Immunology*, *35*(2), 499–512.

Ray, S., (2016). Levels of toxicity screening of environmental chemicals using aquatic invertebrates-a review. *Invertebrates-Experimental Models in Toxicity Screening: InTech*. DOI: 10.5772/61746

Salánki, J., Farkas, A., Kamardina, T., & Rózsa, K. S., (2003). Mollusks in biological monitoring of water quality. *Toxicology Letters*, *140*, 403–410.

Sarkar, U., Pathak, A., Sinha, R., Sivakumar, K., Pandian, A., Pandey, A., et al., (2012). Freshwater fish biodiversity in the River Ganga (India): Changing pattern, threats and conservation perspectives. *Reviews in Fish Biology and Fisheries*, *22*(1), 251–272.

Singh, R. P., (2011). Varanasi, India's cultural heritage city: contestation, conservation & planning. *Heritages Capes and Cultural Landscapes*, 205–254.

Sinha, R., Sinha, S. K., Kedia, D., Kumari, A., Rani, N., & Sharma, G., (2007). A holistic study on mercury pollution in the Ganga River system at Varanasi, India. *Current Science*, *92*(9), 1223–1228.

Strayer, D. L., & Dudgeon, D., (2010). Freshwater biodiversity conservation: Recent progress and future challenges. *Journal of the North American Benthological Society*, *29*(1), 344–358.

Strong, E. E., Gargominy, O., Ponder, W. F., & Bouchet, P., (2008). Global diversity of gastropods (Gastropoda, Mollusca) in freshwater. *Hydrobiologia*, *595*(1), 149–166.

Subba, R. N., (1989). *Handbook, Freshwater Mollusks of India.* Zoological Survey of India. Ed. Director, Zoological Survey of India. Calcutta, India.

CHAPTER 9

SPATIAL VARIABILITY IN THE WATER QUALITY OF CHILIKA LAGOON, EAST COAST OF INDIA

SADAF NAZNEEN and N. JANARDHANA RAJU

School of Environmental Sciences, Jawaharlal Nehru University, New Delhi–110067, India,
E-mail: sadafnazneen01@gmail.com

ABSTRACT

Wetlands provide a range of ecological services which depends on the optimum health of the ecosystem. Chilika lagoon lying on the east coast of India is the largest lagoon in Asia and a biodiversity hotspot sustaining rich fishery resources. Freshwater inflows from the drainage basin along with saline water flow from the ocean results in a wide range of fresh, brackish, and saline water environments within the lagoon which gives rise to a very productive ecosystem. Various processes affecting the water quality of the lagoon system include agricultural drainage from the catchment area, municipal, and domestic waste and sewage intrusion and freshwater discharged into the lagoon from various rivers and rivulets. In the present study, an attempt has been made to understand the spatial variation in the water quality of Chilika lagoon. A total of 26 water samples were collected from different hydro-ecological regions of the lagoon during the 1st week of June 2013. The four regions remained significantly different from one another with respect to many parameters. Physicochemical properties like pH, salinity, EC (Electrical Conductivity), DO (Dissolved Oxygen), DIC (Dissolved Inorganic Carbon), DOC (Dissolved Organic Carbon), and nutrients like PO_4^{3-}, NO_3^-, $Si(OH)_4$ varied significantly between the sectors. A strong positive correlation between salinity, EC, Na^+, K^+, Ca^{2+}, and Mg^{2+} is a result of seawater dominance into the lagoon. Results of

the Principal Component Analysis (PCA) suggest that all the sampling stations can be classified into three groups based on the spatial variations of salinity, EC, nutrients, and other physiochemical parameters. Lagoon's connections with the Bay of Bengal, residual fertilizers washed away from the agricultural fields, domestic sewage, biological activity and allochthonous materials brought by the river discharge play a significant role in governing the water quality of the lagoon. The non-conservative nature of the nutrients in the lagoon suggests that the lagoon is well mixed which gives rise to rich biodiversity.

9.1 INTRODUCTION

Lagoons comprise 13% of the earth's coastlines and are considered to be the most productive ecosystems in the biosphere with a very complex environment (Beltrame et al., 2009). Lagoon hydrodynamics is governed by the circulation and mixing caused by freshwater inputs via river discharge and inflow of saline waters through tidal flows (Statham, 2011). Coastal lagoons exhibit high variability in their physical, chemical, and biological characters, thus they tend to be typically unstable environments and the short and long-term variations that occur in these ecosystems are large in comparison to other saline environments. Lagoons usually exhibit estuarine characteristics and are regions of high primary productivity (Panigrahy et al., 2009). Salinity is an important factor, which is having direct and indirect control over the nutrient availability and their transformations in the saline aquatic environments. Tropical coastal lagoons are under huge anthropogenic pressures but have been studied to a lesser extent when compared to temperate estuaries (Burford et al., 2008). The rapid increase of human activities has increased nutrient transport from land to sea in the past decades, resulting in environmental deterioration and changes to biogeochemical processes. The nutrient-laden effluent discharged from shrimp farming is also a cause of eutrophication of coastal water, and its impacts have been a significant concern (Balasubramanian et al., 2004).

In Chilika, lagoon changes in land use, pattern, and agricultural practices in the catchment basin, as well as adjoining areas, has led to the addition of an enormous amount of nitrogen and phosphorous as residual fertilizers. Another important factor for the addition of nutrients is direct disposal of untreated wastewater from Bhubaneshwar City and the villages in and around Chilika. The discharge of fresh water into the lagoon is quite high during monsoon and post-monsoon while it is negligible or absent during

other periods (Mohanty and Panda, 2009). This heavy discharge brings enormous amounts of nutrients into the lagoon. Water balance calculations indicate that an average 72% of the total freshwater inflow to the lake is due to runoff from the rivers, 15% from direct rainfall and 13% through drainage from the western catchment.

9.2 MATERIALS AND METHODS

9.2.1 STUDY AREA

Chilika lake is the largest tropical lagoon of Asia spread between latitude 19°28'–19°54'N and longitude 85°05'–85°38'E. It is a semi-enclosed, coastal lagoon on the east coast of India in the state of Odisha. The pear-shaped lagoon is about 65 kms long and varies in width from 18 km in the north to 5 km in the south (Figure 9.1). The lagoon is situated on the southern part of the Mahanadi delta-complex. The lagoon is cut off from the Bay of Bengal by a continuous sandy barrier-spit measuring 60 km in length and150 m in breadth, where backshore dunes are developed in the southern half of the spit in two or three parallel groups (Khandelwal et al., 2008). According to earlier estimates, the average water spread area of the lake is 906 km^2 in pre-monsoon and 1165 km^2 in the monsoon (Ghosh and Pattnaik, 2006). Present studies have estimated the lagoon area to be nearly 704 km^2 during summer which spreads to 1020 km^2 in monsoon (Gupta et al., 2008). The water depth in the lake varies from 0.9 to 2.6 m in the dry season and from 1.8 to 3.7 m in the rainy season. Chilika was designated a wetland of international importance under Ramsar convention in 1981. The lagoon is connected to the Bay of Bengal in the east. The barrier spit separates the lagoon from the Bay of Bengal and provides an inlet at its northeast extremity which remains open due to continuous flushing action brought by waves and currents. Changes in the position, shape, and breadth of the inlet have occurred from time to time depending on the interplay of available energy from land and sea and also due to the silt brought by the tributaries of Mahanadi Daya and Bhargavi rivers. At present, the lagoon is connected with the Bay of Bengal near Satapada (Sipakuda) by means of an artificial opening made in September 2000. The lagoon has several hydrological influences; the most important is its connection to the Bay of Bengal in the east and freshwater flow in the north due to the joining of tributaries of Mahanadi River. Many rivers and rivulets join the lagoon through its western catchment. Almost 52 small rivers and streams join the lagoon. The

main tributaries of Mahanadi (such as Bhargavi, Daya, and Makara) account for almost 61% (850 m^3 s^{-1}) of the total freshwater.

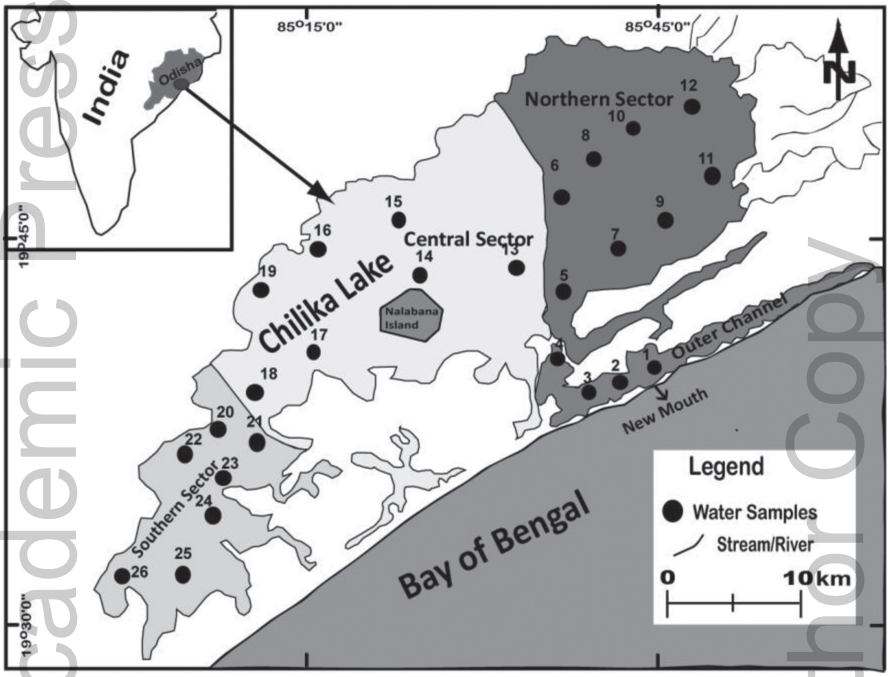

FIGURE 9.1 Study area with sampling points.

9.2.2 METHODOLOGY

A total of 26 surface water samples were collected from four hydro-ecological different sectors of the lagoon during pre and post-monsoon seasons (Figure 9.1). The pre-monsoon sampling was conducted in the 1st week of June 2013, and post-monsoon sampling was conducted in January 2014. The water samples were collected in 500 ml clean propylene bottles. Cleaning of all the plastic bottles was carried out by soaking in 5 % nitric acid (HNO_3 v/v) for 24 hours and then rinsing with doubled distilled water (DDW). After collection, the water samples were poisoned with $HgCl_2$ for nutrients and DIC analysis Another set of samples were collected in 100ml bottles for dissolved metals analysis. The water samples were filtered through 0.45µm nylon filters and acidified below pH < 2 by addition of concentrated HNO_3. The samples were transferred to the laboratory in the boxes and stored at 4°C

until analysis. All the analysis was completed within 15 days of sampling. In every analysis, appropriate blanks were run as controls. pH, salinity, and EC in the water samples were analyzed on the field with portable multiparameter kit after calibrating with respective buffers for pH and EC. The parameters like DO, DIC, DOC, NO_3^-, PO_4^{3-}, H_4SiO_4 were analyzed by standards procedure for surface water.

- The Dissolved oxygen (DO) was measured by Wrinkler's method.
- HCO_3^- by titrimetric method.
- DOC was analyzed by TOC analyzer (Shimadzu TOC–5000 analyzer).
- NO_2^- by indophenol method.
- NO_3^- by cadmium reduction method PO_4^{3-} by the ascorbic acid method.
- H_4SiO_4 (dissolved silica) molybdosilicate method.
- SO_4^{2-} by the turbidimetric method.
- Na^+ and K^+ by Flame photometer (Elico Flame Photometer, CL–378).
- Ca^{2+} titration method and.
- Mg^{2+} by calculation method.
- The heavy metals were analyzed on Atomic Absorption Spectrophotometer (Thermoscientific M series).

9.3 RESULTS AND DISCUSSIONS

The distribution of nutrients and other physio-chemical parameters have been described through spatial diagrams.

9.3.1 pH

The lagoon water is alkaline in nature. The mean pH value in was 8.1 (7.5–8.6). Spatial distribution map shows that the highest pH values were observed in the southern sector of the lagoon (Figure 9.2). High pH values in southern sector are because of greater photosynthetic activity by algae and phytoplankton which remove dissolved CO_2 from the surface water and shift the equilibrium towards alkaline **(**Hennemann and Petrucio, 2011; Jayakumar et al., 2013). The pH value remained low in the northern sector due to large freshwater input into the lagoon. Rest of the sectors had saline water dominance; thus the pH is higher when compared to the northern sector.

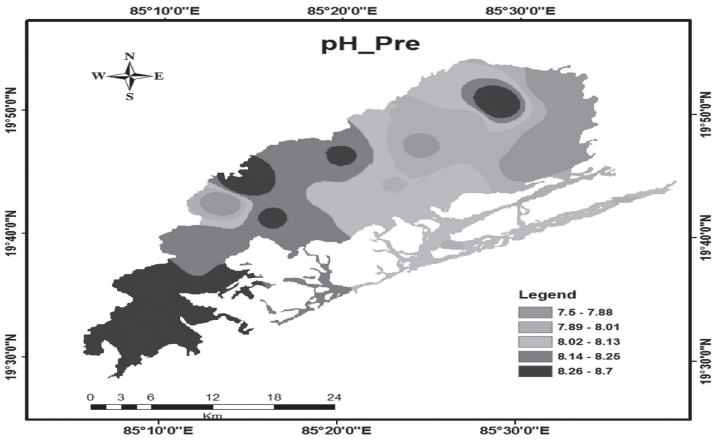

FIGURE 9.2 Spatial distribution of pH in pre-monsoon season.

9.3.2 ELECTRICAL CONDUCTIVITY (EC)

The mean EC value was 34750.4 µS/cm (2720–51,400 µS/cm). The conductivity of water is the ability to conduct electric current by means of the dissolved ions present in its milieu. Electrical conductivity is mainly governed by the ion concentration of the liquid. Since in the month of June saline water is dominant in the lagoon, so is the EC, as seawater contains much more ions when compared to the freshwater. Spatial distribution of EC showed the lowest values in the northern sector (Figure 9.3). This is due to the large freshwater influx in this region brought by the tributaries of Mahanadi River which discharge a significant amount of freshwater in the northern part of the lagoon throughout the year.

9.3.3 SALINITY (SAL)

Salinity is one of the most important factors which determine the concentration of other nutrients in a brackish water system. The mean salinity value was 21.44 PSU (1.3–32.8). The salinity value in the pre-monsoon period was similar to the previous studies in this lagoon (Panigrahy et al., 2007; Panigrahy et al., 2009; Muduli et al., 2013). The higher and comparatively stable salinity values observed in the southern sector could be a result of the input of saline water from Rushikulya estuary through the enclosed Palur canal throughout the year which maintains an even salinity value (Figure

9.4). Another reason for higher and stable salinity values in the southern sector could be less freshwater discharge. Moderate salinity values observed in the central sector is due to good circulation and mixing of both marine and freshwater in this region. This region is well mixed due to the freshwater discharge from small rivulets and streams joining the western catchment of the lagoon and entry of the seawater from the inlets present in the outer channel region.

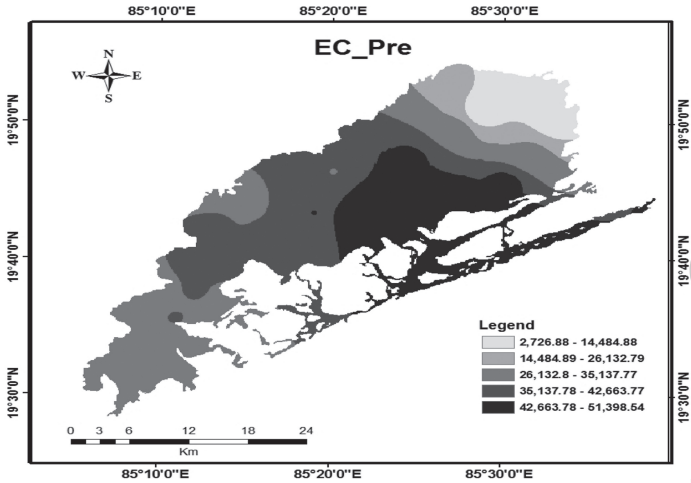

FIGURE 9.3 Spatial distribution of EC in pre-monsoon season.

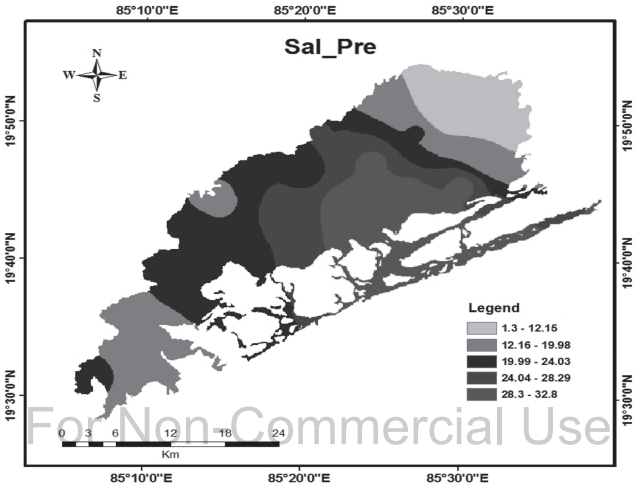

FIGURE 9.4 Spatial distribution of salinity in pre-monsoon season.

9.3.4 DISSOLVED INORGANIC CARBON (DIC)

DIC mean value during the pre-monsoon period was 170.4 mgl^{-1} (132–203.6 mgl^{-1}). In aquatic systems, DIC concentration is governed by chemical, physical, and biological processes. Spatial and temporal variation of DIC could be related to the catchment area characteristics and variability in hydrology (Figure 9.5). The spatial and temporal variability of DIC is mostly due to the weathering of the bedrock in the drainage basin. However, biological activity also has a large influence in controlling the DIC values in Chilika Lake (Gupta et al., 2008). Exchange of CO_2 with atmosphere, pH, salinity, carbonates, respiration, and photosynthesis are some of the factors that govern DIC concentration in a water body. Photosynthetic uptake of CO_2 and precipitation of calcareous material lowers DIC (Muduli et al., 2013). Moderate to high values of DIC has been observed in most parts of southern and some parts of the central sector during the pre-monsoon season as these regions do not have higher plants which make use of dissolved carbon for photosynthesis. Lower values of DIC observed could be a result of primary production and bacterial respiration of carbon which causes variations in DIC concentration (Muduli et al., 2012; Kanuri et al., 2013).

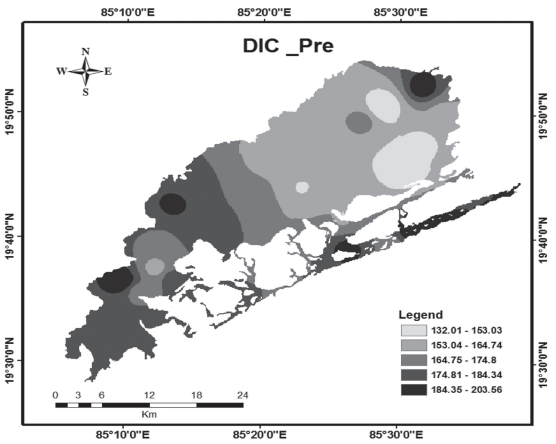

FIGURE 9.5 Spatial distribution of DIC in pre-monsoon season.

9.3.5 DISSOLVED ORGANIC CARBON (DOC)

The mean DOC value was 5.65 mgl^{-1} (3.87–7.89 mgl^{-1}). The chief sources of organic carbon to these environments are allochthonous materials exported

from the land through rivers and autochthonous production of organic matter by algae through photosynthesis and intertidal vegetation (Kanuri et al., 2013). The combination of primary production of plant matter and decomposition rates controls the amount of DOC in water. Spatial distribution of DOC has been presented in Figure 9.6. DOC fluxes from sediments are also an important carbon source in many estuaries, and benthic remobilization is expected to be an internal source of DOC in shallow systems. Rivers draining into Chilika carry higher DOC concentration; thus Chilika has appreciable DOC load (Gupta et al., 2008).

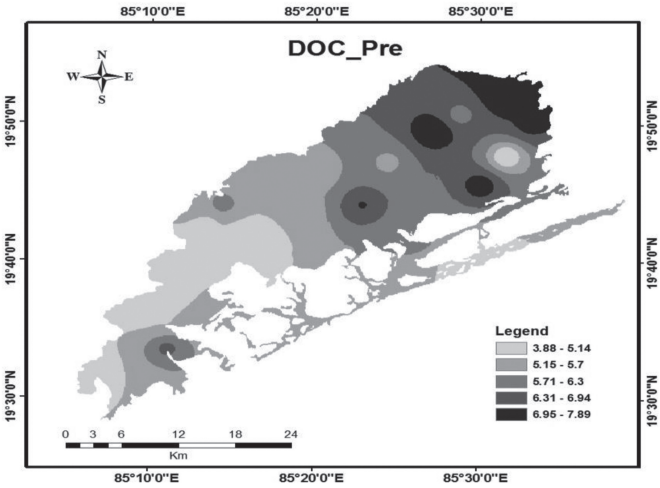

FIGURE 9.6 Spatial distribution of DOC in pre-monsoon season.

9.3.6 DISSOLVED OXYGEN (DO)

The mean DO value was 7.34 mgl^{-1} (2.34–13.43 mgl^{-1}). The spatial distribution of DO shows higher values in the northern sector when compared to the other sectors except near the Balugaon town in the central sector (Figure 9.7). Northern sector is dominated by a large number of freshwater macrophytes which engage in active photosynthesis. Oxygen is released as a by-product of photosynthesis. Therefore, the northern sector remains well oxygenated. Higher DO concentration near the Balugaon region could be a result of high concentrations of nutrients like NO_3^+ and PO_4^{3+} entering the lagoon from Balugaon township which gives rise thick algal mats. Presence of plants leads to photosynthetic activity and release of oxygen (Bose et al., 2012).

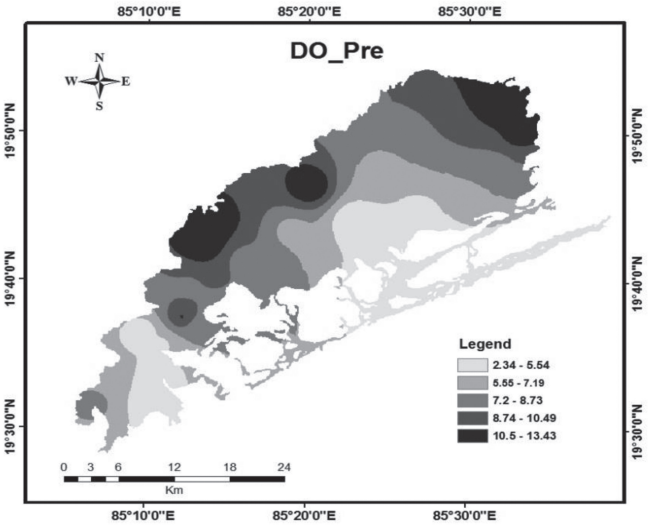

FIGURE 9.7 Spatial distribution of DO in pre-monsoon season.

9.3.7 NITRATE (NO_3^-)

Mean value for NO_3^- was 2.2 mgl^{-1} (0.2–7.5 mgl^{-1}). Nitrate in aquatic environments is mainly derived from terrestrial runoff. Concentration and rate of supply of nitrate are related to land use practices in the drainage basin since NO_3^- moves easily through soils and is rapidly lost from land through natural drainage systems. NO_3– is the most stable form of inorganic nitrogen in well-oxygenated waters. It is added through nitrogenous fertilizers, industrial effluents, human, and animal wastes through the biochemical activity of nitrifying bacteria, such as Nitrosomonas and Nitrobacter (Raju et al., 2009). The spatial distribution of NO^{3-} has been presented in Figure 9.8. These patches may be witnessing NO_3^-inputs due to agricultural runoff, untreated sewage discharge, aquaculture ponds, and other household wastes being directly dumped into the lagoon water. Organic nitrogen present in domestic sewage is bound to carbon-containing compounds as proteins ($R\text{-}NH_2$). Decomposition of organic nitrogen in the sewage soil by a variety of microorganisms slowly transforms the organic nitrogen to ammonia (NH_3) by a process called "mineralization" (Raju et al., 2012). Further, during the nitrification process NH_3 gets converted to NO_2^- first and then NO_3^-. NO_2^- is unstable therefore its gets oxidized to NO_3^-. Nitrate is quite soluble in water and being stable does not get adsorbed to soil particles as

well. The majority of agricultural fertilizers contain nitrogen in the forms of ammonium and nitrate, often as ammonium nitrate (NH_4NO_3), which could be the prime source of nitrogen species in the coastal water (Newton and Mudge, 2005). High NO_3^- concentration in the post-monsoon season may be due to a large amount of nitrate brought about from the agricultural fields by the large freshwater flow into the lagoon. One of the major reasons for high nitrates in certain pockets during post-monsoon may be due to aquaculture ponds and domestic wastes directly released into the water by the fishing villages around the lagoon. Moreover, in winter the rates of nitrification and denitrification become slow which may have lead to NO_3^- accumulation at some places in the lagoon.

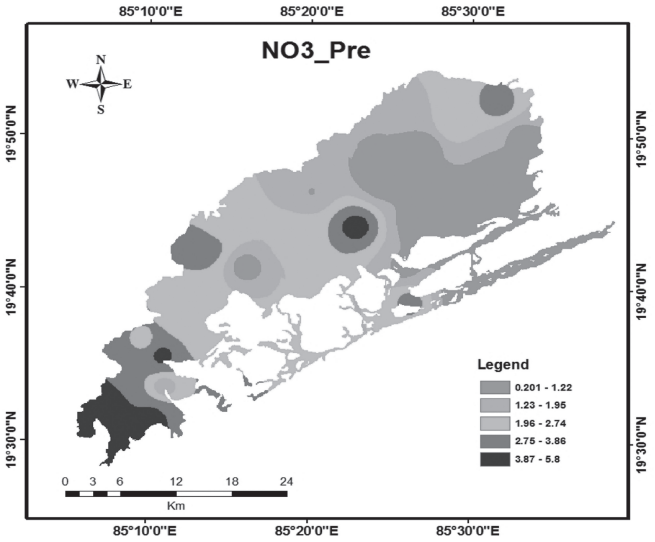

FIGURE 9.8 Spatial distribution of NO_3^- in pre-monsoon season.

9.3.8 PHOSPHATE (PO_4^{3-})

The mean value of PO_4^{3-} was 0.03 mgl^{-1} (0.0–0.09 mgl^{-1}) in the pre-monsoon season 0.04 mgl^{-1}(0.01–0.09 mgl^{-1}) in the post-monsoon. Phosphate is one of the major nutrients responsible for biological production in aquatic ecosystems. PO_4^{3-} is also the limiting nutrient in most of the aquatic ecosystems. As compared to NO_3^- the concentration of PO_4^{3-} is quite low in both the seasons (Figure 9.9). Phosphate is mainly derived from agricultural runoff and domestic sewage, part of it is also derived from weathering of P bearing

minerals as apatite and fluorapatite. Domestic sewage is a major source of ammonium and phosphate. Phosphate is also added through fertilizers which contain di-ammonium phosphate (Chauhan and Ramanathan, 2008). Low phosphate concentration may be due to its rapid assimilation by the micro and macrophytic vegetation in the lagoon or due to its adsorption on the surface of sediments. Other reasons for PO_4^{3-} removal from the water column is its microbial incorporation. The spatial distribution of PO_4^{3-} shows a higher value in some parts of the northern sector and in small patches in the central sector during pre-monsoon (Figure 9.9). Highest PO_4^{3-} concentrations are ranging from 0.07–0.09 mgl^{-1} observed in the inner portion of the lake during pre-monsoon season might have been primarily influenced by external sources as well as contributions from sediment fluxes. This could be a result of PO_4^{3-} addition from the river runoff in the northern and western boundaries of the lagoon. During post-monsoon moderately higher values ranging from 0.04–0.06 mgl^{-1} prevails in most parts of the lagoon. The values observed in both the seasons are comparable to the values observed in previous studies (Panigrahy et al., 2007; Panigrahy et al., 2009).

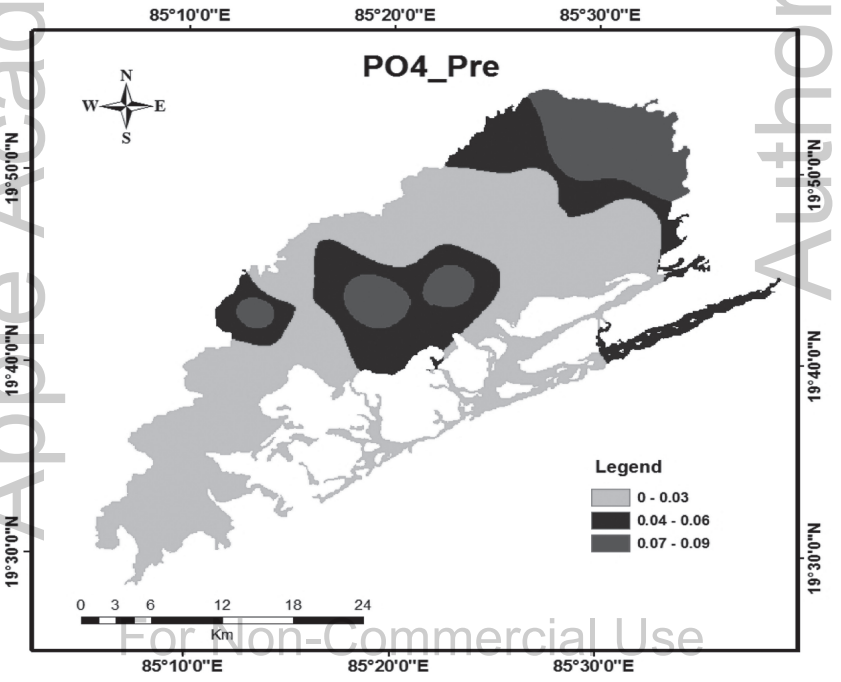

FIGURE 9.9 Spatial distribution of PO_4^{3-} in pre -monsoon season.

9.3.9 DISSOLVED SILICA (H_4SIO_4)

The mean concentration of dissolved silica (DSi) was 3.33 mgl^{-1} (0.3–10.3 mgl^{-1}) in pre monsoon seasons. The spatio-temporal variations of DSi in coastal water is influenced by several factors, including the proportional physical mixing of seawater with fresh water, adsorption of reactive silicate into sedimentary particles, chemical interaction with clay minerals (Gouda and Panigrahy, 1992), co-precipitation with humic compounds and iron and biological removal by phytoplankton, especially by diatoms and silico flagellates (Beucher et al., 2004;Sahoo et al., 2014). The DSi was found to be highest in the northern sector due to maximum river discharge in this region (Figure 9.10).

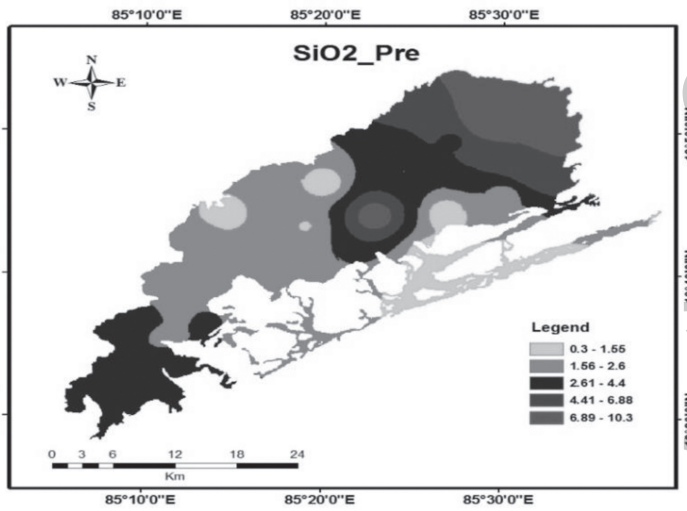

FIGURE 9.10 Spatial distribution of DSi in pre -monsoon season.

9.3.10 CORRELATION ANALYSIS

A bivariate correlation analysis is applied to describe the relationship between the two geochemical parameters. A correlation value above 0.5 between two parameters is considered good whereas a correlation value around 1 (either positive or negative) between two parameters renders them very high relative relationship. The correlation between various parameters has been presented in during the pre-monsoon season has been presented in Table 9.1.

TABLE 9.1 Correlation Analysis for Pre-Monsoon

	pH	**EC**	**Sal**	**DIC**	**DOC**	**DO**	**NO_2-**	**NO_3-**	**$PO_4$3-**	**DSi**	**$SO_4$2-**	**Cl-**	**Na+**	**K+**	**Ca2+**	**Mg2+**
pH	1															
EC	–0.13	1														
Sal	–0.13	**0.99**	1													
DIC	0.03	–0.01	0.01	1												
DOC	–0.28	–0.35	–0.31	–0.25	1											
DO	–0.13	–0.62	–0.61	–0.06	0.13	1										
NO_2	–0.01	–0.37	–0.38	0.18	0.07	0.40	1									
NO_3^-	–0.07	–0.44	–0.43	0.18	0.20	0.43	**0.97**	1								
PO_4^{3-}	–0.26	–0.45	–0.40	0.05	0.39	0.27	0.18	0.29	1							
DSi	–0.19	**–0.69**	–0.68	–0.24	0.53	0.27	0.27	0.36	**0.62**	1						
SO_4^{2-}	–0.17	0.12	0.12	0.12	0.07	0.02	0.21	0.19	–0.05	–0.13	1					
Cl^-	–0.12	**0.98**	**0.99**	0.01	–0.30	**–0.60**	–0.36	–0.41	–0.41	**–0.68**	0.11	1				
Na^+	–0.16	**0.99**	**0.99**	–0.02	–0.29	**–0.59**	–0.39	–0.43	–0.38	**–0.66**	0.12	**0.98**	1			
K^+	–0.05	**0.86**	**0.88**	0.22	–0.41	**–0.51**	–0.34	–0.36	–0.24	**–0.64**	0.05	**0.89**	**0.89**	1		
Ca^{2+}	–0.20	**0.98**	**0.97**	–0.04	–0.32	**–0.58**	–0.44	–0.48	–0.41	**–0.67**	0.13	**0.96**	**0.98**	**0.83**	1	
Mg^{2+}	–0.03	**0.80**	**0.79**	0.06	–0.38	–0.44	–0.23	–0.35	**–0.57**	**–0.64**	0.15	**0.79**	**0.75**	**0.62**	**0.77**	1

In pre-monsoon season a strong positive correlation between Sal, EC, Cl^-, Na^+, K^+, Ca^{2+} and Mg^{2+} indicates that seawater is the major source of these ions. The correlation value of salinity denotes a moderate negative correlation with DO and DSi. DO decreases with salinity because high salinity waters are low in DO. Negative relation indicates that DSi is mainly brought by the freshwater since tropical rivers have high DSi concentration. A strong positive correlation between NO_2^- and NO_3^- is because NO_2^- being unstable is converted to NO_3^-in aquatic systems. A positive correlation between PO_4^{3-} and DSi indicates their terrigenous source. The probable sources of PO_4^{3-} could be fertilizer residue from the agricultural field. Studies have indicated SiO_2 was reaching water bodies from the agricultural field along with other nutrients. DSi has a negative correlation with Cl^-, Na^+, K^+, Ca^{2+}, and Mg^{2+}, which shows its freshwater source, as the other ions are predominantly from the seawater. Different sources of PO_4^{3-} (freshwater) and Mg (seawater) could be a reason for the negative correlation between PO_4^{3-} and Mg. Salinity and EC are positively related to Cl^-, Na^+, K^+, Ca^{2+}, and Mg^{2+}. All these ions are present in major quantity in seawater. This relation is also an indication of seawater dominance in the lake.

9.3.11 PRINCIPAL COMPONENT ANALYSIS

Principal Component Analysis (PCA) is a technique for taking high dimensional data and reducing it to more manageable, lower dimensional form without significant information (Table 9.2). The PCA enables a reduction in data and description of a given multidimensional system by means of a small number of new variables (Loska and Weichula, 2003). Relevant components are those whose eigenvalue is higher than 1. The application of varimax rotation of standardized component loadings enables us to obtain a clear system as a result of the maximization of component loadings variance and elimination of less valid components (Chakrapani and Subramanian, 1993). In the pre-monsoon season, three factors are formed which show 74% of the total variance. PCA 1 is explained by 47.7% of the variance. PC2 and PC3 show 13 % of variance each (Table 9.2).

Factor 1: Factor 1 account for 47.7% of the total variability. Factor 1 shows positive loadings of salinity, EC, Cl^-, Na^+, K^+, Ca^{2+}, and Mg^{2+}. This factor can be explained by the influence of seawater. EC is governed by the concentration of ions in a solution. Na^+, Cl^-, Ca^{2+} and Mg^{2+} are the dominant ions in seawater; hence they show a positive loading with salinity and EC.

TABLE 9.2 Principal Component Analysis for Pre-Monsoon Season

Rotated Component Matrix			
	Components		
	1	**2**	**3**
pH	–0.234	–0.231	–0.715
EC	**0.980**	–0.083	–0.100
Sal	**0.982**	–0.079	–0.076
DIC	0.046	0.468	–0.376
DOC	–0.275	–0.059	**0.734**
DO	–0.586	0.314	0.096
NO_2^-	–0.350	**0.851**	0.010
NO_3^-	–0.399	**0.827**	0.126
PO_4^{3-}	–0.448	0.101	**0.631**
DSi	–0.665	–0.030	**0.569**
SO_4^{2-}	0.235	**0.528**	0.192
Cl^-	**0.978**	–0.064	–0.078
Na^+	**0.982**	–0.088	–0.033
K^+	**0.870**	–0.010	–0.157
Ca^{2+}	**0.973**	–0.125	–0.043
Mg^{2+}	**0.796**	0.019	–0.287

Factor 2: Factor 2 shows a positive loading of NO_2^-, NO_3^- and SO_4^{2-}. A high positive loading between NO_2^- and NO_3^- is an indication of the oxidizing environment which oxidizes unstable nitrite to nitrate. Slightly positive loading of NO_2^-, NO_3^- and SO_4^{2-} could be an indication of their anthropogenic source. Like NO_3^-, SO_4^{2-} can also be added into the system from agricultural fields (Singh et al., 2015).

Factor 3: This factor depicts high positive loadings of DOC, PO_4^{3-} and DSi. A positive relation between these components suggests their allochthonous source. DOC is mainly transported into estuarine systems by rivers which carry carbon in the dissolved form to the coastal waters (Gupta et al., 2008). Similarly PO_4^{3-} and DSi are usually brought by the land and river runoff into the lagoon.

9.4 CONCLUSIONS

Distinct spatial variation of water quality parameters was observed in different parts of the lagoon. The lagoon water was alkaline. The salinity

was largely governed by freshwater discharge and mixing of the Bay of Bengal water with the lagoon. The water was well oxygenated owing to the photosynthetic activities of various micro and macrophytes. The NO^{3-} and PO_4^{3-} in some parts were higher due to runoff from agricultural fields and wastewater discharge. DSi is mainly from land through river discharge. A strong positive correlation between Sal, EC, Cl^-, Na^+, K^+, Ca^{2+} and Mg^{2+} indicates that seawater is the major source of these ions. The correlation value of salinity denotes a moderate negative correlation with DO and DSi. DO decreases with salinity because high salinity waters are low in DO. Negative relation indicates that DSi is mainly brought by the freshwater since tropical rivers have high DSi concentration. The PCA shows that some parameters are governed by seawater whereas others are brought from the land by river discharge. The macro and microphytic vegetation also play a significant role in governing the water quality of the lagoon.

KEYWORDS

- **Chilika lagoon**
- **dissolved nutrients**
- **DOC**
- **salinity**

REFERENCES

Balasubramanian, C. P., Pillai, S. M., & Ravichandran, P., (2004). Zero-water exchange shrimp farming systems (extensive) in the periphery of Chilka lagoon, Orissa, India. *Aquaculture International*, *12*, 555–572.

Beltrame, M. O., De Marco, S. G., & Marcovecchio, J. E., (2009). Dissolved and particulate heavy metals distribution in coastal lagoons. A case study from Mar Chiquita Lagoon, Argentina. *Estuar. Coast. Shelf Sci.*, *85*, 45–56.

Beucher, C., Tréguer, P., Corvaisier, R., Hapette, A. M., & Elskens, M., (2004). Production and dissolution of biosilica, and changing microphytoplankton dominance in the Bay of Brest (France). *Marine Ecology Progress Series*, *267*, 57–69.

Bose, R., De, A., Sen, G., & Mukherjee, A. D., (2012). Comparative study of the physico-chemical parameters of the coastal waters in rivers Matla and Saptamukhi: Impacts of coastal water coastal pollution. *Journal of Water Chemistry and Technology*, *34*(5), 246.

Burford, M. A., Alongi, D. M., McKinnon, A. D., & Trott, L. A., (2008). Primary production and nutrients in a tropical macrotidal estuary, Darwin Harbor, Australia. *Estuarine, Coastal and Shelf Science*, *79*, 440–448.

Chakrapani, G. J., & Subramanian, V., (1993). Heavy metal distribution and fractionation in sediments of the Mahanadi River basin, India. *Environ. Geol*., *22*, 80–87.

Chauhan, R., & Ramanathan, A. L., (2008). Evaluation of water quality of Bhitarkanika mangrove ecosystem, Orissa, east coast of India. *Indian Journal of Marine Sciences*, *37*(2), 153–158.

Gouda, R., & Panigrahy, R. C., (1992). Seasonal distribution and behavior of silicate in the Rushikulya estuary, East coast of India. *Indian Journal of Marine Sciences*, *24*, 111–115.

Gupta, G. V. M., Sarma, V. V. S. S., Robin, R. S., Raman, A. V., Kumar, M. J., Rakesh, M., & Subramanian, B. R., (2008). Influence of net ecosystem metabolism in transferring riverine organic carbon to atmospheric CO2 in a tropical coastal lagoon (Chilka Lake, India). *Biogeochemistry*, *87*, 265–285.

Hennemann, M. C., & Petrucio, M. M., (2011). *Spatial and Temporal Dynamic of Trophic Relevant Parameters in a Subtropical Coastal Lagoon in Brazil*, 347–361.

Jayakumar, R., Steger, K., Chandra, T. S., & Seshadri, S., (2013). An assessment of temporal variations in physicochemical and microbiological properties of barmouths and lagoons in Chennai (Southeast coast of India). *Marine Pollution Bulletin, 70*(1/2), 44–53.

Kanuri, V. V., Muduli, P. R., Robin, R. S., Kumar, B. C., Lovaraju, A., Ganguly, D., et al., (2013). Plankton metabolic processes and its significance on dissolved organic carbon pool in a tropical brackish water lagoon. *Continental Shelf Research*, *61/62*, 52–61.

Loska, K., & Wiechuła, D., (2003). Application of principal component analysis for the estimation of source of heavy metal contamination in surface sediments from the Rybnik Reservoir. *Chemosphere*, *51*, 723–733.

Mohanty, P. K., & Panda, U. S. B., (2009). Circulation and mixing processes in Chilika lagoon. *Indian Journal of Marine Sciences*, *38*(2), 205–2014.

Muduli, P. R., Kanuri V. V., Robin, R. S., Kumar, B. C., Patra, S., Raman, A. V., et al., (2013). Distribution of dissolved inorganic carbon and net ecosystem production in a tropical brackish water lagoon, India. *Continental Shelf Research*, *64*, 75–87.

Muduli, P. R., Kanuri, V. V., Robin, R. S., Kumar, C., Patra, S., Raman, A. V., Rao G. N., & Subramanian, B. R., (2012). Spatio-temporal variation of CO2 emission from Chilika Lake, a tropical coastal lagoon, on the east coast of India. *Estuarine, Coastal and Shelf Science*, *113*, 305–313.

Newton, A., & Mudge, S. M., (2005). Lagoon-sea exchanges, nutrient dynamics and water quality management of the Ria Formosa (Portugal). *Estuarine, Coastal and Shelf Science*, *62*, 405–414.

Panigrahi, S. N., Wikner, J., Panigrahy, R. C., Satapathy, K. K., & Acharya, B. C., (2009). Variability of nutrients and phytoplankton biomass in a shallow brackish water ecosystem (Chilka Lagoon), India. *Limnology*, *10*, 73–85.

Panigrahi, S., Acharya, B. C., Panigrahy, R. C., Nayak, B. K., Banarjee, K., & Sarkar, S. K., (2007). Anthropogenic impact on water quality of Chilika lagoon RAMSAR site: A statistical approach. *Wetlands Ecol. Manage.*, *15*, 113–126.

Raju, N. J., (2012). Evaluation of hydrogeochemical processes in the Pleistocene aquifers of Middle Ganga Plain, Uttar Pradesh, India. *Environ. Earth Sci.*, *65*, 1291–1308.

Raju, N. J., Ram, P., & Dey, S., (2009). Groundwater quality in the lower Varuna River Basin, Varanasi District, Uttar Pradesh. *Journal Geological Society of India*, *73*, 178–192.

Sahoo, S., Baliarsingh, S. K., Lotliker, A. A., & Sahu, K. C., (2014). Imprint of cyclone Phailin on water quality of Chilika lagoon. *Current Science*, *107*(9), 1380–1381.

Singh, S., Raju, N. J., & Nazneen, S., (2015). Environmental risk of heavy metal pollution and contamination sources using multivariate analysis in the soils of Varanasi environs, India. *Environ. Monit. Assess.*, *187*, 345.

Statham, P. J., (2011). Nutrients in estuaries: An overview and the potential impacts of climate change. *Science of the Total Environment*, *434*, 213–227.

CHAPTER 10

PRECISION IRRIGATION AND FERTIGATION FOR THE EFFICIENT WATER AND NUTRIENT MANAGEMENT

P. K. SINGH

Professor, Department of Irrigation and Drainage Engineering, College of Technology, G. B. Pant University of Agriculture & Technology, Pantnagar – 363145, Uttarakhand, India
E-mail: singhpk68@gmail.com

ABSTRACT

Significant progress has been made in irrigation and fertilizer application technologies and in the implementation of water and nutrient management practices such as scientific irrigation and fertilizer scheduling under conventional and modern irrigation techniques. However, scientists report that irrigation inefficiency remains the rule rather than the exception. Gains in water and nutrient use efficiency can be achieved when water application is precisely matched to the site-specific (spatially distributed) crop demand, a central principle underlying *precision irrigation* and *fertigation*. This site-specific crop water demand is present in agricultural fields mainly because of variability in soil properties and topography but may also result from variable rainfall or crop variation associated with multiple crops planted in the same field or plants growing at different phonological stages induced by natural or manmade causes. This chapter deals with the various aspect of the precise application of irrigation water and nutrients for the efficient utilization of the two most important agricultural inputs.

10.1 INTRODUCTION

Application of irrigation water and nutrients at the right time, in the right amount, in the right manner at the right place, is the crux of precision irrigation water and nutrient management. Micro irrigation, a technique that provides crops with water through a network of pipelines at a high frequency but with a low volume of water (drips) applied directly to the root zone in a quantity that approaches consumptive use of the plants, can be combined with fertilizer application, to offer fertigation. Fertigation enables the farmer to meet the specific water and nutrient needs of the crops with great precision, thus minimizing losses of both precious water and nutrients. The direct delivery of fertilizers through drip irrigation demands the use of soluble fertilizers and pumping and injection systems for introducing the fertilizers directly into the irrigation system. Fertigation allows an accurate and uniform application of nutrients to the wetted area, where the active roots are concentrated. The nutrients are applied as per the crop need at different growth stages in a split manner. The problem of mobility of non-mobile nutrients is also addressed using fertigation. Planning the irrigation system and nutrient supply to the crops according to their physiological stage of development, and consideration of the soil and climate characteristics, result in high yields and high-quality crops with minimum pollution. In India more than 9.0 Mha of land have been brought under sprinkler and micro-irrigation; i.e., pressurized irrigation (Malhotra, 2017). Most of the crops irrigated under micro-irrigation are horticultural crops. However, field crops such as sugarcane, groundnut, cotton, etc., are also being brought under micro-irrigation. Efforts are going on to develop the economical design of a micro-fertigation system for the efficient water and nutrient management in a crop like paddy and wheat. The fertilizer applications to these micro-irrigated crops are partially through fertigation in open field condition. However, most of the crops under polyhouse condition are under fertigation. In this chapter, an effort has been made to discuss various issues of fertigation for the precision nutrient management for achieving high nutrient use efficiency.

Applications of agricultural inputs at uniform rates across the field without due regard to in-field variations in soil fertility and crop conditions does not yield desirable results in terms of crop yield. The management of in-field variability in soil moisture, fertility, and crop conditions for improving the crop production and minimizing the environmental impact is the crux of precision farming. It's about doing the right thing, in the right place, in the right way, at the right time. It requires the use of new technologies, such as global positioning system (GPS), sensors, satellite or aerial images, and

information management tools (GIS) to assess and understand variations. Precision farming may be used to improve a field or a farm management from several perspectives. There are many examples of precision irrigation over the last two decades in the western world particularly in the USA and also in Israel. In India and other developing countries, the term precision irrigation means efficient methods of water application through the sprinkler and drip irrigation. However, few systems of micro irrigation and sprinkler irrigation have been installed in an automated mode based on time, volume, and real-time soil moisture feedback system.

10.1.1 PRECISION IRRIGATION

Better irrigation (precision irrigation) is one of the engineering perspectives of precision farming. We first need to establish a common understanding to clarify or explain the term precision irrigation. The traditional meaning of precision irrigation has been that of given in the literature, is referred to as irrigation scheduling. That is, schedule based on environmental data, whether that data comes from local field sensors or from more global sources such as regional meteorological information at precise locations (within the soil profile) or at precise times. Perhaps a good example of this traditional definition of drip irrigation, which is generally accepted as a very precise irrigation technique because water can be precisely controlled with regard to application rate, timing, and location with respect to the plant. This definition continued to be used today in many countries except in USA and western world where more than 60% irrigated area is under sprinkler irrigation (center pivot system). However, in this paper we define precision irrigation as site-specific irrigation water management, specifically the application of water to a given site (right place) in a given volume (right amount) at right time (when) in a right manner (irrigation method) needed for optimum crop production, profitability, and other management objectives at the specific site. This is in contrast with a simultaneous application of the single amount of water to the entire area of the irrigation system/methods. During nineties in USA precision irrigation concept have been initiated at few locations (Camp et al. 2006) mostly concerning to the hardware development and only a few concerning to the site-specific irrigation (Lu et al., 2004(a); Lu et al., 2004(b); Lu et al., 2005). This method of water management continues to be more or less research issues. Development of hardware is mostly in the area of variable rate applicators (sprinkler nozzles, control valves, pumps, sensors, etc.), and software to operate the system. However, an existing

commercial self-propelled system such as center-pivot and lateral-move machines are particularly amenable to cite specific approaches because of their central level of automation and a large area of coverage with a single pipe lateral. This is reflected in some commercial irrigation systems that have recently been modified for precision irrigation. In addition to irrigation, these machines offer an outstanding platform for mounting sensors that can provide real-time monitoring of plant and soil conditions and serve as a transport device for nutrients and other agro-chemical application systems. Adoption of micro (drip/trickle) irrigation and fertigation systems are at an accelerated rate in the developed and developing world for the wide spared horticultural and row crops. This system also offers site-specific management of water and nutrients in a precise manner with the application of controllers and sensors. The development of efficient and cost-effective hardware and software shall be able to accelerate the adoption of a complete precision irrigation system by all category growers.

10.1.1.1 ADVANTAGES AND LIMITATIONS

Applying precision irrigation practices offers significant potential for saving water, nutrient energy, and money. Further, it has the potential to increases crop yield. There is an additional positive environmental impact from precision irrigation in that farm runoff, a major source of water pollution, can be reduced. The major limitation associated with precision irrigation is the limited application of self-propelled center-pivot sprinklers for small land holdings, high initial cost, operation, and maintenance needs a skilled workforce.

10.1.1.2 PRECISION IRRIGATION APPLICATION SYSTEM

In conventional types of irrigation valves, emission devices, sprinkler nozzles, application rates have been altered by manual operations. Similarly, the movement of the lateral line, travel speed were also controlled/ adjusted manually. In newer systems use of controller and software has made these jobs automatically in dynamic mode as per the requirement of the crop and field, i.e., site-specific.

Sprinkler Irrigation: Numerous innovative technologies have been developed to apply the irrigation water in dynamic mode (variable rate) to meet anticipated whole-field management needs in precision irrigation

primarily with center-pivot and lateral-move irrigation systems. In general, the operation criteria for these systems include the case of retrofit to the existing commercial irrigation system, good water application uniformity within and between management zone, robust electronics, compatibility with existing irrigation system equipment, bi-directional communication, and flexible expansion for future development and functional requirement. In addition, management of precision water application must include the interactions between individual sprinkler wetted diameters, the start/stop movement of towers, and solenoid valve cycling. These new precision water application technologies generally can be classified as either (1) a multiple of discrete fixed-rate application devices operated in combination to provide a range of application depths, (2) flow interruption to fixed-rate devices to provide a range of application depths that depend upon pulse frequency, or (3) a variable aperture sprinkler with time proportional control. Multiple sprinklers, pulsing sprinklers, and variable-orifice sprinklers have been developed in different part of the world for the precision application of water to the crops.

Micro-Irrigation: In low-pressure irrigation system (drip, microsprinkler, etc.) constant and variable discharge emitters have been developed by manufacturers to provide variable flow rate at the specific site in the field. In micro-irrigation there may be single or multiple emitters at a point, the operation of one or more than one emitters could be possible with the precision irrigation system. The operation time of emitters/lateral is possible through automatic hydraulic valves controlled by the microprocessor/controller.

10.2 SYSTEM CONTROL

Various forms of control systems has been developed for the surface, sprinkler, and micro-irrigation system for the control of the self-propelled sprinklers, emitters on the basis of time, volume, and real-time feedback. The control system generally consists of a microprocessor/controller, communication system (wire/wireless), control valve and sensors. For example, Remote Irrigation Monitoring and Control System (RIMCS) have been developed for continuous move irrigation systems that integrate localized wireless sensor networks for monitoring soil moisture and weather and provide control for individual or groups of nozzles with wireless access to the Internet to enable remote monitoring and control. The *RIMCS* uses a Single Board Computer (SBC) using the Linux operating system to control solenoids connected to individual or groups of nozzles based on prescribed application maps. The main control box houses the SBC connected to a sensor network radio, a

GPS unit, and an Ethernet radio creating a wireless connection to a remote server. A C-software control program resides on the SBC to control the on/off time for each nozzle group using a "time on" application map developed remotely. The SBC also interfaces with the sensor network radio to record measurements from sensors on the irrigation system and in the field that monitor performance and soil and crop conditions. The SBC automatically populates a remote database on the server in real time and provides software applications to monitor and control the irrigation system from the Internet. Another example of the irrigation control system is EIT irrigation control system is a data collection and SCADA based control system which utilizes EIT data telemetry products as well as third-party supplied soil sensors for monitoring and scheduling irrigation activities. The system is designed for flexibility and ease of use. The Human Machine Interface (HMI) provides easy to use functions for setting the selecting irrigation modes and soil moisture set points. The system comprises of three main components. These are the central PC, a sensor for monitoring soil moisture and telemetry for data collection, valve, and pump control.

Sensors: Sensors are the most important component of a precision irrigation control system which provides the desired information for the control of the sprinkler nozzles/emitters, control valve, etc. Field environmental sensors and soil moisture sensors are the most common type of environmental sensor employed for determining a crop's water requirements. However, sensors for ambient temperature and humidity in the crop's field are also common. As stated above, full weather stations may even be included in local sensors. Sensors are strategically located at a number of points within a crop's field in a way that covers variations in soil type and climate. Pressure transducers may also be employed in the field for monitoring the water pressure of irrigation zones. For crops that require continuous flood conditions, such as rice, water level sensors at various points in the field may be used. They may be used as direct real-time feedback for automatic controls (discussed below) and/or data collection and logging. Sensor data collection sensors may be queried manually or automatically by a data collection system. Automatic data collection systems will query at regular intervals (generally every 5–15 minutes or so) and then log the data into a database for subsequent reference. Also, automatic data collection systems generally require a wireless communications network of very low power data collection nodes with solar cells and rechargeable batteries. Any node within the network may have one to several sensors attached. Some nodes may be used only as a communication relay within the wireless network. In addition to the wireless nodes, the network may also include switching hubs, routers, and gateways. Viewing

of real-time data as well as data in the database archive may be limited to a local network on the farm or may be accessible from the Internet.

10.2.1 OPTIONAL SYSTEM COMPONENTS

10.2.1.1 LOCATION AND ALIGNMENT

The control system for most site-specific application systems use some form of spatiality indexed data to determine the appropriate application rate for specific sites. The basis for these spatially indexed data is typically a widely accepted geo-reference system, such as latitude and longitude. Consequently, it is necessary to know the precise location of all elements of the application system at all times during operation if accurate site-specific applications are expected. Various approaches have been used, but the greatest challenge is cost. Although it is often desirable to have multiple location sensors along the truss length of a moving irrigation system, the cost would be prohibitive. A general solution has been to use one or two sensors to locate one or both ends of the moving system and to calculate the location intermediate location points. Because moving irrigation systems consist of multiple segments or spans, with each end of the span moving independently but within confined limits, the truss is not always linear. This is not a significant problem for small systems, but misalignment can be significant for a large system. Fortunately, in many cases, the shape of the truss is consistent, predictable, and describable for specific operational conditions. The determination of precise locations for lateral move system is similar to that of center pivot systems concept that is more difficult because both ends move. The laser alignment system is also used for such a system. Although the travel path is constrained by the guidance system, some variation usually exists in repeatability. The issues of tissue misalignment are similar for a lateral move and center-pivot systems. In general, more sensors are required for determining locations in lateral move systems than in center pivot systems. Most lateral move precision irrigation systems have used one or more GPS sensor to determine location.

10.2.1.2 MANAGEMENT DATABASE AND DECISION SUPPORT

Any information to be used in the precision management application must be indexed by its geographical location and stored in an electronic format that can be readily accessed by a computer or computer-based controller. As such,

it operates as special purpose GIS. This management database houses the data with which the control system operates the irrigation machines, records the actual application amounts for later use or documentation, and provides the framework on which a decision support system can operate. Data that may be stored could include user-entered soil characteristics, cultural operations, or application maps. It could also include historical geo-referenced data such as yield maps, past application maps, or cultural histories. Spatial arrays of sensors either mounted on the system or in the field could potentially feed information directly into the management database.

10.2.1.3 VARIABLE WATER SUPPLY

Most conventional moving irrigation systems are designed for and operate with a constant water flow rate and pressure to the system in which all sprinklers operate most of the time. With precision irrigation, in which variable flow rates are required for several management zones within the total system, water must be applied to the system at constant pressure but at a variable flow rate. The magnitude of the flow rate variance depends upon the system design and operation characteristics, but in extreme cases, it can vary from full design flow rate to almost zero.

10.3 FERTIGATION FOR PRECISION MANAGEMENT OF NUTRIENTS

The precise management of nutrients in the soil is possible through application of the right amount of fertilizers /nutrients and other chemicals at the right time, at the right place and in the right manner to achieve high yield and the quality of produce along with minimum / no loss to the groundwater caused due to nutrient leaching. Fertigation (application of fertilizer/chemical solution with irrigation) has the potential to ensure that the right combination of water and nutrients is available at the root zone, satisfying the plants total and temporal requirement of these two inputs. Fertilizer application through irrigation can be conducted using a micro (drip/trickle), surface (border, basin, and furrow), pipe, and sprinkler irrigation systems. Micro and subsurface system of irrigation can only be used for fertigation of soil-applied agricultural fertilizers/ chemicals. Surface irrigation methods can, at times, present problems with the uniformity of fertilizer/chemical application and may limit some chemical applications. Sprinkler irrigation system (impact, rain gun, pop-up, center pivots, lateral

move, etc.) can be used both for soil and over canopy/ foliar application of nutrients/chemicals.

There are various benefit and risk associated with the application of fertilizers, chemicals, and other nutrients under fertigation/chemigation/ nutrition. Proper management and efficient application of these nutrients/ chemicals offer a significant saving of these chemicals, better scheduling as per crop need, improvement in yield and nutrient use efficiency and less impact on the environment which is an important component of sustainable soil management. The main drawbacks associated with fertigation are the initial set-up costs and the need to monitor the operation carefully to ensure that irrigation and injection systems are working correctly. Water quality can limit the use of fertigation; irrigation waters that are high in salts are not suitable for fertigation. Generally, the concentration of salts in the fertigation solution should not exceed 3000 micro Siemens per centimeter (μs/cm). The most significant risk when utilizing fertigation/chemigation is for water source contamination due to back siphoning, backpressure, over-irrigation and untimely application of N fertilizers, which reduces the efficiency of fertilizer use and compounds N losses to the environment (Ng Kee Kwong and Devile, 1987). In addition, nutrient depletion within plant root zone and soil acidification were reported (Peryea and Burrows, 1999; Mmolawa and Or, 2000; Neilsen et al., 2004) if proper care has not taken during fertigation. Fertigation may favor NO_3-N leaching, which requires a careful calculation of the fertilizer dose to minimize the risk of groundwater contamination.

A well-designed fertigation system can reduce fertilizer application costs considerably and supply nutrients in precise and uniform amounts to the wetted irrigation zone around the tree where the active feeder roots are concentrated. Applying timely doses of small amounts of nutrients to the trees throughout the growing season has significant advantages over conventional fertilizer practices. Fertigation saves fertilizer as it permits applying fertilizer in small quantities at a time matching with the plants nutrient need. Besides, it is considered eco-friendly as it avoids leaching of fertilizers. Liquid fertilizers are best suited for fertigation. In India, inadequate availability and the high cost of liquid fertilizers restrict their uses. Fertigation using granular fertilizers poses several problems namely, their different levels of solubility in water, compatibility among different fertilizers and filtration of undissolved fertilizers and impurities. Different granular fertilizers have different solubility in water. When the solutions of two or more fertilizers are mixed together, one or more of them may tend to precipitate if the fertilizers are not compatible with each other. Therefore, such fertilizers

may be unsuitable for simultaneous application through fertigation and would have to be used separately. This article reports on the various issues of fertigation, i.e., advantages, and limitations, selection of water-soluble fertilizers (granular and liquid), fertigation scheduling in various crops and fertigation system for efficient fertigation programme and response of plants to fertigation; and it is economic.

10.3.1 IMPORTANCE OF FERTIGATION

- The fertigation allows applying the nutrients exactly and uniformly only to the wetted root volume, where the active roots are concentrated, which eliminates the over and underfeeding of nutrients.
- Remarkably increase in the application efficiency of the fertilizer, which saves the significant amount of fertilizers.
- Reduction in the production costs and groundwater pollution caused by the fertilizer leaching.
- Fertigation allows adapting the amount and concentration of the applied nutrients in order to meet the actual nutritional requirement of the crop throughout the growing season. Timely application of fertilizers and chemical significantly increases the crop yield.
- Fertigation reduces the operator's exposures to fertilizers and chemicals.
- Mechanical damage to crop by manual/tractors application of fertilizers is reduced by fertigation.
- Many fertilizers/chemical required to be placed at a particular location in the plant root zone which is possible through fertigation.
- Saving of energy and labor.
- Flexibility of the moment of the application (nutrients can be applied to the soil when crop or soil conditions would otherwise prohibit entry into the field with conventional equipment).
- Convenient use of compound and ready-mix nutrient solutions also containing small concentrations of micronutrients which are otherwise very difficult to apply accurately to the soil, and
- The supply of nutrients can be more carefully regulated and monitored. When fertigation is applied through the drip irrigation system, crop foliage can be kept dry thus avoiding leaf burn and delaying the development of plant pathogens.

10.3.2 SELECTION OF FERTILIZERS

Effective fertigation requires an understanding of plant growth behavior including nutrient requirements and rooting patterns, soil chemistry such as solubility and mobility of the nutrients, fertilizers chemistry (mixing compatibility, precipitation, clogging, and corrosion) and water quality factors including pH, salt, and sodium hazards, and toxic ions. The granular and liquid fertilizers used in fertigation are available in various chemical formulations, solubility, and different types of coatings; therefore the selection of fertilizer is an important issue in fertigation programme. The selection of granular fertilizer will depend on the nutrient that is applied, fertilizer solubility and ease of handling.

An essential pre-requisite for the solid fertilizer use in fertigation is its complete dissolution in the irrigation water. Examples of highly soluble fertilizers appropriate for their use in fertigation are: ammonium nitrate, potassium chloride, potassium nitrate, urea, ammonium monophosphate, and potassium monophosphate. The solubility of fertilizers depends on the temperature. The fertilizer solutions stored during the summer form precipitates when the temperatures decrease in the autumn, due to the diminution of the solubility with low temperatures. Therefore, it is recommended to dilute the solutions stored at the end of the summer. Fertilizer solutions of smaller degree specially formulated by the manufacturers are used during the winter.

To ensure the fertilizers selected will not precipitate in irrigation pipe, mix the fertilizer solution with a sample of irrigation water in the same proportions as and when they are mixed in the irrigation system. If the chemical stays in the solution, then the product is safe to use under fertigation. Liquid fertilizers offer many intrinsic advantages over granular fertilizers for fertigation. It is considered as most suitable for of fertigation under micro and sprinkler irrigation. These are available as fertilizers solutions and suspension, both of which may contain single or multi-nutrient materials. To avoid damage to the plant roots high fertilizer concentrations, the fertilizer concentration in irrigation water should not exceed 5%. Although, the susceptibility to root burning from concentrated fertilizers varies with crops, fertilizers, and accompanying irrigation practices. Therefore, it is safer to keep the fertilizer concentration of 1–2% in the irrigation water during fertigation.

10.3.3 IMPORTANT POINTS TO BE CONSIDERED DURING FERTIGATION

10.3.3.1 WATER QUALITY

The interaction of water having pH values (7.2–8.5) with fertilizers can cause diverse problems, such as the formation of precipitates in the fertilization tank and clogging of the drippers and filters. In waters with high calcium content and bicarbonates, use of sulfate fertilizers causes the precipitation of $CaSO_4$ obtruding drippers and filters. The use of urea induces the precipitation of $CaCO_3$ because the urea increases pH. The presence of high concentrations of calcium and magnesium and high pH values lead to the precipitation of calcium and magnesium phosphates. Recycled waters are particularly susceptible to precipitation due to its high bicarbonate and organic matter content. The resultant precipitates are deposited on pipe walls and in orifices of drippers and can completely plug the irrigation system. At the same time, P supply to the roots is impaired. When choosing P fertilizers for fertigation with high calcium and magnesium concentrations, acid P fertilizers (phosphoric acid or monoammonium phosphate) are recommended.

Fertigation under saline conditions: Crops vary widely in their tolerance to plants, reference tables are available defining individual crop sensitivity to total soluble salts and individual toxic ions (Maas and Hoffman, 1977). When brackish waters are used for irrigation, we must bear in mind that fertilizers are salts and Therefore, they contribute to the increase of the EC of the irrigation water. Nonetheless, calculation of the contribution of chloride from KCl to the overall load of chloride from irrigation water shows its relative by low share (Tarchitzky and Magen, 1997). When irrigation water has an EC > 2 dS/m (with high salinization hazard), and crop is sensitive to salinity, we must decrease the amount of accompanying ions added with the N or K. For example, in avocado—a very sensitive crop to chloride—KNO_3 is preferred on KCl to avoid Cl accumulation in the soil solution. This practice diminishes leaf burning caused by Cl excess. Also in greenhouse crops grown in containers with a very restricted root volume, we must choose fertilizers with low salt index. Sodium fertilizers as $NaNO_3$ or NaH_2PO_4 are unsuitable due to the adverse effect of sodium on the hydraulic conductivity and the performance of the plant. A correct irrigation management under saline conditions includes water application over the evaporation needs of the crop, so that there is excess water to pass through and beyond the root zone and to carry away salts with it. This leaching prevents excessive salt

accumulation in the root zone and is referred to as leaching requirement (Rhoades and Loveday, 1990).

10.3.3.2 FERTILIZERS COMPATIBILITY

When preparing fertilizer solutions for fertigation, some fertilizers must not be mixed together. For example, the mixture of $(NH_4)_2SO_4$ and KCl in the tank considerably reduce the solubility of the mixture due to the K_2SO_4 formation. Other forbidden mixtures are:

- Calcium nitrate with any phosphates or sulfates.
- Magnesium sulfate with di- or mono- ammonium phosphate.
- Phosphoric acid with iron, zinc, copper, and manganese sulfates.

10.3.4 FERTIGATION SYSTEM

System EU shall not be less than 85 percent where fertilizer or pesticides are applied through the system. Injectors (chemical, fertilizer, or pesticides) and other automatic operating equipment shall be located adjacent to the pump and power unit, placed in accordance with the manufacturer's recommendation and include integrated backflow prevention protection. Fertigation/nutrigation/chemigation shall be accomplished in the minimum length of time needed to deliver the chemicals and flush the pipelines. Application amounts shall be limited to the minimum amount necessary, as recommended by the chemical label. A number of different techniques are used to introduce the fertilizers into the irrigation system. Generally, fertilizers are injected into irrigation systems by three principal methods namely, (1) fertilizer tank (the by-pass system), (2) the venturi pump and (3) the injection pump (piston or destron pump). Non-corrosive material should be used for the fertilizer containers and for the injection equipment.

10.4 CONCLUSIONS

The precision farming and hi-tech agriculture for the improved input use efficiency, more yield, and quality produce in a sustainable manner is incomplete without efficient irrigation and fertilizer application techniques. Application of water at the right time, in the right amount at the right place

with right manner is the crux of precision irrigation. Fertigation is the most efficient techniques of fertilizer application in a split manner as per crop need at different stages of crop development. The fertilizers used for fertigation must be 100% water soluble, and it should not precipitate while making the solution. The selection of fertilizers should be in accordance with the pH of the soil. The concentration of fertilizer should not be more than 2% during fertigation. The fertilizer requirement should be determined based on soil analysis and if soil analysis not possible certain correction factors must be applied depending on the soil texture. The fertilizer use efficiency can be maximized by adopting drip-fertigation to the level of 95%. The drip- fertigation system should be appropriately designed to achieve at least 85% of uniformity of water and fertilizer application. The piston pump type of fertigation unit is the most efficient system of fertilizer application. However, fertilizer tank and ventury type of fertigation unit are most common at the farmer's field because of its low cost.

KEYWORDS

- **fertigation**
- **micro irrigation**
- **saline condition**
- **sprinklers**

REFERENCES

Camp, C. R., Sadler, E. J., & Evans, R. G., (2006). Precision water management: Current realities, possibilities and trends In: *Handbook of Precision Agriculture*, Haworth, 153–185.

Lu, Y. C., Camp, C. R., & Sadler, E. J., (2004a). Efficient allocation of irrigation water and nitrogen fertilizer in corn production. *Journal of Sustainable Agriculture*, *24*(4), 97–111.

Lu, Y. C., Camp, C. R., & Sadler, E. J., (2004b). Optimal levels of irrigation in corn production in the southeast coastal plains. *Journal of Sustainable Agriculture*, *24*(1), 95–106.

Lu, Y. C., Sadler, E. J., & Camp, C. R., (2005). Economic feasibility study of variable irrigation of corn production in southeast coastal plains. *Journal of Sustainable Agriculture*, *26*(3), 69–81.

Maas, E. V., & Hoffman, G. J., (1977). Crop salt tolerance - current assessment. *J. Irrig. Drainage Div. ASEC*, *103*, 115–134.

Malhotra, S. K., (2017). *Initiative and Option in Transition for Doubling Farmer's Income*. Keynote lecture delivered at the occasion of National Conference on "Technological

changes and innovations in agriculture for enhancing farmer's income," held at JAU, Junagadh, Gujrat during May 28–30.

Mmolawa, K., & Or, D., (2000). Root zone salute dynamics under drip irrigation: A review. *Plant Soil*, *222*, 163–190.

Neilsen, G. H., Neilsen, D., Herbert, L. C., & Hogue, E. J., (2004). Response of apple to fertigation of N and K under conditions susceptible to the development of K deficiency. *J. Am. Soc. Hortic. Sci.*, *129*, 26–31.

Ng Kee, K. K. F., & Devile, J., (1987). Residual nitrogen as influenced by the timing and nitrogen forms in silty clay soil under sugarcane in Mauritius. *Fertil. Res*., *14*, 219–226.

Peryea, F. J., & Burrows, R. L., (1999). Soil acidification caused by four commercial nitrozen fertilizer solutions and subsequent soil pH rebound. *Commun. Soil Sci. Plant Anl.*, *30*, 525–533.

Rhoades, J. D., & Loveday, J., (1990). Salinity in irrigated agriculture. In: Stewars, B. A., & Nielsen, D. R., (eds.), *Irrigation of Agricultural Crops* (pp. 1089–1142). ASA-CSAA-SSSA, Madison, WI.

Tarchitzky, J., & Magen, H., (1997). *Status of Potassium in Soils and Crops in Israel, Present K Use Indicating the Need for Further Research and Improved Recommendations*. Presented at the IPI Regional Workshop on Food Security in the WANA Region, May, Bornova, Turkey.

CHAPTER 11

IDENTIFICATION OF URBAN HEAT ISLANDS FROM MULTI-TEMPORAL MODIS LAND SURFACE TEMPERATURE DATA: A CASE STUDY OF THE SOUTHERN PART OF WEST BENGAL, INDIA

PRITI KUMARI[1], NAVAL KISHOR YADAV[2], ABHISEK SANTRA[2], and UTKARSH UPADHAYAY[3]

[1]Department of Civil Engineering, GGSESTC, Bokaro, Jharkhand, India, E-mail: priti.9407@gmail.com

[2]Department of Civil Engineering, Haldia Institute of Technology, Haldia, West Bengal, India

[3]Centre for Water Engineering and Management, Central University of Jharkhand, Ranchi, Jharkhand, India

ABSTRACT

Land surface temperature (LST) is the temperature of the earth's ground surface and is crucial for climate studies in different aspects like hydrology, geology, engineering, phenology, etc. Research on Urban Heat Island (UHI) is mainly dependent upon the LST studies and is highly useful for studying its impact over the surrounding environment, precipitation, and water quality of the area. An attempt has been made here to study the spatiotemporal dynamics of the LST and associated UHIs in the southern part of West Bengal, India. The authors extracted the major UHIs from mean monthly time series MODIS Land Surface Temperature datasets for the period from 2010 to 2015 and identified the pattern of change of LST in the study area.

It has been observed that the temperature values of the four summer months have less variance with the mean summer temperature values. The range of temperature adopted is below 30°C, 30–35°C, 35–40°C, and 40°C onwards. The prevailing aridity shows the high LST in and around Purulia district. The year 2010 and 2014 shows the high spatial distribution of the very high-temperature class probably due to environmental and climatic reasons. The result also reveals a four-yearly cyclic pattern of LST change in the study area and two heat islands in and around Kolkata and Haldia areas. Among the urban agglomerations, only two Kolkata-Howrah and Haldia areas can be visible as UHI at the coarse spatial resolution from the thermal image. The UHI patterns have also been correlated with the classified land use and land cover information of the same area.

11.1 INTRODUCTION

The temperature of an area is greatly affected by its land use/land cover. Over the past several decades, the global process of urbanization has progressed dramatically rapid, thus gave rise to many problems for the urban environment and climate. When a large fraction of natural land cover in an area are replaced by a built surface, it traps incoming solar radiation during the day and reradiates at night, the resulting phenomenon is known as Urban Heat Island (UHI). UHI was considered as the most well-documented example of anthropogenic climate modification within the field of urban climate (Arnfield, 2003). In recent years UHI has become a topic of great interest both among the academicians and the governing bodies. Researchers are interested in understanding the various aspects of this phenomenon including its causes (Huang et al., 2011), impacts (Imhoff et al., 2010) and complexity (Mirzaei and Haghighat, 2010). UHI is increasingly gaining interest as it directly affects both environmental (Ferguson and Woodburry, 2007; Sharma et al., 2012) as well as human health (Lo and Quattrochi, 2003; Tomilson et al., 2011). UHI affects the environment through heat pollution (Papanastasiou and Kittas, 2012), it increases the number of smog events (Sham et al., 2012), higher energy consumptions (Kolokotroni et al., 2012), while from human health perspectives it causes a larger number of heat-related health problems (Harlan and Ruddell, 2011) and adversely impact human comfort (Steeneveld et al., 2011). Therefore, it is very essential to understand the UHI phenomena and its ill effect on the environment in order to mitigate this effect to some extent for the betterment of the environment and the human race. UHI manifests itself in two basic forms (i) the Surface UHI (SUHI) and

(ii) the Atmospheric UHI (AUHI). SUHI is the phenomenon of the temperature difference between surfaces of urban and surrounding rural areas. The phenomenon revealed high spatial and temporal variability (Stathopoulou and Cartalis, 2009). SUHI is studied using land surface temperature (LST) regained from thermal satellite sensors (Schwarz et al., 2011). AUHI includes the difference in the pattern of air temperature between urban and rural settings. AUHI further falls in one of the two categories viz., Canopy layer or Boundary layer. The atmosphere is extending from the surface to mean building height or tree canopy are influenced by Canopy layer UHI, while the Boundary layer UHI accounts for air beyond canopy layer (Weng, 2003). AUHI is studied using meteorological data (Saaroni et al., 2000). Such data have frequently been explored to study monthly or seasonal variations in AUHI (Jongtanom et al., 2011; Cayan and Douglas, 1984; Fujibe, 2009; Jauregui, 1997; Liu et al., 2007; Gaffin et al., 2008; Hua et al., 2008). Gallo and Owen (1999) for illustration analyzed urban-rural temperature (using observation stations) and Normalized Difference Vegetation Index (NDVI) (using NOAA-AVHRR, National Oceanic and Atmospheric Administration–Advanced Very High-Resolution Radiometer) of 28 cities on a monthly and seasonal basis to study UHI. UHI intensity in Bangkok, Chiang Mai, and Songkhla cities were investigated using urban and rural meteorological station data (Jongtanom et al., 2011). Cayan and Douglas (1984), Fujibe (2009), Jauregui (1997), Liu et al., (2007), Gaffin et al., (2008), and Hua et al., (2008) have also conducted similar researches. Thus it is evident that detailed work is available on seasonal studies of AUHI, but such detailed literature for SUHI is lacking. However, a dearth of such literature exists for SUHI studies. Seasonal analysis of SUHI requires temporal LST (Hu and Brunsell, 2013; Buyantuyev and Wu, 2010). Very few and recent work is available on SUHI seasonal analysis with a huge gap in this research existing for Indian cities. Researchers have proposed various approaches to quantify UHI in terms of intensity or area. Keramitsoglou et al., (2011) have used the difference between LST and reference LST (RLST) to assess UHI intensity. Zhang et al., (2009) calculated LST differences between different impervious surface area categories and water as an estimate for UHI intensity. Zhang and Wang (2008) proposed hot island area (HIA) as UHI intensity estimate that is based on standard deviation segmentation of LST image. In this chapter, an attempt has been made to identify the spatio-temporal pattern of summertime UHI of the southern part of West Bengal. Also, the surface extents of the UHIs have been compared from the land use land cover information of the area.

11.2 MATERIALS AND METHODS

11.2.1 STUDY AREA

The study area is south Bengal and mainly focused on Kolkata, North, and South 24 Parganas, East Midnapur, West Midnapur, Birbhum, Bankura, Purulia, Hooghly, Howrah, and Durgapur districts. In south Bengal, there are several town and villages with a high population (such as Kolkata) and industrial hubs like Haldia, Kharagpur, and Durgapur, etc. The study area (West Bengal) is located about 17 feet above MSL, and it ranks 14th as per land area and 4th in population (India). The highest day temperature of the area ranges from 38°C to 45°C. This high temperature in summer is a combined consequence of high population density and never-ending emission of industries. As urbanization and industrialization will continue, it is very important to identify Heat Islands because the further increase in population and industries in those areas may lead to bad consequences over agriculture, living life and climatic cycle (Figure 11.1).

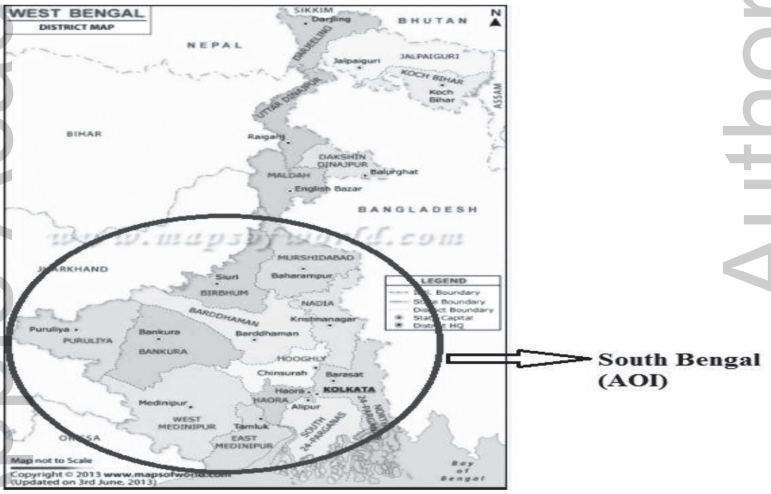

FIGURE 11.1 Study area.

11.2.2 DATABASE AND METHODOLOGY

LST of the southern part of the Bengal is estimated from the MODIS monthly LST images acquired for the period from 2010 to 2015. The data

has been freely acquired from NASA Earth Observation (NEO) website. The spatial resolution of the data is 11.132 km (0.1 degrees). The data is a geo-referenced product in geographic latitude/longitude coordinate system and WGS84 datum plane. Since UHI is distinct in the summer season, only four months from March to June have been considered for the identification and understanding of the dynamics of UHI for the study area. The downloaded data were stacked considering four months for each year. After that, data for each year consisting of four layers have been clipped with the exact boundary of the study area using the ERDAS Imagine software package. The exact boundary of the study area (AOI) has been digitized and extracted from the published maps of the Census of India (2011). ArcGIS software package has been used to reclassify the set of images in terms of different LST classes. After that, the classified image of the study area collected from ENVISAT MERIS Globcover was considered to cross-validate the spatial locations of UHIs. The classified data also clipped using the same study area of interest (AOI) layer in Erdas Imagine software. The methodology flow diagram (Figure 11.2) simplifies the broad framework of the research.

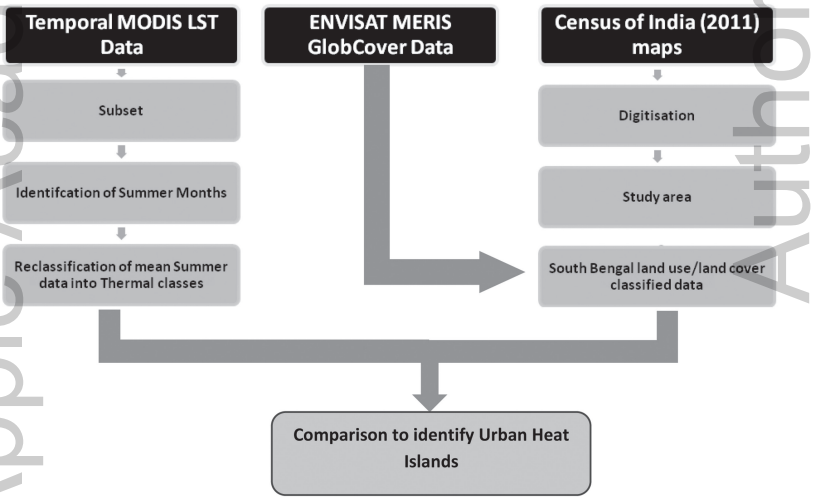

FIGURE 11.2 Methodology flowchart.

11.3 RESULTS AND DISCUSSIONS

As a good indicator of the earth's energy balance at the surface of the earth, LST controls the physics of the land surface processes directly or indirectly

both on a global and regional scale. It integrates the surface atmospheric interactions and energy fluxes between the atmosphere and the ground surface. The reclassified area gives the number of pixels contained in each temperature range. It has been observed that the temperature values of the four summer months have less variance with the mean summer temperature values. The mean summer temperature of the study area for 2010 to 2015 was calculated using the modeler tool of Erdas Imagine software package. The range of temperature adopted is below 30°C, 30–35°C, 35–40°C and 40°C onwards. Here it would be more relevant to draw the comparison among the class 4 area values as this class is a high-temperature range (Table 11.1).

TABLE 11.1 Year Wise Land Surface Temperature Values for the Highest Land Surface Temperature Class

Year	Area under class 4 (km2)
2010	16481.36
2011	991.36
2012	1239.20
2013	7806.96
2014	15985.68
2015	247.84

The maps generated (Figure 11.3) show the spatiotemporal dynamics of the LST. The prevailing aridity shows the high LST in and around Puruliya district. The years 2010 and 2014 show the high spatial distribution of the very high-temperature class probably due to environmental and climatic reasons. The results also reveal a four-yearly cyclic pattern of LST change in the study area. However, it is clear from the Figure 11.3; two heat islands have evolved in and around Kolkata and Haldia areas surrounded by cooler temperature. These two are the possible results of high urbanization and industrial development in those areas.

The land use and land cover data of the area depicts mostly cultivated and irrigated lands (Figure 11.4). Some patches of forested lands can also be seen. Mangroves dominate at the lower parts of South 24 Parganas district. Four urban areas can be distinctly located at Kolkata – Howrah, Barddhaman – Asansol – Durgapur, Kharagpur – Medinipur and Haldia. These four areas are of primary concern from UHI point of view. However, among these four urban agglomerations, only two – Kolkata – Howrah, and Haldia areas can be visible as UHIs at the coarse spatial resolution from the thermal images. The prevailing aridity and small scale of the data are probably hindering the visibility of the

other two urban regimes and heat islands. However, high spatial resolution thermal images at the larger scale may isolate them as heat islands.

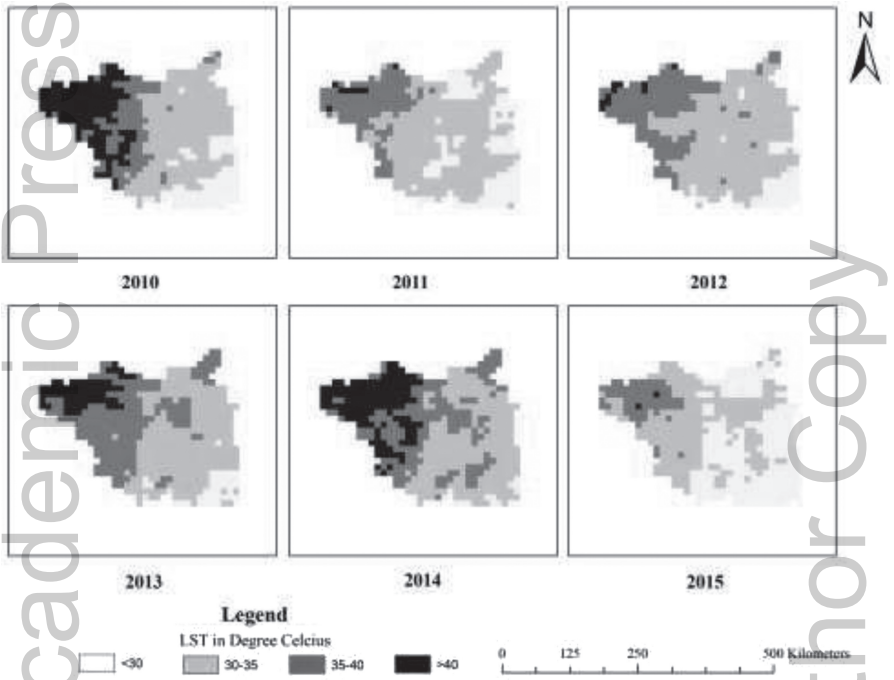

FIGURE 11.3 Spatio-temporal pattern of the land surface temperature.

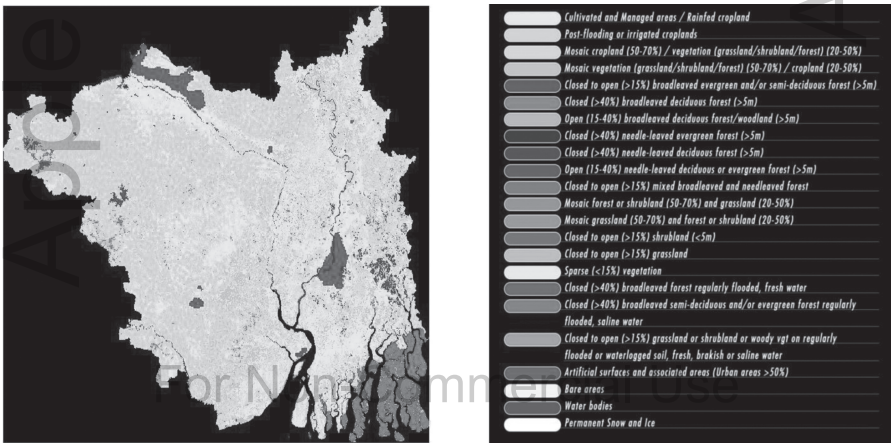

FIGURE 11.4 **(See color insert.)** Land use and land cover.

11.4 CONCLUSIONS

The present work demonstrates the importance of thermal remote sensing as a valuable source of temperature information for cities and urban agglomerations. However, the scale of the images is the first and foremost criteria in this regard to fill up the gaps of lack of information. The paper identifies the spatiotemporal changes of LST in this area. It also pinpoints the impact of summer months on LST. However, for a large area, the coarser resolution images may be used to identify probable UHIs. After that, the high-resolution satellite images with thermal bands may be applied to see the small UHIs within an urban area. In this way, the temperature characteristics of the cities can be identified in relation to the urban land use and expansion. The relevance of such studies is not immediately obvious and deserves closer inspection.

KEYWORDS

- **Arc-GIS**
- **globcover**
- **land surface temperature**
- **MODIS**
- **Urban Heat Island**

REFERENCES

Arnfield, A. J., (2003). Two decades of urban climate research: A review of turbulence, exchanges of energy and water, and the urban heat island. *International Journal of Climatology*, *23*, 1–26.

Buyantuyev, A., & Wu, J., (2010). Urban heat islands and landscape heterogeneity: Linking spatiotemporal variations in surface temperatures to land-cover and socioeconomic patterns. *Landscape Ecol.*, *25*, 17–33.

Cayan, D. R., & Douglas, A. V., (1984). Urban influences on surface temperatures in the southwestern United States during recent decades. *J. Climate Appl. Meteorol.*, *23*, 1520–15330.

Ferguson, G., & Woodbury, A. D., (2007). Urban heat island in the subsurface. *Geophys. Res. Lett.*, *34*, 2192–2201.

Fujibe, F., (2009). Urban warming in Japanese cities and its relation to climate change monitoring. In: *The Seventh International Conference on Urban Climate*, Yokohama, Japan.

Gaffin, S. R., Rosenweig, C., Khanbilvardi, R., Parshall, L., & Mahani, S., (2008). Variations in New York city's urban heat island strength over time and space. *Theor. Appl. Climatol.*, *94*, 1–11.

Gallo, K. P., & Owen, T. W., (1999). Satellite-based adjustments for the urban heat island temperature bias. *J. Appl. Meteorol*., *38*, 806–813.

Hu, L., & Brunsell, N. A., (2013). The impact of temporal aggregation of land surface temperature data for surface urban heat island (SUHI) monitoring. *Remote Sens. Environ.*, *134*, 162–174.

Hua, L. J., Ma, Z. G., & Guo, W. D., (2008). The impact of urbanization on air temperature across China. *Theor. Appl. Climatol.*, *93*, 179–194.

Huang, G., Zhou, W., & Cadenasso, M. L., (2011). Is everyone hot in the city? Spatial pattern of land surface temperatures, land cover and neighborhood socioeconomic characteristics in Baltimore, MD. *J. Environ. Manage*., *92*, 1753–1759.

Imhoff, M. L., Zhang, P., Wolfe, R. E., & Bounoua, L., (2010). Remote sensing of the urban heat island effect across biomes in the continental USA. *Remote Sens. Environ*., *114*, 504–513.

Jauregui, E., (1997). Heat island development in Mexico City. *Atmos. Environ*., *31*, 3821–3831.

Jongtanom, Y., Kositanont, C., & Baulert, S., (2011). Temporal variations of urban heat island intensity in three major cities, Thailand. *Mod. Appl. Sci.*, *5*, 105–110.

Keramitsoglou, I., Kiranoudis, C. T., Ceriola, G., Weng, Q., & Rajasekar, U., (2011). Identification and analysis of urban surface temperature patterns in Greater Athens, Greece, using MODIS imagery. *Remote Sens. Environ*., *115*, 3080–3090.

Liu, W., Ji, C., Zhong, J., Jiang, X., & Zheng, Z., (2007). Temporal characteristics of the Beijing urban heat island. *Theor. Appl. Climatol.*, *87*, 213–221.

Lo, C. P., & Quattrochi, D. A., (2003). Land-use and land-cover change, urban heat island phenomenon, and health implications: A remote sensing approach. *Photogramm. Eng. Remote Sens*., *69*, 1053–1063.

Mirzaei, P. A., & Haghighat, F., (2010). Approaches to study urban heat island – abilities and limitations. *Build. Environ*., *45*, L23743(1–4).

Papanastasiou, D. K., & Kittas, C., (2012). Maximum urban heat island intensity in a medium-sized coastal Mediterranean city. *Theor. Appl. Climatol.*, *107*, 407–416.

Sham, J. F. C., Lo, T. Y. L., & Memon, S. A., (2012). Verification and application of continuous surface temperature monitoring technique for investigation of nocturnal sensible heat release characteristics by building fabrics. *Energy Build.*, *53*, 108–116.

Sharma, R., & Joshi, P. K., (2012). Monitoring urban landscape dynamics over Delhi (India) using remote sensing (1998–2011) inputs. *J. Ind. Soc. Remote Sens.*, 1–10.

Tomilson, C. J., Chapman, L., Thomes, J., & Baker, C. J., (2011). Including the urban heat island in spatial heat health risk assessment strategies: a case study for Birmingham, UK. *Int. J. Health Geographics.*, *10*, 14.

Weng, Q., (2003). Fractal analysis of satellite-detected urban heat island effect. *Photogramm. Eng. Remote Sens.*, *69*, 555–566.

Zhang, Y., Odeh, I. O. A., & Han, C., (2009). Bi-temporal characterization of land surface temperature in relation to impervious surface area, NDVI and NDBI, using a sub-pixel image analysis. *Int. J. Appl. Earth Obs. Geoinf.*, *11*, 256–264.

CHAPTER 12

DERIVATION OF AN OPTIMAL OPERATION POLICY OF A MULTIPURPOSE RESERVOIR

PRABEER KUMAR PARHI

Centre for Water Engineering and Management, Central University of Jharkhand, Jharkhand, India
E-mail: prabeer11@yahoo.co.in

ABSTRACT

Zone-wise operating policy for conservation and flood control zones has been developed for Maithon Reservoir, on Barakar River, a major tributary of Damodar River, which is managed by Damodar Valley Corporation (DVC) in India. The operating policy for conservation and flood control zones has been designed respectively to confirm adequate water supply to different sectors and for real-time flood protection/management. For design, the concept of hedging rule, i.e., rationing of water through Monte-Carlo simulation (MCS) is applied. Further three storage performance indicators, i.e., reliability, resilience, and vulnerability have been tested. It is observed that the three system performance indicators are satisfactory.

12.1 INTRODUCTION

Multipurpose reservoirs are designed and operated to satisfy domestic and industrial water supply, irrigation, hydropower generation, navigation, recreation, environmental flow as well as flood control requirements. Most of the reservoirs are divided into three storage zones (a) dead storage zone, (b) conservation zone, and (c) flood control zone having each zone have its specific objective and operating characteristic. Among the above storage zones, the conservation zone is responsible for water supply to different

sectors and organizations whereas flood control zone is used to control and mitigate the flood in monsoon period.

In the available literature, many researchers have discussed on a different policy of reservoir operations like Standard Operating Policy (SOP), Linear Decision Rule (LDR), Pack Rule, Space Rule and different forms of the Hedging Rule in the area of water supply for conservation zone of the multipurpose reservoir. Among the above policies, SOP (Loucks et al., 1981; Stedinger, 1984; Marien et al., 1994) is the simplest policy which aims at releasing the water according to the demand (if possible) and preserve water for future needs if the water is available only after meeting the demands. However, SOP neglects the consideration of potential shortage vulnerability during later periods which is the main limitation of this rule. To overcome this limitation hedging rule (Masse, 1946; Bower et al., 1962; Klemes, 1977; Loucks et al., 1981; Shih and ReVelle, 1994, 1995) came into operation which is based on equal value margin principle. In a recent discussion, Draper and Lund (2004) explained the hedging rule analytically as, at optimality, the marginal benefit of storage (S) must equal the marginal benefits of release (D), which can be expressed as:

$$\frac{\partial C(S)}{\partial S} = \frac{\partial B(D)}{\partial D} \tag{1}$$

where, C(S) = carryover storage function, and B(D) = benefit delivery function. This shows that if B(D) is linear, then SOP is the best optimal policy for reservoir operation and if B(D) is non-linear then hedging rule is the optimal policy. Extending this work of Draper and Lund, (2004), You and Cai (2008) explicitly included uncertain future reservoir inflow in the future marginal value expression and discussed factors that influence hedging rule. Incorporating Monte-Carlo Simulation (MCS) with hedging rule with a different parameter of hedging, Srinivasan and Philipose (1998) investigated reservoir storage performance indicators. In the case of reservoirs with limited capacities and significant perennial water supply demands, the conservation zone usually overlaps with the flood control zone. This overlap yields a normal level that is higher than the initial level, thus prompting the necessary prerelease prior to the actual beginning of a flood. One of the most important aspects of mitigating the damaging impacts of floods is the real-time operation of flood control systems. According to Chow and Wu (2010), flood control includes three flood stages, (a) stage prior to flood arrival, in which water releases are to be managed in such a manner that enough reservoir capacity is available for the upcoming flood; (b) stage preceding peak flow, in which floodwater releases are for disaster mitigation; and (c) stage after

peak flow, in which releases are to be regulated such that the storage at the end of the flood are available for future use. Further, the performance of a reservoir operation policy is usually expressed in terms of three performance indicators such as reliability, resiliency, and vulnerability (Vogel and Bolognese, 1995; Kundzewicz and Kindler, 1995; Jain and Bhuniya, 2008; Raje and Majumdar, 2010).

In the above context, the present study attempts to: (a) formulate a zone-wise reservoir operation policy such that the available water is rationally used in such a manner (both in conservation zone and flood control zone) that the water requirement for different purpose is satisfied adequately along with flood mitigation; and (b) evaluate different performance indices such as reliability (volume reliability, time reliability, and annual reliability), resiliency, and vulnerability with respect to two important reservoir functions (water supply and flood control). As a case study, the proposed methodology is applied to the Maithon Reservoir, situated in the States of Jharkhand and West Bengal under Damodar Valley Corporation (DVC) in India.

12.2 MATERIALS AND METHODS

For the purpose of analysis the Maithon Reservoir on Barakar River, a major tributary of Damodar River is considered. The reservoir is situated in the States of Jharkhand and West Bengal and managed by DVC in India. The catchment area of the reservoir is 5309.4 km^2 and is primarily designed to control flood during the monsoon and provide irrigation, domestic, and industrial water supply along with hydropower generation. For reservoir analysis, the inflow and outflow time series has been collected and the combined time-series over the time period 1981 to 2013 has been plotted. Figure 12.1 shows the combined time-series of inflow and outflow for the Maithen Reservoir over the time period 1981 to 2013.

12.2.1 METHODOLOGY

12.2.1.1 MONTE-CARLO SIMULATION-BASED HEDGING MODEL

In the present study, a hedging based simulation model has been developed for the Maithon reservoir which states that the marginal benefit of release is equal to the marginal benefit of storage. For a water supply reservoir, the available storage (AS_t) is calculated which is equal to initial storage (S_t) for

time period *t* plus current inflow (I_t) for time period *t* minus evaporation loss (Et) for that time which is represented by Eq. (2).

$$ASt = St + It - Et \quad (2)$$

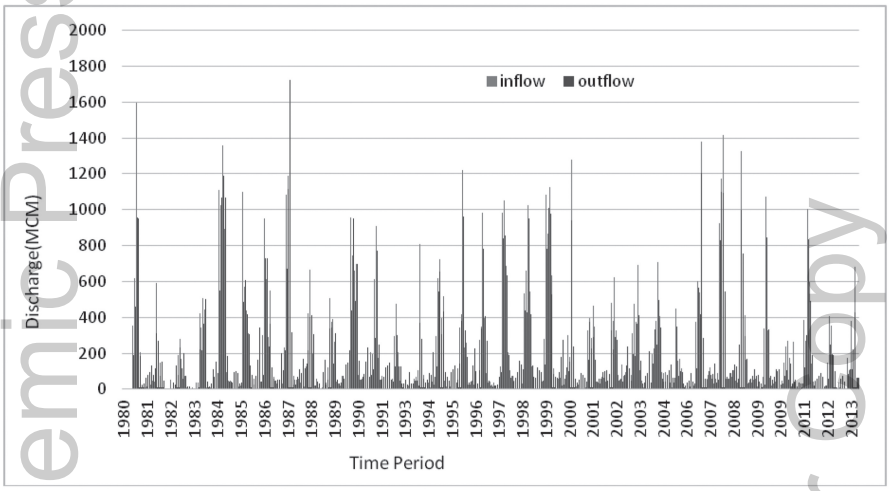

FIGURE 12.1 Combined time-series of inflow and outflow overtime period 1981 to 2013.

The time *t* lies between 0 and K, where K is active reservoir capacity.

This AS_t can be multiplied by hedging factor (H_f) so that some amount of AS_t water can be hedged for future use. The hedging factor can be taken as a discrete random variable (Rv) for the respective month. However, due to the availability of low storage during the months of May to June Rv may be taken as less and relatively more during July to April. In the present study the MCS model has been developed taking hedging factor as random variable divided by 10,000 such that:

$$H_f = Rv/10{,}000 \quad (3)$$

If $5000 < Rv < 10{,}000$, than for July to April $0.5 < H_f < 1$ and if $1000 < Rv < 2000$, than for May to June $0.1 < H_f < 2$.

Using MCS, 15 runs are being conducted for different random variables. Figure 12.2 shows the changing trajectory of random variable in MCS. Now available water for release (A_w) is equal to hedging factor multiplied by AS_t.

$$A_w = ASt * H_f \quad (4)$$

If these random variable change then the value of available water for release will also change, and this can be done through MCS. Now if available water

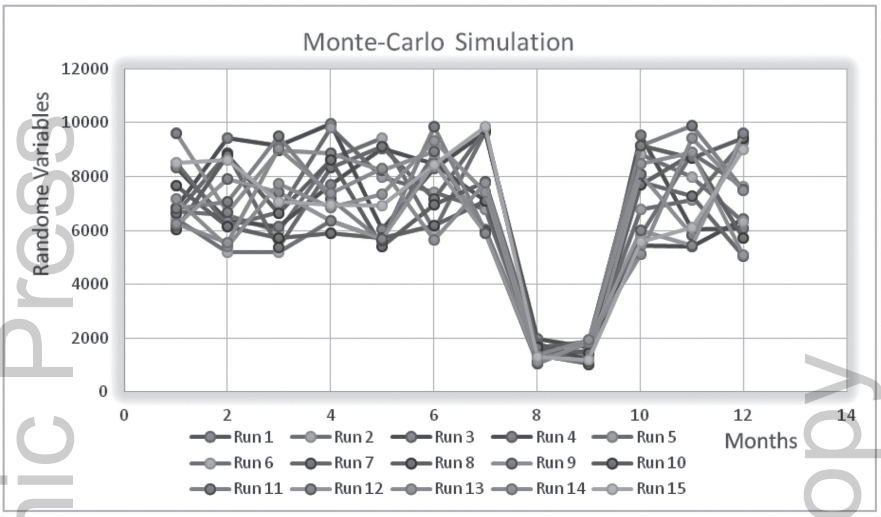

FIGURE 12.2 (See color insert.) Changing the trajectory of a random variable in Monte-Carlo simulation.

for release is less than the total demand (D_t), then water to be released (R_t) is equal to available water for release, and if available water for release is greater than the total demand, then water released is equal to total demand. Mathematically it can be represented as:

If $A_w \leq D_t$, then $R_t = Aw$, thus the hedged water (Hw) = A_w – ASt *H_f. And also

If $A_w \geq D_t$, then $R_t = D_t$, thus the hedged water (Hw) = $A_w - R_t$

The above theory implies that the water available at time *t* is either allocated to the projected demand at a time *t* or stored in the reservoir for possible future use. The water available after water release (A_{w1}) at a time *t* is equal to the sum of the water hedged for storage plus available water for release (A_w) minus water released (R_t) in the reservoir at the end of time 't.' This can be expressed as:

$$A_{w1} = A_w - R_t + Hw \tag{5}$$

Now the reservoir storage for next period (S_{t+1}) can be calculated using the hedged water as:

If, $A_{w1} \geq S_{max,}$ the outflow (O_t) = $A_{w1} - S_{max,}$ where S_{max} is the reservoir capacity. And

if, $A_{w1} \leq S_{max}$, the outflow (O_t) = $A_{w1} - S_{max}$. Hence

$$S_{t+1} = A_{w1} - R_t - O_t \tag{6}$$

Eq. (6) predicts AS_t for next time period. This storage will be used to estimate the AS_t of the reservoir for further next time period and so on. Thus the model has been developed through hedging rule for 12 months through MCS by changing the random variable, i.e., hedging factor by 5000 times. The best operating policy for water supply has been chosen among the 5000 iteration results with maximum reliability of Maithon Reservoir.

12.2.1.2 STATISTICAL MODEL FOR FLOOD MITIGATION

The chances of flood occurrence become more when the flood control zone provided is not sufficient to accommodate the expected flood. The flood control zone can be managed optimally by managing the outflow of water to reduce the water level with respect to inflow.

A relationship can be derived between water level (L) and the ratio of outflow to inflow (O_{t+1}/I_t) by multiple linear regression equation from historical data as:

$$(Y_i) = \beta\ (X_i) \tag{7}$$

where i = 1, 2, 3,…., n, Y = water level, X = (O_{t+1}/I_t) and β is constant which is calculated by multiple linear regression equation. The ratio of outflow to inflow at any time *t* (O_{t+1}/I_t) can be represented by a function 'α' known as flood reduction ratio and is represented by:

$$\alpha = \beta * (O_{t+1}/I_t)$$

$$\text{Or, } O_{t+1} = (\alpha/\beta)*I_t \tag{8}$$

The value of 'α' varies from 0 to 1, such that when the value of 'α' is '0,' $Ot_{+1} = 0$, i.e., all the inflow is retained in the reservoir and when the value of 'α' is '1,' $Ot_{+1} = I_t$, i.e., all the inflow is released as the outflow from reservoir. For flood control, the value of 'α' is calculated by linear interpolation between 0 and 1 at a different level of flood control zone using Eq. (8).

12.2.1.3 PERFORMANCE EVALUATION OF THE MODEL

The performance of the simulation model is evaluated using three statistical performance indices, viz. reliability with respect to water supply and flood control and vulnerability with respect to flood damages and water supply.

Reliability with respect to water supply: The reliability of a system can be described by the frequency or probability that a system is in a satisfactory

state. Three reliability indices are generally considered in water resources planning and management.

Time reliability (R_t) is estimated by a number of failure periods (fp) for a particular demand out of the total periods (Tp).

$$R_t = 1 - (fp/Tp) \text{ such that } fp \leq Tp \tag{9}$$

Volume or quantity-based reliability (R_v) is expressed as:

$$R_v = V_s/V_d \tag{10}$$

where V_s is the volume of water supplied and V_d the volume of water demanded during a given period. Annual reliability is an analogous way to express time reliability. But the difference is that the time period is one year. Annual reliability can be estimated by:

$$Ra = 1 - (Fy/Ty) \tag{11}$$

where Fy is the number of failure years when the annual supply is less than the annual demand over a total duration of Ty years.

A vulnerability with respect to flood damages and water supply: The mean vulnerability was simplified by Kjeldsen and Rosbjerg (2004) as:

$$V_{mean} = \frac{1}{M}\sum_{j=1}^{M} Vj \tag{12}$$

where, vj is the excess volume over the maximum live storage (for flood control purpose)/deficit volume than the particular demand (water supply purpose) of the j^{th} failure event and M is the number of failure events.

12.3 RESULTS AND DISCUSSION

12.3.1 MONTE-CARLO SIMULATION-BASED HEDGING

Applying the hedging rule based on MCS to the Maithon reservoir in which 75% of dependable monthly inflow has been taken for model development, 5000 iterations are carried out to choose the best hedging policy among 5000 results. The derived hedging policy based on MCS is shown in Figure 12.3 for Maithon Reservoir. Accordingly, an operation rule curve is designed based on the derived policy through an algorithm that is altered according to the alternative adaptation strategies. The rule curve is designed based on this derived policy through an algorithm that is altered according to the alternative adaptation strategies. This is based on the algorithm as A = f(Q), where

A is a set of monthly reservoir storage levels and Q = $\{q_1, q_2, ..., q_n\}$ is a set of daily inflow sequences. Thus based on this policy, a rule curve is developed for the conservation zone of Maithon Reservoir.

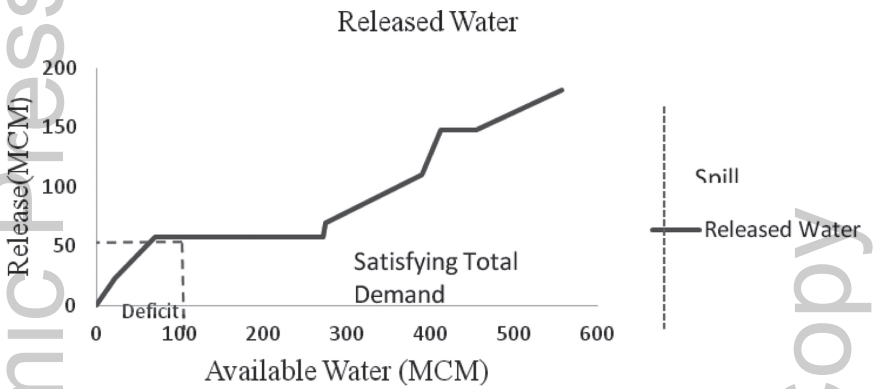

FIGURE 12.3 Hedging policy based on Monte-Carlo simulation for Maithon reservoir.

12.3.2 FLOOD MITIGATION POLICY FOR MAITHON RESERVOIR

Eq. (8) has been derived from a statistical approach is used to derive a flood mitigation policy. In Eq. (8), the value of β and α is calculated according to interpolation at a different level of flood control zone, i.e., between 146.31m and 151m. After putting the ratio of α/β and inflow at a particular height, the value of outflow can be estimated. Table 12.1 shows the different levels of flood control and their corresponding α/β value.

This method of flood mitigation is very simple and easy. As the occurrence of the flood is mainly due to flood peak, this model reduces the flood peak in a manner that the reservoir storage is reduced to optimum storage and optimal water is released to mitigate downstream flooding without allowing water surface level of the reservoir to exceed the acceptable safety level of the flood control zone.

12.3.3 EVALUATION OF PERFORMANCE INDICATORS

The performance of the simulation model has been assessed by estimating various statistical performance indices, i.e., time reliability, volume reliability and annual reliability with respect to water supply, resilience, and

vulnerability in connection with water supply and flood damages. From the results, water supply reliability for fulfilling municipal and industrial demands was found to be 100%. The results of other parameters for Monte-Carlo based hedging model are presented in Table 12.2.

TABLE 12.1 Level of Flood Control and Their Corresponding α/β Value

Level (m)	Value of α/β	Level (m)	Value of α/β	Level (m)	Value of α/β	Level (m)	Value of α/β	Level (m)	Value of α/β
146.3	0.000	147.3	0.219	148.3	0.4387	149.3	0.658	150.3	0.877
146.4	0.022	147.4	0.241	148.4	0.4606	149.4	0.680	150.4	0.899
146.5	0.044	147.5	0.255	148.5	0.4826	149.5	0.702	150.5	0.921
146.6	0.066	147.6	0.277	148.6	0.504	149.6	0.724	150.6	0.943
146.7	0.088	147.7	0.298	148.7	0.526	149.7	0.746	150.7	0.965
146.8	0.110	147.8	0.319	148.8	0.548	149.8	0.768	150.8	0.987
146.9	0.132	147.9	0.351	148.9	0.570	149.9	0.790	150.9	1.008993
147	0.154	148	0.373	149	0.592	150	0.812	151	1.030928
147.1	0.175	148.1	0.395	149.1	0.614	150.1	0.834		
147.2	0.197	148.2	0.417	149.2	0.636	150.2	0.855		

TABLE 12.2 Various Performance Indicators for Monte-Carlo Based Hedging Model

Performance Indicators	Reliability (%)			Resilience	Vulnerability (For water supply in MCM)		Vulnerability (For Flood damages in MCM)	
MCS based Hedging Model	Volume	Time	Annual	0.83	Mean	Max	Mean	Max
	86.74	83.33	82.35		126.60	87.80	33.656	33.65

From the above analysis it is found that as more water becomes available to meet the demands, the reliability of the system increases and the system becomes less vulnerable with respect to water supply but more vulnerable with respect to flood damages. As the percentage dependability of inflow increases that is the availability of water decreases the slope of reliability with respect to water supply also decreases but vulnerability with respect to water supply increases and with respect to flood damages decreases. However, the resiliency does not follow the same trend; it measures the relative recovery speed of the system from an unsatisfactory state. Hence as more water becomes available, the unsatisfactory periods are eliminated or shortened. But, as resiliency is a relative measure, if the recovery time is

long, relative to the total unsatisfactory period, the resiliency decreases even though the reliability of the system improves.

12.4 CONCLUSIONS

This paper discusses the optimality conditions for reservoir operation with evaluation of performance indicators including optimal release policy for conservation zone and flood mitigation policy for flood control zone. Implications for optimal reservoir operation for conservation zone have been derived through Monte Carlo Simulation-based hedging model whereas flood mitigation policy has derived on the basis of statistical approach and testing with Maithon reservoir under Damoder Valley Corporation in India. The result shows that the Maithen Reservoir is capable of satisfying the water requirement in terms of volume is 86.74%, and the reservoir can satisfy the demands 83.33% times, and its annual reliability is 82.35%. Similarly, the resilience which stands for the ratio of the number of times the system moved from failure to success, to the total number of periods the system was in failure state is 83. The vulnerability, i.e., the maximum period deficit is 87.87 MCM for water supply and 33.65 MCM for the flood.

KEYWORDS

- **hedging rule**
- **Monte-Carlo simulation**
- **performance indicators**
- **reservoir operation policy**
- **statistical method**

REFERENCES

Bower, B. T., Hufschmidt, M. M., & Reedy, W. W., (1962). In: Maass, A., et al., (eds.), *Operating Procedures: Their Role in the Design of Water-Resources Systems by Simulation Analyses, in Design of Water-Resource Systems* (pp. 443–458). Harvard Univ. Press, Cambridge, Mass.

Chou, F. N. F., & Wu, C. W., (2010). Stage-wise optimizing operating rules for flood control in a multi-purpose reservoir. *Journal of Hydrology*, *521*, 245–260.

Draper, A. J., & Lund, J. R., (2004). Optimal hedging and carryover storage value. *J. Water Resour. Plan Manag.*, *130*(1), 83–87.

Jain, S. K., & Bhunya, P. K., (2008). Reliability, resilience, and vulnerability of a multipurpose storage reservoir. *Hydrological Sciences Journal*, *53*(2), 434–447.

Klemes, V., (1977). Value of information in reservoir optimization, *Water Resour. Res*., *13*(5), 850–857, doi: 10.1029/WR013i005p00837.

Kundzewicz, Z. W., & Kindler, J., (1995). Multiple criteria for evaluation of reliability aspects of water resources systems. In: *Modeling and Management of Sustainable Basin-scale Water Resources* (pp. 217–224). IAHS Publ. 231. IAHS Press, Wallingford, UK.

Loucks, D. P., Stedinger, J. R., & Haith, D. A., (1981). *Water Resources Systems Planning and Analysis*, Prentice-Hall, Englewood Cliffs, NJ.

Marien, J. L., Damáio, J. M., & Costa, F. S., (1994). Building flood control rule curves for multipurpose multireservoir systems using controllability conditions, *Water Resour. Res.*, *30*(4), 1135–1144, doi: 10.1029/93WR03100.

Masse, P., (1946). *Les Reserves et la Regulation de l'Avenir Dans la vie Economique* (Vol. I), Avenir Determine (in French), Hermann and Cie, Paris.

Raje, D., & Mujumdar, P. P., (2010). Reservoir performance under uncertainty in hydrologic impacts of climate change. *Adv. Water Resour.*, *33*, 312–326.

Shih, J. S., & ReVelle, C., (1994). Water supply operations during drought: Continuous hedging rule. *J. Water Resour. Plan. Manage*, *120*(5), 613–629.

Shih, J. S., & ReVelle, C., (1995). Water supply operations during drought: A discrete hedging rule, *Eur. J. Oper. Res*., *82*, 163–175.

Srinivasan, K., & Philipose, M. C., (1998). Effect of hedging on over-year reservoir performance, *Water Resources Management*, *12*(2), 95–120.

Stedinger, J. R., (1984). The performance of LDR models for preliminary design and reservoir operation, *Water Resource Research*, *20*(2), 215–224.

Vogel, R. M., & Bolognese, R. A., (1995). Storage–reliability–resiliency–yield relations for over-year water supply systems. *Water Resour. Res*., *31*(3), 645–654.

You, J. Y., & Cai, X., (2008). Hedging rule for reservoir operations: A numerical model. *Water Resources Research*, *44*, 1–11.

CHAPTER 13

GLACIERS AND GLACIAL LAKE OUTBURST FLOOD RISK MODELING FOR FLOOD MANAGEMENT

NITY TIRKEY[1], P. K. PARHI[2], and A. K. LOHANI[3]

[1]*Research Scholar, Central University of Jharkhand, Ranchi, India, E-mail: nitytirkey@gmail.com*

[2]*Assistant Professor, Centre for Water Engineering and Management, Central University of Jharkhand, Ranchi, India*

[3]*Scientist G, National Institute of Hydrology, Roorkee, Jharkhand, Ranchi, India*

ABSTRACT

Global temperature rise has been responsible for the depletion of glaciers and consequently creation of lakes on their terminus. Several of these lakes had burst and caused flooding or Glacial Lake Outburst Floods (GLOFs) in the recent past. GLOFs have the potential of releasing millions of cubic meters of water in a very small time period causing catastrophic flooding downstream and damaging whatever comes into their way. Study of GLOFs hazard in Sutlej River basin using geospatial techniques consisting of satellite remote sensing, geographical information system, is proposed in this chapter. The outcomes of the proposed study will be helpful for GLOFs risk management and for developing an overall strategy to address possible risks from future GLOF events in the country.

13.1 INTRODUCTION

Worldwide receding of mountain glaciers is one of the most reliable evidence of the changing global climate. Globally, the impacts of climate

change include rising temperatures, shifts in rainfall pattern, melting of glaciers and sea ice, the risk of glacial lake outburst floods (GLOFs), sea level rise and increased intensity and frequency of extreme weather events (Ganguly et al., 2010). The climatic change/variability in recent decades has made considerable impacts on the glacier lifecycle in the Himalayan region. The Himalayas are geologically young and fragile and are vulnerable to even insignificant changes in the climatic system (Lama et al., 2009). Glaciers and glacial lakes play an important role in maintaining ecosystem stability as they act as buffers and regulate runoff water supply to plains during both dry and wet seasons. The glaciers and glacial lakes are generally located in remote and inaccessible areas. The inventories are only possible using time series remote sensing data and geographic information system (GIS) technology. The mountain ecosystems are fragile and highly susceptible to global climate changes. GLOF occurs when a dam containing a glacial lake fails. This is mainly due to the glaciers retreat. As glaciers retreat, glacial lakes are formed behind moraine or ice dams or inside the glaciers. A sudden breach in its walls may lead to a discharge of huge volumes of water and debris. Several of such lakes have been burst in the recent past resulting in a loss of human lives and destruction and damages of infrastructure in the valleys below. Glacier-outburst floods cannot be predicted, and therefore, continuous monitoring and mapping, both spatial and temporal, as opposed to a limited frequency point measurement can reduce the devastating impact of such hazards. Sometimes it is not easy to avoid natural phenomena causing disasters such as GLOFs, but a prior knowledge about their nature and possible extent can develop a capacity of disaster management authorities to respond and recover from emergency and disaster events. Similarly, hazard maps cannot stop a disastrous event from happening, but an effective use of hazard maps can prevent an extreme event from becoming a disaster. Himachal Pradesh is a mountain state in Indian Himalayas covering an area of 55,673 km^2. Himachal Pradesh has four major river basins namely Satluj, Beas, Chenab, and Ravi. Satluj basin alone covers 45% of the total geographical area of the state (923,645 km^2). The basin is very active and experiences regular floods causing widespread damage in the down valleys.

Due to global climate fluctuations, the water resources of the river basin are going to be altered over time. Hence a systematic study of water resources in the basin is pre-requisite for embarking on development plans. Keeping these facts in view the present study on the inventory of glaciers and glacial lakes in Satluj basin was undertaken to see the changes in the glacier lakes.

13.2 MATERIALS AND METHODS

13.2.1 STUDY AREA

The study area of the Satluj river basin lies between 30°22′ to 32°42′ N Longitude and 75°57′ to 78°51′ East Latitude in Himachal Pradesh. The basin constitutes parts of the districts of Lahaul & Spiti, Kinnaur, Shimla, Kullu, Mandi, Bilaspur, Solan, Sirmour, and Una. The basin exists in the topographic maps published by the Survey of India (SOI) vide numbers 53A, 53E, 52H, 52L, 53I, and 53F published in the 1960's–1970's on the scale of 1:50,000. The river Sutlej is one of the main tributaries of Indus and has its origin near Manasarowar and Rakas lakes in Tibetan plateau at an elevation of about 4,500 m (approx.). The entire Satluj basin has been divided into three sub-basins viz. Spiti as sub-basin number 1, Upper Tibet as 3 and Lower Satluj as sub-basin number 2 (Figure 13.1).

FIGURE 13.1 Different river basin.

13.2.2 METHODOLOGY

A digital database of glaciers and glacial lakes is necessary to identify the potentially dangerous glacial lakes. To identify the individual glaciers and glacial lakes, different image enhancement techniques are useful. The

ERDAS imagine 9.3 and Arc GIS 10.2.2 have been used for the processing of satellite data and GIS analysis.

13.3 RESULTS AND DISCUSSION

In the Himalayas, during the retreating phase, a large number of lakes are being formed either at the snout of the glacier as a result of damming of the moronic material known as moraine-dammed lakes or supraglacial lakes formed in the glacier surface area. Most of these lakes are formed by the accumulation of vast amounts of water from the melting of snow and by blockade of end moraines located in the down valleys close to the glaciers. In addition, the lakes can also be formed due to landslides causing artificial blocks in the waterways. The sudden break of a moraine/block may generate the discharge of large volumes of water and debris from these glacial lakes and water bodies causing flash floods namely GLOF. The sudden bursts of lakes can happen due to erosion, a buildup of water pressure, an avalanche of rock or heavy snow, an earthquake, or if a large enough portion of a glacier breaks off and massively displaces the waters in a glacial lake at its base (Figure 13.2).

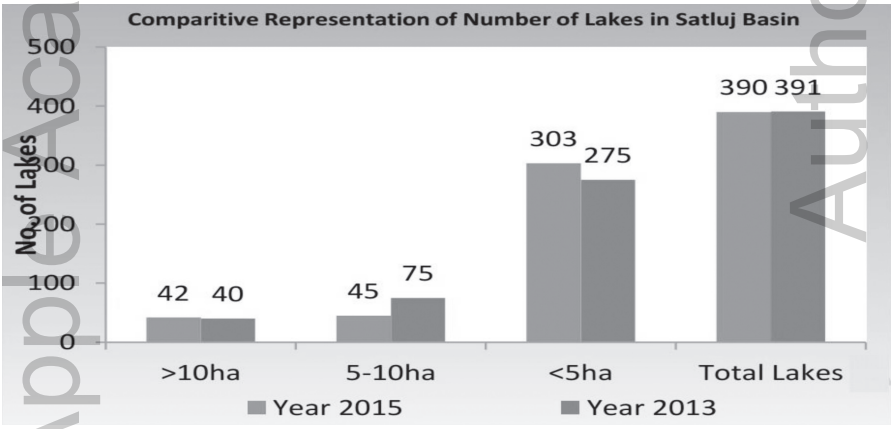

FIGURE 13.2 Number of lakes formed during the year 2013 and 2015.

There is a considerable increase in the number of moraine-dammed lakes (GLOFs) in Satluj basin which reflects that formation of such lakes in the Higher Himalayan region is indicating an increasing trend. The higher number of smaller lakes, i.e., lakes with an area less than 5 hectares indicates that the effect of the climatic variations is more pronounced on the glaciers

of the Himalayan region resulting in the formation of small lakes in front of the glacier snouts due to the damming of the moronic material. The lakes with an area more than 10 hectares and those with the area between 5–10 hectares are more vulnerable sites for causing damage in case of the bursting of any one of them. Therefore, a proper monitoring and change analysis of all such lakes in the higher Himalayan region of the State is critical for averting any future eventuality in Himachal Pradesh, so that the precious human lives are saved.

13.4 SUMMARY

The study indicated that eighty percent of Satluj river catchment is snow fed. The glaciers were found to be mostly distributed in the northeastern part of the basin. A total of 38 moraine-dammed lakes were identified in the Satluj basin (Kulkarni et al., 2001), out of which 14 lakes were in the Himachal part, and the remaining 24 lakes were in the Tibetan part which has been increased to 391 which includes the Spiti and the Baspa basins.

KEYWORDS

- **GIS**
- **glacier lake outburst flood**
- **glacier lakes**

REFERENCES

Ganguly, K., & Panda, G. R., (2010). *Adaptation to Climate Change in India: A Study of Union Budgets*. Oxfam India working papers series – OIWPS – I.

Randhawa, S. S., Sood, R. K., & Kulkarni, A. V., (2001). Delineation of moraine-dammed lakes in Himachal Pradesh using high-resolution IRS LISS III satellite data. *Proc. National Symposium on Advances in Remote Sensing Technology With Special Emphasis on High-Resolution Imagery*, SAC Ahmadabad.

CHAPTER 14

DETERMINATION OF DESIGN PARAMETERS FOR THE BORDER IRRIGATION METHOD

GARIMA JHARIYA[1], RAJEEV RANJAN[2], PRATIBHA WARWADE[3], K. L. MISHRA[2], and V. K. JAIN[4]

[1]*Institute of Agricultural Sciences, Banaras Hindu University, Varanasi (U.P.), 221005, India, E-mail: garima2304@gmail.com*

[2]*Collage of Agricultural Engineering, Jawaharlal Nehru Krishi Vishva Vidhyala Jabalpur (M.P.) – 480661, India*

[3]*Center for Water Engineering and Management, Central University of Jharkhand, Brambe, Ranchi–835205, India*

[4]*Subject Matter Specialist, KVK, RVSKVV, Ashok Nagar, Madhya Pradesh, India*

ABSTRACT

Surface irrigation analysis and design require the knowledge of the variation of the cumulative infiltration water (per unit area) into the soil as a function of the infiltration time. The purpose of this study is to evaluate Design parameters for border irrigation system water infiltration and storage under surface irrigation in a cultivated field. The factors affecting the design parameter are infiltration, slop, roughness time of pounding, etc. The infiltration characteristics are shown by plotting graph between accumulated infiltration and average infiltration rate against elapsed time by the data obtained from concentric cylindrical infiltrometer and the values of b = –2.42, α = 0.3131 and a = 0.2268 which is desirable in sandy loam soil. The slope is found out to be 0.20%, the time of ponding is approximately 27.03 min, hydraulic resistance is 0.0274, the Manning's roughness coefficient is 0.01219. The application efficiency is found out to be 55.99%.

14.1 INTRODUCTION

Border irrigation is an old surface irrigation system used in the western part of the United States to irrigate alfalfa, wheat, other small grains, and sometimes close growing row crops. The concept is to flush a large volume of water over a relatively flat field surface in a short period of time. Borders are raised beds or levees constructed in the direction of the field's slope. The idea is to release water into the area between the borders at the high end of the field. The borders guide the water down the slope as a shallow sheet that spreads out uniformly between the borders.

The crop should be flat planted in the direction of the field slope or possibly at a slight angle to the slope. The spacing between borders is dependent on soil type, field slope, pumping capacity, and field length and field width. A clay soil that cracks is sometimes difficult to irrigate, but with borders, the cracking actually helps as a distribution system between the borders. The border-spacing on sandy and silt loam soils that tend to seal or crust over is more of a challenge than with the cracking clays. The pumping capacity and field dimensions (length and width) are used to determine the number of borders needed and how many can be irrigated in a reasonable time.

The general most of the methods of surface irrigation include four phases advance, storage, depletion, and recession (Walker and Skogerboe, 1987; Alazba, 1999; Amer, 2004) with the objective to maximize a measure of merit (performance criterion) while minimizing some undesirable consequences. This border irrigation has no of advantage over other surface irrigation methods If can be used on a field that is usually flood irrigated. The aim of this work is to study the suitability of border irrigation system for the dusty area farm of J.N.K.V.V. Jabalpur and to determine the different parameters of the border irrigation system of that area.

14.2 MATERIALS AND METHODS

The area proposed for the study is dusty area farm of J.N.K.V.V. Jabalpur at the distance of about 6 km from district headquarter. The area received an average annual rainfall 1354 mm; most of which occurs July to be the south-west monsoon. This indicated that the area has a sub-tropical climate. Maximum temperature is 45°C in the month of May and minimum of 9.3°C in December. Longitude –78°21' E to 80°58'E & Latitude –22°29' N to 24°48'N. The surface texture of majority of the area is Sandy loam soil.

14.2.1 INFILTRATION MEASUREMENT

The infiltration rate (I) is the volume of water infiltrating through a horizontal unit area of soil surface at any instant (infinitely small period of time) (the unit is L T^{-1}, cmh^{-1}). The main aim of preparing infiltration curve through this test is to obtain basic infiltration which is constant infiltration rate for medium. Using the field data as t_1 and t_2 obtained from infiltration measurement experiment the rectifying value of t is found from the relation

$$t_3 = \sqrt{(t_1 * t_2)} \quad (1)$$

where, t is the elapsed time. The corresponding value of Y_3 was determined from the graph plotted between accumulated infiltration rates against elapsed time based on data presented in Table 14.1. The value of constant b is obtained as follows:

$$b = \frac{\left(y_1 y_2 - y_3^{\,2}\right)}{\left(y_1 + y_2 - 2 * y^3\right)} \quad (2)$$

The value of b is subtracted from each value of y. The logarithmic form of the equation

$$y = at^a + b \quad (3)$$

$$\text{Log } (y - b) = \log a + \alpha \log t$$

Initial soil moisture content was measured before measuring the infiltration rate. Infiltration (cumulative and/or rate) of the soil was measured using double ring method (Ankeny, 1992; Reynolds et al., 2002) before irrigation for more than location along border furrow.

14.2.2 LAND SLOPE

Irrigation border and furrows have a uniform downfield gradient. The maximum land slope is limited by consideration of soil erosion by the irrigation stream and rainfall. A dumpy level, a level rod (staff) and a measuring chain or tape are required for the survey to determine land slope border strips. When the land slope is uniform, the percentage slope is determined as follows:

$$\text{Percentage slope} = \frac{\text{Difference in elevation between the first and last point}}{\text{Distance between the first and last point}}$$

14.2.3 OPPORTUNITY TIME

The time interval during which infiltration of water into the soil can occur is bounded by the advance and recession functions and is defined as the infiltration opportunity time (Holizapfel et al., 1984; DeTar, 1989; Foroud et al., 1996; Rodriguez, 2003). The infiltration opportunity time of the selected area is calculated by plotting advance and recession curves. The difference between the times, the waterfront reaches a particular point along the border (or furrow) and the time at which the tailwater recesses from the assumed point is the infiltration opportunity time.

14.2.4 HYDRAULIC RESISTANCE

The Darcy-Weisbach resistance coefficient for the non-vegetated border strips was calculated from the modified form of the Blasiu's formula applicable to border strips which are expressed as follows:

$$f = \frac{0.316}{(49q|\upsilon)^{\frac{1}{4}}} \tag{4}$$

where, f is Darcy-Weisbach resistance coefficient, q is the discharge (liter/sec), and υ is the Kinematics' viscosity of water (cm^2/sec).

$$\upsilon = \mu / \rho$$

where, μ is given as dynamic viscosity of water (dyne-sec/cm^2), and ρ is the mass density of water (gm/cm^3)

$$\mu = \frac{0.0179}{(1 + 0.03368T + 0.000221T^2)} \tag{5}$$

where, T = temperature of water.

14.2.5 MANNING'S ROUGHNESS CO-EFFICIENT

In non-vegetated borders, when the hydraulic resistance is expressed by the Darcy-Weisbach friction factor 'f,' the equivalent value of Manning's 'n' is calculated using the following relationship:

$$n = \frac{\left(R^{2/3} \times \sqrt{f}\right)}{\left(\sqrt{8} \times \sqrt{g}\right)} \quad (6)$$

where, R is the hydraulic radius in meters, g is the acceleration due to gravity in ms^{-2}, and t is the Darcy-Weisbach friction factor.

14.2.6 APPLICATION EFFICIENCY

The application efficiency is determined by conducting the experiment in the field, by using the method to take moisture sample in borders strips before and after irrigations, and find out the moisture reach in the zone supplied in the field. The water application efficiency is influenced by the factors like amount of water applied in unit time (stream size), infiltration characteristics of the soil, and the rate of advancing front in the furrow.

$$\text{Application efficiency} = \frac{\text{Water stored in the root zone}}{\text{Water applied to the field}}$$

14.2.7 SOILBULK DENSITY

For calculating bulk density core cutter method was used and is given by:

$$\text{Bulk Density= Mass/Volume (gm cm}^{-3}\text{)}$$

14.3 RESULTS AND DISCUSSION

The result obtained from the investigation carried on the sites stated as before are categorized into infiltration characteristics of the project site, opportunity time, slope, hydraulic resistance, meanings roughness co-efficient, and application efficiency.

14.3.1 INFILTRATION CHARACTERISTICS

Infiltration test was performed at two different places in the same field at dusty area J.N.K.V.V. farm. The infiltration started with the very high infiltration rate (18 cm h^{-1}), which decreased very rapidly to 9 cm h^{-1} within 5 min. It further went on decreasing till the constant rate of 1.65 cm h^{-1}

was achieved at the end of 70 min, time period of the test. Studies made on infiltration are presented in Figures 14.1 and 14.2. Figure 14.1 indicates the two curves, i.e., average infiltration rate & accumulated infiltration depth as a function of time was found out to be 18.70 and the constants b = –2.42, α = 0.3131 and a = 2.2268. The values observed and calculated accumulated infiltration rate are given in Table 14.1.

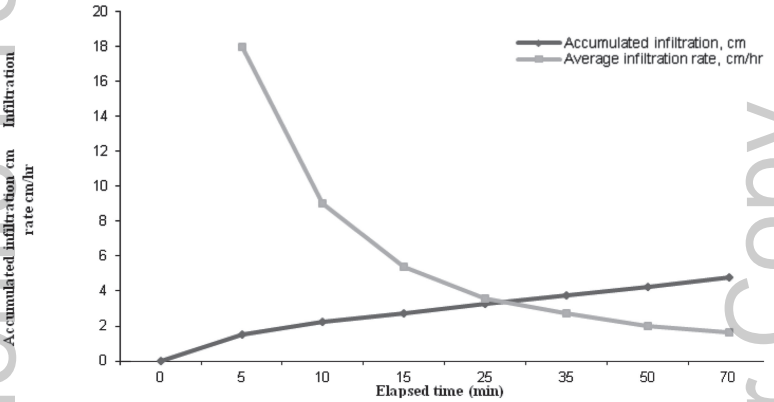

FIGURE 14.1 Plots of average accumulated infiltration and average infiltration rate against elapsed time-based.

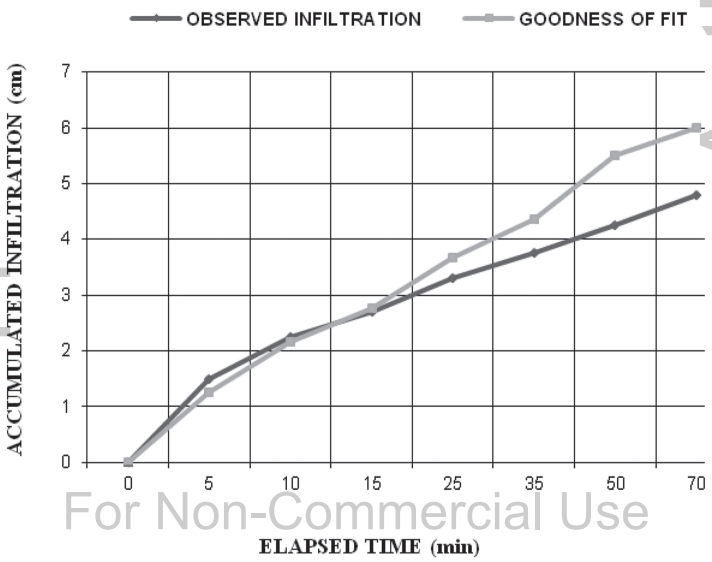

FIGURE 14.2 Compare of observed accumulated infiltration and goodness of fit against elapsed time.

TABLE 14.1 Average Infiltration Test Performed in Two Different Plots

S. No.	Elapsed Time *t* (Min)	Average Infiltration Rate (cm/hr)	Average Accumulated Infiltration 'Y' (cm)	Goodness of Fit 'Y' (cm)
1	0	-	-	-
2	5	18	1.5	1.266
3	10	9	2.25	2.159
4	15	5.4	2.7	2.770
5	25	3.6	3.3	3.680
6	35	2.7	3.75	4.358
7	50	2.0	4.25	5.506
8	70	1.65	4.8	6.001

14.3.2 HYDRAULIC RESISTANCE

The hydraulic resistance in non-vegetated border strip is expressed as Darcy-Weisbach resistance coefficient "f." The value of "f" is obtained 0.0274 by using Blasius empirical equation.

14.3.3 ROUGHNESS CO-EFFICIENT

The Manning's 'n' Roughness coefficient is found in the dusty area of JNKVV farm is 0.01219 and bulk density obtained in this field is 1.7 gm cc^{-1} which is more clearly explained from the Table 14.2 sowing the data obtained for bulk density.

TABLE 14.2 Average Bulk Density Performed in Two Different Sites for Different Depth

S. No	Depth (cm)	Weight of Wet Soil (gm)	Weight of Dry Soil (gm)	Bulk Density (gm cm^{-3})
1	0–17.5	2663	2324	1.657
2	17.5–35	2680	2392	1.7060
3	35–52.5	2.715	2433	1.735
Average Bulk Density				1.6994 ≈1.70

14.3.4 INFILTRATION OPPORTUNITY TIME

The infiltration opportunity time at any point along a border is the vertical distance between the advance and recession curve at the point. In the

Figure 14.3, the average time of pounding is 27 min 3 sec at the distance of 11 m. The graph represented shows that the relationship between the time of advance and time of recession. When irrigation started in border strip, pump discharge is 3.37 l/sec first water advance time up to 10m is very rapid and it took only 63 sec. After that the time of advance is slow and the total time taken by the water to reach the end of the strip is 16 min. 3 sec. Avg. Recession time is 27 min. 3 sec (Table 14.3).

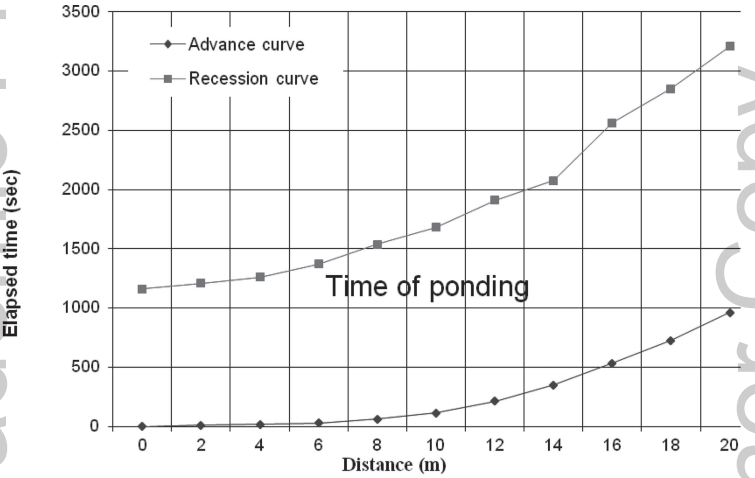

FIGURE 14.3 Advance and recession curves against distance.

TABLE 14.3 Water Advanced Front for Border Size (Average Depth of Water = 7.72 cm)

S. No.	Border Length (M)	Water Advance Time (Min-Sec)	Recession Time (Min-Sec)	Time of Ponding (Min-Sec)	Deviation From Average time of Ponding (Min-Sec)
1	0	0	19–22	19–22	+7–41
2	2	0–8	20–08	20–00	+7–03
3	4	0–16	21–02	20–46	+6–17
4	6	0–29	22–52	22–23	+4–40
5	8	1–03	25–37	24–34	+2–29
6	10	1–52	28–03	26–11	+0–52
7	12	3–32	31–52	28–20	–1–17
8	14	5–48	34–35	29–13	–2–10
9	16	8–54	42–42	33–48	–6–45
10	18	12–05	47–33	35–28	–8–25
11	20	16–03	53–30	37–27	–10–24

14.3.5 APPLICATION EFFICIENCY

The application efficiency determined by conducting an experiment in dusty area field of JNKVV farm is found to be 55.99%.

14.4 CONCLUSIONS

A design procedure for border irrigation system based on the conservation of mass has been developed. The present method presumes that the border has a free overfall outlet and uniform field parameters, slope, roughness, and infiltration. The design criterion is to select the appropriate inflow rate and time of cutoff so that the maximum or possibly desired efficiency is obtained efficiency which is the primary criterion in border irrigation system design and management. The study sites selected for the present study in the dusty area of J.N.K.V.V. farm, which come under Jabalpur (M.P.). The study area composed of mostly by cultivated field, which uses for border irrigation easily adopted in the field. The infiltration characteristics are shown by plotting graph between accumulated infiltration and average infiltration rate against elapsed time by the data obtained from concentric cylindrical infiltrometer are desirable in sandy loam soil. Designed hydraulics of border irrigation system shows it is well adapted for this area.

KEYWORDS

- **application efficiency**
- **border irrigation**
- **infiltration rate**
- **time of pounding**

REFERENCES

Alazba, A. A., (1999). Dimensionless advance curves for infiltration families. *Agricultural Water Management*, *41*, 115–131.

Amer, A. M., (2004). *Soil Hydro-Physics* (2nd Part, p. 438, in Arabic). Agricultural irrigation and drainage. El-Dar Al Arabia for Publish. & Distrib. Cairo, Egypt.

Ankeny, M. D., (1992). Methods and theory for unconfined infiltration measurements. In: Topp, G. C., (ed.), *Advances in Measurement of Soil Physical Properties: Bringing Theory Into Practice* (pp. 123–141). SSSA Spec. Publ. 30. SSSA, Madison, WI.

DeTar, W. R., (1989). Infiltration functions from furrow stream advance. *Journal of Irrigation and Drainage Engineering – ASCE, 115*(4), 722–730.

Foroud, N., George, E. S., & Entz, T., (1996). Determination of infiltration rate from border irrigation advance and recession trajectories. *Agricultural Water Management, 30*, 133–142.

Holizapfel, E. A., Marino, M. A., & Morales, J. C., (1984). Comparison and selection of furrow irrigation models. *Agricultural Water Management*, *9*, 105–111.

Reynolds, W. D., Elrick, D. E., & Young, E. G., (2002). Single-ring and double-ring or concentric-ring infiltrometers. In: Dane, J. H., & Topp, G. C., (eds.), *Methods of Soil Analysis* (Part 4, pp. 821–826). Physical Methods, SSSA, Madison, WI.

Rodriguez, J. A., (2003). Estimation of advance and infiltration equations in furrow irrigation for untested discharges. *Agricultural Water Management*, *60*, 227–239.

Walker, W. R., & Skogerboe, G. V., (1987). *Surface Irrigation: Theory and Practice* (p. 386). Prentice-Hall, Englewood Cliffs, NJ 07632.

CHAPTER 15

ENSO ASSOCIATION WITH RAINFALL

PRATIBHA WARWADE

Assistant Professor, Center for Water Engineering and Management, Central University of Jharkhand, Brambe Ranchi–835205, India, E-mail: pratibhawarwade@gmail.com

ABSTRACT

This study is mainly focused on Dikhow catchment which is a part Brahmaputra river basin, located between 94°28'49"E to 95°09' 52" E longitude and 26°52' 20"N to 26°03' 50" N latitude. The geographical area of Dikhow catchment is about 3100 km^2, which encompasses around 85% of Nagaland, ten percent of Assam and five percent of Arunachal Pradesh. This study is more precise to find out the relationship using between El Niño-Southern Oscillation (ENSO) and rainfall for Dikhow catchment, using statistical techniques. Monthly rainfall data of six stations of study area from 1950–2002 were acquired from the Indian Meteorological Department Pune and monthly SST anomalies of Niño of 3.4 regions (5°N to 5°S and 170°W to 120°W) during the study period (1950–2002) were downloaded from the NOAA, National Weather Service (NWS), and National Center for Environmental Prediction (NCEP), Climatic Prediction Center (CPC) (http://www.cpc.noaa.gov/data/indices), to classify ENSO events. Results showed that the significant correlation was found for monsoon rainfall only while winter and summer rainfall showing insignificant correlation. Sibsagar, Tirap, and Mon stations portrayed the significant correlation between monsoon rainfall with ENSO and insignificant correlation observed between remaining three stations. Further, the probability of exceedance of long-term average monsoon precipitation was also lower during El Niño episodes than La Niña and neutral years for these stations (Sibsagar, Tirap, and Mon).

15.1 INTRODUCTION

The El Niño-Southern Oscillation (ENSO) pattern is driven partly by alternating warmer and cooler temperatures of the sea surface in the eastern and central tropical Pacific Ocean, which themselves are caused by changes in upwelling currents. It changes to rain and temperatures over a large portion of the globe, with severe consequences to human activities like agriculture and fishing, which depend on meteorological conditions and ocean fluxes. In turn, the changes in weather and atmospheric circulation change in the ocean currents (Ward and Richardson, 2011). ENSO is a set of anomalously warm ocean water temperatures that infrequently develops off the western coast of South America and can cause climatic changes across the Pacific Ocean. Many of the researchers (Khandekar and Neralla, 1984; Ropelewaski and Halpert, 1987; Glantz et al., 1991; Diaz and Markgraf, 1992) found that the ENSO associated with climate irregularities all over the globe. Kousky et al. (1984) depicted that in Australia, Indonesia, India, and West Africa drought is strongly associated with ENSO. Investigators have been working on this issue (ENSO's connection with climate anomalies) since the late 1800s. El Niño (La Niña) is one of the environment related phenomena in the equatorial Pacific Ocean characterized by a five consecutive three-month running mean of sea surface temperature (SST) anomalies in the Niño 3.4 region of the threshold of ± 0.5°C. This standard of measure is known as the Oceanic Niño Index (ONI). As per the Census 2011, 54 percent of the Indian workforce is still occupied in agriculture, and 53 percent of the gross cropped area is about rainfed. ENSO has been known to exert the most important external forcing on Indian summer monsoon rainfall (ISMR) (Kumar et al., 1999; Rasmusson and Carpenter, 1983; Webster and Yang, 1992; Ropelewaski and Halpert, 1987; Chiew et al., 1998; Khole, 2000; Lau and Nath, 2000; Ashok et al., 2001; Krishnamurthy and Kirtman, 2009). The interannual variations of ISMR have motivated studies of the ENSO since the turn of the twentieth century (Walker, 1923; Barnett, 1984). ENSO studies have been used either to mitigate the impacts of adverse conditions or to take advantage of favorable conditions (Selvaraju, 2003).

Historically, scientists have classified the intensity of El Niño based on SST anomalies exceeding a pre-selected threshold in a certain region of the equatorial Pacific. The most commonly used region is the Niño 3.4 region, and the most commonly used threshold is a positive SST departure from normal greater than or equal to +0.5°C. Since this region encompasses the western half of the equatorial cold tongue region, it provides a good measure of important changes in SST and SST gradients that result in changes in the

pattern of deep tropical convection and atmospheric circulation. The criterion that is often used to classify El Niño episodes is that five consecutive 3-month running mean SST anomalies exceed the threshold.

Studies have shown that a necessary condition for the development and persistence of deep convection (enhanced cloudiness and precipitation) in the Tropics is that the local SST be 28°C or greater. Once the pattern of deep convection has been altered due to anomalous SSTs, the tropical and subtropical atmospheric circulation adjusts to the new pattern of tropical heating resulted in anomalous patterns of precipitation and temperature that extend well beyond the region of the equatorial Pacific. SST anomaly of +0.5°C in the Niño 3.4 region is sufficient to reach this threshold from late March to mid-June. During the remainder of the year a larger SST anomaly, up to +1.5°C in November-December-January, is required in order to reach the threshold to support persistent deep convection in that region.

Many investigations regarding ENSO Association with rainfall over Indian region are discussed here: Kirtman and Shukla, (2000) found a strong negative correlation between ENSO and ISMR using 100 years of historical record. A negative correlation is strongest during the months of December to March for east Pacific SSTA. Results show that monsoon variability and ENSO variability related to each other, strong (weak) monsoon results in a strengthening (weakening) of the trade winds over the tropical Pacific. Kripalani et al. (2003) examined the decadal variability and inter-annual for monsoon rainfall over India and its teleconnections using observed data for a period of 131 years (1871–2001). The study indicated that the inter-annual variability showed year-to-year variation, and the decadal variability showed distinct alternate epochs of above and below normal rainfall. Further, they studied the links between the ENSO phenomenon, the surface temperature of the Northern Hemisphere and Eurasian snow with Indian monsoon rainfall and stated that the correlations are not only weak but have altered signs in the early 1990s, suggesting that the IMR (Indian Monsoon Rainfall) has linked not on1y with the Pacific but with the Northern Hemisphere/Eurasian continent also. The fact that temperature/snow relationships with IMR are weak further suggests that global warming may not be responsible for the recent ENSO-Monsoon weakening. Further, they conveyed that warm phase (El Nino) is connected with the weakening of the Indian monsoon, and cold phase (La Niña) is connected with the strengthening of the Indian monsoon. Kumar et al. (2006) exposed that severe droughts in India always go along with El Niño events using 132 data of past rainfall. El Niño events along with SST anomalies in the central equatorial Pacific are very effective for producing drought subsidence in India than the events of warmest SSTs

in the eastern equatorial Pacific. Kumar et al. (2007) reported the inverse relationship between ENSO and southwest monsoon rainfall has weakened during the current years and positive relationship between ENSO and North East Monsoon (NEM) rainfall, which has strengthened and developed statistically significant after the mid-1970s. Epochal changes in the regional circulation features are one of the causes of this variation in the relationship. During the recent El Niño years, above normal NEM rainfall is experienced due to stronger easterly wind anomalies and anomalous low-level moisture convergence along with associated changes in the circulation regime throughout the troposphere and across the southern parts of India and Sri Lanka. Ihara et al., (2007) observed the relationship between the ENSO, state of the equatorial Indian Ocean, and ISMR data from 1881 to 1998 of 36 stations in India. SST anomalies and zonal wind anomalies over the equatorial Indian Ocean were used to reflect the situation of the Indian Ocean. Negative correlation with ISMR was observed, while significant with wind index during El Niño years. Krishnamurthy and Kirtman (2009) studied the relationship between the intra-seasonal modes of the South Asian monsoon and the SST in the tropical oceans on a daily timescale. The strong relation of the persistent modes, which mainly determine the seasonal mean monsoon, when the SST leads, provides hope for long-term prediction of the seasonal mean monsoon. The strong relationship between the monsoon and the SST, when the monsoon leads, points toward the strong influence of the monsoon on the variability of ENSO and IOD. Kumar et al. (2013) suggested that the major portion of the drought variability is influenced by the ENSO. Global warming, especially the warming of the equatorial Indian Ocean represents the second coupled mode and is responsible for the observed increase in the intensity of droughts during the recent decades over India. Krishnamurthy and Krishnamurthy (2014) studied decadal-scale oscillations and trend in the Indian monsoon rainfall: Using a long record of high-resolution Indian rainfall data, this study has established the existence of three decadal scale nonlinear oscillations and a nonlinear trend in the IMR. The monsoon rainfall decadal oscillations were shown to be associated with the decadal variability of the North Atlantic and North Pacific oceans. This paper associate's only rainfall with the variability of SST. Parida and Oinam, (2015) conveyed that drought associated with El Niño was not so strong; however, increasing temperature and increased monsoon season rainfall variability have an impact on global climate change. This may cause warming-induced drought leading to an adverse impact on agriculture and food security in the NER (North Eastern Region) of India.

The research on the links between ENSO and rainfall (Achuthavarier et al., 2012), at the regional scale only began in recent years. However, the ENSO does not display the same degree of correlation with different homogeneous regions of India on a longer timescale. Some regions are least impacted by ENSO, while others are moderate to strongly correlated with the phenomenon (Ashok and Saji, 2007). For managing water resources systems such study of regional scale is essential for water authority over the region as well as the country. Hence this study is more precise to present the relationship between ENSO and rainfall using statistical analysis.

15.2 MATERIALS AND METHODS

15.2.1 STUDY AREA

The study area is Dikhow catchment which is a part of the larger Brahmaputra river basin, Dikhow river which originates from the hills of the state Nagaland. It is a south bank tributary of river Brahmaputra contributing 0.7 % runoff. A lower Brahmaputra river basin, a region where the hydrological impact of climate change is expected to be particularly strong, and population pressure is high (Gain and Giupponi, 2015). Brahmaputra river is the biggest trans-Himalayan river basin (Sharma and Flugel, 2015). Figure 15.1 presents the location map and demonstrates with the drainage map of the study area situated between 94°28'49"E to 95°09' 52" E longitude and 26°52' 20"N to 26°03' 50" N latitude. The geographical area of Dikhow catchment is about 3100 km^2, which encompasses around 85% of Nagaland, 10% of Assam and 5% of Arunachal Pradesh. The river traverses towards the north along the border of Mokokchung and Tuensang districts. The main tributaries of river Dikhow are Yangyu of Tuensang district and Nanung in the Langpangkong range in Mokokchung district. The river flows further northward and leaves the hill near Sibsagar and finally merges with the Brahmaputra River in the plains of Assam.

The study area is remote and largely inaccessible, land cover changes by practicing *shifting* cultivation (slash and burn) predominantly. Stations considered for the present study are Sibsagar, Mokokchung, Mon, Tirap, Tuensang, and Zunheboto portrayed in Table 15.1 with their geographical location and elevation. Altitude of the study area varies from 98m to 1818 m (Sibsagar to Zunheboto). It is highly diversified in terms of elevation hence divided into three physiographic zones namely; Low Elevated Zone (LEZ), Moderate Elevated Zone (MEZ) and High Elevated Zone (HEZ),

because it is expected that each zone will respond differently. Stations below than 100 m from m.s.l., fall under LEZ also known as alluvial plain, stations between 101–1000 m elevation from m.s.l., covers the MEZ and stations between 1001 to 2000 m elevations from m.s.l., were classified as HEZ.

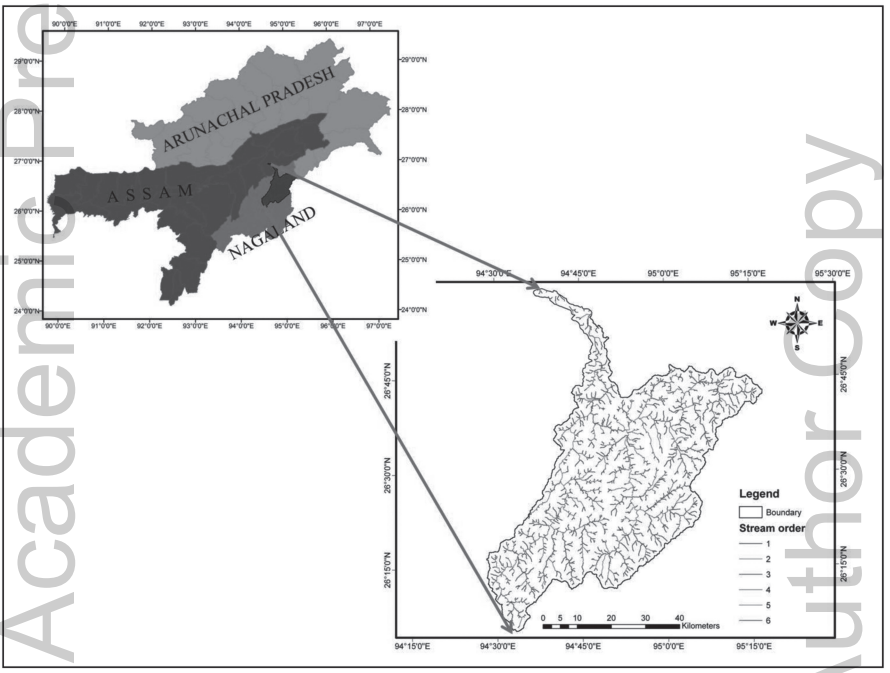

FIGURE 15.1 Location map of Dikhow catchment.

TABLE 15.1 Selected Stations of Study Area

S.N.	State	Station	Longitude (° 'N)	Altitude (m) (° 'E)	Latitude
1	Assam	Sibsagar	26° 5' 42"	94° 37' 42"	98
2	Nagaland	Mokokchung	26° 19' 20"	94° 30' 53"	1323
3	Nagaland	Mon	26° 43' 21"	94° 01' 52"	720
4	Arunachal Pradesh	Tirap	26° 59' 43"	95° 32' 27"	776
5	Nagaland	Tuensang	26° 14' 9"	94° 48' 46"	1570
6	Nagaland	Zunheboto	26° 00' 35"	94° 31'42"	1818

15.2.2 DETAILS OF DATA

The monthly precipitation data of six stations of Dikhow catchment for the years 1950–2002 were obtained from Indian Meteorological Department Pune. The monthly SST anomalies of Niño of 3.4 regions (5°N to 5°S and 170°W to 120°W) during the study period (1950–2002) were downloaded from the NOAA, National Weather Service (NWS), and National Centre for Environmental Prediction (NCEP), Climatic Prediction Centre (CPC) (http://www.cpc.noaa.gov/data/indices), to classify ENSO events.

15.3 METHODOLOGY

The methodology adopted for to find out the relationship between ENSO and rainfall are Pearson's Correlation Analysis, and Cumulative Distribution Frequency (CDF) discussed below.

15.3.1 PEARSON'S CORRELATION ANALYSIS

The correlation coefficient measures the strength of association between two continuous variables. Among several correlation analyses, three methods are common in use, i.e., Kendall's tau (τ), Spearman's rho and Pearson's correlation (r). The first two are based on ranks and measure all monotonic relationships. Also, these are resistant to the effect of outliers. In this study, Pearson's (r) correlation coefficient was calculated. Pearson's correlation (Crichton, 1999) is the most commonly used method to measure the correlation. As (r) measure the linear association between two variables, so it is also called linear correlation coefficient. Pearson's correlation was calculated using the formula:

$$r = \frac{1}{n-1}\sum_{i=1}^{n}\left(\frac{x_{i-\bar{x}}}{S_x}\right)\left(\frac{y_i - \bar{y}}{S_y}\right) \quad (1)$$

where x and y are precipitation and SST anomalies, respectively. The $\bar{x}$ and $\bar{y}$ are the mean, and S_x and S_y are the standard deviation of x and y, respectively, and n is the total number of years of analysis.

15.3.2 CUMULATIVE DISTRIBUTION FREQUENCY (CDF)

Cumulative frequency distribution (CDF) is a function that gives the probability that a random variable is less than or equal to the independent variable of the function. Steps to calculate CDF are given below:

Step 1: In the first step, precipitation data were first standardized by deducting the mean value from the observed value and dividing by the standard deviation. Note that the standardized time series has a zero mean and a unit standard deviation.

Step 2: In the next step, precipitation data for each El Nino, La Niña and neutral year time series were separated for each station and probability of exceedance for each event was calculated using a Weibull's formula. To calculate the probability of exceedance, the standardized data were arranged in descending order and rank (m) was assigned. For the first entry m = 1; for second m = 2 and so on till the last value as m = n. Then the experience of probability can be calculated by using many methods, but the most common formula was used, i.e., Weibull's formula of exceedance of probability as $(100\times m)/(n+1)$, where m is the m^{th} value in order of magnitude of the series and n is the number of data series.

Step 3: Now a plot was drawn between the probability of exceedance (in %) on the vertical axis and standardized precipitation data on the horizontal axis and the exceedance probability corresponding to zero precipitation was identified for each El Nino, La Niña and neutral years time series.

Step 4: The same procedure was repeated for each station to calculate the CDF. It was computed for monsoon season.

15.4 RESULTS AND DISCUSSIONS

The Southern Oscillation Index (SOI) and the SST are the two most widely used indicators of ENSO. The monthly time series of SST anomaly are used in this study. Teleconnection between ENSO and rainfall first requires the definition of "El Niño/Lal Niña" as years. Trenberth, 1997 stated that El Niño is an ocean-atmosphere phenomenon where the cooler Eastern Pacific warms up once in every two to seven years. Increase in Eastern Pacific SST is due to the weakening of the easterly trade wind that resulted in the warm water from the western Pacific moving to the east. NOAA, 2008 classified an ENSO event on the basis of SST. An average deviation of ±0.5°C from the historical mean of SST and for three consecutive months result shows an ENSO event. A positive anomaly indicates El Niño and a negative anomaly indicates La Niña.

15.4.1 ENSO EPISODES

Since in the 1950s, globally there has been 23 El Niño, 15 La Niña and 16 Neutral years occurred as presented in Table 15.2. Out of which we categorized as strong, moderate, and weak El Niño years on the basis of sea surface temperature anomalies (SSTA) presented in Table 15.3. SSTA of greater than 1.5 categorize as strong, SSTA ranges from 1–1.5 as moderate and SSTA ranges 0.5–1.0 categorized as weak El Niño years. Twelve strong, thirteen moderate, and nine weak El Niño years were obtained and are shown in Table 15.3.

TABLE 15.2 ENSO Episodes

S.N.	El Niño	La Niña	Neutral
1	1951	1950	1952
2	1953	1954	1960
3	1956	1955	1961
4	1957	9561	1962
5	1958	1964	1966
6	1959	1970	1967
7	1963	1971	1979
8	1965	1974	1980
9	1968	1975	1981
10	1969	1985	1984
11	1972	1988	1990
12	1973	1989	1993
13	1976	1998	1994
14	1977	1999	1995
15	1978	2000	1996
16	1982		2001
17	1983		
18	1986		
19	1987		
20	1991		
21	1992		
22	1997		
23	2002		

TABLE 15.3 Classification of El Niño Years.

Categories of El Niño years from 1950–2002			
S.N.	**SSTA>1.5**	**SSTA Ranges 1–1.5**	**SSTA Ranges 0.5–1**
	Strong	**Moderate**	**Weak**
1	1957	1951	1953
2	1958	1952	1954
3	1965	1963	1958
4	1966	1964	1959
5	1972	1968	1969
6	1973	1969	1970
7	1982	1986	1976
8	1983	1987	1977
9	1987	1991	1978
10	1988	1992	
11	1997	1994	
12	1998	1995	
13		2002	

15.4.2 PRECIPITATION RELATIONSHIP WITH ENSO

In the study area, three seasons viz., winter (November–February), summer (March–May), and monsoon (June–October) were defined to analyze the rainfall relationship with El Niño. The running mean of monthly anomalies of SST for each station was used to identify the number of years during El Niño, La Niña and neutral phase for the span of 1950–2002. Number of years in each ENSO phase during the study period in different seasons are presented in Table 15.4, and the number of El Niño episodes was higher during the winter followed by monsoon and summer.

TABLE 15.4 Number of Years in Each El Niño, La Niña, and Normal Phase During 1950–2002

Phase	Winter	Summer	Monsoon
El Niño	18	9	13
La Niña	17	11	15
Neutral	18	33	25

15.4.2.1 VARIATION OF PRECIPITATION DURING ENSO PHASES

The mean annual and seasonal precipitation during El Niño, La Niña and Neutral phase at different stations revealed in Table 15.5. The comparison of results of three ENSO phases shows that the mean of El Niño precipitation was less than the mean of La Niña and Neutral phase precipitation during monsoon season at all the stations. However, in winter season the mean of El Niño precipitation was more than La Niña and neutral phase precipitation. Moreover, the mean of El Niño precipitation was less than the mean of Neutral phase's precipitation in the summer season at all the stations. Results showed that the ENSO influences the seasonal precipitation in the study area which is also revealed by the study of Mooley and Parthasarathy (1983).

TABLE 15.5 Precipitation Variability in Each El Niño, La Niña and Normal Phase During 1950–2002

	Mean Precipitation During ENSO								
Station	**Winter**			**Summer**			**Monsoon**		
	El Niño	**La Niña**	**Normal**	**El Niño**	**La Niña**	**Normal**	**El Niño**	**La Niña**	**Normal**
Sibsagar	114.1	82.8	92.9	516.1	508.5	537.6	1450.4	1560.8	1499.8
Mokokchung	105.8	73.1	85.5	472.6	466.8	494.5	1460.9	1517.6	1479.7
Mon	104.4	75.2	86.1	453.9	444.8	472.5	1426.6	1504.9	1462.3
Tirap	100.4	74.8	83.8	420.6	412.6	438.2	1364.7	1463.0	1414.3
Tuensang	99.1	69.2	81.8	391.8	385.3	412.3	1454.4	1487.8	1464.7
Zunheboto	103.1	70.4	83.7	426.8	421.6	450.7	1487.4	1509.4	1486.8

15.4.2.2 CORRELATION ANALYSIS

The results of Pearson's correlation coefficient between ENSO and precipitation at 5% level of significance are shown in Table 15.6. The bold values are indicating a significant correlation. The results indicate a significant negative correlation between precipitation and ENSO during the monsoon season at Sibsagar, Mon, and Tirap. Remaining stations showed a non-significant positive correlation. During winter and summer, non-significant positive correlation between ENSO and precipitation were observed at all the stations. Negative correlations mean lower precipitation during El Niño and higher during the La Niña and vice-versa during positive correlation. Further analysis was performed only for monsoon season precipitation at all the stations because of significant correlation obtained for monsoon precipitation.

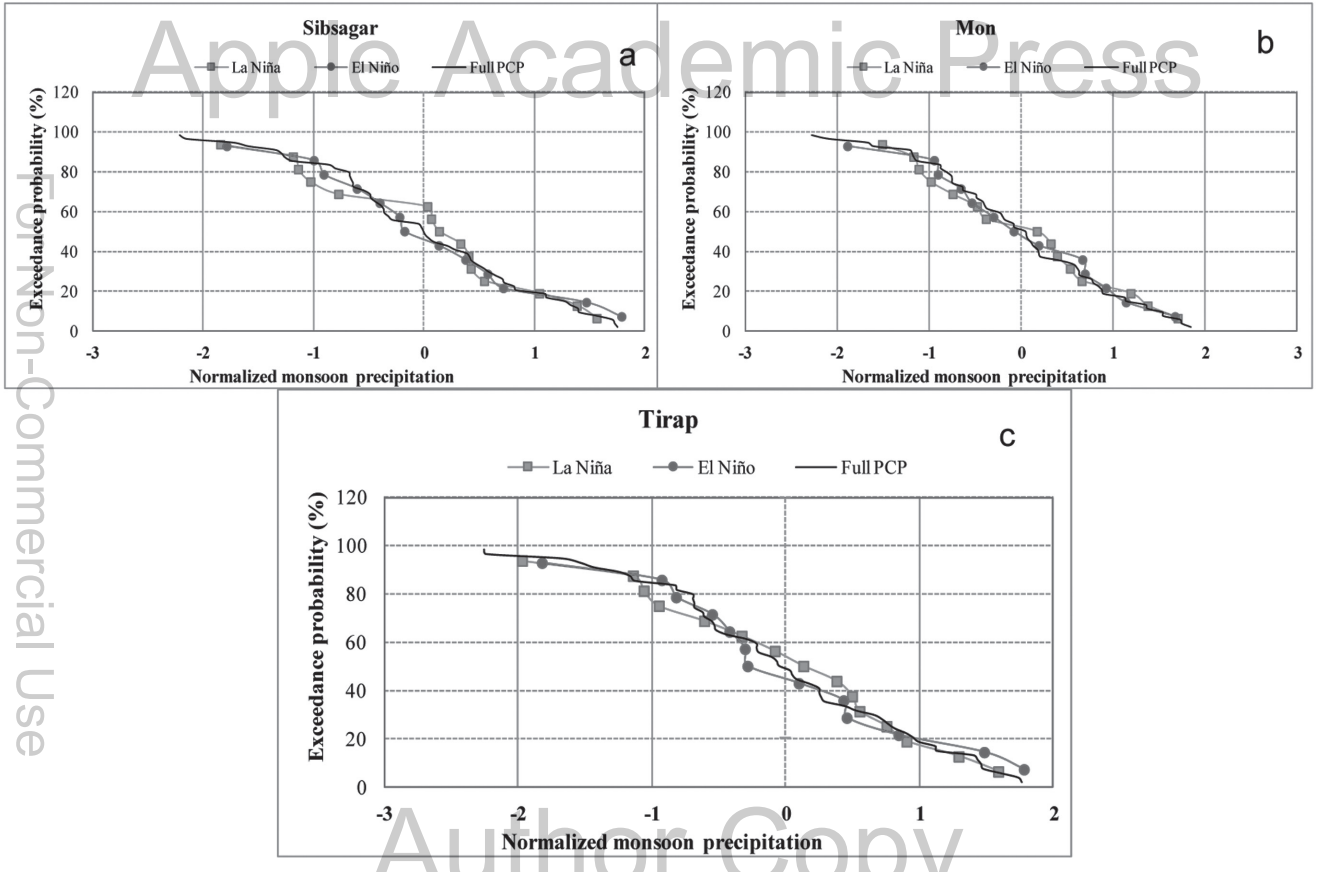

FIGURE 15.2 **(See color insert.)** Graph of the cumulative distribution of normalized monsoon precipitation during El Niño, La Niña and Normal phase for (a) Sibsagar, (b) Mon and (c) Tirap.

TABLE 15.6 Result of Pearson's Correlation Between ENSO and Precipitation

Station	Winter	Summer	Monsoon
Mokokchung	0.411	0.032	0.195
Sibsagar	0.321	0.023	–0.275
Tuensang	0.406	0.05	0.182
Zunheboto	0.418	0.043	0.158
Tirap	0.306	0.026	–0.270
Mon	0.353	0.036	–0.273

15.4.2.3 CUMULATIVE FREQUENCY DISTRIBUTION (CDF)

The CDF of normalized monsoon precipitation for El Niño, La Niña, and Normal series are shown in Figure 15.2a–c and Figure 15.3a–c, the black line represents the probability of normal series, while the red line with a circle and green line with square shows the probability of El Niño and La Niña series. For the normalized time series, the long-term average monsoon precipitation corresponds to zero. Figure 15.2a shows the probability of exceedance during El Niño years drops up to 45%, while for the La Niña years, this exceedance probability of long-term average rainfall reaches to 62% at Sibsagar. At Mon, the probability of exceedance during El Niño years was 46%, and during La Niña years it was 55% (Figure 15.2b), similarly at Tirap probability of exceedance during El Niño years was less (45%) than the exceedance probability during La Niña years (56%).

On the contrary, Figure 15.3a–c shows the exceedance probability of long-term average precipitation at Mokokchung, Tuensang, and Zunheboto. The probability of exceedance is 50%, 50% and 49% for El Niño, Neutral, and La Niña series for Mokokchung respectively. For Tuensang it was 52%, 49% and 45% for El Niño, Neutral, and La Niña series respectively. And for Zunheboto 54%, 48% and 45% probability of exceedance for El Niño, Neutral, and La Niña series respectively were obtained. It can be concluded that the probability of exceedance of average precipitation drops at Sibsagar, Mon, and Tirap during El Niño. Whereas for Mokokchung, Tuensang, and Zunheboto does not show the same (although the correlation of these stations between ENSO and precipitation were not significant). These results show that the effect of ENSO on the first three stations (Sibsagar, Mon, and Tirap). Although theses station were classified topographically into different zones, on this basis, it can be concluded that LEZ and HEZ shows the ENSO effect as reported in the study of Kripalani and Kulkarni (1997); Krishnamurthy

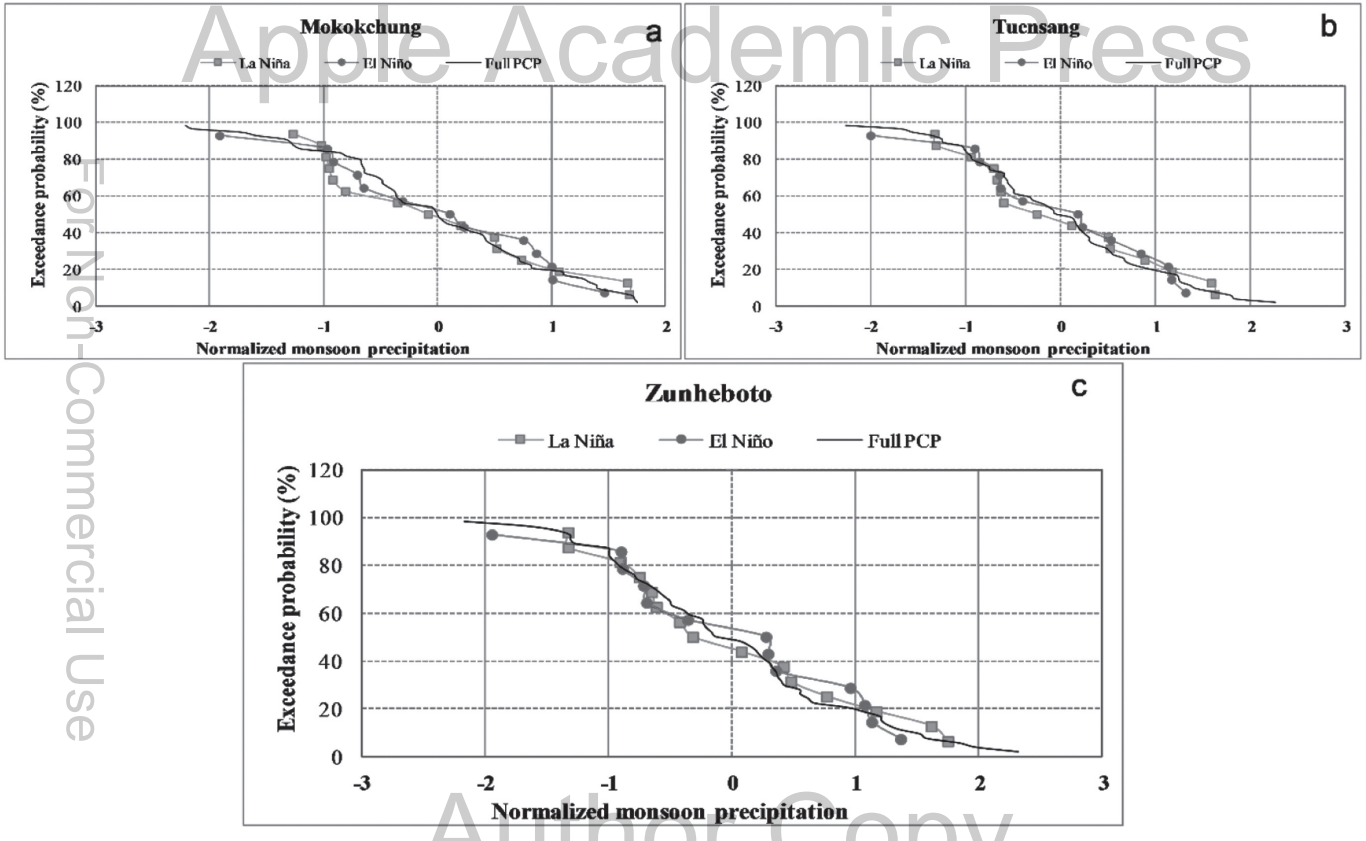

FIGURE 15.3 **(See color insert.)** Graph of the cumulative distribution of normalized monsoon precipitation during El Niño, La Niña and Neutral phase for (a) Mokokchung, (b) Tuensang and (c) Zunheboto.

and Goshwami (2000); Ashok et al. (2001) and Maity and Kumar (2006), wherein they reported that El Niño (La Niña) is associated with lower (higher) normal precipitation. Results are also in conformity with Walker (1924) in which he found that the relation between the Southern Oscillation and seasonal (June–September, JJAS) mean summer monsoon rainfall over India is one of the earliest observed teleconnections. The result shows, the influence of ENSO on monsoon precipitation observed over LEZ and MEZ of study region but not over the HEZ. There can be other factors too, such as mid-latitude circulation feature (Raman and Rao, 1981; Tanaka, 1982), wind speed at a point in the Arabian Sea (10° N 65° E) (Shukla and Mishra, 1977), Darwin pressure anomaly before monsoon season (Shukla and Paolino, 1983) and topography might have some role over the variability of rainfall in the region.

15.5 CONCLUSIONS

Region-specific study of the most important climatic variable, i.e., rainfall is essential to reduce the adverse effects of climate change in developing countries. Correlation analysis between ENSO and precipitation indicated a significant negative correlation in monsoon season for three stations (Sibsagar, Mon, and Tirap) in the catchment. Therefore, further analysis was carried out for monsoon season precipitation only. The CDF of standardized monsoon precipitation during El Niño, La Niña, and full-time series shows that the exceedance probability for average monsoon precipitation is less in El Niño years and more in La Niña years. It can also be concluded in terms of elevation that the LEZ and HEZ show the ENSO effect while there is no effect of ENSO over HEZ.

KEYWORDS

- **cumulative distribution frequency**
- **ENSO**
- **Nino 3.4 region**
- **Pearson's correlation coefficient**
- **SST**

REFERENCES

Achuthavarier, D., Krishnamurthy, V., Kirtman, B. P., & Huang, B., (2012). Role of the Indian Ocean in the ENSO-Indian summer monsoon teleconnection in the NCEP climate forecast system. *Journal of Climate*, *25*(7), 2490–2508.

Ashok, K., & Saji, N. H., (2007). On the impacts of ENSO and Indian Ocean dipole events on sub-regional Indian summer monsoon rainfall. *Natural Hazards*, *42*(2), 273–285.

Ashok, K., Guan, Z., & Yamagata, T., (2001). Impact of the Indian Ocean dipole on the relationship between the Indian monsoon rainfall and ENSO. *Geophysical Research Letters*, *28*(23), 4499–4502.

Barnett, T. P., (1984). Interaction of the monsoon and Pacific trade wind system at interannual timescales. Part III: A partial anatomy of the Southern Oscillation. *Monthly Weather Review*, *112*(12), 2388–2400.

Chiew, F. H., Piechota, T. C., Dracup, J. A., & McMahon, T. A., (1998). El Nino/Southern Oscillation and Australian rainfall, streamflow and drought: Links and potential for forecasting. *Journal of Hydrology*, *204*(1), 138–149.

Diaz, H. F., & Markgraf, V., (1992). *El Niño: Historical and Paleoclimatic Aspects of the Southern Oscillation*. Cambridge University Press.

Glantz, M. H., Katz, R. W., & Nicholls, N., (1991). *Teleconnections Linking Worldwide Climate Anomalies* (p. 535). Cambridge: Cambridge University Press.

Ihara, C., Kushnir, Y., Cane, M. A., & De La Peña, V. H., (2007). Indian summer monsoon rainfall and its link with ENSO and Indian Ocean climate indices. *International Journal of Climatology*, *27*(2), 179–187.

Khandekar, M. L., & Neralla, V. R., (1984). On the relationship between the sea surface temperatures in the equatorial Pacific and the Indian monsoon rainfall. *Geophysical Research Letters*, *11*(11), 1137–1140.

Khole, M., (2000). Anomalous warming over the Indian Ocean during 1997 El-Nino. *Meteorology and Atmospheric Physics*, *75*(1/2), 1–9.

Kirtman, B. P., & Shukla, J., (2000). Influence of the Indian summer monsoon on ENSO. *Quarterly Journal of the Royal Meteorological Society*, *126* (562), 213–239.

Kousky, V. E., Kagano, M. T., & Cavalcanti, I. F., (1984). A review of the Southern Oscillation: Oceanic-atmospheric circulation changes and related rainfall anomalies. *Tellus A.*, *36*(5), 490–504.

Kripalani, R. H., & Kulkarni, A., (1997). Climatic impact of El Nino/La Niña on the Indian monsoon: A new perspective. *Weather*, *52*(2), 39–46.

Kripalani, R. H., Kulkarni, A., Sabade, S. S., & Khandekar, M. L., (2003). Indian monsoon variability in a global warming scenario. *Natural Hazards*, *29*(2), 189–206.

Krishnamurthy, L., & Krishnamurthy, V., (2014). Decadal-scale oscillations and trend in the Indian monsoon rainfall. *Climate Dynamics*, *43*(1/2), 319–331.

Krishnamurthy, V., & Goswami, B. N., (2000). Indian monsoon-ENSO relationship on interdecadal timescale. *Journal of Climate*, *13*(3), 579–595.

Krishnamurthy, V., & Kirtman, B. P., (2009). Relation between Indian monsoon variability and SST. *Journal of Climate*, *22*(17), 4437–4458.

Kumar, K. K., Rajagopalan, B., & Cane, M. A., (1999). On the weakening relationship between the Indian monsoon and ENSO. *Science*, *284*(5423), 2156–2159.

Kumar, K. K., Rajagopalan, B., Hoerling, M., Bates, G., & Cane, M., (2006). Unraveling the mystery of Indian monsoon failure during El Niño. *Science*, *314*(5796), 115–119.

Kumar, K. N., Rajeevan, M., Pai, D. S., Srivastava, A. K., & Preethi, B., (2013). On the observed variability of monsoon droughts over India. *Weather and Climate Extremes*, *1*, 42–50.

Kumar, P., Kumar, K. R., Rajeevan, M., & Sahai, A. K., (2007). On the recent strengthening of the relationship between ENSO and northeast monsoon rainfall over South Asia. *Climate Dynamics*, *28*(6), 649–660.

Lau, N. C., & Nath, M. J., (2000). Impact of ENSO on the variability of the Asian-Australian monsoons as simulated in GCM experiments. *Journal of Climate*, *13*(24), 4287–4309.

Maity, R., & Nagesh, K. D., (2006). Bayesian dynamic modeling for monthly Indian summer monsoon rainfall using El Nino–Southern Oscillation (ENSO) and Equatorial Indian Ocean Oscillation (EQUINOO). *Journal of Geophysical Research: Atmospheres*, *111*(D7), 1–12.

Mooley, D. A., & Parthasarathy, B., (1983). Variability of the Indian summer monsoon and tropical circulation features. *Monthly Weather Review*, *111*(5), 967–978.

CHAPTER 16

EFFICIENT RESERVOIR OPERATION WITH A MULTI-OBJECTIVE ANALYSIS

PRITI SAGAR[1] and PRABEER KUMAR PARHI[2]

[1]*Research Scholar, Central University of Jharkhand, Centre for Water Engineering & Management, Bramby, 835205, Jharkhand, India, E-mail: sagarpriti68@gmail.com*

[2]*Assistant Professor, Central University of Jharkhand, Centre for Water Engineering & Management, Brambe, 835205, Jharkhand, India*

ABSTRACT

During the past several decades numerous major multiple-purpose reservoir systems have been constructed throughout the nation. About 5,500 large reservoir system exists in India, and generally, their operation is done through the rule curve. As demands on reservoir system is increasing day by day and along with this a continuously changing pattern of various factors like temperature, rainfall, land use land cover, etc. has been observed since the past several decades, evaluation of refinements and modifications in the existing operating rule or development of new policy of the reservoir systems is becoming an increasingly important activity. In the present study, an optimal operation policy has been developed for a multi-purpose reservoir, namely, Maithon Reservoir in order to maximize the hydropower production subject to the condition of satisfying the irrigation water demands (IWDs), domestic and industrial water demand (DIWD) with an eye on sustainable sediment management using a non-linear programming model (NLP). The operation policies have been derived by dividing the entire operation year into three segments, i.e., pre-monsoon (April to May), monsoon (June to October) and post-monsoon (November to March) in order to analyze the different possibilities during real-time operation. In each segment the percentage fulfillment of various purposes like IWD,

DIWD, and corresponding hydropower production are determined. The fulfillment of various purposes has been determined under 50%, 60%, and 80% and dependable inflow conditions. The distinguishing feature of this model is that it maximizes hydropower generation along with sustainable sediment management strategy also.

16.1 INTRODUCTION

Water is the most precious gift of nature, as the existence of no any flora or fauna is possible without water on this earth. It is a basic human need and a prime natural resource with finite dimensions which cannot be created and has no any other substitute. Although there is plenty of water present on the surface of the earth, only 3% of total water resources are fresh, and the rest 97% is contained in the seas and ocean as saline water. Out of the total fresh water, 75% occurs as polar ice and glaciers, and 24% remains in the subsoil. Only 1% of fresh water accounts for water in lakes and rivers.

The average annual rainfall in India is about 1170 mm, which corresponds to an annual precipitation (including snowfall) of 4000 billion m^3. Nearly 75% of this, i.e., 3000 billion m^3 occurs during monsoon season (June-September) in a year. Regional variations are also extreme in the country as the rainfall varies from 100 mm in Western Rajasthan to over 11000 mm in Meghalaya in Northeastern side of India. The extreme variability in the distribution of water (both temporally and spatially) makes the situation more complicated and seeks greater concern among water resource engineers and scientists, encouraging them for in-depth study and development of efficient surface water management systems and techniques.

During the past several decades, one of the most important advances made in the field of water resources engineering has been the development of optimization techniques for planning, design, and management of complex water resource system. Reservoirs are the most important component of a water resources development scheme, which serve to regulate natural stream-flow thereby modifying the temporal and spatial availability of water according to human needs. Optimal operation of reservoirs is crucial in the present context of water scarcity being faced by the country, due to a perceivable overall increase in water demands from various sectors like agricultural water demand, industrial and domestic water demand, hydropower generation demand, water pollution, and environmental concerns, flood mitigation concern, etc.

Due to continuously changing the pattern of land cover and land use in the upstream catchment the reservoir systems are becoming more vulnerable

to increased sediment load which reduces the live storage capacity of the reservoir. The multipurpose reservoir systems are subjected to intensive water management efforts due to competing demands from irrigation, domestic, industrial water supply, and hydropower production. With an eye on the above needs of the hour, there is a necessity to rethink the way for the refinement and modification to the existing operation policy accounting for changing hydrologic conditions and also for a sustainable sediment management strategy.

16.2 MATERIALS AND METHODS

16.2.1 STUDY AREA DESCRIPTION

In the present study, an optimal operation reservoir operation model has been developed and applied on the Maithon multi-purpose reservoir system, located at Maithon, 48km from Dhanbad district, in the state of Jharkhand, India. The reservoir is built on the river Barakar, a tributary of Damodar River (catchment area of 6294 km^2) and designed for flood control, hydropower generation, irrigation, navigation, municipal water supply, etc. for the states of Jharkhand and West Bengal State. Figure 16.1 describes the details of Damodar Basin.

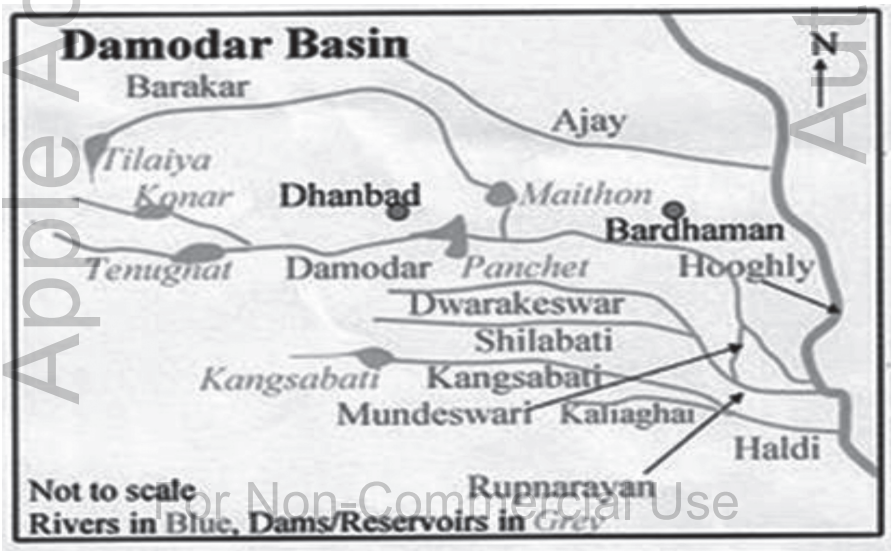

FIGURE 16.1 Index map of Damodar basin.

16.2.2 METHODOLOGY FOR HYDROPOWER OPTIMIZATION USING NLP

The present study attempts to develop an optimal operating policy which satisfies domestic, industrial, irrigation, and environmental flow demands optimally simultaneously producing optimum hydropower, optimum flood space with sustainable sediment management strategy. Optimal policy has been developed considering different dependable inflow levels for dry scenario (50% dependable inflow), normal scenario (60% dependable inflow) and wet scenario (80% dependable inflow), so that different possible operating policies can be generated, which will be helpful to the reservoir authorities in managing the real-time operation of the reservoir.

16.2.2.1 MODEL DESCRIPTION

In past time several optimization techniques have been applied to derive the optimal reservoir operational rules like linear programming (LP), non-linear programming (NLP), goal programming (GP), chance constraint linear programming (CCLP), dynamic programming (DP), and recently, the soft computing techniques. Among several techniques, NLP is widely applied for optimizing hydropower systems (Gagnon et al., 1974; Tejada-Guibert et al., 1990), since it is most accurate, involves no approximation and uses the physically based non-linear function (Barros et al., 2003). The software package LINGO (Language for Interactive General Optimizer) has been used to optimize hydropower generation from the reservoirs under consideration as both objective function and constraints are nonlinear.

16.2.2.2 OBJECTIVE FUNCTION

The various needs fulfilled by the Maithon dam operation has been modeled using the following objective function and constraints.

Objective: Maximize monthly hydropower production. Production of hydropower has been defined as:

$$Maximize\ (HP_t) = \sum_{t=1}^{12} [H_t \times R_t \times \eta \times \Upsilon_w] \quad (1)$$

where,

HP_t = monthly hydropower production in terms of kilowatt hours; (kWh) during month t;

H_t = monthly average head available during month *t*;
R_t = monthly release to powerhouse during month *t*;
η = combined turbine and generation efficiency;
Υ_w = specific weight of water.

16.2.2.3 CONSTRAINTS

Reservoir Water Mass Balance Constraint: The theory of conservation of mass has to be satisfied as mass can neither be created nor be destroyed.

$$S_{t+1} = S_t + I_t - R_t - Q_t - E_t - S_{pt} \quad (2)$$

where,

S_{t+1} = Final storage in MCM during month *t*;
S_t = Initial storage in MCM during month *t*;
I_t = Dependable inflow in MCM during month *t*;
R_t = Release in MCM during month *t*;
Q_t = Release through gates in MCM during month *t*;
E_t = Evaporation Loss in MCM during month *t*;
S_{pt} = Spill in MCM during month *t*.

Municipal and Industrial Demand Constraints: Generally, the average water requirements for Municipal and Industrial (M&I) purposes are quite constant throughout the year, as compared to the water requirements for irrigation or hydropower.

$$Q_t \geq IR_t + O_t \quad (3)$$

where,

O_t = Release made during any month *t* in MCM;
IR_t = Irrigation water demand (IWD) during any month *t* in MCM;
Q_t = Water requirement of sub-basin other then IWD at any time *t* in MCM.

Flood Control Constraint: The strategy adopted for controlling flood is that every month some free space must be allocated in the reservoir to handle uncertainties.

$$S_{max} - S_t \geq 50\% \textit{ of Flood Zone Space} \quad (4)$$

where,

S_t = Storage at the beginning of month 't';
S_{MAX} = Maximum reservoir capacity.

Channel Capacity Constraint: The water release through the power plant should not exceed the channel carrying capacity. This can be written as:

$$R_t \leq C \tag{5}$$

where,

C = Maximum carrying capacity of penstock during a month;
R_t = Release made during a month through penstock.

Bounds on Storage Constraint: The reservoir storage in any time should not be more than the maximum capacity of the reservoir and cannot fall below the dead storage level (DSL).

$$S_{MIN} \leq S_t \leq S_{MAX} \tag{6}$$

where,

S_{MAX} = Maximum capacity of the reservoir;
S_t = Storage capacity of the reservoir at the beginning of month *t*;
S_{MIN} = Minimum head required to produce electricity which is above the dead storage level.

Sediment Management Constraint: In reservoir planning, allowance is made for the storage of sediment. The volume provided for is known as dead storage. In this study, the allowance provided is equal to the minimum drawdown level (MDDL).

$$S_6 = 93\text{MCM} \tag{7}$$

where, S_6 = Storage at the starting of month June.

16.3 RESULTS AND DISCUSSION

In the present study, a monthly time step basis NLP model has been used to optimize the operational plans of Maithon reservoir to maximize the hydropower production with an eye on sustainable sediment management strategy. The above formulated NLP model is solved using LINGO/Global solver (Lingo User Guide Lindo Systems, Inc., Illinois, 2011). The developed NLP model is optimized for 50%, 60% and 80% dependable inflows, estimated by Weibull's method (Subramanya, 2008). Based on the constraints of the above formulated NLP model, several policies have been generated for each dependable inflow condition by varying the irrigation demands in each policy. These policies will be helpful to the reservoir operators in assessing the full potential of the reservoir system.

16.3.1 UNDER 50% DEPENDABLE INFLOW CONDITION

Under this condition, five policies have been made. Policy 1 says, keeping all the demands fully satisfied in all three segments except irrigation demand in monsoon and pre-monsoon season which satisfies 95% times. Policy 2 says, keeping all the demands fully satisfied in all three segments except irrigation demand in monsoon and pre-monsoon season which satisfies 85% times. Policy 3 says, keeping all the demands fully satisfied in all three segments except irrigation demand in monsoon and pre-monsoon season which satisfies 75% times. Policy 4 says, keeping all the demands fully satisfied in all three segments except irrigation demand in monsoon and pre-monsoon season which satisfies 65% times. Policy 5 says, keeping all the demands fully satisfied in all three segments except irrigation demand in monsoon and pre-monsoon season which satisfies 55% times.

16.3.2 UNDER 60% DEPENDABLE INFLOW CONDITION

Under this condition also five policies have been generated. Policy 1 says, keeping all the demands fully satisfied in all three segments except irrigation demand in monsoon and pre-monsoon season which satisfies 95% and 45% times respectively. Policy 2 says, keeping all the demands fully satisfied in all three segments except irrigation demand in monsoon and pre-monsoon season which satisfies 65%& 35% times, respectively. Policy 3 says, keeping all the demands fully satisfied in all three segments except irrigation demand in monsoon and pre-monsoon season which satisfies 55% and 25% times respectively. Policy 4 says, keeping all the demands fully satisfied in all three segments except irrigation demand in monsoon and pre-monsoon season which satisfies 35% and 15% times respectively. Policy 5 says, keeping all the demands fully satisfied in all three segments except irrigation demand in monsoon and pre-monsoon season which satisfies 25% and 0% times respectively.

16.3.3 UNDER 80% DEPENDABLE INFLOW CONDITION

For 80% inflow condition only one policy was found to be feasible. Keeping all the demands fully satisfied in all three segments except irrigation demand which satisfies 15% and 0% times in monsoon and pre-monsoon season, respectively.

16.3.4 OPTIMAL RESERVOIR OPERATION POLICY

The results shows that at 50% dependable inflow, the policy 1 satisfies all the requirements during all the segments 100% times (except pre-monsoon irrigation demand which is satisfied 90% times) and produces minimum annual hydropower of 94653.45 mWh and trial 5 produces maximum annual hydropower of 98270.39 mWh satisfying all the requirements during all the segments 100% times (except pre-monsoon and monsoon irrigation demand which is satisfied 55% times). In a similar way considering different dependable inflows (60% and 80%) various feasible trials have been derived and corresponding annual hydropower generation have been shown in Table 16.1.

TABLE 16.1 Annual Hydropower Production From Various Policies for Different Inflow Conditions

Policy	Annual hydropower (mWh/yr) for dependable inflow conditions		
	50%	**60%**	**80%**
1	94653.45	64503.42	42312.06
2	95410.64	65310.83	-
3	97009.48	66057.95	-
4	97536.36	66805.95	-
5	98270.39	66819.27	-

For 80% inflow condition only one policy was found to be feasible. On comparing all the five policies, it was found that on relaxing the irrigation release slightly the power production can be increased. The derived policy of tradeoffs between irrigation release and hydropower generation will be helpful to the reservoir operators and engineers in assessing the full potential of the reservoir system.

16.4 SUMMARY

A wide range of researches has been carried out in the field of reservoir operation policies. Among those researches, optimizing hydropower production was found to be the main point of focus by many researchers. One of the key feature of this model which distinguishes it from the other one is that it focuses on optimizing hydropower production with the aim of sediment management strategy also. The study also indicates that there is a good scope for further research and development in this field.

Following conclusions are derived based on the above study:

- In the present study, the Maithon reservoir operation policies have been optimized for hydropower production while satisfying all other demands using the NLP model.
- The derived policy is capable of producing maximum hydropower of 98270.39, 66819.27, and 42312.06 mWh/year for 50%, 60%, and 80% dependable inflow conditions, respectively.
- The derived model can be useful in minimizing sediment deposit and thus increasing the reservoir life.

KEYWORDS

- **efficient reservoir operation**
- **operation policy**
- **optimal hydropower generation**
- **sustainable sediment management**

REFERENCES

Arunkumar, R., & Jothiprakash, V., (2012). Optimal reservoir operation for hydropower generation using Non-linear programming model. *Journal of Institution of Engineers, India*, *93*(2), 111–120.

Barros, M. T. L., Tsai, F. T. C., Yang, S. L., Lopes, J. E. G., & Yeh, W. W. G., (2003). Optimization of large-scale hydropower system operations. *Journal of Water Resource Planning and Management, ASCE*, *129*(3), 178–188.

Gagnon, C. R., Hicks, R. H., Jacoby, S. L. S., & Kowalik, J. S., (1974). A nonlinear programming approach to a very large hydroelectric system optimization. *Math Program*, *6*, 28–41.

Husain, A., (2012). An overview of reservoir systems operation techniques. *International Journal of Engineering Research and Development*, *4*(10), 30–37.

Lingo User Guide, (2011). (Lindo Systems, Inc., Illinois), p. 834.

Subramanya, K., (2008). *Engineering Hydrology* (3rd edn., p. 452). Tata McGraw-Hill Education Pvt. Ltd.

Tejada-Guibert, J. A., Stedinger, J. R., & Staschus, K., (1990). Optimization of value of CVP's hydropower production. *Journal of Water Resource Planning and Management, ASCE*, *116*(1), 52–70.

CHAPTER 17

AN ANALYSIS OF FLOOD CONTROL IN EASTERN SOUTH ASIA

AMARTYA KUMAR BHATTACHARYA

Chairman and Managing Director, MultiSpectra Consultants, 23, Biplabi Ambika Chakraborty Sarani, Kolkata – 700029, West Bengal, India, E-mail: dramartyakumar@gmail.com

ABSTRACT

This chapter studies the causes and features of floods and measures for the control of floods in eastern India and Bangladesh. Structural as well as non-structural measures are being emphasized for flood management in both India and Bangladesh. It has been proved that non-structural measures have a significant effect on flood damage minimization.

17.1 INTRODUCTION

The northeastern region of India comprises seven states, namely Assam, Meghalaya, Mizoram, Manipur, Nagaland, Tripura, and Arunachal Pradesh and the region borders the countries of Bhutan, China, Bangladesh, and Myanmar. The entire region is one of the most hazard-prone regions in the Asian continent, with different areas being prone to multi-hazards like earthquakes, floods, landslides, and cyclonic storms. The rivers Brahmaputra and Barak drain the region. The Brahmaputra river has a catchment area of 5,80,000 km in Tibet, Bhutan, India, and Bangladesh and in terms of discharge is the third largest river in the world, in terms of sediment load it is second after the Hwang-Ho river of China. The river flows for a length of 918 km in India of which 720 km is in through the plains of Assam. In this valley, about 20 major tributaries on its North bank and about 13 on its South Bank join the river Brahmaputra. The precipitation here is mainly due

to the South-West monsoon. Heavy rainfall occurs from June to September. Average annual rainfall in the region is very high and ranges from 1750 mm in the plains to about 6400 mm in the hills, this huge volume of water rushes through the narrow bowl-shaped valley of Assam to the Bay of Bengal ravaging the area through floods and land erosion. The recurring floods on an average devastate about 20% of the total area of the plain districts of the state of Assam, and in the high floods years, the devastation has been recorded to be as high as 67%. The region lies at the junction of the Himalayan arc to the north and the Burmese arc to the east and is one of the six most seismically active regions of the world.

The monsoon in the region normally commences around the months of April, May, and is active until the end of October. The pre-monsoon period is often marked by severe cyclonic storms and hailstorms. The annual cyclonic depressions in the Bay of Bengal along the coast of Bangladesh cause severe storms to hit the bordering states of Meghalaya and Tripura. Bangladesh stretches between latitudes 20°34'N and 26°38'N and longitudes 88°01'E and 92°41'E. The country contains the confluence of a distributary of the Ganga (the other distributary, also called Ganga, passes through West Bengal and drains into the sea at Ganga Sagar), Brahmaputra, and Meghna Rivers and their tributaries, which originate in the Himalayas (except the Meghna, which in its upstream portion is called the Barak) and discharge into the Bay of Bengal. The terrain is mainly flat, and with 90% of its landmass, up to 10 meters above the mean sea level, is a primarily low-lying riverine country. It is frequently hit by natural disasters, particularly floods, riverbank erosion, cyclones, and droughts. Each affects the livelihoods of those affected, but with different severity. Displacement due to flood, erosion, and inadequate facilities during and after major floods, as shown in Figure 17.1, can create major hardship and health problems.

The climate of Bangladesh is a tropical monsoon, influenced by the Himalaya Mountains in the north and the Bay of Bengal in the south. High monsoon rains associated with Bangladesh's unique geographical location in the eastern part of the delta of the world's second largest river basin make it extremely vulnerable to recurring floods. Agriculture is the dominant land use in the country covering about 59% of the land, rivers, and other water bodies constitute about 9% (BBS, 2002). Monsoons with varying degrees of associated flooding are anticipated annual events in Bangladesh.

The state of West Bengal lies in the eastern part of India and is flood-prone with floods occurring with a depressing regularity. A number of factors combine to cause floods in southern West Bengal. There is

extremely high rainfall in the monsoon season. The seaward slope of southern West Bengal is very low, and the Ganga delta is tidal in nature. There are several low-lying areas where water lies stagnant. There is silting of several outlet canals reducing carrying capacity. In addition, there is human encroachment on some channels hampering renovation of those channels (Figure 17.2).

FIGURE 17.1 Erosion and inadequate facilities during and after major floods in Bangladesh (*Source*: The Daily Prothom Alo, 2004).

FIGURE 17.2 Flood in Assam, India (*Source*: Assam_Disaster_Management.htm).

17.2 TYPES OF FLOODS

The term flood is generally used when the flows in the rivers and channel cannot be contained within natural or artificial riverbanks. By spilling the riverbanks, when water inundates floodplains and adjoining high lands to some extent or when the water level in the river or channels exceeds certain stage, the situation then termed as flood (Hossain, 2004). Important river basins and type of floods are shown in Figures. 17.3–17.8.

FIGURE 17.3 Ganga Basin in India and Bangladesh.

17.2.1 FLASH FLOOD FROM HILLY AREAS

Flash flood-prone areas of the India and Bangladesh are at the foothills. Intense local and short-lived rainfall often associated with mesoscale convective clusters is the primary cause of flash floods. These are characterized by a sharp rise followed by a relatively rapid recession. Often with high velocities of on-rush flood damages crops, properties, and fish stocks of the wetland. Flash flood can occur within a few hours and are particularly frequent in the months of April and May.

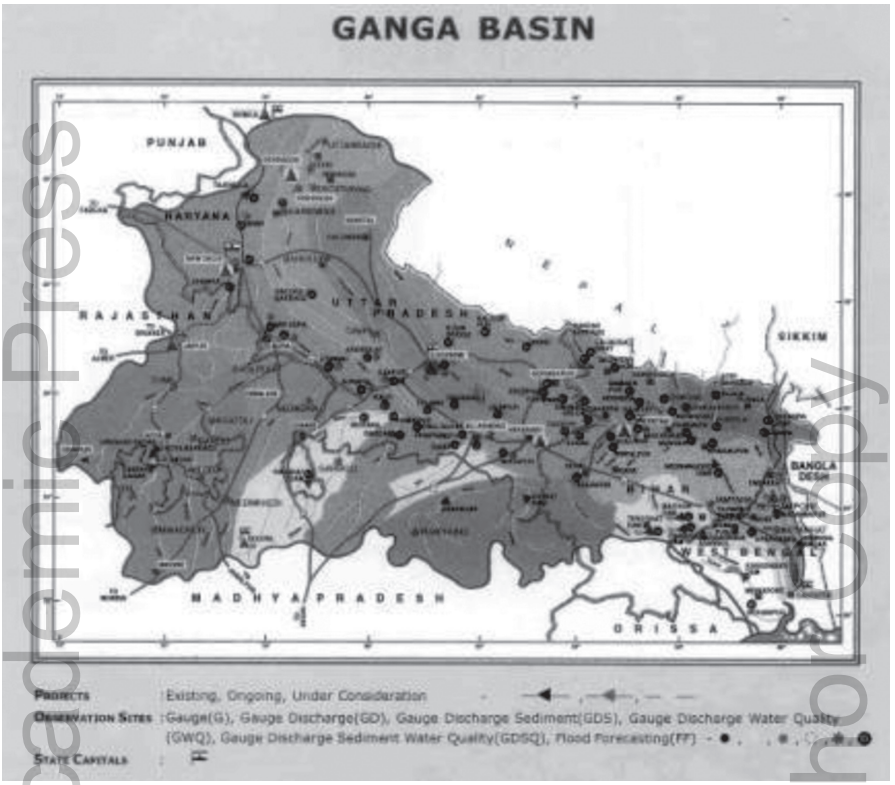

FIGURE 17.4 Ganga river basin in India (*Source*: www.wrmin.nic.in).

17.2.2 MONSOON FLOODS OR NORMAL FLOOD FROM MAJOR RIVERS

River flood is a common phenomenon in India and Bangladesh and is caused by bank overflow. Of the total flow, around 80% occurs in the 5 months of monsoon from June to October (WARPO, 2004). A similar pattern is observed in case of rainfall also. Therefore, to these skewed temporal distributions of river flow and rainfall, India, and Bangladesh suffer from an abundance of water in monsoon, frequently resulting into floods and water scarcity in other parts of the year, developing drought conditions.

In the Brahmaputra, maximum discharge occurs in an early monsoon in June and July whereas in the Ganga maximum discharge occurs in August and September. Synchronization of the peaks of these rivers results in devastating floods in India and Bangladesh. The rivers of Bangladesh drain about 1.72

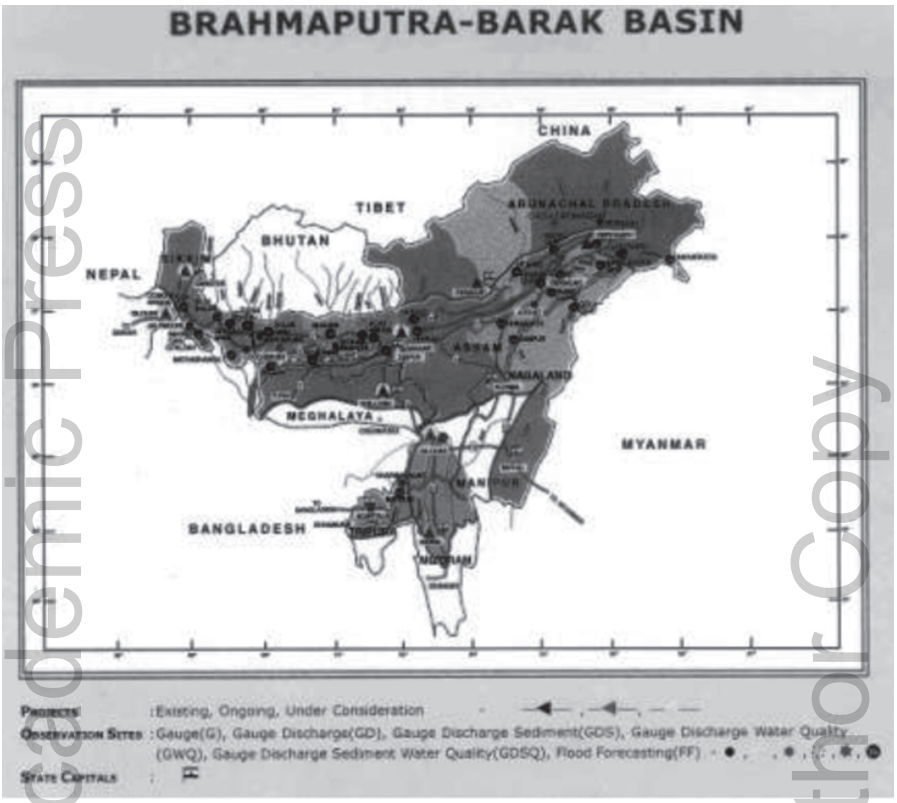

FIGURE 17.5 Brahmaputra and Barak river basins in India (*Source*: www.wrmin.nic.in).

million sq km area of which 93% lies outside its territory in India, Nepal, Bhutan, and China. The annual average runoff of the transboundary rivers of Bangladesh is around 1200 cubic kilometers (WARPO, 2004). A major impediment is the lack of accurate data on a real-time basis on stream flow in the vast upper reach of the Brahmaputra in Tibet in China (the river is called Tsangpo there) and the IRS (Indian Remote Sensing) series of satellites launched from, first the ASLV, and now the PSLV series of rockets from Shriharikota in southern India have to be used to get data. Considering that the floods in the Brahmaputra affect the state of Assam in India as well as Bangladesh, very accurate data on streamflow into India from China on a real-time basis would indubitably be very helpful. However, some streamflow data is being made available to India by China. A cause of concern for the subcontinent as a whole is the Chinese River Linking Plan in which the waters of the Brahmaputra would be diverted northwards via the Yangtze-Kiang River to the Hwang-Ho

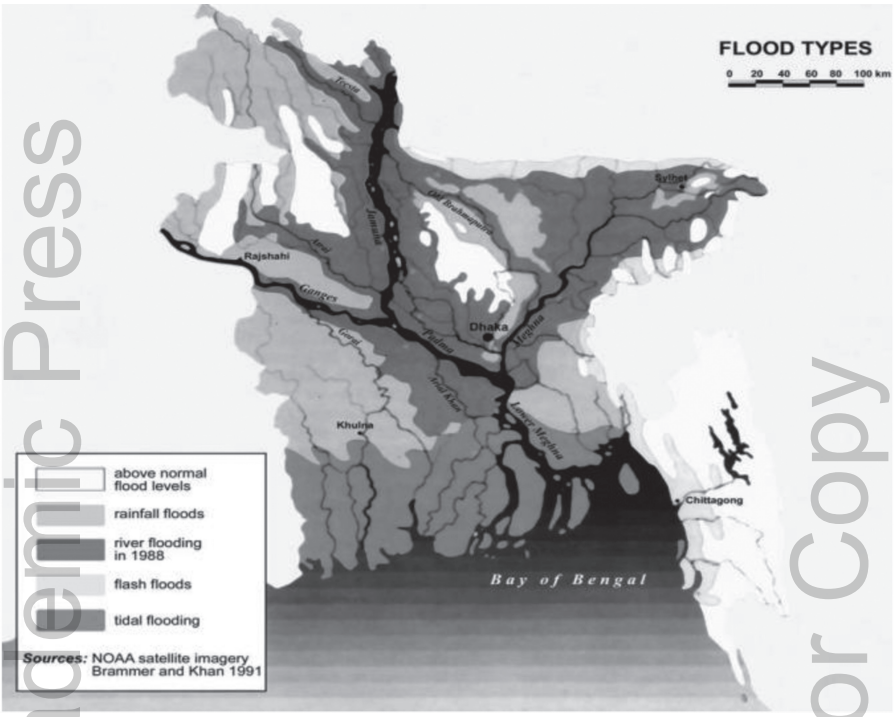

FIGURE 17.6 Types of the flood in Bangladesh (*Source*: FFWC, Dhaka).
(**Note:** Rivers outside the boundaries of Bangladesh are not shown in the figure).

river. This plan, if implemented excluding the water needs of the subcontinent, would result in severe water deficit in the subcontinent.

It may be mentioned that India too has a River Linking Plan (NWP, 2002) to ensure equitable distribution of water and control of floods but much debate is on this issue and Bangladesh, Nepal, and Bhutan would certainly be included in the plan, if it is at all implemented, so that all the countries can get their share of the benefits of this integrated and holistic sub-continental River Linking Scheme. With reference to Figures 17.3 and 17.8, the Indus River Basin and the Ganga River Basin are separated by a low watershed. As per the India-Pakistan Treaty, 1961, the waters of the Indus River Basin are to be shared by the two countries such that India gets the full share of water flowing through the basin via the Sutlej, Beas, and Ravi rivers while Pakistan gets the full share of water flowing through the basin via the Chenab, Jhelum, and Indus Rivers. It is envisaged to construct a canal connecting the Sutlej River in the Indus basin with the Ganga basin so as to divert some water

FIGURE 17.7 Confluence of a distributary of the Ganga, Brahmaputra, and Meghna (lower Barak) River Basins in Bangladesh (*Source*: FFWC, Dhaka).

FIGURE 17.8 Indo-Gangetic basin (*Source*: IWMI).

from the Indus Basin to the Ganga Basin without, in any way, impinging on the water rights of Pakistan because the waters of the Sutlej are fully allocated to India. The objective is to augment and increase the discharge in the Ganga to meet the needs of the Ganga basin fully.

17.2.3 FLOODS DUE TO STORM SURGES

This kind of flood mostly occurs along the coastal areas of Bangladesh and West Bengal. Continental shelves in this part of the Bay of Bengal are shallow and extend to about 20–50 kms. Moreover, the coastline in the eastern portion is conical and funnel-like in shape. Because of these two factors, storm surges generated due to any cyclonic storm is comparatively high compared to the same kind of storm in several other parts of the world. In case of the super-cyclones maximum height of the surges were found to be 10–15 m, which causes flooding in the entire coastal belt. The worst kind of such flooding was on 12 Nov 1970 and 29 April 1991, which caused loss of 300,000 and 138,000 human lives respectively (FFWC, 2005). Coastal areas are also subjected to tidal flooding during the months from June to September when the sea is in spate due to the southwest monsoon wind.

17.3 GENERAL PATTERN

The Brahmaputra starts rising in March due to snowmelt on the Himalayas, which causes the first peak in May or early June. It is followed by subsequent peaks up to the end of August caused by the heavy monsoon rains over the catchments. The response to rainfall is relatively quick, resulting in rapid increases in the water level. The Ganga starts rising gradually in May-June to a maximum sometime in August. High water levels are normally sustained until mid-September. The Meghna may not attain its annual peak until August-September. The upper Meghna carries only about 10% of the flow in the Ganga and Brahmaputra. The total volume of runoff in the GBM is determined by the net precipitation over all the catchments. The normal sequence of floods with flash floods in the eastern hill streams during the pre-monsoon period in the months of April and May. High floods occur if the peaks of the Ganga and Brahmaputra coincide; this may happen during August-September (Rahman et al., 2007).

17.3.1 FLOOD DAMAGES IN BANGLADESH

The terrain has experienced seventeen highly damaging floods in the 20th century. Since independence in 1971, Bangladesh has experienced floods of vast magnitudes in 1974, 1984, 1987, 1988, 1998, 2000, and 2004 (FFWC, 2005). The largest recorded flood in depth and duration of flooding in its history occurred in 1998 when about 70% of the country was under water for several months (FFWC, 2005; Nishat et al., 2000). The area affected in percent of the total area during major flood event inundating more than 20% of the country's land area of the country is presented in Figure 17.9. The damages during some severe floods are presented in Table 17.1.

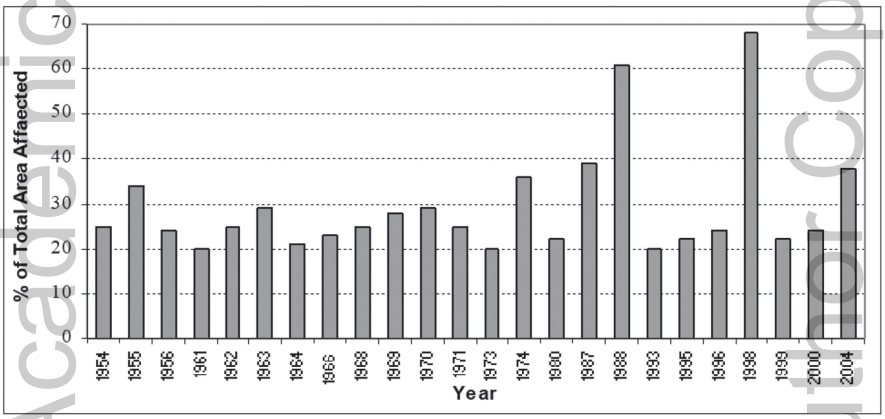

FIGURE 17.9 Area of Bangladesh affected during major flood events (in percent of the total area).

17.4 FLOOD MANAGEMENT IN BANGLADESH

Bangladesh tries to deal with flood and disaster with structural and non-structural measures. Systematic structural measures began by implementing flood control projects in the sixties after the colossal flood of 1963. Non-structural measures have introduced in the seventies. Flooding is a natural phenomenon, which cannot be prevented. Complete flood control is not in the interests of most Bangladeshi farmers. The flood control measures and policies should be directed to mitigation of flood damage, rather than flood prevention. Resources should be allocated to help people adopt a lifestyle that is conformable to their natural environment. Indigenous solutions such as changing the housing structures and

TABLE 17.1 Some Notable Flood and Cyclone Induced Storm Surge Events in Bangladesh

Event	Impact
1974 flood	Inundated 36% of the country (FFWC, 2005), estimated damages US$ 57.9 Million, over 28,700 deaths, (http://www.em-dat.net/disasters/Visualisation/profiles/natural-table-emdat.php?country=Bangladesh dated 2.3.2006)
1987 flood	Inundated over 57,000 sq-km area, estimated damage US$ 1.0 billion and human death 2055 (The World Bank, 2002)
1988 flood	Inundated 61% of the country, persons affected 45 million, 2300 deaths, damage worth about US$ 1.2 billion (The World Bank, 2002)
1998 flood	Inundated 100,250 sq-km (68%) of the country, 1100 deaths, persons affected 31 million, damaged 500,000 homes, 23,500 km roads and 4500 km embankment, destroyed crops of 500,000 ha of land, damage worth about US$ 2.8 billion (The World Bank, 2002)
2004 flood	Inundated 38% of the country, 750 deaths, persons affected 36 million, damaged 58,000 km roads and 3,100 km embankment, crop damage 1.3 million ha, damage worth about US$ 2.2 billion (ADB-World Bank, 2004)

crop patterns can help reduce flood damage. Moreover, good governance, appropriate environmental laws, acts, and ordinances will be necessary to achieve sustainable economic development and to reduce any environmental degradation. In addition, implementation of an improved real-time flood and drought control warning system can reduce the damage caused by floods (http://www.bytesforall.org/8th/control_flood.htm dated 2.3.2006). In recent years, improved forecasting, early warning system, and preparedness measures have helped to reduce the number of lives lost by natural disasters.

17.4.1 FLOOD MANAGEMENT BY STRUCTURAL MEASURES

The structural option provided some benefits especially increase in agricultural production (BWDB, 2005; BBS, 2002) at an earlier period but some adverse effects were observed later on (Nishat et al., 2000). Notably, the construction of a high embankment along both banks of the rivers in some cases resulted in a rise in bed levels due to siltation causing obstruction to drainage. In the coastal areas, although the construction of polders prevented salinity intrusion, but resulted in restriction of the movement of the tidal prism, sedimentation of tidal rivers and obstruction to the gravity drainage. Another important impact on agriculture was found that the farmers in most cases opted for production of cereal crops, especially HYV rice enjoying

a flood free situation rather than going for crop diversification. Structural measure caused many adverse effects on the aquatic lives, especially on open water fisheries. National and regional highways and railways, to the extent feasible, have been raised above flood level. Raising feeder and rural roads will be determined in the context of disaster management plans. River maintenance through dredging is also going on in a limited case due to the high cost. Efforts are continued for erosion control on medium and small rivers. Several Flood Control, Drainage, and/or Irrigation (FCD/I) projects have been constructed. FCD/I project are of two types, namely, (i) full flood control facilities; and (ii) partial flood control. Until date, FCD/I projects provide facilities in about 5.38 million ha which is about 59% of the country's net cultivated land (BWDB, 2000). Flood control and drainage structures have also been provided in major cities to make the cities flood free.

17.4.2 FLOOD MANAGEMENT BY NON-STRUCTURAL MEASURES

Introduction of non-structural option, i.e., Flood Forecasting and Warning System I Bangladesh started from the early '70s and contributed to the improvement of the capacity for flood preparedness and mitigation/ minimization of flood losses. Other non-structural measures are discussed in the following.

Flood cum Cyclone Shelter: School buildings are so constructed that they can be used as flood-cum cyclone shelter especially in the coastal zone with the highest risk of flood and storm surge. These structures are not intended to change the flood regime, and therefore, considered as no-structural measures of flood management.

Floodproofing: Efforts have been made to provide vulnerable communities with mitigation by raising homesteads, schools, and marketplaces in low-lying areas (rather than flood control) and in the charred land so that peasants can save their livestock and foodstuff.

The concept of *flood zoning* and *flood insurance* are not practiced in the country until date. Flood zoning will facilitate development in a co-coordinated way to avoid expensive investments in vulnerable areas. Proper land development rules need to be developed based on the flood-zoning map.

Other non-structural measures practiced are:

- Working with communities to improve disaster awareness.
- Developing disaster management plans.
- Relief and evacuation.

17.4.3 FLOOD FORECASTING AND WARNING IN BANGLADESH

A flood warning is concerned to reduce sufferings to human life and damages of economy and environment. Flood Forecasting and Warning Service of Bangladesh was established in 1972 as a permanent entity under Bangladesh Water Development Board (BWDB). Initially, co-axial correlation, gauge-to-gauge relationship, and Muskingum-Cunge Routing Model were used for forecasting. From the early nineties, a numerical modeling based approach has been applied for flood forecasting and warning. Using the principal concept of mass transfer based on the continuity and momentum equations, dynamic computation has been used in this method. Very briefly, it comprises of estimating water levels using hydrodynamic simulation model (MIKE 11). Research on Modeling System and capacity building in the forecasting is currently emphasized. During the severe flood in Bangladesh and West Bengal, India, in 1998, loss of lives and damage of FCD/I projects in Bangladesh were minimum mainly because of flood forecasting and early warning (Islam and Dhar, 2000).

17.5 DISASTER MITIGATION

Disaster management (including disaster preparedness) involves prevention and mitigation measures, preparedness plans and related warning systems, emergency response measures, and post-disaster reconstruction and rehabilitation. The main aims for water-related disaster management are to provide the means by which, through a combination of structural and non-structural measures and to the extent feasible and affordable, people are adequately warned of an approaching disaster, and are adequately supported in rebuilding their lives thereafter. The vulnerability to natural disasters combined with the socio-economic vulnerability of the people living in the different states of India poses a great challenge for the government machinery and underscores the need for a comprehensive plan for disaster preparedness and mitigation. The Government of India since the last decade has been actively supporting programs for the reduction of vulnerabilities and risks. UNDP has been a partner of the Government of India in such efforts. Vulnerability reduction and linking with sustainable development efforts have been one of the key approaches of UNDP. Strengthening capacities for disaster risk reduction and sustainable recovery process across the country and bringing together skills and resources for making communities disaster resistant is one of the

first steps taken in the long term for achieving a reduction in loss of lives and protecting the development gains.

Quite a few measures may be taken to reduce floods in West Bengal. The network of drainage canals is to be increased, and silted drainage canals are to be dredged to augment channel capacity and allow free flow of excess water through those channels. More dykes are to be built to prevent floodwater from entering low-lying areas, and existing dykes are to be strengthened to prevent their breaching. If possible, human habitation is to be evacuated from flood-prone areas. Pumps of adequate capacity are to be kept on standby to pump out water particularly from low areas. Better meteorological forecasting is necessary so that the water levels in the Damodar Valley Corporation reservoirs can be brought down early enough to accommodate high inflows from upstream in flood periods. Adequate discharge channels are to be provided in the lower Damodar basin; this area is suffering from flood due to inadequate discharge channels. The capacity of the Mayurakshi river also needs to be augmented. Floods in West Bengal can be prevented or reduced by taking adequate structural and non-structural measures.

The Disaster Management Department, Government of West Bengal, India, (MOFM, 2006) has emphasized that during floods, large tracts of land get inundated and, thereby, disconnected from the adjoining areas resulting in disruption of normal day-to-day activity in that area. Though natural calamities like a flood cannot be avoided, its impact in terms of loss of lives and damage to properties can be minimized by undertaking appropriate management practices for preparedness, prevention, and mitigation measures. This constitutes a holistic approach towards management of flood with emphasis not only on the traditional post-disaster response; but also on pre-disaster preventive/mitigation preparedness as well, thereby, laying down a Standard Operating Procedure (SOP) for a Disaster Manager for flood management (www.wbgov.com).

The Government of Bangladesh (GoB) established the Disaster Management Bureau (DMB) in 1993, which has prepared comprehensive Disaster Management Plans. DMB is working under the Ministry of Disaster Management and Relief. Standing orders on Disaster have been prepared in 1997 and upgraded in 1999 by the DMB (Chowdhury, 2003). At the central level, a National Disaster Management Council (NDMC) has formed headed by the Honorable Prime Minister including Ministers from different ministries as a member. Inter-Ministerial Disaster Management Co-ordination Council (IMDMCC) has also been formed which guided by the NDMC. Beside this,

District, Thana (area under the jurisdiction of a Police Station) and Union (lowest level of local government) level committees have also formed with the participation of local community for post-disaster management and mitigation. Task and responsibilities of each committee are stated in the standing order (MoDMR, 1997). By all these steps GoB has strengthened the disaster response capacity through institutional capacity building activities; community disaster response simulation drills; and stockpiling of essential relief items.

Forecasting facilities, preparedness planning, during, and post-disaster relief efforts have reduced the severity of flood disaster impacts. Non-Government Organizations (NGOs) have also responded in an important way. It has been observed that emergency flood fighting during peak flood, evacuation, and relief operation can best be achieved with peoples' participation along with deployment of the army.

17.6 CONCLUSIONS

Structural as well as non-structural measures are being emphasized for flood management in both India and Bangladesh. It has been proved that non-structural measures have a significant effect on flood damage minimization. Flood and disaster cannot fully be controlled, prevented or eliminated, but damages can be reduced significantly by the integration of measures and coordination of agencies. Flood forecasting and early warning are very important. Co-operation is needed at all levels for research and development for improvement of flood mitigation measures.

KEYWORDS

- **Bangladesh**
- **flood control**
- **flood damages**
- **flood mitigation**
- **India**

REFERENCES

Assam Disaster Management. www.AssamDisasterManagement.htm (accessed on XX-XX-XXXX).

Bangladesh Bureau of Statistics (BBS), (2002). *Ministry of Planning*, Bangladesh.

Bangladesh Water Development Board, (BWDB), (2000). Annual Report, Dhaka, Bangladesh.

Chowdhury, J. R., (2003). *Technical Paper Presented in the 47th Annual Convention of the Institution of Engineers Bangladesh (IEB)*, Chittagong, Bangladesh.

FFWC, (2005). *Consolidation and Strengthening of Flood Forecasting and Warning Services* (Vol. II). Final Report, Monitoring, and evaluation, Bangladesh Water Development Board, Dhaka, Bangladesh.

Flood Forecasting and Warning Centre (FFWC), (2005). *Annual Flood Report*, BWDB, Dhaka, Bangladesh.

Hossain, A. A. N. H., (2004). *Flood Management: Issues and Options*. Presented in the International Conference organized by the Institution of Engineers, Bangladesh.

India-Pakistan Water Treaty, (1961). New Delhi, India and Islamabad, Pakistan.

International Water Management Institute (IWMI), (2007). Colombo, Sri Lanka.

Islam, S. R., & Dhar, S. C., (2000). *Bangladesh Floods of 1998: Role of Flood Forecasting & Warning Centre*. BWDB, Dhaka, Bangladesh.

Joint ADB-World Bank, (2004). *Emergency Flood Damage Rehabilitation Project*. Joint ADB-World Bank damage and need assessment, Dhaka, Bangladesh.

Ministry of Disaster Management and Relief (MoDMR), (1997). *Standing Order for Disaster Management*. Dhaka, Bangladesh.

Monograph on Flood Management, (2006). *Department of Disaster Management*. Government of West Bengal, Kolkata, India.

National Water Policy, (2002). India.

Nishat, A., (2000). *The 1998 Flood: Impact on Environment of Dhaka City*. Ministry of Environment & Forest and IUCN Bangladesh, Dhaka, Bangladesh.

Rahman, M. M., (2005). Geo-informatics approach for augmentation of lead time of flood forecasting- Bangladesh Perspective, Proceedings of International Conference on Hydrological Perspectives for Sustainable Development in the Department of Hydrology. Indian Institute of Technology, Roorkee, Uttaranchal, India.

Rahman, M. M., Hossain, M. A., & Bhattacharya, A. K., (2007). Flood management in the floodplain of Bangladesh. *Proceedings, International Conference on Civil Engineering in the New Millennium: Opportunities and Challenges*. Bengal Engineering and Science University, Shibpur, Howrah, India, Paper No. WRE 015.

The World Bank, (2002). Bangladesh Disaster & Public Finance, Paper no 6, Dhaka, Bangladesh.

Water Resources Planning Organization (WARPO), (2004). National Water Management Plan (NWMP), Ministry of Water Resources, Bangladesh, Dhaka, Bangladesh.

www.em-dat.net/disasters/Visualisation/profiles/natural-table-emdat.php?country=Bangladesh dated 2.3.2006 (accessed on XX-XX-XXXX).

www.wbgov.com (accessed on XX-XX-XXXX).

www.wrmin.nic.in (accessed on XX-XX-XXXX).

PART III
Groundwater Management

CHAPTER 18

HYDRO-GEOLOGICAL STATUS OF THE CORE AND BUFFER ZONE OF BEEKAY STEEL INDUSTRIES LIMITED, ADITYAPUR INDUSTRIAL AREA, SARAIKELA, KHARSAWAN, JHARKHAND

UTKARSH UPADHYAY[1], NISHANT KUMAR[2], RANDHIR KUMAR[3], and PRITI KUMARI[4]

[1]Research Scholar (PhD), Center for Water Engineering and Management, Central University of Jharkhand, Ranchi, India, E-mail: utkarsh.wem.cuj@gmail.com

[2]Technical Specialist, Drinking Water and Sanitation Department, Government of Jharkhand, Ranchi, India

[3]Research Scholar (PhD), Center for Water Engineering and Management, Central University of Jharkhand, Ranchi, India

[4]Assistant Professor, Department of Civil Engineering, GGSESTC, Bokaro, Jharkhand, India

ABSTRACT

It has become imperative on the part of water planners to adopt techniques for quantifying the available groundwater resources for sustainable development and management keeping in mind the scarcity of available water resources versus its demand in the near future. The apparent heterogeneities and complexities present in the hard rock aquifers make it a challenge to tackle groundwater problems. The intricacy increases manifold for the management of groundwater when the hard rock aquifers are situated in arid or semi-arid regions. This study was taken up to generate hydro-geological

data through field investigations to prepare a groundwater assessment report for the expansion and increase in groundwater extraction of Beekay Steel Plant, Adityapur Industrial Area, Saraikela-Kharswana, so as to study the existing groundwater scenario and impact of the withdrawal of groundwater on groundwater regime in and around the plant area.

The geology and subsurface conditions were studied and interpreted based on the groundwater exploratory data and geological studies made by GSI and AMD. Well inventory with a collection of water samples were done to evaluate the status of groundwater level and water quality in the buffer zone within 10 Km radius from the plant area. The average seasonal fluctuation of the water table works out to be 3.96m. The perusal of concentration of various chemical constituents of water indicates that groundwater is suitable for all the purposes viz. drinking, and domestic purposes. Pumping tests were conducted within the plant area to know the aquifer characteristics, and subsequently, aquifer parameters were calculated. ΔS calculated from drawdown-time curve has been found to be 2.00 m and transmissivity calculated from Jacob's Method has been found to be 12.096 m^2d^{-1}. The value of the radius of influence (R) comes as 169 m. Low permeability and small radius of influence indicate the marginal impact of pumping on local water regime. It is found that the stage of groundwater development in which the core zone fall, does not exceed 20% and marginal changes occur in the buffer zone after the proposed increase in groundwater extraction, which is a positive factor for taking up groundwater abstraction for the expansion.

18.1 INTRODUCTION

M/s Beekay Steel Industries Ltd. (BSIL) a Public Limited Company incorporated under 'Companies Act, 1956' having its registered office at Lansdowne Towers, 2/1A, Sarat Bose Road, 4th Floor, Kolkata, West Bengal, India intends to expand its Rolling Mill unit at its existing premises which is located Large Scale Sector, Adityapur Industrial Area, Gamharia, and District-Seraikela - Kharswan, in Jharkhand. BSIL believes in producing its quality products in an eco-friendly manner. BSIL will be in a very competitive position having control over all the major inputs required to produce TMT Bar. Power and Billets are the major inputs for production of TMT Bar. Looking at the projection of demand for Steel in the present market, it can be realized that there remains a considerable gap between demand and supply of steel by 2015–2016. To meet the demand, BSIL is expanding its

production and as a resulting requirement of groundwater will increase from 40 cumd^{-1} to 160 cumd^{-1}.

Presently there is moderate utilization of water within the plant area for domestic and industrial consumption only. However, it is proposed to meet the primary requirement of industrial as well as domestic water from groundwater sources. The daily water requirement is estimated to increase from the present requirement of 40 cumd^{-1}to 160 cumd^{-1}. A per prevailing groundwater legislations it is mandatory to obtain the permission of the concerned regulating authority prior to any abstraction of water from the sub-soil sources beyond 100 cumd^{-1}. In order to obtain the permission and fulfill the statutory requirements hydro-geological report over an area of 10 km radius surrounding the project site is a prerequisite.

18.1.1 STATUTORY COMPLIANCE

As per prevailing groundwater legislation, it is mandatory to obtain due permission of the concerned Government controlling/regulating authority prior to any abstraction of water from the sub-soil sources. In order to obtain the required permission, submission of a hydro-geological report with evaluation of groundwater potential over an area of 10 km radius surrounding the project site is a prerequisite. The present report has been prepared after field studies and analysis of various hydrological data collected through secondary sources to fulfill the conditions for submitting the application to obtain permission for groundwater abstraction. As per the prevailing groundwater regulations, i.e., guidelines/criteria for evaluation of proposals/requests for groundwater abstraction (with effect from November 15, 2012), it is mandatory to obtain due permission of the concerned Government controlling/regulating authority prior to any abstraction of water from underground. In order to get the environmental clearance from the concerned authorities' environmental impact assessment studies are being carried out by different consulting agencies.

A field visit was made for collecting hydro-geological data of key wells for studying the present groundwater conditions, estimating the long-term groundwater recharge, the present status of groundwater development. The post-monsoon hydro-geological data from 12 well was collected for November 2017. The present report has been prepared after field studies for core and buffer zones of Beekay Steel Industries Limited and the impact of groundwater abstraction on the water regime and analysis of various hydro-geological data collected through secondary sources to fulfill the condition

for submitting, the application to obtain permission for required groundwater abstraction.

18.1.2 OBJECTIVE

The following objectives were taken into account for hydro-geological investigation of the study area:

1. To assess the present hydrological scenario of the study area.
2. To find out aquifer geometry in the area.
3. To evaluate the status of groundwater condition in the area.
4. To evaluate the hydraulic behavior of the aquifer system in the area.
5. To assess the groundwater resources of the area.
6. To assess the impact of present withdrawal on groundwater regime.
7. To find out the hydrochemical character of water resources in the present area.

18.2 METHODOLOGY

To achieve the goal, it becomes essential to evaluate the exact hydro-geological conditions, aquifer parameters, and aquifer geometry, etc. for this purpose data were collected from the reports available in Central and State Government departments. The geology of the area and subsurface conditions has been interpreted based on the exploratory data and geological studies made by G.W.D & C.G.W.B. Intensive well inventory of the area have been undertaken to measure the status of the water table in the study area. The water samples were collected for analysis in order to establish the water quality. To evaluate the aquifer parameter pump test have been conducted in a surrounding area where the rate of depletion in water level at constant pumping rate were observed. The aquifer parameters were calculated using the standard analytical technique to field conditions of the testing site. The groundwater resources and its utilization have been worked out as per the norms prescribed by the groundwater estimation committee, Govt. of India. The impact of groundwater abstraction, on groundwater storage, has been estimated based on field data analysis and interpretation. The hydro-chemical behavior of groundwater has been evaluated based on the analytical results of the water sample collected in the field.

18.2.1 STUDY AREA (BUFFER ZONE)

For hydro-geological and hydrochemical study point of view an area of 314 Km^2 has been chosen as circular area of 10 km radius keeping place of large industrial area in Adityapur Industrial Area (22° 49' 39.44"N and 86° 04' 30.55"E) of Gamharia block of Saraekela- Kharsawa district in the centre. The area falls under Survey of India Toposheet No.73/F/13, 73J/1 & 73 J/2. The Latitude and Longitude of the proposed site are 22° 49' 39.44"N and 86° 04' 30.55"E, respectively.

It is bounded by coordinates 85°59'02" E to 86°09'56" E longitudes and from 22°44'14" N to 22°55'04" N latitudes. It is bounded by Katia, Manikul, Thakrudiand Salgodih villages in the north and Aunlataur, Nayadih villages and Tamadungri (pahar) in the south. In the east, it is bounded Kagainagar and Shatrinagar urban township of Jamshedpur city and Satnala, while by the western flank of Patubara hills in the west. A major part of the area falls under Gamharia block, but also covers a very little part of Rajnagar and Chandil blocks of Sareikela district and Gulmuri and Potka blocks of East Singhbhum district. The block-wise area coverage is given in Table 18.1. The total area under study is 314 Km^2, and here it is called a buffer zone.

TABLE 18.1 Block Wise Area Coverage in Buffer Zone

Sl. No.	District	Block	Area	% of Area
1	Sareikela	Gamharia	233.37	74.28
2		Rrajnagar	23.68	7.57
3		Chandil	18.72	5.96
4	East Singhbhum	Gulmuri	25.88	8.24
5		Potka	12.52	3.99

18.2.2 CLIMATE AND METEOROLOGY

The mean annual temperature remains at about 26°C. The temperature ranges from 16°C in winter months to 44°C in the summer months. It experiences tropical and humid climate which shows three distinct seasons viz. hot and dry summer season, humid, and warm rainy season and winter season. The summer is very hot and dry starting from March and continues till mid of June (Figure 18.1). The rainy season lasts from mid-June to end to September October, and November are the post-monsoon months followed by a cold winter which lasts till the middle of March. The district belongs

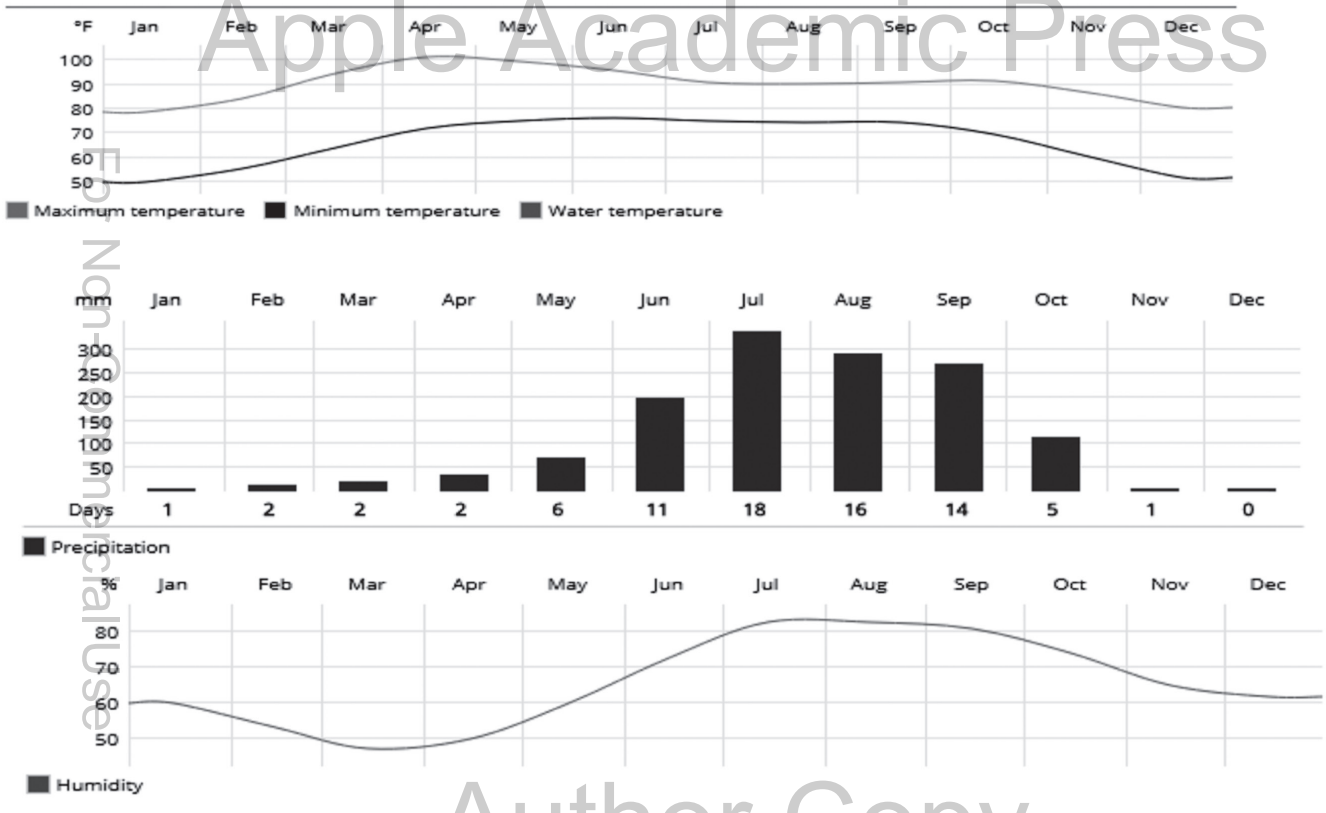

FIGURE 18.1 Monthly temperature, rainfall, and humidity pattern of Gamharia block, Saraikela-Kharsawan.

to one of the 13 districts of Jharkhand, which falls in the Agro climatic sub-zone-IV. The district falls in the rain shadow of the Santhal Pargana plateau. The average annual precipitation is 1307.6 mm and the average number of rainy days is 59. Even this meager precipitation is erratic which coupled with long inter-spell forces the district to suffer from drought (Figure 18.2).

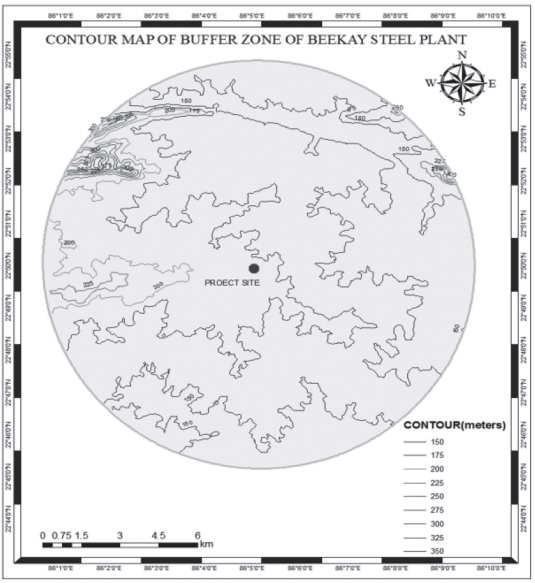

FIGURE 18.2 Contour map of the buffer zone of the beekay steel plant.

18.2.3 GEOMORPHOLOGY AND SOIL TYPES

The predominant physical feature over the major part of the district is the rolling topography dotted with isolated inselbergs except in the Borijore and Sundarpahari blocks. A substantial part of Borijore and Sundarpahari block is under forest cover. The altitude of the land surface increases from west to the east. The major hills are confined to the eastern part of the district comprising the Gandeshwari Pahar (238.41m) and Kesgari Pahar (268.29 m) while in the western part of the district isolated hills are in the form of the inselbergs and other small hillocks. The soil is mostly acidic, reddish yellow; light textured and highly permeable with poor water holding capacity.

18.2.4 DRAINAGE

The present area under study falls under the Subarnarekha river basin. Its main tributaries Sanjai and Kharkai River Subarnarekha originates 15 kms south of Ranchi on the Chhotanagpur plateau draining the states of Jharkhand, Orissa, and West Bengal before entering the Bay of Bengal. The total length of the river is 450 kms, and its important tributaries include the Raru, Kanchi, Kharkai, and Garra rivers. River Subernarekha flows from NW – SE in the northern part of the buffer zone. Its main tributary Kharkai River which flows in the southern part of study area joins Subernarekha river near village Saharbera. Other river and nalas which constituted the drainage in the area are- Sanjai River (flow from W-E), Kharkai River (W-E), Kanki jhor (W-E, and SW-NE) Sanjai River joins Kharkai river. The rivers and nalas show highly meandering features as the area has been suffered prolonged weathering. The drainage pattern is dendritic. Beside the rivers and nalas, there are many small water tanks among which Sitarampur reservoir is prominent. Drainage map of the area has been shown in Figure 18.3.

18.2.5 GEOLOGY

The area is underlain by rocks belonging to Precambrian age. The most common rock types are Granite and granitic -gneisses, Quartzites, Mica Schist, and quartz-mica-schists. At places, sporadic distribution of unclassified rocks such as amphibolites and epidiorites are found in narrow strips. Recent alluvium occurs as thin discontinuous, elongated manner along both sides of the river. A generalized stratigraphic sequence of the area is given Table 18.2.

TABLE 18.2 Geological Succession in the Area

Age	Series	Stage	Lithology
Recent	Alluvium		Sand, silt, and clay
	----------	**Unconformity** ----------	
Pre-Cambrian	Iron Ore Series	Chaibasa Stage	Quartzites, Mica Schist, and Quartz-mica-schist
		Singhbhum shear zone	Granite and granitic –gneisses

18.2.6 HYDRO-GEOLOGY

Geological setting, climate, and topography play important roles in occurrence and movement of groundwater. Depending upon the varied geological setup, the hydro-geological features in the area too register wide spatial

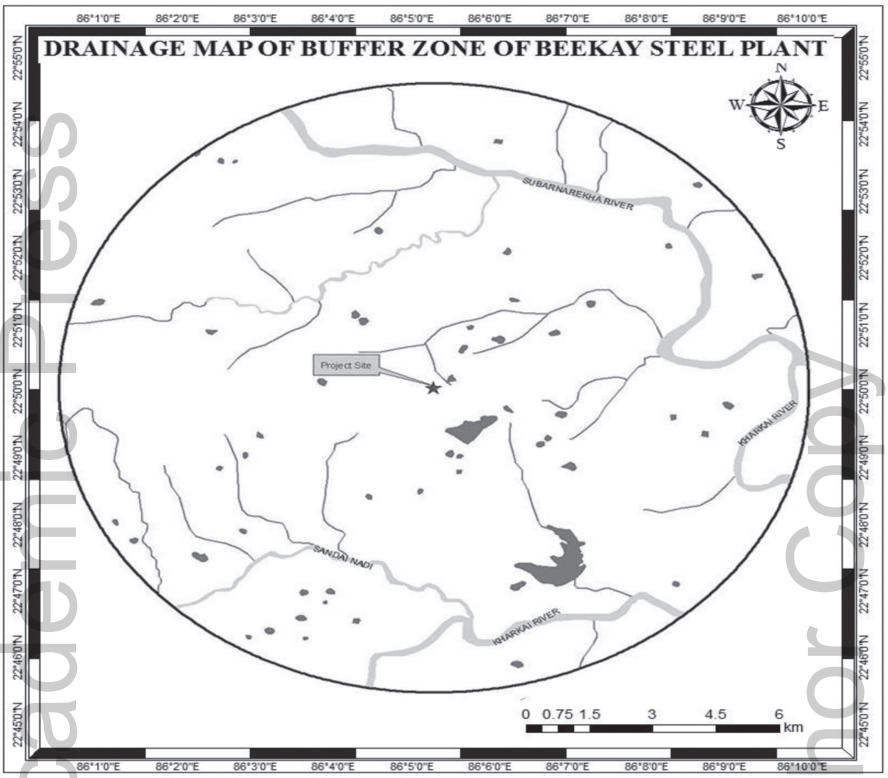

FIGURE 18.3 Drainage map of the buffer zone of the Beekay steel plant.

variations. The geological setting primarily controls the occurrence and movement of groundwater. The composition and structure of the geological formation influence certain inherent properties like porosity, permeability, and hence water holding and water-yielding capacity of aquifers, thereby playing a vital role in the hydro-geological regime.

The occurrence and movement of, by and large, depend on the hydro-geological condition of the subsurface formation. These natural deposits vary greatly in their lithology, thickness of weathering, texture, and structure which in turn influence their hydro-geological characteristics. Depending upon the geological setup of the study area, and water-yielding properties, two major hydro-geological units have been identified in the area. These are:

1. Consolidated formation; and
2. Un-consolidated formations.

As far as the hydro-geological property of underlying rocks is concerned, it is depicted through various groundwater abstractions structures. Most of the open wells are circular in shape. Total 12 nos. of open wells have established an observation well in the area. Hydro-geological properties of each unit are discussed in the following subsections.

18.2.6.1 CONSOLIDATED FORMATIONS

The major part of the area is occupied by consolidated formations comprising granites and granite-gneisses, quartzites, and mica-schists, etc. of Iron Ore series belonging to Precambrian age. These rocks are very hard and compact and lack primary porosity. Groundwater is stored mainly in the secondary porosity resulting from weathering and fracturing of the rocks. The aquifer materials are highly heterogeneous in character showing both vertical and lateral variations. The weathered residuum from the main repository of groundwater, which occurs under water table conditions and circulates through deeper fractures and fissures. Groundwater occurs under an unconfined condition in phreatic aquifers and semi-confined to confined conditions in the deeper fractures zones. The water-yielding capacity of fractured rocks largely depends on the extent of fracturing, openness, and size of fractures and extent of their interconnections into the near-surface weathered zone. These interconnected joints and fractures in the underlying hard rock's facilitate circulation of groundwater and in turn from deeper aquifers.

18.2.6.2 WATER BEARING PROPERTIES OF MAJOR LITHO UNITS

Hydro-geological characteristics of different rock formations are described in the following paragraphs based on the data collected and generated through groundwater survey and investigations.

Granite Gneiss: These are the most predominate formations occupying the northern part of Subernarekha River and central part of the buffer zone. These rocks occur in pediments and pediplains and denudational hills and other smaller hillocks and undulating plains. The rocks are well foliated, jointed, and are weathered easily. Weathering in these rocks is pronounced and fissures and joints, etc., are well developed and can be observed even in exposures. Granite gneisses are also traversed by numerous veins of

quartz and pegmatites. The depth of weathering is found in a range of 21.40 to 24.30 meters in general. The weathered zone forms the main repository of groundwater in the hard rocks occupying area of present study and are tapped by dug wells. Groundwater can be developed through dug well, dug-cum-bore well and bore well. The available data generated during a survey reveals that the development of groundwater is being done through all types of groundwater structures, i.e., dug wells and as well as bore wells. Both structures are used for drinking as well as irrigation and industrial purposes.

Quartzites: Quartzite is the second dominating formations in the buffer zone. It is generally associated with Quartz mica-schists of Iron Ore Series of rock. These rocks are quite massive and compact and occupy hill ranges. Weathering is quite prominent. The weathered residuum and the fracture zones constitute the main repository of groundwater. Weathered part of quartzite forms the repository of groundwater and facilitates supply and storage of groundwater for dug well.

Mica schist: These are the least dominating rock types in the area and found generally in association with quartzites and granitic formations and occupy the lower parts of denudational hills and pediplanes in central parts also. Due to its sporadic and poor occurrence, no open wells were found in the area. However, shallow as well as deeper bore wells data indicate underlying formation as mica-schists. It is also confirmed by its outcrops exposed along nalas. These rocks are moderately weathered. Schistosity in these rocks itself controls the movement of groundwater in weathered residuum and at depth formed deeper aquifer. Details of the observation wells are given in the Table 18.3.

18.2.6.3 UNCONSOLIDATED FORMATION

Unconsolidated formation comprises alluvium deposits are brought by Subernarekha River and its tributaries in the area. Alluvium deposits are in a narrow strip and elongated way along the river courses. Due to its limited occurrence that too along river coarse only two monitoring wells were established for measurement. The depth of alluvium is from 15 to 40 m and forms a good potential zone for the shallow and middle aquifer. Hydro-geological features of the buffer zone have been shown in Figure 18.4.

18.2.7 DEPTH TO WATER TABLE

To decipher the status of groundwater detailed inventory of the existing wells falling within the study area has been carried out. The limited well inventory of 12 nos. of open wells has been given in Table 18.3.

TABLE 18.3 Post-Monsoon Water Level Data of Open Wells

S. No.	Location	Elevation (mamsl)	Dia. of Well (ft)	Water Level (mbgl)
1.	Barkatand (22°48’36.530” N, 86 °03’25.190” E)	176.0	10	2.2
2.	Ramjivanpur (22°48’31.67” N, 86 °03’06.890” E)	167.3	10	0.9
3.	Ramjivanpur (22°48’28.240” N, 86 °03’04.220” E)	173.9	3	1
4.	Ramjivanpur (22°48’25.00” N, 86 °03’03.400” E)	162.5	3	2.1
5.	Gamharia (22°49’01.300” N, 86°05’55.760” E)	148.5	6	4
6.	Gamharia (22°48’58.785” N, 86°06’00.25” E)	167.0	8	2.41
7.	Ramchandrapur (22°49’49” N, 86°04’46.550” E)	160.0	6	3.9
8.	Ramchandrapur (22°49’50” N, 86°04’45.400” E)	175.5	6	4.2
9.	Srirampur (22°49’58.200” N, 86°03’47.115” E)	204.35	4	2.85
10.	Hariharpur (22°49’52.750” N, 86°03’36.135” E)	186	5	1.35
11.	Hariharpur (22°49’54.700” N, 86°03’28.950” E)	209.9	10	1.95
12.	Birajpur (22°49’16.750” N, 86°03’57.900” E)	191.5	4	2.08

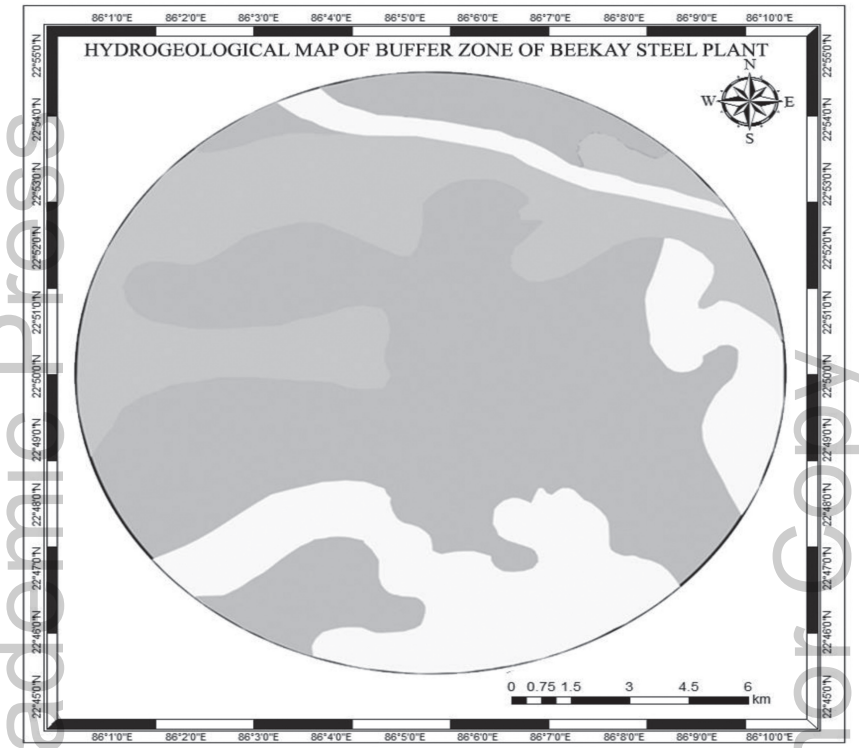

LEGEND	AGE & FORMATION	LITHOLOGY	HYDROGEOLOGICAL CONDITION	GROUND WATER POTENTIAL
	Quaternary	Alluvium	Ground Water occurs in in primary porosity	Yield Range from 7.5 to up to 20 m^3/day With an average of 10^3/day
	Pre Cambrian	Quartzites and mica-schists	Ground Water in weathered residuum and in fracture zones with secondary porosity	Yield Range from 6.3 to up to 25.2m^3/hr With an average of 9^3/hr
	Pre cambrian	Granite gneiss	Ground Water in weathered residuum and in fracture zones with secondary porosity	Yield Range from 5.4 to up to 18 m^3/hr With an average of 10^3/hr

FIGURE 18.4 Hydro-geological map of the buffer zone of the Beekay steel plant.

18.2.7.1 GROUNDWATER FLOW REGIME

The depth to water levels was observed during Nov-2017 reflect post-monsoon water levels. The review of the data indicates moderate variation in depth to water table in the area. Such a variation is mainly due to variation in topography, and partly it is structurally controlled. Using the observed

water level, depth to water level map has been prepared. The water table elevation contour map has been drawn based on observed pre-monsoon level and elevation of observation well. The review of the map shows a regional flow towards south-east over the study area that is towards the flow direction of Khakhai River. The surface water flow regime and the groundwater flow regime are similar.

18.2.7.2 FLUCTUATION OF WATER TABLE AND LONG-TERM TREND

The pre-monsoon water level was evaluated by a local enquiry by people having owned well and found to be in the range of 5.5 to 10 meters below ground level, being minimum at Hariharpur village and maximum at Ramchandrapur Village. Post- monsoon water level varies from 0.9 meters below ground level to 4.2 meters below ground level, being minimum at Ramjivanpur village and maximum at Ramchandrapur village. The average water level (post-monsoon period) is 2.41 meters below ground level. The minimum fluctuation has been observed at Ramchandrapur with 3.1 m, and maximum groundwater fluctuation has been observed at Gamharia with 7.59 m (Table 18.4 and Figures 18.5–18.7). As per the local enquiry, significant water table declining trend has not been observed in the area.

18.2.8 EVALUATION OF AQUIFER PARAMETERS

The aquifer character is the vital parameter of the groundwater study especially to evaluate flow regime and quantify subsurface groundwater flow. The Pumping test is the most effective tool to estimate the aquifer parameters. Consequently, short duration pumping test was conducted on bore well existing within the project area, which is presently used for domestic purposes. The pump was kept shut for 12 hours before the start of pumping test. The test details and the observations are discussed subsequently. During the test period, the water levels were observed in the well at regular intervals which are given in Tables 18.5–18.7.

18.2.9 QUALITY OF GROUNDWATER

Quality of water is as important as quantity. A suitable quality of water is whose characteristics make it acceptable to the needs of a particular purpose,

TABLE 18.4 Pre-Monsoon Water Level Data of Open Wells

S. No.	Location	Elevation (mamsl)	Dia. of Well (ft)	Water Level (mbgl)
1.	Barkatand (22°48'36.530" N, 86 °03'25.190" E)	176.0	10	7.3
2.	Ramjivanpur (22°48'31.67" N, 86 °03'06.890" E)	167.3	10	5.5
3.	Ramjivanpur (22°48'28.240" N, 86 °03'04.220" E)	173.9	3	5.5
4.	Ramjivanpur (22°48'25.00" N, 86 °03'03.400" E)	162.5	3	7.5
5.	Gamharia (22°49'01.300" N, 86°05'55.760" E)	148.5	6	9.5
6.	Gamharia (22°48'58.785" N, 86°06'00.25" E)	167.0	8	10.0
7.	Ramchandrapur (22°49'49" N, 86°04'46.550" E)	160.0	6	7.0
8.	Ramchandrapur (22°49'50" N, 86°04'45.400" E)	175.5	6	8.0
9.	Srirampur (22°49'58.200" N, 86°03'47.115" E)	204.35	4	6.0
10.	Hariharpur (22°49'52.750" N, 86°03'36.135" E)	186	5	7.0
11.	Hariharpur (22°49'54.700" N, 86°03'28.950" E)	209.9	10	6.0
12.	Birajpur (22°49'16.750" N, 86°03'57.900" E)	191.5	4	8.5

be it industrial or domestic. Whenever any industry is established towards serving the mankind, it is always a prerequisite to determining the quality of water which will be utilized for the industry as well for domestic use for people engaged in the industry. During the field study, two number of water samples from dug and bore well were collected to know the suitability of water for domestic as well as industrial use. The location and source of water samples collected have given in Table 18.8.

FIGURE 18.5 Depth to water level map of the buffer zone of the Beekay steel plant.

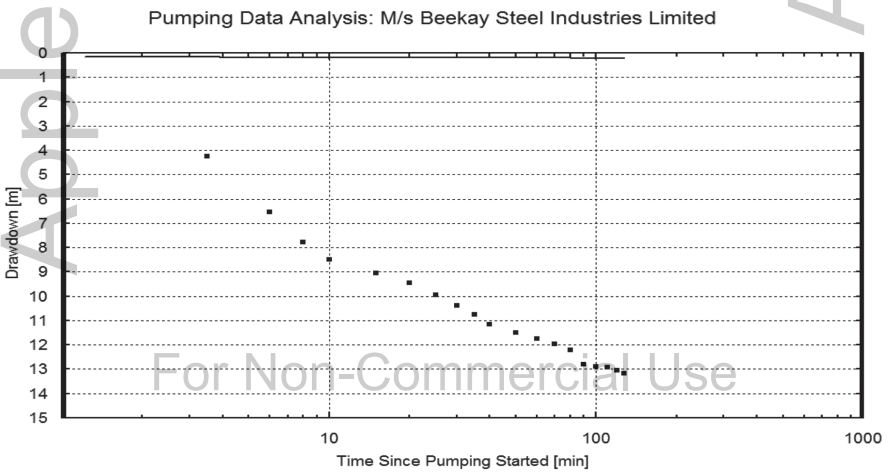

FIGURE 18.6 The data plot of bore well pumping test (Jacob's method).

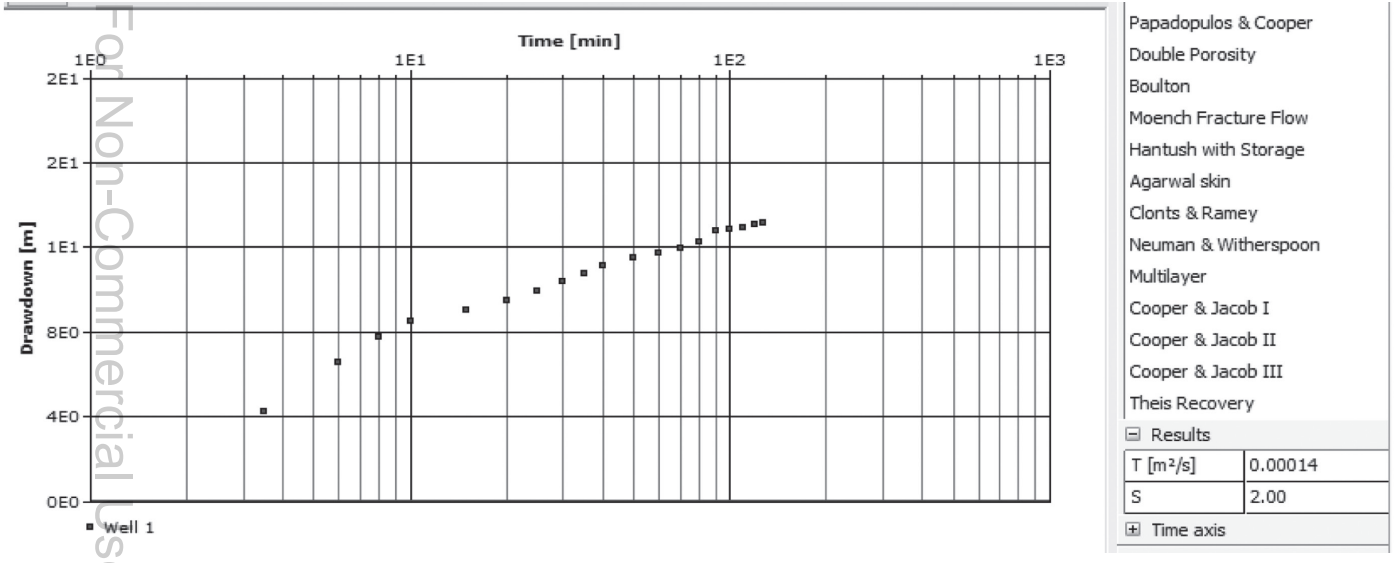

FIGURE 18.7 The data plot of bore well pumping test (Jacob's straight-line method).

TABLE 18.5 Details of Bore Well at Beekay Steel Industries Limited, Adityapur Industrial Area, Gamharia, Saraikela-Kharsawan, Jharkhand

Site Name	M/S Beekay Steel Industries Private Ltd.	Location	Plant Site (22°49'32.32" N, 86°4'33.1" E)
Well Depth	77 mbgl	Pump lowered at	60 mbgl
Dia of well	6"	pump (HP)	3 HP
MP	0.76 magl	Pumping rate	1.532 LPS
DTWL	8.08 mbgl	Temp	28ºC

TABLE 18.6 Pumping Test Data of Bore Well at Beekay Steel Industries Limited, Adityapur Industrial Area, Gamharia, Saraikela-Kharsawan, Jharkhand

Sl. No.	Time (min)	Hold (m)	Cut (m)	DTWL (mbmp)	DTWL (mbgl)	Drawdown (m)
1.	0	25	16.16	08.84	8.08	0
2.	3.5	25	11.90	13.10	12.34	4.26
3.	6	25	9.61	15.39	14.63	6.55
4.	8	25	8.39	16.61	15.85	7.77
5.	10	25	7.66	17.34	16.58	8.50
6.	15	25	7.11	17.89	17.13	9.05
7.	20	25	6.71	18.29	17.53	9.45
8.	25	25	6.20	18.80	18.04	9.96
9.	30	25	5.77	19.23	18.47	10.39
10.	35	25	5.41	19.59	18.83	10.75
11.	40	25	5.01	19.99	19.23	11.15
12.	50	25	4.67	20.33	19.57	11.49
13.	60	25	4.40	20.60	19.84	11.76
14.	70	25	4.19	20.81	20.05	11.97
15.	80	25	3.94	21.06	20.30	12.22
16.	90	25	3.36	21.64	20.88	12.80
17.	100	25	3.27	21.73	20.97	12.89
18.	110	25	3.24	21.76	21.00	12.92
19.	120	25	3.12	21.88	21.12	13.04
20.	127	25	3.00	22.00	21.24	13.16

TABLE 18.7 Recuperation Data of Bore Well at Beekay Steel Industries Limited, Adityapur Industrial Area, Gamharia, Saraikela-Kharsawan, Jharkhand

Sl. No.	Time Since Pumping Started (t) in min	Time Since Pumping Stopped (t') in min	(t/t')	Hold (m)	Cut (m)	D.T.W.L (mbmp)	D.T.W.L (mbgl)	Residual Draw-down (m)
1.	127	0		25	3.00	22.00	21.24	13.16
2.	130	3	43.33	25	3.90	21.10	20.34	12.26
3.	132	5	26.4	25	6.57	18.43	17.58	9.5
4.	134	7	19.14	25	8.11	16.89	16.10	8.02
5.	136	9	15.11	25	19.91	15.09	14.33	6.25
6.	140	13	10.76	25	10.22	14.78	14.02	5.94
7.	145	18	8.05	25	10.73	14.27	13.51	5.43
8.	150	23	6.52	25	11.32	13.68	12.92	4.84
9.	155	28	5.53	25	11.97	13.03	12.27	4.19
10.	160	33	4.84	25	12.55	12.45	11.69	3.52
11.	170	43	3.95	25	12.77	12.23	11.47	3.39
12.	180	53	3.39	25	13.50	11.50	10.74	2.66
13.	190	63	3.01	25	14.09	10.91	10.15	2.07
14.	200	73	2.73	25	14.54	10.46	9.70	1.62
15.	210	83	2.53	25	14.90	10.10	9.34	1.26
16.	217	90	2.41	25	15.02	9.98	9.22	1.14

$T = (15.8 \times Q)/\Delta S$

ΔS calculated from drawdown-time curve (Theis recovery method) has been found to be

$T = (15.8 \times 1.532)/2.00 = 12.096$

TABLE 18.8 Location of Water Samples Collected in Buffer Zone of M/s Beekay Steel Industries Limited, Gamharia, Saraikela-Kharsawan, Jharkhand

Sl. No.	Type of Well	Location/Village Name	Depth (mbgl)	Temp (°C)	Parameters for chemical analysis: pH, E.C, Ca, Mg, K, F, NO_3, HCO_3, Cl, SO_4, CO_3, As & TDS
1.	Bore Well	22°49'48.900" N, 86°04'46.850" E	77	26	—do—
2.	D1	22°49'32.520" N, 86°04'33" E	31	26	—do—

Quality of water is as important as quantity. pH of groundwater is to slight alkaline in nature. pH varies between 6.47–6.57. Total dissolved solids are within permissible limits prescribed by Bureau of Indian Standards (BIS). Total dissolved slid of groundwater varies between 310.50 to 320.80 mg/l. The value of chloride varies between 31.80 to 32.78 mg/l. The value of sulfate varies from 15.26 to 16.27 mgl^{-1}. The value of calcium varies from 46.60 to 47.42 mgl^{-1}. The value of magnesium varies from 3.97 to 4.96 mgl^{-1}. The total hardness as calcium carbonate varies between 132.70 to 138.72 gl^{-1}. The range of different chemical constituents has been given in given Table 18.9.

Groundwater and surface water of core and buffer zone has been found suitable for domestic as well as industrial uses. The remarks on different samples collected have been given in Table 18.10 and result summarized in table.

A perusal of concentration of various chemical constituents of water indicates that groundwater is suitable for all the purposed viz. drinking, and domestic purposes (Table 18.11).

TABLE 18.9 Comparison of Bis Standards with Chemical Analysis Results of Water Samples Collected From Buffer Zone of M/S Beekay Steel Industries Limited, Gamharia, Saraikela-Kharsawan, Jharkhand

S. No.	Chemical Constituent	Range	Unit	BIS
1.	pH	6.5–8.5		6.47–6.57
2.	TDS	500.0	mgl^{-1}	310.50–320.80
3.	Cl	250.0	mgl^{-1}	31.80–32.78
4.	SO_4	200.0	mgl^{-1}	15.26–16.27
5.	Total Alkalinity as $CaCO_3$	200.0	mgl^{-1}	106.82–111.18
6.	Total Hardness as $CaCO_3$	300.0	mgl^{-1}	132.70–138.72
7.	Ca	75.0	mgl^{-1}	46.60–47.42
8.	Mg	30.0	mgl^{-1}	3.97–4.96
9.	Fe	0.3	mgl^{-1}	0.08–0.10
10.	Turbidity	5.0 NTU	NTU	<1.0

TABLE 18.10 Remarks on Chemical Analysis of the Water Samples Collected

S. No.	Well No.	Location in Buffer Zone	Remarks
1.	Bore Well	Beekay Steel (Plant Area)	Water sample after chemical analysis found satisfactory
2.	D1	Sikardih	Water sample after chemical analysis found satisfactory

TABLE 18.11 Results of Chemical Analyses of Water Samples Collected in and Around Plant of M/S Beekay Steel Industries Limited, Adityapur Industrial Area, Gamharia, Saraikela-Kharsawan, Jharkhand

Sample No.	D1	Bore Well	Testing Method	BIS
Location/Village	Sikardih	Beekay Steel (Plant Area)		
pH	320.80	310.50	Digital pH	500.0
TDS	32.78	31.80	Digital TDS Meter	250.0
Cl	16.27	15.26	EDTA Titration Method	200.0
SO_4	111.18	106.82	PhotoMetric Method	200.0
Total Alkalinity as $CaCO_3$	138.72	132.70	EDTA Titration Method	300.0
Total Hardness as $CaCO_3$	47.42	46.60	EDTA Titration Method	75.0
Ca	4.96	3.97	Photometric Method	30.0
Mg	0.10	0.08	Photometric Method	0.3
Fe	<1.0	<1.0	3500 Fe –B	5.0 NTU
Turbidity	6.57	6.47	3500 Mg –B	6.5–8.5
T. Coliform	Not Detected	Not Detected	9221 B	
E. Coliform	Absent	Absent	9221 F	

18.3 GROUNDWATER RESOURCES

Precise quantification of exploitable groundwater resource is essential before any program for its development. It involves quantification and identification of various factors affecting groundwater recharge, discharge, and demarcation of areas suitable for recharge. The principal sources of recharge to groundwater are rainfall, seepage from canals, return flow from applied irrigation seepage from tanks and ponds. The buffer zone of the project area of M/s Beekay Steel Industries Limited, which is the area with 10 km radius from the proposed site, falls in Gamharia, Rajnagar, and Chandil block of Saraikela-Kharsawan district and Potka block of East Singhbhum district. Availability of groundwater resources of these blocks has been estimated based on norms recommended by Groundwater Estimation Committee (G.E.C 1997) by CGWB, which has been presented below in Table 18.12. It is found that the stage of groundwater development in which the core zone of the proposed project fall, does not exceed 20 %, which is a positive factor for taking up groundwater abstraction for the increased demand.

TABLE 18.12 Groundwater Resources in Gamharia Administrative Block Falling in the Buffer Zone of the Proposed Plant

Block	Gamharia (ham)	Rajnagar (ham)	Chandil (ham)	Potka (ham)
Total Annual Groundwater Recharge	2138.52	3521.70	2647.55	4012.70
Net Groundwater Availability	1924.66	3345.62	2382.79	3894.50
Annual Net Draft Through Existing Structures for Irrigation	87.894	90.63	73.53	96.05
Annual Net Draft Through Existing Structures for Domestic and Industrial Supply	282.2	197.1	192.6	287.72
Allocation for Domestic and Industrial Requirement Supply	376.20	262.84	256.82	435.48
Net Groundwater Availability for Future Irrigation	1460.58	2992.15	2052.44	3362.98
Stage of Groundwater Development (%)	19.23	8.60	11.17	9.85

The block in which core zone of the project is situated has been categorized as safe by CGWB, Govt. of India depending upon water table behaviors and stage of groundwater development which has been given in Table 18.13.

TABLE 18.13 Categorization of The Block Falling in the Core Zone of M/s Beekay Steel Industries Limited, Adityapur Industrial Area, Gamharia, Saraikela-Kharsawan, Jharkhand

S. No.	Assessment Unit	Stage of Groundwater Development	Is there any significant decline of pre-monsoon level	Is there any significant decline of post-monsoon level	Categorization of future groundwater development
1.	Gamharia	19.23%	No	No	Safe
2.	Rajnagar	8.60	No	No	Safe
3.	Chandil	11.17	No	No	Safe
4.	Potka	9.85	No	No	Safe

18.3.1 GROUNDWATER RESOURCE OF THE BUFFER ZONE OF THE PROPOSED PROJECT

1. Area of the buffer zone = 314 km^2
2. Area of the water bodies = Nil
3. Hilly area (area not suitable for recharge) = 28.90 km^2
4. Area suitable for recharge under different rock types

(a) Singhbhum Granite – 44.78 km^2
(b) Mica Schist – 216.93 km^2.
(c) Shale, Phyllites – 23.39 km^2

5. Groundwater Fluctuation in (m)
(a) Average Fluctuation in Singhbhum Granite – 3.65 m
(b) Average Fluctuation in Mica Schist – 3.89 m
(c) Average Fluctuation in Shale, Phyllites – 5.00 m

6. Specific Yield –
(a) Shale, Phyllited – 0.03
(b) Mica Schist – 0.015
(c) Singhbhum Granite – 0.03

7. Monsoon Recharge under different formation in the Buffer Zone (Water Table Fluctuation Method)
= Singhbhum Granite + Mica Schist + Shale & Phyllites
= (44.78 x 3.65 x 0.03) + (216.93 x 3.89 x 0.015) + (23.39 x 5.00 x 0.03)
= 4.90 + 12.66 + 3.50
= 21.06 MCM

8. Rainfall Infiltration factor of different rock types in the buffer zone
(a) Shale, Phyllites – 0.04
(b) Mica Schist – 0.08
(c) Singhbhum Granite – 0.11

9. Annual Rainfall = 1307.60 mm
(a) Monsoon Rainfall = 1131.70 mm
(b) Non-monsoon Rainfall = 175.90 mm

10. Groundwater Recharge by Rainfall Infiltration Factor (Monsoon Season)
(a) R_{rf} (Singhbhum Granite) = Infiltration factor of singhbhum granite x Area x Normal rainfall in the monsoon season
= 0.11 x 44.78 x 1.131
= 5.571 mcm
(b) R_{rf} (Mica Schist) = Infiltration factor of mica schist x Area x Normal rainfall in the monsoon season
= 0.08 x 216.93 x 1.131
= 19.627 mcm
(c) R_{rf} (Shale, Phyllites) = Infiltration factor of Shale, Phyllites x Area x Normal rainfall in the monsoon season
= 0.04 x 23.39 x 1.131
= 1.05 mcm

Monsoon Recharge by Rainfall Infiltration Factor = 26.248 mcm

Monsoon Recharge due to water table fluctuation = 21.06 mcm

The rainfall recharge for normal monsoon season rainfall is finally adopted as per criteria are given below:

(a) If PD is greater than or equal to –20%, and less than or equal to +20%; R_{rf} (normal) is taken as the value estimated by the water table fluctuation method.
(b) If PD is less than –20%; R_{rf} (normal) is taken as equal to 0.8 times the value estimated by the rainfall infiltration factor method.
(c) If PD is greater than +20%; R_{rf} (normal) is taken as equal to 1.2 times the value estimated by the rainfall infiltration factor method.

$$\text{P.D.} = (21.06–26.248)/26.248 \times 100$$
$$= –19.76\ \%$$

Because PD is greater than or equal to –20%, and less than or equal to +20%; R_{rf} (normal) is taken as the value estimated by the water table fluctuation method

R_{rf} (normal) = 21.06 mcm

11. Groundwater Recharge by Rainfall Infiltration Factor (Non-monsoon Season)

(a) R_{rf} (Singhbhum Granite) = Infiltration factor of singhbhum granite x Area x Normal rainfall in non-monsoon season
= 0.11 x 44.78 x 0.175
= 0.862 mcm
(b) R_{rf} (Mica Schist) = Infiltration factor of mica schist x Area x Normal rainfall in non-monsoon season
= 0.08 x 216.93 x 0.175
= 3.037 mcm
(c) R_{rf} (Shale, Phyllites) = Infiltration factor of Shale, Phyllites x Area x Normal rainfall in non-monsoon season
= 0.04 x 23.39 x 0.175
=0.163 mcm

Total Non-monsoon Recharge by Rainfall Infiltration Factor = 4.062 mcm

Total Annual recharge = Monsoon Recharge + Non-monsoon Recharge
= 21.06 +4.062
= 25.122 mcm

12. Draft
Total Draft = Total draft of Gamharia + Rajnagar + Chandil + Potka
= 13.62 + 0.86 + 0.35 + 0.06
= 14.89 MCM (including industrial/drinking/irrigation)

13. Net Annual Groundwater Availability
= Total replenishable resources – Natural non-monsoon discharge
= 25.122 – 1.48
= 23.642

14. **S**tage of Groundwater Development
= (Total Draft/Net Annual Groundwater Availability) x 100
= (14.89/23.642) x 100
= 62.98 % (Say 63%)

18.4 IMPACT OF PUMPING ON LOCAL GROUNDWATER SYSTEM

18.4.1 PREVIOUS AND INCREASED WATER DEMAND OF THE PLANT

Total water requirement for the proposed project is estimated to be 160m^3d^{-1}. Present water requirement and the additional requirement will be obtained from groundwater through bore well within the premises (Table 18.14).

Water System

- The proposed project requires water for manufacturing as well as domestic consumption.
- The company will use groundwater through bore well to meet its requirement. The company has implemented the Rain Water Harvesting System for recharge of groundwater through 3 Nos. of recharge pit.
- Water is mainly required for cooling operations, where it is re-used
- As such wastage of water will be negligible, and there is no need of any water treatment arrangement.

TABLE 18.14 Water Requirements (Existing and Additional) of Beekay Steel Plant

S. No.	Particulars	Existing in KLD	Proposed in KLD	Total in KLD
1.	Industrial	33	99	132
2.	Domestic	4	12	16
3.	Others	3	9	12
	TOTAL	40	120	160

18.4.2 EFFECT ON STAGE OF GROUNDWATER DEVELOPMENT

The stage of groundwater development as assessed in the buffer zone of the project is 62.98 %. For meeting the existing as well as the increased water demand, it is proposed to withdraw water of 160m^3/day from the bore wells to be drilled within the plant premises.

Daily Water Requirement – 160 m^3d^{-1}

Annual Consumption – 160 x 365 = 58,400 m^3 = 0.0584 MCM

Total Draft = existing total draft + draft from the proposed bore wells

= 14.89 MCM + 0.0584 MCM = 14.9484 MCM

Expected stage of groundwater development

= Total Draft/Net Groundwater Resources x 100

= 14.9484/23.642 x 100

= 63.22%

So the stage of groundwater development after withdrawal of required quantity of groundwater for meeting the increased water demand of project will be increased to only 63.22 % from existing 62.98%.

18.4.3 RADIUS OF INFLUENCE

As per the studies carried out by CGWB in the district and pumping test carried out within the plant premises the storativity has been found to be 3.2 x 10^{-4} and the transmissivity has been found to be 12.096 m^2/day Due to the low permeability of the aquifer units, the impact of pumping on local water regime will be marginal and the radius of influence will be limited to a small distance. However, to estimate a probable zone of influence, the finding of CGWN studies have been considered for assessing the radius of influence. To evaluate the radius of influence the c-efficient of storage (S) value of 3.2 x 10^{-4} has been taken from the studies of Central Groundwater Board in the adjoining area of the buffer zone of the plant. The radius of influence has been arrived at using the following equation: $R^2 = (2.25Tt)/S$.

The time (t) has been considered as 8 hours of continuous pumping at a time and transmissivity 12.096 m^2d^{-1}. The value of the radius of influence (R) comes as 169 m. So it is found that there will be no effect of pumping in the local groundwater system at a distance of 169 m from pumping well in and around the plant area.

18.5 CONCLUSIONS AND RECOMMENDATIONS

The proposed project of M/s Beekay Steel Industries Limited falls within the administrative jurisdiction of Gamharia, Rajnagar, and Chandil Block of Saraikela-Kharsawan district and Potka Block of East-Singhbhum district. The stage of groundwater development in Gamharia block in which the core zone falls is 19.23% as assessed by CGWB (2013). There is no significant decline of pre-monsoon water level, as well as post-monsoon water levels in all the blocks and blocks, are categorized as "Safe" for future groundwater development as per CGWB published a report of Central Groundwater Board, Govt. of India on "Dynamic groundwater resources of Jharkhand." This leaves the scope of groundwater development for meeting the water demand of the proposed project. Again it is to mention that the stage of groundwater development after withdrawal of a required quantity of groundwater for meeting the water demand of the proposed project will be increased to only 63.22% from existing 62.98%.

To assess the impact on water levels in time and space, it is recommended to develop a close monitoring network in the zone of influence and quarterly monitoring of the water levels. For observing the impact on the aquifer system, shallow, and deeper piezometers will be constructed for monitoring the unconfined and confined aquifers respectively. The location and design of the piezometers will be finalized in close coordination with CGWB. They will be constructed in a protective place and will be monitored periodically. The water quality is monitored under routine monitoring. Creation of awareness among workers and local people about rainwater harvesting and conservation of water will be helpful. Monitoring the water quality of local nala and in domestic water intake structures will be regular. On analyzing the monitoring data, if any area is found to have any deleterious impact (qualitative or quantitative) due to industrial activity, suitable control and remedial measures will be taken by the project authorities.

KEYWORDS

- **BSIL**
- **CGWB**
- **TMT**

REFERENCES

ATLAS of Jharkhand State, (2008).

Dynamic Groundwater Resource of Jharkhand, Published by CGWB, (2011). Govt. of India and GWID, Govt. of Jharkhand.

Groundwater Information Booklet, Saraikela District, Published by CGWB, (2011). Govt. of India, State Unit Office-Ranchi, Mid-Eastern Region, Patna.

Karanth, K. R., (2016). *Groundwater Assessment Development and Management*, Tata McGraw Hill, New Delhi.

CHAPTER 19

SIMULTANEOUS BIOLOGICAL REMOVAL OF ARSENIC, IRON, AND NITRATE FROM GROUNDWATER BY A TERMINAL ELECTRON ACCEPTING PROCESS

ARVIND KUMAR SHAKYA and PRANAB KUMAR GHOSH

Department of Civil Engineering, IIT Guwahati, India – 781039,
E-mail: a.shakya@iitg.ernet.in

ABSTRACT

Groundwater contamination, natural, and/or anthropogenic is a major concern to human health. There are several reports of arsenic and iron co-contamination of groundwater from many parts of the world including northeastern states of India. Along with arsenic and iron, there are reports on co-occurrence of nitrate in groundwater of Assam, Jharkhand (India) and many other areas of the world. Several groundwaters contain increased concentrations of these pollutants that are observed either isolated or in pairs, or all three together. Although several physicochemical and/or biological processes have been established for the removal of one of the above-mentioned contaminants, but till now very few studies have been performed on the efficient and cost-effective simultaneous removal of two or more contaminants from groundwater.

In the present study, the performance of suspended growth batch bioreactors on simultaneous removal of arsenic, iron, and nitrate by mixed bacterial culture was evaluated by means of terminal electron accepting process in the presence of sulfate. A series of conical flasks were used as batch reactors were inoculated with mixed bacterial culture mainly collected from a wastewater treatment plant and acclimatized in the presence of arsenic, nitrate, and sulfate. The reactors were fed with real contaminated groundwater containing 30–125 μgl^{-1} of arsenic, 1.5–3.0 mgl^{-1} of iron, 50 mgl^{-1} of

nitrates, 25 mgl^{-1} of sulfate, along with 105 mgl^{-1} of COD. The reactors were operated for a period of 7 days at 30°C in an incubator shaker. The removal approach consists of reduction of arsenic and nitrate coupled with oxidation of an electron donor (acetic acid). Complete nitrate removal was observed whereas arsenic and iron were below drinking water permissible limits of 10 μgl^{-1} and 0.3 mgl^{-1}, respectively within 3–4 days of operation. The insoluble bio-precipitates of arsenic and/or iron sulfides were the main arsenic and iron removal mechanism in the studied system.

19.1 INTRODUCTION

Arsenic is a common groundwater pollutant affecting more than 150 million people around the world. Long-term consumption of arsenic in drinking water causes adverse effects on human health including cancer (skin, lung, bladder), neurological problems, gastrointestinal disorders, reproductive problems and muscular weakness (Singh et al., 2015). Due to health risks associated with arsenic, the World Health Organization and other state agencies have imposed a maximum contaminant level (MCL) guideline of 10 μgl^{-1}. Under reducing conditions, those prevailing in groundwater, arsenite [As (III)] is the prevalent form of arsenic. Arsenic (III) is 25–60 times more toxic than arsenic (V). Iron is common contaminant often present in groundwater with arsenic, for example, in groundwater of Mekong Delta in Vietnam (Buschmann et al., 2008) and in several districts of Assam (India). Iron is not considered to cause severe health problems in humans; rather its presence in potable water can cause different types of nuisance problems. Recently, due to regular intake of high iron containing groundwater, some adverse health effects like hemochromatosis, liver cirrhosis, and siderosis is observed in people of Assam, India (Chaturvedi et al., 2014). The MCL of iron in drinking water is 0.3 mgl^{-1} (WHO, 2011). Nitrate is another common contaminant of groundwater often coexists with arsenic and iron (Rezaie-Boroon et al., 2014). High nitrate concentrations are reported elsewhere, for example, Australia, USA, China, and India (Kapoor and Viraraghavan, 1997). The major source of nitrate in groundwater are extensive use of nitrogenous fertilizers, discharge from septic tanks, spreading of sewage sludge and seepage from pit latrines. Ingestion of high nitrate levels in drinking water causes "blue baby syndrome" in infants and cancers, reproductive problems, infectious diseases and diabetes (Bhatnagar and Sillanpaa, 2011). Keeping in mind the link between serious health problems and excessive concentration of nitrate in drinking water, WHO recommended nitrate concentration

limit of 50 mg NO_3^-/L (WHO, 2011). The combined occurrence of arsenic, iron, and nitrate is reported from many regions of the world including Argentina (Gimenez et al., 2013) India (Chakrabarty and Sarma, 2011), and Myanmar (Bacquart et al., 2015). The co-occurrence of these contaminants in groundwater is either due to natural geogenic sources or anthropogenic origin such as industrial activities in that nearby area, for example, high level of iron, nitrate, and fluoride in Angul-Talcher (Orissa) and Drain Basin Area, Najafgarh (Delhi) (CPCB, 2007). Although much work has been done on the individual removal of these common pollutants with different conventional methods to provide a suitable mitigation approach, little attention was paid on combined removal of them using an effective and sustainable process. Conventional methods for removing nitrate, arsenic, and iron include sorption on to various materials, ion exchange, membrane filtration and electrocoagulation (Bhatnagar and Sillanpaa, 2011; Singh et al., 2015; Khatri et al., 2017). All these methods have specific disadvantages. For example, ion exchange and membrane filtration are generally costly and produces large quantities of spent sludge which requires further treatment and disposal problems (Chung et al., 2007). Similarly, electrocoagulation suffers from the replacement of electrodes at a regular interval, high cost and anode passivation (Kumar and Goel, 2010). The research for sustainable and effective treatment options has focused attention on the biologically mediated process. Terminal electron accepting process based bioreactors is an emerging alternative option to existing methods used to remove multi-contaminants from groundwater (Brown et al.,2008). Chung et al. (2007) demonstrated simultaneous bio-reduction of nitrate, arsenic, and other contaminants in a membrane bioreactor. Membrane bioreactors inoculated with mixed bacterial culture removed nearly 100% nitrate and 80% arsenic from an initial concentration of 21 mg-Nl^{-1} and 7.3 μgl^{-1}, respectively. Zhao et al., (2014) studied the performance of a two-stage membrane biofilm reactor treating groundwater containing nitrate, perchlorate, sulfate, and oxygen. They reported 100% nitrate and 97% perchlorate removal from an initial concentration of 9 mgl^{-1} and 200 μgl^{-1}, respectively. Upadhyaya et al., (2012) demonstrated two stage fixed film bioreactor system for combined removal of arsenic and nitrate. At an influent arsenic concentration of 300 μgl^{-1} and nitrate of 50 mgl^{-1}, the nitrate removal efficiency was 100 %. However, the arsenic removal efficiency was 90% and treated water was not meeting drinking water MCL of 10 μgl^{-1}. In their study, the main arsenic removal mechanism was precipitation of biogenic arsenic and iron sulfides resulting from biosulfidogenesis.

Although few studies have investigated the combined removal of arsenic and nitrate using indigenous mixed microbial culture, the combined removal of arsenic, nitrate, and iron from real contaminated groundwater has not been yet studied. Hence, the present study investigates the efficiency of simultaneous biological removal of arsenic, iron, and nitrate in acetate fed suspended growth reactors in which sulfate serves as an electron acceptor for the biogenic sulfide and the subsequent removal of arsenic and iron. Particular importance was attached to the effects of real groundwater on mixed bacterial culture performance on contaminant removal. The biogenic precipitate was characterized by field emission scanning electron microscopy (FESEM).

19.2 MATERIALS AND METHODS

19.2.1 EXPERIMENTAL SETUP

High-density polyethylene conical flasks with the effective volume of 250 mL were used as the bioreactors. The cap was butyl synthetic rubber, with air tightness, and the solution volume was 100 mL, including feed medium (real groundwater) and inoculation sludge. Real groundwater was added into the reactor with a sterile syringe. Residual air in the reactor was expelled by purging oxygen-free nitrogen gas for 5 minutes. The reactors were covered with black paper and incubated in a shaking incubator at 120 rpm.

19.2.2 REAL GROUNDWATER COLLECTION

Real groundwater was collected from the well of two locations at (26°16.45′N and 90°41.22′E; 26°16.53′N and 90°40.79′E, depth of well 160 ft.) near New Bongaigaon district, Assam (India), where arsenic and iron concentrations were varied in the range of 30–125 μgl^{-1} and 1.5–3.0 mgl^{-1}, respectively. Groundwater collected after adequate purging (10–15 min.) were stored in pre-acidified (with HCl at pH 2) high-density polyethylene containers for metal analysis. The characterization of other water quality parameters is done with non-acidified groundwater sample. The real groundwater quality parameters are given in Table 19.1. Containers were filled to overflowing and sealed with thread seal tape immediately to further minimize contact of oxygen. All groundwater samples were transported to the Environmental Engineering Laboratory, IIT Guwahati, within 6 h and subsequently kept at 10°C until analysis.

TABLE 19.1 Composition of the Real Groundwater

Components	Unit	Concentration	
		RGW–1	RGW–2
Temperature	°C	27.8°C	27.5
pH	-	6.6	6.62
EC	$Mscm^{-1}$	862	872
ORP	mv	87.3	84
Fe_{tot}	mgl^{-1}	1.68	3.2
SO_4^{2-}	mgl^{-1}	5.2	4.4
As_{tot}	μgl^{-1}	29.2	124.4
NO_3^{2-}	mgl^{-1}	2.6	3.2
PO_4^{3-}	mgl^{-1}	1.14	0.86
Cl^-	mgl^{-1}	10.6	12.4
HCO_3^-	mgl^{-1}	176	170
CO_3^{2-}	mgl^{-1}	19.2	17.6
Na	mgl^{-1}	9.8	8.2
Ca	mgl^{-1}	51.8	38.2
Mg	mgl^{-1}	4.82	5.1
D.O.	mgl^{-1}	4.1	4.3

19.2.3 INOCULUM AND STARTING UP

Anoxic sludge was collected from the anoxic pond of IIT Guwahati Sewage Treatment Plant (Guwahati, India). Seed culture for inoculation of reactors was obtained by mixing sludge collected from IIT Guwahati sewage treatment plant and a bench scale sulfate anoxic removal bioreactor. Acclimatized sludge (100 mgl^{-1} as MLVSS) was added as inoculum in the experiments. Based on carbon required for complete removal of all electron acceptors (i.e., residual DO, nitrate, arsenate, and sulfate) and average net yield of 0.4 g biomass/g COD acetate, 105 mgl^{-1} COD as carbon was supplemented in synthetic groundwater with a safety factor of 1.5. All the chemicals used were of analytical grade and purchased from Merck. To investigate the potential for bio-adsorption of arsenic (V) and iron on to biomass and any volatilization loss of contaminants a control group was examined containing only real groundwater (RGW–2) mixed bacterial culture and no carbon source. Two test groups were investigated with three replications, fed with type–1 and type–2 groundwater, to ensure the

reliability of results. The reactors were fed solely with real groundwater except for the addition of 50 mgl^{-1} nitrate, 25 mgl^{-1} sulfate and 105 mg^{-1} COD. Experiments were also conducted with simulated groundwater at higher concentrations of arsenic (200 and 300 μgl^{-1}), iron (4 and 5 mg^{-1}) and nitrate (75 and 100 mg^{-1}) to evaluate mixed culture performance. COD in the influent media was increased at higher concentrations of nitrate to meet carbon requirements. All groups were examined at natural pH of real groundwater and 35°C for 7 days. The experiments were conducted in an incubator shaker in self-scarifying mode.

19.2.4 ANALYTICAL METHODS

Liquid samples were centrifuged at 6000 rpm for 10 min using a REMI R–24 centrifuge, and then filtered prior to nitrate, sulfate, COD, iron, and arsenic measurements in the supernatant. In general, standard techniques as given in Standard Methods for the Examination of Water and Wastewater (APHA, 2005) have been followed unless otherwise stated. Samples for pH, nitrate, sulfate, and residual COD were analyzed promptly on the same day. The pH of the medium from the reactor was measured using pH meter (Thermo Scientific). Nitrate was measured using an UV-visible spectrophotometer (Varian, Cary 50 Bio) at 220 and 275 nm. Sulfate analysis was done using digital nephelo-turbidity meter (132, Systronics). Residual COD was measured by using closed reflux titrimetric method (Hach DRB 200). Prior to COD determination, samples were acidified to a pH less than 2 by addition of concentrated H_2SO_4 and then purged with N_2 gas for approximately 5 minutes to remove H_2S. Samples for total arsenic and iron were acidified to a final concentration of 0.02 N HCl to solubilize any precipitates and stored at 4°C after filtering through 0.2 µm filters. Total arsenic samples were analyzed within 48 h by using an atomic absorption spectrometer (Varian, SpectrAA Analyst 800). A continuous flow hydride generation system was used for detection of arsenic concentration with detection limits of 1 μgl^{-1} As (T). Iron was measured using the phenanthroline method. All measurements were performed in duplicate and mean values of the results are presented. Biogenic precipitates were analyzed using field emission scanning electron microscope-energy dispersive X-ray spectroscopy (FESEM-EDX). After centrifugation the pellets were collected and frozen at –20°C for 12 h, and then freeze-dried. The freeze-dried samples were examined using a FESEM (Sigma, Carl Zeiss, Germany). The elemental composition of precipitate was analyzed using EDX (Oxford Instruments, Germany).

19.3 RESULTS AND DISCUSSION

19.3.1 BIOMASS ADSORPTION STUDIES

The adsorption of arsenic and iron on to 100 mgl^{-1} of biomass (MLVSS) from the "control" is shown in Figure 19.1. After 7 days, from an initial 124 μgl^{-1}, only about 11%, removal of arsenic was noticed from control. The total amount of iron adsorbed was found to be 26.8%. Reduction in arsenic concentration in control might be due to loss of arsenic by adsorption on to biomass, adsorption on to ferrous iron and/or volatilization. Teclu et al., (2008) reported about 6.5% and 10% bio-sorption of As (III) and As(V), respectively, from an initial of 1000 and 5000 μgl^{-1}.

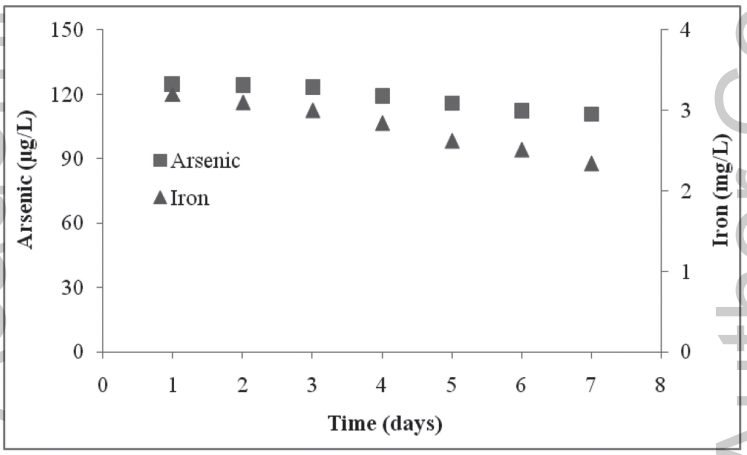

FIGURE 19.1 Arsenic removal due to adsorption on to biomass and/or iron.

Similarly, the loss of iron might be associated with biomass adsorption and/or formation of adsorption complex with arsenic. Low removal of arsenic through bio-sorption could have been due to the fact that the isoelectric point of most microbes is around pH 2. Therefore, bio-sorption of arsenic near neutral pH was very low (Teclu et al., 2008).

19.3.2 PROFILES OF NITRATE, SULPHATE, COD, PH, AND MLVSS

Figure 19.2(a) represents the performance of mixed bacterial culture in batch reactors on nitrate removal. Irrespective of initial iron and arsenic

concentration, nitrate in the treated water was always less than the detection limit within 24 h of reactor operation. These results also confirmed that the high nitrate concentration of 75 and 100 mg/L, had not affected the arsenic and iron removal (Figure 19.2a). The sulfate and COD were reduced gradually during an entire period of 7 days operation; reduction rate decreased after about 3–4 days of reaction. Sulfate of only 3–5 mgl^{-1} and 2–3 mgl^{-1} was left out in the treated water after 4 days and 7 days of operation respectively (Figure 19.2a). COD removal was rapid on the first day, and about 70±2% COD was removed (Figure 19.2b). This is in compliance with the complete nitrate removal. Most of the COD was removed in the reactors and only 22–24 mgl^{-1} and 16–18 mgl^{-1} remained in the treated water after 7 days of operation, respectively. The pH of the treated water always remained between 7.25–8.0. pH of the treated water (Figure 19.2c) increased with the removal of nitrate and sulfate. This could have been due to the formation of alkalinity due to the reduction of nitrate and sulfate. Variation in biomass (MLVSS) concentration is shown in Figure 19.2(d). Biomass concentration started decreasing after an initial increase for the first 3–4 days of operation. The increase in MLVSS suggests that mixed microbial consortia grew well-using nitrate, sulfate, and arsenate as the terminal electron acceptor under an anoxic condition in the presence of acetate as an electron donor.

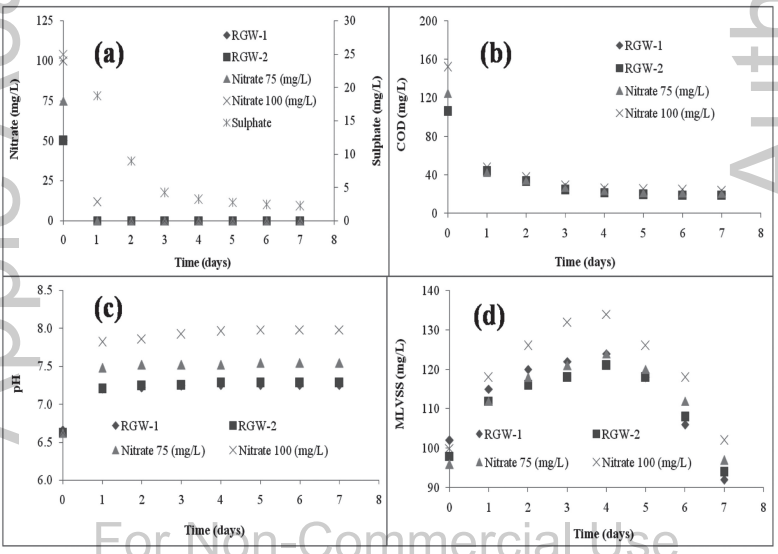

FIGURE 19.2 (a) Change of nitrate and sulfate (b) COD, (c) pH, and (d) MLVSS concentrations in the medium inoculated with mixed culture as a function of incubation time in the presence of variable concentrations of nitrate in the batch reactors.

The decrease in MLVSS after day 5 of reactor run could be associated with unavailability of carbon source in the medium as a result of the reduction of all electron acceptors present in the system.

19.3.3 PROFILES OF ARSENIC AND IRON

Figure 19.3(a) represents the performance of mixed bacterial culture in batch reactors at four different initial arsenic concentrations of 29.2 μgl^{-1} (RGW–1), 124 µg/L (RGW–2), 200 μgl^{-1} and 300 μgl^{-1}, respectively. Irrespective of initial concentration, arsenic in the treated water was reduced below the permissible limit (10 μgl^{-1}) in 4–5 days of reaction and finally averaged 4±2 $\mu gl^{-1}$with 98.5% removal efficiency. Figure 19.3(b) represents effects of initial iron concentration of 1.68, 3.2, 4.0 and 5.0 mgl^{-1}, respectively. Irrespective of initial iron concentration (up to 5.0 mgl^{-1}), nitrate, and arsenic removal was not affected in batch reactors. Up to an initial 3.2 mgl^{-1}, iron in the treated water was always below the detection limit. However, 0.52 mgl^{-1} (87% removal) and 0.84 mgl^{-1} (83% removal) of iron concentration was observed in the treated water at 4.0 mgl^{-1} and 5.0 mgl^{-1} of initial iron. The possible reason for this higher iron concentration (0.84 mgl^{-1}) in treated water might be due to unavailability of sufficient sulfides for precipitation as iron sulfides. As it can be clearly seen in Figures 19.3a and 3b arsenic and iron removal are associated with sulfate reduction. Furthermore, with respect to the effect of initial arsenic concentration on arsenic removal, arsenic removal was always with in accordance with drinking water guidelines.

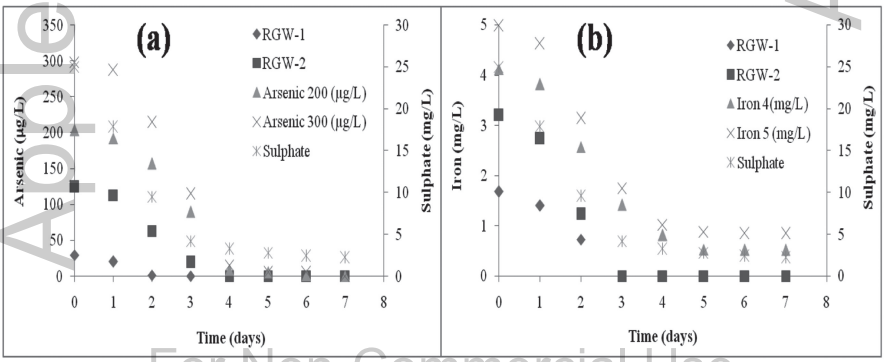

FIGURE 19.3 (a) Change of arsenic, sulfate (b) iron and sulfate concentrations in the medium inoculated with mixed culture as a function of incubation time in the presence of various concentrations of arsenic and iron.

Arsenic removal percentages by the mixed microbial consortia were not affected by high arsenic concentration (up to 300 μgl^{-1}), also indicating the mixed culture viability was not inhibited by arsenite toxicity in the experimental concentration range. The high arsenic and iron concentration had no impact on the nitrate removal. As most of the arsenic and iron was removed during sulfate reduction period which confirmed the precipitation of arsenic and iron with the biogenic sulfides formed as a result of biosulfidogenesis. In summary, mixed culture and sulfate were essential. Once these conditions were met, the arsenic and iron removal was possible.

19.3.4 CHARACTERIZATION OF BIOGENIC PRECIPITATES

The FESEM image of precipitates formed in the inoculated medium is shown in Figure 19.4a. EDS analysis showed that the precipitates were mainly composed of As (39.9%), iron (49.7%) and sulfur (10.3%) (Figure 19.4b). The results indicated that reduced arsenic was probably precipitated with sulfide and/or get adsorbed on to iron sulfide and biomass.

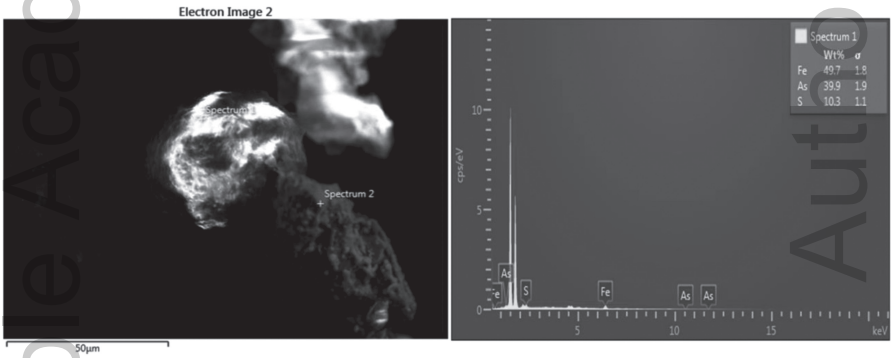

FIGURE 19.4 (See color insert.) FESEM image (a) and EDS analysis of precipitate (b) formed in the batch reactor.

The reduction of electron acceptors (DO, nitrate, sulfate, and arsenate) was coupled to the oxidation of an electron donor (acetate). Thus batch reactors employed in this study relies on terminal electron accepting processes (TEAPs) similar to those occurring in deep subsurface groundwater environment. (Lovley and Chapelle, 1995). The acetic acid was selected as a carbon source as it has been approved for drinking water treatment (National

Sanitation Foundation product and service listings, www.nsf.org) and was previously found to be effective for perchlorate removing bioreactors (Choi et al., 2007). In addition, acetic acid can be effectively utilized by many nitrate and sulfate-reducing bacteria as an electron donor (Calderer et al., 2010, Rabus et al., 2013). Many reports are available on the presence of anaerobic nitrate and sulfate-reducing bacteria in habitats such as activated sludge and sewage waters (Nielsen and Nielsen, 1998, Liu et al., 2008). After nitrate is depleted from the reactors, arsenic, and sulfate was removed from the reactors which were the next most thermodynamically favorable TEAP in the studied system. This segregation of TEAPs also explains the presence of different type of microbes in the bioreactors (Lovley and Chapelle, 1995, Macy et al., 1996). In treated water sample analyses, sulfate reduction corresponded with arsenic and iron removal. Hence, it is possible that arsenic and iron was removed through the precipitation of their respective metal sulfides. The EDS results were consistent with results found by other investigators. They reported arsenic precipitation as orpiment (As_2S_3) (Newman et al., 1997) and realgar (AsS) (O'Day et al., 2004), and confirmed the formation of arsenic sulphides by extensive X-ray absorption near edge structure and thermodynamic modeling (Onstott et al., 2011, Rodriguez-Freire et al., 2014). Some amount of arsenic may also get adsorbed on to biomass as reported by Teclu et al. (2008). In the present study, although the exact arsenic removal processes are not clear, the possible removal mechanism of iron was removal as iron sulfides precipitation and arsenic was removed either as arsenosulfides precipitation and or adsorption on to iron sulfides.

19.4 SUMMARY

In conclusion, the TEAP based batch bioreactors were successfully applied for simultaneous removal of arsenic, iron, and nitrate removal from polluted drinking water supplies to levels below the MCL of 10 μgl^{-1} and 0.3 mgl^{-1}, respectively. Complete nitrate removal was achieved up to 150 mgl^{-1} of nitrate. The presence of high nitrate did not affect arsenic and iron removal in TEAP based process in studied concentration ranges of contaminants. Together with high efficiency, sustainability of the process, environment-friendliness, and the ease of multi-contaminant removal, the present method is having great potential for rural applications in developing countries.

ACKNOWLEDGMENTS

The authors acknowledge the funding by the Ministry of Drinking Water and Sanitation (Government of India), through the project (Ref. No. W.11017/44/2011-WQ) to carry out this work at IIT Guwahati. Authors are also thankful to the central instrument facility of IIT Guwahati for providing facilities for FESEM/EDS analysis of some samples.

KEYWORDS

- **biogenic sulfide**
- **co-contaminant**
- **TEAP**

REFERENCES

APHA, (2005). *Standard Methods for the Examination of Water & Wastewater* (21st edn.). American Public Health Association, Washington DC.

Bacquart, T., Frisbie, S., Mitchell, E., Grigg, L., Cole, C., Small, C., & Sarkar, B., (2015). Multiple inorganic toxic substances contaminating the groundwater of Myingyan Township, Myanmar: Arsenic, manganese, fluoride, iron, and uranium. *Science of the Total Environment*, *517*, 232–245.

Bhatnagar, A., & Sillanpaa, M., (2011). A review of emerging adsorbents for nitrate removal from water. *Chemical Engineering Journal, 168*, 493–504.

Brown, J. C., (2008). Biological treatments of drinking water.

Buschmann, J., Berg, M., Stengel, C., Winkel, L., Sampson, M. L., Trang, P. T. K., & Viet, P. H., (2008). Contamination of drinking water resources in the Mekong delta floodplains: Arsenic and other trace metals pose serious health risks to the population. *Environment International, 34*, 756–764.

Calderer, M., Gibert, O., Marti, V., Rovira, M., De Pablo, J., Jordana, S., Duro, L., Guimera, J., & Bruno, J., (2010). Denitrification in presence of acetate and glucose for bioremediation of nitrate-contaminated groundwater. *Environmental Technology*, *31*, 799–814.

Chakrabarty, S., & Sarma, H. P., (2011). Fluoride, iron and nitrate-contaminated drinking water in Kamrup district, Assam, India. *Archives of Applied Science Research, 3*, 186–192.

Chaturvedi, R., Banerjee, S., Chattopadhyay, P., Bhattacharjee, C. R., Raul, P., & Borah, K., (2014). High iron accumulation in hair and nail of people living in iron affected areas of Assam, India. *Ecotoxicology and Environmental Safety*, *110*, 216–220.

Choi, Y. C., Li, X., Raskin, L., & Morgenroth, E., (2007). Effect of backwashing on perchlorate removal in fixed bed biofilm reactors. *Water Research, 41*, 1949–1959.

Chung, J., Rittmann, B. E., Wright, W. F., & Bowman, R. H., (2007). Simultaneous bio-reduction of nitrate, perchlorate, selenate, chromate, arsenate, and dibromochloropropane using a hydrogen-based membrane biofilm reactor. *Biodegradation, 18*, 199–209.

CPCB, (2007). *Status of Groundwater Quality in India*. Central Pollution Control Board, Ministry of Environment and Forests, Govt. of India.

Gimenez, M. C., Blanes, P. S., Buchhamer, E. E., Osicka, R. M., Morisio, Y., & Farias, S. S., (2013). Assessment of heavy metals concentration in arsenic contaminated groundwater of the Chaco Plain, Argentina. *ISRN Environmental Chemistry.*

Kapoor, A., & Viraraghavan, T., (1997). Nitrate removal from drinking water—Review. *Journal of Environmental Engineering, 123*, 371–380.

Khatri, N., Tyagi, S., & Rawtani, D., (2017). Recent strategies for the removal of iron from water: A review. *Journal of Water Process Engineering, 19*, 291–304.

Kumar, N. S., & Goel, S., (2010). Factors influencing arsenic and nitrate removal from drinking water in a continuous flow electrocoagulation (EC) process. *Journal of Hazardous Materials, 173*, 528–533.

Liu, X., Gao, C., Zhang, A., Jin, P., Wang, L., & Feng, L., (2008). The nos gene cluster from gram-positive bacterium Geobacillus thermodenitrificans NG80–2 and functional characterization of the recombinant NosZ. *FEMS Microbiology Letters, 289*, 46–52.

Lovley, D. R., & Chapelle, F. H., (1995). Deep subsurface microbial processes. *Reviews of Geophysics, 33*, 365–381.

Macy, J. M., Nunan, K., Hagen, K. D., Dixon, D. R., Harbour, P. J., Cahill, M., & Sly, L. I., (1996). Chrysiogenes arsenatis gen. nov., sp. nov., a new arsenate-respiring bacterium isolated from gold mine wastewater. *International Journal of Systematic Bacteriology, 46*, 1153–1157.

Newman, D. K., Kennedy, E. K., Coates, J. D., Ahmann, D., Ellis, D. J., Lovley, D. R., & Morel, F. M., (1997). Dissimilatory arsenate and sulfate reduction in Desulfotomaculum auripigmentum sp. nov. *Archives of Microbiology, 168*, 380–388.

Nielsen, J. L., & Nielsen, P. H., (1998). Microbial nitrate-dependent oxidation of ferrous iron in activated sludge. *Environmental Science & Technology, 32*, 3556–3561.

ODay, P. A., Vlassopoulos, D., Root, R., & Rivera, N., (2004). The influence of sulfur and iron on dissolved arsenic concentrations in the shallow subsurface under changing redox conditions. *Proceedings of the National Academy of Sciences of the United States of America, 101*, 13703–13708.

Onstott, T. C., Chan, E., Polizzotto, M. L., Lanzon, J., & DeFlaun., M. F., (2011). Precipitation of arsenic under sulfate-reducing conditions and subsequent leaching under aerobic conditions. *Applied Geochemistry, 26*, 269–285.

Rabus, R., Hansen, T. A., & Widdel, F., (2013). Dissimilatory sulfate-and sulfur-reducing prokaryotes. *The Prokaryotes* (pp. 309–404). Springer.

Rezaie-Boroon, M. H., Chaney, J., & Bowers, B., (2014). The source of arsenic and nitrate in Borrego valley groundwater aquifer. *Journal of Water Resource and Protection, 6*, 1589.

Rodriguez-Freire, L., Sierra-Alvarez, R., Root, R., Chorover, J., & Field, J. A., (2014). Biomineralization of arsenate to arsenic sulfides is greatly enhanced at mildly acidic conditions. *Water Research*, *66*, 242–253.

Singh, R., Singh, S., Parihar, P., Singh, V. P., & Prasad, S. M., (2015). Arsenic contamination, consequences, and remediation techniques: A review. *Ecotoxicology and Environmental Safety, 112*, 247–270.

Teclu, D., Tivchev, G., Laing, M., & Wallis, M., (2008). Bioremoval of arsenic species from contaminated waters by sulfate-reducing bacteria. *Water Research*, *42*, 4885–4893.

Upadhyaya, G., Clancy, T. M., Snyder, K. V., Brown, J., Hayes, K. F., & Raskin, L., (2012). Effect of air-assisted backwashing on the performance of an anaerobic fixed-bed bioreactor that simultaneously removes nitrate and arsenic from drinking water sources. *Water Research*, *46*, 1309–1317.

WHO Guidelines for Drinking-Water Quality, (2011). *World Health Organisation,* Geneva, *4*, 315–318.

Zhao, H. P., Ontiveros-Valencia, A., & Tang, Y., (2014). Removal of multiple electron acceptors by pilot-scale, two-stage membrane biofilm reactors. *Water Research, 54*, 115–122.

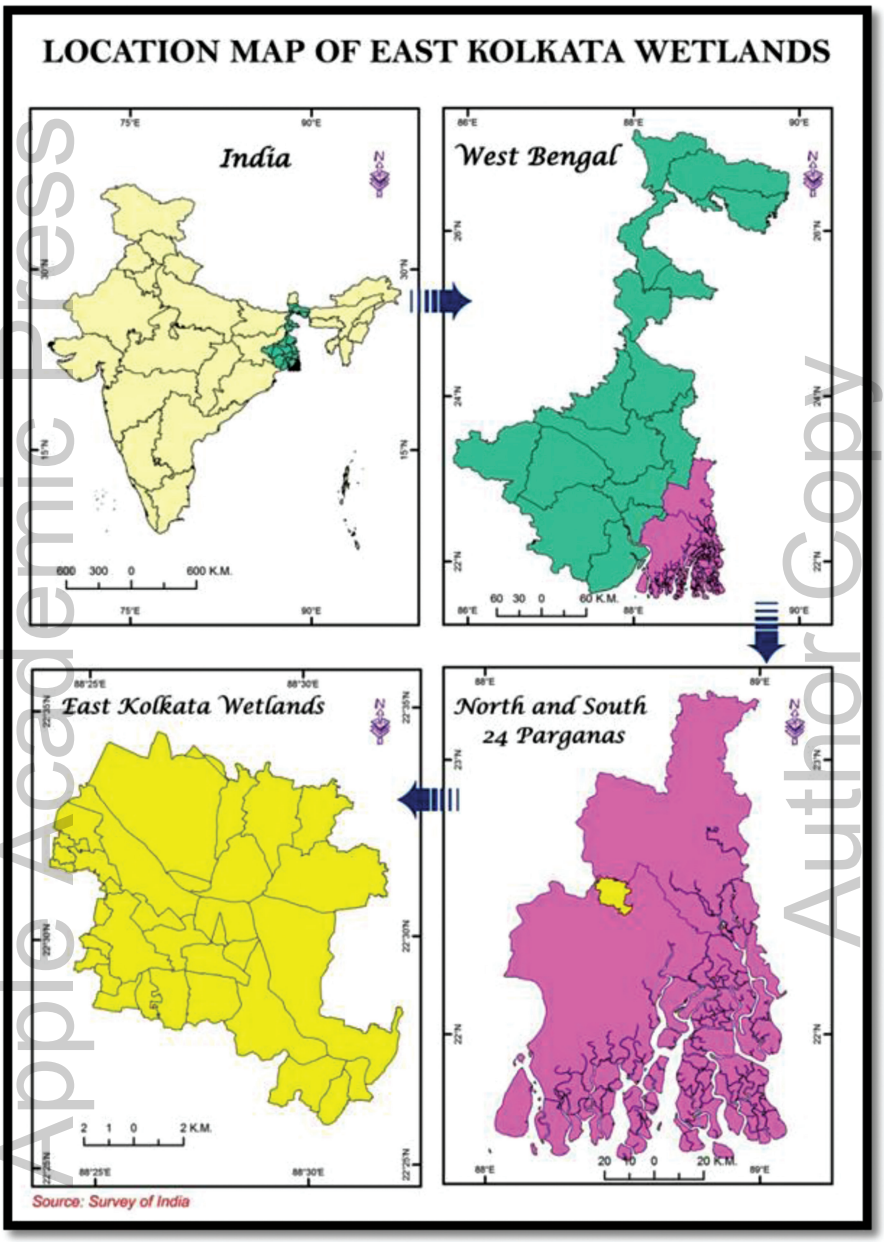

FIGURE 3.1 Location map of EKW, Kolkata.

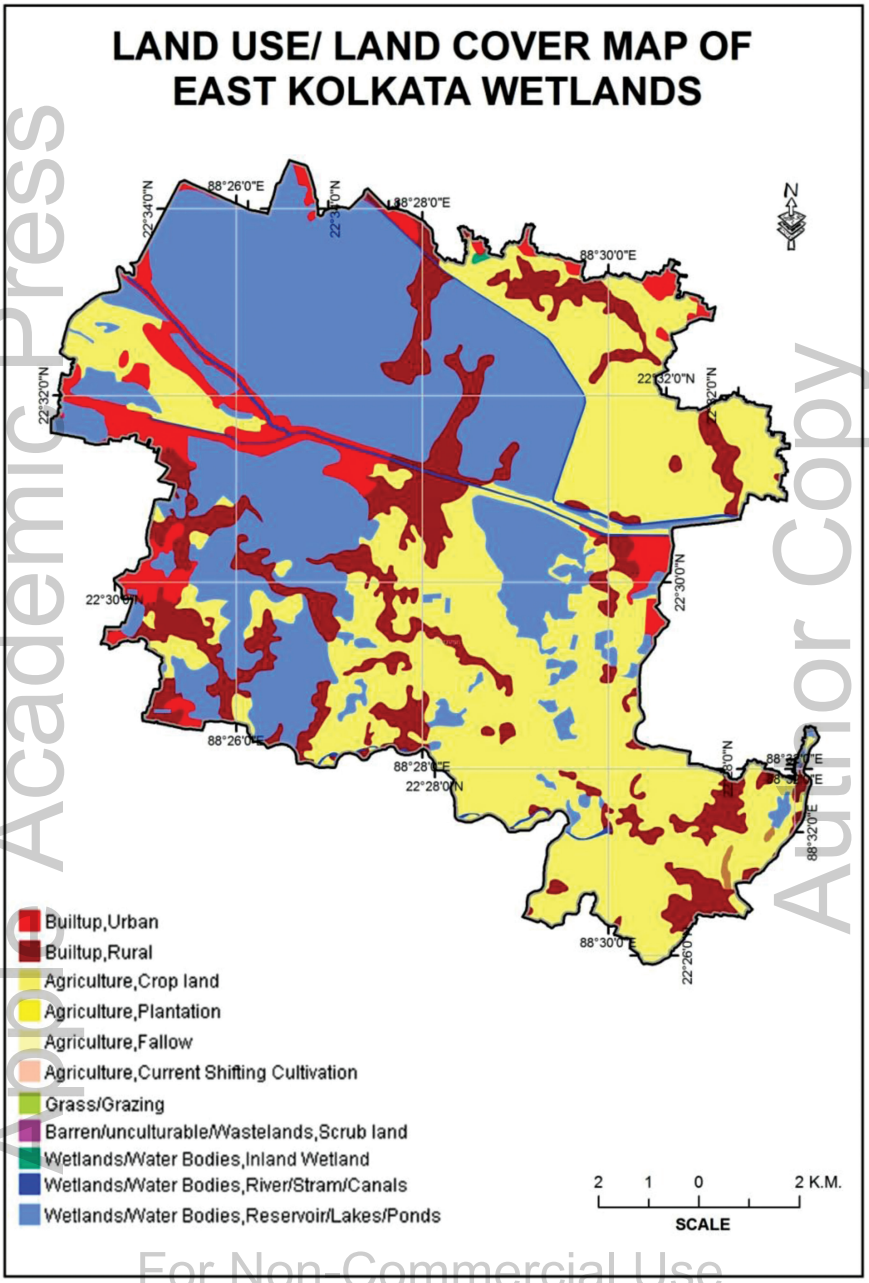

FIGURE 3.2 Current land use and land cover of EKW.

FIGURE 4.3 IWRM planning cycle.

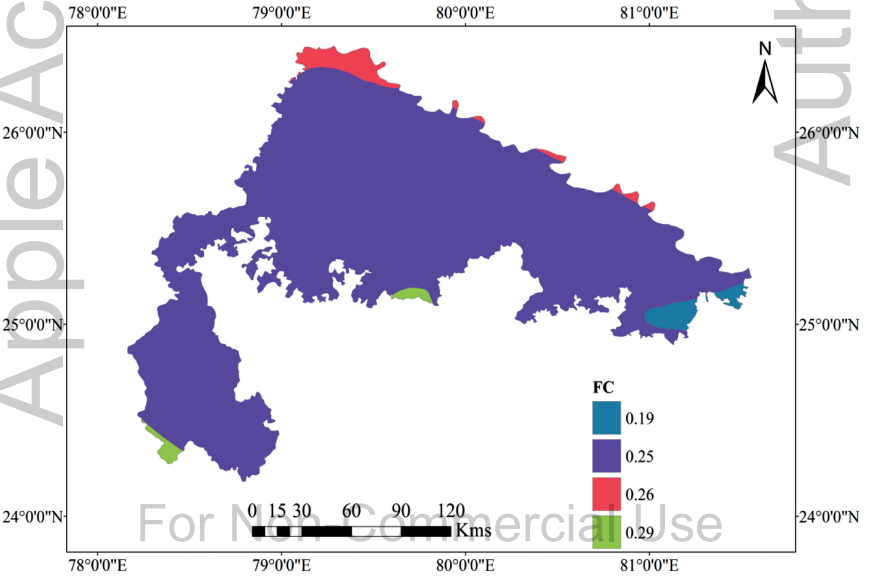

FIGURE 6.2 Field capacity map of study area.

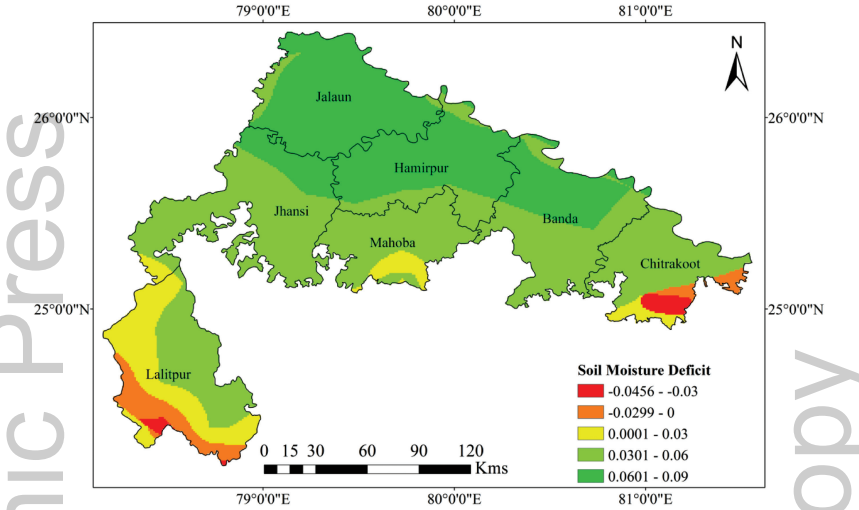

FIGURE 6.4 Soil moisture deficit (SMD) of the study area.

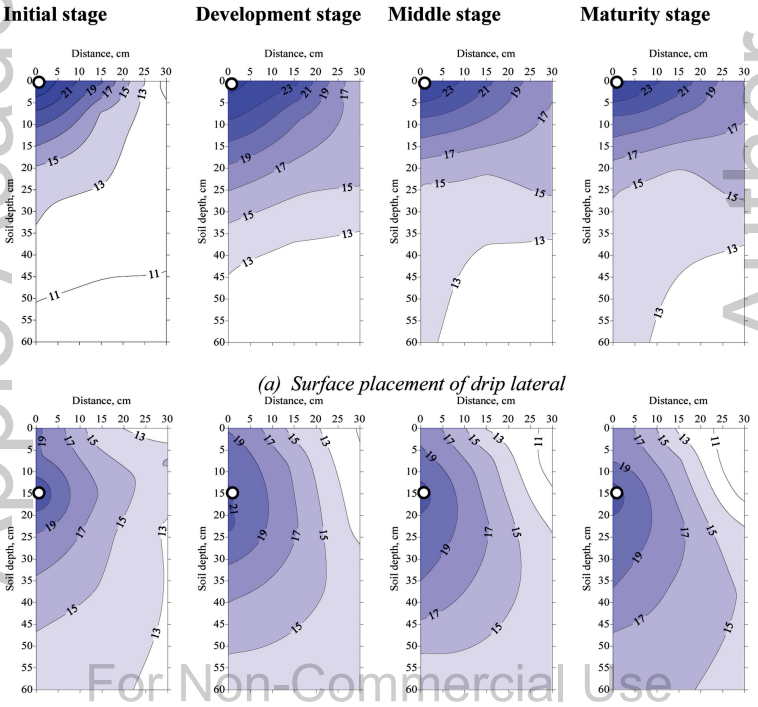

FIGURE 7.1 Observed soil water (volumetric in percent) distribution in the field.

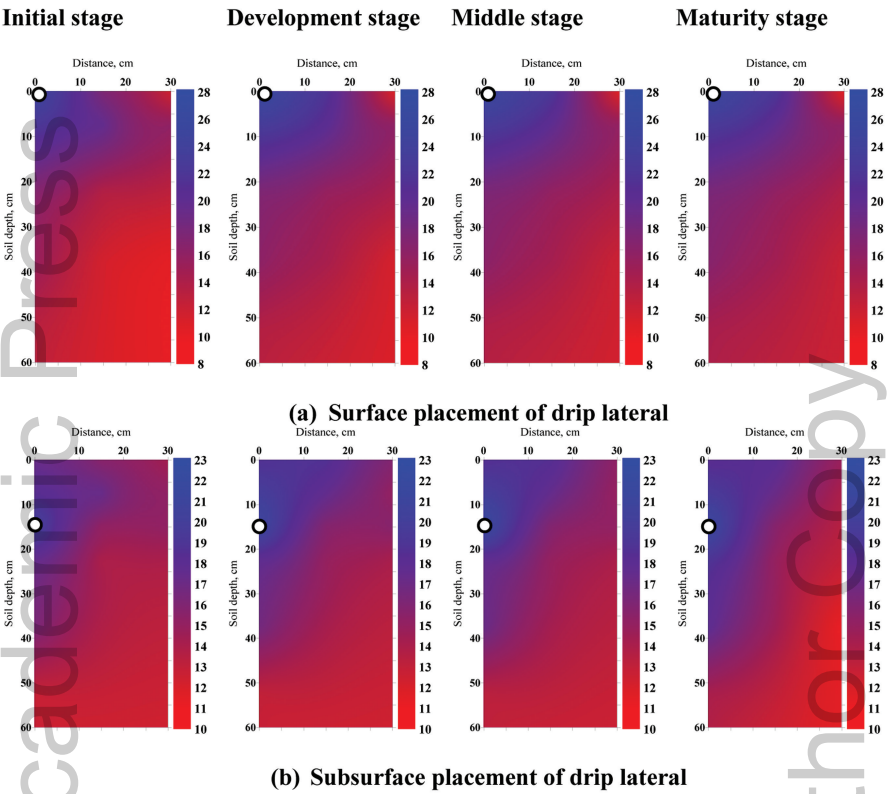

FIGURE 7.2 Simulated soil water (volumetric in percent) distribution with the model.

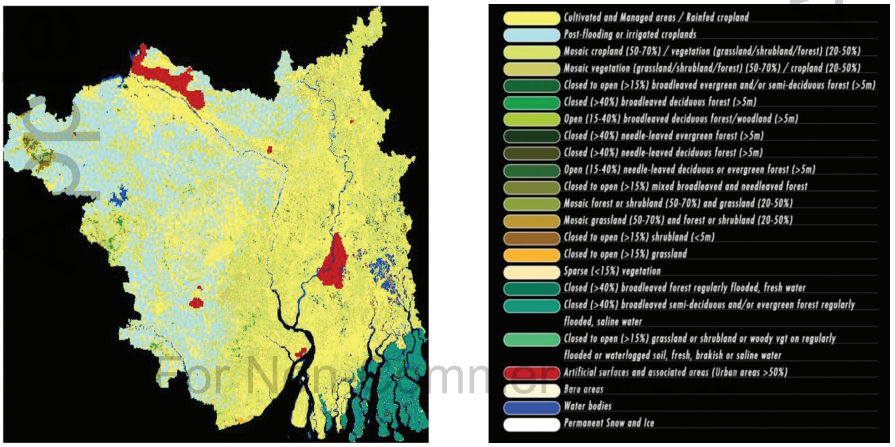

FIGURE 11.4 Land use and land cover.

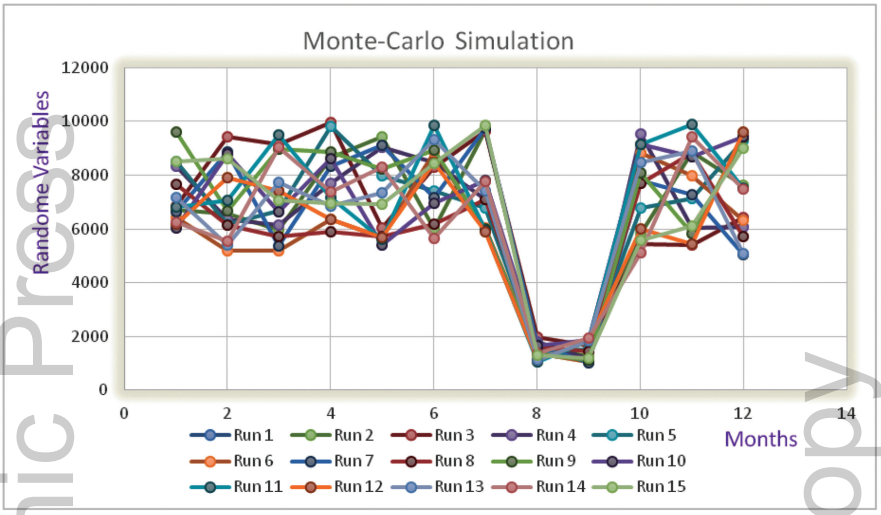

FIGURE 12.2 Changing the trajectory of a random variable in Monte-Carlo simulation.

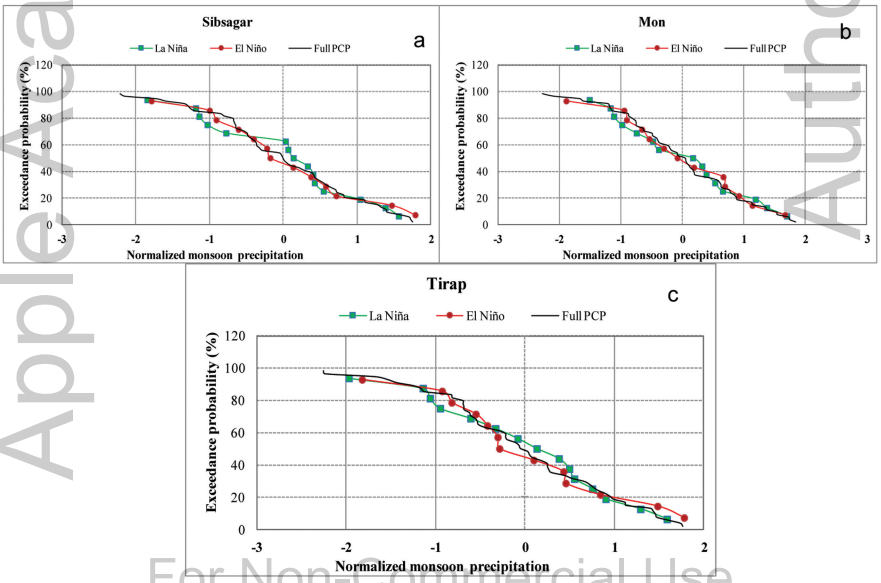

FIGURE 15.2 Graph of the cumulative distribution of normalized monsoon precipitation during El Niño, La Niña and Normal phase for (a) Sibsagar, (b) Mon and (c) Tirap.

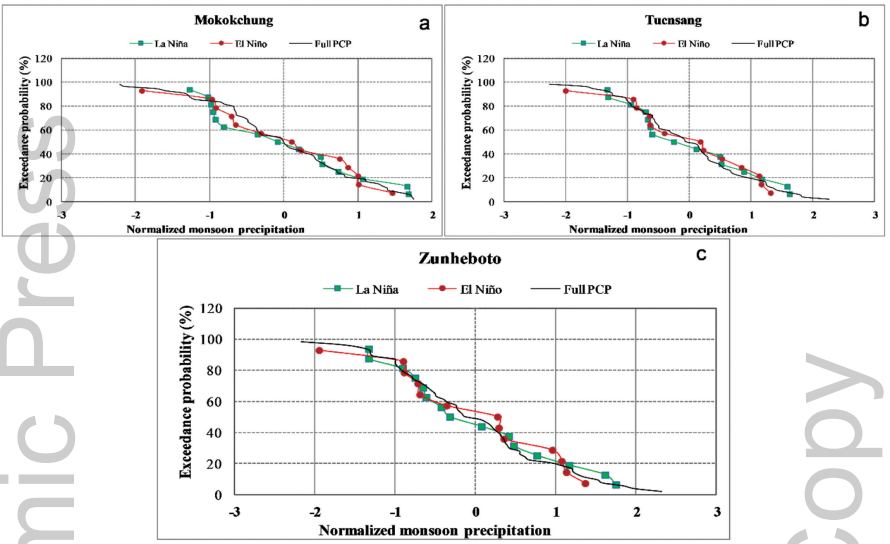

FIGURE 15.3 Graph of the cumulative distribution of normalized monsoon precipitation during El Niño, La Niña and Neutral phase for (a) Mokokchung, (b) Tuensang and (c) Zunheboto.

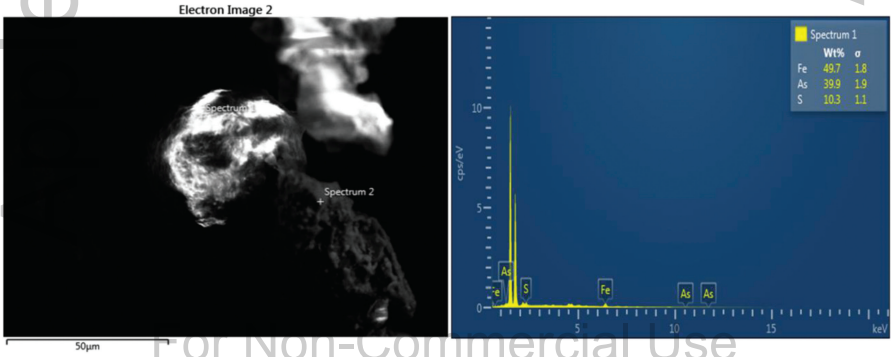

FIGURE 19.4 FESEM image (a) and EDS analysis of precipitate (b) formed in the batch reactor.

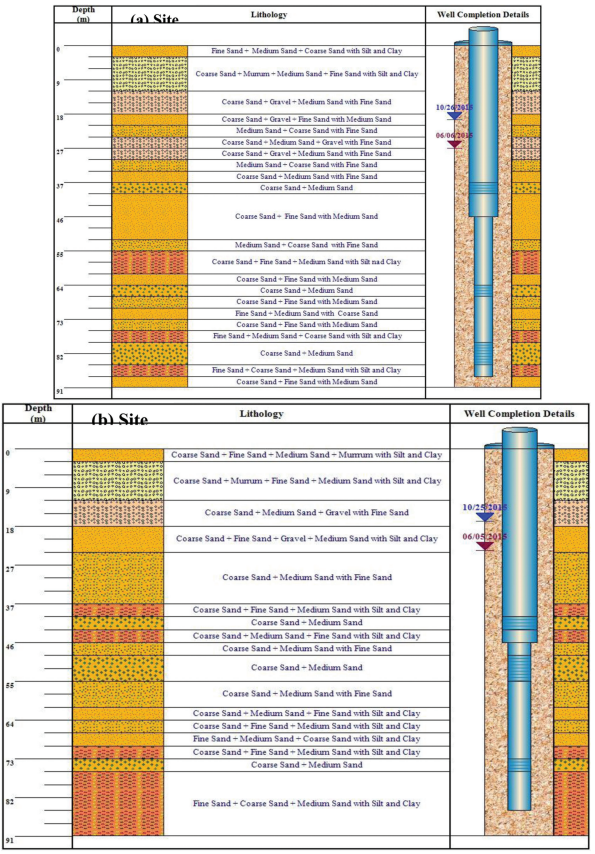

FIGURE 20.3 Well logs and well completion details at: (a) site PHTC and (b) site PFDC (Kharagpur, India).

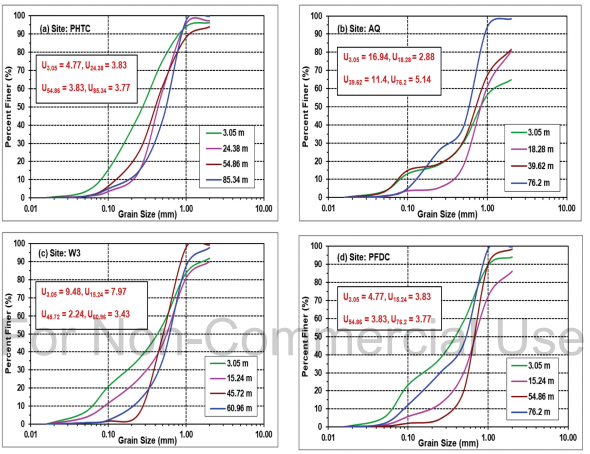

FIGURE 20.4 Grain-size distribution curves for the geologic samples of different depths.

CHAPTER 20

SCIENTIFIC FRAMEWORK FOR SUBSURFACE CHARACTERIZATION AND EVALUATION OF GRAIN-SIZE ANALYSIS METHODS

SABINAYA BISWAL and MADAN KUMAR JHA

AGFE Department, Indian Institute of Technology Kharagpur, Kharagpur – 721 302, West Bengal, India, E-mail: sabin9937@gmail.com

ABSTRACT

Subsurface formations are highly variable with depth and space, which poses challenges in their characterization at a catchment scale. This study demonstrates a scientifically sound approach for lithology exploration and the relative performance of salient grain-size analysis (GSA) methods in estimating hydraulic conductivity of subsurface formations. Test drillings were carried out at eight locations, and geologic samples were collected at a regular interval of 3.05 m (10 feet). All the geologic samples were subjected to sieve analysis. Thereafter, grain-size distribution curves (GSDC) were prepared for individual geologic samples. The physical characteristics of subsurface formations such as porosity, uniformity coefficient, and effective grain diameter were computed using GSDC and empirical formulae. Hydraulic conductivity of subsurface formations was estimated by using four popular GSA methods, and their relative performance was evaluated. The analysis of GSDC revealed that the geologic samples at deeper depths (≥40 m) have S-shape curves compared to the geologic formations present at shallow depths (<40 m). The values of uniformity coefficient range from 2.43 to 16.94 for shallow-depth geologic samples, whereas they vary from 2.24 to 11.40 for deeper depth geologic samples. The lithologic analysis indicated that shallow aquifer layers exist at depths ranging from 9 to 40 m with thickness varying from 3 to

6 m. Besides shallow aquifers, deep aquifer layers of 3 to 34 m thickness exist at 40 to 79 m depths. The average values of hydraulic conductivities (K) based on the four GSA methods range from 2.52 to 208.38 m/day for the deeper aquifer layers and 0.98 to 285.5 m/day for the shallow aquifer layers, thereby suggesting considerable aquifer heterogeneity. Among the four GSA methods, the Hazen and Kozeny methods consistently overestimate the mean K with higher standard deviation at all the sites, while the Slitcher method provides the least mean K values with a less standard deviation. These estimates are useful for a preliminary assessment of subsurface K in the absence of field-based estimates.

20.1 INTRODUCTION

Groundwater is a globally important and valuable renewable natural resource, which supports, human life and health, economic development and ecological diversity. Among various sectors, agriculture accounts for 89% of the total water consumption and domestic consumption account for about 5%. According to the fourth United Nations World Water Development Report, India is the largest consumer of groundwater in the world. Due to excessive human activities and climate change impacts, over-exploitation of groundwater resources has been a major issue in the present condition. In addition, groundwater pumping is often unmonitored and unregulated particularly in the developing country like India resulting a drastic decrease in groundwater levels in several parts of the country. These facts pose a challenging task for the researchers and scientific community to prevent aquifer depletion due to over-exploitation and to supply water in a sustainable way to the society. Thus, it is needed to manage the groundwater resources in a proper way for long-term use.

Hydrogeologic investigation is the prerequisite for groundwater studies and hence plays a central role in the development and management of the vital groundwater resources. The use of empirical grain-size analysis (GSA) models to compute hydraulic conductivity is an indirect and cost-effective method, which has attracted several researchers (Lu et al., 2012; Rosas et al., 2015; Devlin, 2015). The GSA methods estimate subsurface hydraulic conductivity (K) based on the statistical distribution of the soil particles of different sizes. Also, during the sampling procedure, the geologic samples get distorted from its natural structure and don't represent the actual field conditions. Due to these facts, estimates obtained from GSA methods contain some error. Despite the well-accepted limitations of K estimates

from grain-size analyses, there are no simpler or more economical measurement-based techniques for obtaining K estimates from aquifer samples. The results obtained from GSA methods are pretty much important for the areas, where other standard methods like pumping test, slug test, etc. are not easily accessible.

In the present study, an attempt has been made to develop a methodology to characterize the hydrogeology of subsurface formations in a more accurate way as compared to many past studies where feel method (without the use of sieve analysis) or indirect method like resistivity survey were used for classifying the subsurface formations. In addition, the performance evaluation of widely used GSA methods has been carried out for estimating the hydraulic conductivity of different subsurface formations.

20.2 MATERIALS AND METHODS

20.2.1 COLLECTION OF GEOLOGIC SAMPLE

Borehole drilling was conducted up to 91 m depth at eight sites namely, PHTC, AQ, RB, TG, W1, W2, W3 and PFDC over the study area. The area selected for this study was Experimental Farm of Indian Institute of Technology Kharagpur, West Bengal, India, and is located 22° 19' 10.97" N latitude and 87° 18' 35.87" E longitude (Figure 20.1). During drilling, the geologic samples were collected at a regular depth interval of 3.05 m (10 feet) up to the drilling depth. Properly designed well screens were placed at appropriate depths to tap the potential aquifer layers and to prevent entering of fine particles to the borehole. After installation of these observation wells, development was carried out with the help of air compressor. The installation and development procedure is shown in Figures 20.2 (a–d).

20.2.2 ANALYSIS OF GEOLOGIC SAMPLES

Sieve analysis of the geologic samples was carried out with the sieve of different sizes varying from 0.05 to 2 mm. Thereafter, Grain-size distribution curves (GSDC) were prepared for each geologic sample and thus, the physical parameters like characteristic grain diameter, porosity, and uniformity coefficients were estimated. Finally, well logs were constructed for the drilled sites by using the state-of-the-art software package "Hydro-GeoAnalyst" developed by Waterloo Hydrogeologic, Inc. (WHI), Canada.

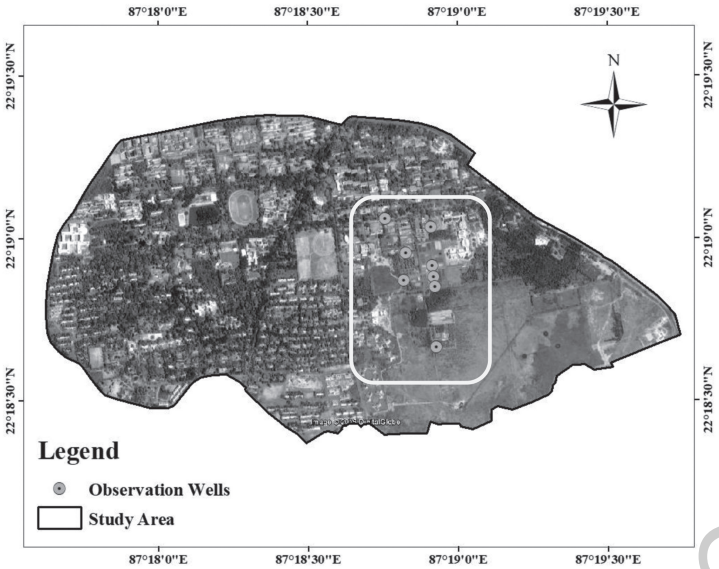

FIGURE 20.1 Location map of the study area.

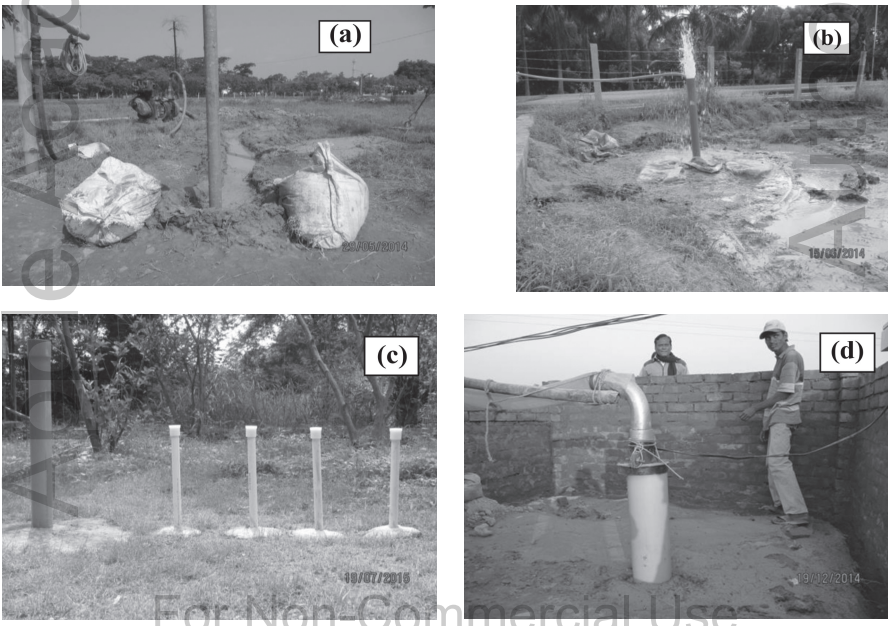

FIGURE 20.2 (a) Installation of observation well, (b) Development of observation well, (c) Field view of developed observation well with a nest of piezometers and (d) Field view of developed pumping well.

20.2.3 ESTIMATION OF HYDRAULIC CONDUCTIVITY BY GSA METHODS

In this study, four widely used GSA methods having varying applicability criteria were selected for the estimation of hydraulic conductivity of different subsurface formations. According to Vukovic and Soro (1992), porosity (n) value may be derived from the empirical relationship with the coefficient of grain uniformity (U) as follows:

$$n = 0.255 \times (1 + 0.83^{U}) \tag{1}$$

where, U = coefficient of grain uniformity, and it is given by:

$$U = \frac{d_{60}}{d_{10}} \tag{2}$$

Here, d_{60} and d_{10} in the Eq. (2) represent the grain diameter in (mm) for which, 60% and 10% of the sample respectively, are finer than. A succinct description of the selected GSA methods is given below.

20.2.3.1 HAZEN METHOD

The Hazen method represents a simpler relationship between the hydraulic conductivity and the effective grain diameter and was initially developed for the design of sand filter (i.e., loose and clean sand) for water purification (Hazen, 1892). The equation is given as:

$$K = 6 \times 10^{-4} \times [1 + 10 \times (n - 0.26)] \times {d_{10}}^2 \tag{3}$$

where, K = hydraulic conductivity (cm/s), d_{10} = effective grain diameter (cm), and n = porosity of the soil sample.

20.2.3.2 HAZEN SIMPLIFIED METHOD

Freeze and Cherry (1979) developed an empirical relation due to Hazen (1892) for estimating hydraulic conductivity. The equation is given as:

$$K = A \times {d_{10}}^2 \tag{4}$$

where, K = hydraulic conductivity (cm/s), d_{10} = effective grain diameter (mm), and A = constant (usually taken as 1).

20.2.3.3 SLITCHER METHOD

Slitcher (1898) developed a simple relationship between grain size and hydraulic conductivity which depends on the porosity of the soil sample. The equation is given as:

$$K = \frac{\rho g}{\mu} \times 1 \times 10^{-2} \times n^{3.287} \times d_{10}{}^{2} \tag{5}$$

where, K = hydraulic conductivity (cm/s), d_{10} = effective grain diameter (cm), and n = porosity of the soil sample.

20.2.3.4 KOZENY METHOD

Kozeny (1953) has specified the simpler non-linear equation to calculate the value of hydraulic conductivity, which is a function of effective grain diameter (d_{10}) and porosity.

$$K = \frac{\rho g}{\mu} \times 8.3 \times 10^{-3} \times \frac{n^{3}}{(1-n)^{2}} \times d_{10}{}^{2} \tag{6}$$

where, K = hydraulic conductivity (cm/s), and d_{10} = effective grain diameter (cm).

20.3 RESULTS AND DISCUSSION

20.3.1 AVAILABILITY OF AQUIFER LAYERS

Well logs were constructed for all the drilled sites over the study area. As an example, the developed well logs for the sites PHTC and PFDC are shown in Figure 20.3 (a, b). The analysis of the developed well logs indicated the presence of *murrum* (reddish brown colored hard geologic material) along with coarse sand at different depths. The first aquifer layer in the study area exists at depths ranging from 9 to 21 m with varying thickness (3 to 6 m). Following the first aquifer layer, the second aquifer layer resides at a depth ranging from 15 to 40 m, and the thickness varies between 3 to 6 m. Beside these two shallow aquifer layers, deeper aquifer layers also exist at depths varying from 40 to 79 m. The thickness of the deep aquifer layer varies from 3 to 34 m. Overall, it can be seen that the thickness of the deeper aquifer layers is higher than the shallow aquifer layers. It was found that there is an appreciable variation in the lithology over the study area, which suggests significant heterogeneity in subsurface formations.

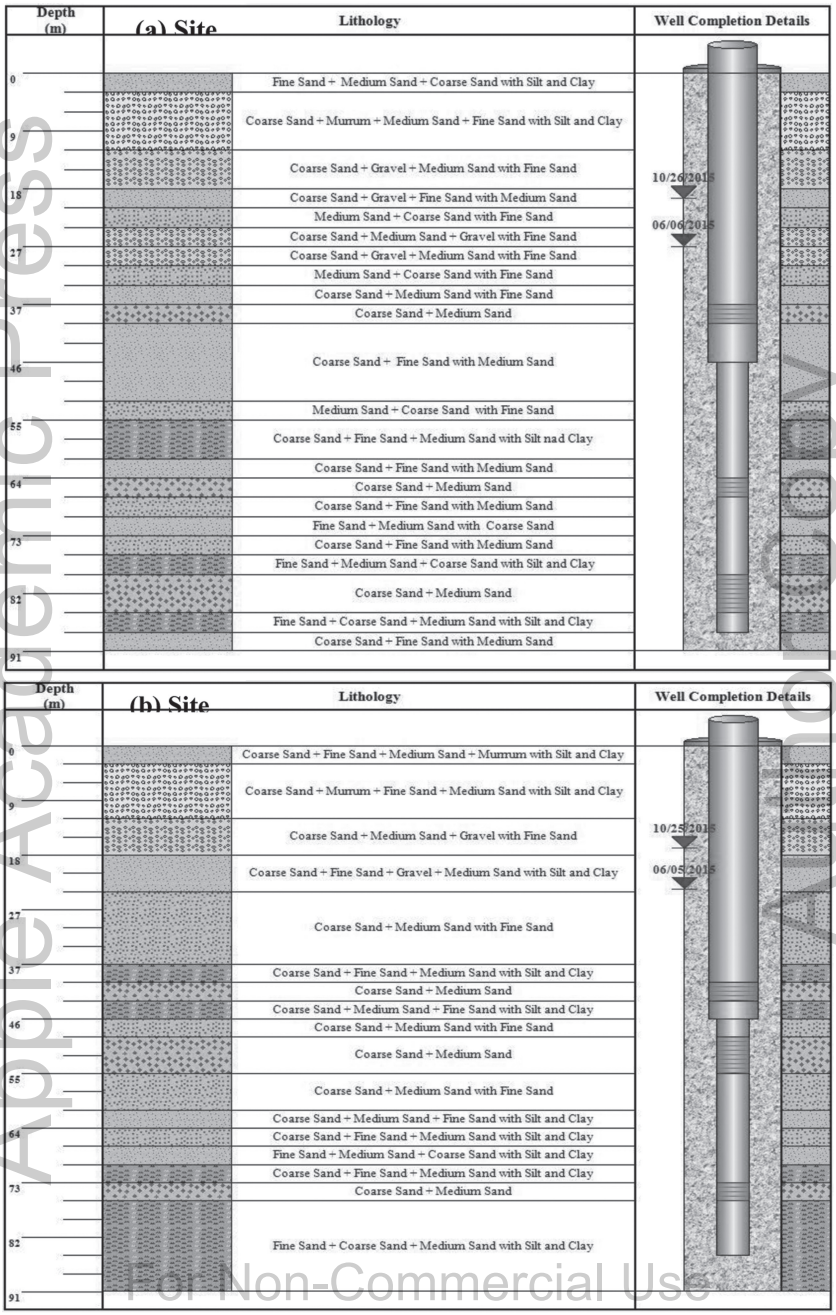

FIGURE 20.3 (See color insert.) Well logs and well completion details at: (a) site PHTC and (b) site PFDC (Kharagpur, India).

20.3.2 CHARACTERISTICS OF SUBSURFACE FORMATIONS

GSDC for the top geologic sample, i.e., 3.05 m depth and at selected depths are shown in Figure 20.4 (a–d) for the four sites as an example. It is apparent from these figures that the uniformity coefficient (U) varies from a minimum value of 2.24 at a depth of 45.72 m (for site W7) to a maximum value of 16.94 at 3.05 m depth (for site W2). It is also evident from these figures that the shallow depth geologic samples (< 40 m) have a low value of U ranging from 2.43 to 16.94 as compared to the U values (2.24 to 11.40) of geologic samples of deeper depth (≥ 40 m). Thus, the deeper depth geologic samples can be considered as uniform or poorly graded compared to the shallow depth geologic samples. Thus, the deep aquifers are supposed to have a high value of porosity as compared to the shallow aquifer layers.

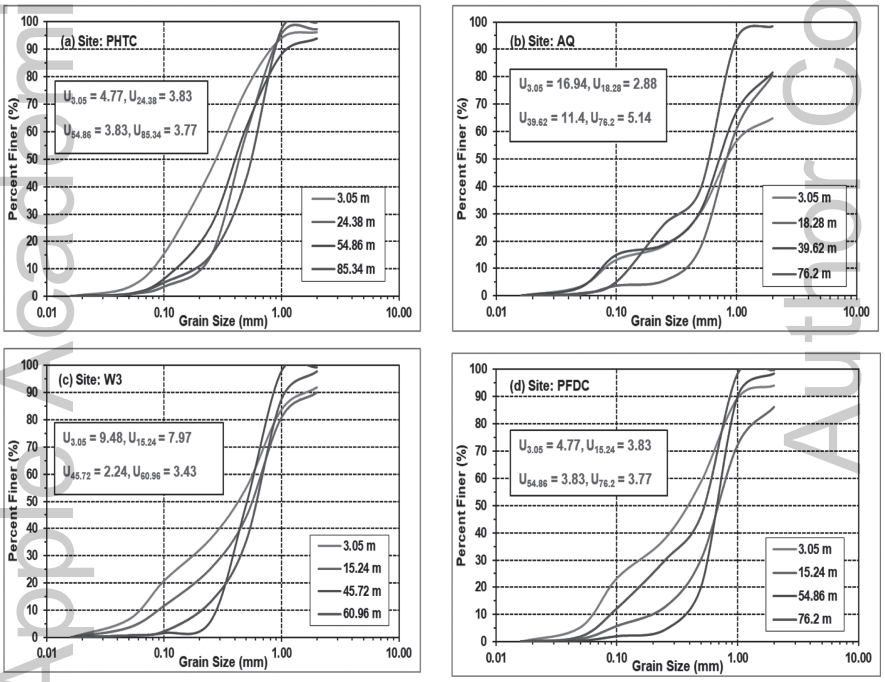

FIGURE 20.4 (See color insert.) Grain-size distribution curves for the geologic samples of different depths.

20.3.3 HYDRAULIC CONDUCTIVITY OF SUBSURFACE FORMATIONS

Hydraulic conductivity (K) values estimated by the four GSA methods vary from a minimum value of 0.98 m/day to a maximum value of. 285.50 m/day

for the aquifer layers, whereas it ranges from 0.67 to 165.41 m/day for the non-aquifer layers. As the non-aquifer layers contain a higher percentage of fine particles compared to coarser particles, low values of K is obvious. Further, the shallow aquifer layers have K values varying from 0.98 to 285.50 m/day, while the deeper aquifer layers have K values in the range of 2.52 to 208.38 m/day.

20.3.4 EFFICACY OF GSA METHODS

The performance of the GSA methods is evaluated in terms of statistical indicators and is tabulated in Table 20.1. It is inferred from this table that the Hazen and Kozeny methods have estimated consistently high mean K values (11.91 to 122.88 m/day) with higher standard deviation (25.4 to 144.65 m/day) as compared to the other two methods for all the sites. On the other hand, lowest K values are obtained from the Slitcher method which varies from 0.27 m/day at site W1 to 171.44 m/day at site TG over the study area. Also, the Slitcher method has the lowest standard deviation ranging from 9.12 m/day at site W1 to 43.05 m/day at site TG. Overall, it could be considered that the Slitcher method and Hazen Simplified methods are performing reasonably well for the study area.

20.4 CONCLUSIONS

Based on the findings of this study, the following conclusions can be drawn:

- The shallow aquifer layers are present at depths varying from 9 to 40 m with the thickness 3 to 6 m, and the deep aquifer layers exist at 40 to 79 m depths with a considerable variation in the thickness (3 to 34 m).
- The geologic samples of the deeper depth (> 40 m) were found to be uniform (U = 2.24 to 11.4) as compared to those of the shallow depth (U = 2.43 to 16.94).
- The average values of K for the shallow and deep aquifer layers vary from 0.98 to 285.50 m/day and 2.52 to 208.38 m/day, respectively.
- Out of the four GSA methods used in this study, the Slitcher method and Hazen Simplified methods were found to estimate K values reasonably.

TABLE 20.1 Basic Statistics of the GSA Methods

Methods	Statistics	Sites							
		PHTC	**AQ**	**RB**	**TG**	**W1**	**W2**	**W3**	**PFDC**
1. Hazen Simplified	Min (m/day)	3.95	4.09	3.42	5.08	1.77	3.22	3.30	3.42
	Max (m/day)	95.94	179.83	101.23	245.12	80.86	96.63	64.18	97.94
	Mean (m/day)	23.11	33.75	17.23	74.49	10.81	31.57	23.28	18.73
	SD (m/day)	22.60	45.48	22.08	65.88	14.82	28.62	23.17	21.28
2. Hazen	Min (m/day)	4.06	3.35	3.03	4.40	1.32	3.22	3.07	3.46
	Max (m/day)	157.15	322.53	170.16	423.44	136.61	169.88	113.40	171.41
	Mean (m/day)	33.04	48.40	22.02	**113.98**	**14.19**	50.18	35.47	27.37
	SD (m/day)	37.30	74.41	34.11	108.34	**25.40**	51.15	41.16	36.87
3. Slitcher	Min (m/day)	0.97	0.71	0.67	0.93	**0.27**	0.76	0.69	0.82
	Max (m/day)	54.48	122.65	60.53	**171.44**	48.84	63.26	42.45	63.54
	Mean (m/day)	10.40	15.71	6.51	39.66	4.24	17.37	11.96	8.82
	SD (m/day)	13.03	26.91	11.75	43.05	9.12	19.01	15.31	13.40
4. Kozeny	Min (m/day)	2.38	1.65	1.58	2.16	0.62	1.81	1.66	2.00
	Max (m/day)	164.96	395.52	186.41	578.87	150.93	201.01	135.38	201.25
	Mean (m/day)	29.95	46.46	18.22	**122.88**	**11.91**	52.98	36.07	25.76
	SD (m/day)	39.60	84.81	35.74	**144.65**	28.21	60.14	48.53	41.87

- It is recommended that the scientific framework should be adopted for the efficient characterization of subsurface formations, which in turn can ensure improved information about the potential of groundwater in an area or a region.

KEYWORDS

- **grain-size analysis methods**
- **grain-size distribution curve**
- **hydraulic conductivity**
- **sieve analysis**
- **subsurface characterization**
- **test drilling**

REFERENCES

Devlin, J. F., (2015). Hydrogeosieve XL: An Excel-based tool to estimate hydraulic from the grain-size analysis. *Journal of Hydrogeology*, *23*, 837–844.

Freeze, R. A., & Cherry, J. A., (1979). *Groundwater* (p. 604). Prentice-Hall Inc., Englewood Cliffs, New Jersey.

Hazen, A., (1892). *Some Physical Properties of Sands and Gravels* (pp. 539–556). Massachusetts State Board of Health, 24th Annual Report.

Kozeny, J., (1953). Das wasser im boden. Grundwasserbewegung. *Hydraulik: Ihre Grundlagen und Praktische Anwendung* , 380–445. The water in the ground: groundwater flow, Springer, Heidelberg, Germany.

Lu, C., Chen, X., Cheng, C., Ou, G., & Shu, L., (2012). Horizontal hydraulic conductivity of shallow streambed sediments and comparison with the grain-size analysis results. *Hydrological Processes*, *26*(3), 454–466.

Rosas, J., Jadoon, K. Z., & Missimer, T. M., (2015). New empirical relationship between grain-size distribution and hydraulic conductivity for ephemeral streambed sediments. *Environmental Earth Science*, *73*(3), 1303–1315.

Slichter, C. S., (1898). *Theoretical Investigations of the Motion of Groundwaters* (pp. 295–384). 19th Annual Report, US Geological Survey, Reston, VA.

Vukovic, M., & Soro, A., (1992). *Determination of Hydraulic Conductivity of Porous Medium from Grain-Size Composition*. Water Resources Publications, Littleton, Colorado, USA.

CHAPTER 21

STUDY OF CHEMICAL NATURE OF GROUNDWATER IN THE WESTERN PARTS OF JHARKHAND WITH A FOCUS ON FLUORIDE

NEETA KUMARI and GOPAL PATHAK

Department of Civil and Environmental Engineering,
B.I.T. Mesra, Ranchi–835215, India,
E-mail: neetak@bitmesra.ac.in, neeta.sinha2k7@gmail.com

ABSTRACT

The present study aims to find the groundwater chemical nature with respect to the fluoride in the groundwater. The sample data analysis indicated that fluoride content in groundwater increases with depth. The comparison of fluoride concentration of groundwater from the shallow dug wells, and deeper bore wells from the same location indicated that the deeper aquifers have a higher concentration of fluoride than the shallow aquifers. Due to continuous rock-water interaction in aquifers the fluoride concentration is found higher in dug well (DW) and hand pump (HP) than in shallow aquifers. The shallow aquifers have more discharge and recharge rate but is prone to anthropogenic pollution. The pH of the study area belongs to the alkaline in origin. An alkaline pH ranging from 7.4–8.8 resulted in high fluoride concentration (1.7–6.1 mgl^{-1}) in groundwater sources. The high pH of water displaces fluoride ions from mineral surface. In this study minimum 330 μmhos $cm^{-1}$to maximum 2580 μmhos cm^{-1} is observed. Thus all samples have a high electrical conductivity (EC).

In this sample analysis, total hardness has a minimum value of 105 mgl^{-1} and a maximum of 890 mgl^{-1}. So in hard water, calcium, and magnesium carbonate and bicarbonate are found. Therefore, water will be calcium deficient, and fluoride leeching will be more. The carbonates are completely

absent in the study area which suggests the occurrence of bicarbonates due to weathering of silicate minerals. In this study, calcium content has minimum-maximum value range as 36–198 mgl^{-1}. Magnesium content has minimum-maximum value range as 2.4–353 mgl^{-1}. Sodium content has minimum-maximum value range as 14–565 mgl^{-1}. Sodium and calcium are the major cations that influence the fluoride level in groundwater. The average chloride content of sedimentary rocks is about the same as the evaporate rocks 150 ppm and indicating sedimentary depositional environment in the study area. The significance of this study is that it helps in understanding the fluoride mobility in groundwater of the study area.

21.1 INTRODUCTION

Groundwater is a primary natural resource which supports all types of life forms (Singhal et al., 2013). Fluoride mainly presents in groundwater in the form of dissolved ions. Major sources of fluoride in groundwater are fluoride-bearing rocks such as fluorspar, cryolite, fluorite, fluorapatite, and hydroxyapatite (Agarwal et al., 1997). The fluoride content in groundwater is a function of many factors such as the presence of fluoride minerals and their solubility in water, the velocity of flowing water, pH, temperature, and concentration of Ca and HCO_3^- ions in water (Chandra et al., 1981; Largent et al., 1961). The problem of high fluoride concentration in ground water is an international problem. Many countries, like India, Srilanka, and China, East Africa, the rift valley countries, Turkey, and parts of South Africa (Pol et al., 2012) are facing this problem at a large scale. In India, the most affected states are Rajasthan, Gujarat, and Andhra Pradesh (Susheela and Mujumdar, 1992) but the problem is most pronounced in Andhra Pradesh, Bihar, Gujarat, Madhya Pradesh, Punjab, Rajasthan, Tamil Nadu, and Utter Pradesh. (Rao et al., 1992). As per the CGWB survey in 2010, in Jharkhand, districts like Palamu, Ranchi, Gumla, Godda, Giridih, Bokaro are affected with fluoride problem in their groundwater. Studies pertaining to fluoride concentration in groundwater of Jharkhand have been conducted by various researchers (Srikanth and Priyadarshi, 2008; Avishek et al., 2010; MacDonald et al., 2011; Pandey et al., 2012). The fluoride pollution is mainly geogenic (because of the geology of the area) in origin, and less rainfall (arid climate) tends to provide longer residence time to the groundwater with fluoride in aquifers.

In 1984, WHO estimated that more than 260 million people living all over the world consume water with fluoride concentration above 1mg/l (WHO, 1984; Smet et al., 1990). High concentrations of F^- in groundwater

are found in many places of the world, but notably in Asia and Africa (Appelo and Postma, 2005). Fluorosis is the most severe and widespread in the two largest countries – India and China. As per UNICEF, the disease fluorosis is endemic in at least 25 countries, and around 200 million people from 25 nations have health risks because of high fluoride in groundwater (Ayoob and Gupta, 2006). As per the WHO standards, the prescribed maximum level for fluoride in drinking water is 1.5 $mgl^{-1}$and the permissible limit is 1.0 mgl^{-1} (WHO, 1971). Indian standard specifications for drinking water IS 10500 specifies required a desirable limit of fluoride concentration in drinking water as 0.6–1.0 $mgl^{-1}$and if the limit is below 0.6 mgl^{-1}, water should be rejected, the maximum limit is extended to 1.5 mgl^{-1}. Bureau of Indian Standards (BIS, 1992) has recommended a desirable upper limit of 1.0 $mgl^{-1}$of fluoride as a desired concentration in drinking water, which can be extended to 1.5 $mgl^{-1}$of fluoride in case no alternative source of water is available.

21.2 MATERIALS AND METHODS

The water samples were collected from the dug well (DW), hand pump (HP), and shallow aquifers. They were brought to the laboratory and analyzed as per the standard methods. The compiled data is then plotted using Origin software.

21.3 RESULTS AND DISCUSSION

Observed fluoride values associated with the type of well is shown in Figure 21.1. On an average, shallow aquifers have less fluoride level than DW and HP. Although many points have reported above 1.5 mgl^{-1} but the fluoride range is high in DW and HP in comparison to shallow aquifers.

21.3.1 FLUORIDE AND DEPTH

In Figure 21.2, a variation of fluoride values with depth is shown. The fluoride content is increasing with depth. The comparison of fluoride concentration of groundwater from the shallow DWs and deeper bore wells from the same location indicated that the deeper aquifers have a higher concentration of fluoride than the shallow aquifers (Wodeyar and Sreenivasan, 1996). The

variation in the concentration of fluoride in groundwater with respect to the depth of the aquifer may depend upon the lithology, amount, and duration of rainfall, and the level of groundwater exploitation of the area.

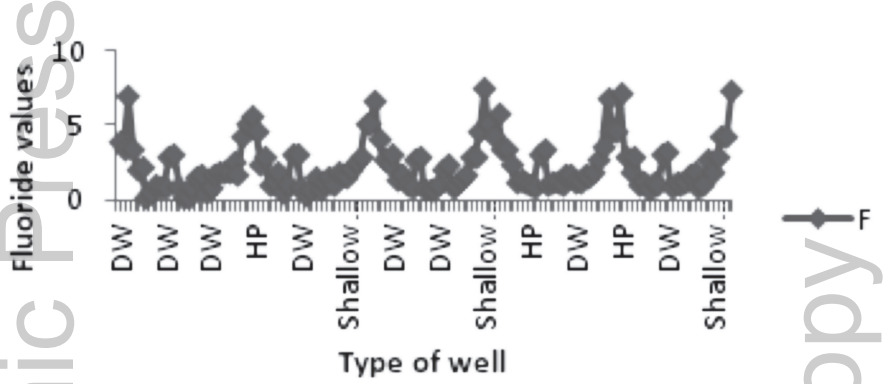

FIGURE 21.1 Observed fluoride values associated with the type of well (X-axis- a type of well and on Y-axis –fluoride level).

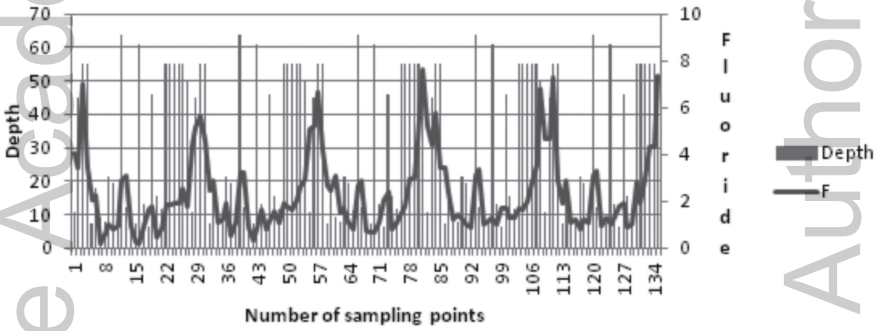

FIGURE 21.2 Variation of fluoride with respect to depth.

At higher depth groundwater contact time with aquifer media increases as velocity decreases. Due to geology and less recharge of groundwater may also cause a high level of fluoride. This is also a reason why high fluoride groundwaters are associated with the arid and semi-arid environment (Kumar et al., 2014). The study area geology has aquifers surrounded with granitic and gneisses rocks which have fluoride-containing minerals like fluorite and fluorapatite (Srikanth et al., 2008). Due to continuous rock-water interaction in aquifers the fluoride concentration is found higher in DW and HP than in shallow aquifers. The shallow aquifers have more discharge and recharge

rate but is prone to anthropogenic pollution. Groundwater velocity is also high in comparison to the deeper aquifer (www.igrac.com). The concentration of fluoride largely depends upon the geology of the area. Geologically the area is comprised of hard rock and sedimentary formations. Groundwater in the hard rock area is controlled by the depth and degree of weathering (Kumar et al., 2014).

21.3.2 FLUORIDE AND pH

pH is considered as an important ecological factor and provides an important piece factor and piece of information on many types of geochemical equilibrium or solubility calculation (Shyamala et al., 2008). When compared with the standard values of WHO and IS 10500, 6.5–8.5, the water samples are found to be in the permissible limit at all locations. In groundwater, the fluoride solubility is pH dependent (Chandio et al., 2015). The pH of the study area belongs to the alkaline in origin. Saxena and Ahmed (2001) reported that an alkaline pH ranging from 7.4–8.8 resulted in high fluoride concentration (1.7–6.1 mgl^{-1}) in groundwater sources in India. Most of the samples in the study area have pH in this range only (Figure 21.3). The high pH of water displaces fluoride ions from the mineral surface (Laxen and Harrison, 2005).

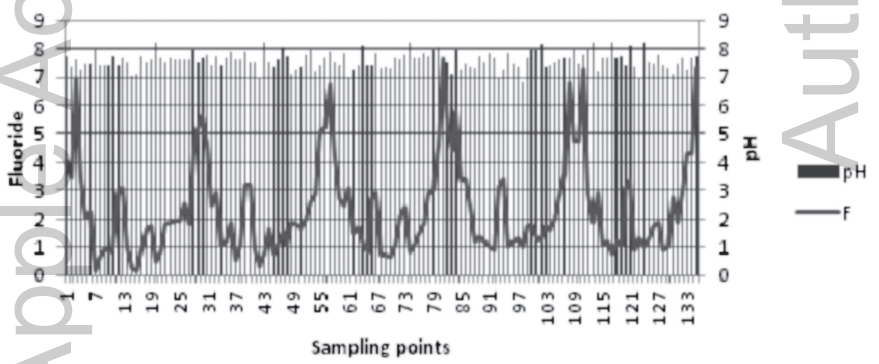

FIGURE 21.3 Variation of fluoride with respect to pH.

21.3.3 FLUORIDE AND HCO3

The carbonates are completely absent in the study area which suggests the occurrence of bicarbonates due to weathering of silicate minerals (Rajmohan

and Elango, 2004). It is composed primarily of carbonate $(CO3)^{-2}$ and bicarbonate $(HCO3)^{-}$; alkalinity acts as a stabilizer for pH. Alkalinity, pH, and hardness affect the toxicity of many substances in the water. In Figure 21.4, fluoride values with higher range have bicarbonates 400–600 mgl^{-1}.

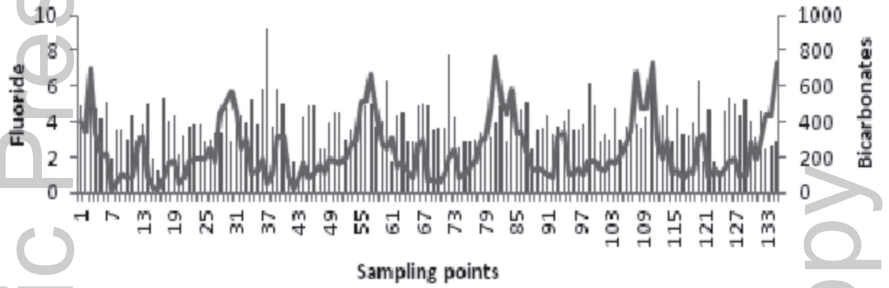

FIGURE 21.4 Variation of fluoride with respect to HCO_3

21.3.4 FLUORIDE VS. CA

Calcium is directly related to hardness and is the chief cation in the water. Low Magnesium and Calcium values indicate the non-carbonaceous aquifers as the source of the groundwater. The ionic strength of the water increases the solubility of fluoride minerals (Kumar et al., 2014). In this study, calcium content has minimum-maximum value range as 36–198 mgl^{-1}. In Figure 21.5, where more calcium is found, fluoride values are in the lower range.

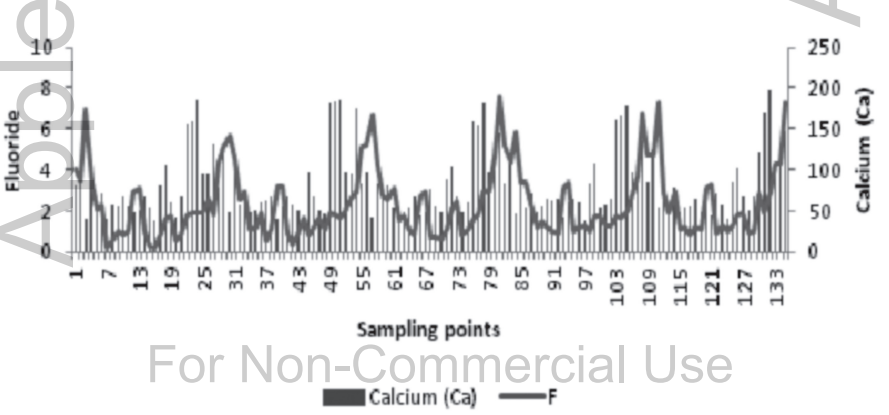

FIGURE 21.5 Variation of fluoride with respect to calcium.

21.3.5 FLUORIDE AND SODIUM

Sodium content has minimum-maximum value range as 14–565 mgl^{-1}. Sodium and calcium are the major cations that influence the fluoride level in groundwater (Rao et al., 2003). The range of sodium content is higher than the Ca and Mg in groundwater, which is a favorable point for fluoride leeching (Rao et al., 1993). This is may be due to the precipitation of $CaCO_3$ and $MgCO_3$. Ca is negatively correlated with the fluoride; therefore, calcium gets precipitated out in the form of $CaCO_3$. Sodium readily forms NaF and remains in solution. It favors fluoride enrichment in the unconfined aquifers (Rao et al., 1993). Most of the samples have high sodium content (Figure 21.6).

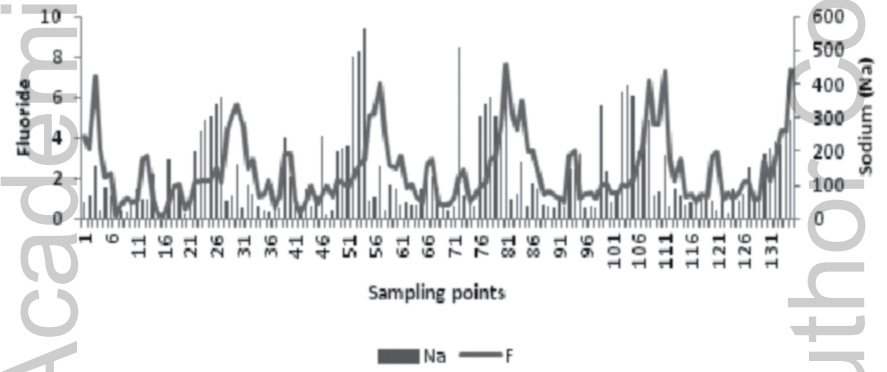

FIGURE 21.6 Variation of fluoride with respect to sodium.

21.3.6 FLUORIDE AND TOTAL HARDNESS

The possible source of Ca^{+2} and Mg^{+2} ions in the groundwater is the geology which suggests the presence of Ca-Mg rich minerals like feldspar, amphiboles (Subramani et al., 2010). The hardness of water mainly depends upon the amount of calcium or magnesium salts or both. Water with hardness up to 75 mgl^{-1} is classified as soft, 76–150 mgl^{-1} is moderately soft, 151–300 mgl^{-1} as hard and more than 300 mgl^{-1} as very hard (Saravanakumar and Ranjith Kumar, 2011). The total hardness is due to the presence of calcium and magnesium carbonate and bicarbonate. The decrease in hardness, resulting in higher fluoride concentration contributed to calcium complexion effect (Kumar and Seema, 2016). In this sample analysis, total hardness has

a minimum value of 105 mgl^{-1} and a maximum of 890 mgl^{-1} (Figure 21.7). So in hard water, calcium, and magnesium carbonate and bicarbonate are found. Therefore, water will be calcium deficient, and fluoride leeching will be more (Rao et al., 1993). WHO has recommended the safe permissible limit for hardness, i.e., 100–500 mgl^{-1}.

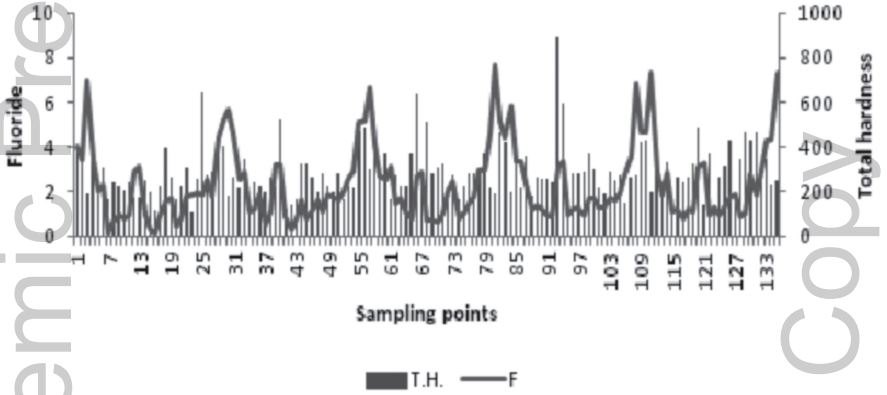

FIGURE 21.7 Variation of fluoride with respect to total hardness.

21.3.7 FLUORIDE VS. ELECTRICAL CONDUCTIVITY (EC)

EC is a numerical expression ability of an aqueous solution to carry electric current (Alagumuthu and Rajan, 2008). It signifies the amount of total dissolved salts (Dahiya and Kaur, 1999) and is a useful tool to evaluate the purity of water (Acharya et al., 2008), indicating the presence of high amount of dissolved inorganic substances in ionized form. Permissible limit for total dissolved solids as per BIS: 10500 is 500 mg/l. USPH recommended a permissible limit for electrical conductivity (EC) is 300 μmhos/cm (Alagumuthu and Rajan, 2008). In this study minimum 330 μmhos/cm to maximum 2580 μmhos/cm is observed (Figure 21.8). Thus all samples have high EC.

21.3.8 FLUORIDE VS. CHLORIDE

Chloride in water sources resulted from agricultural activities, industries, and chloride rich rocks (Dahiya and Kaur, 1999). The chloride concentration serves as an indicator of pollution by sewage. People accustomed to

higher chloride in water are subjected to laxative effects (Dahiya and Kaur, 1999; Guruprasad et al., 2005). This chloride may be supplied by the local leaching of sedimentary rocks (Prasad et al., 2014). The average chloride content of sedimentary rocks is about the same as the evaporate rocks 150 ppm and indicating sedimentary depositional environment in the study area (Prasad et al., 2014). The fluoride values in Figure 21.9, varies with total hardness in equal proportionate. Barring one or two points, chloride is within permissible limit. Fluoride and chloride values increase/decrease in a proportionate way.

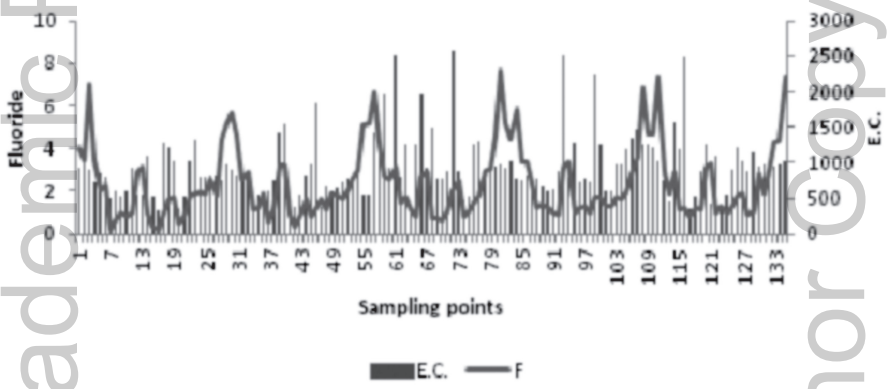

FIGURE 21.8 Variation of fluoride with respect to E.C.

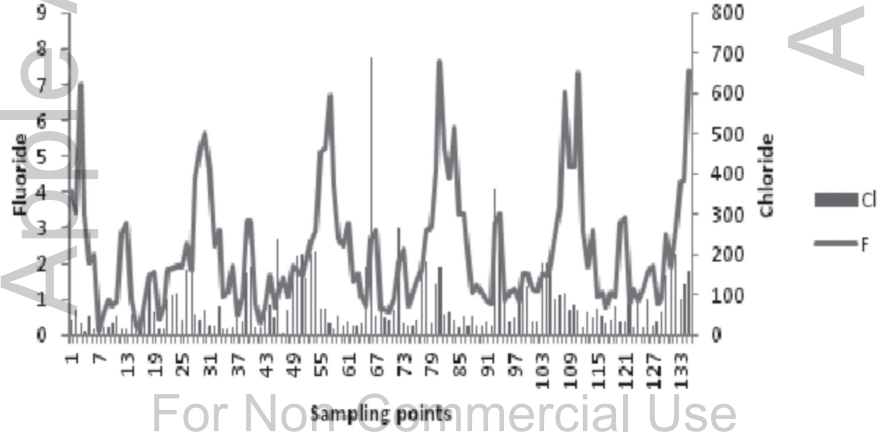

FIGURE 21.9 Variation of fluoride with respect to chloride.

21.3.9 FLUORIDE VS. MAGNESIUM

Magnesium content has minimum-maximum value range as 2.4–353 mgl^{-1} (Figure 21.10). Calcium and Magnesium showed a negative correlation with fluoride. This is probably due to the low solubility of fluoride with these ions (Nemade and Srivastava, 1996). Samples with less magnesium have higher values of fluoride and vice versa.

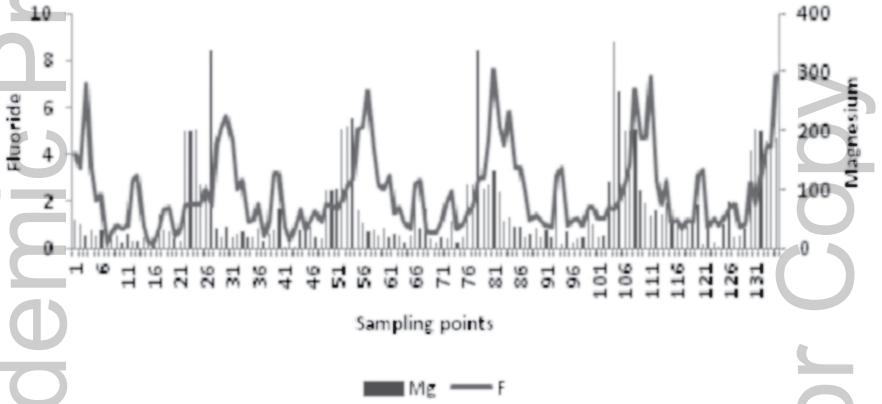

FIGURE 21.10 Variation of fluoride with respect to magnesium.

21.3.10 FLUORIDE VS. POTASSIUM (K)

In Figure 21.11, the higher value of fluoride is associated with lower values of potassium.

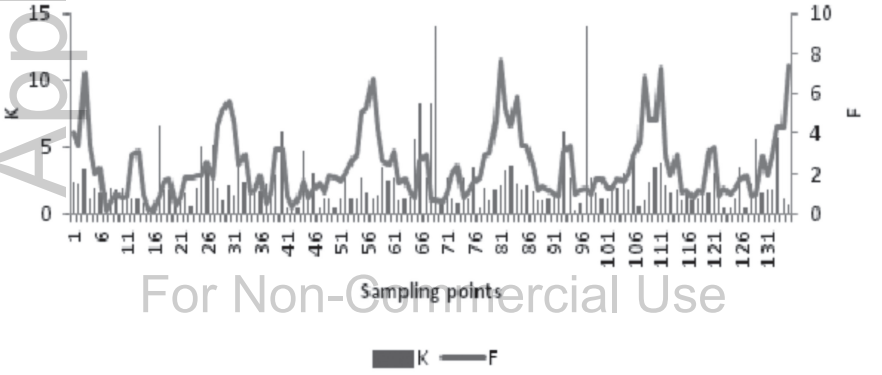

FIGURE 21.11 Variation of fluoride with respect to potassium.

21.4 SUMMARY

With the increasing depth, fluoride content was found to be increasing. The comparison of fluoride concentration of groundwater from the shallow, DWs and deep bore wells from the same location indicated that the deeper aquifers have a higher concentration of fluoride than the shallow aquifers. The pH of the study area belongs to the alkaline in origin. All the samples have high EC. The carbonates are completely absent in the study area which suggests the occurrence of bicarbonates due to weathering of silicate minerals. Soft to hard water is found in the area. The range of sodium content is higher than the Ca and Mg in groundwater, which is a favorable point for fluoride leeching from minerals.

KEYWORDS

- **bicarbonates**
- **carbonates**
- **chloride**
- **depth**
- **electrical conductivity**
- **pH**
- **rock-water interaction**

REFERENCES

Acharya, G. D., & Mathi, M. V., (2010). Fluoride contamination in groundwater sources of Modasa Tehsil of Sabarkantha district, Gujarat, India. *Pollution Research, 29*(1), 43–45.

Agrawal, V., Vaish, A. K., & Vaish, P., (1997). Groundwater quality: Focus on fluoride and fluorosis in Rajasthan., *Current Science*, *73*, 743–746.

Alagumuthu, G., & Rajan, M., (2008). Monitoring of fluoride concentration in groundwater of Kadayam block of Tirunelveli district, India: Correlation with physic-chemical parameters. *Rasayan Journal of Chemistry*, *1*(4), 920–928.

Appelo, C. A. J., & Postma, D., (2005). *Geochemistry, Groundwater, and Pollution* (2nd edn.). Balkema, Amsterdam, the Netherlands.

Avishek, K., Pathak, G., Nathawat, M. S., Jha, U., & Kumari, N., (2010). Water quality assessment of Majhiaon block of Garhwa District in Jharkhand with special focus on fluoride analysis. *Environmental Monitoring Assessment*, *167*, 617–623.

Ayoob, S., & Gupta, A. K., (2006). Fluoride in drinking water: A review on the status and stress effects. *Critical Reviews in Environmental Science and Technology*, *36*, 433–487.

BIS (Bureau of Indian Standards), (1992). *Indian Standard Specifications for Drinking Water*, IS: 10500.

Chandio, T. A., Khan, M. N., & Sarwar, A., (2015). Fluoride estimation and its correlation with other physicochemical parameters in drinking water of some areas of Balochistan, Pakistan. *Environment Monitoring Assessment*, *187*, 537–539.

Chandra, S. J., Thergaonkar, V. P., & Sharma, R., (1981). Water quality and dental fluorosis. *Indian Journal of Public Health*, *25*, 47–51.

Chate, G. T., Yun, S. T., Mayer, B., Kim, K. H., Kim S. Y., Kwon, J. S., Kim, K., & Koh, Y. K., (2007). Fluorine geochemistry in bedrock groundwater of South Korea." *Science of Total Environment*, *385*, 272–283.

Dahiya, S., & Kaur, A., (1999). Physicochemical characteristics of underground water in rural areas of Tosham subdivisions, Bhiwani district, Haryana. *Journal of Environmental Pollution, 6*(4), 281.

Guruprasad, B., (2005). Assessment of water quality in canals of Krishna delta area of A. P. *Nature of Environment and Pollution Technology*, *4*(4), 521–523.

Kumar, P. J. S., Jegathambal, P., & James, E. J., (2014). *Factors Influencing the High Fluoride Concentration in Groundwater of Vellore District*, South India, 2437–2446.

Largent, E. J., (1961). *Fluorosis: The Health Aspects of Fluoride Compounds.* Ohio State University Press, Columbia, OH. 2nd edition, pp. 140.

Laxen, D. P. H., & Harrison, R. M., (2005). Cleaning methods for polythene containers prior to the determination of trace metals in freshwater samples. *Analytical Chemistry*, *53*, 345–352.

MacDonald, L. H., Pathak, G., Singer, B., & Jaffe, P. R., (2011). An integrated approach to address endemic fluorosis in Jharkhand, India. *Journal of Water Resource and Protection, 3*, 457–472.

Nemade, P. N., & Shrivastava, V. S., (1996). Radiological skeletal changes due to chronic fluoride intoxication in Udaipur. *Journal of Environmental Protection*, *16*(12), 43–46.

Nezli, I. E., Achour, S., Djidel, M., & Attalah, S., (2009). Presence and origin of fluoride in the complex terminal water of Ouargla Basin (Northern Sahara of Algeria). *American Journal of Applied Sciences*, *6*(5), 876–881.

Pandey, A. C., Shekhar, S., & Nathawat, M. S., (2012). Evaluation of fluoride in groundwater sources in Palamu district of Jharkhand. *Journal of Applied Sciences, 12*(9), 882–887.

Pol, P. D., Sangannavr, M. C., & Yadawe, M. S., (2012). Fluoride contamination status of groundwater in Mudhol taluk, Karnataka, India: Correlation of fluoride with other physicochemical parameters. *Rasayan Journal of Chemistry*, *5*(2), 186–193.

Prasad, S., Anoop, A., Riedel, N., Sarkar, S., Menzel, P., Basavaiah, N., et al., (2014). Prolonged monsoon droughts and links to the Indo-Pacific warm pool: A Holocene record from Lonar Lake, central India. *Earth and Planetary Science Letters*, 391, 171–182. doi:10.1016/j.epsl.2014.01.043.

Priyadarshi, N., (2008). *Fluoride Toxicity in the Jharkhand State of India*. www. fluoridealert. org.

Rao, N. S., (2003). Groundwater quality: Focus on fluoride concentration in rural parts of Guntur district, Andhra Pradesh, India. *Hydrological Sciences Journal – Des Sciences Hydrologiques, 48*(485), 835–847.

Rao, N. V. R., Rao, N., Rao, K. S. P., & Schuiling, R. D., (1993). Fluorine distribution in waters of Nalgonda District, Andhra Pradesh, India. *Environmental Geology, 21*, 84–89.

Saravanakumar, K., & Ranjith, K. R., (2011). Analysis of water quality parameters of groundwater near Ambattur Industrial Area, Tamil Nadu, India. *Indian Journal of Science and Technology, 4*(5), 560–562.

Saxena, V. K., & Ahmed, S., (2001). Dissolution of fluoride in groundwater: A water-rock interaction study." *Environmental Geology*, *40*, 1084–1087.

Shyamala, R., Shanthi, M., & Lalitha, P., (2008). Physicochemical analysis of Borewell water samples of Telungupalayam area in Coimbatore District, Tamil Nadu, India. *Environmental Journal of Chemistry, 5*(4), 924 929.

Singhal, D. C., (2013). Groundwater resource assessment in India- some emerging issues. *Journal of Groundwater Research, 2*(2), 43–48.

Smet, J., (1990). Fluoride in drinking water. In: Frencken, J. E., (ed.), *Proc. Symposium on Endemic Fluorosis in Developing Countries: Causes, Effects and Possible Solutions* (pp. 51–85). Chapter 6, NIPG-TNO, Leiden.

Srikanth, R., Tripathi, R. C., & Kumar, B. R., (2008). Endemic fluorosis in five villages of the Palamau district, Jharkhand, India. *Fluoride*, *41*(3), 206–211.

Susheela, A. K., & Majumdar, K., (1992). Fluorosis control programme in India. *Water Environment and Management: 18th WEDC Conference* (pp. 229–233). Kathmandu, Nepal.

Umarani, P., & Ramu, A., (2014). Fluoride contamination status of groundwater in an east coastal area in Tamil Nadu, India. *International Journal of Innovative Research in Science, Engineering and Technology*, *3*(3), 10045–10051. ISSN: 2319–8753.

WHO, (1971). *International Standards for Drinking Water*" (3rd edn.). WHO, Geneva.

WHO, (1984). Guidelines for drinking water quality. In: *Health Criteria and Other Supporting Information"* (2nd edn.). World Health Organization, Geneva.

Wodeyar, B. K., & Sreenivasan, G., (1996). Occurrence of fluoride in the ground waters and its impact in Peddavankahalla basin, Bellary District, Karnataka – A preliminary study. *Current Science, 70*, 71–73.

www.igrac.com, https://www.un-igrac.org/sites/default/files/resources/files/IGRAC-SP2007–1_Fluoride-removal.pdf

CHAPTER 22

GEOHYDROLOGICAL INVESTIGATION USING VERTICAL ELECTRICAL SOUNDING AT CHINAMUSHIDIWADA VILLAGE IN VISAKHAPATNAM, ANDHRA PRADESH, INDIA

KIRAN JALEM

Assistant Professor, Centre for Land Resource Management, Central University of Jharkhand, Ranchi, India, E-mail: jalemkiran@gmail.com

ABSTRACT

Geohydrological investigations are performed to assess the groundwater parameters for locating suitable sites for groundwater exploration and resource management at Chinamushidiwada Village in Visakhapatnam, Andhra Pradesh, India. Thirty vertical electrical soundings (VES) using Schlumberger configurations were carried out at selected locations in the vicinity of Chinamushidiwada Village. The interpretation of sounding data has been accomplished using both curves matching as well as computer-assisted automatic iterative resistivity sounding ipi2win (2008) software. On the basis of interpreted sounding results, three to four geoelectrical cross sections have been generated along the profiles. The interpretation of data revealed four layers, generally one top thin layer overlying the other three thick layers. Interpreted results are corroborated with the borehole data. The results depict proper geohydrological conditions for the existence of good aquifers suggesting the continued supply of groundwater in the study area for the extended period.

22.1 INTRODUCTION

Groundwater is very important natural resources for sustainable development of a region. It is the only viable source of water in many areas where the development of surface water is not economically viable. Groundwater in alluvial and sedimentary rocks occurs in pore spaces between grains, while in hard rocks, it is largely due to secondary porosity and permeability resulting from weathering, fracturing, jointing, and faulting activities. The area of investigation is the Chinamushidiwada village of Visakhapatnam urban environment. The recent urban expansion in Visakhapatnam (India) following the increased population growth has resulted in increased developmental activities and shrinking of surface water bodies in Visakhapatnam urban environment.

With increased infrastructure development and irregularity and failure of monsoon, it has been vaguely reported that the groundwater level in Visakhapatnam urban environment is depleting fast. Therefore, with aim of examining the groundwater level and locating the potential aquifers for their management, geohydrological investigations at suitably chosen sites in and around Chinamushidiwada village were carried out with vertical electrical sounding (VES) at thirty sites in the vicinity of Chinamushidiwada village microwatershed of Visakhapatnam, Andhra Pradesh, India urban environment and have interpreted the results for estimating the parameters which may be useful for management of groundwater aquifers in the Chinamushidiwada village microwatershed vicinity to cope with the sustained development of groundwater source in the study area.

22.2 MATERIALS AND METHODS

22.2.1 DESCRIPTION OF THE STUDY AREA

Geographical location of the study area of investigation lies in the Chinamushidiwada village microwatershed of Visakhapatnam district of Andhra Pradesh, India (Figure 22.1). The study area lies between 170 47’ 02” N to 170 48’ 38” N latitudes and 830 11’ 51” E to 830 14’ 45” E longitudes, covering an aerial extent of 9.18 km^2. It is a part of Survey of India (SOI) Toposheets – 65 O/1 SE (Figure 22.2) of 1:25,000 scale and is within the administrative boundaries of Greater Visakhapatnam Municipal Corporation (GVMC) of Visakhapatnam, Andhra Pradesh.

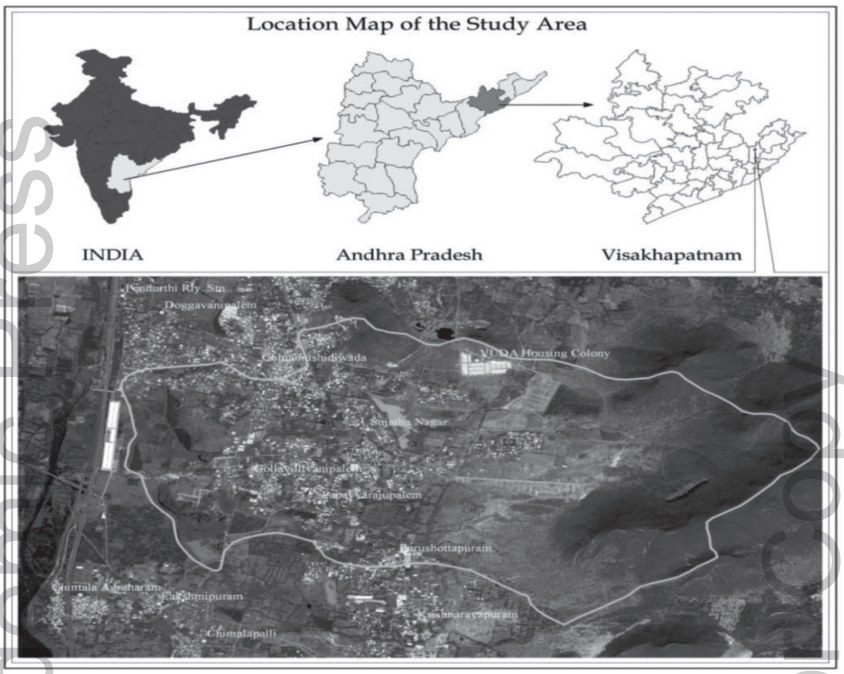

FIGURE 22.1 Location map of the study area.

FIGURE 22.2 Locations of 30 VES data sampling stations.

In this study, the VES method has been adopted, and VES surveys have been carried out at thirty locations in the area (Figure 22.2) using Schlumberger electrode configuration. For resistivity sounding using Schlumberger array, the current electrodes are spaced much farther apart as compared to the potential electrodes. Although, a number of electrode arrangements for current electrodes (C1, C2) and potential electrodes (P1, P2) have been suggested for this purpose, we used the symmetrical Schlumberger arrangement for the VES survey. In the symmetrical arrangement the points C1, P1, P2, C2 are taken on a straight line such that points P1 and P2 are symmetrically placed about the center of the spread (Figure 22.3).

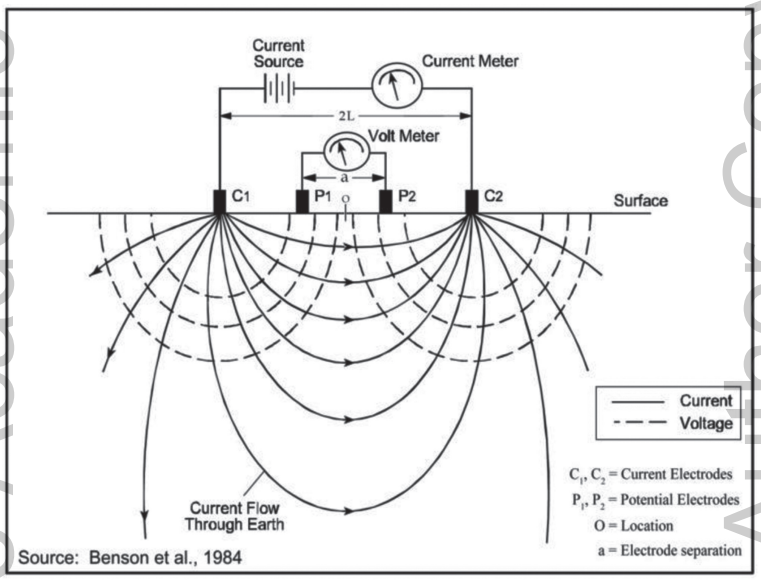

FIGURE 22.3 Symmetrical Schlumberger electrode arrangements.

$$\rho_a = \pi * \left(\left(L^2 - a^2 \right) / 2a \right) * \frac{\Delta V}{I} \quad (1)$$

where,

ρ_a = Apparent resistivity (Ωm);
L = Distance between center point and a current electrode;
ΔV = Potential deference in millivolts;
a = Distance between Potential electrodes;
I = Current input in milliamps;
O = VES location.

In order to determine the exact thickness and true resistivity of each layer, field curves are interpreted and matched with the set of model curves for two layer, three layer and multilayer cases prepared by Ipi2Win 2008 and broadly 3 to 4 layers are demarcated, which are classified into topsoil, weathered rock, fractured rock, hard fractured rock and hard rock. In total, 30 numbers of VES data has been interpreted to determine the subsurface lithology, and the corresponding elevations for weathered, fractured, hard fractured and hard rock surfaces are determined, which are tabulated in Table 22.1.

TABLE 22.1 The Results of the Fieldwork That Was Carried Out During the Vertical Electrical Sounding Experiment for Exploring Groundwater for Part of Visakhapatnam Urban Area, Andhra Pradesh, India

VES No	Type of Curve	Resistivity Ω-m	Thickness (Meter)	Depth (meter)	Lithological Units
1	H	38	1.19	1.19	Red Loamy Soil
		13.2	12	13.2	Weathered Rock
		220	-	-	Fractured Rock
2	QH	35.4	0.5	0.5	Red Loamy Soil
		18.7	2.46	2.96	Gravel
		8.01	16.9	19.9	Weathered Rock
		2219	-	-	Hard Rock
3	H	37.1	2	2	Red Loamy Soil
		14.7	19.4	21.4	Weathered Rock
		3804	-	-	Hard Rock
4	HA	137	1.34	1.34	Gravel & Boulder
		41.2	2.23	3.57	Weathered Rock
		181	23.5	27.07	Fractured Rock
		269	-	-	Hard Fractured Rock
5	H	1436	0.5	0.5	Gravel & Boulder
		244	12	12.5	Fractured Rock
		486	-	-	Hard Fractured Rock
6	H	247	1.92	1.92	Gravel & Boulder
		123	10.6	12.52	Weathered Rock
		357	-	-	Hard Fractured Rock
7	QH	563	0.524	0.52	Gravel & Builder
		236	5.92	6.44	Gravel
		47.2	8.14	14.58	Weathered Rock

TABLE 22.1 *(Continued)*

VES No	Type of Curve	Resistivity Ω-m	Thickness (Meter)	Depth (meter)	Lithological Units
		364	-	-	Hard Fractured Rock
8	HA	1872	0.8629	0.86	Gravel & Boulder
		75.159	0.9943	1.86	Gravel
		558.21	49.121	50.98	Hard Fractured Rock
		1071	-	-	Hard Rock
9	H	355	1.29	1.29	Gravel & Boulder
		88.4	9.38	10.67	Weathered Rock
		327	-	-	Hard Fractured Rock
10	QH	122	0.672	0.67	Gravel & Boulder
		54.9	1.84	2.51	Gravel
		29.9	14.1	16.61	Weathered Rock
		148	-	-	Fractured Rock
11	HA	28.9	1.34	1.34	Red Loamy Soil
		9.69	2.23	3.57	Clay
		21	22.2	25.77	Weathered Rock
		3070	∞	-	Hard Rock
12	QHK	27.7	0.91	0.91	Red Loamy Soil
		895	7.89	8.6	Weathered Rock
		2926	∞	-	Hard Rock
13	H	48.9	1.01	1.01	Red Loamy Soil
		20.2	18.1	19.11	Weathered Rock
		382	∞	-	Fractured Rock
14	HA	128	0.5	0.5	Gravel & Boulder
		17.9	4.54	5.04	Weathered Rock
		47.9	61.7	66.74	Fractured Rock
		6480	∞	-	Hard Rock
15	H	85.1	2.59	2.59	Gravel & Boulder
		14.7	3.13	5.72	Weathered Rock
		146	∞	-	Fractured Rock
16	HA	191	1.7	1.7	Gravel & Boulder
		28.9	3.7	5.4	Weathered Rock
		89.9	43.8	49.2	Fractured Rock
		4663	∞	-	Hard Rock
17	HKH	816	1.02	1.02	Gravel & Boulder

TABLE 22.1 *(Continued)*

VES No	Type of Curve	Resistivity Ω-m	Thickness (Meter)	Depth (meter)	Lithological Units
		44.4	1.25	2.27	Weathered Rock
		1280	2.3	4.57	Boulder
		119	7.68	12.25	Fractured Rock
		722	∞	-	Hard Fractured Rock
18	HK	1677	1.81	1.81	Gravel & Boulder
		661	11.5	13.3	Fractured Rock
		1356	∞	-	Hard Fractured Rock
19	H	468	1.99	1.99	Gravel & Boulder
		53.7	2.38	4.37	Fractured Rock
		1168	∞	-	Hard Fractured Rock
20	H	2138	0.961	0.96	Gravel & Boulder
		436	7.84	8.8	Fractured Rock
		1442	∞	-	Hard Fractured Rock
21	HA	249	1.34	1.34	Gravel & Boulder
		71.1	2.23	3.57	Fractured Rock
		363	21.9	25.47	Hard Fractured Rock
		629	-	-	Hard Rock
22	HA	203	1.58	1.58	Gravel & Boulder
		47.9	2.29	3.87	Weathered Rock
		216	35.5	39.37	Fractured Rock
		24848	-	-	Hard Rock
23	QH	203	0.744	0.74	Gravel & Boulder
		136	4.41	5.15	Hard Fractured Rock
		28.8	8.81	13.96	Fractured Rock
		318	-	-	Hard Fractured Rock
24	HA	162	1.34	1.34	Gravel & Boulder
		30.3	2.23	3.57	Weathered Rock
		117	22.2	25.77	Fractured Rock
		435	-	-	Hard Fractured Rock
25	H	1046	1.11	1.11	Boulder
		162	6.07	7.18	Fractured Rock
		498	-	-	Hard Fractured Rock
26	HA	12.3	0.938	0.94	Red Loamy Soil
		2.93	1.36	2.3	Clay

TABLE 22.1 *(Continued)*

VES No	Type of Curve	Resistivity Ω-m	Thickness (Meter)	Depth (meter)	Lithological Units
		27.1	63.6	65.9	Weathered Rock
		1164	-	-	Hard Fractured Rock
27	H	3.01	2.04	2.04	Clay
		7.82	15.2	17.24	Weathered Rock
		11377	-	-	Hard Rock
28	H	47.9	1.2	1.2	Gravel
		13.4	4.46	5.66	Weathered Rock
		229	-	-	Fractured Rock
29	QHA	46.3	0.5	0.5	Red Loamy Soil
		23.6	1.53	2.03	Gravel
		4.1	2.2	4.23	Clay
		25.3	16.1	20.33	Weathered Rock
		14887	-	-	Hard Rock
30	H	370	1.26	1.26	Gravel & Weathered
		161	6.38	7.64	Fractured Rock
		608	-	-	Hard Fractured Rock

22.3 RESULTS AND DISCUSSIONS

For better understanding, the results of the investigation are usually presented in the form of geoelectrical cross-sections and isopach map (Figure 22.10) of the aquifer in the study area. Therefore, in accordance with above fact, four geoelectrical cross-sections (Figures 22.5–22.8) are prepared along AA″, BB″, CC″ and DD″ shown in the study area map (Figure 22.4) are interpreted as given in the following subsections.

22.3.1 GEOELECTRICAL CROSS-SECTION AA'

Along the cross section AA,' the area represented in blue in the Figure 22.5 is weathered rock extending from VES location 27 to 11 and this area identified as potential aquifer zone. The green and yellow color in the figure represents Fracture and Hard fracture rock respectively. The red color having high apparent resistivity in the figure is hard rock.

FIGURE 22.4 Traverse along the sections A, B, C, and D.

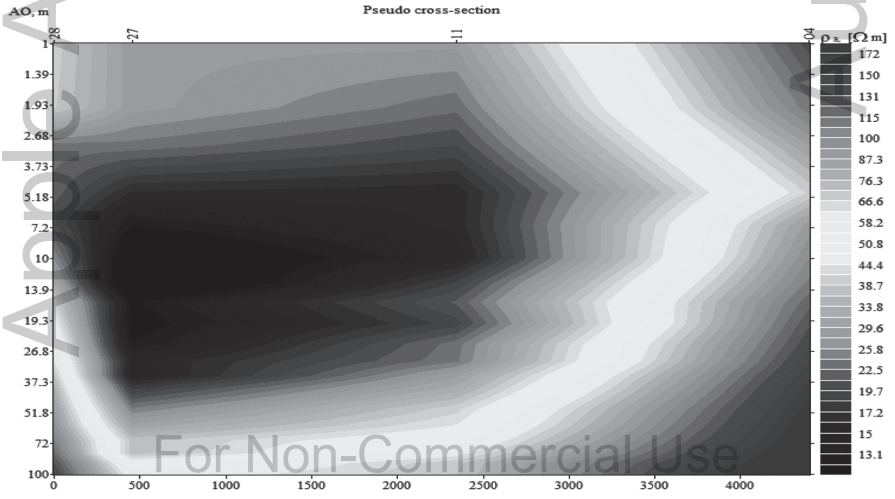

FIGURE 22.5 Geoelectrical cross-section along the line AA.'

22.3.2 GEOELECTRICAL CROSS-SECTION BB'

Along the cross-section BB,' the area represented in blue in the Figure 22.6 is weathered rock extending from VES location 29 to 14 and this area identified as potential aquifer zone. The green and yellow color in the figure represents Fractured and Hard fractured rock, respectively. The red color having high apparent resistivity in the figure is hard rock. The VES location 10 and 9 are in the foothill region of Yerrakonda hill; hence the area has low aquifer potential.

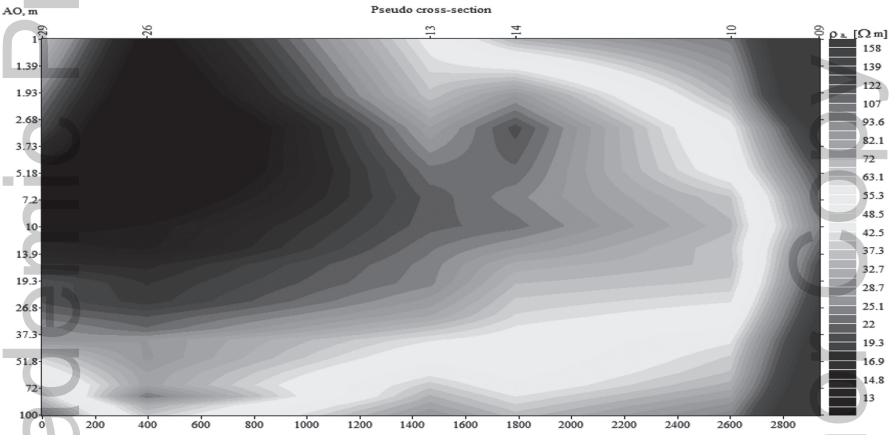

FIGURE 22.6 Geoelectrical cross-section along the line BB.'

22.3.3 GEOELECTRICAL CROSS-SECTION CC'

Along the cross section CC,' the area represented in blue in the Figure 22.7 is weathered rock extending from VES location 24 to 16 and this area identified as potential aquifer zone, but if compared to other cross-sections, the area is not highly potential. The green and yellow color in the figure represents Fractured and Hard fractured rock respectively. The red color having high apparent resistivity in the figure is hard rock.

22.3.4 GEOELECTRICAL CROSS-SECTION DD'

Along the cross section DD,' the area represented in blue in the Figure 22.8 is weathered rock extending from VES location 13 to 03 and this area identified as potential aquifer zone, but if compared to other cross-sections, the area has high potential aquifer zone. The green and yellow color in the

figure represents Fractured and Hard fractured rock respectively. The red color having high apparent resistivity in the figure is hard rock.

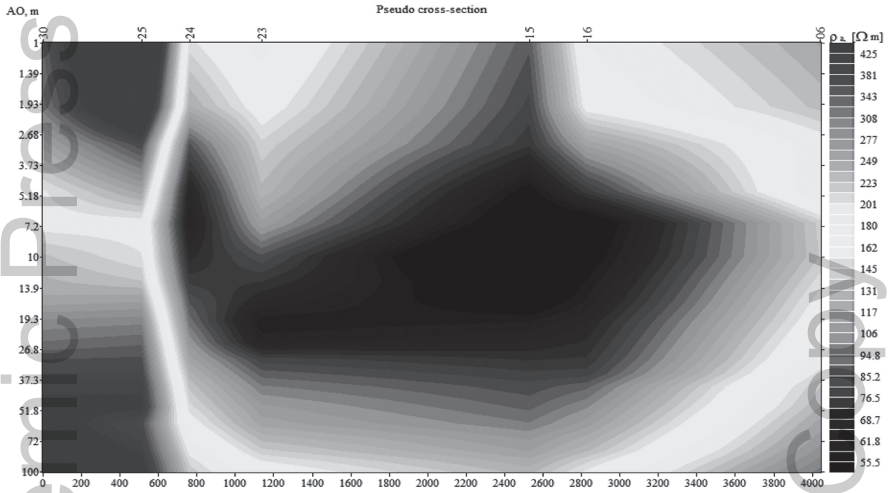

FIGURE 22.7 Geoelectrical cross-section along the line CC.'

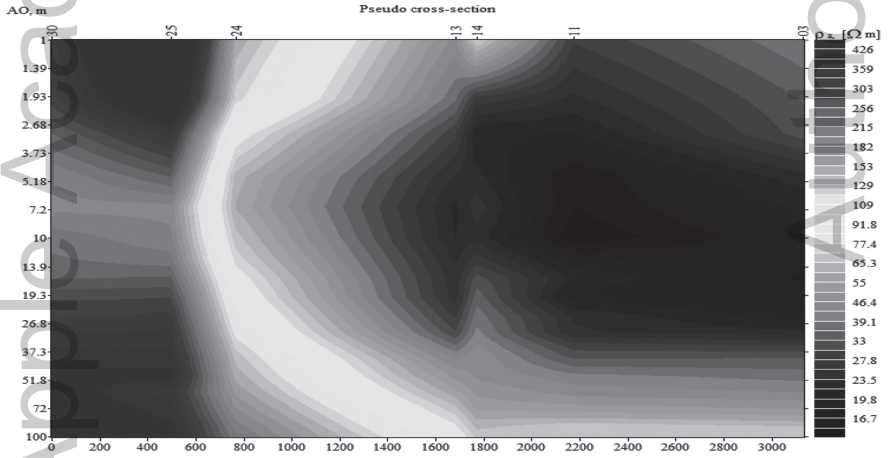

FIGURE 22.8 Geoelectrical cross-section along the line DD.'

From all the vertical cross-sections, it is clear that the thickness of the water-bearing formations, i.e., weathered, and fractured rock zones have increased from the foothill regions to the low lying areas of the study area. Over the hill slopes and hill ridges, hard rock is present immediately below the top soil. Even though there are some fractured rock zones noticed over

the hill slopes, these may not contain aquifer system but may guide the rainwater to percolate from the topsoils into the aquifer system down below. However, the hill slopes are useful to retain rainwater for some time and release it into the aquifer system existing down below the foothill region. Therefore, this zone is considered to be suitable for constructing harvesting structures, like contour trenches.

22.4 SUMMARY

22.4.1 BOREHOLE LITHOLOGICAL INFORMATION IN AND AROUND THE STUDY AREA

The borehole lithological information is collected from various locations in and around the study area. Total four borehole investigations were conducted at VUDA Colony, Laxmipuram, Drivers Colony and Sujatha Nagar, respectively (Figure 22.9).

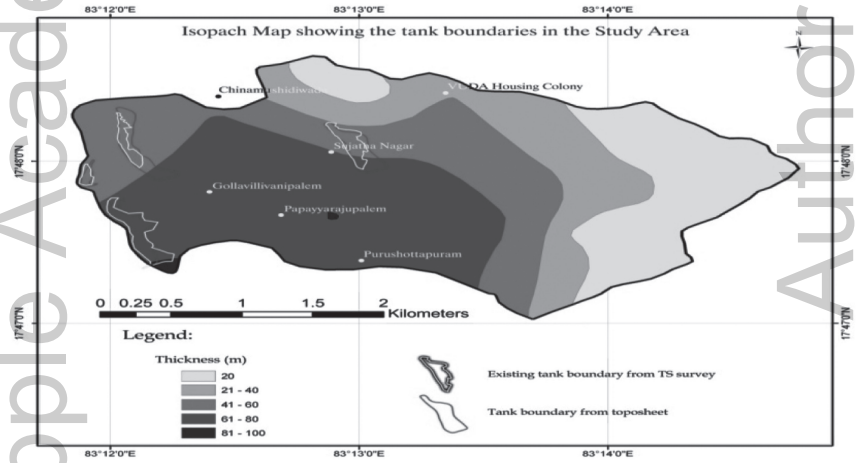

FIGURE 22.9 Isopach map of the study area.

Borehole in VUDA Colony is done for Vishakha urban development authority revealed four layers, first layer extending from ground to 10 meters below revealed Gravel and Boulder, second layer extending till 50 meters reveal weathered rock, third layer extending from 50 to 80 meter below revealed fractured rock and last layed which beyond 80 meter depth is hard rock. Borehole in Laxmipuram is done for Rural Water Supply

Scheme of Panchayati Raj (RWSP) Vishakhapatnam, revealed four layers, first layer extending from ground to 3 meters below revealed soil, second layer extending till 30 meters revealed weathered rock, third layer extending from 30 to 90 meters below revealed fractured rock and last layer beyond 90 meter depth is hard rock. Borehole data collected from local inhabitant Mr N. Nookaraju for household purpose, revealed four layers, first layer extending from ground to 0.5 meter below revealed soil, second layer extending till 15 meters revealed gravel, third layer extending from 15 to 50 meter below revealed fractured rock and last layer beyond 50 meters depth is hard rock. Borehole data from Sujatha Nagar is done for Bharat Heavy Plates & Vessels (BHPV) Vishakhapatnam, revealed four layers, first layer extending from ground to 2 meters below revealed soil, second layer extending till 20 meters reveal weathered rock, third layer extending from 80 to 90 meters below revealed fractured rock and last layed which beyond 80 meter depth is hard rock. The collected borehole data is given below in Table 22.2 with bore log profiles of four locations in Figure 22.10. The borehole data were analyzed with VES data nearest to the location of borewell and identified that the VES data is almost similar to borewell data. The result is strongly proven that VES data are more accurate for identifying potential groundwater aquifers.

TABLE 22.2 Lithological Information of Borehole Stations

Borehole Stations	Location	Depth (m)	Lithological Units
1	VUDA Colony	0 to 10	Gravel& Boulder
	(VUDA)	10 to 50	Weathered Rock
		50 to 80	Fractured Rock
		> 80	Hard Rock
2	Laxmipuram	0 to 3	Soil
	(RWSP Scheme, VSP)	3 to 30	Weathered Rock
		30 to 90	Fractured Rock
		> 90	Hard Rock
3	Drivers Colony	0 to 0.5	Soil
	(N. Nookaraju	0.5 to 15	Gravel
	House Purpose)	15 to 50	Fractured Rock
		> 50	Hard Rock
4	Sujatha Nagar	0 to 2	Soil
	(BHPV-VSP)	2 to 20	Weathered Rock
		20 to 80	Fractured Rock
		> 80	Hard Rock

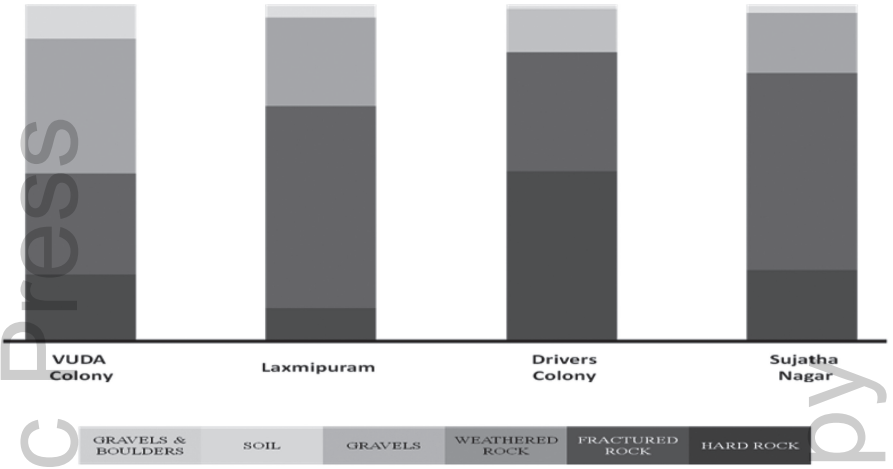

FIGURE 22.10 Borelog profile of four locations.

KEYWORDS

- **borehole**
- **geoelectrical cross section**
- **geohydrological investigations**
- **groundwater**
- **vertical electrical sounding**

REFERENCES

Breusse, J. J., (1963). Modern geophysical methods for subsurface water exploration. *Geophysics*, *28*, 663.

Davis, G. H., (1982). Prospect risk analysis applied to groundwater reservoir evaluation, *Groundwater*, *20*(6), 657–662.

El-kadi, A. I., Oloufa, A. A., Eltahan, A. A., & Malic, H. U., (1994). Use of a geographic information system in site-specific groundwater modeling. *Ground Water*, *32*, 617–625.

Goyal, S., Bharawadaj, R. S., & Jugran, D. K., (1999). *Multicriteria Analysis Using GIS for Groundwater Resource Evaluation in Rawasen and Pilli Watershed*, U.P., http://www.GIS development net Cited 17 Dec 2003.

Jaiswal, R. K., Mukherjee, S., Krishnamurthy, J., & Saxena, R., (2003). Role of remote sensing and GIS techniques for generation of groundwater prospect zones towards rural development-an approach. *International Journal of Remote Sensing, 24*, 993–1008.

Krishnamurthy, J. N., Venkatesa, K., Jayaraman, V., & Manivel, M., (1996). An approach to demarcate potential groundwater zones through remote sensing and geographical information system. *International Journal of Remote Sensing, 17*, 1867–1884.

Masvopo, T. H., David, L., & Hodson, M. *Evaluation of the Ground Water Potential of the Malala Alluvial Aquifer*, Lower mzingwane river, Zimbabwe.

Musa, G., Abdullahi, M. E., Toriman, G., & Mohd, B., (2014). Application of vertical electrical sounding (VES) for groundwater exploration in Tudun Wada Kano state, Nigeria. *International Journal of Engineering Research and Reviews*, *2*(4), 51–55.

Nageswara Rao, K., Rao, U. B., & Venkateswara Rao, T., (2008). Estimation of sediment volume through geophysical and GIS analysis – A case study of the red sand deposit along Visakhapatnam coast. *Journal of Indian Geophysical Union*, *1*(12), 23–30.

Novaline, J., Saibaba, J., & Prasada, R. P. V. S. P., (1999). *Groundwater Modeling for Sustainable Development Using GIS Techniques*. Preconference volume, Geoinformatics Beyond 2000, Dehradun, India.

Obi Reddy, G. P., Chandra, M. K., Srivastav, S. K., Srinivas, C. V., & Maji, A. K., (2000). Evaluation of groundwater potential zones using remote sensing data: a case study of Gaimukh watershed, Bhandara district, Maharashtra. *Journal of Indian Society of Remote Sensing*, *281*, 19–32.

Orellana, E., & Mooney, H. M., (1966). *Master Tables and Curves for Vertical Electrical Soundings Over Layered Structures: Interciencia*, Madrid.

Pratap, K., Ravindran, K. V., & Prabakaran, B., (2000). Groundwater prospect zoning using remote sensing and geographical information system: A case study in Dala-Renukoot Area, Sonbhadra district Uttar Pradesh. *Journal of Indian Society of Remote Sensing, 284*, 249–263.

Rokade, V. M., Kundal, P., & Joshi, A. K., (2007). Groundwater potential modeling through remote sensing and GIS: A case study from Rajura Taluka, Chandrapur district, Maharastra. *Journal of Geological Society of India, 69*, 943–948.

Saraf, A. K., Choudhury, P. R., Roy, B., Sarma, B., Vijay, S., & Choudhury, S., (2004). GIS-based surface hydrological modeling in the identification of groundwater recharge zones. *International Journal of Remote Sensing, 25*(24), 5759–5770.

Saraf, A., & Choudhary, P. R., (1998). Integrated remote sensing and GIS for groundwater exploration and identification of artificial recharge sites. *International Journal of Remote Sensing*, *19*(10), 1825–1841.

Schueler, T. (2011). *The Impervious Cover Model: Stream Classification*, Urban Subwatershed Management, and Permitting, Chesapeake Stormwater Network. www.cwp.org/Our_Work/Training/Institutes/icm_and_watershed_mgmt.pdf.

Shahid, S., & Nath, S. K., (1999). GIS Integration of remote sensing and electrical sounding data for hydrogeological exploration. *Journal of Spatial Hydrology*, *21*, 1–12.

Shahid, S., Nath, S. K., & Roy, J., (2000). Groundwater potential modeling in soft rock area using GIS. *Journal of Remote Sensing, 21*, 1919–1924.

Shaver, E., Maxted, J. Curtis, G., & Carter, D., (1994). Watershed protection using an integrated approach. In: *Stormwater NPDES Related Monitoring Needs. Proc. of an Eng. Foud. Conf. held in Mount Crested Butte*. Colorado.

Singh, A. K., & Prakash, S. R., (2002). *An Integrated Approach of Remote Sensing, Geophysics and GIS to Evaluation of Groundwater Potentiality of Ojhala Sub Watershed*. Mirzapur District, U. P., India http://www.GISdevelopment.net).

Srinivasa, R. Y., & Jugran, K. D., (2003). Delineation of groundwater potential zones and zones of groundwater quality suitable for domestic purposes using remote sensing and GIS. *Hydro-geology Society Journal*, *48*, 821–833.

Subba, R. N., Chakradhar, G. K. J., & Srinivas, V., (2001). Identification of groundwater potential zones using remote sensing techniques in and around Guntur town, Andhra Pradesh, India. *Journal of the Indian Society of Remote Sensing*, *29*(12), 69–78.

Teeuw, R. M., (1995). Groundwater exploration using remote sensing and a low-cost geographical information system. *Hydrogeology Journal, 3*, 21–30.

Tuinhof, A., Olsthoorn, T., Heederik, J. P., & De Vries, J., (2002). *Management of Aquifer Recharge and Subsurface Storage: A Promising Option to Cope with Increasing Storage Needs* (p. 4). Netherlands National Committee of theInternational Association of Hydrogeologists.

Venkateswa, R. V., Srinivasa, R., Prakasa, R. B. S., & Koteswara, R. P., (2004). Bedrock investigation by seismic retraction method – A case study. *Journal of Indian Geophysical Union*, *8*(3), 223–228.

Venkateswara, R. V., Amminedu, E., Venkateswara, R. T., & Ramprasad, N. D., (2009). *Water Conservation Structures in the Urban Environment, Management of Urban Runoff Through Water Conservation Methods*.

Venkateswaran, S., & Jayapal, P., (2013). Geoelectrical Schlumberger investigation for characterizing the hydrogeological conditions using GIS in Kadavanar sub-basin, Cauvery River, Tamil Nadu, India. *International Journal of Innovative Technology and Exploring Engineering*, *3*(2).

CHAPTER 23

DELINEATION OF GROUNDWATER POTENTIAL ZONES IN HARD ROCK TERRAIN USING REMOTE SENSING AND GEOGRAPHICAL INFORMATION SYSTEM (GIS) TECHNIQUES

D. NANDI[1], P. C. SAHU[2], and S. GOSWAMI[3]

[1]*Assistant Professor, Department of RS & GIS: North Orissa University, Baripada, Odisha, India, E-mail: debabrata.gis@gmail.com*

[2]*Reader, Department of Geology: MPC Autonomous Colleges, Baripada, Odisha, India*

[3]*Professor, Department of Earth Science, Sambalpur University, Sambalpur, Odisha, India*

ABSTRACT

Integration of Remote Sensing data and the Geographical Information System (GIS) for targeting of groundwater resources has become an advanced technique in the field of hydrological research, which assists in measuring, monitoring, and conserving groundwater resources. In the present chapter, various groundwater potential zones in Rairangpur block have been delineated using Remote Sensing and GIS techniques. Survey of India (SOI) toposheets and LISS-III satellite imageries are used to preparing various thematic layers viz. Lithology, slope, landuse, lineament, drainage, soil, and geomorphology and were transformed to raster data using the feature to raster converter tool in ArcGIS. The raster map of these factors is allocated a fixed score and weight computed from Multi Influencing Factor (MIF) technique.

Moreover, each weighted thematic layer is statistically computed to get the potential groundwater potential zones. Thus, five different groundwater

potential zones were identified, namely 'very good,' 'good,' 'moderate,' 'poor,' and 'very poor.' The villages under good groundwater potential zone and the villages under very good groundwater potential zone have found out in our study area. The above study has clearly demonstrated the capabilities of Remote Sensing and GIS in the demarcation of the different groundwater potential zones in hard rock terrain.

23.1 INTRODUCTION

Groundwater is a purest, dynamic, and replenishing natural resource. It meets the overall demand for water supplies in all climatic regions including developed and developing countries (Todd and Mays, 2005). In India, more than 90% of the rural and nearly 30% of the urban population depend on groundwater for meeting their drinking and domestic requirements (Reddy et al., 1996). Mapping groundwater potential zones are essential for planning the location of new abstraction wells to meet the increasing demand for water. The groundwater occurrence, distribution is dependent upon the geological and hydro-geomorphological features of the area. Remote sensing techniques are used for groundwater exploration, especially for delineating hydrogeomorphological units (Anonymous, 1979, 1986, 1988; Baldev et al., 1991; Krishnamurthy and Srinivas, 1995). GIS has been found to be one of the most powerful techniques, and it is easier to establish the baseline information for groundwater potential zones (de Zurria et al., 1994; Kadam et al., 2016; Abdul et al., 2016). In the past, several researchers have used RS and GIS techniques for the delineation of groundwater potential zones (Nag and Anindita, 2011; Basavaraj and Nijagunappa, 2011; Krishnamurthy and Srinivas 1995; Kamaraju et al., 1995; Krishnamurthy et al., 1996; Sander et al., 1996; Edet et al., 1998; Saraf and Choudhury, 1998; Jaiswal et al., 2003; Rao and Jugran, 2003; Sener et al., 2005; Ravi Shankar and Mohan, 2006; Solomon and Quiel, 2006; Madrucci et al., 2008; Chowdhury et al., 2009; Jha et al., 2010; Sahu et al., 2017)

The study was conducted to find out the potential groundwater zones in Rairangpur block of Mayurbhanj district, Odisha, India. Different types of thematic maps such as geology, geomorphology, soil texture, land use/land cover, drainage, lineament map were prepared for the study area. The groundwater potential zones were obtained by overlaying all the thematic maps in terms of weighted overlay methods using the spatial analysis tool in Arc Gis10.2.2.

23.2 MATERIALS AND METHODS

23.2.1 STUDY AREA

Rairangpur block of Mayurbhanj District lies between 22° 11′ 30” to and 22° 26′ 30” latitude and 86° 06′ 30” to and 86° 21′ 15” longitude (Figure 23.1). The block falls in the Survey of India (SOI) topographic sheet no 73J/3, 73J/4, 73J/7, 73J/08. The block is covering an area of 258 km^2. According to the 2011 Indian census, the total population is 69374. The average rainfall of this area is 445.47 mm. The block is characterized by the presence of Granite and Epidiorite of pre-Cambrians age. The maximum temperature of the block is 45°C and minimum temperature is 30°C. During the summer, the groundwater level in this block lowers beyond the economic lift, which constitutes the main source of drinking water for this region. The study area is severely suffering from water scarcity, and the sustainability of water supply is threatened. The water scarcity has a direct impact on the livelihood, health, and sanitation of the local people.

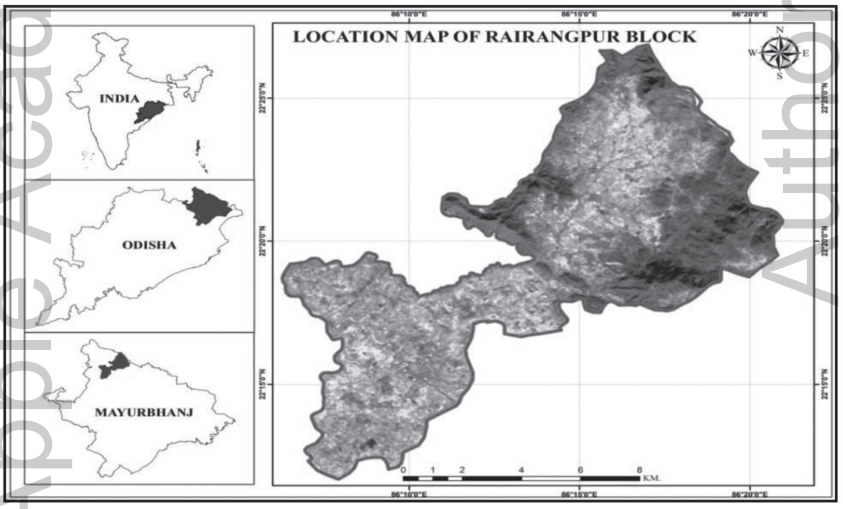

FIGURE 23.1 Location map of the study area with a satellite image.

23.2.2 METHODOLOGY

The administrative base map of Rairangpur block was prepared based on SOI toposheets 73J/3, 73J/4, 73J/7, 73J/08 on a 1:50,000 scale. The

drainage system for the study area was digitized in ArcGIS 10.2.2 from SOI toposheets. The slope map was prepared from CARTOSAT DEM data in ArcGIS spatial analyst module. The drainage density and lineament density maps were prepared using the line density analysis tool in ArcGIS. For the preparation of thematic layers such as land-use, lithology, lineament, and soil types satellite images from IRS–1C, LISS-III sensor has been used. All the thematic layers were converted to a raster format. The groundwater potential zones were calculated by overlaying all the thematic maps in terms of weighted overlay methods using the spatial analysis tool in ArcGIS 10.2.2. During weighted overlay analysis, the ranking was given for each individual parameter of each thematic map, and weights were assigned according to the information in groundwater occur acne (Figure 23.2). Cumulative score index (CSI) was used for this classification. CSI was calculated by multiplying the rank and weight age of each thematic layer as expressed in the following equation.

CSI = ∑ (Geology rank x weight + Geomorphology rank x weight + Soil rank x weight, Lineament density rank x weight + Drainage density rank x weight + Slope rank x weight + Land use rank x weight)

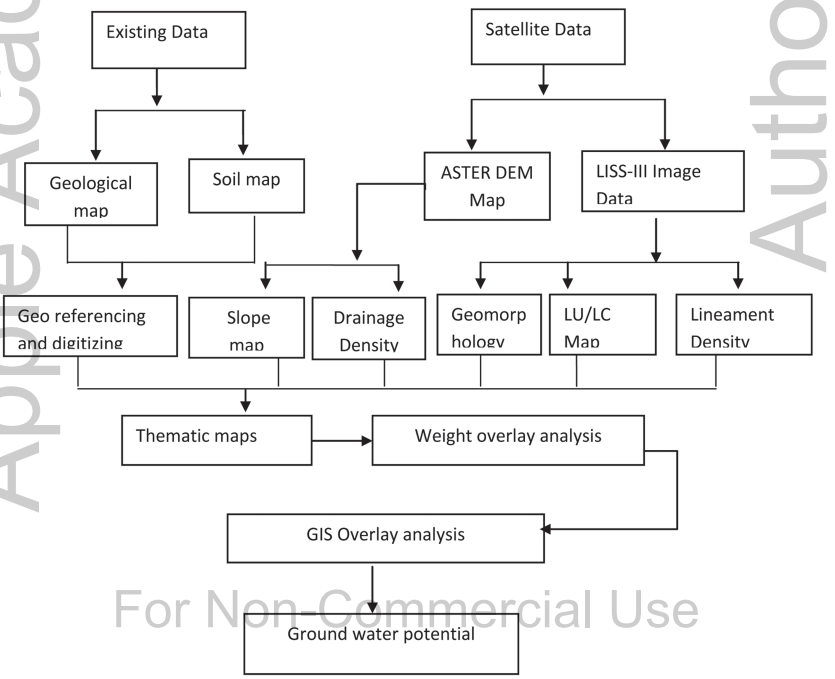

FIGURE 23.2 Flowchart for potential groundwater zone using Geospatial techniques.

23.3 RESULT AND DISCUSSION

23.3.1 GEOLOGY

The study area is characterized by the presence of Epidiorite and Granite of Precambrian age. The main rock type granite and epidiorite (Figures 23.3 and 23.4). Percentage of Granite and Epidorite is 83% and 17%, respectively. These rocks lack Primary porosity. Groundwater occurrence is restricted to weathered and fractured zone. Groundwater occurs in unconfined and confined aquifer condition.

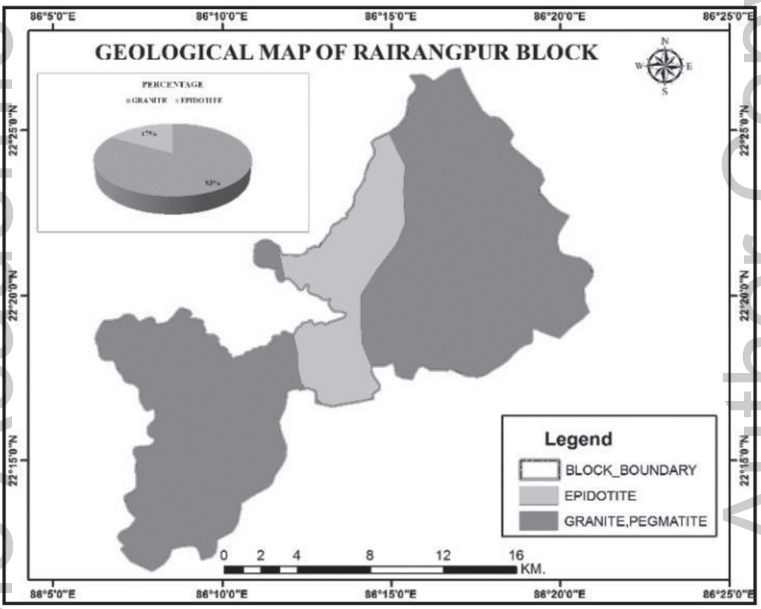

FIGURE 23.3 Geological map of Rairangpur.

23.3.2 HYDRO GEOMORPHOLOGY

The hydrogeomorphological study shows that there is a close relationship between the hydrogeomorphic units and groundwater resources (Rao and Devada, 2003). Geomorphological units are extremely helpful for delineating potential groundwater zones and artificial recharge sites (Elango et al., 2003). By taking image interpretation characteristics such as tone, texture, shape, color, and association over the geocoded FCC image, the

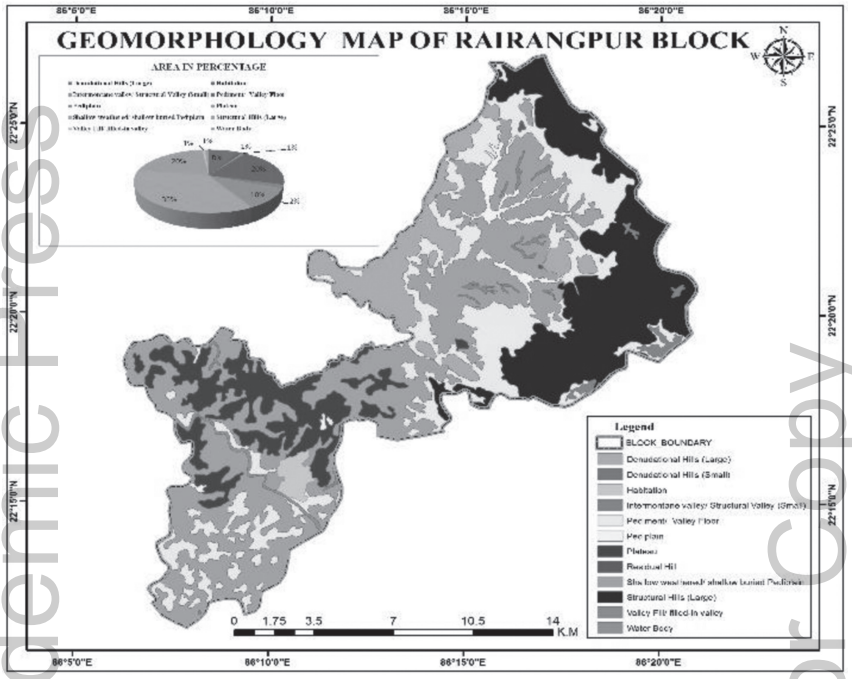

FIGURE 23.4 Geomorphological map of Rairangpur.

geomorphologic units and landforms are interpreted. The geomorphological feature of the Rairangpur block are Denotational Hill (8%), Habitation (1%), Intermontane Valley (1%), Paddy plain (1%), Plateau (10%), Shallow weathered/ shallow buried Pediplain (36%), Structural Hills (Large) (20%), Valley Fill/ filled-in valley (0.74%), Water Body (1%). The Physical Characters of the different landform is present in Table 23.1.

23.3.3 LINEAMENT DENSITY

Lineaments are structurally controlled linear or curvilinear surface expression of zones of weakness or structural displacement in the crust of the earth features, which are identified from the satellite imagery by their relatively linear alignments. Lineament density of an area has a major role for the groundwater potential. High lineament density is good for potential groundwater zones. In hard rock terrain lineaments and fractures act as principal conduits in movement and storage of groundwater. In the Rairangpur block, 33% of the area has very low density, 45% has low

density, 18% has moderate density, and 2% has high-density lineament (Figures 23.5 and 23.6).

23.3.4 DRAINAGE DENSITY

Drainage density is indicated as the closeness of spacing of stream channels. It is a measure of the total length of all the orders per unit area. The drainage density is inversely proportional to permeability. The less permeable rock is which conversely tends to be concentrated in surface runoff. Drainage density of the study area is calculated using Arc GIS Spatial analysis tools of line density tool. The study area is divided into five groups, i.e., very high, high, moderate, low, and very low.

TABLE 23.1 Image and Physical Characteristics of Different Landform in the Study

Geomorphic unit	Image elements	Landform Characteristics (Ground observation)	Area (km2)
Structural hills	Dark red tone coarse texture irregular shape	Linear to arcuate hills dissected, khondalite group rocks mostly dendritic drainage, jointed ridges, average height 300 m. strong to very steep slopes	52.4999
Denudational hills	Dull red tone, coarse texture irregular shape	Weathered khondalite, dendritic drainage, moderate to steep slopes, sparse vegetation	19.8984
Residual hills	Dark grey tone, coarse texture shape and size-irregular and rounded	Erosional surfaces, isolated mounds which have undergone the process of denudation, Steep slopes, radial drainage act as runoff zones	0.16309
Pediments	Light red to red tone, moderate to fine texture	Gentle to moderate slopes, devoid of vegetation with various depths of weathering material, shallow sediment cover rocky and gravely surfaces, dendritic to sub-dendritic drainage, mostly vegetated or cultivated lying at foothills	52.1056
Shallow Weathered pediplains	Green-bluish mixed tone moderate to fine texture	These units are characterized by the presence of relatively thicker weathered material. The thickness of the weathered material is (up to 5 m. These hydrogeomorphic units are developed mostly upon Mayurbhanj Granite	93.0976
Intermontane Valley	Green-bluish mixed tone moderate to fine texture	A linear or curvilinear depression valley within the hills, filled with colluvial deposits of IOG sediments	1.9768
Plateau	Dark red tone coarse texture irregular shape	Tableland shaped hill with a flat surface at the top with sloping sides	26.8315

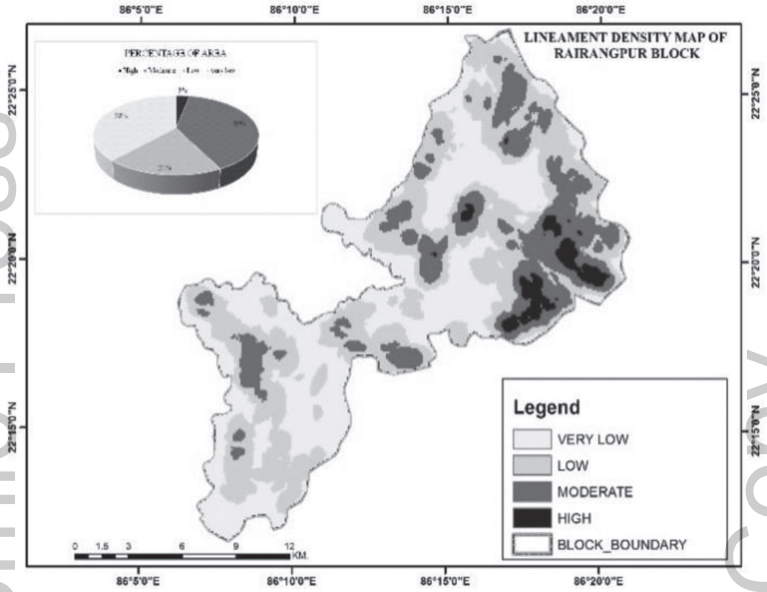

FIGURE 23.5 Lineament density map of the study area.

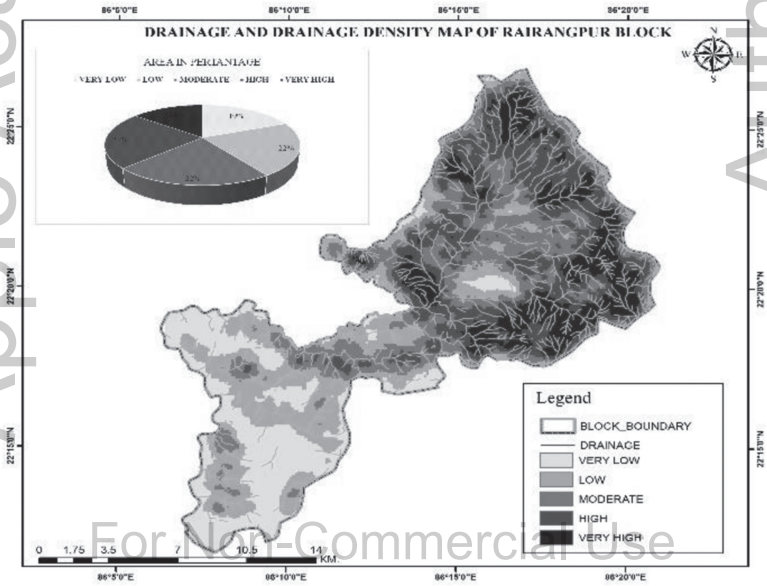

FIGURE 23.6 Drainage map of study area.

23.3.5 SLOPE

The slope has an important role in the identification of potential groundwater zones. Steep slope area facilitates high runoff allowing increased erosion rate with feeble recharge potential whereas, less residence time for rainwater to percolate and hence comparatively less infiltration. The slope map of the study area was prepared based on SRTM data using the 3D analysis tool in Arc Gis10.2.2. Base on a slope the study area is divided into four classes. The area under 0 degree to 4 degrees is very low, 4 degrees to 11 degrees is low, 11 degrees to 21 degree highly moderate, > 21 degrees considered as very poor due to high slope and runoff.

23.3.6 SOIL

The soil is one of the important factors for delineating potential groundwater potential zone. The soil acts as a natural filter and penetration of surface water into an aquifer system and directly related to rates of infiltration, percolation, and permeability (Donahue et al., 1983). The movement and penetration of surface water into the ground is based on the porosity and absorbency of soil. The result of soil classification found that the study area has six types of soils such as, laterite soil, sandy loam, sandy clay, clay, clay loam, and sticky clay (Figure 23.7).

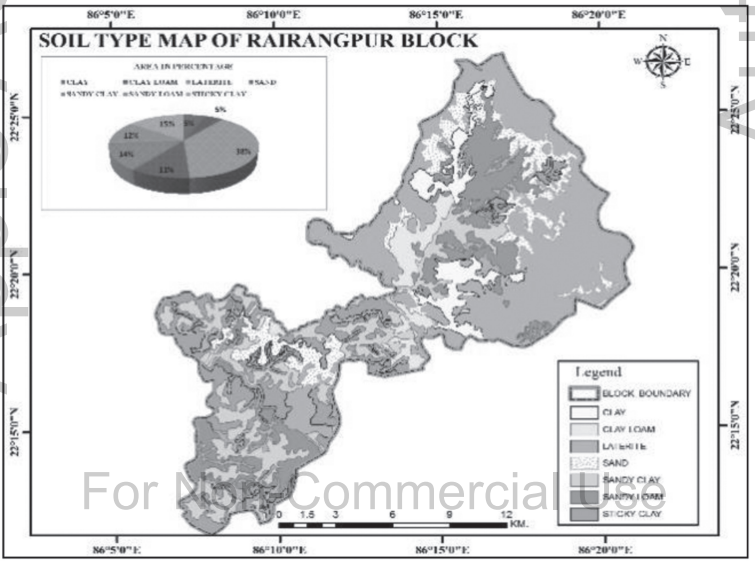

FIGURE 23.7 Soil type map of Rairangpur block.

23.3.7 LAND USE LAND COVER

Land use/land cover map was prepared using LISS-III image Carto Sat Remote Sensing Data. The data was digitally classified in ERDAS 10.0 Software package using a supervised classification technique. The parallelepiped supervised classification technique was applied to extract different types of thematic layers. The study area has five major land use class, i.e., forest (28%), agriculture land (61%) Wasteland (3%), Built-up land (7%) and water bodies (1%). The weights were assigned according to the influence on groundwater occurrence. Water bodies are coming under good categories and lands which are not used for any purpose classified as a wasteland, and built-up land is categorized as poor for groundwater prospects. Agriculture is categorized as moderate categories groundwater occurrence, holding, and recharge (Figure 23.8).

23.3.8 WEIGHT ASSIGNMENT AND GEOSPATIAL MODELING

Suitable weights were assigned to the seven themes according to their hydrogeological importance in groundwater occurrence in the study area. The normalized weights of the individual themes and their different features were obtained through the Saaty's analytical hierarchy process (AHP). The weights assigned to different themes are presented in Table 23.2. After deriving the normal weights of all the thematic maps are converted into raster format and superimposed by weighted overlay method, and all the thematic layers were integrated with one another using spatial analysis of Arc-GIS software to delineate potential groundwater potential zones in the study area. The final integrated layer was divided into five classes, i.e., 'very good,' 'good' 'moderate,' 'poor' and 'very poor' in order to delineate potential groundwater potential zones (Figure 23.9).

23.4 SUMMARY

Delineation of groundwater potential zones in Rairangpur block of Mayurbhanj district using remote sensing and GIS techniques is found efficient to minimize the time, labor, and money and thereby enables quick decision-making for sustainable water resources management. Satellite imageries, topographic maps, and conventional data were used to prepare the thematic layers of lithology, lineament density, drainage density, slope, soil, land-use, and slope. The various thematic layers are

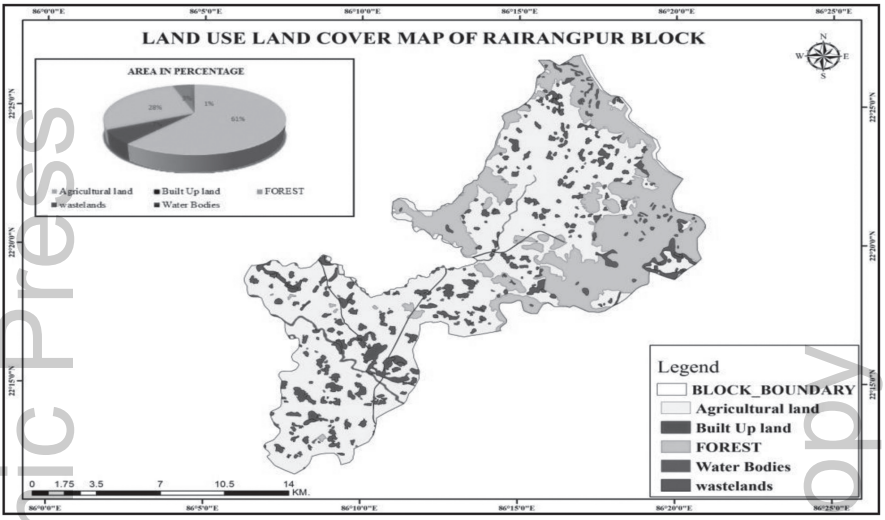

FIGURE 23.8 Land use land cover map of Rairangpur block.

TABLE 23.2 Ranks Assigned to Different Parameters Used for Overlay

Sl No	Parameters	Classes	Feature score	Map Weight
1	Geomorphology	Denudational Hills (Large)	1	25
		Denudational Hills (Small)	1	
		Habitation	1	
		Intermontane valley/ Structural Valley (Small)	8	
		Pediment/ Valley Floor	8	
		Pediplain	2	
		Plateau	7	
		Shallow weathered/ shallow buried Pediplain	2	
		Structural Hills (Large)	6	
		Valley Fill/ filled-in valley	6	
		Water Body	2	
			8	
			10	
2	Slope classes (Degree)	0 to 4	8	15
		4 to 11	6	
		11to 21	3	
		>21	1	

TABLE 23.2 *(Continued)*

Sl No	Parameters	Classes	Feature score	Map Weight
3	Drainage density (Km/Km^2)	0–93	9	10
		93–186	7	
		186–280	6	
		280–373	4	
		373–467	3	
4	Lineament density (Km/Km^2)	0–0.9	9	15
		0.9–1.9	8	
		1.9–2.9	6	
		2.9–3.9	3	
5	Land use/land cover	Agriculture Land	8	15
		Built-up land	2	
		Forest land	6	
		Waterbody	9	
		Wasteland	3	
6	Geology	Granite	2	15
		Epidote	3	
7	Soil	Clay	1	5
		Clay loam	2	
		Laterite	4	
		Sand	8	
		Sandy clay	3	
		Sandy loam	2	
		Sticky clay	1	

assigned proper weight age through MIF technique and then integrated into the GIS environment to prepare the groundwater potential zone map of the study area. According to the groundwater potential zone map, the block is categorized into four different zones, namely 'very good,' 'good,' 'moderate,' 'poor,' and 'very poor.' The villages potential underground zone are Dangapani, Raunsi, Guhaldangri, Mochianetra, Mahedebdihi, Dhatikidihi, Kusumghaty, Jamuban, Teleijhari, Dandbose, Pokhoria, Sansimila, Palasbani, Badpakhana, Tamalbandh, Niranjan, and the villages under very good groundwater potential zone are Naupada, Udayapur, Tolak, Kukudimundi, Sanmauda, Kalsibhanga, Chhatramandal, Badsimila, Kalarda, Katupit, Petepani, and Purunapani. The results of the present study can serve as guidelines for planning future

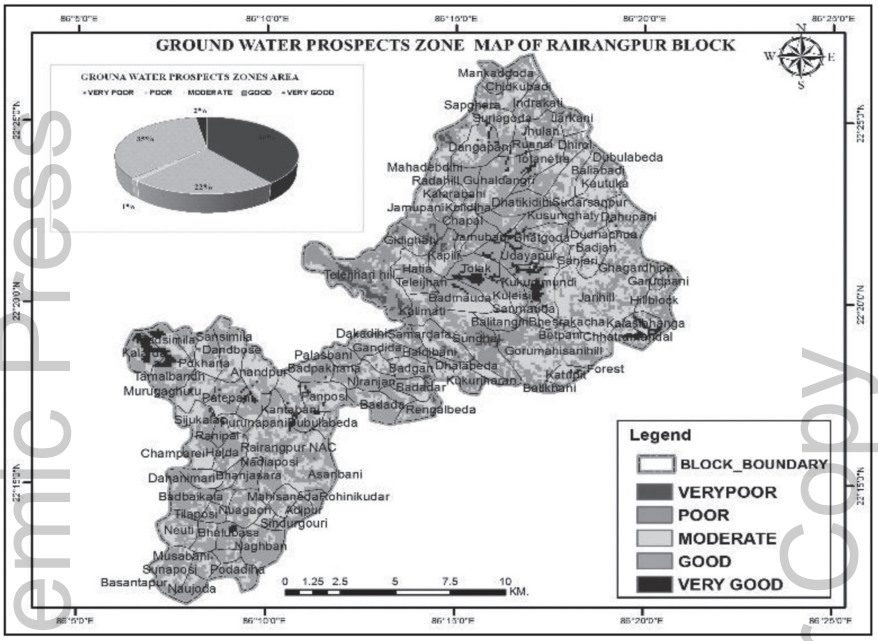

FIGURE 23.9 Groundwater prospect zone map of Rairangpur Block.

artificial recharge projects in the study area in order to ensure sustainable groundwater utilization. This is an empirical method for the exploration of groundwater potential zones using remote sensing and GIS, and it succeeds in proposing potential sites for groundwater zones. This method can be widely applied to a vast area with rugged topography for the exploration of groundwater resources.

KEYWORDS

- **geospatial technology**
- **groundwater**
- **hydrogeomorphology**
- **lineament**

REFERENCES

Anonymous, (1979). Satellite remote sensing survey: southern part of Tamil Nadu (Vol. I and II). Project Report, National Remote Sensing Agency, Department of Space, Hyderabad, India.

Anonymous, (1986). Report on the groundwater potential maps of Karnataka prepared based on visual interpretation of Landsat Thematic Mapper data, NRSA, Department of Space, Government of India, and Hyderabad.

Anonymous, (1988). Preparation of hydrogeomorphological maps of India on 1: 250000 scale using satellite imagery, project report, Department of Space, Bangalore, India.

Bhattacharyaa, B., & Hegde, V. S., (1991). IRS–1A application for groundwater targeting, special issue on remote sensing for National Development. *Journal of Current Science*, *61*, 172–179.

Burrough, P. A., (1989). *Principles of Geographical Information Systems for Land Resources Assessment*, Oxford: Oxford University Press.

Chi, K. H., & Lee, B. J., (1994). Extracting potential groundwater area using remotely sensed data and GIS techniques. In: *Proceedings of the Regional Seminar on Integrated Application of Remote Sensing and GIS for Land and Water Resource Management* (pp. 64–69). Bangkok.

Chowdhury, A., Jha, M. K., Chowdary, V. M., & Mal, B. C., (2009). Integrated remote sensing and GIS-based approach for assessing groundwater potential in West Medinipur district, West Bengal, India. *Int. J. Remote Sens., 30*(1), 231–250.

Clavre, B., Maldonado, J. O., & Valenzuela, C. R., (1994). A conceptual approach to evaluating watershed hazards: The Tunari watershed, Cochabamba, Bolivia. *ITC Journal, Special GIS Issue Latin America, No.3*, 283–291.

Elango, L., Kumar, S., & Rajmohan, N., (2003). Hydrochemical studies of groundwater in Chengalpet region, South India. *Indian Journal of Environmental Protection*, *23*(6), 624–632.

Hussein, A. A., Govindu, V., & NiGusse, A. G. M., (2016). Evaluation of Groundwater potential using Geospatial Techniques. *Journal of Applied Water Science*.

Hutti, B., & Nijagunappa, R., (2011). Identification of potential groundwater zone using geoinformatics in Ghataprabha basin, North Karnataka, India. *International Journal of Geomatics and Geosciences, 1*(2), 91–109.

Jaiswal, R. K., Mukherjee, S., Krishnamurthy, J., & Saxena, R., (2003). Role of remote sensing and GIS techniques for generation of groundwater prospect zones towards rural development – an approach. *International Journal of Remote Sensing*, *24*(5), 993–1008.

Jha, M. K., Chowdary, V. M., & Chowdhury, A., (2010). Groundwater assessment in Salboni Block, West Bengal (India) using remote sensing, geographical information system, and multi-criteria decision analysis techniques. *Hydrogeology Journal, 18*(7), 1713–1728.

Kadam, A. K., Sankhua, R. N., & Umrikar, B. N., (2016). *Assessment of Groundwater Potential Zones Using GIS Technique: A Case Study of Shivganga River Basin* (pp. 70–77). Pune, Maharashtra, India Conference: IGWC–2015, At Chennai.

Kamaraju, M. V. V., Bhattacharya, A., Reddy, G. S., Rao, G. C., Murthy, G. S., & Rao, T. C. M., (1995). Groundwater potential evaluation of West Godavari District, Andhra Pradesh State, India—a GIS approach. *Ground Water*, *34*(2), 318–325.

Krishnamurthy, J., & Srinivas, G., (1995). Role of geological and geomorphological factors in groundwater exploration: A study using IRS LISS data. *International Journal of Remote Sensing, 16*(4), 2595–2618.

Krishnamurthy, J., Venkatesa, K. N., Jayaraman, V., & Manuvel, M., (1996). An approach to demarcate potential groundwater zones through remote sensing and a geographical information system. *International Journal of Remote Sensing, 17*(10), 1867–1884.

Krishnamurty, J., & Srinivas, G., (1995). Role of geological and geomorphological factors in groundwater exploration a study through remote sensing technique. *International Journal of Remote Sensing, 16*, 2595–2618.

Madrucci, V., Taioli, F., & De Araújo, C. C., (2008). Groundwater favorability map using GIS multicriteria data analysis on crystalline terrain, São Paulo State, Brazil. *Journal of Hydrology, 357*, 153–173.

Nag, S. K., & Anindita, L., (2011). An integrated approach using remote sensing and GIS techniques for delineating potential groundwater zones in Dwarakeswar watershed, Bankura district, West Bengal. *International Journal of Geomatics and Geosciences, 2*(2), 430–442.

Nandi, D., & Mishra, S. R., (2014). Groundwater quality mapping by using geographic information system (GIS): A case study of Baripada city, Odisha, India. *International Journal of Conservation Science*, *5*(1), 79–84.

Rao, Y. S., & Jugran, D. K., (2003). Delineation of groundwater potential zones and zones of groundwater quality suitable for domestic purposes using remote sensing and GIS. *Hydrology Science Journal, 48*(5), 821–833.

Ravi, S. M. N., & Mohan, G., (2006). Assessment of the groundwater potential and quality in Bhatsa and Kalu river basins of Thane district, western Deccan Volcanic Province of India. *Environmental Geology, 49*, 990–998.

Sahu, P. C., (2017). Groundwater resource conservation and augmentation in hard rock terrain: An integrated geological and geospatial approach. *International Journal of Conservation Science*, *8*(1), 145–156.

Sander, P., Chesley, M. M., & Minor, T. B., (1996). Groundwater assessment using remote sensing and GIS in a rural groundwater project in Ghana: Lessons learned. *Hydrogeology Journal*, *4*(3), 40–49.

Saraf, A. K., & Choudhury, P. R., (1998). Integrated remote sensing and GIS for groundwater exploration and identification of artificial recharge sites. *International Journal of Remote Sensing, 19*(10), 1825–1841.

Sener, E., Davraz, A., & Ozcelik, M., (2005). An integration of GIS and remote sensing in groundwater investigations: A case study in Burdur, Turkey. *Hydrogeology Journal*, *13*(5–6), 826–834.

Shaban, A., Khawlie, M., & Abdallah, C., (2006). Use of remote sensing and GIS to determine potential recharge zone: The case of Occidental Lebanon. *Hydrogeology Journal, 14*, 433–443.

Solomon, S., & Quiel, F., (2006). Groundwater study using remote sensing and geographic information systems (GIS) in the central highlands of Eritrea. *Hydrogeology Journal*, *14*, 729–741.

Subba, R. N., & John, D. D., (2003). Fluoride incidence in groundwater in an area of peninsular India. *Environmental Geology*, *45*, 243–251.

Suja, R. R. S., & Krishnan, N., (2009). Spatial analysis of groundwater potential using remote sensing and GIS in the Kanyakumari and Nambiyar Basins, India. *Journal of the Indian Society of Remote Sensing*, *37*, 681–692.

Todd, D. K., & Mays, L. W., (2005). *Groundwater Hydrology* (3rd edn.). New Jersey: John Wiley & Sons.

Zuviria, M. D., & Valenzuela, C. R., (1994). Mapping land suitability for coffee with ILWIS. *ITC Journal*, *Special GIS Issue Latin America*, *3*, 301–307.

CHAPTER 24

AN ANALYSIS OF SALINE WATER INTRUSION INTO COASTAL NIGERIA

AMARTYA KUMAR BHATTACHARYA

Chairman and Managing Director, MultiSpectra Consultants, 23, Biplabi Ambika Chakraborty Sarani, Kolkata – 700029, West Bengal, India, E-mail: dramartyakumar@gmail.com

ABSTRACT

The present chapter gives an overview of saline water intrusion into coastal Nigeria. This chapter places saline water intrusion into coastal Nigeria in the context of geology, hydrogeology, meteorology, and land use of coastal Nigeria. This chapter suggests ways and means to manage the problem of saline water intrusion into coastal Nigeria.

24.1 INTRODUCTION

Groundwater dynamics that is the movement of groundwater through geological formations and it can be linked to different phenomena that occur in deep aquifers such as the upward advance of saline waters of geologic origin; surface waste discharges into shallow aquifers and the invasion of saline water into coastal aquifers. In recent years, considerable interest has been evinced in the study of flow through porous media, because of their natural occurrence and importance in many engineering problems such as movement of water, oil, and natural gas through the ground, saline water intrusion into the coastal aquifers, flow through packed towers in some chemical processes and filtration. Therefore, the physical understanding of flow through porous media is essential to scientists and engineers working in the related areas. The proposed work as the reported herein is on the movement of groundwater as related to saltwater intrusion into coastal aquifers

and submarine discharge of freshwater into the sea. The mechanism responsible for this phenomenon involves the reduction or reversal of groundwater gradients, which permits denser saline water to displace freshwater and vice-versa. This situation commonly occurs in a coastal aquifer in hydraulic continuity with the sea when pumping of wells disturbs the natural hydrodynamic balance.

Saline water intrusion in fresh groundwater takes place in the vicinity of coastal regions whenever saline water displaces or mixes with freshwater. This situation usually occurs in coastal regions having hydraulic continuity with the sea when the pumping rate in the wells disturbs the natural hydrodynamic balance. The intrusion of saline water into the freshwater coastal aquifer is likely to cause a problem when such aquifer is tapped for domestic water supply or for irrigation. The coast of Nigeria is located in West Africa, part of the Gulf of Guinea. The coastline of Nigeria stretches for about 850km, from the Republic of Benin in the west to Cameroon in the east. It forms part of the West African groundwater region. River Niger discharges into the Gulf of Guinea via a delta as the major river, thereby, dividing the coastline into two parts. Other rivers discharge through estuaries either into the lagoon of directly into the ocean. The surface strata of the coastline of Nigeria consist of unconsolidated coastal plain sands. Lagoons, estuaries, creeks, and delta dominate the Nigerian coastline. The vegetation of the area is mangrove swamp forest that is being cleared for wood and to give room for other economic activities. The western of the coastline is highly populated with total dependence on groundwater to meet domestic and industrial demands. Thousands of private boreholes have been drilled in the area to extract groundwater for drinking. Continuous pumping or heavy extractions of groundwater have led to increment of chloride content in groundwater. The chloride/bicarbonate ratio is a very good indicator of saline water contamination in groundwater. High chloride content in groundwater may also be caused by the presence of chloride-containing minerals in the area, or there are pollutants being discharged into groundwater. The major cause of saline water pollution into groundwater in this area is as a result of saline water intrusion. Upcoming occurs below wells as a result of continuous pumping of freshwater. The entire coastline of Nigeria is divided into seven administrative units (Lagos, Ogun, Ondo, Delta, Bayelsa, Rivers, and Akwa Ibom states).

Saline water intrusion is one of the most common forms of groundwater contamination in coastal areas (Bear et al., 1999). Saline water intrusion is the movement of salty water into an aquifer or surface water with the consequent mixing or displacement of fresh water. When groundwater is

pumped from aquifers that are in hydraulic connection with the sea, and the piezometric surface of the fresh water is lowered, the balance between the saline water/freshwater interface is disturbed, the hydraulic gradients so created induce seawater to encroach the freshwater aquifer (Domenico and Schwartz, 1998; Walton, 1970).

Saline water intrusion has been a major water resource problem in the urban coastal areas of the Niger Delta, and it has therefore been and continues to be a focus of considerable research efforts over time. This is because a scientific understanding of the occurrence of salt and fresh waters in a particular coastal area is essential for the development and management of the water resource. Nigeria has a coastline that is about 1000 km long with the Atlantic Ocean bordering eight States. These are: Rivers, Bayelsa, Akwa Ibom, Cross Rivers State, Delta, Ondo, Ogun, and the Lagos States. Potable water supply to inhabitants in some of the communities in the coastal belt (especially in the saline mangrove swamp) has been a major problem due to saltwater intrusion. Water wells and boreholes drilled have been abandoned in many communities due to high salinity. They, therefore, depend on rain harvesting and purchasing water from water merchants. In Nigeria, there have been few studies aimed at assessing freshwater resources in coastal areas of the country. This forms the main thrust of the proposed research.

The quality of water is the main constraint of groundwater in the coastal aquifers in Nigeria. Like all coastal aquifers worldwide, saline water intrusion into aquifers is the major source of quality impairment in the coastal aquifers in Nigeria. This is followed by pollution from spillages of crude and refined petroleum and lastly by leachates from municipal and other industrial wastes. Most of the confined aquifers in the coastal areas of Nigeria have high iron concentration such that treatment for the removal of iron has to be undertaken. Saline water intrusion into unconfined and confined aquifers occurs in Niger Delta. In Coastal beach ridges or sandy islands within the saline mangrove belt, freshwater lens floating above saline water-bearing sands are found to occur in the unconfined aquifers (Oteri, 1990). The growth of industrial development within the urban coastal areas of the Niger Delta and the attendant population explosion places a very heavy demand on the lean supply of fresh water. According to Frank Briggs (2003) “indiscriminate abstraction of groundwater from the first aquifer has resulted in saltwater intrusion in several coastal wells….” This limits the supply of potable drinking water in the area, which can have detrimental effects on human health, wildlife habitat and increase the cost of water treatment (Domenico and Schwartz, 1998).

24.1.1 GEOGRAPHY AND METEOROLOGY OF COASTAL NIGERIA

In Nigeria, eight states are bounded to the south by the Atlantic Ocean. They include from West to East – Ogun, Lagos, Ondo, Delta, Bayelsa, Rivers, Akwa Ibom, and the Cross River States. The states are contiguous and are in direct contact with the sea. They are located between latitude 7° and 4° 10' N and longitudes 2° 30' and 8 30' East. There are a number of highly populated cities situated within the coastal area of these states which include Port Harcourt, Warri, Yenagoa, Lagos, Uyo, and Calabar. The coastal states of Nigeria fall within the humid tropical zone of the country. Rainfall is copious and lasts for eight to nine months of the year (mid-March to early-November) with a mean annual value often exceeding 3000 mm at the coastal fringes at Akasa and Brass. Seasonal changes of wet and dry are as a result of the interplay of two contrasting air masses – the moisture-laden SW monsoon winds blowing into the country from the Atlantic Ocean and the dry North East Trade winds from the Sahara desert. The two main rivers in the southwestern part of Nigeria are Ogun and Oshun which drain into the ocean.

24.1.2 GEOLOGY OF COASTAL NIGERIA

Geologically, coastal Nigeria is made up of two sedimentary basins-the Dahomey Basin and the Niger Delta Basin separated by the Okitipupa Ridge. The Dahomey Basin covers the southern areas of Lagos, Ogun, and the Ondo States in Nigeria and stretches into the neighboring countries of Benin, Togo, Ghana, and Ivory Coast. The present study is centered on the Niger Delta area of Nigeria. The geological formations of primary interest for the evaluation of the groundwater resources potential of the study area are the sedimentary formations deposited in the Niger Delta during the Eocene-Quaternary periods. The stratigraphic sequence under consideration comprises, from oldest to youngest formations, the Imo Shale Group, the Ameki Formation, the Benin Formation, and the Quaternary deposits as described by Amajor and Agbaire (1989).

The Imo Shale Group is made up of marine clay, shale, and limestone. The formation is estimated to have a thickness of up to 1,000 m, and it outcrops in a belt more than 100 km north of the study area. The formation, due to its impermeable texture, is believed to constitute the base of the groundwater aquifers under consideration in the study area. The Ameki Formation overlies the Imo Shale Group. It comprises numerous alternations

of marine shales and fine to coarse, very heterogeneous, coastal – deltaic sands and sandstones. The formation is estimated to have a thickness of up to 1,700m and is out-cropping in an east-west and north-west – south-east oriented belt, approximately 100km north of the study area. The groundwater resources potential of the formation is believed to be good (Tahal, 1998). The present-day Niger Delta is defined geologically by three subsurface sedimentary sequences consisting of Benin, Agbada, and Akata Formations (Short and Stauble, 1967).

24.2 BENIN FORMATION

The Benin Formation overlies the Ameki Formation. The formation is an extensive stratigraphic unit in the Southern Sedimentary Basin, with an average thickness of about 1,900 m (Short and Stauble, 1967). The formation is recognized throughout the delta due to its few shale streaks, the absence of brackish water and a high percentage of sand. The Benin Formation, which consists mainly of coastal plain sands, extends from the west across the whole Niger Delta area and southward beyond the present coastline. The sediments comprise yellow and white sands with pebbly gravels. The clays and sandy clays occur in lenses of 3m to as much as 10m, and they make the groundwater formation a multi-aquifer system. The formation is massive porous fresh water-bearing sandstone with localized thin beds. The formation is, due to its coarse texture and huge outcrop area, believed to constitute a very good groundwater aquifer. The aquifer in this basin has a southwest gradient towards the Delta, and it thickens seawards in the same direction of groundwater movement. It is thus the most prolific aquifer in the region. It is overlain by the Quaternary deposits, which ranges in thickness in between 133 – 500ft (Etu – Efeotor and Akpokodje, 1990). The Quaternary deposit, which comprises recent deltaic sediments made up of sand, silt, and clay beds, overlies the Benin Formation in the swampy delta areas. The formations have a seaward dip resulting in confined aquifers.

The sandstones of the Benin Formation are coarse-grained, locally fine -grained, poorly sorted and sub angular to well rounded. The age of the Benin Formation lies between Oligocene and Recent. This formation constitutes the major aquifer in the Niger Delta area (Udom et al., 1999). Whiteman (1982) notes that a formation such as the Benin Formation, deposited in a continental fluviatile environment has a highly variable lithology, can be recognized because of its high sand percentage (70–100%), few minor shale intercalations and the absence of brackish water and marine faunas.

To date, very little oil has been found in the Benin Formation (mainly minor oil shows).

24.3 AGBADA FORMATION

The Agbada Formation underlies the Benin Formation and forms the second of the three strongly diachronous Niger Delta complex formations. It comprises mainly of alterations of sands, silts, and shales in various thicknesses and proportions, indicative of cyclic sequences of off-lap cycles, better called off-lap rhythms (Weber, 1971). The characteristic features of the sandstones here are poor sorting, calcareous matrix and shell fragment occurrences. The grain size varies from fine to coarse. The approximate total thickness of the Agbada Formation lies between 10,000 ft and 12,000 ft (Kogbe, 1976). The top of the Agbada Formation is sandy whereas the bottom is shaley because it grades into the Akata shales gradually. The shales are denser at the base of the formation due to the compaction process. The sandy parts constitute the main hydrocarbon reservoirs in the delta oil fields. The shales constitute seals to the reservoirs and as such are very important because the formation is rich in hydrocarbon. Paralic clastics of the Agbada Formation represent the true deltaic portions of the delta top-set and fluvio-deltaic environment (Short and Stauble, 1967; Weber and Dakoru, 1975). However, Whiteman (1982) notes that the Agbada Formation, as defined by Short and Stauble (1967), contains beds laid down in a variety of sub-environments grouped together under the heading-paralic environment. The age of the Agbada Formation ranges from Eocene to Recent.

24.4 AKATA FORMATION

This formation is the basal major time-transgressive lithological unit of the Niger Delta Complex. It is composed mainly of marine shales, but contains sands and silty beds which are thought to have been laid down as turbidites, and continental slope channel fills. The shales are typically under-compacted and over-pressured, forming diapric structures. Whiteman (1982) contributes that the Akata Formation is rich in planktonic foraminifera, which indicates deposition on a shallow marine shelf environment. The formation occurs between depths of 0–6000 m below the Agbada Formation and ranges in age from Paleocene to recent. It represents the prodelta mega facies (Tahal, 1998).

24.5 HYDROGEOLOGY AND AQUIFERS OF THE STUDY AREA

In the study area, groundwater is abstracted from the Benin Formation, mainly from its upper section. Lenses of silty clay of some few meters thickness have been recorded in the borehole penetrating the Benin Formation (Tahal, 1998). To the south of Port Harcourt, belts rich in shales lying at a depth of 10m to 200m have been observed. These lenses create several sub-aquifers in the Benin Formation, the upper sub-unconfined, while the deeper aquifers range from leaky to confined and are isolated from the ground surface. The natural recharge comes mainly from the northern high coastal plain. Generally, the sediments of the Benin Formation dip seawards at a low gradient. The upper section of these sediments is being utilized in the development of groundwater.

The sandy components, in most layers, are about 90% of the lithological sequences (Tahal, 1998). The size distribution of the sedimentary particulates does not vary significantly from place to place in the study area. There is a steady gradation in quantity between coarse sands and clay beds. Locally to some extent, the clay beds separate hydraulically between the sub-aquifers.

Groundwater abstracted from the upper Benin Formation is characterized by low p^H (acidity), high carbon dioxide (CO_2) content, and hence it is corrosive and soft. In addition, the groundwater contains high concentrations of iron and therefore requires treatment. The water tables of all sub-aquifers penetrated by boreholes are relatively shallow and range between 5m to 15m where hydrostatic water levels increase with the depth (Tahal, 1998). According to Etu – Efeotor, and Odigi (1983), three main zones have been differentiated as follows:

i) A northern zone is consisting shallow aquifer of predominantly continental deposits.
ii) A transitional zone of marine and continental materials.
iii) A coastal zone of predominantly marine deposits.

Aquifer distributions in the Niger Delta are controlled by the geology. Table 24.1 is the summary of the properties and behavior of hydrostratigraphic units in the Niger Delta Basin. In most parts of the Niger Delta, including the study area, a multi -aquifer system is encountered, and the aquifer lies within the arenaceous Benin Formation. The depth to water table of the Benin Formation ranges between 3–5 m below ground level (Offodile, 1984). Ngah (1990) also identified three main aquifer zones in the Niger Delta Viz:

i) An upper unconfined aquifer is extending throughout the Benin Formation with its thickness ranging between 15–80 m while the Static Water Level (SWL) varies between 4m and 21 m.
ii) A middle aquifer system, semi -confined and consisting of thick medium to coarse-grained, sometimes pebbly sands with thin clay lenses. Its thickness varies between 30–60m.
iii) A lower aquifer system that extends from 220–300 m and consists of coarse -grained sands and gravels with some interlayer clay. The majority of the groundwater wells abstract water from the first and second aquifers (<100 m deep). The very few industrial and municipal groundwater supply wells tap deeper aquifers.

24.5.1 AQUIFER RECHARGE IN THE STUDY AREA

Precipitation is the main source of recharge to aquifers. The rate of recharge depends to a large extent on the infiltration capacity of the soil, evaporation rate and the overland drainage characteristics. In places where sandy clay forms a part of soil layers, recharge usually occurs mainly through a distant outcrop of the porous formation and partially through the lateritic sand. The northern and the southern movement of air masses and pressure belts characterize the rainfall regime of the coastal plain. The amount of rainfall decreases inland from the coast. The isohyets run parallel to the coast up to a line through Ahoada-Degema-Port Harcourt. From this line inland, the decrease in rainfall is much slower. According to the lithologic profile of some boreholes, in some places, there are few meters of lateritic sandy clay under the soil. Tahal (1998) observed that about 30% to 40% of the yearly average of rainfall (2,280mm) could infiltrate and recharge the Benin Formation. To the north, sandy, and porous outcrops exist, where the replenishment can be 60% to 70% of rainfall. The estimated annual recharge to the aquifer in the study area from the Northern High Coastal Plain is about 100 mcm to 150 mcm (Tahal, 1998).

24.5.2 PROBLEMS AFFECTING THE COASTAL AQUIFER ECOSYSTEM IN NIGERIA

The major constraint to the water resource in the aquifers of the coastal Nigeria is quality. The saline water intrusion is both natural and man-made. For the natural saline water intrusion, the problem is exacerbated by:

TABLE 24.1 Summary of Properties and Behavior of Hydrostratigraphic Units in the Niger Delta Basin

Hydrogeological basin	Hydrostratigraphic units	Lithologic details	Aquifer type and characteristics	Water quality	Economic importance
Niger Delta Basin	Alluvial plains aquifer	Sands, clays, silt	Unconfined	Saline water	Domestic Municipal Industrial uses
	Meander Belt aquifer	Sands, gravel, clays		Corrosion	
	Mangrove swamp aquifer	Sands, clay, swamps	Good, water table is confined	Iron-rich saline water intrusion	
	Abandoned Ridges aquifer, Sombrero	Sands and pebbles, yellow sands, clays	Poor aquifer		
	Benin aquifer	Sand, clays	Prolific		
	Delta Ogwashi – Asaba Ameki aquifer	Clays, shale, lignite, silty sand, clay siltstone	Aquitard	Problematic with iron and saltwater encroachment, Low Ph	
	Imo shales Deep oceanic Agbada – Akpata Shales	Shalestone, claystone lenses of sands	Aquitard Aquitard		

- The lack of willingness to carry out necessary studies or utilize such studies when carried out.
- Lack of appreciation of the need for water resources assessment and management groundwater resources of the coastal aquifers resulting in over-exploitation of the aquifers.
- The activities of man have also led to increased saline water intrusion through.
- Uncontrolled development of both unconfined and confined aquifers especially in Port Harcourt Metropolis, Lagos, Warri, and Bonny. In Lagos which is the commercial capital of Nigeria, the problem is particularly acute as many boreholes which were producing fresh water after drilling becomes salty a few months after especially in Ikoyi, Victoria Island and Apapa.
- Lack of proper sealing of disused boreholes or those abandoned due to saltwater intrusion.
- The groundwater in most of the confined aquifers in coastal Nigeria is corrosive, and casing corrosion is a major source of borehole failures. There is a need to determine the best material for casing and screens and also best completion techniques that will prevent saline water ingress into fresh water yielding boreholes especially in situations where the freshwater aquifers underlie saline water-bearing sands.
- Sea water level rise (as a result of global warming); the building of dams in upstream areas of the rivers leading to low flows and decrease in river sediments to the coast by the rivers have all led to increased coastal erosion.
- Construction of drainage canals, transportation canals.
- Urbanization – In the Lagos area for example. The rate of Urbanization is so high that the recharge area has been converted to concrete zones, while swamps and streams are being reclaimed and turned into cities. This decreases the amount of recharge to the aquifers, thereby increasing saline water intrusion.
- Oil spillage from both upstream and downstream operations of the oil industry is the next major problem affecting both the aquifers and the environment of coastal areas in general.
- Finally, disposal of wastes from industries and municipal areas is a threat to the coastal aquifer ecosystem.

24.6 CONCLUSIONS

The control of saline water intrusion demands knowledge of the hydraulic conditions within aquifer; it also demands knowledge of the source of the saline water. It is, therefore, necessary to identify the extent of the problem and to assess the behavior of the saline water body under various conditions of recharge and discharge, such that efficient water resources management plans can be implemented. The optimum solution to the problem of saline water intrusion is prevention, by which the encroachment of saline water is controlled to an acceptable degree. But in many cases, the problem is a legacy of the past; therefore, management must concentrate on minimizing further intrusion, and/or reducing the extent of the existing saline water, it may be that the aquifer in question is too badly polluted so reclamation may be the only viable option. In extreme cases, if the resource for potable water supply, it may be abandoned, although the water may still be utilized for certain industrial or agricultural applications.

KEYWORDS

- **coastal regions**
- **Nigeria**
- **saline water intrusion**

REFERENCES

Amajor, L. C., & Agbaire, D. W., (1989). Depositional history of the reservoir sandstones, Akpor and Apara Oilfields, Eastern Niger Delta, *Nigeria Journal of Petroleum Geology, 12*(4), 453–464.

Bear, J., Cheng, A. H. D., Sorek, S., Ouazar, D., & Herrer, T. J. B., (1999). *Saltwater Intrusion in Coastal Aquifers–Concepts, Methods, and Practices, in Theory, and Application in Porous Media* (p. 625). Kluwer Academic Publishers. Dordrecht.

Domenico, P. A., & Shwartz, F. W., (1998). *Physical and Chemical Hydrogeology,* John Wiley and Sons Inc., New York.

Etu–Efeotor, J. O., & Akpokodje, G. E., (1990). Aquifer systems of the Niger delta. *Journal of Mining and Geology*, *26*(2), 264–266.

Etu–Efeotor, J. O., & Odigi, M. I., (1981). Water supply problems in the Eastern Niger Delta. *Journal of Mining and Geol., 20*(1), 182–192.

Frank-Briggs, I. N., (2003). The geology of some Island Towns in the Eastern Niger Delta, Nigeria. *An Unpublished PhD Thesis Submitted to the Department of Geology*, University of Port Harcourt.

Kampsax–Krüger, (1985). *Final Report on Hydrological Site Studies for Water Well Development*, *Phase 1*, 118.

Kogbe, C. A., (1976). *The Cretaceous and Paleocene Sediments of Southern Nigeria* (pp. 237–252). Elizabethan Publishing Coy, Lagos.

Ngah, S. A., (1990). *Groundwater Resource Development in the Niger Delta: Problems and Prospects.* 6th IAEC Congress.

Offodile, M. E., (1982). The Problems of Water Resources Management in Nigeria, *Journal of Mining and Geology, 20th Anniversary edn.*, *19*(1).

Oteri, A. U., (1990). Delineation of seawater intrusion in a coastal beach ridge of Forcados. *Journal of Mining and Geology, 26*(2), 225–229.

Short, K. C., & Stauble, A. J., (1967). Outline of the geology of the Niger Delta. *AAPG Bull*., *51*, 761–779.

Tahal Consultant Engineers Ltd., (1998). Final report on multistate water supply project, feasibility study of rivers state capital (Port Harcourt and Environs and selected Urban Communities), 2–4.

Udom, G. J., Etu-Efeotor, J. O., & Esu, E. O., (1999). Hydrochemical evaluation of groundwater in parts of Port Harcourt and Tai-Eleme Local Government Area, rivers state: *Global Journal of Pure and Applied Sciences*, *5*, 546–552.

Walton, W. C., (1970). *Groundwater Resource Evaluation*, McGraw–Hill, 375.

Weber, K. J., & Dakoru, E., (1975). *Petroleum Geology of the Niger Delta* (pp. 109–221). Ninth World Petroleum Congress.

Weber, K. J., (1971). Sedimentological aspects of oil fields in the Niger Delta. *Journal of Environmental Geology, Minbouw, 50*(3), 559–576.

Whiteman, A., (1982). *Nigeria: Its Petroleum Resources and Potentials*. Graham and Trotman, *1*, 63–78.

CHAPTER 25

SALINE WATER INTRUSION IN COASTAL AREAS: A CASE STUDY FROM INDIA

AMARTYA KUMAR BHATTACHARYA

Chairman and Managing Director, MultiSpectra Consultants, 23, Biplabi Ambika Chakraborty Sarani, Kolkata – 700029, West Bengal, India, E-mail: dramartyakumar@gmail.com

ABSTRACT

An innovative method of control of saltwater intrusion into the coastal aquifers has been suggested in this paper. A new method consists of withdrawal by Qanat-well structures with reasonable compensation by rainwater harvesting by means of recharge ponds and recharges well. The salient features of the methodology are described by considering a design example adopted in the Contai Polytechnic Institute Campus of the district of Purba Midnapur in the state of West Bengal, India.

25.1 INTRODUCTION

Groundwater is the second largest reserve of fresh water on earth. About 2 billion people, approximately one-third of the world's population, depend on groundwater supplies, withdrawing about 20% of global water (600–700 km) annually—much of it from shallow aquifers (Patra et al., 2006). India cities located near coastlines with a large population can experience saline water intrusion due to over-exploitation of groundwater, causing this significant threat to freshwater resources. Sustainability strategies adopted to retard or halt the rate of saline water intrusion are necessary to protect the resources from further damage. The complexity of hydrogeological setup in the concerned area calls for scientific management techniques to be adopted in the groundwater development. This requires a clear understanding

of the hydrogeology of the area concerned, appreciation of the possible consequence of over or under developments and a coordinated approach of the planners, hydrogeologists, irrigation engineers, social scientists in the field (Bhattacharya et al., 2004). Excessive withdrawal of groundwater in coastal zones will lead to depression of water table with associated hazards like putting the well out of use, rendering the abstraction uneconomic with increased lift. A sustained regional groundwater drawdown below sea level runs the risk of saline water intrusion, even for confined coastal aquifers. A careful pumping and rest schedule may help in avoiding many such problems. An uncontrolled groundwater development may lead to a reversal of fresh water gradient thereby resulting in saline water ingress into the coastal aquifers. For example, reports of salinization of wells subjected to continuous heavy pumpage in the coastal district of Purba Midnapur, West Bengal, India though few, are not uncommon.

As suggested by various Scientists and Engineers, there are several established methodologies to control and minimize the problems associated with groundwater extraction followed by saline water intrusion. Some of the popular methods adopted are: the creation of a hydraulic barrier, rainwater harvesting, artificial recharge, canal irrigation, desalination, and reverse osmosis, etc. However, the author has developed an innovative, cost-effective technique to control saltwater intrusion into coastal aquifers; the techniques include withdrawal of coastal fresh water by means of qanat-well structures associated with artificial recharge through rainwater harvesting aided with percolation pond and recharge well. A case study on a selected location of the coastal zone of Purba Midnapur has been carried out. Adequate quantifications of the effectiveness of this new methodology have been incorporated, and relevant conclusions are drawn therefrom.

25.2 MATERIALS AND METHODS

25.2.1 NEW APPROACH FOR CONTROL OF SALINE WATER INTRUSION IN COASTAL AREAS

While a numerical simulation method like the finite difference or finite element scheme might be very illuminating from a research point of view, it is unlikely that field engineers will be able to capture the intricacies of such an approach. Keeping this in view; an innovative analytical method which is appropriate and at the same time easily implemental; is adopted as a new

approach for groundwater withdrawal and control of saline water intrusion in the study area.

It is evident that any withdrawal of groundwater from a coastal aquifer results in the advancement of the saltwater-freshwater interface from the shoreline towards to the point of withdrawal (Todd, 1976) unless the withdrawal is compensated by an equivalent artificial recharge. The rainwater harvesting is one of the most popular recharge techniques followed worldwide (UNEP Report, 2009). In the proposed methodology for reduction of saline water intrusion into the coastal aquifer and subsequent safe withdrawal of groundwater, the adoption of qanat-well structure associated with artificial recharge by rainwater harvesting through recharge ponds and recharge wells is hereby studied as one of the useful and cost-effective techniques. The salient features of the methodology are described by considering a design example adopted by the author in the Contai Polytechnic Institute Campus of the district of Purba Medinipur in the state of West Bengal.

25.2.1.1 ADOPTION OF QANAT-WELL STRUCTURE

The inland aquifers are suffering from the maladies of over-exploitation of groundwater by way of unscrupulous pumping; the coastal aquifers encounter the danger of seawater intrusion and saline water upconing. Due to saltwater intrusion, deep tube-well is not recommended because of the upconing problem. However, adoption of the shallow well is also inappropriate because of significantly lower discharge. It is well established (Raghu Babu et al., 2004) that adoption of qanats in such conditions not only yields higher discharge but also reduces the upconing problem significantly. Horizontal wells are more efficient than conventional vertical wells for environmental remediation of groundwater for a number of reasons such as:

- Greater reservoir contact with the well screen increases the productivity of the well.
- Geometry of the groundwater zone is conducive to greater access with a horizontal well than a series of vertical wells.
- Access to groundwater zones with vertical wells are often hindered by obstacles such as buildings, paved surfaces, or other topographical obstructions.

Beljin and Losonsky (1992) provided a generalized solution, based on the work of Joshi (1986), for estimating steady-state discharge for withdrawal of

groundwater from a vertical aquifer by means of horizontal water well. The solution provided was given by:

$$Q=\frac{2\pi k_h Hs}{ln[(\frac{\sqrt{1+\sqrt{1+64R^4/L^4}}+\sqrt{-1+\sqrt{1+64R^4/L^4}}}{\sqrt{2}})\frac{(\frac{\frac{\beta H^2}{2}+2\beta\delta^2}{Hr_w})^{\beta H}}{L}]} \quad (1)$$

where,

Q = Steady state discharge.
s = Drawdown above the well center.
L = Length of the horizontal well.
r_w = Well radius.
k_h = Hydraulic conductivity of the aquifer along the horizontal direction.
H = Aquifer thickness.

$$\beta=\sqrt{\frac{k_h}{k_v}}$$

k_v = Hydraulic conductivity of the aquifer along the vertical direction.
δ = Off-centered eccentricity of the well-center in the vertical aquifer plane.
R = Radius of the influence of the equivalent vertical well in the same aquifer for the same drawdown, which can be reasonably estimated using the available correlations (for example, Sichardt's formulae).

The above equation has been modified, applying the method of super-imposition, to reasonably estimate the steady-state discharge by means of a 4-legged qanat. The final expression is obtained as:

$$Q_q=\frac{2\pi k_h Hs}{ln[(\frac{\sqrt{1+\sqrt{1+4R^4/L_{q^4}}}+\sqrt{-1+\sqrt{1+4R^4/L_{q^4}}}}{\sqrt{2}})\frac{(\frac{\frac{\beta H^2}{2}+2\beta\delta^2}{Hr_q})^{2\beta H}}{L_q}]} \quad (2)$$

where, Q_q = Steady state discharge from the qanat.
L_q = Length of a qanat leg (Figure 25.1)
r_q = Inner radius of qanat legs

The maximum discharge from the qanat under full flow condition can be obtained by putting $s = d - 2r_q$ (neglecting the wall thickness of the qanat legs) in the Eq. (2). Thus,

$$Q_q(max) = \frac{2\pi k_h H(d-2r_q)}{ln[(\frac{\sqrt{1+\sqrt{1+4R^4/L_{q^4}}}+\sqrt{-1+\sqrt{1+4R^4/L_{q^4}}}}{\sqrt{2}})\frac{(\frac{\frac{\beta H^2}{2}+2\beta\delta^2}{Hr_q})^{2\beta H}}{L_q}]} \quad (3)$$

where, $Q_{q(max)}$ = Maximum possible discharge from the qanat.

d = Depth of the bottom surface of the qanat legs below the undisturbed water table.

Using Sichardt's formulae $R = 3000(d - 2r_q)k_h$ in Eq. (3), where all terms should essentially be in SI units, the Eq. (3) can be written as:

$$Q_q(max) = \frac{2\pi k_h H_f(d-2r_q)}{In[\xi\frac{(\frac{\frac{BH^2}{2}+2\beta\delta^2}{H_f r_q})_f^{2\beta H}}{L_q}]} \quad (4)$$

where $\xi = \frac{\sqrt{1+\sqrt{1+4[3000(d-r_q)\sqrt{k_h}]^4/L_q}}+\sqrt{-1+\sqrt{1+4[3000(d-r_q)\sqrt{k_q}]^4/L_{q\Leftarrow}}}}{\sqrt{2}}$

Although upconing in case of qanat-well structures is apparently not practical specifically when the saltwater-freshwater interface is situated at a significant depth below the bottom of the structures, the upconing problem may be catastrophic for shallow depth of interface in the area near the sea. Therefore, the present analysis is extended considering upconing as well (Figure 25.2). After the recommendation of Dagan and Bear (1968):

$$Z_\alpha = \frac{Q_q}{2\pi\left(\frac{\rho_s}{\rho_f}-1\right)K_h(H_f-d)} \quad (5)$$

where, Z_∞ = the value of Z at infinite time. The value of Q attains the maximum value when $Z_\infty = H_f - d$

$$Q_{q(\max)} = 2\pi k_h\left(\frac{\rho_s}{\rho_f}-1\right)(H_f-d) \quad (6)$$

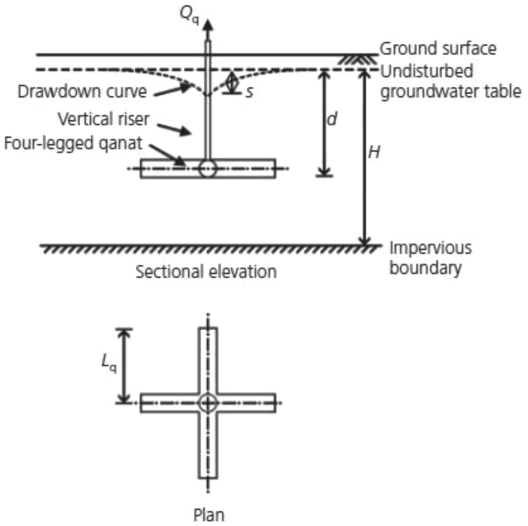

FIGURE 25.1 A typical 4-legged qanat.

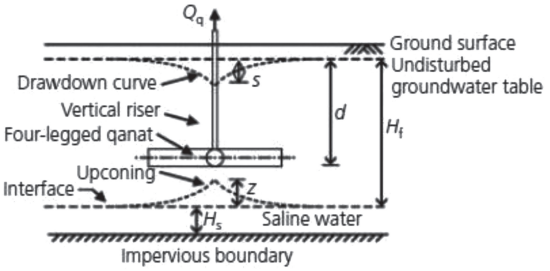

FIGURE 25.2 Withdrawal of groundwater by qanat in salinity affected aquifer.

The optimum values of $Q_{q(max)}$ shall be the least of the two values obtained from the Eq. (4) and (6). It is hereby mentioned that the design values of the depth of qanat-well structures are calculated as unrealistically high, therefore not feasible, the number of such qanat-well structures may be reasonably increased as required.

25.2.2 GROUNDWATER RECHARGE BY RAINWATER HARVESTING

A hybrid method considering ponds and recharge wells is adapted to: (i) combine the best of both, (ii) providing only ponds would eat up a huge amount of unnecessary spaces, and (iii) providing only wells would necessitate pressure injection

into the aquifer. Therefore, since due to space constraint in the locality under consideration, the full recharge may not be affected by the pond, recharge wells are needed. The withdrawal of groundwater by qanat should be suitably compensated by a recharge with rainwater harvesting, the salient features of this new approach with adequate quantification is described in the following subsections.

25.2.2.1 RECHARGE AREA

If fresh water in a coastal area is withdrawal regularly, the saltwater-freshwater interface is progressively advanced horizontally as well as vertically unless the withdrawal is subsequently compensated by a suitable artificial groundwater recharge techniques. The method proposed herein includes rainwater harvesting by means of recharge ponds and recharge wells design.

Usually for a particular community, neglecting the area of recharge well,

$$A_t = A_{roof} + A_{road} + A_{pond} + A_1 \tag{7}$$

where, A_t = Total area of the community;
A_{roof} = Total roof cover area for all building in the community;
A_{road} = Total road area in the community;
A_{pond} = Total pond area of the community;
A_1 = Total area of vacant land in the community.

25.2.2.2 FACTOR OF SAFETY FOR RAINFALL RECHARGE

For a particular community in a coastal area, the net volume of freshwater withdrawal in a certain period of time should not exceed the available volume of recharge for that period. With this conception, the corresponding factor of safety for the particular community has been formulated for the volumetric constancy as:

$$F = \frac{Volume\ of\ water\ annually\ available\ for\ recharge}{Volume\ of\ water\ annually\ extracted} = \frac{\left[\left(A_t - A_{roof}\right)\eta + \alpha A_{roof}\right]R}{365WP} \tag{8}$$

where,

W = Average water consumption of people in the community in liter per capita per day = 140 lit/capita/day;

P = Population of the community;
R = Design annual rainfall in mm;
η = Recharge coefficient;
α = Fraction of rainwater collected at roof which is directed towards the recharge well.

It is hereby mentioned that this technique is most effective when the value of the factor of safety is slightly higher than unity. The excessively high value of the factor of safety may be necessitated adequate drainage facility in the area under consideration to avoid the undesirable circumstance like water logging and flooding. Conversely, when the value of the factor of safety is less than unity, the situation can be compensated either by reducing the withdrawal of groundwater or by increasing the catchments area for rainfall recharge.

25.2.2.3 PERCOLATION POND

The design precipitation chosen depends on the design return period of the precipitation. The longer the design returns period, the greater the precipitation. After recommendation by Sarkar (2007), the water collected from the roof area in the community is partly allowed to percolate through recharge chamber cum recharge well, and the remaining portion is stored for future usages like firefighting and domestic use, etc. Therefore, the total area of recharge pond for the community under consideration may be estimated reasonably considering the net volume of water to be stored in the pond during the monsoon period. Therefore,

$$A_p = \frac{\left[\left(A_t - A_{roof} - A_{road}\right)\eta_1 + A_{road}\right]R_m}{1000\,H_p - (1-\eta_1)R_m} \tag{9}$$

where, A_p = Area of the pond;
R_m = Design monsoon rainfall in mm;
η_1 = Runoff coefficient relevant to the area;
H_p = Depth of pond to be excavated.

25.2.2.4 RECHARGE CHAMBER WITH RECHARGE WELL

As already mentioned earlier Sarkar (2007) designed a rainwater harvesting scheme for TCS building Salt Lake, Kolkata, India. Following his

recommendations, the dimensions and number of recharge chamber fitted with 100 mm diameter recharge well for the community under consideration may be reasonably estimated by:

$$\frac{V_w\ N_w}{V_{w\,s}\ N_{w\,s}} = \frac{\alpha\ R\ A_{roof}}{\alpha_s\ R_s\ A_{roof\,s}} \tag{10}$$

where V_w = Volume of the recharge chamber in the community.
N_w = Nos. of recharge chamber fitted with 100 dia. recharge well adopted in the community.

The suffix 's' denotes the corresponding parameter for the relevant to Sarkar (2007). From the field investigation, SP reading is observed to move towards negative side indicating the presence of sand aquifer below. As observed, the average depth freshwater-saltwater interface is situated at a depth of about 40m below the ground surface. It is advisable not to go for 'Deep Tube Well' construction; Qanat-Well Structures is preferable in this situation. The input parameters necessary for design in the locality under consideration are summarized below in Table 25.1.

TABLE 25.1 Values of Variables Determined From Hydrogeological Investigation

Input Parameter	Values
Maximum design discharge, $Q_{q(max)}$	Calculated using Eqs. (4) and (6)
Aquifer thickness, H	40 m
Horizontal hydraulic conductivity, K_h	3.512 x 10^{-4} m s^{-1} (Laboratory test)
Vertical hydraulic conductivity, K_v	3.614 x 10^{-4} m s^{-1} (Laboratory test)
Conductivity contrast, $\beta = \sqrt{\frac{K_h}{K_v}}$	0.9857
Well eccentricity, δ	0
Population in Contai Polytechnic College Campus, P	300
Total Area of the College Campus, A_t	90,169 m^2
Total Roof Area including Student Hostels, A_r	12,000 m^2
Total road area, A_r	1010 m^2
Total area of pond, A_p	1204 m^2
Area of vacant land, A_1	75,955 m^2
Design annual precipitation, R	Various values are taken
Design monsoon precipitation, R_m	Various values are taken
Per capita water consumption, W	140 liters/capita/day
Recharge coefficient, η	Chosen from available literature
Runoff coefficient, η_1	-do-

25.3 APPLICATION OF NEW APPROACH

From the available groundwater data, the coastal areas in the district of Purba Medinipur mostly consist of unconfined aquifers, with the average freshwater table of 2–3 m below the ground surface (Goswami, 1968; Sarkar, 2005) and the average saline water and fresh water interface varies in the range of 0–100 m. The aquifer is unconfined having an average hydraulic conductivity of k_h =3.512 x 10^{-4} m s^{-1} and k_v =3.614 x 10^{-4} m s^{-1}. From the available data (UNDP Report, 2006; WHO/UNICEF Report, 2010), the value of W (water demand) has been chosen as 140 liters/capita/day. The average population in the campus is 250. Considering a 20% increase, the value of P is taken as 300. On the basis of water demand per day for the college campus with pumping operation per day such as 2, 3, 4, and 5 hours, the qanat-well structures with a different parameter such as length, radius, and depth of qanat is calculated using the Eq. (4). The $Q_{q(max)}$ is calculated as follows:

$$Q_{q(\max)} = \frac{W\ P}{t \times 3600 \times 10^3} \tag{11}$$

where, t = hourly pumping rate in the college campus per day.

Using Eq. (4), the values of the depth of the qanat base for the chosen value of L_q and r_q is calculated. This value of 'd' is back-figured in the Eq. (6) to check for upconing. If the discharge calculated from the Eq. (6) exceeds the design discharge as estimated previously, upconing does not take place. Otherwise, the depth 'd' may be calculated by using Eq. (6). It is observed that at the college campus, the upconing does not occur. As observed from Figure 25.3, the parameter d decreases following a curvilinear pattern with the length of leg L_q. The variation is quite sharp in the range of $1m \le L_q \le 3m$ and assumes a linear pattern for $L_q > 3$ m. The above curves will be helpful for Design Engineer to adopt suitable values of the qanat parameter r_q, L_q, d, and t considering other design aspects such as, maximum depth of water table, the feasibility of construction, etc.

25.3.1 RECHARGE STRUCTURES

25.3.1.1 RAINFALL RECHARGE

From the available literature (State Forest Report, 2008–2009 and Annual Climate Summary, 2010), the total annual rainfall in the district of Purba Medinipur of the state of West Bengal, India for the decade 2001–2010

varies in the range of 1296–2259 mm. For the design of recharge pond equipped with recharge-wells for the given community, the factor of safety F for recharge may be estimated using the Eq. (8), using the following data:

$A_t = 90{,}169\ m^2$

$A_{ROOF} = 12000\ m^2$

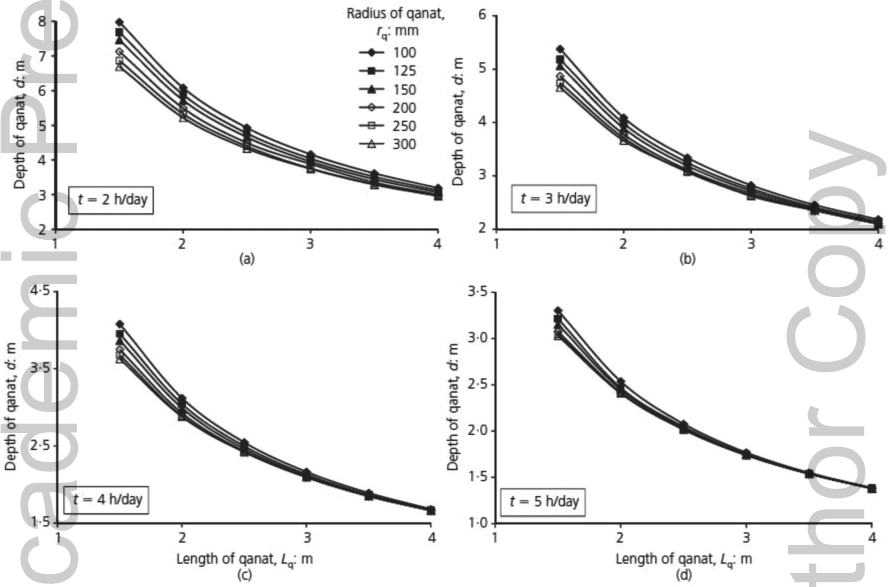

FIGURE 25.3 Variation of the depth of qanat at base versus length of qanat leg for pumping duration (in hours per day), t: (a) 2; (b) 3; (c) 4; and (d) 5.

The value of the recharge coefficient η may be reasonably estimated from the available literature (Wu and Zhang, 1994; Chaturvedi, 1936; Kumar, 2002). Wu and Zhzng (1994) calculated the effective precipitation P_e and the total amount of recharge P_e produced by P_e. By performing a regression analysis on P_e and R data available in China, a functional relationship between them was obtained as:

$$R_e = 0.87(P_e - 27.4) \tag{12}$$

where R_e = Infiltration Recharge in mm;

P_e = Effective Rainfall in mm.

Chaturvedi (1936) derived an empirical relationship to arrive at the recharge as a function of annual precipitation in Ganga-Yamuna doab basin as follows:

$$R = 2.0\ (P - 15)^{0.4} \tag{13}$$

where, R = net recharge due to precipitation during the year (inch);
P = annual precipitation (inch).

The formula of Chaturvedi (1936) was later modified further by Kumar and Seethapathi (2002), and the modified form of the formula is:

$$R = 1.35\ (P - 14)^{0.5} \tag{14}$$

As observed from Figure 25.4, the factor of safety increases linearly with an increase in annual precipitation, which is well in agreement with the Eq. (8). Also, the curves relevant to those of Chaturvedi (1936) and Kumar and Seethapathi (2002) almost coincide. Both the magnitudes and the slope of the curve relevant to that of Wu and Zhzng (1994) are significantly high.

25.3.1.2 PERCOLATION POND

The runoff should be assessed accurately for designed the recharge structures and may be assessed by the following formula.

Runoff = Catchments area x Rainfall x Runoff coefficient

Runoff coefficient plays an important role in assessing runoff availability, and it depends upon the catchments characteristics. It is the factor that accounts for the fact that not all rainfall falling on catchments can be collected. Some rainfall will be lost from the catchments by evaporation and retention on the surface itself. The required area of recharge pond decreases in a hyperbolic manner with the depth of pond to be excavated, which is well in agreement with Eq. (9).

Recharge chamber with recharge well: The relevant calculations for recharge chamber with recharge well are described below. As observed from Figure 25.5, the number of recharge chambers N_W decreases fairly exponentially with the volume V_W of the recharge chambers. The rate of decrease is pronounced in the range of V_W, 5, beyond which a stabilizing tendency is noted.

Appropriate Engineering Design: The appropriate site-specific engineering design is suggested by the author following the analysis described above in details.

Qanat-well Structure: The following parameters are suggested:

- t = 3 hours.
- r_q = 125 mm

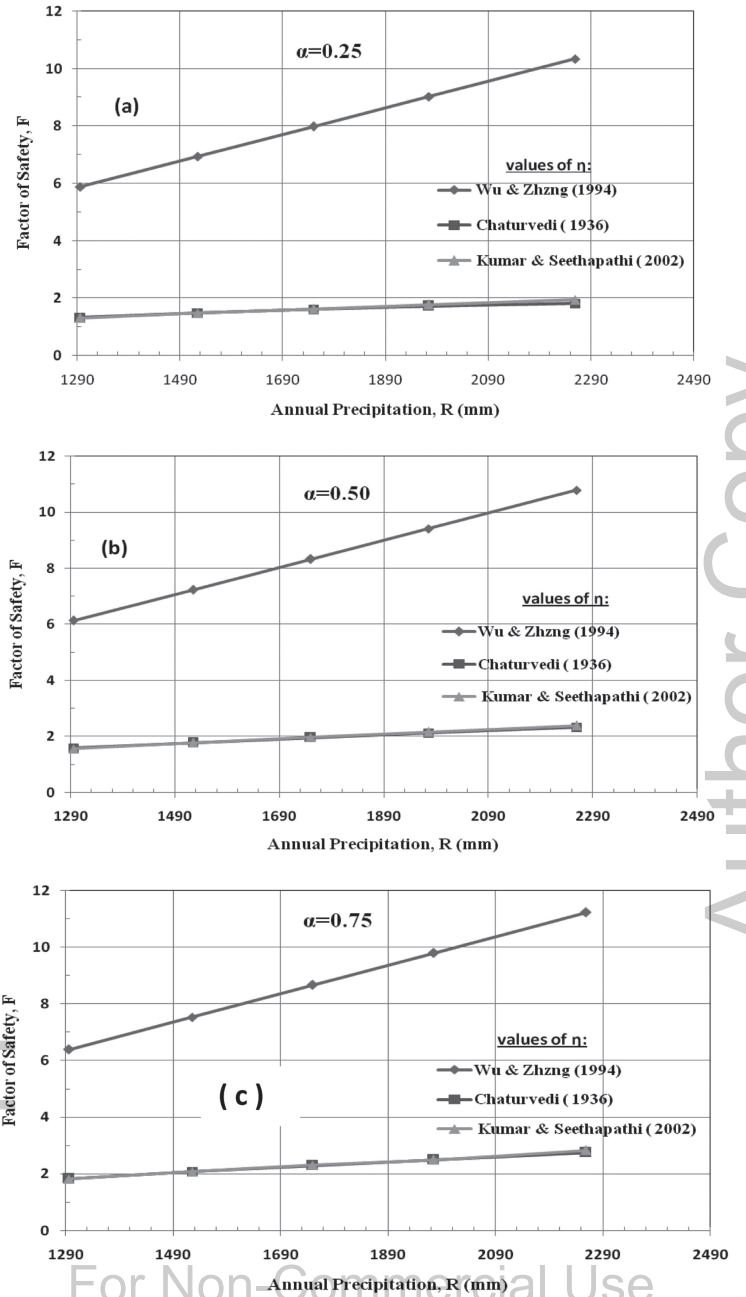

FIGURE 25.4 Variation of the factor of safety F with annual precipitation R for: (a) α = 0.25. (b) α = 0.50, and (c) α = 0.75.

- L_q = 2.5 m
- d = 3.25 m

(For future safety provision, 2 qanat-well structures are recommended for alternative use). Therefore, design depth of the qanat below G.L. = d + maximum depth of G.W.T. = 3.25 + 3 = 6.25 m.

Factor of Safety: The factor of safety for minimum and maximum rainfall are obtained as

Rainfall	Factor of Safety
Minimum	6.135 (after Wu and Zhzng, 1994)
	1.586 (after Chaturvedi, 1936)
	1.565 (after Kumar and Seethapathi, 2002)
Maximum	10.786 (after Wu and Zhzng, 1994)
	2.321 (after Chaturvedi, 1936)
	2.387 (after Kumar and Seethapathi, 2002)

For the Indian condition, the recommended value as per Kumar and Seethapathi (2002) is mostly suitable. It is also mentioned here that the value of factor of safety under minimum rainfall in the last 10 years should not fall below 1.0., therefore satisfactory in terms of reasonable compensation of withdrawal of groundwater. Also, under maximum rainfall in the last 10 years, the factor of safety exceeds 2.0, which may introduce sufficient pushback of saline water interface. It should also be mentioned here that for the excessively high value of factor of safety, adequate drainage should be facilitated at the site towards nearby stream channel.

Area and depth of Percolation Pond: The design rainfall data has been chosen as R_M = 367.1 mm. The depth of the pond is chosen as H_p = 3 m. Therefore, the area of pond required may be interpolated as, A_p = 1202.436 m^2. Hence, in the Contai Polytechnic College Campus, 4 ponds of area 301 m^2 each are provided, the depth of each pond is 3.0 m. Figure 25.6 illustrates the plots of recharge pond area versus pond depth for monsoon precipitation of (a) 350 mm, (b) 500 mm, and (c) 750 mm.

Recharge Chamber with Recharge Well: Adopting a total roof area in the site as 12000 m^2, α = 0.5 and R = 2259 mm (maximum rainfall in last 10 years), keeping the recharge chamber dimensions as: L= 2 m, B= 2 m, H= 1.2 m, the number of recharge chamber with recharge well has been obtained as N_W = 12. It is also mentioned that the dimension of the recharge wells adopted here are as per the recommendation of Sarkar (2007) and are as follows:

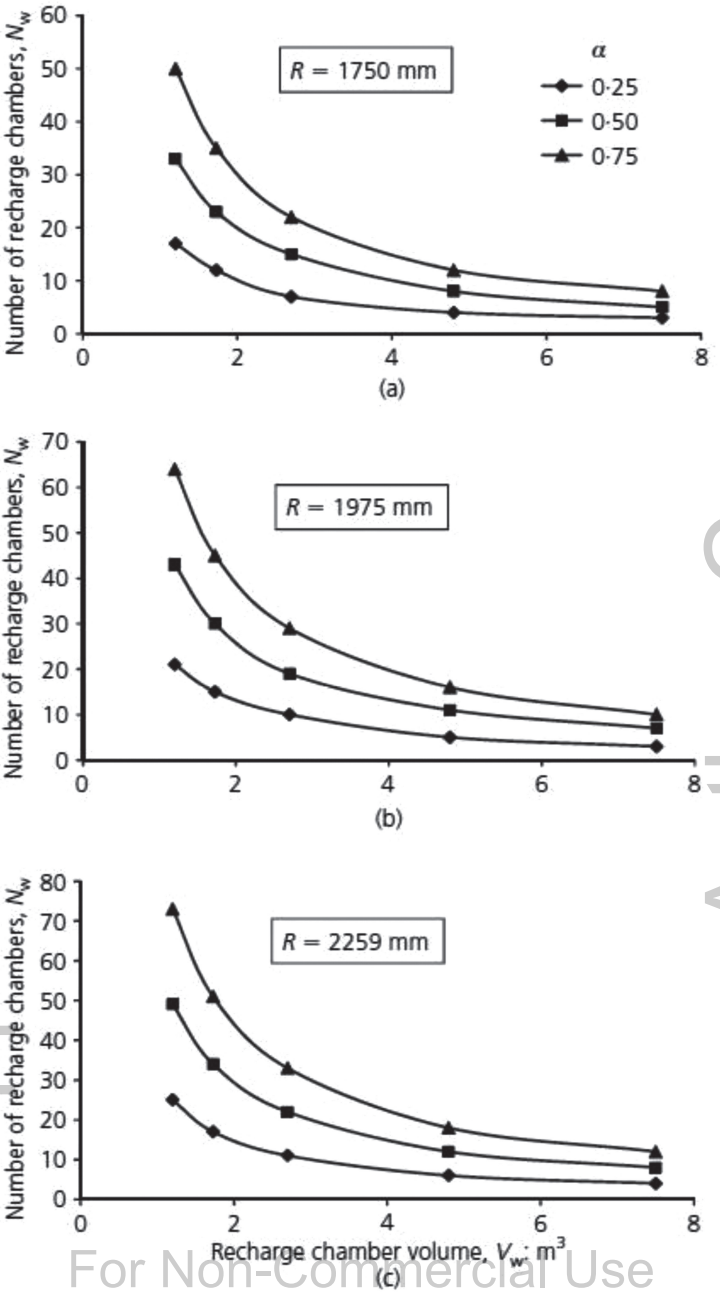

FIGURE 25.5 Variation of recharge chamber volume with number of chambers for (a) R = 1750 mm, (b) R = 1975 mm, (c) R = 2249 mm.

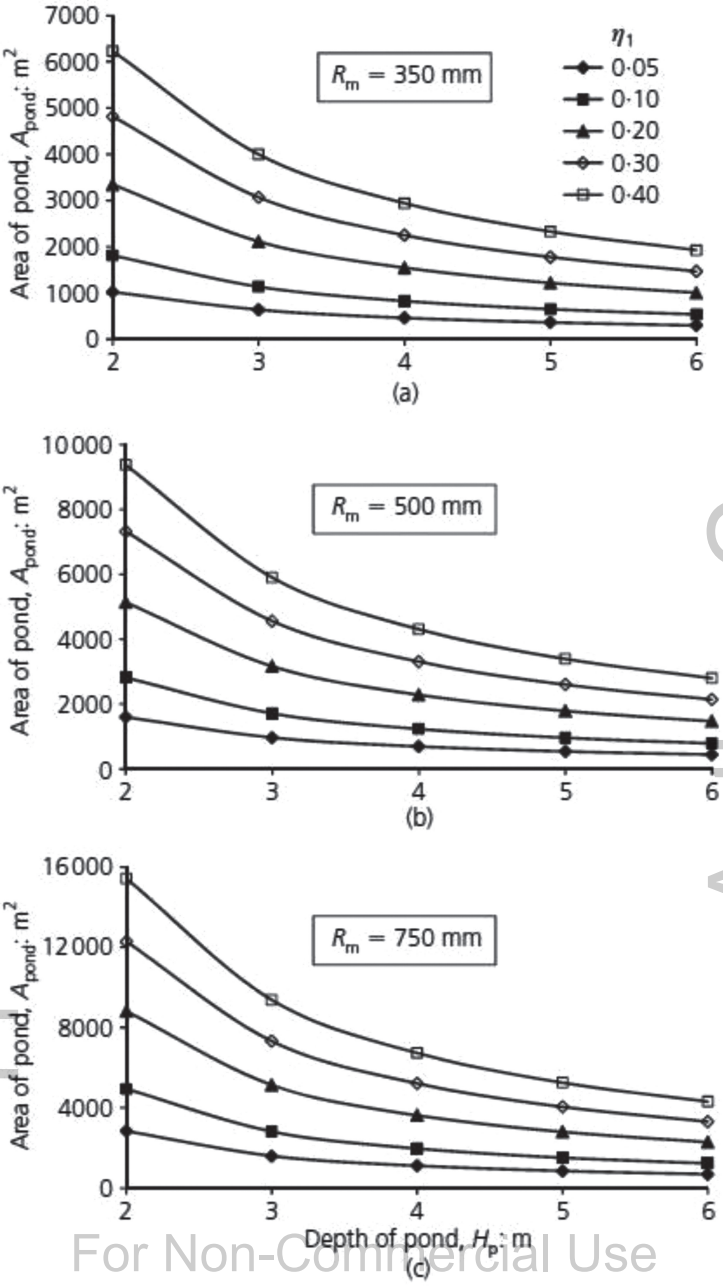

FIGURE 25.6 Plots of recharge pond area versus pond depth for monsoon precipitation of (a) 350 mm, (b) 500 mm, and (c) 750 mm.

Diameter of the well	100 mm
Strainer dia in the aquifer	100 mm
Length of strainer	12 m
Dia of the inlet strainer placed in the recharge chamber	150 mm
Length of 150 mm strainer	800 mm

As per design recommendation, the plan of the site provided with the new methodology has been given in Figure 25.7. The Contai Polytechnic College Campus area is shown with the location of qanat-well structures, percolation ponds and recharge chambers with recharge wells. The cross-section of recharge well adopted and methodology of recharge through recharge wells and recharging chambers are also shown inthe Figure 25.7. It is hereby mentioned that the parameters for recharge, well, etc. used in the design are highly site-specific. Successful application of the entire methodology is possible only when the design parameters are adequately chosen for a specific site.

25.4 CONCLUSIONS

The following significant conclusions are drawn:

An innovative method has been developed by the author for coastal zone groundwater management which involves withdrawal by qanat-well structures associates with equivalent artificial recharge by rainwater harvesting through percolation pond and recharges well. If adequately applied and design the proposed methodology is expected to be quite useful and convenient, for the unconfined condition of the coastal aquifers. As the suggested methodology has been applied to a selected coastal site located at Purba Midnapur district to study the various quantitative aspects of the method, it was observed that depth of qanat d decreases following a curvilinear pattern with the length of leg L_q. The variation is quite sharp in the range of $1m \leq L_q \leq 3m$ and assumes a linear pattern for $L_q > 3$ m.

The factor of safety for rainwater recharge in the selected location increases linearly with an increase in annual precipitation. Also, the curves relevant to those of Chaturvedi (1936), and Kumar and Seethapathi (2002) almost coincide. Both the magnitudes and the slopes of the curves relevant to that of Wu and Zhzng (1994) are significantly high. This technique is most effective when the value of the factor of safety is slightly higher than unity. The required area of recharge pond decreases in a hyperbolic manner with the depth of pond to be excavated.

The number of recharge chambers N_W decreases fairly exponentially with the volume V_W of the recharge chambers. The rate of decrease is pronounced

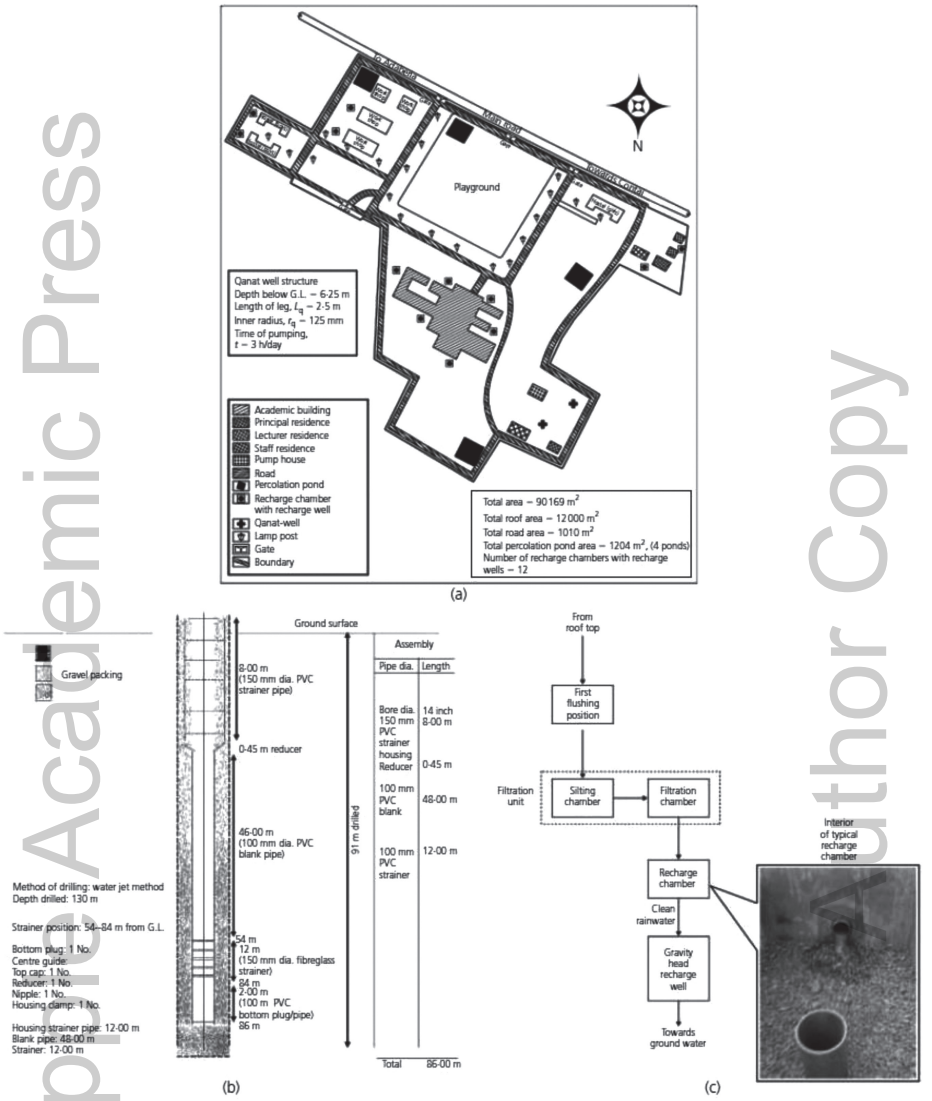

FIGURE 25.7 (a) Contai Polytechnic College Campus area showing the location of qanat-well structures, percolation ponds and recharge chambers with recharge wells; (b) Cross section of recharge well adopted; (c) Methodology of recharge through recharge wells and recharging chambers.

in the range of $V_W < 5$, beyond which a stabilizing tendency is noted. It is hereby mentioned that the model suggested is highly site-specific. Successful

application of the entire methodology is possible only when the design parameters are adequately chosen for the particular site under consideration.

KEYWORDS

- **coastal environment**
- **geotechnical investigation**
- **management and control of saline water intrusion**
- **mathematical analysis**
- **quantitative analysis**

REFERENCES

Annual Climate Summery (2010). India Meteorological Department, Ministry of Earth Sciences, Government of India.

Bhattacharya, A. K., (2002). Saline water Intrusion into Coastal Aquifers of West Bengal, India. *International Conference on Low Lying Coastal Areas Hydrology and Coastal Zone Management, Bremerhaven* (pp. 197–200). The Federal Republic of Germany.

Bhattacharya, A. K., & Basack, S., (2003). *Analysis and Control of Saline Water Intrusion in Coastal Aquifers with Special Emphasis on East Coast of India.* Final Technical Report, AICTE No. 8022/RID/NPROJ/RPS–82–4 dated 22/3/2004.

Bhattacharya, A. K., & Basack, S., (2003). Chloride and arsenic contamination in groundwater in coastal areas of West Bengal. *Tenth West Bengal State Science and Technology Congress* (2nd edn.), Midnapur, West Bengal, India.

Bhattacharya, A. K., Basack, S., & Maity, P., (2004). A feasible method of groundwater extraction in the United Arab Emirates and Qatar. *Proceedings of, the International Conference on Water Resources – Flood Control, Irrigation, Drinking Water, Waterways, Electric Power and Transmission System* (pp. 170–175). New Delhi.

Bhattacharya, A. K., Basack, S., & Maity, P., (2004). Groundwater extraction in the United Arab Emirates under the constraint of saline water intrusion, *Journal of Environmental Hydrology, 12*(6), 1–5.

Bhattacharya, A. K., Basack, S., & Maity, P., (2010). Groundwater extraction in coastal arid regions-A design methodology using qanats, *Electronic Journal of IETECH, Journal of Civil and Structures, 3*(1), 017–020.

Blair, D. A., Spronz, W. D., & Ryan, K. W., (1999). Brackish groundwater desalination—A community's solution to water supply and aquifer protection, *Journal of the American Water Resources Association, 35*(5), 1201–1212.

Chaturvedi, R. S., (1973). A note on the investigation of groundwater resources in western districts of Uttar Pradesh. *Annual Report, U.P. Irrigation Research Institute,* 86–122.

Dagan, G., & Bear, J., (1968). Solving the problem of local interface upconing in a coastal aquifer by the method of small perturbations, *Journal Hydraulic Research, 6*(1), 15–44.

Drabbbe, J., & Ghyben, B., (1888). *Nota in verband met de voorgenoment putboring nabji Amsterdam, Tijdschrift van het koninklijk institute van ingenieurs* , The Hague, Netherlands.

Ghyben, W. B., (1888). Nota in verband met de voorgenomen putboring nabij Amsterdami , *Tijdschrift Kon. Inst. Ing.,* 8–22.

Herzberg, B., (1901). Wasserversorgung Einiger Nordseebader *, Journal of Gasbeleuchtung and Wasserversorgung,* Munich, *44.*

http://www.rainwaterharvesting.org/.

http://www.tn.gov.in./dtp/rainwater.htm.

Joshi, S. D., (1986). Augmentation of well productivity using slant and horizontal wells, *Paper SPE 15375, Presented at 61st Annual Technical Conference and Exhibition of the Society of Petroleum Engineers.* New Orleans, LA.

Karanth, K. R., (1990). *Groundwater Assessment Development and Management*," Tata McGraw-Hill Publishing Co. Ltd., New Delhi.

Kumar, C. P., & Seethapathi, P. V., (2002). Assessment of natural groundwater recharge in upper Ganga canal command area, *Journal of Applied Hydrology, Association of Hydrologists of India, XV*(4), 13–20.

Lee, C. H., & Chang, T. S., (1974). On sea water encroachment in coastal aquifers, *Water Resources Research, 10*, 1039–1043.

Mays, L. W., (2001). *Water Resources Engineering*, John Wiley & Sons, N. Y.

Patra, M. N., (2006). *Localized and Generalized Subsidence and Swelling of the Ground Surface Due to Change in Groundwater Piezometric Level With a Special Reference to Calcutta*. PhD thesis, Bengal Engineering and Science University, Shibpur, Howrah, India.

Raghu, B. M., Prasad, B. R., & Srikanth, I., (2004). Subsurface skimming techniques for coastal sandy soils, *Bulletin No. 1/04: 18. A I C R P Saline Water Scheme*, Bapatla.

Raghunath, H. M., (1987). *Ground Water* (2nd edn.), Wiley Eastern Ltd., New Delhi.

Sarkar, A., (2007). Design of rainwater harvesting scheme for water conservation for firefighting and others and artificial recharge to groundwater at TCS main building campus, Salt Lake, Kolkata, *A Scheme Design Report as a Consultancy Submitted to Tata Consultancy Services Limited, Dec.*

Sarkar, S., (2005). *A Field Study on Saline Water Intrusion Into Coastal Aquifer of Purba Medinipur, M.E. Thesis*. Bengal Engineering and Science University, Howrah, India.

State Forest Report 2008–2009 Office of the Principal Chief Conservator of Forests, Kolkata, Directorate of Forests, Government of West Bengal, India.

United Nations Development Programme Report, (2006). Human Development Report 2006 Beyond Scarcity: Power, Poverty and Global Water Crisis, ISBN 0-230-50058-7.

United Nations Environment Programme Report, (2009). *Rainwater Harvesting: A Lifeline for Human Well-Being*, A report prepared for UNEP by Stockholm Environment Institute, ISBN: 978-92-807-3019-7, Job No. DEP/1162/NA.

Wood, E. F., Sivapalan, M., & Beven, K., (1986). Scale effects in infiltration and runoff production, *Proceedings of the Budapest Symposium, IAHS, No., 156*, 375–387.

World Health Organization Report, (2010). *Progress on Sanitation and Drinking Water – 2010 Update, WHO/UNICEF Joint Monitoring Programme for Water Supply and Sanitation*. ISBN 978-92-4-156395-6, NLM classification: WA 670.

Wu, J., & Zhang, R., (1994). Analysis of rainfall infiltration recharge to groundwater. *Proceedings of Fourteenth Annual American Geophysical Union: Hydrology Days* (pp. 420–430). Colorado, USA.

PART IV
Watershed Development and Management

CHAPTER 26

MORPHOMETRIC ANALYSIS AND PRIORITIZATION OF SUB-WATERSHEDS IN THE KOSI RIVER BASIN FOR SOIL AND WATER CONSERVATION

RAJANI K. PRADHAN, SWATI MAURYA, and PRASHANT K. SRIVASTAVA

Institute of Environment and Sustainable Development, Banaras Hindu University, Varanasi–221005, India, E-mail: rkpradhan462@gmail.com

ABSTRACT

Remote sensing and Geographical Information System are efficient techniques for prioritization of sub-watershed through morphometric analysis and positioning water harvesting structures. The morphometric analysis provides a quantitative description of a watershed for evaluating and estimation of drainage characteristics. The present study focused on Kosi River Basin (KRB), situated in Indo-Gangetic plains, Bihar state, India for soil and water conservation. The Digital Elevation Model (DEM) estimated from Shuttle Radar Topographic Mission (SRTM) is utilized for calculating the morphometric parameters in terms of basic, linear, and shape parameters and compound factor. KRB have been divided into 13 sub-watersheds and prioritized accordingly based on compound factor analysis to meet the need of water and soil conservation. The overall results indicate that the sub-watershed nos. 5, 8 and 4 require utmost attention and conservative practices because of their high erodibility characteristics. This study can be very useful in the identification of erosion-prone areas and implementation of conservation practices for water resources.

26.1 INTRODUCTION

The morphometric analysis involves the mathematical analysis of the configuration of the earth surface, form, and dimension of landforms (Ganie et al., 2016). Morphometric analysis of subbasin can be estimated through the measurement of liner, aerial, and relief aspects of the basin and slope contribution (Nag and Chakraborty, 2003). It is well established that the influence of drainage morphometry is very useful in understanding the landform process, soil physical properties and erosional characteristics (Rai et al., 2017). Morphometric analysis of the river basin also provides a quantitative description of the study area, which is an important aspect of the characterization of the basin (Magesh et al., 2013; Strahler, 1964). In addition, the hydrological process of a basin can be correlated with various morphometric parameters like size, shape, drainage density, size, and shape of the contributories (Rama, 2014).

Nowadays, remote sensing and GIS evolved as a promising technique for various watershed management and soil water conservation studies. It is a very effective tool for integration of various spatial data, preparation of various thematic layers and to derive useful outputs for modeling (Patel et al., 2013; Srivastava et al., 2012). Satellite products like digital elevation model (DEM) obtained from Shuttle Radar Topographic Mission (SRTM) can be used for the generation of the elevation model and stream network of the landscape. Number of studies have been conducted in morphometric analysis of river basin using both convention (Horton, 1945; Smith, 1950; Strahler, 1957; Strahler, 1964) and GIS and Remote sensing approach (Harini et al., 2017; Patel et al., 2013; Rai et al., 2017; Rao et al., 2010; Siddaraju et al., 2017). The morphometric analysis will provide a quantitative description of the basin for hydrological investigations like groundwater potential, watershed management, and environmental assessment. Thus, the detailed analysis of morphometric parameters of the river basin is of immense help in understanding the influence of drainage morphometry on landforms and their characteristics.

The main objectives of the present study are to prioritize the KRB for soil and water conservation. The linear and aerial parameters were estimated using various mathematical equations to analyze the morphometric parameters for the better planning and sustainable management of the river basin. It may also be useful in integrated decision making studies like soil erosion assessment, water management, and flood management.

26.2 MATERIALS AND METHODS

26.2.1 STUDY AREA

The river Kosi was also known as the "Sorrow of Bihar" is a tributary of river Ganga. It originates at an altitude of 7000 m from the Himalayas and meets the river Ganga near Kursela, in district Katihar of Bihar (Figure 26.1). Generally the entire catchment of river is divided into two parts, i.e., Upper catchment which is lies in Tibet and Nepal characterized by hilly area (constitute about 80% of total catchment area), whereas the lower catchment, falls in floodplain of north Bihar, India (about 20% of total catchment area). The ridge lines surround the Kosi river basin (KRB), and these ridgelines it from the Mahananda catchment in the east and from Gandak and Tsangpo (Brahmaputra) catchments in west and north respectively, whereas river Ganga bounds it in the in the south. From the past records, it concluded that that the river has laterally shifted westward about 150 km in last 200 years (Bapalu and Sinha, 2005; Gole and Chitale, 1966; Wells and Dorr, 1987) and this shifting has caused extensive damage to local inhabitants, their livelihood, infrastructure, and property. Following Nepal and Himalaya, it finally enters into the alluvial plains of state Bihar and travels nearly 320 kilometers from Chatra before it joins with Ganga. The current research work is carried out in part of the lower catchment of the Kosi which geographically lies between 86° 20' to 87° 10' East longitude and 25° 30' to 26° 30' north latitude and covering an area of 4062 km^2 in Bihar. The high intense rainfall (1200–2000 mm) in most parts (Sinha and Friend, 1994) is the main reason for the most of hydrological processes like soil erosion and thus a high amount of sediment load in the Kosi basin.

26.2.2 METHODOLOGY

The SRTM based digital elevation model (DEM; 90m resolution) is used for the extraction of topographic characteristics (relief) in this study. With the help of Arc GIS 10.1 spatial analysis extension and Arc Hydro tool, further analysis is carried out. The detail methodologies followed is presented in Figure 26.2. The pre-processing of DEM was performed and followed by post-processing as generating the DEM fills and flow direction, and flow accumulation was calculated for the individual pixel of the DEM using the Arc Hydro tool of ArcGIS10.1. Later a total of 13 sub-watersheds were

delineated from the study area, and the morphometric parameters were analyzed for each subwatershed. Due to the simplicity and wide application of the Strahler's (1964) method of stream ordering, the same method was applied in this study. Further details of the formula and method used in this study for analysis of various morphometric parameters were listed in Table 26.1. Finally, a compound factor is used to rank the watershed for the prioritization of the various sub-watersheds.

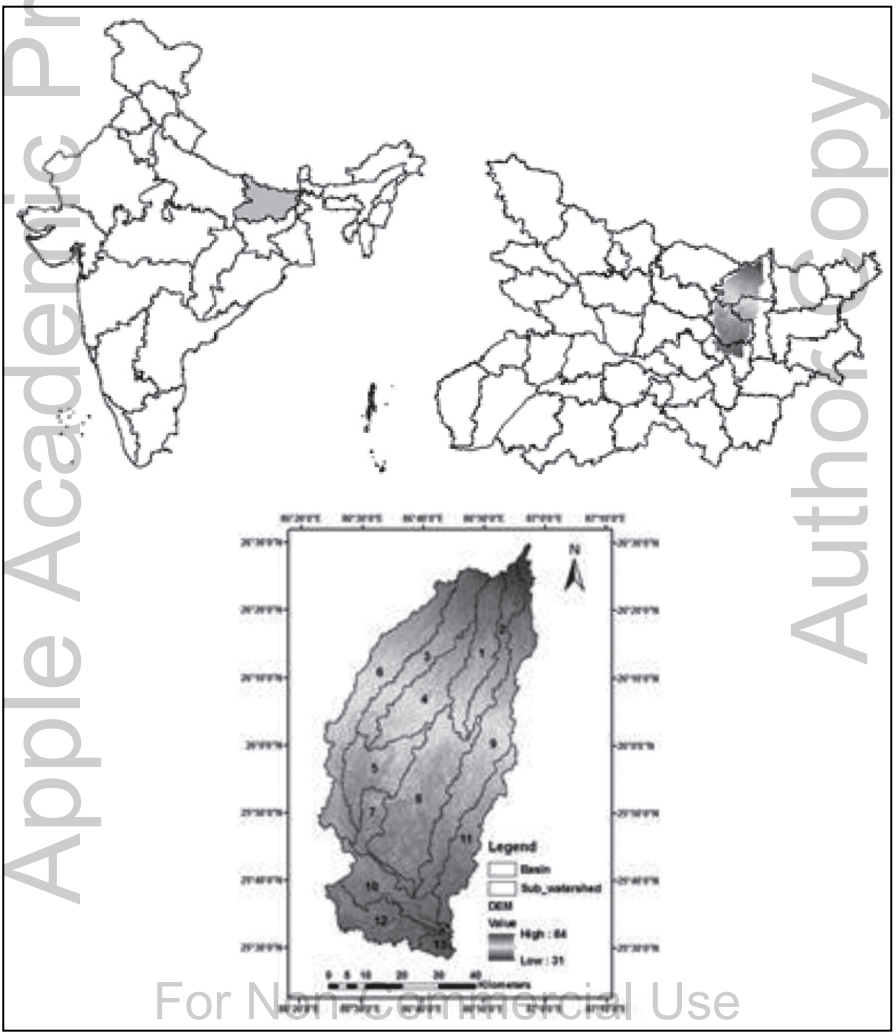

FIGURE 26.1 Location map of the study area.

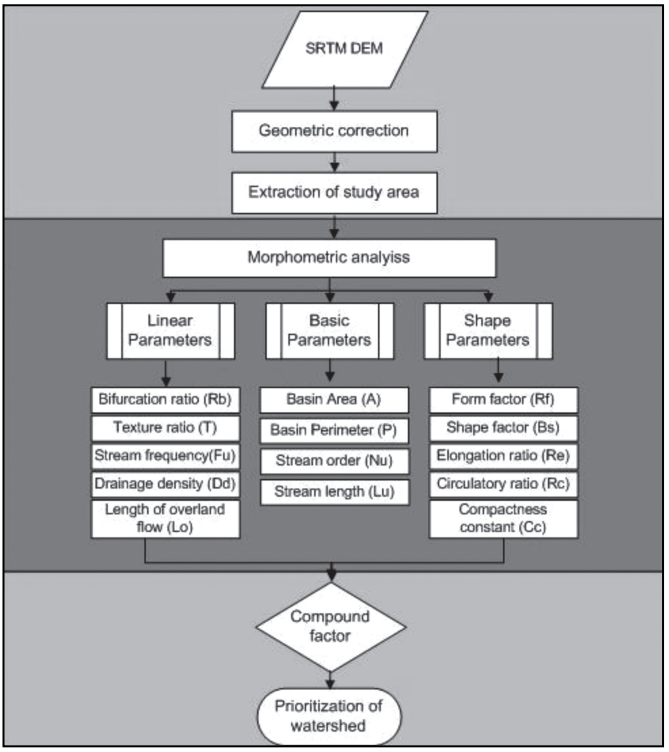

FIGURE 26.2 Methodology flowchart of the study.

26.3 RESULTS AND DISCUSSION

Morphometric analysis is a quantitative process, which constitutes the measurement of configurations of earth surface and dimensions of landforms. The morphometric parameters considered in this study for characterization of the Kosi watershed includes basic parameters, linear parameters and shape parameters. The formulas and equation used in this study for the analysis of various morphometric parameters were listed in Table 26.1.

26.3.1 BASIC PARAMETERS

The main basic parameters considered in this study for morphometric analysis includes drainage area, perimeter, stream order, stream length, and basin length.

TABLE 26.1 Morphometric Parameters Estimated for Kosi River Basin

S. No.	Parameters	Formula	References
1	Stream order (u)	Hierarchical rank	(Strahler, 1964)
2	Number of streams (Nu)	Total number of stream segment of the order u	(Strahler, 1957)
3	Stream length (L_u)	Total length of the stream segment of a particular order	(Horton, 1945)
4	Stream frequency (Fu)	$Fu = \sum Nu/A$	(Horton, 1932)
5	Length of overland flow (Lo)	Lo = 1/2 * Dd	(Horton, 1945)
6	Bifurcation ration (R_b)	$(R_b) = N_u/N_u + 1$	(Schumm, 1956)
7	Drainage density (D_d)	$D_d = \sum L_u/A$	(Horton, 1932)
8	Texture ratio (T)	T = Nu/p	(Horton, 1945)
9	Elongation ratio (R_e)	$R_e = D/L = 1.128\sqrt{A}/L$	(Schumm, 1956)
10	Circularity ratio (Rc)	$Rc = 4\pi A/P^2$	(Strahler, 1964)
11	Form factor (Rf)	$R_f = A/L^2$	(Horton, 1945)
12	Shape factor (Bs)	$Bs = L^2/A$	(Horton, 1932)
13	Basin length (Lb)	$Lb = 1.312 \times A^{0.5}$	(Ratnam, et al. 2005)
14	Compactness Constant (Cc)	$Cc = 0.282IP/A^{0.5}$	(Horton, 1945)

26.3.1.1 DRAINAGE AREA (A) AND PERIMETER (P)

Drainage area is the most important parameters of any watershed, and it is used to estimate the total volume of runoff and sediment load can be created from the basin. According to the result sub-watershed, no. 8 has the maximum area of 598.21 km^2 while the sub-watershed no. 13 has the minimum area of 51.54 km^2. The basin perimeter cab defined as the length of the line that defines the surface divide of the basin. In the present case, the maximum value of 376 km is found in sub-watershed no. 9, whereas the minimum of 51.08 km in sub-watershed no. 13.

26.3.1.2 STREAM ORDER (N_U)

Hierarchical position of the streams within the drainage basin can be defined through analysis of stream order. In this research work, stream order analysis is performed using Strahler method: where the first order streams does not

consist of any tributaries, and the confluence of the two first-order streams formed the second order streams and so on. However, as the stream orders increase the total number of streams of the particular order decreases. The result outlines that the study area is a fifth order drainage basin and having a total number of 502 streams, sprawl over 4021.41 km^2. Among the 13 subwatershed, the subwatershed no.8 has the maximum number of streams of 79 followed by 70 in sub-watershed 9, while the sub-watershed no.13 has the lowest number of streams of 7. Further details about the number of streams in each order are presented in Table 26.2.

TABLE 26.2 Stream Order of Kosi River Basin

Sub-Watershed	I Order	II Order	III Order	IV Order	V Order	Total no. of streams
1	22	11	10	0	0	43
2	12	9	0	0	0	21
3	20	10	11	0	0	41
4	23	12	9	0	0	44
5	21	13	1	8	0	43
6	24	11	5	0	0	40
7	8	2	0	4	0	14
8	40	18	13	8	0	79
9	37	16	14	3	0	70
10	19	7	0	6	2	34
11	23	15	5	0	0	43
12	16	5	2	0	0	23
13	3	2	0	0	2	7

26.3.1.3 STREAM LENGTH (L_U) AND BASIN LENGTH (L_B)

Stream length has been computed by adding all the stream lengths of a particular order. Generally, streams having relatively smaller length indicate of the high slope, while the length of the large streamlength is of flatter gradient. In the present study subwatershed, no. 8 has the maximum stream length of about 268.60 km while the minimum of 15.52 km in sub-watershed no. 13. Basin length can be defined as the distance measured along the main channel from the watershed outlet to the basin divide. It is an important factor in the estimation of various morphometric analysis, and it is proportional to

the drainage area. As per the result, the basin length of sub-watersheds varies from 49.5 km (sub-watershed no. 8) to 12.3 km (sub-watershed no. 13).

26.3.2 LINEAR PARAMETERS

It includes bifurcation ratio, drainage density, stream frequency, length of overland flow and texture ratio.

26.3.2.1 BIFURCATION RATIO (R_B)

It is the ratio between the number streams of a given order to a number of streams of the next higher order. It is a dimensionless property which measures the degree of distribution of stream network in the basin (Mesa, 2006; Soni, 2016) and is highly influenced by the geological characteristics of the drainage basin. The higher value of bifurcation ratio indicates a strong structural control on the drainage pattern, whereas the lower value reflects the basin less affected by structural disturbances. In the present study the maximum Bf ratio of 4.9 found in subwatershed no. 5, whereas the minimum of 1.2 in sub-watershed no. 13, which indicates low structural control on the basin drainage pattern. Table 26.3 shows the list of sub-watersheds and their corresponding bifurcation ratio in KRB.

26.3.2.2 DRAINAGE DENSITY (D_D) AND STREAM FREQUENCY (F_U)

Drainage density (Dd) is the ratio of the total length of the streams of the watershed to the total area of that watershed. It is an important factor for characterizing the degree of drainage development of the basin. High Dd of basin indicates impermeable surface, sparse vegetation, and steep slope while low Dd values reflect the permeable surface, dense vegetation, and flat relief. As per the result, the Dd values range from 0.6 to 0.29 which indicates permeable sub-surface material with low to intermediate drainage and relief. Stream frequency is the ratio of the total number of streams of all orders to the total area of the basin (Horton, 1932). Mainly stream frequency depends on the lithology of the basin, and the higher values of stream frequency indicate higher runoff and the steep ground surface, and a higher chance of flood occurrences. The values of stream frequency show a positive correlation with drainage density. In the present study stream frequency values varies from 0.158 to 0.05 and further details are presented in Table 26.3.

TABLE 26.3 Analyzed Morphometric Parameters

Sub-Watershed	Area (km^2) (A)	Perimeter (km) (P)	Length (km) (Lb)	Bifurcation ratio (Rb)	Texture ratio (T)	Stream frequency (Fu)	Drainage density (Dd)	Length of over land flow (Lo)	Form factor (Rf)	Shape factor (Bs)	Elongation ratio (Re)	Circulatory ratio (Schaap et al.)	Compactness constant (Cc)
1	274.32	177.80	31.832	1.550	0.124	0.157	0.466	0.233	0.271	3.694	0.587	0.109	2.067
2	203.42	182.75	26.859	1.333	0.066	0.103	0.600	0.300	0.282	3.547	0.599	0.077	2.518
3	333.61	228.87	35.574	1.455	0.087	0.123	0.455	0.227	0.264	3.793	0.579	0.080	2.381
4	317.81	180.27	34.607	1.625	0.128	0.138	0.485	0.242	0.265	3.768	0.581	0.123	1.928
5	286.79	169.31	32.646	4.913	0.124	0.150	0.509	0.255	0.269	3.716	0.585	0.126	1.920
6	514.93	318.83	45.521	2.191	0.075	0.078	0.356	0.178	0.249	4.024	0.562	0.064	2.592
7	127.53	144.22	20.602	2.250	0.055	0.110	0.539	0.269	0.300	3.328	0.618	0.077	2.591
8	598.21	253.62	49.566	1.744	0.158	0.132	0.457	0.228	0.243	4.107	0.557	0.117	1.894
9	568.29	376.80	48.143	2.707	0.098	0.123	0.473	0.236	0.245	4.078	0.559	0.050	2.897
10	238.96	166.13	29.432	1.905	0.114	0.142	0.401	0.200	0.276	3.625	0.592	0.109	2.089
11	269.91	207.49	31.540	2.267	0.111	0.159	0.368	0.184	0.271	3.686	0.588	0.079	2.435
12	236.09	168.08	29.231	2.850	0.095	0.097	0.327	0.164	0.276	3.619	0.593	0.105	2.128
13	51.54	51.08	12.315	1.250	0.059	0.136	0.297	0.149	0.340	2.943	0.658	0.248	1.535

26.3.2.3 LENGTH OF OVERLAND FLOW (LO) AND TEXTURE RATIO (T)

Length of overland flow is the length of the water flow over the ground before it combines into the mainstream and it is also expressed as half of reciprocal of the drainage density (Horton, 1945). It is one of the important independent variable, which affecting both hydrologic and physiographic development of the drainage in the basin. The lower the values of length of overland flow, the faster the runoff from the streams (Rama, 2014). In the present study, the values of length of overland flow varies from 0.3 to 0.14, and the mean is 0.22 which indicate ground slope with moderate infiltration and runoff. Texture ratio is defined as the ratio of first-order streams segments to the perimeter of the basin (Horton, 1932). It is an important factor in the morphometric analysis of drainage and is depend on the underlying lithology, infiltration capacity and relief of the basin or terrain. The values of texture ratio vary from 0.158 to 0.05 reflect low erosivity.

26.3.3 SHAPE PARAMETERS

26.3.3.1 SHAPE FACTOR (B_S)

Shape factor is the ratio of the square of basin length to the area of the basin. It reflects the shape irregularity of the drainage basin, and it is inversely related with the form factor. In this study area, shape factor ranges from 2.9 to 4.10, which indicates the shape of the basin is elongated. The form factor can be defined as the ratio between the areas of the basin to the square of the basin length. The form factor varies from 0 to 1, however mostly the values are less than 0.79 (for a perfectly circular basin) (Chopra et al., 2005). The lower the value of form factor the more the elongated of the basin, and have lower peak flow in longer duration, while the higher value indicates the more circular shape of the basin with higher peak flow in short duration. In the present case, the values of form factor vary from 0.24 to 0.33, which indicates the more elongated shape of the basin and thus may take a longer time duration for peak flow.

26.3.3.2 ELONGATION RATIO (R_E)

It is defined as the ratio of the diameter of a circle of the same area as the basin to the maximum basin length (Schumm, 1956). It is a most

significant index for the analysis of the basin shape. According to Strahler these values varies from 0.6 to 1.0 for a wide range of climatic and geological conditions (Strahler, 1964). Further the lower the value of this factor means the more elongated the basin shape. In the present case, the values of elongation ratio lie between 0.55 to 0.65 reflect the elongated shape of sub-basins

26.3.3.3 COMPACTNESS COEFFICIENT (C_c) AND CIRCULATORY RATIO (R_c)

Compactness coefficient can be expressed as, basin perimeter divided by the circumference of a circle to the same area of the basin. It is quite the opposite (inversely related) to the elongation ratio a basin and responsible for causing erosion in the basins. The lesser the value of compactness coefficient means the more elongated the shape of the basin and less erosion while, a higher value indicates less elongated and more erosion-prone of the basin. It was also observed that the values of compactness coefficient exhibit a variation from 2.89 to 1.535, shown in Table 26.3. Circularity ratio is the ratio between the basin areas to the area of a circle having the same circumference as the perimeter of the basin. It is equivalent to 1 when the basin is perfectly circular, and it lies between 0.4–0.5 when the basin shape is more elongated in shape and very permeable with homogeneous materials. As per result, the maximum circularity ratio was observed in subwatershed no.13 (0.248) while the minimum in subwatershed no.9 (0.05), which reflects the highly elongated shape of the basins.

26.3.4 COMPOUND FACTOR AND PRIORITIZED RANKS

In this study, a compound factor is used for the prioritization of subwatershed in the KRB. For this, both Shape parameters and linear parameters are taken into consideration. Linear parameters are directly correlated to the erosion (higher the value, the more erodible), whereas as in the case of shape parameters it is vice versa (lower the value, the more erodible). First of all individual ranking is assigned to both linear and shape parameters depending on the parameters values and afterward, finally, a compound factor is obtained by summing up all the parameters ranking divided by the number of parameters. From the compound factor, the first rank is assigned to the lowermost value, and the last rank to the higher most value. In the present case, watershed no.

5 ranked first (4.9) followed by watershed no. 8 and 4 with second and third respectively, whereas the watershed no. 13 have last rank (9.7) and details are demonstrated in Table 26.4 and Figure 26.3 as well.

TABLE 26.4 Calculation of Compound Factor and Prioritized Ranks

Sub-Watershed	Rb	Dd	Fu	T	Lo	Rf	Bs	Re	Rc	Cc	Compound factor	Prioritized rank
1	10	6	2	4	6	7	7	7	9	5	6.5	5
2	12	1	11	11	1	11	3	11	3	10	7.4	9
3	11	8	9	9	8	4	10	4	6	8	7.7	10
4	9	4	5	2	4	5	9	5	11	4	5.8	3
5	1	3	3	3	3	6	8	6	12	3	4.9	1
6	6	11	13	10	11	3	11	3	2	12	8.2	11
7	5	2	10	13	2	12	2	12	4	11	7.3	8
8	8	7	7	1	7	1	13	1	10	2	5.4	2
9	3	5	8	7	5	2	12	2	1	13	6.0	4
10	7	9	4	5	9	9	5	9	8	6	7.1	7
11	4	10	1	6	10	8	6	8	5	9	6.7	6
12	2	12	12	8	12	10	4	10	7	7	8.3	12
13	13	13	6	12	13	13	1	13	13	1	9.7	13

26.4 CONCLUSIONS

The quantitative analysis of morphometric parameters of the river basin is an immense help in evaluations of the hydrological process of the basin (runoff, infiltration capacity, etc.), effective management of the natural resources and prioritization of the sub-watershed. Remote sensing satellite data integrated with GIS evolved as a promising technique for various water management studies at the watershed level. In the present study, a detailed morphometric analysis of the KRB is carried out using the integration of GIS and Remote sensing techniques for the prioritization sub-watershed. There are a total of 13 sub-basin delineated in the catchment. According to the result, the river basin has a well-drained structure with a fourth order basin. The basin characterized with an elongated shape and flattered slope, which indicates a lower chance of flooding. The overall analysis indicates that the sub-watershed nos. 5, 8, and 4 require utmost attention for the conservation measure, while the sub-watershed nos. 13, 12 and 6 have lowered priority. This study can be utilized for implementation effective conservation measures to the

vulnerable sites, which will reduce the high runoff and soil erosion, thus for the flood control in the KRB.

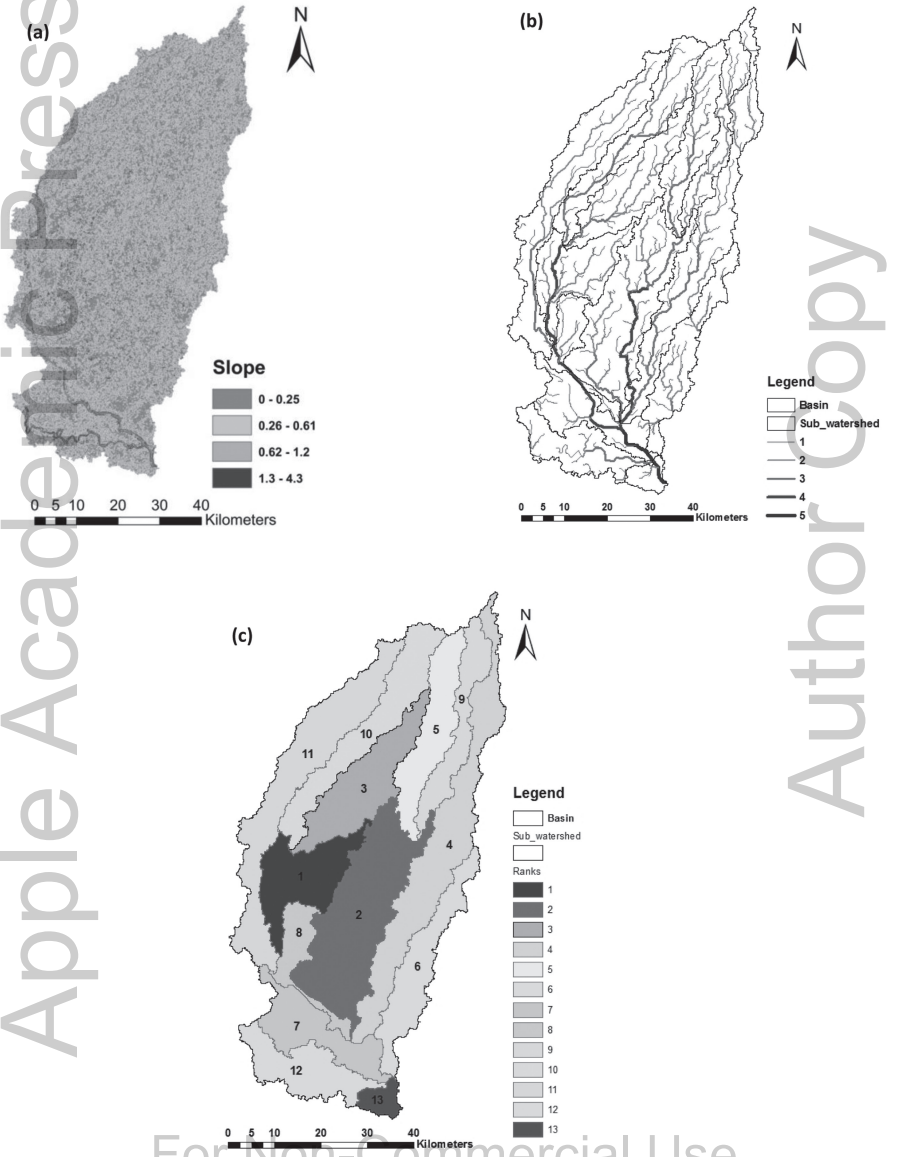

FIGURE 26.3 (a) Slope (b) Drainage order and (c) Prioritization of sub-watersheds from Compound factor.

KEYWORDS

- **GIS**
- **Kosi river basin**
- **morphometric analysis**
- **prioritization**
- **SRTM (DEM)**

REFERENCES

Bapalu, G. V., & Sinha, R., (2005). GIS in flood hazard mapping: A case study of Kosi River Basin, India. *GIS Development Weekly*, *1*(13), 1–3.

Chopra, R., Dhiman, R. D., & Sharma, P., (2005). Morphometric analysis of sub-watersheds in Gurdaspur district, Punjab using remote sensing and GIS techniques. *Journal of the Indian Society of Remote Sensing*, *33*(4), 531–539.

Ganie, P. A., Posti, R., Kumar, P., & Singh, A., (2016). Morphometric analysis of a Kosi River Basin, Uttarakhand using geographical information system. *Int. J. of Multidisciplinary and Current Research*, *4*.

Gole, C. V., & Chitale, S. V., (1966). Inland delta building activity of Kosi river, *Journal of the Hydraulics Division*, *Proceedings of the American Society of Civil Engineers*, 111–126.

Harini, P., Manikyamba, C., Kumar, S. D., Durgaprasad, M., & Nandan, M., (2017). Geographical information system based morphometric analysis of Krishna River Basin, India. *Journal of Applied Geochemistry*, *19*(1), 44.

Horton, R. E., (1932). Drainage-basin characteristics. *Eos, Transactions American Geophysical Union*, *13*(1), 350–361.

Horton, R. E., (1945). Erosional development of streams and their drainage basins, hydrophysical approach to quantitative morphology. *Geological Society of America Bulletin*, *56*(3), 275–370.

Magesh, N., Jitheshlal, K., Chandrasekar, N., & Jini, K., (2013). Geographical information system-based morphometric analysis of Bharathapuzha river basin, Kerala, India. *Applied Water Science*, *3*(2), 467–477.

Mesa, L., (2006). Morphometric analysis of a subtropical Andean basin (Tucuman, Argentina). *Environmental Geology*, *50*(8) 1235–1242.

Nag, S., & Chakraborty, S., (2003). Influence of rock types and structures in the development of drainage network in hard rock area. *Journal of the Indian Society of Remote Sensing*, *31*(1), 25–35.

Patel, D. P., Gajjar, C. A., & Srivastava, P. K., (2013). Prioritization of malesari mini-watersheds through morphometric analysis: A remote sensing and GIS perspective. *Environmental Earth Sciences*, *69*(8), 2643–2656.

Rai, P. K., Mohan, K., Mishra, S., Ahmad, A., & Mishra, V. N., (2017). A GIS-based approach in drainage morphometric analysis of Kanhar River Basin, India. *Applied Water Science*, 1–16.

Rama, V. A., (2014). Drainage basin analysis for characterization of 3rd order watersheds using geographic information system (GIS) and ASTER data. *J. Geomatics*, *8*(2), 200–210.

Rao, N. K., Latha, S. P., Kumar, A. P., & Krishna, H. M., (2010). Morphometric analysis of Gostani River basin in Andhra Pradesh state, India using Spatial information technology. *International Journal of Geomatics and Geosciences*, *1*(2), 179.

Ratnam, K. N., (2005). Check dam positioning by prioritization of micro-watersheds using SYI model and morphometric analysis—remote sensing and GIS perspective. *Journal of the Indian Society of Remote Sensing*, *33*(1), 25.

Schumm, S. A., (1956). Evolution of drainage systems and slopes in badlands at Perth Amboy, New Jersey. *Geological Society of America Bulletin*, *67*(5), 597–646.

Siddaraju, K., Nagaraju, D., Bhanuprakash, H., Shivaswamy, H., & Balasubramanian, A., (2017). Morphometric evaluation and sub-basin analysis in Hanur watershed, Kollegal Taluk, Chamarajanagar district, Karnataka, India, using remote sensing and GIS techniques. *International Journal of Advanced Remote Sensing and GIS*, 2178–2191.

Sinha, R., & Friend, P. F., (1994). River systems and their sediment flux, Indo-Gangetic plains, Northern Bihar, India. *Sedimentology*, *41*(4), 825–845.

Smith, K. G., (1950). Standards for grading texture of erosional topography. *American Journal of Science*, *248*(9), 655–668.

Soni, S., (2016). Assessment of morphometric characteristics of Chakrar watershed in Madhya Pradesh India using the geospatial technique. *Applied Water Science,* 1–14.

Srivastava, P. K., Han, D., Gupta, M., & Mukherjee, S., (2012). Integrated framework for monitoring groundwater pollution using a geographical information system and multivariate analysis. *Hydrological Sciences Journal*, *57*(7), 1453–1472.

Strahler, A. N., (1964). Quantitative geomorphology of drainage basin and channel networks. In: Ven Te Chow, editor. *Handbook of Applied Hydrology.* New York (NY): McGraw-Hill; p. 4–39.

Strahler, A. N., (1957). Quantitative analysis of watershed geomorphology. *Eos, Transactions American Geophysical Union*, *38*(6), 913–920.

Wells, N. A., & Dorr, J. A., (1987). Shifting of the Kosi river, northern India. *Geology*, *15*(3), 204–207.

CHAPTER 27

ANALYSIS OF URBAN DRAINAGE SIMULATIONS OF AN IMMENSELY URBANIZED WATERSHED USING THE PCSWMM MODEL

SATISH KUMAR[1], D. R. KAUSHAL[2], and A. K. GOSAIN[2]

[1]*PhD Scholar, Indian Institute of Technology Delhi, Hauz Khas, New Delhi–110016, India, E-mail: satish.kumar140@gmail.com*

[2]*Professor, Indian Institute of Technology Delhi, Hauz Khas, New Delhi–110016, India*

ABSTRACT

Flooding has caused immense damage to the people as well as to the property. Flooding in urban areas mostly occurs due to increased urbanization, low rate of infiltration and poor infrastructure for stormwater drainage network. Stormwater Management Model (SWMM) is found to be very dynamic hydrology-hydraulic water quality simulation model for modeling of the urban stormwater drainage network. In the present study, PCSWMM model is used for modeling the stormwater drainage network for the southern part of Delhi, the capital city of India. PCSWMM is developed by Computational Hydraulics International (CHI), Canada. PCSWMM uses the same SWMM engine for the modeling work; the only advantage is that it is GIS compatible software which makes this model more efficient. The model required following input information for simulation, i.e., land-use for calculating impervious and previous area, soil type, 15-minute interval precipitation data, temperature, humidity, and three-dimension cross-sectional geometry of the existing drainage network. A field survey was carried out for data collection, and in the process, it was found that most of the storm-water drains are choked, have improper flow gradient

or damaged. All the collected field details of the storm-water drains were incorporated in ArcMap 10.1 and then imported in PCSWMM to develop a hydrology-hydraulic model for surface runoff. The simulated results of the model were further calibrated and validated with the available flooding locations data obtained from the Delhi Traffic Police Department. The simulated results were in close agreement with the observed flooding locations. Thus PCSWMM model can be applied to any urban/rural areas for designing stormwater drains or drainage network.

27.1 INTRODUCTION

Urban drainage is described as the process of collecting and transporting wastewater, rain /stormwater or a combination of both. Urban sewer or stormwater is a part of the urban infrastructure. Urban drainage is gaining importance in recent years. Properly designed and operated urban drainage systems with its interactions with other urban water systems are a crucial element of the healthy and safe urban environment. Urban flooding problems range from minor one where water enters the basements of a few houses to major incidents where large parts of cities are inundated for several days. Most modern cities in the industrialized part of the world usually experience small-scale local problems mainly due to insufficient capacity in their drainage systems during heavy rainstorms (Schmitt et al., 2004). Cities in other regions, including those in South/South-East Asia, often have more severe problems because of much heavier local rainfall and lower drainage standards. This situation continues to get worse because many cities in the developing countries are growing rapidly but without the funds to extend and rehabilitate their existing drainage systems. Moreover, New Delhi, capital of India, due to fast urbanization and rapid migration without simultaneous progress in drainage condition is suffering from serious waterlogging issues which result in loss of the property, infrastructure, and severe traffic jams. For solving such big and complex watershed problems, various type of mathematical models is used nowadays by the researchers/designers.

For managing runoff generated in the urban catchments, several models are available like MOUSE (DHI), HEC–1(US army), Hydro works (HRWL), SWMM (Storm Water Management Model) and PCSWMM (CHI). Out of this PCSWMM was identified as the GIS-based powerful model for modeling urban drainage networks because it precisely matches the simulated results with the observed data. PCSWMM used SWMM model for modeling stormwater drainage systems. SWMM is a dynamic rainfall-runoff model for the

simulation of quantity and quality complications related to urban catchments runoff (Huber and Dickinson, 1992). EPA had developed SWMM (Storm Water Management Model) in the year 1791 (Metcalf and Eddy Inc., 1971), which is extensively used to simulate all features of urban hydrologic and water cycles. The features include surface runoff, rainfall, and drainage network's flow routing, snowmelt, and pollution concentrations (Huber and Dickinson, 1992). Further, simulation through single or continuous events can be executed for the catchments where combined sewer drains or natural drains or stormwater drain exists.

For managing the urban stormwater system, distributed rainfall-runoff models are used. But the main difficulties in using these models are that developing of these models is a time taking the process and also about the model accuracy. PCSWMM is the most dynamic rainfall-runoff model in which runoff and pollution are generated from the subcatchments goes directly to manholes or to the downstream subcatchments. Thus, spatial discretization of the catchments is required by the rainfall-runoff model for developing runoff model computationally. Yu et al. (2001) reported that for developing rainfall-runoff model three essential elements are considered, i.e., characteristic of catchments, loss due to abstraction and simple equations of flow. In the urban subcatchments complicated processes like infiltration rate of surfaces, flows through overflow, the concentration of runoff due to depression is involved in modeling surface runoff. The factors like a watershed, surface area, flow streams, and outlets play an important role in forecasting the runoff in urban catchments. Traditional methods of discretizing in which the urban catchments were done manually on the basis of topographic maps which is a very slow process as well as not accurate. Geographic Information System (GIS) is a very powerful tool which has the spatial analysis function. GIS can be used for developing the hydrological model. For modeling urban stormwater, the GIS application can be used for storage, handling, evaluating, and demonstrating data in GIS form (Seth et al., 2006). GIS technology can help us in generating input parameters like digital elevation models (DEM), land-use maps, soil imperviousness maps and drainage network maps for developing a rainfall-runoff model (Seth et al., 2006). However, some of the parameters can be taken directly from GIS layers which can be used in SWMM for modeling rainfall-runoff. For developing a rainfall-runoff model, many researchers had used GIS for generating subcatchments (Yu et al., 2001; Du, 2007). But the above concepts cannot be used for the urban areas due to the complexity of the surface. Zaghloul (1981) reported that for obtaining better modeling results from SWMM largely depends on the catchment's discretization. PCSWMM is found to

be the efficient tools for modeling urban stormwater system because it is a GIS-based tool. All the GIS layers can be imported into PCSWMM and also subcatchments discretization for an urban area is done very accurately.

In this present study, PCSWMM has been used for the first time for modeling stormwater drains of the urban area (Delhi city, India) and the results obtained from simulation is in good agreement with the observed data.

27.2 MATERIALS AND METHODOLOGY

27.2.1 STUDY AREA

Delhi is located in northern India between the latitudes of 28°24'17" and 28°53'00" North and longitudes of 76°50'24" and 77°20'37" East having an average elevation of 233 m (ranging from 213 to 305 m) above the mean sea level. A study area is a small catchment in Barapullah basin which come under Aravalli hills ranges in the southern part of Delhi is shown in Figure 27.1. Delhi is a monsoon-influenced humid subtropical with high variation between summer and winter temperatures and precipitation. Summers start in early April and peak in May, with average temperatures near 32°C, although occasional heat waves can result in highs close to 45°C on some days and therefore higher apparent temperature. The monsoon starts in late June and lasts until mid-September, with about 797.3 mm of rain. The average temperatures are around 29°C, although they can vary from around 25°C on rainy days to 32°C during dry spells. The monsoons recede in late September, and the post-monsoon season continues until late October, with average temperatures sliding from 29 C to 21°C. The catchment covers an area of 5.79 Sq Kms and has a population of about 1.8 lacs and is a typical commercial/residential area. The Digital Elevation Model (DEM), land-use layer and soil type used in the present study was provided by the Geospatial Delhi Limited (GSDL). The lands of the study area are completely urbanized, and soil type is loam soil. Rainfall data for the last 5 years (2009 to 2013) obtained from the Indian Meteorological Department, Lodhi Road, New Delhi, India was used for the simulation process.

27.2.1.1 STORMWATER DRAINAGE SYSTEM

From stormwater drainage point of view, Delhi can be divided into six drainage basins, ultimately discharging into river Yamuna, namely–Najafgarh Drain, Barapulaah Nallah, Wildlife sanctuary area discharging thro` Haryana, Drainage of Shahdara area and other drains directly out falling into

river Yamuna. The NCT of Delhi is prone to flooding from river Yamuna via Najafgarh drain. The low-lying Yamuna floodplains (Khadar) are also prone to recurrent floods.

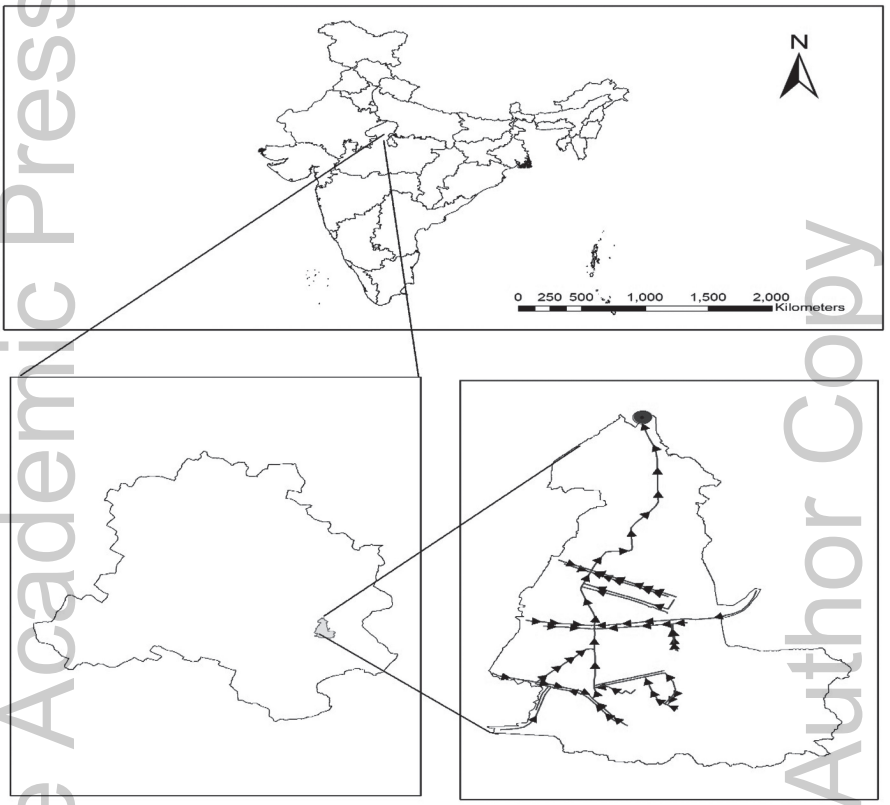

FIGURE 27.1 Location of study area.

Due to fast urbanization in Delhi during last four decades resulting in an increase in paved area and a decrease in the agricultural land which used to act as a percolation (Net Agriculture area shown in 1950–51 was 97,067 ha in 2005–2006 is just 25,000 ha out of total 148,300 ha). Delhi normally remained flooded to the extent of 70,000 ha (50% of its geographical area of 148,300 ha from 1953 to 1984). The Capital of India has suffered floods as back as in 1924, 1947, 1967, 1971, 1975, 1976, 1978, 1988, 1993, 1995, 1998, 2010, etc. The 1978 was the worst ever flood in Delhi when the water level reached at 207.49 m (danger level is 204.83 m) with discharge 2.53 lac cusec at old railway bridge (7.0 lac cusec discharge was released from Tajewala).

Barapullah Nallah is the main stormwater drain which is carrying all the water from Barapullah basin of south Delhi to Yamuna River. The stormwater drainage system in South Delhi is distributed between South Delhi Municipal Corporation, New Delhi Municipal Council, Public Works Department, and Delhi Development Authority. The major challenges caused by the stormwater drainage system in the city is due to the poor infrastructure of the drainage networks.

27.2.2 PCSWMM

PCSWMM software was developed by Computational Hydraulics Int. (CHI) in collaboration with the Environmental Protection Agency (EPA). PCSWMM is the graphical decision support system for the USEPA SWMM program. This software offers a wide range of files and time series management, model development and calibration, demonstration of dynamic output obtained from simulation and other related tools to the stormwater designer. More GIS attributes had been added to the new version of PCSWMM. In the latest version, anything related to stormwater modeling can be obtained. PCSWMM is developed by six elements, i.e., rainfall, runoff, temperature, extran, and storage. PCSWMM helps in dividing the urban areas into subcatchments on the basis of DEM and landuse. Infiltration takes place when the water is received by the subcatchments can be explained by Green Ampt, SCS curve number or Horton methods. Surface runoff takes place if water is not taken by the subcatchments and transported to the final outfall points via conduits and manholes. Steady flow, kinematics flow, and dynamic flow routing are the three types of flow routing processes which are used in the PCSWMM are same as in SWMM. Manning's equation explains the relation among cross-section area, discharge, gradients, and hydraulic radius. A full description of PCSWMM can be found in the theoretical documentation by James et al. (2010). The incident rainfall intensity is the input to the control volume on the surface of the plane; the output is a combination of the runoff Q and the infiltration f. Considering a unit breadth of the catchment the continuity and dynamic equations which have to be solved are as shown in equations below.

$$Q = B\frac{C_m}{n}S^{1/2}(y - y_d)^{5/2} \text{ (Dynamic equation)} \quad (1)$$

$$L = (fL + \frac{Q}{B}) + L\frac{\Delta_y}{\Delta_t} \text{ (Continuity equation)} \quad (2)$$

where, L = overland flow length, B = catchment breadth, C_m = 1.0 for metric units = 1.49 for Imperial or US customary units, n = Manning roughness coefficient, y_d = surface depression storage depth and f = infiltration.

27.2.3 MODEL SETUP

The surveyed data of the stormwater drains for the study area was converted into conduits layers and manholes layers with the help of ArcGIS 10.2. The drains information like invert level, width, depth, latitude, and longitude, conduits length was available in the attributes table. Then the outfall point layers of the drains were generated in ArcGIS. All these layers were imported into the PCSWMM. In PCSWMM, watershed, and sub-catchments were generated from the DEM on the basis of manholes. The subcatchments was delineated in such a fashion that runoff generated from each subcatchments will contribute to single manholes. Further, the land-use and soil were given to the catchments. And finally, rainfall station information and rainfall data were given to the PCSWMM. After loading all the necessary input data required by the PCSWMM, the model was initially run for the day having peak rainfall.

27.3 RESULTS AND DISCUSSION

The rainfall-runoff model was developed using PCSWMM is shown in Figure 27.2. Precipitation data from the years 2008 to 2012 of 15 minutes interval received from the Indian Meteorological Department, New Delhi was used for the simulation. Between 2008 to 2012 years, the maximum rainfall recorded was 109.2 mm on 20th August, 2010. Since, our objective is to find out whether the existing infrastructure is sufficient for extreme events, so the model was simulated and the results obtained was evaluated for the above days. Time series plot of the rate of flow of the drains, flooding rate and velocity of runoff is shown in Figure 27.3. For validating the model efficiency, the waterlogging locations identified by the model was checked with the past records. The waterlogging locations information is available on the Delhi police website. It was found that the simulated results are in close agreement as shown in Figure 27.4. The waterlogging may be caused due to various reasons like inadequate drainage infrastructure like drains are undersized due to which waterlogging takes place at the junctions or downstream. The other reasons are the rainfall intensity and

duration of rainfall. The most important reasons are the improper gradient of drains, i.e., invert levels of the drains is not uniform due to which flow is not able to go forward and hence, backflow takes place causing waterlogging in the upstream.

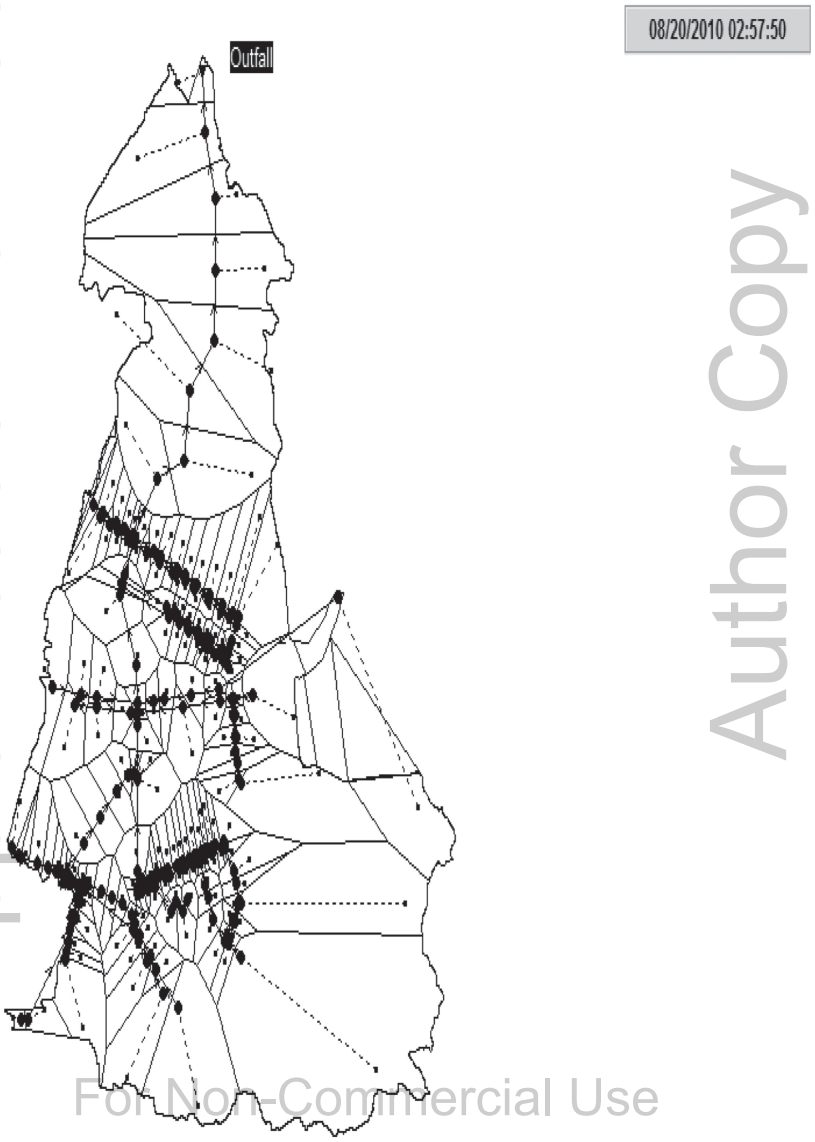

FIGURE 27.2 Rainfall-runoff model.

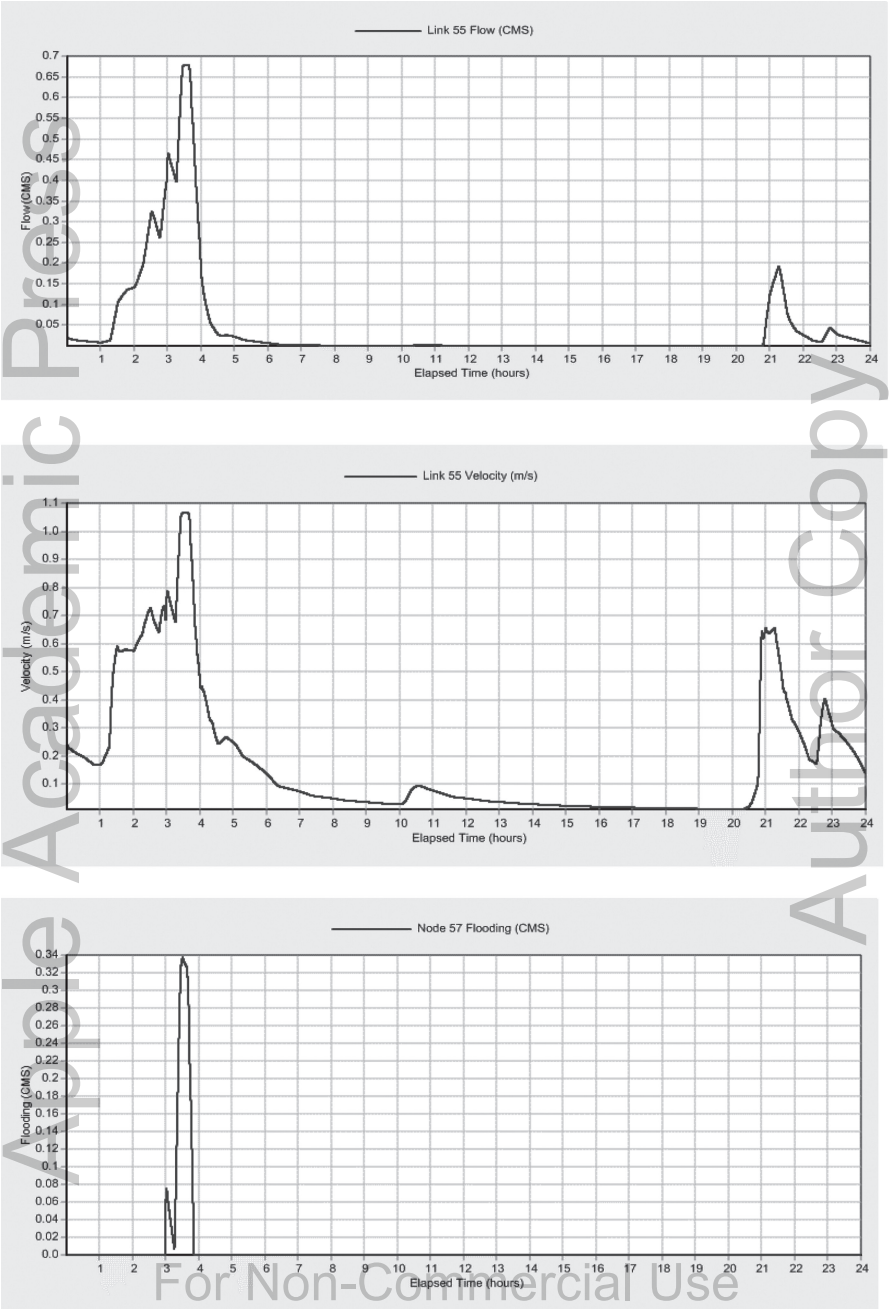

FIGURE 27.3 Showing rate of flow, flooding rate, and velocity.

FIGURE 27.4 Simulated results with observed data.

27.4 CONCLUSIONS

In the present study, PCSWM model was developed for stormwater drains of the small watershed of Delhi city. The model is also identifying the exact location of waterlogging locations. The watershed was divided into

192 subcatchments using DEM which makes PCSWMM a unique model. Thus PCSWMM found to be GIS friendly model which is very efficient for modeling any size of the urban drainage system.

ACKNOWLEDGMENT

The authors would like to thanks, Delhi Government, India for providing data to do this research. The authors would also like to thanks, Computational Hydraulics International (CHI), Canada for providing PCSWMM software as an honorarium to Indian Institute of Technology Delhi. Last but not the least, the author's thanks, Indian Institute of Technology Delhi for all the financial support given during the research.

KEYWORDS

- **GIS**
- **PCSWMM**
- **stormwater drainage**
- **surface runoff**
- **urban flooding**

REFERENCES

Du, J. K., Xie, S. P., Xu, Y. P., Xu, C. Y., & Singh, V. P., (2007). Development and testing of a simple physically-based distributed rainfall-runoff model for storm runoff simulation in humid forested basins. *Journal of Hydrology, 306*, 334–346.

Huber, W. C., & Dickinson, R. E., (1992). *Storm Water Management Model User's Manual, Version 4.* Environmental Protection Agency, Georgia.

Huber, W., (1992). Contaminant transport in surface water. In: Maydment, Dr., (ed.), *Handbook of Hydrology.* McGraw-Hill, New York.

James, W., (2005). *Rules for Responsible Modeling* (4th edn.). Computational Hydraulic International Press, Guelph, Ontario, Canada.

James, W., Rossman, L. A., & James, W. R. C., (2010). *User's Guide to SWMM 5*, Computational Hydraulic International Press, Guelph, Ontario, Canada.

Metcalf and Eddy Inc., (1971). *Storm Water Management Model, Final Report.* US Environmental Protection Agency.

Santhi, C., Arnold, J. G., Williams, J. R., Dugas, W. A., Srinivasan, R., & Hauck, L. M., (2001). Validation of the SWAT model on a large river basin with point and nonpoint sources. *Journal of the American Water Resources Association, 37*(5), 1169–1188.

Schmitt, T. G., Thomas, M., & Ettrich, N., (2004). Analysis and modeling of flooding in urban drainage systems. *Journal of Hydrology*, 300–311.

Seth, I., Soonthornnonda, P., & Christensen, E. R., (2006). Use of GIS in urban storm-water modeling. *Journal of Environmental Engineering, 132*(12), 1550–1552.

Tsihrintzis, V., & Hamid, R., (1998). Runoff quality prediction from small urban catchments using SWMM. *Hydrological Processes, 12*(2), 311–329.

Yu, P. S., Yang, T., & Chen, S. J., (2001). Comparison of uncertainty analysis methods for a distributed rainfall-runoff model. *Journal of Hydrology, 244*, 43–59.

Zaghloul, N. A., (1981). SWMM model and level of discretization. *Journal of the Hydraulics Division, 107*(11), 1535–1545.

CHAPTER 28

RAINFALL FORECASTING USING A TRIPLE EXPONENTIAL SMOOTHING STATE SPACE MODEL

SWATI MAURYA and PRASHANT K. SRIVASTAVA

Institute of Environment and Sustainable Development, Banaras Hindu University, Varanasi–221005, India, E-mail: mauryaswati35@gmail.com

ABSTRACT

The prediction of rainfall is too complex due to its high spatial and temporal variability. Study of variation in rainfall is important as it also influences the hydrological cycle of the Earth. While in India, 60–90% rainfall occurs in the monsoon period (June-September), and our agricultural system is dependent on this for rainfall for most of the water requirements. Therefore, this study focuses on the quantitative method for rainfall forecasting such as triple exponential smoothing state space model (tESM) for rainfall prediction in Dhariawad catchment of Mahi River Basin in Rajasthan, India. The tESM is enriched with model level, trend, and seasonal decomposition for efficient forecasting of meteorological parameters. In this study, the long-term data of rainfall during the period 1997–2012 (16 years) were used for optimization and forecasting of the rainfall. In total 12 years (1997–2008) were used for model calibration and 4 years (2009–2012) were kept separately for validation purpose. The overall data analysis indicates that the tESM performed better in terms of root-mean-square error (RMSE = 75.31 mm), index of agreement (d = 0.86) and percent bias (PBIAS = –35.5). The application of tESM forecast methods indicates that it is easy to implement and provide results that are more appropriate in lesser time.

28.1 INTRODUCTION

Rainfall plays a major role in the hydrological system. Rainfall mainly influences the water resource development, agricultural activities, disasters, economy of the region, etc. (Gajbhiye et al., 2016). Thus, the forecast of rainfall is critically important for understanding the variation in rainfall. The variation in rainfall alters stream flow, groundwater resources, distribution of rainfall, soil moisture content, etc. Therefore, regular monitoring of rainfall is necessary for proper management of natural hazards such as flood, drought, landslide, cloud bursting and in agriculture for improving productivity, irrigation scheduling, etc.

For rainfall forecasting, time series analysis is the most common method used in the recent past, and various technique proved to provide more appropriate results for evaluating the variation of rainfall over the region (Tularam et al., 2010). In time series analysis two forms are very common such as trend and seasonality (Kalekar, 2004). The trend defines as a systematic linear or nonlinear component that changes over time and not repeats in the period of time range captured by the data. The seasonality almost similar nature; but it repeats itself in regular intervals over time. These two basic classes of time series components may coexist in the data. The present works focus on the triple Exponential Smoothing Models (tESM) for rainfall forecasting. The main reason for the popularity of these methods that they are simple and easy to put in practice and don't need a fitting parameter (Gelper et al., 2010). It was based on a repetitive computing scheme for update the forecasts for each new upcoming observation.

28.2 STUDY AREA

The Dhariawad catchment geographical lies in 74.48^0 longitudes, 24.09^0 latitudes of Mahi River Basin in Rajasthan, India. The average annual rainfall is 813 mm. The area of this catchment is 1510 sq km. Maximum rainfall occurs in the monsoon period, and climatic conditions are tropical to sub-tropical. Geographical diversity varies from highly dense forests to hilly terrain and plateau. Major crops are wheat, maize, soya bean, gram, garlic, and opium. The soil types are silt loam to clay loam and greyish brown in color. Further small-scale mining activities are in operation extracting mainly Red Ochre, Calcite, Dolomite, Quartz, Feldspar, and Soapstone. Marble, Building-stone, and Limestone are also available in small quantities. The Shuttle Radar Topography Mission (SRTM) is a collaboration of National

Aeronautics and Space Administration (NASA) and the National Geospatial-Intelligence Agency (NGA) for topographical analysis. It provides elevation datasets for the globe at 1 arcsec (approx. 30 m) and at 3-arcsec (approx. 90 m). For evaluating the drainage, patterns freely available SRTM DEM (90 m) datasets are used (http://www.cgiarcsi.org). Geographical location of the study area shown in Figure 28.1.

28.3 MATERIALS AND METHODS

28.3.1 DSSAT

Decision Support System for Agrotechnology Transfer (DSSAT) of precipitation data of 16 years during the period (1997–2012). DSSAT is a NASA POWER (Prediction of Worldwide Energy Resources) database have 1° latitude by 1° longitude grid with global coverage and provides global modeled meteorological dataset in the standard format of International Consortium for Agricultural Systems Applications (ICASA) and American Standard Code for Information Interchange (ASCII) (White et al., 2011). DSSAT database measures daily meteorological parameters based on satellite observations and assimilation models. The main advantage of DSSAT are required only latitude and longitude of particular regions and provide all meteorological data. Precipitation data were downloaded from http://power.larc.nasa.gov/cgibin/cgiwrap/solar/agro.cgi. In the 16 years of monthly datasets, 12 years (1997–2008) were used for model calibration and 4 years (2009–2012) for validation.

28.3.2 TRIPLE EXPONENTIAL SMOOTHING MODEL

This method is used when the data shows level, trend, and seasonality. These set of equations is called the "Holt-Winters" (HW) method after the names of the inventors (Kalekar, 20004; Willmott, 1981). For Additive seasonality measurement, the following equations are used.

In this model, the time series is represented as below.

$$y_t = b_1 + b_{2t} + S_t + \varepsilon_t \quad (1)$$

where b_1 is the base signal also called the permanent component; b_2 is a linear trend component; S_t is a seasonal additiveseasonal factor; ε_t is the

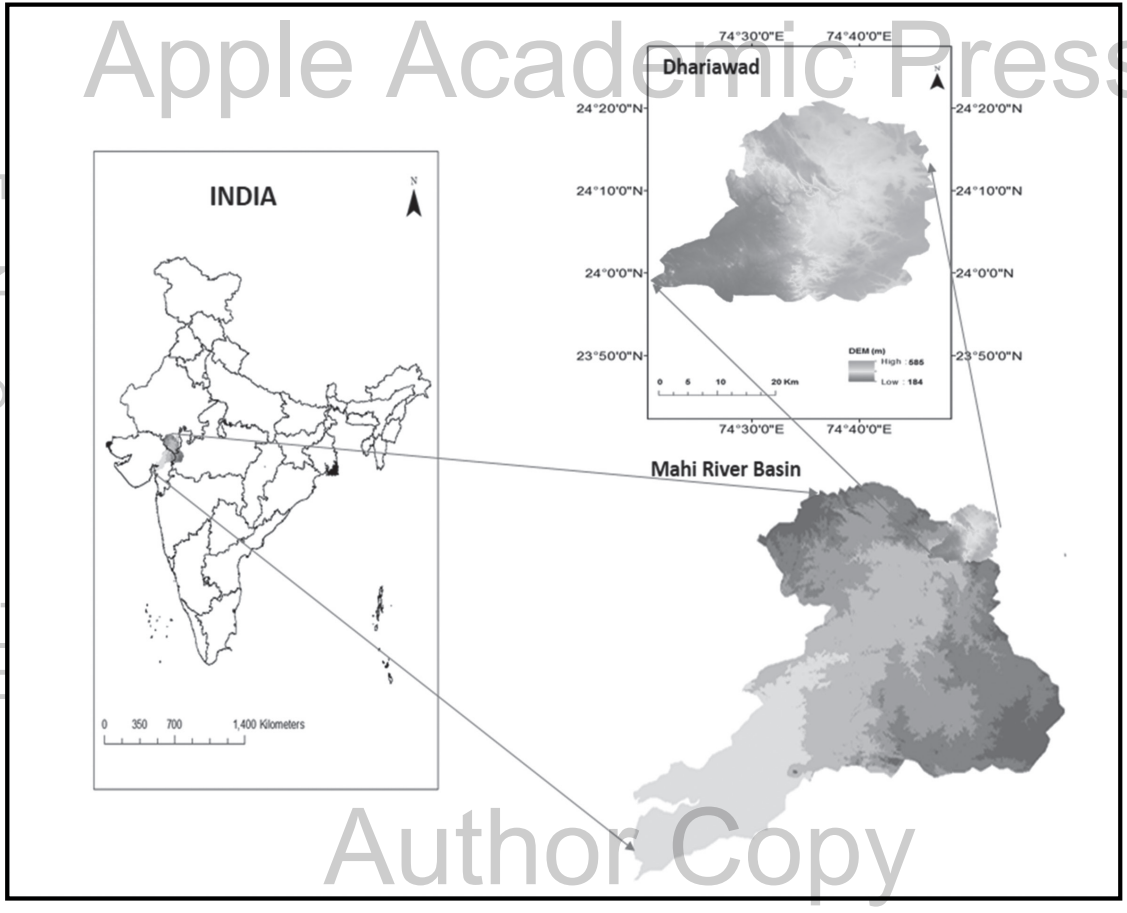

FIGURE 28.1 Geographical location of the study area.

random error component. Let the length of the season be L periods. The seasonal factors are the sum to the length of the season, i.e.

$$\Sigma_{1 \le t \le L} S_t = 0 \quad (2)$$

The trend component b_t if deemed unnecessary, may be deleted from the model. After selecting a model, the next step is its specification. The process of specifying a forecasting model first of all select the variables to be included, selected the form of the equation of relationship, and estimated the values of the parameters in that equations.

28.3.2.1 PROCEDURE FOR UPDATING THE ESTIMATES OF MODEL PARAMETERS

28.3.2.1.1 Overall Smoothing

$$R_t = \alpha(y_t - S_{t-L}) + (1 - \alpha) * (R_{t-1} + G_{t-1}) \quad (3)$$

R_t estimate of the deseasonalized level.
G_t estimate of the trend
S_t estimate of seasonal component (seasonal index)

where $0 < \alpha < 1$ is a smoothing constant.

Dividing y_t by S_{t-L}. It is the seasonal factor for T period calculated the one season (L periods) ago, deseasonalizes the data, and the prior value of the permanent component enters into the updating process for R_t.

28.3.2.1.2 Smoothing of the Trend Factor

$$G_t = \beta * (S_t - S_{t-1}) + (1 - \beta) * G_t - 1 \quad (4)$$

where $0 < \beta < 1$ is a second smoothing constant. Trend component estimated by smoothing the difference between two successive estimates of the deseasonalized level. The estimate of the trend component is the simply smoothed difference between two successive estimates of the deseasonalized level.

28.3.2.1.3 Smoothing of the Seasonal Index

$$S_t = \gamma * (y_t - S_t) + (1 - \gamma) * S_{t-L} \quad (5)$$

where $0 < \gamma < 1$ is the third smoothing constant.

The estimate of the seasonal component is a combination of the most recently observed seasonal factor given by the demand y_t divided by the deseasonalized series level estimate R_t and the previous best seasonal factor estimate for this time period. Since seasonal factors represent deviations above and below the average, the average of any L consecutive seasonal factors should always be 1. Thus, after estimating S_t, it is good practice to renormalize the L most recent seasonal factors such that

$$\sum_{i=t-q+1}^{t} S_t = q \tag{6}$$

28.3.2.1.4 Value of Forecast

The forecast for the next period given by

$$y_t = R_t - 1 + G_{t-1} + S_{t-L} \tag{7}$$

28.3.3 STATISTICAL EVALUATIONS

The three statistics, root-mean-squared error (RMSE), index of agreement (*d*) and percent bias (%Bias) are used. RMSE defined as the average of error magnitude. The index of agreement (d) is the ratio between the mean square error and the "potential error" (Willmott, 1981). The potential error is the sum of the squared absolute values of the distances from the predicted values to the mean observed value and distances from the observed values to the mean observed value. Its range varies from 0 to 1. The calculated value 1 express a perfect agreement between the measured and predicted values, while 0 expresses the no agreement at all (Willmott, 1981). Percent bias (%Bias) measures the average tendency of the simulated values to be larger or smaller than their observed value. The optimal value of %Bias is 0.0; with low-magnitude, values express that accurate model simulation. Root-mean-square error (RMSE) can be defined as;

$$RMSE = \sqrt{\frac{1}{n}\sum_{i=1}^{n}\left[y_i - x_i\right]^2} \tag{8}$$

Degree of Agreement can be defined as;

$$d = 1 - \frac{\sum_{i=1}^{n}(x_i - y_i)^2}{\sum_{i=1}^{n}(|y_i - x| + |x_{i-x}|)^2} \tag{9}$$

Percent Bias can be defined as;

$$\%Bias = 100 * [\Sigma(y_i - x_i)\ \Sigma(x_i)] \quad (10)$$

Where n is the number of observations, x is observed values and y *is* forecasted values.

28.4 RESULTS AND DISCUSSIONS

The trend of rainfall during the period (1997–2012) is shown in Figure 28.2 (a). The pattern of rainfall is variable throughout the years. But the value of rainfall is almost same in 1997–2002 while the value of rainfall suddenly drops down in 2003. After this, the value of rainfall gradually increases as the year progresses from 2003 to 2012. In the seasonal pattern, up, and down steps occur in a regular time interval of whole 17 years. That means repeating pattern obtained over consecutive periods. While scattering plots for validation in between observed and model value shown in Figure 28.2 (b). In this plots, the value indicates a moderate deviation between the observed and model values from the equiline thus resultant in a moderate positive correlation. The rainfall forecasting by tESM is shown in Figure 28.3, with the prediction intervals at 80 and 90%. The values of prediction intervals are necessary because it's defined the uncertainty in the forecasts. Further visual inspection of Figure 28.3 clear that narrow confidence boundary is evident in tESM. That means parameters are concentrated in a smaller area and perform better.

The performances of the tESM model are also evaluated by the three statistical parameters RMSE, d, PBIAS for forecasting the rainfall as shown in Table 28.1. The value of RMSE for tESM is 75.3, which indicate a better agreement in between the observed and forecasted values. Further the value of the degree of agreement (d = 0.8) close to 1, which shows a perfect agreement between the observed and forecasted value. Moreover, the value of percent bias (PBIAS = –33.45) is close to zero; it is indicated that low value had better perform in a model simulation. Thus, the overall analysis indicates that the chosen model provided almost accurate results for forecast rainfall and suggested that rainfall increases gradually in the Dhariawad catchment.

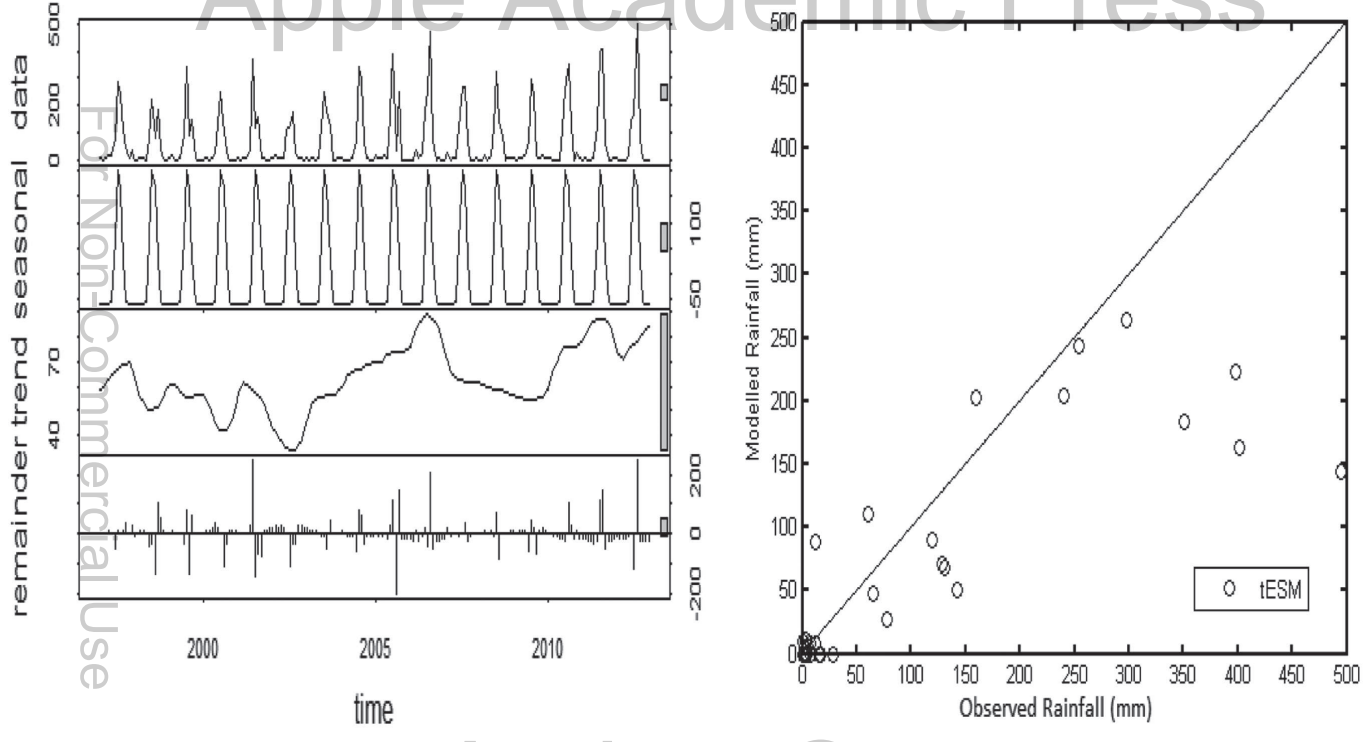

FIGURE 28.2 (a) Rainfall trend of Dhariawad catchment during the period of 1997–2012. (b) Scatter plot of validation datasets.

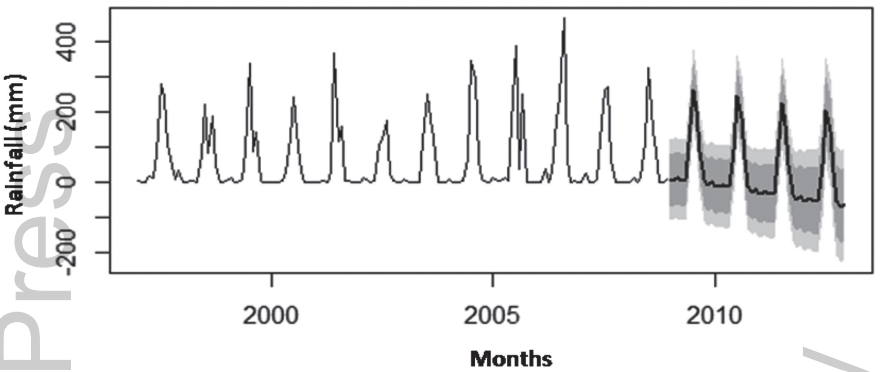

FIGURE 28.3 Forecast results of rainfall (1997–2012) using tESM modeling approach with prediction intervals.

TABLE 28.1 Performance Statistics of the tESM Modeling Approaches for Forecasting Rainfall

		tESM			
RMSE(mm)	75.31	PBIAS	–35.5	d	0.86

RMSE, root-mean-square error; *d*, index of the agreement; PBIAS, Percent bias.

28.5 CONCLUSIONS

Rainfall is a major factor in agriculture and in recent years, interest has increased in learning about precipitation variability and predictability for periods of months to years. The effects of climatic change and variability have been analyzed by many researchers and proved that rainfall pattern uncertain in various region. Therefore, our prime concerned to understand the variability of rainfall time to time. In this study, an overall analysis of long-term series (1997–2012) of rainfall by tESM in the Dhariawad catchment indicated that rainfall time series fluctuate randomly and after 2004 increase gradually. The reason behind the rainfall increases are climate change but not assure because of some other factors also influence the rainfall such as land use, land cover, unlimited growth of population and meteorological parameters, etc. The future aspect of this study helped in various field of hydrology such as flood forecasting, water resource management, etc.

KEYWORDS

- **forecasting accuracy**
- **monsoon rainfall**
- **tESM**

REFERENCES

Gajbhiye, S., (2016). Precipitation trend analysis of Sindh River basin, India, from the 102-years record (1901–2002). *Atmospheric Science Letters*, *17*(1), 71–77.

Gelper, S., Fried, R., & Croux, C., (2010). Robust forecasting with exponential and Holt-Winters smoothing. *Journal of Forecasting*, *29*(3), 285–300.

Kalekar, P. S., (2004). Time series forecasting using holt-winters exponential smoothing. *Kanwal Rekhi School of Information Technology*. *4329008*, 1–13.

Tularam, G. A., & Ilahee, M., (2010). Time series analysis of rainfall and temperature interactions in coastal catchments. *Journal of Mathematics and Statistics. 6,* 372–380.

White, J. W., (2011). Evaluation of satellite-based, modeled-derived daily solar radiation data for the continental United States. *Agronomy Journal, 103*(4), 1242–1251.

Willmott, C. J., (1981). On the validation of models. *Physical Geography*, *2*(2), 184–194.

CHAPTER 29

IMPROVING IRRIGATION WATER USE EFFICIENCY: A SOLUTION FOR FUTURE WATER NEED

PRABEER KUMAR PARHI

Center for Water Engineering and Management, Central University of Jharkhand, Brambe, Ranchi – 835205, India,
E-mail: prabeer11@yahoo.co.in

ABSTRACT

As productive irrigated land base and available fresh water are declining day by day, there is a need for optimal use of land and water resources so that crop yield is maximized per unit volume of water per unit land area per unit time. There is a greater possibility to raise the productivity of water through the management of soil water than with genetic approaches (biotechnology and breeding). Properly and carefully managed deficit irrigation strategies on agronomic crops would provide the greatest potential for substantially reducing agricultural water use. Scientific irrigation scheduling has the potential to improve the ratio of yield to consumptive use primarily because of the optimized quantity and timing of water applications. High-value and early mature crops may also produce some water savings through various deficit irrigation strategies, Geographically relocating certain crops to their most productive areas and soils, thereby minimizing irrigation amounts and maximizing overall efficiencies would be the most economically efficient use of water resources. Advanced irrigation technologies, precision agriculture tools and state-of-the-art delivery systems, needs to be fully implemented for successful deficit irrigation management as water savings under nonstress conditions (maximum yield) using site-specific technologies have a potential to bring down the water need to the order of 15% to 30%.

29.1 INTRODUCTION

The good quality, non-saline fresh water suitable to support human health and enterprise constitutes only about 1% of the water available worldwide. It is estimated that as a major consumer of the total freshwater, irrigation alone accounts for about four-fifths of the total freshwater. With the rapid increase in human population, more, and more water has to be allocated towards irrigated agriculture to satisfy the increasing food needs. Further, the increasing water needs due to rapid urbanization, environmental consciousness, recreation, tourism, and related concerns are to be taken care of. In this context, it is important to mention that an estimated 60% of the global population is going to suffer from water scarcity by 2025 (Qadir et al., 2007). Recently, the United Nations in its report (UNESCO, 2006) has estimated that increased cropping intensity to meet world food needs will require an increase of 40% in the area of harvest crops by 2030, and that the amount of water allocated to irrigated agriculture must increase correspondingly by 14%. However, it not assured that the needed water will be available by that time.

Further, Global climate change is a source of uncertainty having its potential impacts on temperatures, annual precipitation levels, and regional rainfall distribution patterns and increased water demand. Crop producers could face a decrease in the quantity and temporal availability of water supplies. The timing of precipitation and runoff from mountain snowmelt would differ from historical norms, leading to more frequent and sustained intense weather events such as droughts in some areas and floods in others. Hydrologic uncertainties would be compounded leading to modifications in precipitation and temperature having disproportionately larger effects on crop evapotranspiration (ET). The combination of these factors would force changes in the distribution of existing cropping patterns. Hence, it is free from any doubt that the alarming pressure on water resources ensures that water will be the primary natural resource issue of the 21st century (Seckler and Amarasinghe, 2000). Already there are economic and social pressures on all water users to reduce irrigation water amounts. This obviously calls fora novel approaches to water management and systems will be needed to address the declining land base and water allocations to balance production needs. Hence it is the need of the hour to identify measures through which agricultural users can economically adopt advanced irrigation schemes and implement practices to improve irrigation efficiency and water productivity in sustainable agriculture.

In the above context, the objectives of the present study are to review (1) the ability of irrigated agriculture to meet the growing population food

needs, (2) the concepts of water use efficiency, and (3) the ways to improve water use efficiency (WUE).

29.2 BASIC CONCEPTS AND DEFINITIONS OF WUE

The present discussion emphasizes on methods to use less water for crops while maintaining or even increasing total crop productivity by enhancing the efficient use of water through improved management and advanced irrigation technologies. Various strategies to minimize water loss include redesigning total irrigation systems for higher efficiency, successfully treating and reusing degraded waters, reducing evaporation losses, introducing site-specific water applications, implementing managed-deficit irrigations, and employing engineering techniques to minimize leaching.

So far as WUE or the crop water productivity is concerned, it is basically defined as an input/output ratio to measure productivity. In other words, it is also defined as the crop productivity per unit volume of water used. Though many different definitions of WUE have been offered by large number agricultural scientists, WUE is the generally considered as the ratio of the harvested biomass to the water consumed to achieve that yield (Steduto, 1996). According to Viets (1962), WUE is the yield of interest (e.g., grain, biomass) divided by the water used to produce that yield. Howell (2001) pointed out that the denominator (water used) is difficult to measure and suggested that water used to be estimated from effective rainfall plus irrigation plus the change in soil water content. Bos (1980) suggested WUE as the yield benefit from irrigation divided by the irrigation water applied. WUE has also been defined in terms of the dry matter harvest index (ratio of yield biomass to the total cumulative biomass at harvest) as the yield of interest divided by water use (Howell et al., 1990)

Moreover, WUE is primarily considered as biological response ratio rather than an efficiency term, due to which many people are now referring to this concept as crop water production (Howell, 2006; Steduto et al., 2007). Monteith (1984, 1993) criticized the WUE term and pointed out that no theoretical limits exist as a reference, as should be the case for efficiency in an engineering sense. The WUE is alsobe greatly influenced by the timing of water applications as is evident in supplemental irrigations in humid areas. Irrigation at just the right time to avoid water stress can have a very large increase in WUE. Hence as a management practice, this term is very often used as a key indicator to compare values of WUE from different places with similar climatic conditions, geospatial characteristics and crop characteristics.

29.3 OPTIONS TO IMPROVE WATER USE EFFICIENCY (WUE)

29.3.1 IMPROVING MANAGEMENT CAPACITY

Minimization of the negative effects of water deficits on yields and quality through management of soil water (management of appropriate irrigation timing) can raise the productivity of water in irrigated agriculture. This can be achieved through the proper design of water delivery and farm irrigation system, which can help farmers to apply the right amount of water at the right place for all irrigations. While deciding irrigation timing optimal use of available rainwater is important.

Management of irrigation water under severe to moderate soil water deficit conditions during the growing period of crops can increase crop productivity while reducing the amount of water applied. This implies economically optimization of production for each unit of water used can maximize crop productivity while reducing the amount of water applied. Hence it is clear that properly managed deficit irrigation strategies can reduce agricultural and urban water use and conserve water to an appreciable extent. However, it needs excellent control of the timing and amounts of the applied water.

29.3.2 ADOPTING SCIENTIFIC IRRIGATION SCHEDULING

Scientific irrigation scheduling refers to the application of an optimum quantity of water at a most appropriate time so that crop stress and over-application is avoided. The method improves the ratio of yield to consumptive use (water productivity), primarily because of improved timing of water applications. However, it is always essential to combine the effects of scheduling with improved farming practices that typically accompany an on-farm irrigation-scheduling program. The irrigation scheduling can be further improved by converting irrigation system from gravity surface irrigation to pressurized drip or sprinkler systems.

29.3.3 CROP SELECTION

In arid and semiarid areas where there is a scarcity of water resulting in frequent partial season droughts, it is always advisable to choose crops that mature more quickly, such as small grains, cool season oilseeds

(e.g., mustards, camelina), or various pulse crops such as peas and lentils. Shifts to deep-rooted, drought-resistant crops such as sunflower and safflower may also occur to maximize use of precipitation stored in the soil. However, longer season crops such as maize (corn) may have reduced yields.

29.3.4 SUPPLEMENTAL IRRIGATION PRACTICE

Supplemental irrigation is a tactical measure to complement reasonably sufficient rainfall and stabilize production despite short-term droughts. However, this practice is important primarily in arid and semiarid areas where it may be possible to apply only one or two irrigations per season. This is a form of managed deficit irrigation where the impact of the timing and applications of limited water supplies relative to only rain-fed agriculture can be very positive (Sojka et al., 1981; Zhang and Oweis, 1999). These techniques imply applying water during critical growth stages so that there is an optimal benefit per unit volume of water per unit quantity of crops of interest produced.

29.3.5 SPATIALLY OPTIMIZING PRODUCTION

Another option for improving the productivity of water is its spatial optimization. Spatially optimal land use includes geographically relocating certain crops to their most productive areas and soils, thereby minimizing irrigation amounts and maximizing overall efficiencies. Relocating specified crops to climatic regions and soil types best suited to maximal output would be the most economically efficient use of resources.

29.3.6 ADVANCED IRRIGATION TECHNOLOGIES

Almost every aspect of irrigation has seen significant innovation, including diversion works, pumping, filtration, conveyance, distribution, application methods, drainage, power sources, scheduling, erosion control, land grading, soil water measurement, and water conservation. Originally, irrigation was accomplished by methods utilizing gravity to distribute and apply water. Sprinkler technology was enhanced by the development of low-cost aluminum and later PVC pipe, and currently,

more land is irrigated in the United States by sprinklers than by gravity methods. High-frequency drip irrigation and other micro-irrigation methods have been shown to increase the yield and quality of fruit and vegetable crops through reduced water and nutrient stresses. Tied to an effective soil water monitoring program, good design, and appropriate management practices, micro irrigation can have an application efficiency of 95% or better without drought stress, and is now used on about 5% of the irrigated area in the United States (NASS, 2002).

29.3.7 IMPROVED IRRIGATION SYSTEMS

The major reasons to go for system improvements are to reduce labor by automation, minimizing water costs by conservation (higher irrigation efficiencies) and expanding irrigated area with the same diverted water volume (irrigation capacity). Further, there are several management options for reducing water losses. Making small pits or basins (mini reservoirs), commonly called furrow diking, in sprinkler irrigated fields to hold water can be beneficial. Irrigation at night can reduce evaporation losses. Weeds are a major nonbeneficial use of water, and their control is critical, but chemical control is costly and may have unwanted environmental consequences. The use of mulches for weed control may reduce non-beneficial ET and soil evaporation. Reduced tillage techniques can reduce soil evaporation losses. Drip irrigation technologies can conserve water by greatly reducing soil evaporation and maximizing crop water productivity. These strategies could also incorporate alternative cropping systems including winter crops and deep-rooted cultivars that maximize use of stored soil water and some nutrients.

29.3.8 SITE-SPECIFIC IRRIGATION

Site-specific technologies to maximize crop yield per unit volume of water have a great potential in arid and semi-arid regions. Experiments show that potential water savings under non-stress conditions (maximum yield) using site-specific technologies are probably on the order of about 5% or less, but maybe in the range of 15% to 30% (Sadler et al., 2005). By aligning irrigation water application with variable water requirements in the field, total water diversions may be reduced and, almost certainly, deep percolation and surface runoff can be reduced.

29.3.9 MICRO IRRIGATION

Micro-irrigation is an extremely flexible irrigation method, and it offers the potential for high levels of water savings because of precise, high-level management. Due to its high cost and intensive management requirement currently, its use is restricted to relatively small fields. This method can be applied to almost all cropping situation, climatic zone and over a wide range of terrain. This type of irrigation suits best where soils are of very low or very high infiltration rates and salt-affected soils. However micro irrigation is used on less than 1% of lands worldwide, primarily because of its recent development and high initial capital cost. Micro-irrigation has the potential for use on most agricultural crops, although it is most often used with high-value specialty crops such as vegetables, ornamentals, vines, berries, olives, avocados, nuts, fruit crops, and greenhouse plants because of its relatively high cost and management requirements. The use of micro irrigation is increasing around the world, and it is expected to continue to be a viable irrigation method for agricultural production in the near future. With increasing demands on limited water resources and the need to minimize environmental consequences of irrigation, this technology will undoubtedly play an important role in the future irrigation scenario.

29.3.10 SYSTEM-LEVEL OPTIMIZATION

To maximize WUE, integration of all the above components and optimization of the whole system on a specific zone level is needed. The maximum production per unit volume of water is possible if all terms that do not produce yield were eliminated, leaving all water for productive use. However, in the systems perspective, some uses that do not contribute immediately to yield increases can lead to long-term yield. For example, leaching requirement in arid and semiarid areas never contribute to yield immediately, but irrigation without some leaching can eventually lead to soil salination. Similar is the case of evaporation as it helps meet the energy balance, and loss from one system may be the water supply to another system at watershed or catchment level.

29.4 CONCLUSIONS

Irrigated agriculture contributes nearly 40% of total food and fiber production worldwide. But, the paradox is that the productive irrigated land base and

available water is declining day by day. This necessitates the need for optimal use of land and water resources so that crop yield is maximized per unit volume of water per unit land area. Studies show that there is a greater possibility to raise the productivity of water and minimize of the negative effects of water deficits on yields and quality through management of soil water than with genetic approaches (biotechnology and breeding). Properly managed deficit irrigation strategies can reduce agricultural and urban water use and conserve water to an appreciable extent; however, it needs excellent control of the timing and amounts of the applied water.

Scientific irrigation scheduling can improve the ratio of yield to consumptive use primarily because of the optimized quantity and timing of water applications. However, the scientific scheduling and improved farming practices can be combined together to yield best results. Carefully managed deficit irrigation on agronomic crops would provide the greatest potential for substantially reducing agricultural water use. High-value and early mature crops may also produce some water savings through various deficit irrigation strategies. Geographically relocating certain crops to their most productive areas and soils, thereby minimizing irrigation amounts and maximizing overall efficiencies would be the most economically efficient use of water resources.

Advanced irrigation technologies, precision agriculture tools and state-of-the-art delivery systems, needs to be fully implemented for successful deficit irrigation management. Water savings under non-stress conditions (maximum yield) using site-specific technologies have a potential to bring down the water need to the order of 15% to 30%. Hence, in the era of increasing water needs, there is an urgent need to explore the specific knowledge and technologies required to minimize water use while maintaining reasonable production levels to satisfy all the needs for food, fiber, feed, and fuels in addition to environmental, recreation, and municipal requirements.

KEYWORDS

- **advanced irrigation technology**
- **irrigated agriculture**
- **irrigation management**
- **water productivity**
- **water use efficiency**

REFERENCES

Bos, M. G., (1980). Irrigation efficiencies at the crop production level, *ICID Bull*., *29*(2), 18–25, 60.

Howell, T. A., (2001). Enhancing water use efficiency in irrigated agriculture, *Agron. J*., *93*(2), 281–289.

Howell, T. A., (2006). *Challenges in Increasing Water Use Efficiency in Irrigated Agriculture, Paper Presented at International Symposium on Water and Land Management for Sustainable Irrigated Agriculture*, Adana, Turkey.

Howell, T. A., Cuenca, R. H., & Solomon, K. H., (1990). Crop yield response, in the management of farm irrigation systems, *Am. Soc. of Agric. Eng*., 93–122.

Monteith, J. L., (1984). Consistency and convenience in the choice of units for agricultural science, *Exp. Agric*, *20*, 105–117.

Monteith, J. L., (1993). The exchange of water and carbon by crops in a Mediterranean climate, *Irrig. Sci*., *14*(2), 85–91, doi: 10.1007/ BF00208401.

National Agricultural Statistic Service (NASS), (2002). *Ranch Irrigation Survey* (Vol. 3). Special studies Part 1, U.S. Department of Agriculture, Washington, D.C.

Qadir, M., Sharma, B. R., Bruggeman, A., Choukr-Allah, R., & Karajeh, F., (2007). Non-conventional water resources and opportunities for water augmentation to achieve food security in water-scarce countries, *Agric. Water Manage*., *87*(1), 2–22.

Sadler, E. J., Evans, R. G., Stone, K. C., & Camp, C. R., (2005). Opportunities for conservation with precision irrigation, *J. Soil Water Conserv*., *60*(6), 371–379.

Seckler, D., & Amarasinghe, A., (2000). Water supply and demand, 1995 to 2025: Water scarcity and major issues, in Annual Report 1999–2000. *World Water Vision*, *3*, 9–17.

Sojka, R. E., Stolzy, L. H., & Fischer, R. A., (1981). Seasonal drought responses of selected wheat cultivars, *Agron*., *73*, 838–845.

Steduto, P., (1996). In: Pereira, L. S., et al., (eds.), *Water Use Efficiency, in Sustainability of Irrigated Agriculture* (Vol. 312, pp. 193–209). NATO ASI Ser., Ser. E, Kluwer Acad. Dordrecht, Netherlands.

Steduto, P., Hsiao, T. C., & Fereres, E., (2007). On the conservative behavior of biomass water productivity, *Irrig. Sci*., *25*(3), 189–208.

U.N. educational, scientific, and cultural organization, water, a shared responsibility, Rep. 2, World water assess. The programme, Berghann, New York, 2006.

Viets, F. G. Jr., (1962). Fertilizers and the efficient use of water, *Adv. Agron., 14*, 223–264.

Zhang, H., & Oweis, T., (1999). Water-yield relations and optimal irrigation scheduling of wheat in the Mediterranean region, *Agric. Water Manage*, *38*(3), 195–211.

CHAPTER 30

RAINFALL VARIABILITY AND EXTREME RAINFALL EVENTS OVER JHARKHAND STATE

R. S. SHARMA and B. K. MANDAL

Meteorological Centre Ranchi, India Meteorological Department, B. M. Airport Road, Hinoo, Ranchi–834002, India, E-mail: radheshyam84@rediffmail.com

ABSTRACT

Rainfall is the primary source of surface and groundwater recharge. The state receives 91% of its annual rainfall due to the southwest monsoon, which is its principal rainy season. The contribution of winter, Pre-Monsoon, and Post-Monsoon season's rainfall amount to about 2%, 3%, and 4%, respectively, of the annual total rainfall. Therefore, the temporal and spatial distribution of rainfall plays a vital role not only in the agricultural community but also in water resources management. This study investigates the rainfall variability over Jharkhand by using past 116 years data from 1901 to 2016. The extreme annual one-day rainfall depths investigated by using normal frequency distribution. The period examined for extreme rainfall events is 1986–2016. The data showed that the annual daily maximum rainfall received at any time ranged between 34.2 mm (minimum) to 341.0 mm (maximum) over Jamshedpur, indicating a very large range of fluctuation during the period of study. The magnitude of one-day annual maximum rainfall corresponds to return period were investigated. The depth of maximum daily rainfall is found highest over Jamshedpur. The highest rainfall observed in a day is: 224.3 mm at Ranchi, 341.0 mm at Jamshedpur and 240.4 mm at Daltonganj during the study period. The return period of extremely heavy rainfall (greater than or equal to 204.5 mm) in a day is 6 years, and the probability of exceedance is found 18% at Jamshedpur. Heavy rainfall events with more

than 64.5 mm rain in a day was examined by using past 31 years daily rainfall data of Ranchi, Jamshedpur, and Daltonganj stations. To study the presence of a trend in rainfall, a widely used nonparametric Mann-Kendall test is applied. The linear trend line suggests that there is a decreasing trend in seasonal rainfall. The value of Kendall Score is found –2.82, which reveals that the decreasing trend in seasonal rainfall over Jharkhand is significant. An increasing trend is found in annual heavy rainy days over Jamshedpur, and the value of Kendall test statistics Z_s for Jamshedpur is +2.43, which reveals that the increasing trend in an annual number of heavy rainy days is significant at 5% significance level. However, no significant trend is found over Ranchi and Daltonganj.

30.1 INTRODUCTION

Jharkhand is located in the eastern region of India, and it is generously endowed with mineral wealth. It has some of the richest deposits of iron and coal in the world. Forests and woodlands occupy more than 29% of the state. Most of the state lies on the Chota Nagpur Plateau, which is the main source of the Koel, Damodar, Brahmani, Kharkai, and Subarnarekha rivers, whose upper watersheds lie within Jharkhand. Although the territory of Jharkhand holds a rich store of minerals; yet agriculture in Jharkhand is the mainstay for most of the tribal communities. In fact, about 80% of the total population is dependent on agriculture and allied activities for their livelihood. Rainfall is the primary source of surface and groundwater recharge.

The state receives 91% of its annual rainfall due to the southwest monsoon, which is its principal rainy season. The contribution of winter, pre-monsoon, and post-monsoon season's rainfall amount to about 2%, 3%, and 4%, respectively of the annual total rainfall. Therefore, the temporal and spatial distribution of rainfall plays a vital role not only in the agricultural community but also in water resources management.

Hydrological processes are usually regarded as stationary; however, there is growing evidence of trends, which may be related to anthropogenic influences and natural features of the climate system. Serious concerns are drawn on the catastrophic nature of floods, droughts, and storms, caused due to the significant variations in the regional climate including the rainfall pattern taking place on a regional level. The IPCC's (Intergovernmental Panel on Climate Change) fifth climate Assessment Repo (IPCC, 2013) shows that the globally averaged combined land and ocean surface temperature increased by 0.85°C, over the period 1880 to 2012. It is likely that in a warmer climate

heavy rainfall will increase and be produced by fewer more intense events. This could lead to longer dry spells and a higher risk of floods.

The studies of seasonal and annual rainfall on global and local scales suggest that the total rainfall is highly variable and extreme rainfall is highly variable over many regions of the world. Several studies have been made in the past to determine the presence of trend or variability in precipitation and temperature all over the globe. Trends in rainfall in the regional scale over India were investigated by Parthasarathy and Dhar (1974), where the trends in rainfall over 31 subdivisions of India were investigated using the sixty years data. Parthasarathy and Dhar (1974) witnessed positive trends over the central India and parts of Northeast and Northwest India (Mehfooz, 2005). Therefore, there is an urgent need to investigate the rainfall pattern of the state for making the long-term strategic plan to minimize or restore the ecosystem.

30.2 DATA AND METHODOLOGY

This study investigates the South West Monsoon rainfall variability and trend over Jharkhand state by using past 116 years (1901–2016) data. The year wise monthly and seasonal (JJAS) rainfall data has been taken from Meteorological Centre Ranchi & National Data Centre, India Meteorological Department. To investigate the trend a widely used nonparametric Mann-Kendall test is applied at 5% significance level. Daily rainfall data at three different stations distributed in Jharkhand with longtime series were used for heavy rainfall analysis. Period examined for heavy rainfall events is 1986–2016. The extreme annual one-day rainfall depths for selected return periods on the basis of frequency analysis were investigated. The days with more than 64.5 mm was considered as heavy rainy days. Yearly variations of a number of heavy rainy days analyzed correspond to each station.

In the extreme rainfall analysis, first of all, one-day maximum rainfall data were extracted for each year from daily data and tabulated for each selected stations. The annual one-day maximum rainfall data were analyzed by using a software package RAINBOW (Raes et al., 2006). In this study, a commonly used probability distribution functions namely: normal distribution is applied for frequency analysis. The main application of frequency distribution in water resource management involves the assignment of an exceedance probability P_e, of the design event. The average Probability of exceedance and return period is estimated by Weibull method (Weibull, 1939).

To bring out major aspects of rainfall variability and trend in time series data, the common nonparametric Mann-Kendall test is applied. The Mann-Kendall test (Kendall, 1975) is the most common one used in studying hydrologic time series trends. There are two advantages of using non-parametric test over parameter test. First, the non-parametric tests do not require the data to be normally distributed. Second, the test has low sensitivity to abrupt breaks due to inhomogeneous time series.

30.3 DATA ANALYSIS

The design and water management for agricultural activities, flood control system, etc. should be average and extreme rainfall pattern. The seasonal rainfall variability is an important parameter for the agricultural community and water resources management. The southwest monsoon season (JJAS) is a principal rainy season for Jharkhand.

30.3.1 MANN KENDALL TEST

It is a statistical test widely used for the analysis of the trend in climatological and in hydrologic time series. Mann-Kendall test had been formulated by Mann (1945) as a non-parametric test for trend detection, and the test statistic distribution had been given by Kendall (1975) for testing non-linear trend and turning point. According to this test, the null hypothesis H_0 assumes that there is no trend (the data is independent and randomly ordered) in precipitation and this is tested against the alternative hypothesis H_1, which assumes that there is a trend (increasing or decreasing).

The computational procedure for the Mann Kendall test considers the time series of n data points and x_i and x_j as two subsets of data where $i = 1, 2, 3, \ldots\ldots n-1$ and $j = i+1, i+2, i+3 \ldots\ldots n$. Each of the data point x_i is taken as a reference point which is compared with the rest of data points x_j. If a data value from a later time period is higher than a data value from an earlier time period, the statistic S is incremented by 1. On the other hand, if the data value from a later time period is lower than a data value sampled earlier, S is decremented by 1. The net result of all such increments and decrements yields the final value of S.

The Mann-Kendall S Statistic is computed as follows:

$$S = \sum_{i=1}^{n-1} \sum_{j=i+1}^{n} sgn\left(x_j - x_i\right) \tag{1}$$

where,

$$sgn\left(x_j - x_i\right) = \begin{cases} +1, \Delta x > 0 \\ 0, \Delta x = 0 \\ -1, \Delta x < 0 \end{cases}$$

For moderate (n about 10) or larger series lengths, the sampling distribution of the test static in equation (1) is approximately Gaussian, and if the null hypothesis (no trend) is true, this Gaussian null distribution will have zero mean. The variance of this distribution is depends on whether all the x's are distinct, or if some are repeated values. If there are no ties, the variance of the sampling distribution of S is

$$Var\left(S\right) = \frac{n\left(n-1\right)\left(2n+5\right)}{18} \tag{2}$$

Otherwise, the variance is

$$Var\left(S\right) = \frac{n\left(n-1\right)\left(2n+5\right) - \sum_{j=1}^{J} t_j \left(t_j - 1\right)\left(2t_j + 5\right)}{18}$$

where J indicates the number of groups of repeated values, and t_j is the number of repeated values in the j^{th} group.

At certain probability level H_0 is rejected in favor of H_1 if the absolute value of S equals or exceeds a specified value $S_{\alpha/2}$, where $S_{\alpha/2}$ is the smallest S which has the probability less than $\alpha/2$ to appear in case of no trend. A positive (negative) value of S indicates an upward (downward) trend.

The test statistic Z_s is used a measure of the significance of the trend. The test statistic Z_s is given by

$$Z_s = \begin{cases} \dfrac{S-1}{\left[Var\left(S\right)\right]^{1/2}}, S > 0 \\ \dfrac{S+1}{\left[Var\left(S\right)\right]^{1/2}}, S < 0 \end{cases} \tag{3}$$

Test statistic Z_s is used to test the null hypothesis, H_0. If $|Z_s|$ is greater than $Z_{\alpha/2}$, where α represents the chosen significance level (e.g., 5% with Z 0.025 = 1.96) then the null hypothesis is invalid implying that the trend is significant.

30.4 RESULTS

30.4.1 SOUTH-WEST MONSOON RAINFALL VARIABILITY

The mean rainfall observed over the state Jharkhand is 1084.6mm for the period of 116 years from 1901 to 2016 during South-West Monsoon season (JJAS). The seasonal rainfall varied between 1539.0 mm and 578.4 mm in the year 1971 and 2010, respectively. Standard deviation is 165.39 mm for the study period. Seasonal SW-Monsoon rainfall variability and trend over Jharkhand state is represented in Figure 30.1. The linear trend line suggests that there is a decreasing trend in seasonal rainfall. The value of Kendall Score is found –2.82, which reveals that the decreasing trend in seasonal rainfall over Jharkhand is significant at 95% confidence level.

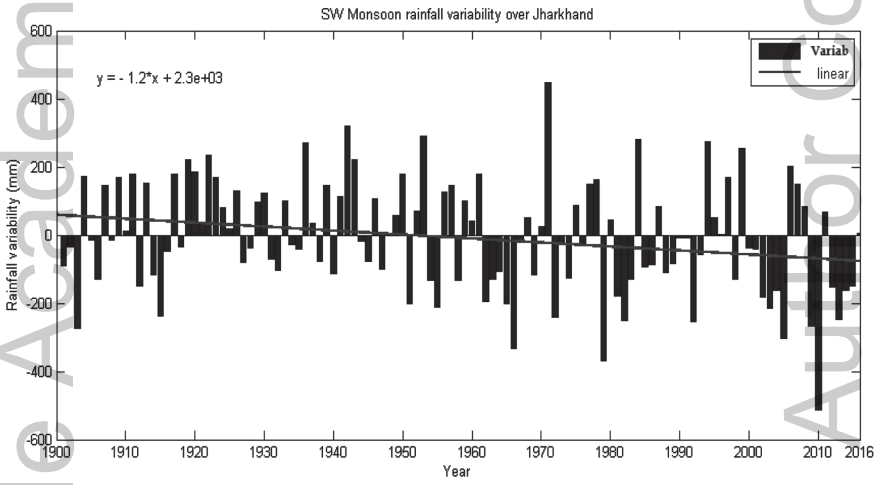

FIGURE 30.1 Southwest Monsoon rainfall variability over Jharkhand (1901–2016).

30.4.2 EXTREME RAINFALL ANALYSIS

Daily rainfall data at three different stations distributed in Jharkhand were analyzed for extreme rainfall analysis for the period of 1986–2016. Annual one-day maximum rainfall data extracted from daily rainfall data of Ranchi, Jamshedpur, and Daltonganj stations. Box plot is shown in Figure 30.2.

Particular rainfall depths that can be expected for a specific period is called the return period, and it is a vital parameter for the management of irrigation and flood control system. Return period for a station is obtained

by using frequency analysis of longtime series rainfall data. In the frequency analysis of extreme rainfall events, first of all, one-day maximum rainfall data extracted for each year from daily data. In this study, the normal distribution is applied for frequency analysis. The average probability of exceedance and return period is estimated by Weibull method (Weibull, 1939).

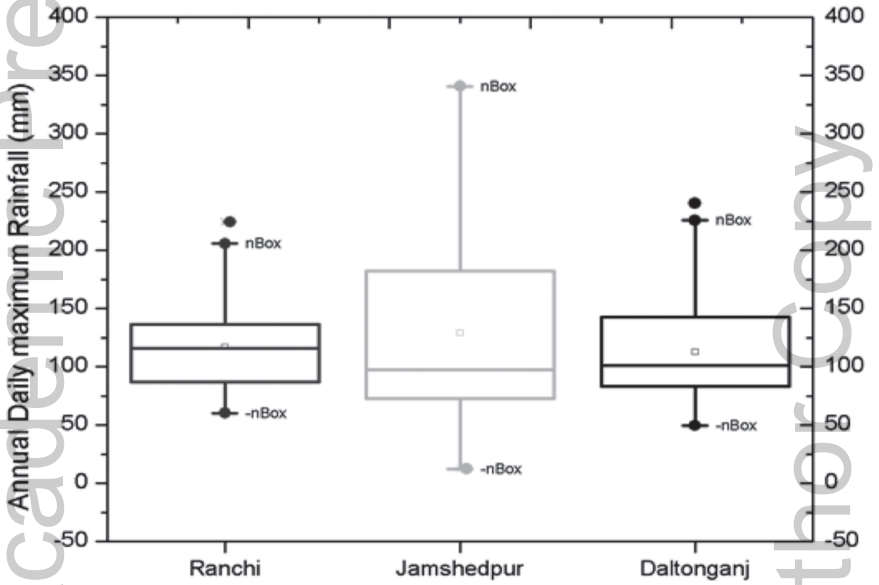

FIGURE 30.2 Box plot of annual daily maximum rainfall (1986–2016).

Weibull estimates the probability of exceedance as:

$$P_e = \frac{r}{n+1}$$

where, r is the rank number and n is the number of observations.

The return period T in years is related to the annual exceedance probability.

$$T = \frac{1}{P_e}$$

Table 30.1 represents the probability of exceedance and return period for all the stations. The return period of extremely heavy rainfall (greater than or equal to 204.5 mm) in a day is 6 years, and the probability of exceedance is about 18% at Jamshedpur.

TABLE 30.1 Probability of Exceedance and Return Period (1986–2016)

Probability of Exceedance (%)	Return Period (Year)	Rainfall (mm)		
		Ranchi	Jamshedpur	Daltonganj
—	25	180.6	267.9	194.7
10	10	163.6	230.7	172.8
20	5	147.6	195.9	152.2
30	3.33	136.1	170.8	137.4
40	2.5	126.3	149.3	124.8
50	2	117.1	129.3	113
60	1.67	108	109.3	101.1
70	1.43	98.2	87.9	88.5
80	1.25	86.7	62.7	73.7
90	1.11	70.7	27.9	53.1

For estimation of the probability of exceedance of annual one-day maximum rainfall, the normal distribution is used in this study. A probability distribution and counts of extreme rainfall events are plotted in Figure 30.3.

To analyses the trend in heavy rainfall events, annual heavy rainy days (more than 64.5 mm) were estimated from daily rainfall data for all the study stations. Highest 13 heavy rainy days in a year were found during 2016 at Jamshedpur. Variability of annual heavy rainy days is represented in Figure 30.4.

The study reveals that there is an increasing trend in annual heavy rainy days over Jamshedpur however; no significant trend is seen over Ranchi and Daltonganj. The linear trend line suggests that there is an increasing trend in annual heavy rainy days over Jamshedpur. The Kendall score for Daltonganj is +2.43 which reveals that the increasing trend in a number of heavy rainy days is significant at 5% significance level. A slight linear decreasing trend in annual heavy rainy days is observed over Ranchi and Daltonganj; however, Man-Kendall suggests that the decreasing trend is not significant. Variations of annual heavy rainy days are represented in Figure 30.5.

30.4.3 NON-PARAMETRIC TESTS

In this study, a non-parametric Mann-Kendall test is applied to investigate the trend in seasonal rainfall and extreme events over Jharkhand. The value of Kendall score for South West Monsoon rainfall over Jharkhand is

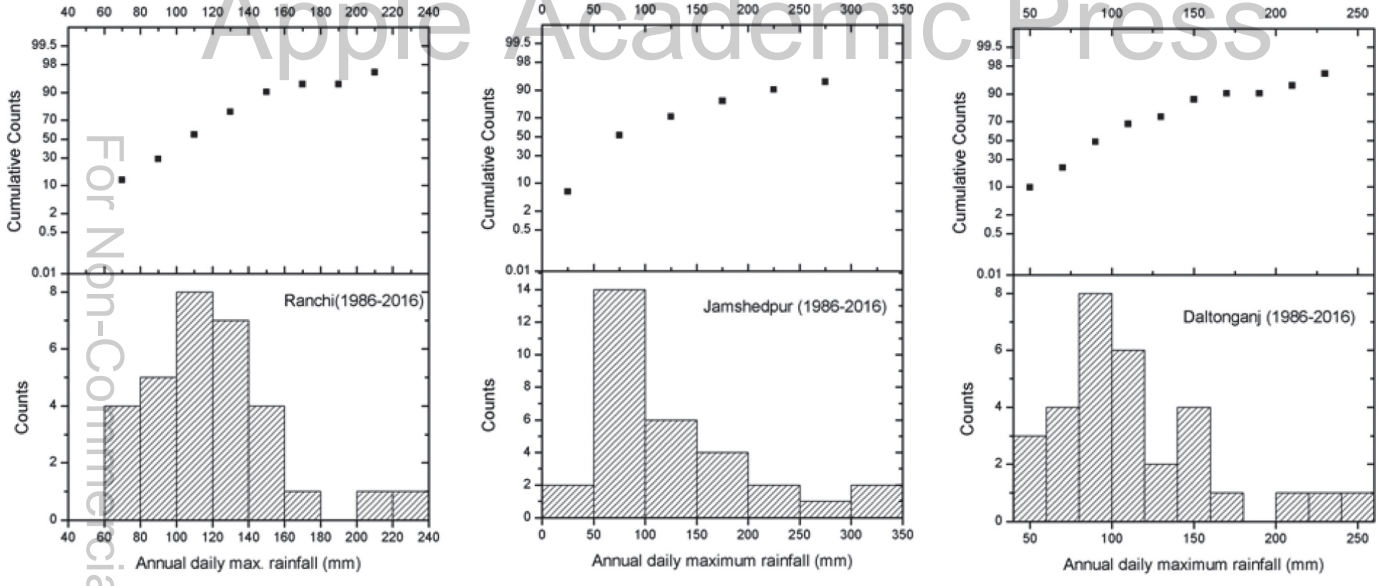

FIGURE 30.3 Cumulative probability and frequency count of annual daily maximum rainfall.

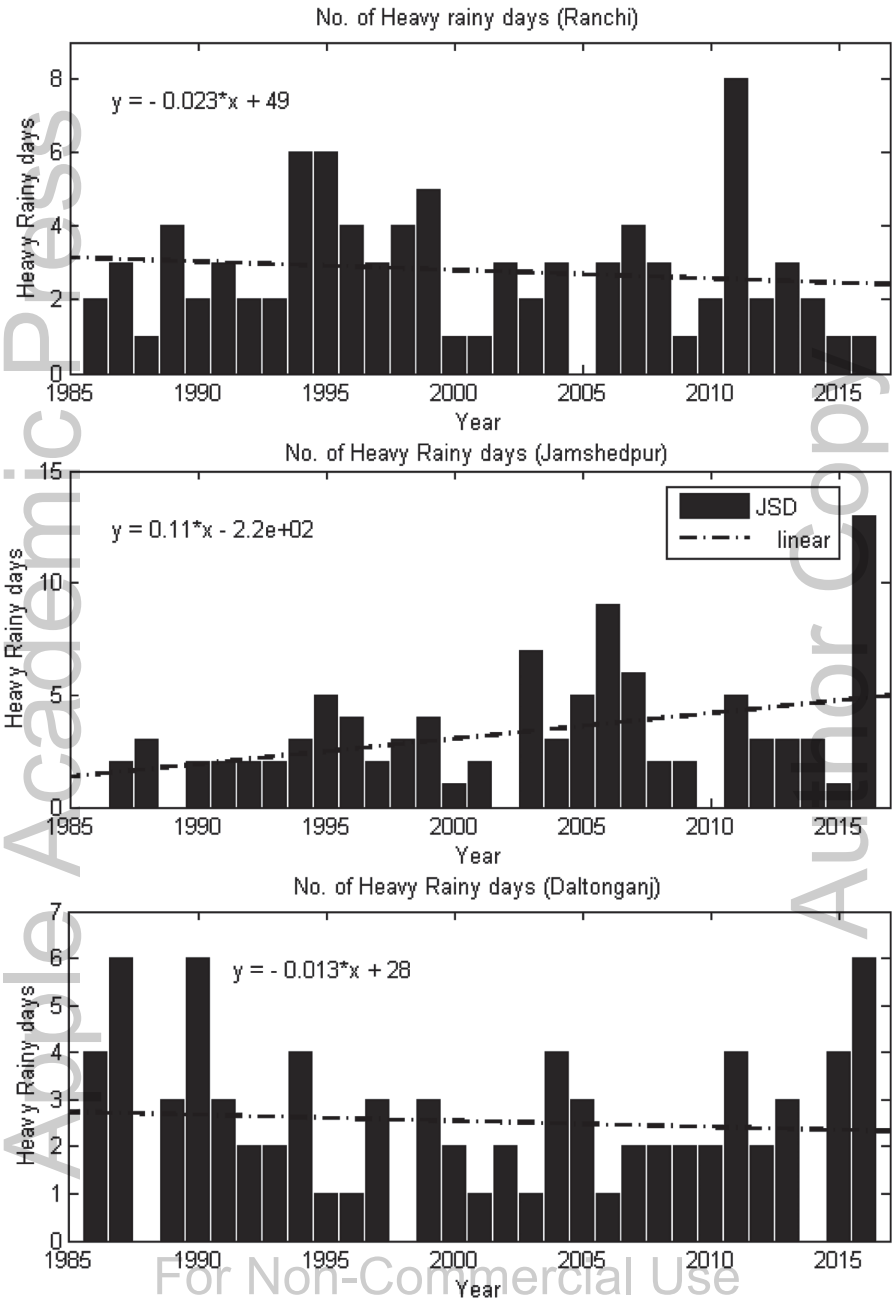

FIGURE 30.4 Annual variation of heavy rainy days. The dashed line shows a linear trend line.

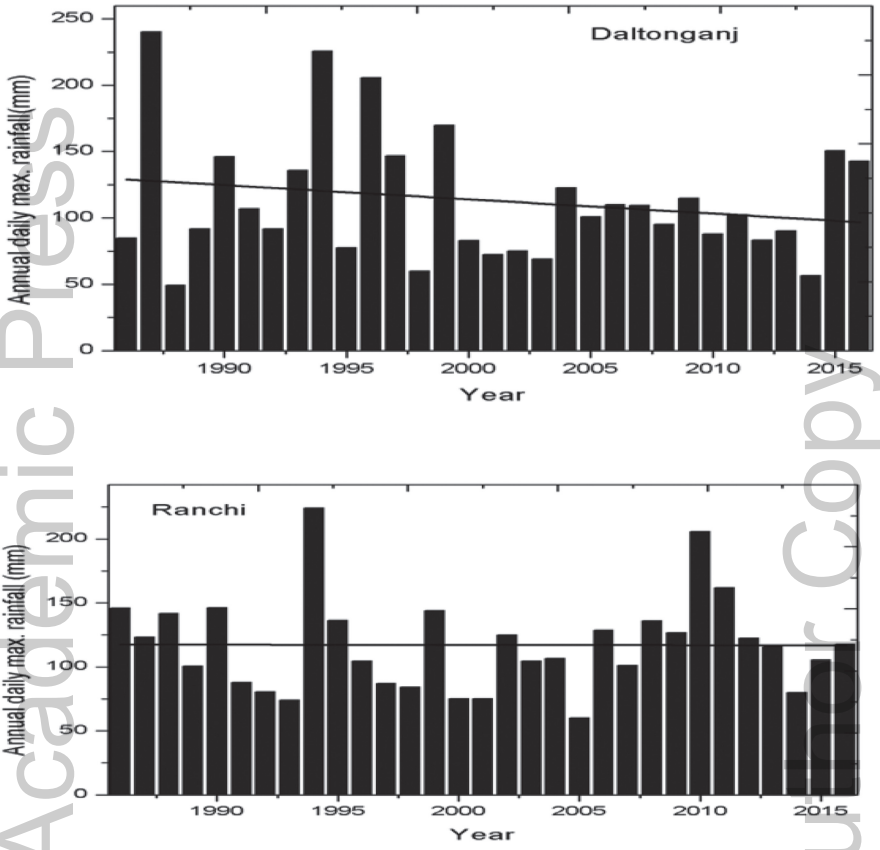

FIGURE 30.5 Variation of annual daily maximum rainfall. The straight line shows a linear trend line.

–1082 and test statistics Z_s is –2.58, which reveals that there is a decreasing trend in seasonal rainfall at significance level 5%. The test is also applied for extreme rainfall events correspond to the stations. The Kendal score of annual daily maximum rainfall is negative over Ranchi and Daltonganj. The negative value of Kendall score represents a decreasing trend; however, the decreasing trend is not significant. The value of Kendall score of annual one-day maximum rainfall over Jamshedpur is 144 and test statistics Z_s is 2.43, which reveals that the increasing trend in extreme rainfall events is significance at level 5%. No other parameters show a significant trend. Various Kendall parameters are shown in Table 30.2.

TABLE 30.2 Mann-Kendall Parameters

Sr. No.	Particulars	Variable	Kendall Score 'S'	Test Statistic Z_s	Hypothesis Test
1.	Jharkhand	SW Monsoon rainfall variability (1901–2016)	–1082	–2.58	H_o accepted
2.	Ranchi	Annual daily max. rainfall (1986–2016)	–13	–0.20402	H_o rejected
		Annual heavy rainy days (1986–2016)	–61	–1.04558	H_o rejected
3.	Jamshedpur	Annual daily max. rainfall (1986–2016)	144	2.432245	H_o accepted
		Annual heavy rainy days (1986–2016)	103	1.77264	H_o rejected
4.	Daltonganj	Annual daily max. rainfall (1986–2016)	–28	–0.45897	H_o rejected
		Annual heavy rainy days (1986–2016)	–14	–0.22628	H_o rejected

30.5 CONCLUSIONS

The depth of maximum daily rainfall is found highest over Jamshedpur. The highest rainfall observed in a day is: 224.3 mm at Ranchi, 341.0 mm at Jamshedpur and 240.4 mm at Daltonganj during the study period. The return period of extremely heavy rainfall (greater than or equal to 204.5 mm) in a day is 6 years, and the probability of exceedance is found 18% at Jamshedpur. The value of Kendall Score is found –2.82, which reveals that the decreasing trend in seasonal rainfall over Jharkhand is significant. An increasing trend is found in annual heavy rainy days over Jamshedpur, and the value of Kendall test statistics Z_s for Jamshedpur is +2.43, which reveals that the increasing trend in a number of heavy rainy days is significant at 5% significance level. However, no significant trend is found over Ranchi and Daltonganj.

ACKNOWLEDGMENT

The authors are grateful to Dr. K. J. Ramesh, Director General of Meteorology, India Meteorological Department for continuously encourage and his support. Authors express their sincere thanks to all staff members and officers of Meteorological Centre Ranchi for their kind and sincere

assistance in preparing this paper. The authors are also grateful to Dr. Sanjiv Bandyopadhyay, DDGM, RMC Kolkata for valuable guidance and support.

KEYWORDS

- **extreme events**
- **Mann-Kendall**
- **normal frequency distribution**
- **probability distribution**
- **rainfall variability**
- **return period**

REFERENCES

IPCC (2013). Summary for Policymakers. In: Stocker, T. F., Qin, D., Plattner, G.-K., Tignor, M., Allen, S. K., Boschung, J., Nauels, A., Xia, Y., Bex, V., & Midgley, P. M., (eds.), *Climate Change, the Physical Science Basis. Contribution of Working Group I to the Fifth Assessment Report of the Intergovernmental Panel on Climate Change*. Cambridge University Press, Cambridge, United Kingdom and New York, NY, USA.

Kendall, M. G., (1975). *Rank Correlation Methods* (4th edn.). Charles Griffin, London, U.K.

Mann, H. B., (1945). Non-parametric tests against trend. *Econometrica*, *33*, 245–259.

Mehfooz, A., Joardar, D., & Loe, B. R., (2005). Variability of South monsoon over Rajasthan and Kerala, *Mausam*., *56*(3), 593–600.

Parthasarathy, B., & Dhar, O. N. (1974). Secular variations of regional rainfall over India. *Quart. J. R. Met. Soc.*, *100*, 245–257.

Raes, D., Willems, P., & Baguidi, G. F., (2006). RAINBOW – a software package for analyzing data and testing the homogeneity of historical data sets. *Proceedings of the 4th International Workshop on 'Sustainable Management of Marginal Drylands.'* Islamabad, Pakistan. Fourth Project Workshop Islamabad Pakistan (27–31 January 2006), pp. 41–55.

Scnetzler, A. E., Market, P. S., & Zeitler, J. W. (2008). *Analysis of Twenty Five Years of Heavy Rainfall Events in the Texas Hill Country.* MS Thesis, University of Missouri.

Zain, Al-Houri, Abbas Al-Omari, & Osama, S., (2014). "Frequency analysis of Annual one-day Maximum rainfall at Amman Zarqa Basin, Jordan." *Civil and Environmental Research*, *6*(3), 44–57.

CHAPTER 31

VARIATION OF CLIMATOLOGICAL PARAMETERS INSIDE AND OUTSIDE NATURALLY VENTILATED POLYHOUSES

RAVISH CHANDRA[1] and P. K. SINGH[2]

[1]*Central Agricultural University, Pusa, Samastipur (Bihar), India, E-mail: ravish.cae@gmail.com*

[2]*Department of Irrigation and Drainage Engineering, College of Technology, Govind Ballabh Pant University of Agriculture and Technology, Pantnagar, India*

ABSTRACT

A field experiment was conducted to study the various climatological parameters taken under the naturally ventilated polyhouse and outside polyhouse during 19th October 2013 to 10th April 2014. Two types of polyhouses, Double Span Naturally Ventilated Polyhouse (DS NVPH) and Walking Tunnel Type Polyhouse were selected for the study. Both the polyhouses were planted with capsicum (*Capsicum annuum L.*). The climatic parameters such as temperature, and solar radiation were measured at 09:00 hrs, and 16:00 hrs. The comparisons were made with the ambient conditions prevailing in outside the open field. Solar intensity was found highest in the open field condition followed by solar radiation inside Walking Tunnel Naturally Ventilated Polyhouse (WT NVPH) and then solar radiation received by DS NVPH. The percentage of solar radiation received by the DS NVPH ranges from 38.40% to 72.13% with an average value of 50.86% and WT NVPH ranges from 55.58% to 87.07% with an average value of 70.58%, of the solar radiation received outside field condition. The maximum and minimum temperatures were higher in WT NVPH followed by DS NVPH and then open field condition. It was observed that the maximum temperature in DS NVPH varied from 16 to 43.6°C with an average value of 33.4°C and

minimum temperature varied from 5.5 to 22.5°C with an average value of 14°C. Similarly, the maximum temperature in WT NVPH varied from 17 to 44°C with an average value of 34.8°C and minimum temperature varied from 6 to 23.5°C with an average value of 15.4°C.

31.1 INTRODUCTION

Among these protective cultivation practices, greenhouse/polyhouse cum rain shelter is useful for the off-season cultivation of vegetables. The greenhouse is generally covered by transparent or translucent material such as glass or plastic. The greenhouse covered with a simple plastic sheet is termed as polyhouse. The greenhouse generally reflects back 43% of the net solar radiation incident upon it allowing the transmittance of the "photosynthetically active solar radiation" in the range of 400–700 Nm wavelength. The sunlight admitted to the greenhouse is absorbed by the crops, floor, and other objects. These objects, in turn, emit longwave thermal radiation in the infrared region for which the glazing material has lower transparency. As a result, the solar energy remains trapped in the greenhouse, thus raising its temperature. This phenomenon is called the "Greenhouse Effect." This condition of a natural rise in greenhouse air temperature is utilized in the cold regions to grow crops successfully. However in the summer season due to the above-stated phenomenon ventilation and cooling is required to maintain the temperature inside the structure well below 35C. The ventilation system can be natural or a forced one. Greenhouses provide protection against biotic and abiotic stresses and ensure high quality produce (Peet and Welles, 2005). Low cost naturally ventilated polyhouse offers a great scope for the off-season cultivation of capsicum for round the year supply in the cold climatic areas of India. A greenhouse is a framed structure made of GI Pipe/MS angle/Wood/Bamboo and covered with transparent material or translucent material fixed to the frame with grippers. It has control/monitoring equipment, which is considered necessary for controlling environmental factors such as temperature, light, relative humidity, etc., which is considered necessary for maximizing plant growth and productivity. Thus, the greenhouse is an enclosed area, in which crops are grown under partially or fully controlled conditions. The cladding material is of plastic (polyethylene) film and acts like a selective radiation filter that allows solar radiation to pass through it but traps thermal radiation emitted by the inside objects to create a greenhouse effect. Greenhouse technology since it protects the crop from adverse weather conditions, attack from insects, pests, diseases,

and thus helps in increasing yield and quantity. At the same time since the inside environment remains under control, carbon dioxide released by the plants during the night is consumed by the plants itself in the morning. Thus plants get about 8–10 times more food than the open field condition. The regulation of temperature, ventilation, adjustment of the amount of entering sunlight, to provide soil moisture, fertilizer, and even facilitate pollination are important for the crop growth. Environmental control systems in controlled environment plant production facilities (including greenhouses and growth chambers) traditionally focus on maintaining the indoor climate according to pre-defined set points (Fleisher, 2002). It is necessary to know the climatic conditions inside and outside of the greenhouse to control the favorable climate for the proper growth of the particular crop. So the objective was to study the various climatological parameters inside and outside the polyhouse.

31.2 MATERIALS AND METHODS

A field experiment was conducted to study the various climatological parameters taken under the naturally ventilated polyhouse and outside polyhouse during 19th October 2013 to 10th April 2014. The study was conducted at experimental field of the Department of Irrigation and Drainage Engineering, College of Technology, G. B. Pant University of Agriculture and Technology, Pantnagar. Two types of polyhouses, Double Span Naturally Ventilated Polyhouse (DS NVPH) and Walking Tunnel Type Polyhouse were selected for the study. Both the polyhouses were planted with capsicum (*Capsicum annuum L.*). The climatic parameters such as temperature, and solar radiation were measured at 09:00 hrs, and 16:00 hrs. The observations of maximum and minimum temperature were taken from Crop Research Centre, 0.5 km away from the experimental field.

31.3 RESULTS AND DISCUSSION

31.3.1 TEMPERATURE

The daily variation of maximum and minimum temperature in DS NVPH, Walking Tunnel Naturally Ventilated Polyhouse (WT NVPH) and open field condition are shown in Figure 31.1. The analysis revealed that the maximum temperature was higher in WT NVPH followed by DS NVPH and then open

field condition. The minimum temperature followed the same trend. It was observed that the maximum temperature in DS NVPH varied from 16 to 43.6C with an average value of 33.4°C and minimum temperature varied from 5.5 to 22.5°C with an average value of 14°C. Similarly, the maximum temperature in WT NVPH varied from 17 to 44°C with an average value of 34.8°C and minimum temperature varied from 6 to 23.5°C with an average value of 15.4°C. The maximum temperature was recorded on 8th April 2014, and the minimum temperature was recorded on 4th January 2014.

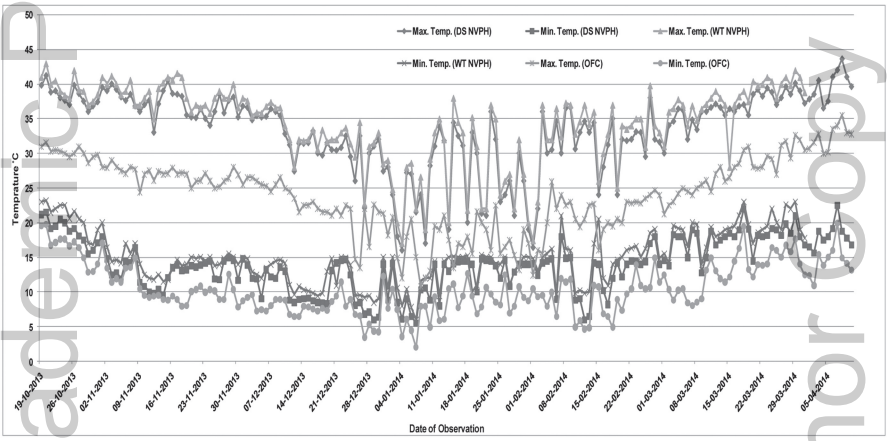

FIGURE 31.1 Daily variation of maximum and minimum temperature in DS NVPH, WT NVPH, and open field condition.

The analysis shows that the lowest maximum temperature inside DS NVPH was recorded during the 4th segment, i.e., from 1st January 2014 to 31st January 2014 with an average maximum temperature value of 26.03°C and the highest maximum temperature was recorded during the last segment, i.e., from 1st April 2014 to 30th April 2014 with an average maximum value of 39.8°C (Table 31.1). When comparison was made for minimum temperature it was found that the lowest minimum temperature inside DS NVPH was recorded during the 3rd segment, i.e., from 1st December 2014 to 31st December 2014 with an average minimum value of 10.64°C and the highest minimum temperature was recorded during the first segment, i.e., from 19th to 31st October 2014 with an average minimum value of 18.8°C. The similar trend was observed for WT NVPH. The lowest maximum temperature inside WT NVPH was recorded during the 4th segment, i.e., from 1st January 2014 to 31st January 2014 with an average maximum temperature value of 27.47°C and the highest maximum temperature was recorded during the last segment,

TABLE 31.1 Maximum and Minimum Temperature in Different Time Segments in DS NVPH, WT NVPH and in Open Field Condition

Time segment		Max. Temp. (°C) DS NVPH	Min. Temp. (°C) DS NVPH	Max. Temp. (°C) WT NVPH	Min. Temp. (°C) WT NVPH	Max. Temp.(°C) Open field	Min. Temp. (°C) Open field
19–31	Lowest	36.00	15.50	37.00	16.80	28.60	12.80
1 October 2013	Highest	41.20	21.50	43.00	23.20	31.60	19.70
	Average	**38.27**	**18.78**	**39.47**	**20.78**	**30.16**	**16.38**
1–30 November 2013	Lowest	33.00	9.50	35.00	11.50	24.40	7.80
	Highest	40.50	18.00	41.60	20.00	29.00	17.00
	Average	**37.22**	**13.07**	**38.67**	**14.42**	**26.88**	**10.55**
1–31 December 2013	Lowest	22.10	6.00	22.70	8.50	13.50	3.40
	Highest	36.80	14.80	38.00	15.00	26.50	12.20
	Average	**31.83**	**10.64**	**32.96**	**11.97**	**22.58**	**7.66**
1–31 January 2014	Lowest	16.00	5.50	17.00	6.00	10.80	2.00
	Highest	36.00	14.80	38.00	15.30	22.50	12.60
	Average	**26.03**	**11.89**	**27.47**	**12.73**	**16.96**	**8.09**
1–28 February 2014	Lowest	16.40	6.00	17.40	9.70	12.40	4.60
	Highest	38.00	18.00	39.80	21.00	25.90	14.90
	Average	**31.19**	**12.94**	**32.83**	**14.78**	**21.06**	**9.17**
1–31 March 2014	Lowest	30.00	12.80	28.00	14.00	21.20	8.00
	Highest	40.10	22.00	42.00	23.00	32.60	19.40
	Average	**36.59**	**17.75**	**37.79**	**19.06**	**27.35**	**13.01**
1–10 April 2104	Lowest	36.50	15.60	37.00	17.60	30.00	10.90
	Highest	43.60	22.50	44.00	23.50	35.50	19.90
	Average	**39.80**	**18.15**	**40.96**	**20.26**	**32.41**	**14.54**

i.e., from 1st April 2014 to 30th April 2014 with an average maximum value of 40.9°C. The similar comparison for minimum temperature revealed that the lowest minimum temperature inside WT NVPH was recorded during 3rd segment, i.e., from 1st December 2014 to 31st December 2014 with an average minimum value of 11.97°C and the highest minimum temperature was recorded during the first segment, i.e., from 19th to 31st October 2014 with an average minimum value of 20.8°C. The maximum temperature decreases from 1st segment to the 4th segment and then increases up to the last segment. The minimum temperature first decreases from 1st segment to 3rd segment and then increases up to the last segment in both DS NVPH and WT NVPH.

31.3.2 SOLAR INTENSITY

The daily variation of solar intensity recorded at 9:00 AM and 2:00 PM in DS NVPH, WT NVPH, and open field condition are shown in Figures 31.2 and 31.3. The analysis revealed that the solar intensity at 9:00 AM was higher in WT NVPH followed by DS NVPH.

The DS NVPH receives solar radiation ranging from 33.33% to 67.14% with an average value of 47.56% of total solar radiation received in open field condition. On the other hand, WT NVPH receives solar radiation ranging from 40.15% to 86.10% with an average value of 69.68% of total solar radiation received in open field condition. The maximum solar intensity observed for WT NVPH was 732 Klux on 9th April 2014 and minimum was 2.70 Klux on January 3, 2014. Similarly, the maximum value for DS NVPH was 59.5 Klux on April 11, 2014, and minimum was 2.0 Klux on January 3, 2014.

The similar trend was observed for solar intensity measured at 2:00 PM. The figure revealed that the solar intensity was highest in the open field condition followed by solar radiation inside WT NVPH and then solar radiation received by DS NVPH. The percentage of solar radiation received by the DS NVPH ranges from 38.40% to 72.13% with an average value of 50.86% and WT NVPH ranges from 55.58% to 87.07% with an average value of 70.58%, of the solar radiation received outside field condition. The maximum solar intensity observed for WT NVPH was 784 Klux on March 21, 2014, and the minimum was 6.8 Klux on January 30, 2014, when measurements were made at 2:00 PM (Figure 31.3). Similarly, the maximum value for DS NVPH was 66.5 Klux on March 21, 2014, and the minimum was 4.8 Klux on January 31, 2014. When comparison was made between solar radiation received at 9:00 AM and 2:00 PM inside DS NVPH, it was found that the minimum

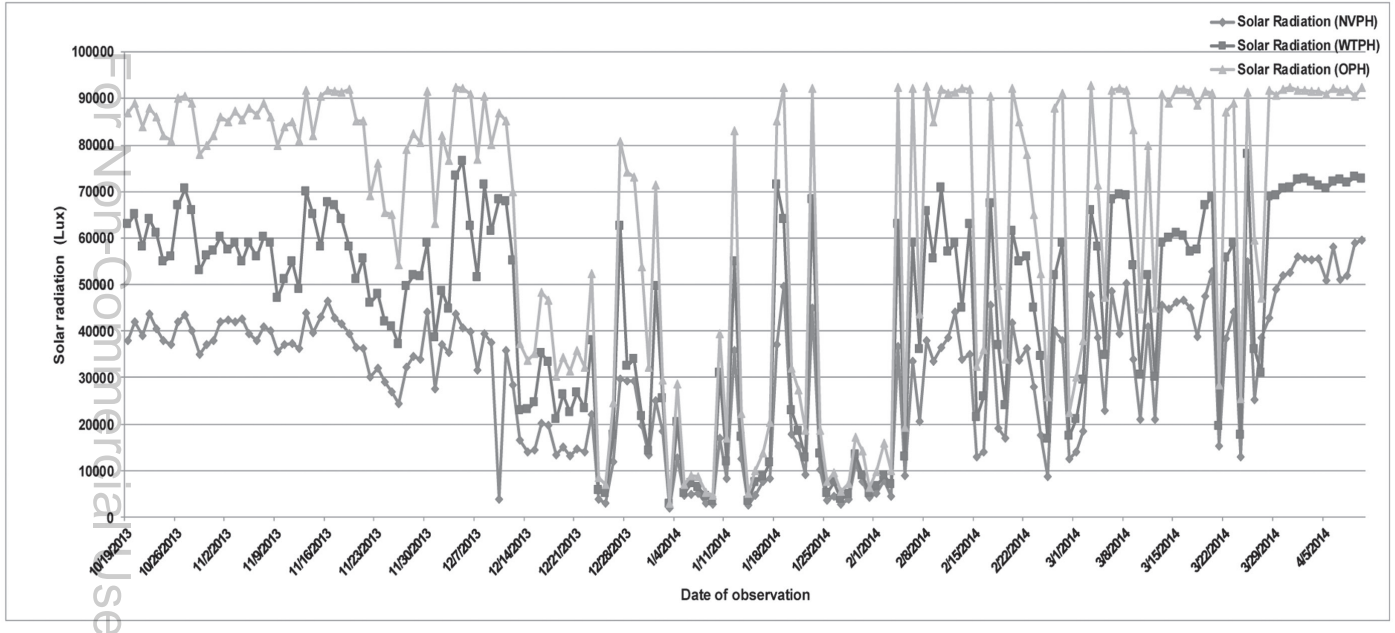

FIGURE 31.2 Daily variations in solar intensity at 9:00 AM in Double Span NVPH, Walking Tunnel NVPH and open field condition.

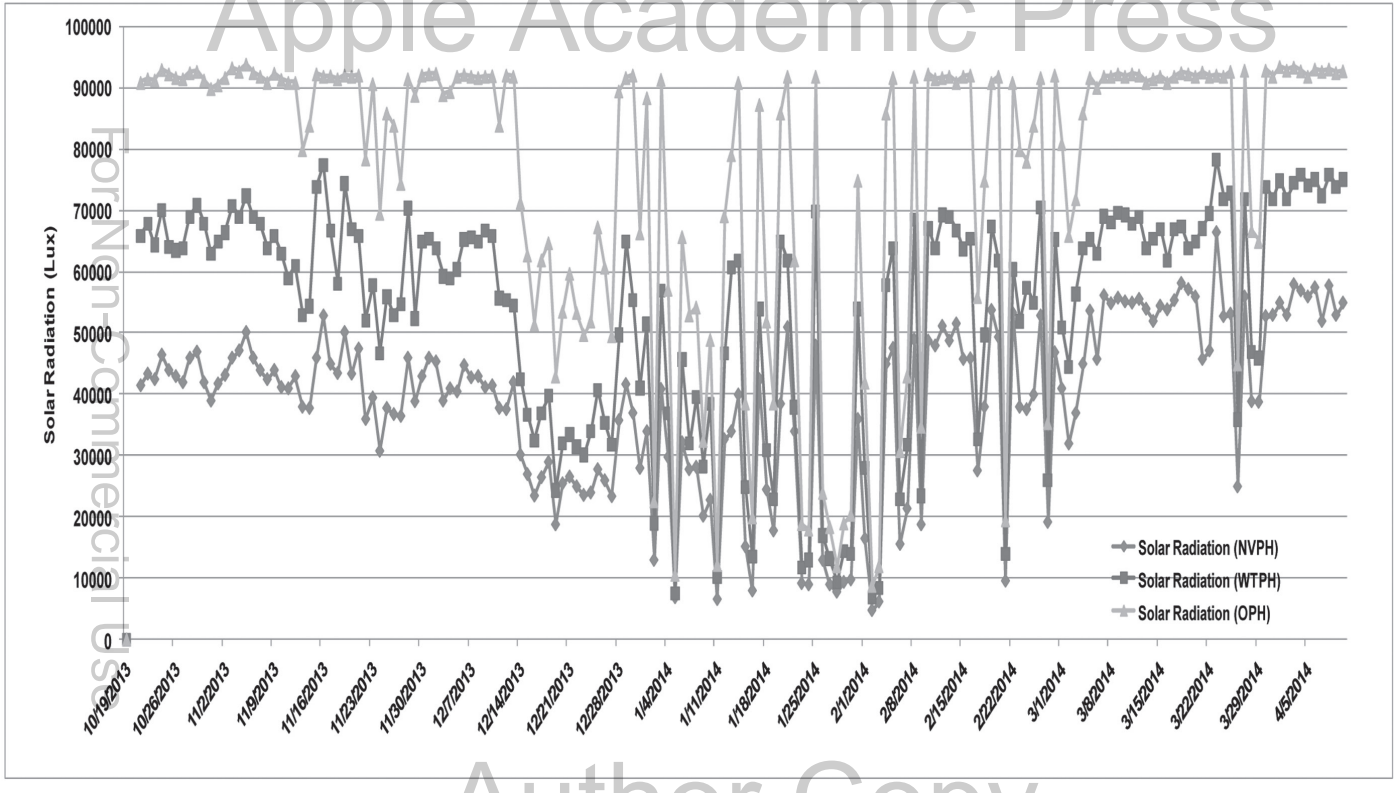

FIGURE 31.3 Daily variation in solar intensity at 2:00 PM in Double Span NVPH, Walking Tunnel NVPH and open field condition.

TABLE 31.2 Solar Radiation Received in Different Time Segments in DS NVPH, WT NVPH and in Open Field Condition

Time segment		Solar Radiation (Lux) inside DS NVPH (9:00 AM)	Solar Radiation (Lux) inside WT NVPH (9:00 AM)	Solar Radiation (Lux) outside (9:00 AM)	Solar Radiation (Lux) inside DS NVPH (2:00 PM)	Solar Radiation (Lux) inside WT NVPH (2:00 PM)	Solar Radiation (Lux) outside (2:00 PM)
19–31	Minimum	35000.00	53000.00	78000.00	39000.00	63000.00	90000.00
2 October	Maximum	43600.00	70500.00	90500.00	47000.00	71000.00	93100.00
3 2013	Average	**39515.38**	**60915.38**	**85115.38**	**43223.08**	**66376.92**	**91700.00**
1–30	Minimum	24450.00	37200.00	54300.00	30800.00	46800.00	69600.00
November 2013	Maximum	46500.00	70000.00	91900.00	52900.00	77500.00	94000.00
	Average	**37688.33**	**55026.67**	**82943.33**	**42870.00**	**63070.00**	**89043.33**
1–31	Minimum	2900.00	5000.00	7000.00	13000.00	19000.00	22600.00
December 2013	Maximum	43750.00	78000.00	92400.00	44800.00	66900.00	92300.00
	Average	**24248.39**	**39174.19**	**56767.74**	**32180.65**	**46387.10**	**72641.94**
1–31	Minimum	2000.00	2500.00	3000.00	4800.00	6800.00	8800.00
January	Maximum	49700.00	71500.00	92400.00	51000.00	70000.00	92000.00
2014	Average	**12814.52**	**19045.16**	**26196.77**	**23422.58**	**33190.32**	**48083.87**
1–28	Minimum	4550.00	6500.00	9800.00	6200.00	8500.00	12000.00
February	Maximum	45500.00	70800.00	92600.00	53800.00	70600.00	92400.00
2014	Average	**26482.14**	**42228.57**	**62957.14**	**38682.14**	**51850.00**	**73800.00**
1–31	Minimum	13000.00	17500.00	25400.00	25000.00	36000.00	45000.00
March	Maximum	55000.00	73500.00	92800.00	66500.00	78400.00	93000.00
2014	Average	**36707.69**	**51334.62**	**73703.85**	**51569.23**	**65373.08**	**88234.62**
1–10	Minimum	50900.00	70500.00	90600.00	52000.00	72000.00	92000.00
April	Maximum	59500.00	73200.00	92400.00	60800.00	76000.00	93800.00
2104	Average	**54775.00**	**71883.33**	**91725.00**	**56241.67**	**74541.67**	**93041.67**

values increased by 15.25%, the maximum value increased by 7.42% and the average value increased by 6.95%. The higher amount of radiation received in WT NVPH might be due to lower control height compared to DS NVPH. Besides this, the inner surface area of WT NVPH is lesser compared to DS NVPH, and hence probably fewer energy losses were there in heating the system. The other researchers reported on similar results for different kind of playhouses (Dhandare et al. 2006, Dhandare et al. 2008). Table 31.2 shows that the minimum average radiation inside DS NVPH was received during the 4th segment, i.e., from 1st January 2014 to 31st January 2014 with a value of 12.8 Klux and the maximum average radiation was received during the last segment, i.e., from 1st April 2014 to 30th April 2014 with a value of 54.8 Klux, when measurement was made at 9:00 AM (Table 31.2). The analysis revealed that average solar radiation was higher for WT NVPH compared to DS NVPH. The minimum average radiation inside WT NVPH was received during the 4th segment, i.e., from 1st January 2014 to 31st January 2014 with a value of 19.0 Klux and the maximum average radiation was received during the last segment, i.e., from 1st April 2014 to 30th April 2014 with a value of 71.8 Klux, when measurement was made at 9:00 AM. A similar trend was found when measurements were made at 2:00 PM. The average solar radiation based on time segment shows that the average solar radiation first decreases from the 1st segment up to 4th segment and then increases gradually in both DS NVPH and WT NVPH. The study suggests that proper ventilation is required in the 1st segment, 2nd segment, 6th and last segment of the study. The study also suggests that there is a need for increasing the photoperiod and strength of radiation in the month of January.

31.4 CONCLUSION

The maximum and minimum temperatures were observed higher in WT NVPH followed by DS NVPH and then open field condition. The solar radiation was observed high in the open field followed by WT NVPH than DS NVPH, also observed high at 16:00 hrs than 09:00 hrs. The percentage of solar radiation received by the DS NVPH ranges from 38.40% to 72.13% with an average value of 50.86% and WT NVPH ranges from 55.58% to 87.07% with an average value of 70.58%, of the solar radiation received outside field condition.

KEYWORDS

- **double span naturally ventilated poly-house**
- **walking tunnel naturally ventilated poly-house**

REFERENCES

Dhandare, K. M., (2006). *Response of Capsicum (Capsicum annuum L.) to Cyclic Irrigation and Fertigation Under Environmental Controlled and Naturally Ventilated Polyhouse* (p. 152). MTech thesis, Department of Irrigation and Drainage Engineering, G. B. Pant University of Agriculture and Technology, Pantnagar, India.

Dhandare, K. M., Singh, K. K., Singh, P. K., Singh, M. P., & Bayissa, G., (2008). Variation of climatological parameters under environmental controlled and naturally ventilated polyhouses. *Pantnagar. Journal of Research, 6*(1), 142–147.

Fleisher, D. H., (2002). Preliminary analysis of plant response to environmental disturbances in controlled environments. *ASAE Paper No: 024076 St. Joseph, Mich.*

Peet, M. M., & Welles, G. W. H., (2005). In: Heuvelink, E., (ed.), *Greenhouse Tomato Production (In) Tomatoes* (pp. 257–304). CABI Publishing, Wallingford, U.K.

CHAPTER 32

DESIGN OF A RAIN WATER HARVESTING STRUCTURE AT ALLAHABAD MUSEUM, ALLAHABAD CITY, U.P., INDIA

VIVEK TIWARI[1], SARIKA SUMAN[2], and H. K. PANDEY[3]

[1]*Banaras Hindu University, Varanasi, India,*
E-mail: viveektiwary@gmail.com

[2]*Banaras Hindu University, Varanasi, India*

[3]*Department of Civil Engineering, MNNIT Allahabad, India*

ABSTRACT

A study has been conducted to design the Rain Water Harvesting system at Allahabad Museum. The Allahabad Museum is centrally located in Allahabad city in the picturesque of Chandrashekhar Azad Park and is a monument of national importance since the pre-historic era. The study was aimed to carry out the assessment of The Allahabad Museum's potential towards Roof Top Rain Water Harvesting (RTRWH) and to design an effective groundwater recharge structure for its main building which can serve as the model site for the scientific study and inspiration to the visitors, apart from the groundwater recharge. It has a sprawling green campus of 21850 m^2 and lies under the zone in which underground water level is declining at the rate of 0.49 m/year since last few years. It receives 950 mm of annual rainfall every year. It is estimated that about 3568.34 m^3 volume of water can be contributed towards groundwater recharging through RTRWH structure at the main building of The Allahabad Museum. It was observed that the Allahabad Museum has enough potential and resources available which can significantly contribute towards the groundwater recharge through cost-effective techniques.

32.1 INTRODUCTION

Groundwater, which is the source for more than 85% of India's rural domestic water requirements, 50% of its urban water requirements and more than 50% of its irrigation requirements is depleting fast in many areas due to its large-scale withdrawal for various sectors (CGWB, 2006). In India even though an average rainfall is 1100 mm there is a scarcity of water that results in water crisis (Hajare et al., 2003). There have been continued efforts in India for development of groundwater resources to meet the increasing demands of water supply. The artificial recharge has now been accepted worldwide as a cost-effective method to augment groundwater resources. Groundwater sources are depleting in quantity due to unregulated extraction of water and reduced replenishment of the groundwater. Quality of existing sources is also deteriorating (Biswas, 2007). Artificial recharge efforts are basically aimed at augmentation of the natural movement of surface water into groundwater reservoir through suitable civil construction techniques (ASCE, 2001). Artificial recharge is achieved by storing water on the land surface where it infiltrates into the soil and moves downward to underlying groundwater (Bouwer, 1997; 1999). Such techniques interrelate and integrate the source water to groundwater reservoir which depends on the hydro-geological situation of the area. Domestic Rainwater harvesting or RTRWH is the technique through which rain water is captured from roof catchments and stored in tanks/reservoirs/groundwater aquifers. It consists of conservation of rooftop rainwater in urban areas and utilized to augment groundwater by artificial recharge. It requires connecting the outlet pipe from rooftop to divert collected water to existing well/tube well/ bore well or a specially designed well. Our study was concerned to carry out an assessment of Allahabad Museum's potential towards Rainwater harvesting and to design an effective groundwater recharge structure for its main building which can serve a model site for scientific study and motivation.

32.2 STUDY AREA

The Allahabad Museum is centrally located in Allahabad city in the picturesque of Chandrashekhar Azad Park and is a monument of national importance (Figure 32.1). It has a sprawling green campus of 5.4 acres and lies under the zone in which underground water level is declining at the rate of 0.49 m/year. Total average precipitation in Allahabad is 950mm, which is equivalent to 0.950 lm^{-2}.

FIGURE 32.1 Location of Allahabad Museum.

32.3 HYDROGEOLOGICAL SETUP

Exploratory drilling data of CGWB and state tube well department show that there are three distinct granular zones, i.e., shallow aquifer ranging from 20 to 50 mbgl, middle aquifer ranging from 70 to 120 mbgl and deeper aquifer lies below 150 mbgl down to 300 mbgl. The extension of individual zones varies over the Allahabad district. A comparative analysis of various hydrological parameters (pre-monsoon groundwater level, post-monsoon groundwater level, and water table fluctuation) has been done for better understanding of changes in groundwater (Singh et al., 2014).

32.3.1 GROUNDWATER CONDITION

The area is characterized by quaternary to recent sediments which act as aquifer (sand of various grades) with intercalations of clay. The groundwater occurs in the porous formation and has different groundwater level and fluctuation in different parts of the city. The groundwater behavior in and around the study area is explained below.

32.3.1.1 GROUNDWATER ELEVATION MAP (2017)

Figures 32.2 and 32.3 present pre-monsoon and post-monsoon groundwater levels for the Allahabad city. The pre-monsoon groundwater elevation map shows that the Allahabad Museum falls in the range of 68 m to 72 m water level elevation and in the post-monsoon, the water level shows slight improvement and comes in a range of 64 m to 72 m. The seasonal fluctuation map (Figure 32.4) for the year 2016–2017 shows that the Allahabad Museum lies in the region where annual groundwater fluctuation is 3 mbgl to 4 mbgl.

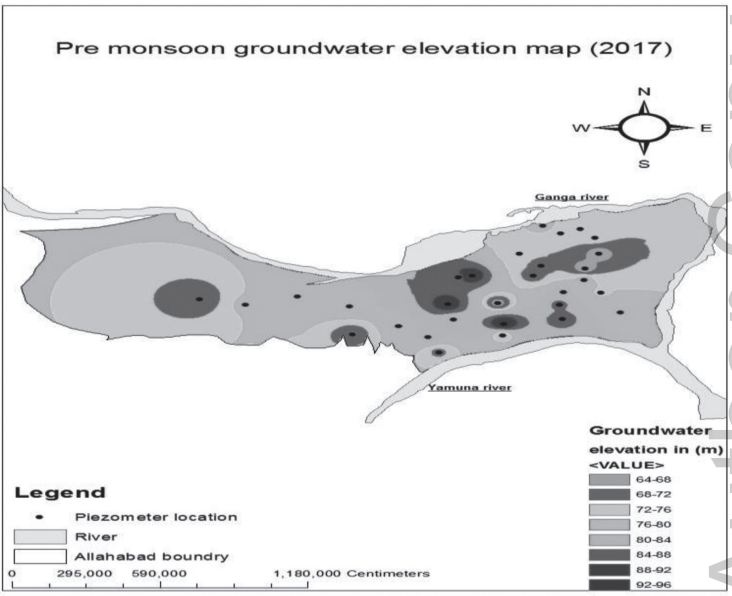

FIGURE 32.2 Pre-monsoon groundwater elevation map (2017).

32.4 MATERIALS AND METHOD

The study aimed at carrying out an assessment of Allahabad Museum's potential towards Rainwater harvesting and to design an effective groundwater recharge structure for its main building which can serve a model site for scientific study and motivation. The Allahabad museum doesn't have a supply of water from Water Board of Allahabad City and is completely dependent on groundwater for its needs. Salient features of the museum campus (Table 32.1) are used to plan the layout of recharge structure network (Figure 32.5).

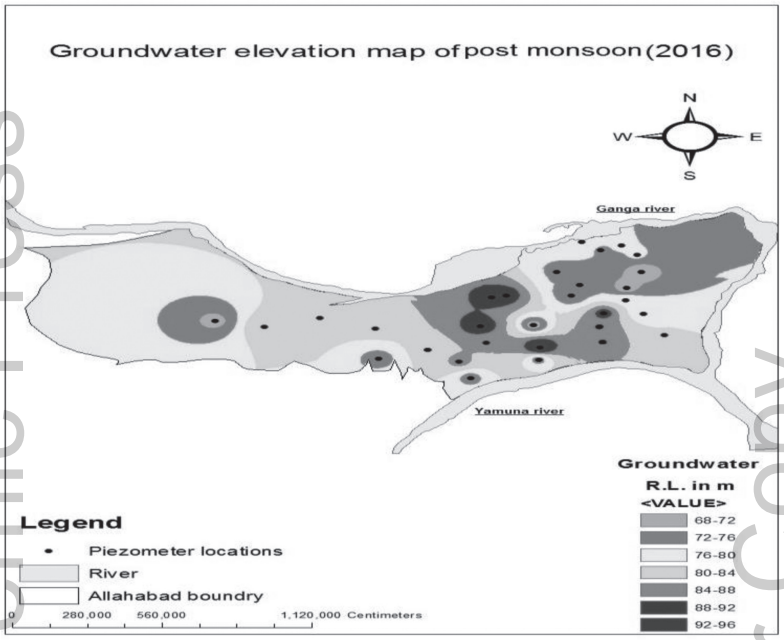

FIGURE 32.3 Post monsoon groundwater elevation map (2016).

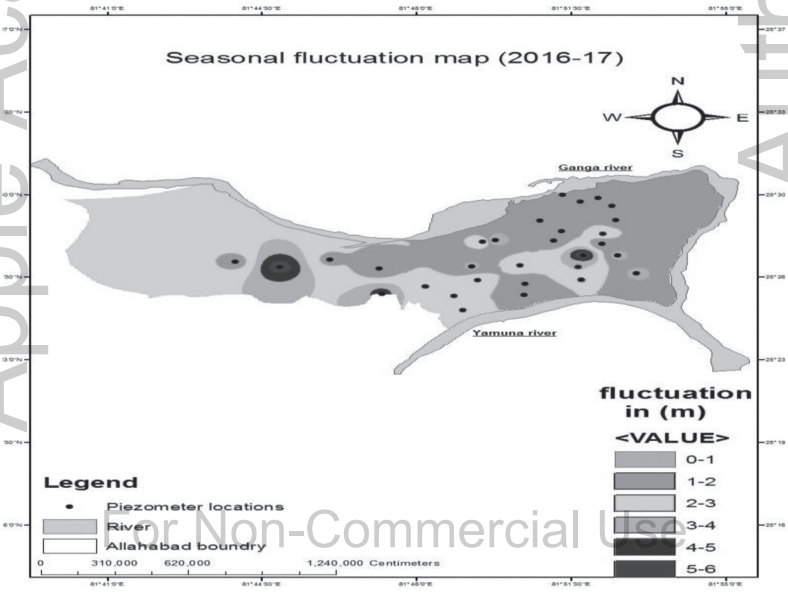

FIGURE 32.4 Seasonal fluctuation groundwater map (2016–17).

TABLE 32.1 Salient Features of the Museum Campus

Natural slope:	**towards the west side**
Rate of decline of groundwater level:	0.49m year^{-1}
Average depth to groundwater level:	16.0 mbgl
Intake capacity of recharge well:	12 m^{3}h^{-1}
Type of aquifer:	Unconfined
Total Roof Area (Main Building area):	4910 m^2 – 10% of the total roof area (Open area) = 4419 m^2
Average annual Rainfall Intensity:	30mm h^{-1}
Runoff Coefficient:	0.85
Water Available for Recharge:	4419 x 0.03 x 0.85 = 112.68 ≈ 113m^3
Expected recharge:	0.950 x 4419 x 0.85 = 3,568.34 m^{3}year^{-1}

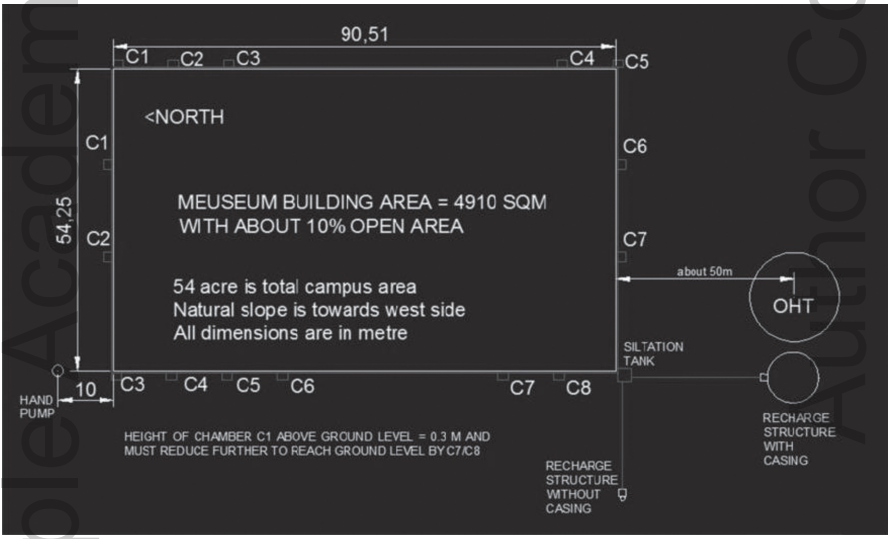

FIGURE 32.5 Layout of recharge structure network plan.

32.4.1 DIAMETER OF PIPE REQUIRED TO CARRY RAIN WATER COLLECTED

We know that Discharge, Q = πr^2 *v

where, r = radius, v = velocity of flow of water

Here, Q = 113 m^{3}h^{-1}, r =?, v =1 m^{2}s^{-1}

Therefore, r = $\frac{\sqrt{Q}}{\sqrt{\pi v}} = \frac{\sqrt{113}}{\sqrt{\pi * 1 * 3600}}$ or, r = 0.09 m

Or, Diameter, d = 2 x r = 2 x 0.09 = 0.19m ≈ 8”

32.4.2 DESIGN OF RECHARGE STRUCTURE HAVING RECHARGE WELL WITH CASING

Location: Adjacent to Over Head Tank at about 50m from Main Building in its South direction Shape of structure: Concentric Cylinder (Figure 32.6).

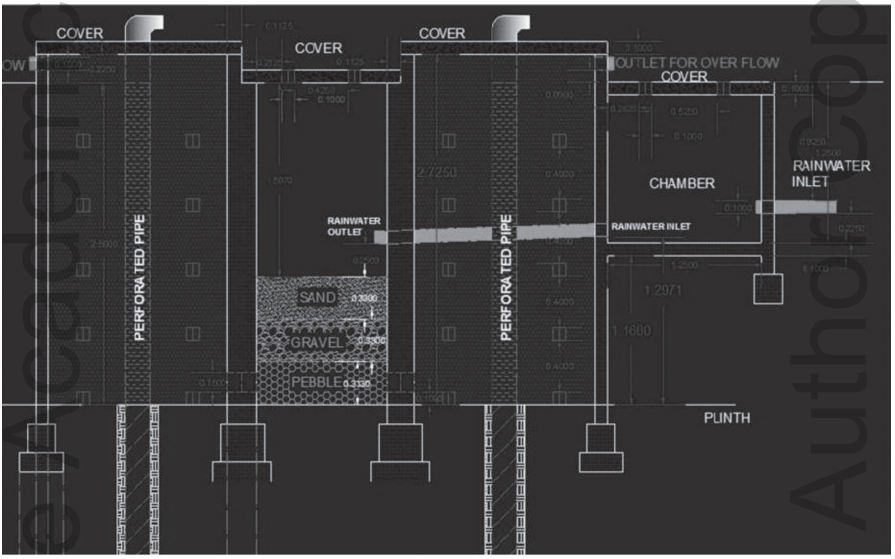

FIGURE 32.6 Design of recharge well with a casing.

32.4.2.1 DESIGN OF FILTER

Total discharge, Q = 113 m^3h^{-1}

Intake capacity of recharge well with casing = 145 lpm = 8.7m^3h^{-1} ≈ 9 m^3h^{-1}

Intake capacity of 4 number of recharge well with casing = 9 x 4 = 36 m^3h^{-1}

Intake capacity of recharge well without casing = 80 lpm = 4.8 m^3h^{-1}

Intake capacity of 10 number of recharge well without casing = 4.8 x 10 = 48 m^3h^{-1}

Available water as discharge = 113 – (36 + 48) = 29 m^3h^{-1}
Hydraulic conductivity in medium, K = 110 lpm = 6.60 m^3h^{-1}
Height of aquifer, L = 4m; Depth of filter, h = 2.5 m
Depth of filter media = to be filled up to 40% the height of filter = 2.5 x 0.4 = 1m
Sand, Gravel, and Pebble are supposed to be in equal length, i.e., 0.33 m each
Provide Nylon Mesh after layer of sand Area, A = $\frac{QL}{kh}$ = (29 x 4)/ (6.6 x 2.5) = 7.03 m^2
Radius of Filter, r = 0.525 m

32.4.2.2 DESIGN OF RECHARGE WELL

Number of recharge wells = 4
Intake Capacity of recharge well with casing = 145 lpm = 8.7 $m^3h^{-1} \approx 9$ m^3h^{-1}
Intake Capacity of 4 number of recharge well with casing = 9 x 4 = 36 m^3h^{-1}
Diameter of Recharge well = 8" = 0.2m
Reaming of bore hole = up to 13" in diameter = 0.325 m in diameter
Depth of Recharge well = 40 m bgl
Depth of pilot hole= 45 m bgl

32.4.2.3 DESIGN OF RECHARGE TANK

Capacity of tank = 113 – (36 + 48) = 29 m^3h^{-1}
Radius of Recharge tank, R = 2.3m

32.4.2.4 COVER

Provide a RCC slab as the cover of 0.1 m in thickness to cover the whole structure.
Here, Radius, R = 2.3 m.

32.4.2.5 CHAMBER

To check the velocity of incoming flow. Its dimension = 1.25 m x 1.25 m x 1 m.

32.4.3 DESIGN OF RECHARGE STRUCTURE HAVING RECHARGE WELL WITHOUT CASING

Location: Southwest of Main building
Shape of structure: Cylindrical (Figure 32.7)

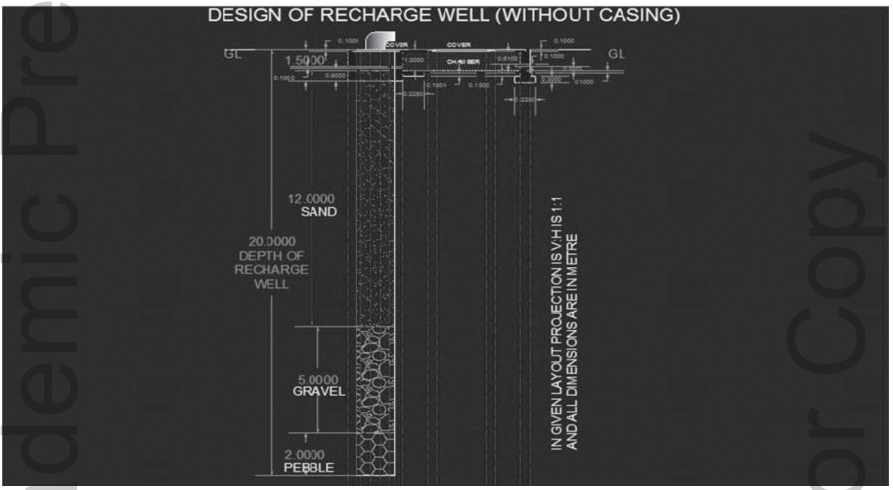

FIGURE 32.7 Design of recharge well without casing.

32.4.3.1 DESIGN OF FILTER AND STRUCTURE

Intake Capacity of recharge well without casing = 80 lpm = 4.8 m^3h^{-1}
Intake Capacity of 10 number of recharge well without casing = 4.8 x 10 = 48 $m^3\ h^{-1}$

Depth of filter, h = 19 m

Total depth of well = 20 m

Diameter of bore well = 12” = 0.3 m

Reaming of bore hole= up to 16” in diameter = 0.4 m in diameter

Provide a lining of 0.1m by brickwork around the circumference of well for 1.5 m in depth

Depth of Sand layer = 12 m

Depth of Gravel layer = 5 m

Depth of Pebble Layer = 2 m

32.4.3.2 COVER

Provide a RCC slab as the cover of 0.1m in thickness to cover the whole structure. Here, Radius, R = 0.25m.

32.4.3.3 CHAMBER

To check the velocity of incoming flow, its dimension = 1.25 m x 1.25 m x 1 m.

32.4.4 OTHER COMPONENTS

Siltation tank: Dimension 2.5m x 2.5m x 1 m (underground).

Leaf screens: Provide screen at all the outlets of rooftop and over holes provided in covers of structures to check impurities.

32.5 RESULT

The study at the Allahabad Museum and its nearby area revealed that there is a need for immediate attention towards the groundwater level as it is declining at an appreciable rate. The premises of Allahabad Museum can be considered to be best in potential to yield significant of rainfall runoff to recharge groundwater table. It is estimated that from the main building about = 3,568.34 $m^3 year^{-1}$ water will be recharged every year. The Allahabad Museum has an enormous and sprawling campus of about 5.4 acres or 21853.02 m^2 (carpet area). If effectively planned then about 17,646.31 m^3 quantity of water can be harvested every year.

32.6 CONCLUSION

There is a need for RTRWH at The Allahabad Museum to ameliorate the groundwater stress condition in the study area. It is rich in potential to yield towards groundwater recharge significantly. Based on preliminary survey and detailed study over the Allahabad Museum, 11 structures under two categories were proposed, i.e., recharge structure having recharge well with casing and recharge structure having well without casing. There is 4 well with casing and 10 well without casing is proposed. The institution

of National importance and being completely dependent on groundwater supply to meet the water demands, must install, promote, and advocate for groundwater recharge practices and techniques.

KEYWORDS

- **groundwater**
- **recharge structure**
- **RTRWH**

REFERENCES

Biswas, R., (2007). Water management in Delhi: Issues, challenges, and options, *Jour. Indian Water Works Assoc*, *39*, 89–96.

Bouwer, H., (1997). Role of groundwater recharge and water reuse in integrated water management, *Arabian Jour. Sci. Engg., 22*, 123–131.

Bouwer, H., (1999). Chapter 24: Artificial recharge of groundwater: systems, design, and management. In: Mays, L. W., (ed.), *Hydraulic Design Handbook* (Vol. 24, pp. 1–24, 44). McGraw Hill, New York.

Central Ground Water Board, (2007). Manual on Artificial Recharge of Ground Water.

Hajare, H. V., Wadhai, P. J., & Khode, B. V., (2003). *Rainwater Conservation, All India Seminar on Challenges in Environmental Protection and Possible Solutions*, 46–50.

Singh, S., Samaddar, A. B., Srivastava, R. K., & Pandey, H. K., (2014). Groundwater recharge in Urban areas – the experience of rainwater harvesting. *Journal of the Geological Society of India*, *83*(3), 295–302.

Standard Guidelines for Artificial Recharge of Ground Water, (2001). American Society of Civil Engineers, EWRI/ASCE 34–01.

CHAPTER 33

DOWNSCALING OF PRECIPITATION USING LARGE SCALE VARIABLES

PRATIBHA WARWADE[1], SURENDRA CHANDNIHA[2], GARIMA JHARIYA[3], and DEVENDRA WARWADE[4]

[1,3]Assistant Professor, Centre for Water Engineering and Management, Central University of Jharkhand, Brambe, Ranchi-835205, India, E-mail: pratibhawarwade@gmail.com / Institute of Agricultural Sciences, Banaras Hindu University, Varanasi (U.P.) 221005, India, E-mail: garima2304@gmail.com

[2]Research Associate, National Institute of Technology, Roorkee, Uttrakhand, India

[4]Assistant Professor, Department of Physics, Government College Sehore, Barktulla University, Bhopal, M.P., India

ABSTRACT

Present study carried to downscale the monthly precipitation using large-scale variables for Dikhow Catchment, North Eastern region of India. Statistical downscaling is performed in this study by employing multiple linear regression (MLR) approach followed by Bias correction. A daily reanalysis dataset of NCEP (scale of 2.5° latitude × 2.5° longitude) re-gridded on a scale of 2.5° latitude × 3.75° longitude, simulated data of HadCM3 on a scale 2.5° latitude × 3.75° and monthly precipitation data from IMD Pune were used for the analysis. Six potential predictors; wind at 500 hPa, wind direction at 500 hPa, geopotential height at 500 hPa, relative humidity at 500 hPa, near-surface relative humidity, and air temperature at 2m are selected. Nash-Sutcliffe Efficiency (NSE) value varies from 0.88 to 0.89 for calibration and 0.88 to 0.92 for validation period. MLR model has performed well over the region. Future precipitation is increasing at all stations for both A2 and B2 scenarios,

the magnitude of increase in precipitation, is higher for A2 scenario than that of B2 scenario (monsoon precipitation 1857.5 mm and 1715.7 mm, summer precipitation 606.3 mm and 559.7 mm whereas winter precipitation 139.8 mm and 144.05 mm).

33.1 INTRODUCTION

Climate change affects the Earth's environments which leads to effect the people's livelihoods and wellbeing. Apart from climate change, economic development, current demographic trends, and land use changes have a direct impact on the growing demand for freshwater resources (Gain et al., 2012). Sustainable development will secure the availability of resources for further generations (Pechstädt et al., 2011). Rainfall is pertinent parameters that are affected by climate change which in turn influences the hydrological cycle, and the rainfall-runoff process has significant importance in Hydrology (Sahu et al., 2007). The constantly increasing demand and probable changes in the way water resources are distributed in future will be a challenge for water resources managers around the world. Local-scale information about the change in precipitation obtained from large-scale GCMs outputs is used to provide as an input for hydrological modeling, which operates on a daily, weekly, and monthly scales (Rosenberg et al., 2003). Direct use of GCM outputs is not acceptable for estimation of hydrological response to climate change due to its coarser spatial resolution.

However, the GCMs are extensively accepted for future climate change prediction (Dibike and Coulibaly, 2005). Downscaling is the methodology used to fill the gap between large-scale GCM outputs and finer-scale (local-scale) requirements (Chen et al., 2010). Basically, statistical downscaling and dynamical downscaling are two downscaling techniques applied to derive the local-scale information from GCM outputs. Dynamical downscaling has a high complexity, high computational cost and require detailed awareness of physical processes of the hydrological cycle, based on nesting RCM into an existing GCM (Anandhi et al., 2008), identification of bias from GCM to RCM is another problem (Giorgi et al., 2001).

Statistical downscaling methods are most widely used to derive the climate information at a regional scale in which statistical relationships are developed between the large scale (predictors) variables and local scale (pedcitands) parameters (Chen et al., 2010). Statistical downscaling has a low computational cost and can apply without knowing information about the physical processes of the hydrological cycle and geography of the study. Statistical downscaling requires long-term observed data for the

model calibration and validation (Heyen et al., 1996) and it assumes that the relationship between coarse-scale and finer-scale climate are constant to generate point/station data of a specific the region using GCMs output variables (Anandhi et al., 2014). Several statistical approaches are available to the description of these relationships are multiple linear regression (MLR), canonical correlation analysis (CCA), and support vector machines (SVMs), etc. (Anandhi et al., 2008, 2009; Chen et al., 2010; Chu et al., 2010). The present study focused on downscale rainfall over a part of the Brahmaputra river basin, India, using the statistical downscaling technique for estimation of average monthly rainfall at six selected stations.

33.2 MATERIALS AND METHODS

33.2.1 STUDY AREA

The study area is Dikhow catchment which is a part of the larger Brahmaputra river basin, Dikhow river which originates from the hills of the state Nagaland. It is a south bank tributary of river Brahmaputra contributing 0.7% runoff. A lower Brahmaputra river basin, a region where the hydrological impact of climate change is expected to be particularly strong, and population pressure is high (Gain & Giupponi, 2015). Brahmaputra river is the biggest trans-Himalayan river basin (Sharma & Flügel, 2015). Study area situated between 94° 28'49"E to 95° 09' 52" E longitude and 26° 52' 20"N to 26° 03' 50" N latitude. The geographical area of Dikhow catchment is about 3100 km^2.

33.2.2 DATA USED

Statistical downscaling assumes the validity of relationships between predictors (GCM outputs) and predictands (observed meteorological variables) under future climate change (Yan et al., 2011). For the present study, NCEP reanalysis datasets used for the predictor selection to downscale precipitation at selected stations. And observed data of monthly precipitation were procured from IMD website.

33.2.2.1 LARGE SCALE ATMOSPHERIC VARIABLES

A daily reanalysis dataset of NCEP (scale of 2.5° latitude × 2.5° longitude) re-gridded on a scale of 2.5° latitude × 3.75° longitude and simulated data

of HadCM3 on a scale 2.5° latitude × 3.75° longitude were downloaded from the website http://www.cics.uvic.ca/scenarios/sdsm/select.cgi and described in Table 33.1. The data were downloaded for two different emission scenarios A2 and B2; both are regionally focused, but the priority of first to economic issues (A2 scenario) and other to environmental issues (B2 scenario). HadCM3 GCM is a complex model of land surface processes; however, it is unique, most popular and does not require flux adjustments to produce a realistic scenario (Toews and Allen, 2009). The A2 and B2 scenarios are applied in this study. The description of both scenarios: A2 describes cultural identities separate for the different regions, making the world more heterogeneous and international cooperation is less likely. "Family values," local traditions and high population growth (0.83% per year) are emphasized with less focus on economic growth (1.65%/year) and material wealth. And B2 describes a heterogeneous society that emphasizes local solutions to economic, social, and environmental sustainability rather than global solutions. Human welfare, equality, and environmental protection have high priority, specified in the Special Report on Emissions Scenarios (SRES).

TABLE 33.1 List of 26 Predictor Variables

Variable	Description	Variable	Description
P5_f	Geostrophic air flow velocity at 500hPa	P8_f	Geostrophic air flow velocity at 850 hPa
P5_u	Horizontal wind at 500 hPa	P8_u	Horizontal wind at 850 hPa
P5_v	Zonal wind at 500hPa	P8_v	Zonal wind at 850 hPa
P5_z	Vorticity at 500 hPa	P8_z	Vorticity at 850 hPa
P5zh	Divergence at 500 hPa	P8zh	Divergence at 850 hPa
P500	Geopotential height at 500 hPa	P850	Geopotential height at 850 hPa
R500	Relative Humidity at 500 hPa	R850	Relative Humidity at 850 hPa
Pf	Surface geostrophic airflow	mslp	Mean sea level pressure
Pu	Surface horizontal wind	rhum	Near-surface relative humidity
P_v	Surface zonal wind	shum	Near-surface specific humidity
P_z	Surface vorticity	Temp2	2 m air temperature
P_zh	Surface divergence	P5th	500 hpa wind direction
P8th	850 hpa wind direction	Pth	Surface wind direction

The daily data of A2 and B2 scenarios for nine grid points, latitude varies from 25° N to 30° N and longitude varies from 89° 59' 6" E to 97° 29' 6" E

revealed in Figure 33.1 were downloaded. As suggested by Tripathi et al. (2006) and Anandhi et al. (2008), they used 6 × 6and 3 × 3 grid respectively in their study, for downscaling (of precipitation and temperature) purpose. Though, there is no rule for the size of atmospheric domain selection; large domain size may allow to identify better relationship (correlations) between predictors and predictand it may also have a drawback to increase computational cost. Predictor variables are listed below. The predictor variables are available at a grid resolution of 2.5° latitude × 3.75° longitude.

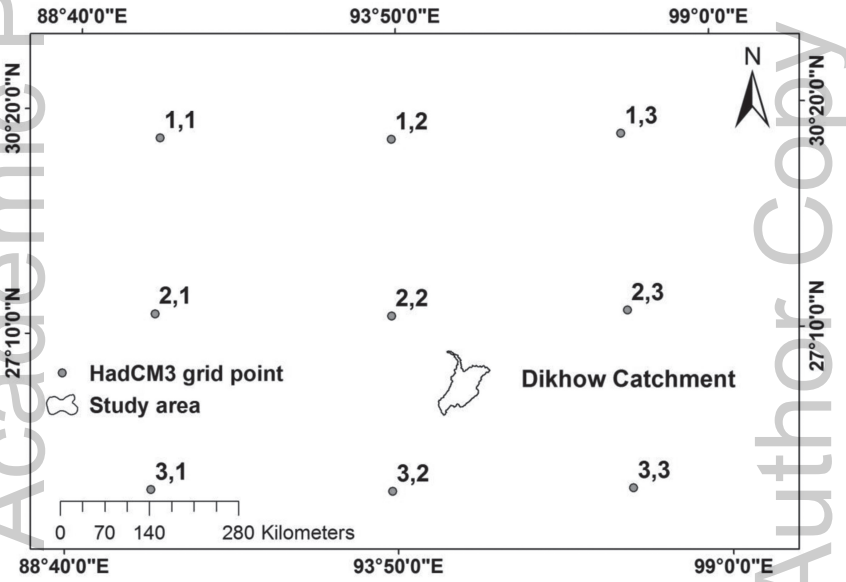

FIGURE 33.1 Spatial domain defined over the Dikhow river catchment.

33.2.3 STATISTICAL DOWNSCALING

Statistical downscaling is performed in this study by employing MLR approach. The procedure of downscaling of precipitation and temperature using MLR are explained in the following subsections.

33.2.3.1 POTENTIAL AND PROBABLE PREDICTORS FOR DOWNSCALING

Selection of predictor variables along with spatial domain plays a key role in statistical downscaling performance; predictor selection should be

on first priority (Wilby and Wigly, 1997; Fowler et al., 2007). Detailed knowledge about the physics of predictors and its relation with predictand may help for the selection procedure. In the present study, twenty-six different atmospheric variables were (listed in Table 33.1), extracted from a daily reanalysis dataset of the NCEP for the years 1961–2001 based on the literature on similar studies. Predictor selection depends on the selected region and physical characteristics of the high-resolution atmospheric circulation. Wetterhall et al., (2005) suggested that predictors selection is strongly based on relationship existence (between the predictor and the predictand).

33.2.3.2 BRIEF DESCRIPTION OF MULTIPLE LINEAR REGRESSION METHOD

MLR technique is most popular in downscaling of large-scale GCM outputs (e.g., Huth, 1999; Murphy, 1999; Schoof and Pryor, 2001; Hay and Clark, 2003) of climate change impact studies. MLR is a statistical technique, which is used to develop a linear relationship between a predictand (dependent variable) and predictors (one or more independent variables), it is a least square-based method, and assumes a linear relationship between variables. Therefore, the MLR model can be expressed as a linear function (Eq. 1).

$$y = \beta_0 + \beta_1 x_1 + \beta_2 x_2 + \beta_3 x_3 \ldots\ldots\ldots + \beta_n x_n \quad (1)$$

where {i= 1…….n}, y is the predictand, β_0 is the intercept, x_i is the i^{th} predictor variable, and β_i is the i^{th} predictor variable coefficient. MLR attempts to find a plane of best fit, and the fit can be assessed by the correlation coefficient (R) expresses the degree to which two or more predictors are related to the predictand.

Bias Correction: The bias correction techniques were applied to remove any bias in future predictands as per need. For precipitation a simple linear correction was used (Eq. 2):

$$P_{meancorr} = P_{gcm} \times \left(\frac{\overline{P_{obs}}}{\overline{P_{gcm}}} \right) \quad (2)$$

where, $P_{meancorr}$ = bias-corrected precipitation monthly, P_{gcm} = uncorrected precipitation monthly, $\overline{P_{obs}}$ = mean of monthly observed precipitation, $\overline{P_{gcm}}$ = mean of uncorrected precipitation monthly.

33.2.3.3 MODEL PERFORMANCE

Monthly reanalysis data of National Center for Environmental Prediction (NCEP) and the predictands (Tmin, Tmax, and precipitation) data from the years 1961 to 1990 were used in the calibration (training) and validation (testing) of the downscaling models. The predictands and NCEP data (treated as an output of a typical GCM) were divided into two data sets (Cannon and Whitfield, 2002): one for the training of the model and another for testing, 70% of data were chosen for training, and remaining 30% for testing of the model. Nash-Sutcliffe Efficiency (NSE), Coefficient of Correlation (R), Root Mean Square Error (RMSE) and graphical representation were used as performance indicators of the model during training and testing period for each station of the study area.

33.3 RESULTS AND DISCUSSIONS

33.3.1 SELECTED PREDICTOR VARIABLES

Pearson correlation coefficients between each probable predictor at each grid point in the spatial domain and predictands (Precipitation, Tmax, and Tmin) were calculated. The probable variables that showed the best, statistically significant (95% confidence level, $p = 0.05$) correlations with the predictands, consistently over the above mentioned period were selected as potential variables. Table 33.2 shows the potential predictors with their grid locations (according to Figure 33.1) used as the final inputs to the MLR based downscaling model for respective predictand variables. Potential predictors used in MLR model consist of horizontal wind at 500 hPa, wind direction at 500 hPa, geopotential height at 500 hPa (Devak and Dhanya, 2014; Anandhi et al., 2008), relative humidity at 500 hPa, near-surface relative humidity, and air temperature at 2 m.

33.3.2 CALIBRATION AND VALIDATION OF MODEL

The selected potential variables were introduced to the MLR model, which showed the best correlation coefficients. The model performances in the calibration and validation were monitored with the original NSE formula, in addition, the correlation coefficient (R) and RMSE were also used. The model that displayed the best NSE in both calibration and validation

was selected as the best model. The model performances were monitored using the raw values of observed and predicted values for each predictand variable. The performance of the downscaling method was also evaluated by comparing data distributions (Cheng et al., 2008) to produce visual comparisons of model predicted values with observed values. The same process was repeated for each of the predictand variable (precipitation, Tmin, and Tmax) for calibration and validation of the MLR model and discussed below separately.

TABLE 33.2 Summary of Selected Large-Scale Predictor Variables Corresponding to Each of the Predictands

Precipitation			
S.N.	**Potential predictor selected**	**Grid location**	**Correlation**
1	Horizontal wind at 500 hPa	(2,1), (2,2), (2,3),(3,2), (3,3)	0.601–0.712
2	Air temperature at 2 m	(2,2), (2,3), (3,1),(3,2), (3,3)	0.791 – 0.812
3	Geopotential height at 500 hPa	(2,1), (2,2), (2,3),(3,2), (3,3)	0.710–0.737
4	Relative Humidity at 500 hPa	(2,2), (2,3), (3,1),(3,2), (3,3)	0.0732 –.794
5	Horizontal wind at 850 hPa	(2,2), (2,3), (3,1),(3,2), (3,3)	0.681–0.704
6	Wind direction at 500 hPa	(2,1), (2,2), (2,3),(3,2), (3,3)	0.412–0.582

33.3.2.1 PRECIPITATION

Rain occurrence and amount of precipitation are stochastic processes; therefore, the downscaling of precipitation is always a difficult problem (Doyle et al., 1997). Table 33.3 shows that for MLR model NSE of 0.88 to 0.89 was obtained for calibration and 0.88 to 0.92 for the validation period. The corresponding RMSE for calibration and validation varies from 14.31 to 18.89 and 14.41 to 19.21 respectively. Correlation coefficient (R) 0.88 to 0.89 was obtained for calibration and 0.87 to 0.92 for validation respectively.

Figure 33.2-f shows the graphical comparison of observed and model predicted monthly precipitation for the calibration (1961–1990) and validation (1991–2001) periods for each station, and graphs were plotted between precipitation in mm at y-axis and time in months at the x-axis. The Red dotted line shows the observed precipitation values, whereas green and blue line shows simulated precipitation for calibration and validation period. The results show under-prediction of the highest precipitation values during the calibration phase (except 1961, 1967, 1997, and 1979) and some

of the years of validation phase (except 1994, 1997, 1999 and 2001) at almost all the stations (Sibsagar, Mokokchung, Mon, Tirap, Tuensang, and Zunheboto). This can be the explanation that the MLR model is unable to capture the extreme values of precipitation but follows good behavior for non-monsoon months.

TABLE 33.3 The Performance of Model for Precipitation During Calibration and Validation Period

Precipitation Calibration (1961–1998)			
Station	**NSE**	**R**	**RMSE**
Sibsagar	0.88	0.88	14.31
Mokokchung	0.89	0.89	15.83
Mon	0.88	0.89	18.84
Tirap	0.88	0.89	15.8
Tuensang	0.89	0.89	17.02
Zunheboto	0.89	0.89	18.89
Precipitation Validation (1991–2001)			
Station	NS	R	RMSE
Sibsagar	0.88	0.87	15.69
Mokokchung	0.91	0.9	15.89
Mon	0.9	0.9	14.66
Tirap	0.91	0.91	14.73
Tuensang	0.92	0.92	19.21
Zunheboto	0.91	0.91	14.41

33.3.3 FUTURE PROJECTION OF PRECIPITATION AND TEMPERATURE TIME SERIES FOR A2 AND B2 SCENARIOS

Figure 33.3 presents the projected precipitation, for the period of 2010–2099 at each station of the study area for both A2 and B2 scenarios. The middle line of the box shows the median values, whereas upper and lower edges show the 75%ile and 25%ile of the dataset, respectively. The difference between 75%ile and 25%ile is known as Inter Quartile (IQR). The red dotted line with circle represents the mean value. Figures 4.6 to 4.8 demonstrate the projected output for A2 and B2 scenarios, A2 having a higher magnitude than the B2 scenario for precipitation. Precipitation was projected uniformly over all the stations of the catchment.

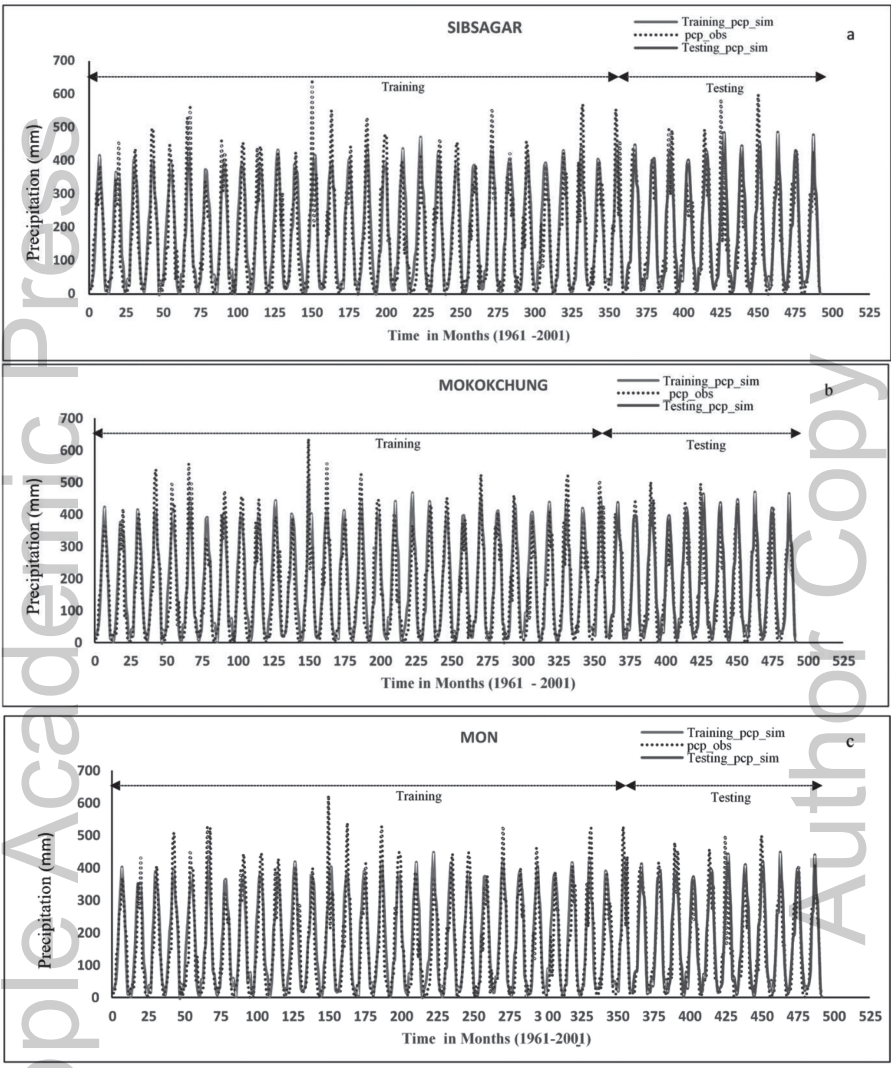

FIGURE 33.2 *(Continued)*

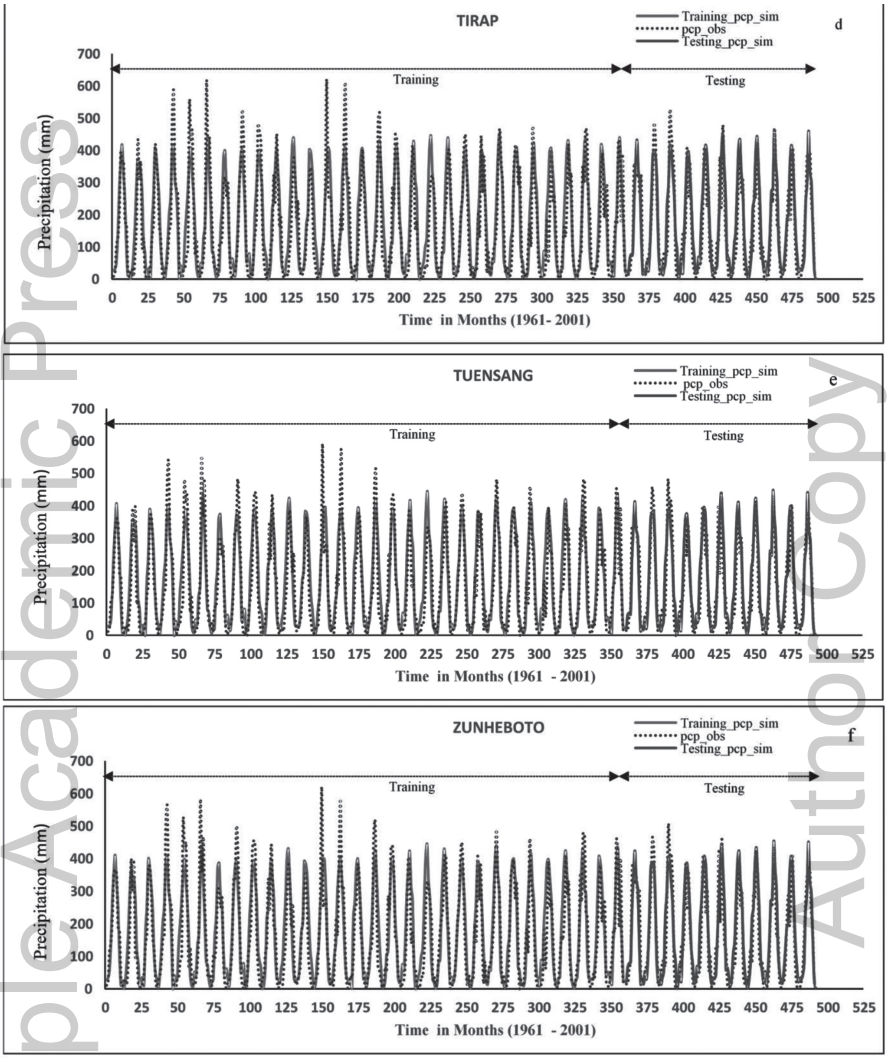

FIGURE 33.2 Comparison of monthly observed and simulated precipitation at stations (a) Sibsagar, (b) Mokokchung, (c) Mon, (d) Tirap, (e) Tuensang, and (f) Zunheboto for training (1961–1990) and validation period (1991–2001).

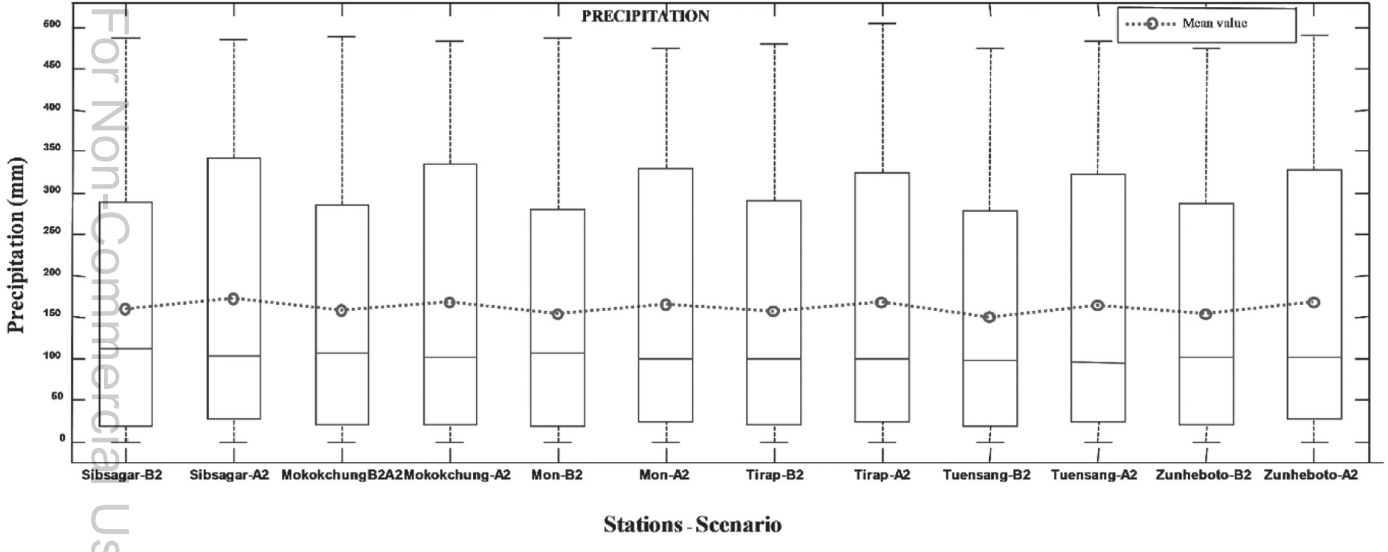

FIGURE 33.3 Projected scenarios A2 and B2 for monthly precipitation from 2010–2099 at each station of Dikhow catchment.

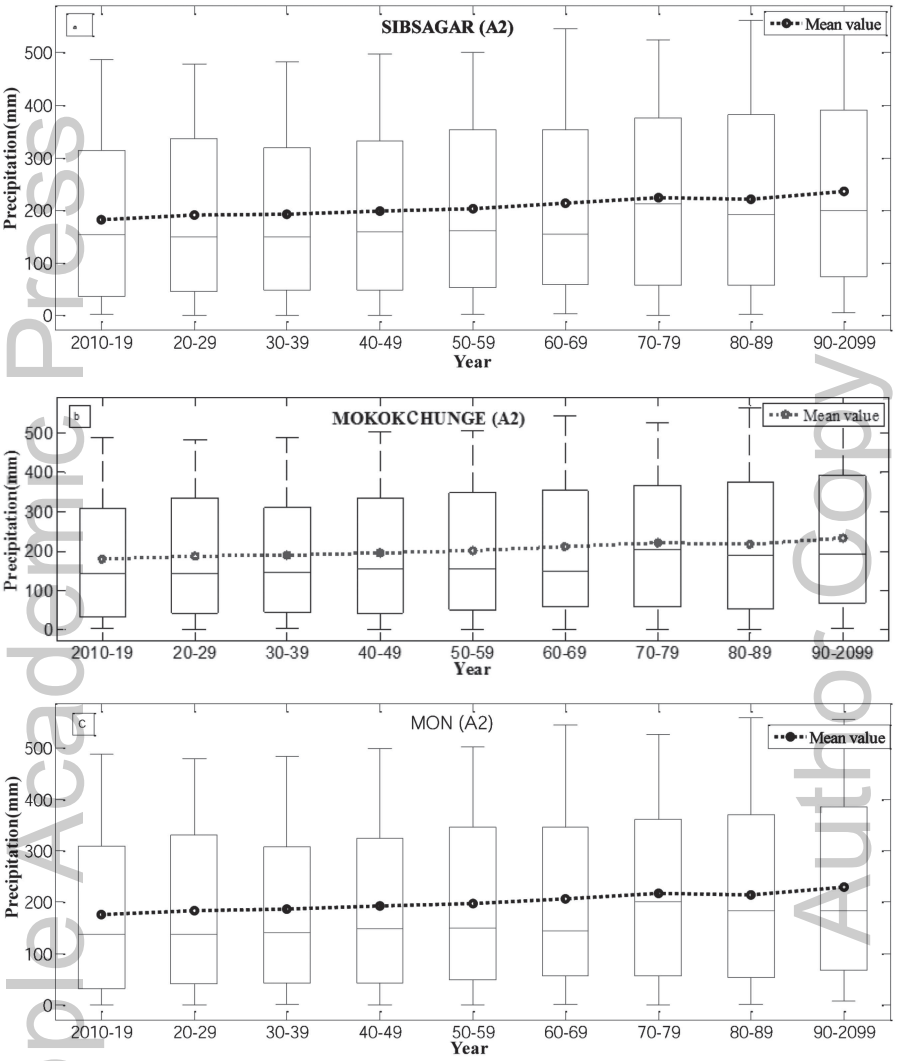

FIGURE 33.4 *(Continued)*

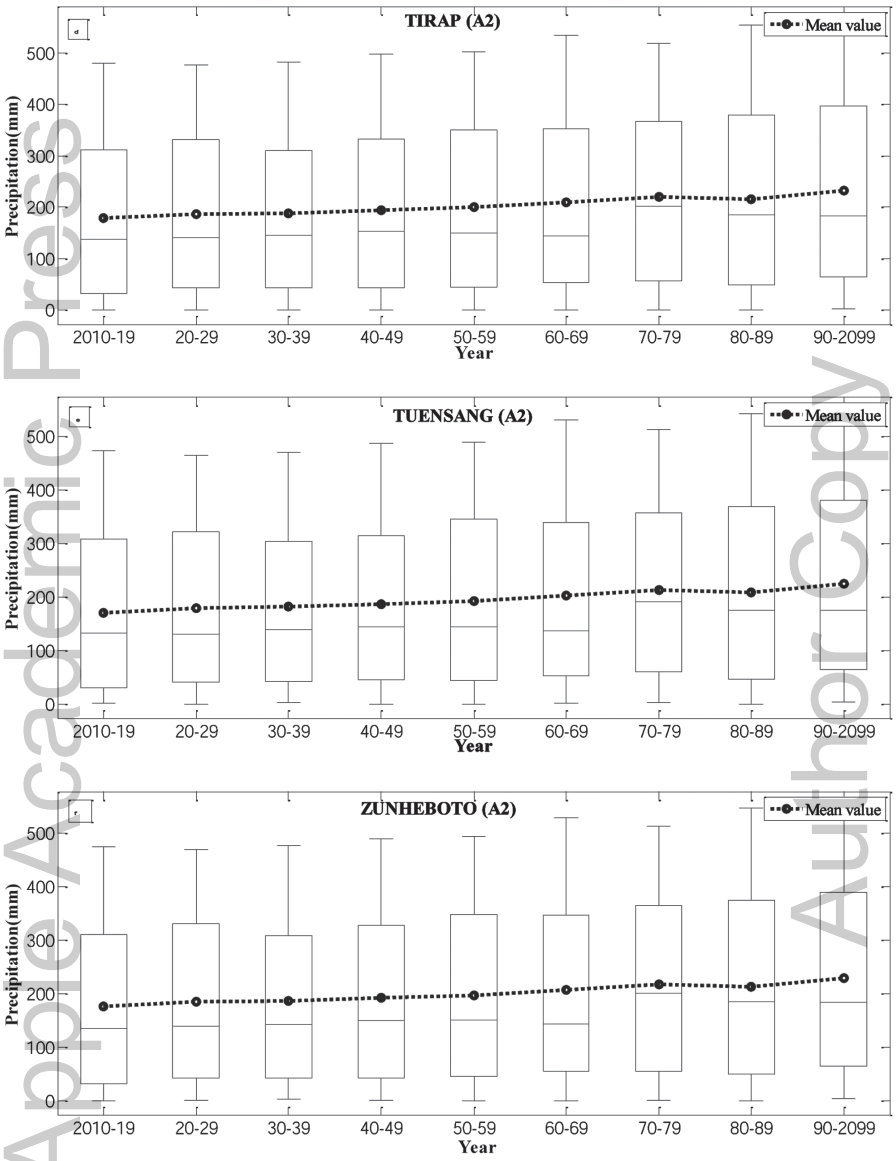

FIGURE 33.4 Box plot depicts the decadal changes in downscaled precipitation from 2010–2099 at (a) Sibsagar, (b) Mokokchung, (c) Mon, (d) Tirap, (e) Tunesang and (f) Zunheboto of Dikhow catchment for emission scenario A2. The red horizontal line in the boxes denotes the median. The red dotted line with circle represents the mean value.

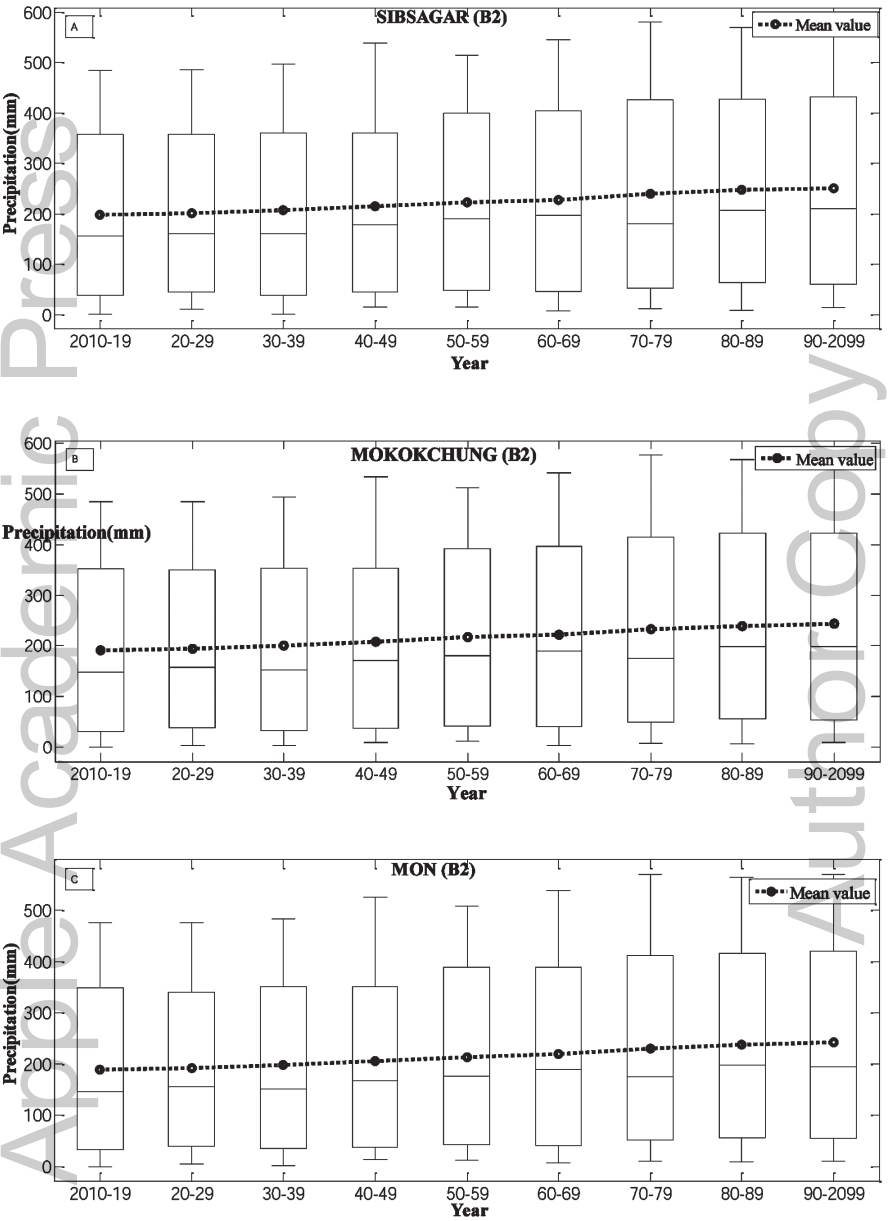

FIGURE 33.5 *(Continued)*

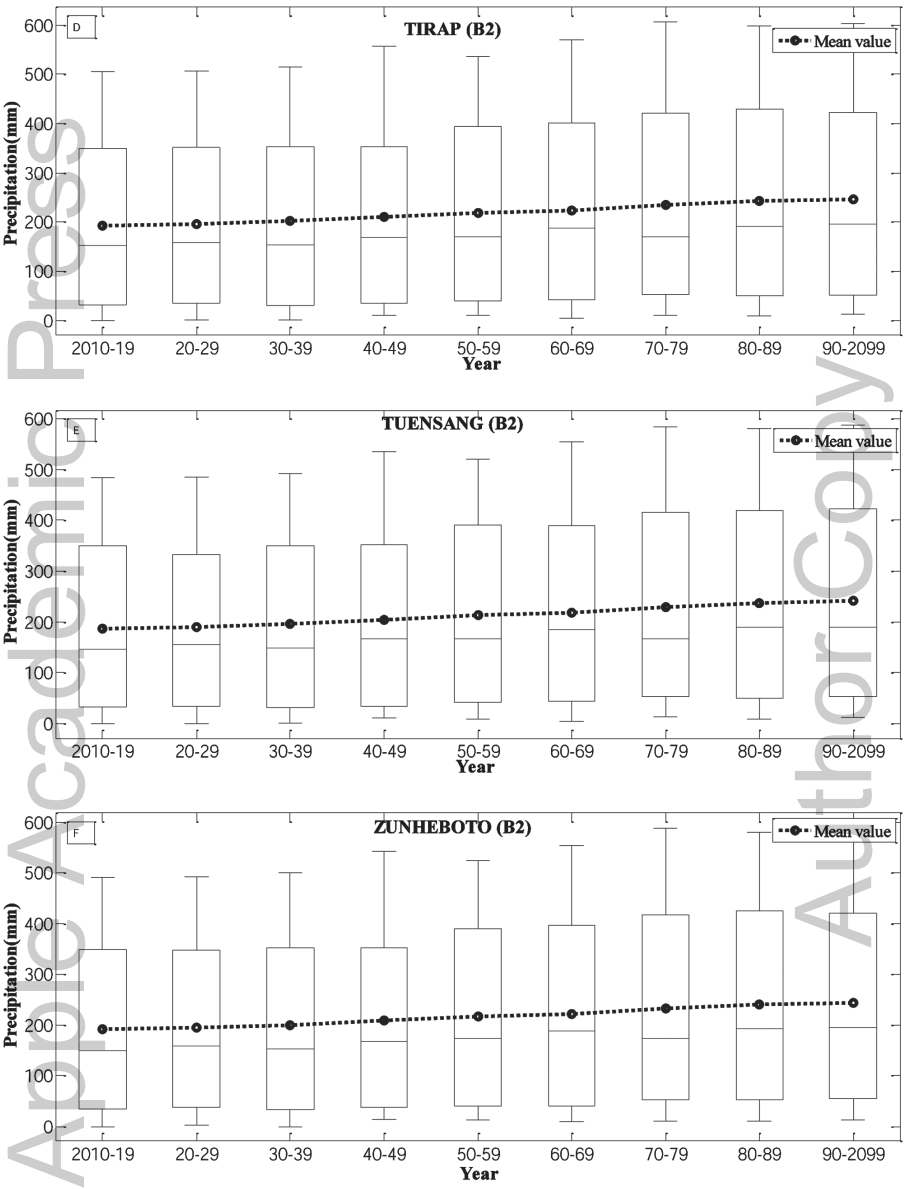

FIGURE 33.5 Box plot depicts the decadal changes in downscaled precipitation from 2010–2099 at (A) Sibsagar, (B) Mokokchung, (C) Mon, (D) Tirap, (E) Tunesang and (F) Zunheboto of Dikhow catchment for emission scenario B2. The red horizontal line in the boxes denotes the median. The red dotted line with circle represents the mean value.

33.3.4 DECADAL CHANGES OF CLIMATE PARAMETER

The box plots of 10-years' time slice are used to determine patterns in predictand. Figures 33.4a–f and 33.5a–f demonstrates the rise in future precipitation at all stations for both A2 and B2 scenarios. Annual future projection of precipitation using MLR model has figured out 2420.3 mm for both A2 and B2 Scenarios over the catchment. Seasonal future projection of precipitation was also figured out; monsoon precipitation 1857.5 mm and 1715.7 mm, summer precipitation 606.3 mm and 559.7 mm whereas winter precipitation 139.8 mm and 144.05 mm were projected at the catchment for A2 and B2 scenarios respectively. Seasonal precipitation was projected more for A2 scenario than the B2 scenario.

Statistical downscaling (Goubanova et al., 2011; Lee et al., 2011) techniques are an effective tool to fill the gap between large-scale climate change and local-scale hydrological response (Chu et al., 2010). Downscaling of local/station-scale monthly meteorological parameters is important to better extend climate change impacts analysis in a variety of environmental assessments (Cheng et al., 2005). MLR (Yan et al., 2011; Sachindra et al., 2013) method was presented to derive station-scale monthly future climate scenarios in terms of various meteorological variables, including precipitation. Performance of the downscaling method was evaluated by (1) analyzing model R, RSME, and NSE, (2) validating downscaling method using cross-validation, (3) comparing data distributions of downscaled GCM historical runs with observations over the same period of 1961–2001. The results showed that MLR-based downscaling methods used in the study performed well in deriving station-scale monthly climate scenarios. However, these methods implicitly assume that historical relationships between GCM-scale synoptic field and station scale responses of the past years would remain constant in the future (Cheng et al., 2008; Ghosh and Mujumdar, 2006). Downscaling shows an increasing trend in precipitation, in general, it was noted that the results show an agreement with the findings of other research works like Duhan et al. (2015); Saraf and Regulwar (2016) over India, and other region. Water resource management (Mahanta, 2006) and planning increasingly need to incorporate the effects of global climate change on regional climate variability in order to assess future water supplies accurately. Therefore, future climate projections, particularly of rainfall is utmost interest to water resource management and water-users (Fu et al., 2011).

33.4 CONCLUSIONS

The following conclusions are drawn from the present study:

1. Six potential predictors wind at 500 hPa, wind direction at 500 hPa, geopotential height at 500 hPa, relative humidity at 500 hPa, near-surface relative humidity, and air temperature at 2 m are selected from 26 large-scale variables.
2. The results of calibration and validation show that the predictands can be downscaled potentially using MLR models, the model has performed well over the region.
3. The future projection shows that precipitation may increase in future at all stations for both A2 and B2 scenarios.
4. The magnitude of increase in precipitation is higher for A2 scenario than that of B2 scenario.

KEYWORDS

- **downscaling techniques**
- **GCM**
- **HadCM3**
- **IPCC 2007**

REFERENCES

Anandhi, A., Srinivas, V. V., Kumar, D. N., & Nanjundiah, R. S., (2009). Role of predictors in downscaling surface temperature to river basin in India for IPCC SRES scenarios using support vector machine. *International Journal of Climatology*, *29*(4), 583–603.

Anandhi, A., Srinivas, V. V., Kumar, D. N., Nanjundiah, R. S., & Gowda, P. H., (2014). Climate change scenarios of surface solar radiation in data sparse regions: a case study in Malaprabha River Basin, India. *Climate Research*, *59*(3), 259.

Anandhi, A., Srinivas, V. V., Nanjundiah, R. S., & Nagesh, K. D., (2008). Downscaling precipitation to river basin in India for IPCC SRES scenarios using support vector machine. *International Journal of Climatology*, *28*(3), 401–420.

Chen, S. T., Yu, P. S., & Tang, Y. H., (2010). Statistical downscaling of daily precipitation using support vector machines and multivariate analysis. *Journal of Hydrology*, *385*(1), 13–22.

Cheng, C. S., Li, G., Li, Q., & Auld, H., (2008). Statistical downscaling of hourly and daily climate scenarios for various meteorological variables in south-central Canada. *Theoretical and Applied Climatology*, *91*(1–4), 129–147.

Cheng, Y. S., Zhou, Y., Irvin, C. M., Pierce, R. H., Naar, J., Backer, L. C., & Baden, D. G., (2005). Characterization of marine aerosol for assessment of human exposure to brevetoxins. *Environmental Health Perspectives*, 638–643.

Chu, J. T., Xia, J., Xu, C. Y., & Singh, V. P., (2010). Statistical downscaling of daily mean temperature, pan evaporation and precipitation for climate change scenarios in Haihe River, China. *Theoretical and Applied Climatology*, *99*(1–2), 149–161.

Devak, M., & Dhanya, C. T., (2014). Downscaling of precipitation in Mahanadi basin, India. *International Journal Civil Engineering Research*, *5*, 111–120.

Dibike, Y. B., & Coulibaly, P., (2005). Temporal neural networks for downscaling climate variability and extremes. In: *Neural Networks, 2005. IJCNN'05, Proceedings, 2005 IEEE International Joint Conference* (Vol. 3, pp. 1636–1641).

Doyle, J. D., & Foley, D. M., (1999). *Veneziani* (2ndpart, p. 438), CA: Edwards.

Duhan, D., & Pandey, A., (2015). Statistical downscaling of temperature using three techniques in the Tons River basin in Central India. *Theoretical and Applied Climatology*, *121*(3/4), 605–622.

Fowler, H. J., Blenkinsop, S., & Tebaldi, C., (2007). Linking climate change modeling to impacts studies: Recent advances in downscaling techniques for hydrological modeling. *International Journal of Climatology*, *27*(12), 1547–1578.

Fu, G., Charles, S. P., Chiew, F. H. S., & Teng, J., (2011). Statistical downscaling of daily rainfall for hydrological impact assessment. In: *MODSIM2011, 19th International Congress on Modeling and Simulation* (pp. 12–16). Perth, Australia.

Gain, A. K., & Giupponi, C. A., (2015). Dynamic assessment of water scarcity risk in the lower Brahmaputra river basin: An integrated approach. *Ecological Indicators*, *48*, 120–131.

Gain, A. K., Giupponi, C., & Renaud, F. G., (2012). Climate change adaptation and vulnerability assessment of water resources systems in developing countries: A generalized framework and a feasibility study in Bangladesh. *Water*, *4*(2), 345–366.

Ghosh, S., & Mujumdar, P. P., (2006). Future rainfall scenario over Orissa with GCM projections by statistical downscaling. *Current Science*, *90*(3), 396–404.

Giorgi, F., Whetton, P. H., Jones, R. G., Christensen, J. H., Mearns, L. O., Hewitson, B., & Jack, C., (2001). Emerging patterns of simulated regional climatic changes for the 21st century due to anthropogenic forcings. *Geophysical Research Letters*, *28*(17), 3317–3320.

Goubanova, K., Echevin, V., Dewitte, B., Codron, F., Takahashi, K., Terray, P., & Vrac, M., (2011). Statistical downscaling of sea-surface wind over the Peru–Chile upwelling region: Diagnosing the impact of climate change from the IPSL-CM4 model. *Climate Dynamics*, *36*(7/8), 1365–1378.

Hay, L. E., & Clark, M. P., (2003). Use of statistically and dynamically downscaled atmospheric model output for hydrologic simulations in three mountainous basins in the western United States. *Journal of Hydrology*, *282*(1), 56–75.

Heyen, H., Zorita, E., & Von Storch, H., (1996). Statistical downscaling of monthly mean North Atlantic air-pressure to sea level anomalies in the Baltic Sea. *Tellus. A*, *48*(2), 312–323.

Huth, R., (1999). Statistical downscaling in central Europe: Evaluation of methods and potential predictors. *Climate Research*, *13*(2), 91–101.

Lee, T. C., Chan, K. Y., & Ginn, W. L., (2011). Projection of extreme temperatures in Hong Kong in the 21st century. *Acta Meteorologica Sinica*, *25*, 1–20.

Mahanta, C., (2006). Water resources of the Northeast: State of the knowledge base. *Background Paper*, *2*.

Murphy, J., (1999). An evaluation of statistical and dynamical techniques for downscaling local climate. *Journal of Climate*, *12*(8), 2256–2284.

Pechstädt, J. O. R. G., Bartosch, A. N. I. T. A., Zander, F. R. A. N., Schmied, H. M., & Flugel, W. A., (2011). *Development of a River Basin Information System for a Sustainable Development in the Upper Brahmaputra River Basin*.

Rosenberg, N. J., Brown, R. A., Izaurralde, R. C., & Thomson, A. M., (2003). Integrated assessment of Hadley Centre (HadCM2) climate change projections on agricultural productivity and irrigation water supply in the conterminous United States: I. Climate change scenarios and impacts on irrigation water supply simulated with the HUMUS model. *Agricultural and Forest Meteorology*, *117*(1), 73–96.

Sachindra, D. A., Huang, F., Barton, A., & Perera, B. J. C., (2013). Least square support vector and multi-linear regression for statistically downscaling general circulation model outputs to catchment streamflows. *International Journal of Climatology*, *33*(5), 1087–1106.

Sahu, R. K., Mishra, S. K., Eldho, T. I., & Jain, M. K., (2007). An advanced soil moisture accounting procedure for SCS curve number method. *Hydrological Processes*, *21*(21), 2872–2881.

Saraf, V. R., & Regulwar, D. G., (2016). Assessment of climate change for precipitation and temperature using statistical downscaling methods in upper Godavari River Basin, India. *Journal of Water Resource and Protection*, *8*(01), 31.

Schoof, J. T., & Pryor, S. C., (2001). Downscaling temperature and precipitation: A comparison of regression-based methods and artificial neural networks. *International Journal of Climatology*, *21*(7), 773–790.

Toews, M. W., & Allen, D. M., (2009). Evaluating different GCMs for predicting spatial recharge in an irrigated arid region. *Journal of Hydrology*, *374*(3), 265–281.

Wetterhall, F., Halldin, S., & Xu, C. Y., (2005). Statistical precipitation downscaling in central Sweden with the analog method. *Journal of Hydrology*, *306*(1), 174–190.

Wilby, R. L., & Wigley, T. M. L., (1997). Downscaling general circulation model output: A review of methods and limitations. *Progress in Physical Geography*, *21*(4), 530–548.

Yan, G., Jian-Ping, L., & Yun, L., (2011). Statistically downscaled summer rainfall over the middle-lower reaches of the Yangtze River. *Atmospheric and Oceanic Science Letters*, *4*(4), 191–198.

CHAPTER 34

GROUNDWATER PROSPECT MAPPING IN UPPER SOUTH KOEL RIVER BASIN JHARKHAND (INDIA) BASED ON GIS AND REMOTE SENSING TECHNOLOGIES

STUTI[1], ARVIND CHANDRA PANDEY[2], and SAURABH KUMAR GUPTA[1]

[1]*Research Scholar, Centre for Land Resource Management, School of Natural Resource Management, Central University of Jharkhand, Brambe, Jharkhand, India, E-mail: stuti@cuj.ac.in*

[2]*Professor, School of Natural Resource Management, Centre for Land Resource Management, Central University of Jharkhand, Brambe, Jharkhand, India*

ABSTRACT

Groundwater is dynamic natural resources which depend on various parameters mainly hydrogeomorphology of an area. In hard rock terrain availability of groundwater is limited. In such terrains groundwater is essentially confined to fractured and weathered zones. Because of undulating topography and hard rock terrain in Upper South Koel river basin the availability of ground water is limited. Multispectral satellite image from LISS-III sensor having resolution 23.5 m is used for the creation of various thematic layers like land-use landcover, lithology, lineaments, and hydrogeomorphology. Cartosat 1 DEM data is used for the creation of a slope map of the area. Field survey data and GPS point records were used to create groundwater yield map and depth to water level map. Overlaying various weighted thematic maps prepared in Arc GIS platform and validated with field surveying data help to demarcate potential groundwaterpotential zones in the area. Very good groundwater prospect zones are mainly located along the valley fills, covering an area of 1.92 sq. km. whereas very poor groundwater prospect zones lies along

dissected pediments, structural hills, relict hills, covering an area of 15 sq. km. Groundwater management and planning must be done in the areas having very poor groundwater prospects to enhance groundwater potential and to combat future drought. Geoinformatics techniques facilitate effective evaluation of groundwater potential for effective watershed development planning.

34.1 INTRODUCTION

Groundwater is the main source of drinking water in India which helps to sustain life on earth. In order to maintain the sustainability of groundwater, there is a need to understand the groundwater prospects, hydrogeomorphology as well as the geological setting of that area. Water scarcity is the major trouble in the modern-day situation, to overcome this proper water management via underground or surface water management need to be done to reduce water shortage and fight drought. It is now felt that to deal with and overcome those issues, the drinking water supply schemes need to be evolved considering the hydrogeological records.

Jharkhand is hard rock terrain regions and the area under study, i.e., part of upper South Koel river basin not having good groundwater prospect zones and faces severe water scarcity. Surface water assets in the area inadequate to satisfy the nearby need, consequently to meet the current need, exploration, and exploitation of groundwater resources require thorough expertise of geology, hydrology, and geomorphology of the location. Hence an assessment of this useful resource is extremely huge for the sustainable control of the groundwater system in this area. A number of works considered within the area of groundwater potential zones. Application of remote sensing (RS) and geographical information systems (GIS) for the exploration of potential groundwater zones is achieved by some of the researchers around the world. Teeuw (1995) relied handiest on the lineaments for groundwater exploration, even as others merged various factors aside from the lineaments like drainage density, geomorphology, geology, slope, land use, rainfall intensity and soil texture (Sander et al., 1996; Sener et al., 2005; Ganapuram et al., 2009). The satellite statistics gives quick and beneficial baseline records about various factors controlling directly or indirectly the occurrence and movement of groundwater which includes geomorphology, soil, land slope, land use/land cover, drainage patterns and lineaments (Waters et al., 1990; Meijerink, 1996; Jha et al., 2007). RS research offers an opportunity for better observation and extra systematic analysis of various hydrogeomorphic units/ landforms/ lineaments capabilities following the synoptic, multispectral, and repetitive

coverage of the terrain (Horton, 1945; Kumar and Srivastava, 1991; Sharma and Jugran, 1992). Remotely sensed information are generally price effective as compared to the traditional techniques of hydrological surveys and specifically are of first-rate significance in remote areas (Machiwal et al., 2011). GIS gives an exquisite framework for efficiently managing big and complicated spatial data for natural asset control, accordingly, it has proved to be a useful tool for groundwater studies (Krishnamurthy et al., 1996; Meijerink, 1996; Nour, 1996; Sander et al., 1996). In the beyond, several researchers have used RS and GIS techniques for the delineation of groundwater potential zones (Chi and Lee, 1994; Kamaraju et al., 1995) with a successful result.

In last two decades, many researchers have found that multi-criteria decision-making (MCDM) presents a powerful tool for water management by using structure, shape, auditability, transparency to the decision (Flug et al., 2000; Joubert et al., 2003). Recently, Hajkowicz and Higgins (2008) counseled that at the same time as the choice of a MCDM approach is important for water resources management, extra emphasis is required at the preliminary structuring of a selective problem which entails selecting criteria and decision alternatives. Integration of RS with GIS for making numerous thematic layers, together with lithology, drainage density, lineament density, rainfall, slope, soil, and land use with assigned weightage in a spatial domain will aid the identification of ability groundwater zones. The present study aims at the identification of groundwater potential zones of the study area as part of upper South Koel river basin, Jharkhand, India using RS, GIS, and weighted overlay analysis for groundwater resources exploration. The predominant goal of this study is to construct groundwater potential map of the hard rock terrain of the study area. This study targets to spatial analyze the connection among groundwater potential and terrain and hydrological parameters which manipulate groundwater accumulation.

34.2 MATERIALS AND METHODS

34.2.1 STUDY AREA

The watershed is a part of South Koel basin with an area of 772 km^2 bounded by latitude 23°17’16”N & 23°32’16”N and longitude 84°14’15”E & 85°46’51”E (Figure 34.1). It lies in SOI toposheet no 73 A/14, 73 A/15, 73 E/2, 73 E/3 covering Lohardaga and Ranchi districts of Jharkhand (Figure 34.2). South Koel is the main river in the study area with Kandani and Saphi River as its major tributaries. The drainage pattern is mainly dendritic. The climate of the area is subtropical. The annual rainfall in the region is

1400 mm, on an average of which 82.1% is received during the periods June to September and the rest 17.9% in remaining months. Temperature is lowest during December and January with a mean minimum of 9°C and highest during April and May with a mean maximum of 37.2°C.

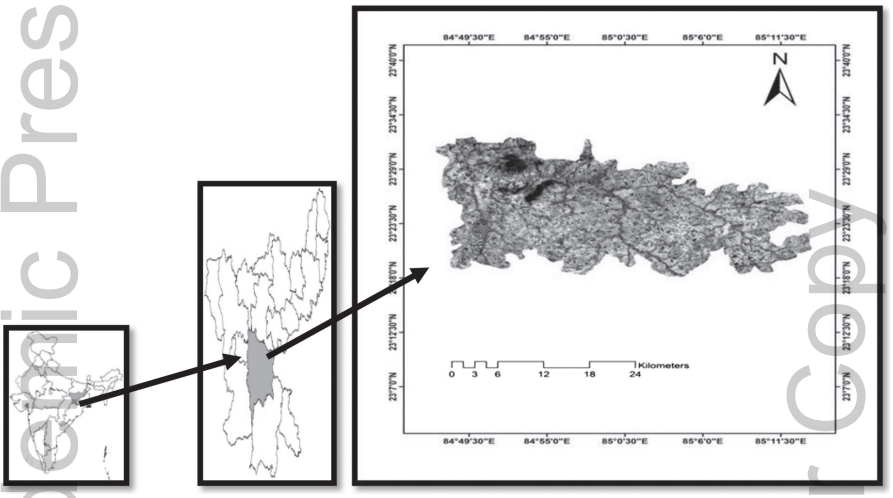

FIGURE 34.1 Map showing a satellite image of study area of LISS III data.

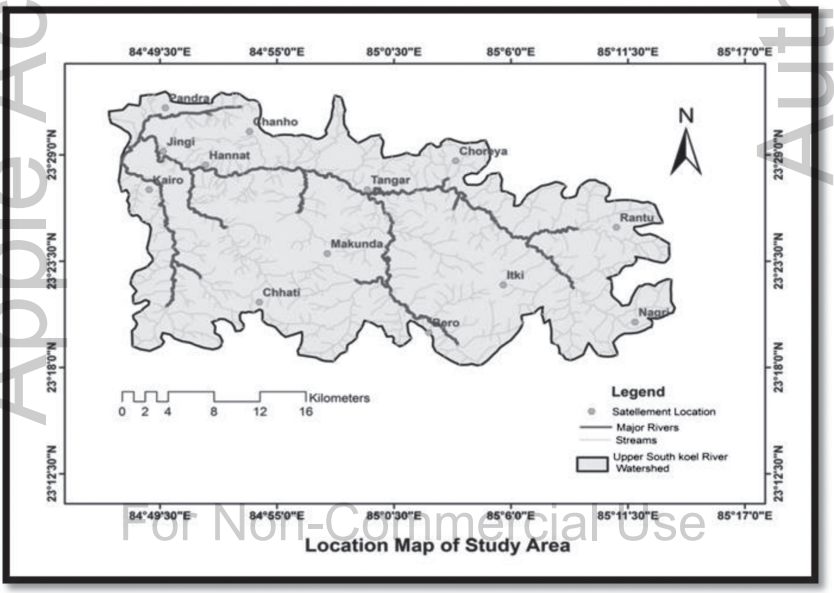

FIGURE 34.2 Location map of the study area.

34.2.2 METHODOLOGY

The details of the steps followed in the study are illustrated in Figure 34.3. Multispectral Satellite image of LISS-III sensor has been used for preparing thematic maps of land-use landcover, lithology, lineament, and geomorphology of the study area with the help of image interpretation keys, i.e., color, shape, size, texture, pattern, shadow, and association. Nine major class of LULC has been identified as Intense agriculture (143.65 km^2), Sparse agriculture (148.72 km^2), Open forest (39.59 km^2), Degraded forest (46.54 km^2), Barren land (91 km^2), Barren land rocky (80.37 km^2), Water bodies/reservoir (9.24 km^2), Built up areas (81.68 km^2) as shown (Figure 34.4) which is further validated with google earth data and survey of India toposheet of 1:50,000. Drainage order map has been prepared with the help of toposheet of 1.50,000 (SOI) which shows 6th order watershed. Lithology map has been prepared which shows mainly five classes as Alluvium, Granite Gneiss, Hornblende Schist and Amphibolite, Schist, metabasic dykes and laterite as shown (Figure 34.5). Lineament map has been prepared which basically shows major lineaments and dissected lineaments as shown in Figure 34.7. Hydrogeomorphology of study area shows nine major types of landforms, i.e., Denudational hills, Structural hills, Relict hills, Inselberg, Pediment inselberg complex, Plateau weathered shallow, Plateau weathered moderate, Pediment shallow buried, Valley fills, lineaments, Waterbodies as shown in Figure 34.6. Cartosat 1 DEM data has been used for slope map. Study area is mainly having a high slope between 0–45 degrees and elevation 766 m as highest and 677 m as lowest. Soil map is taken from National Bureau of soil science mainly showing two types of soil for the area of 772 km^2 i.e., fine loamy, coarse loamy soil which is further divided into seven classes i.e., Fine loamy (Aeric Haplaquents 309.52 km^2), coarse loamy (Haplaquents 230.02 km^2) Fine loamy (Typic Ustochrepts 91.01 km^2) Fine (Ustrochrepts 11.92 km^2), Fine loamy (Aeric 11.09 km^2), Fine loamy (Haplaustalfs 45.89 km^2), Fine (Vertic Ustochrepts 53.62 km^2) as shown in Figure 34.7. A weighted overlay analysis of various thematic maps of various layers has been done in the study area for suggesting the site to identify the areas facing severe water scarcity or less groundwater prospect. The spatial variability of groundwater in upper south koel river basin was obtained by assigning weightage to the various themes such as land-use landcover, geomorphology, slope, soil map and drainage which was overlaid in the platform of Arc GIS software. On the basis of groundwater prospect, each thematic maps were assigned weights from 1 to 10 based on an understanding of groundwater potential with 1 being considered least significant in regard to water potential zone

and highest number, i.e., 10 being assigned for the most potential zone in consideration of groundwater prospect. Maximum weight to reservoir i.e., 10 which is having more probability of water contained and minimum weight to barren land rocky as 2 (Krishnamurthy et al., 1996; Malczewski, 1999; Balachandar, 2010). The given weights for each map were normalized so that the difference in the number of classes in all maps can be brought to the same scale with the value of weights in the range of 0 to 1. For normalization, weights of each class were recalculated by dividing the class weight by cumulative weight of all the classes. The total weight was calculated by multiplying the normalized weight with the theme weight, and on the basis of the total weight, all the themes were rasterized and overlaid in raster calculator of ArcGIS for estimation of groundwater prospect zones. The groundwater prospects map obtained were classified into five zones (viz., very poor, poor, moderate, good, and very good). The assignment of theme weight, unit weight, normalized weight, and total weight for the various thematic layers has been shown in Table 34.1. For validating this result ground truthing and field validation has been done. Field GPS points of different wells and their depth in different geomorphological units and data from Rajiv Gandhi Ground Water Atlas has been taken to prepare a map showing depth of water table and water yield capacity in different places of the Upper south koel river basin as shown in Figures 34.10 and 34.11 which help to validate our work.

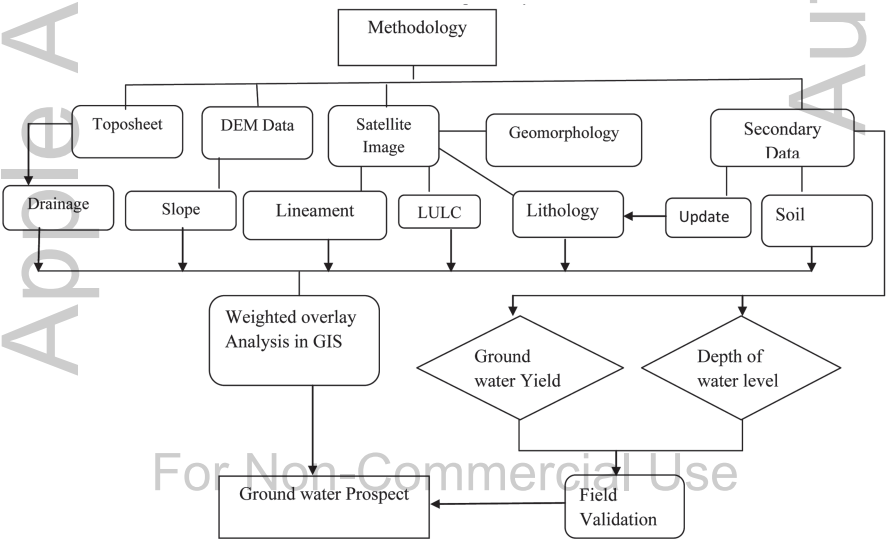

FIGURE 34.3 Flowchart of methodology.

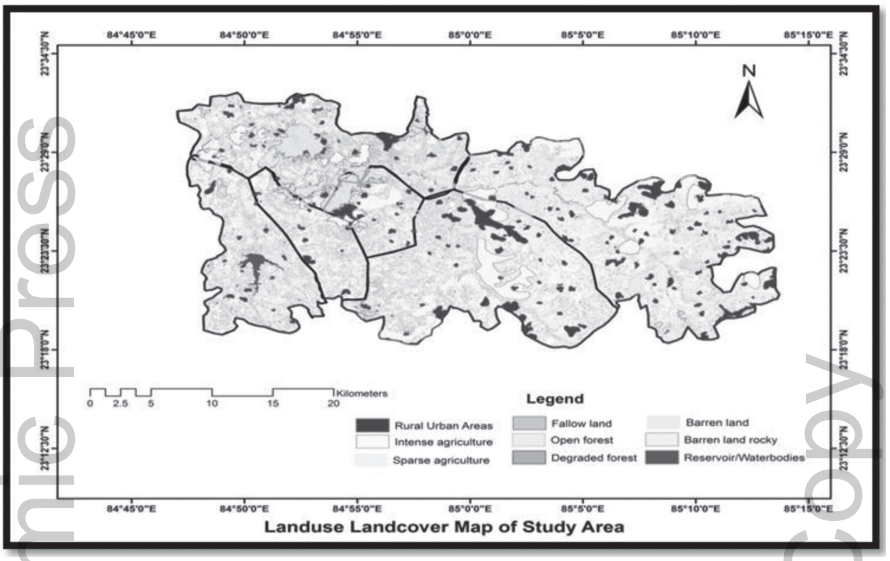

FIGURE 34.4 Map showing land use landcover of study area using LISS III data.

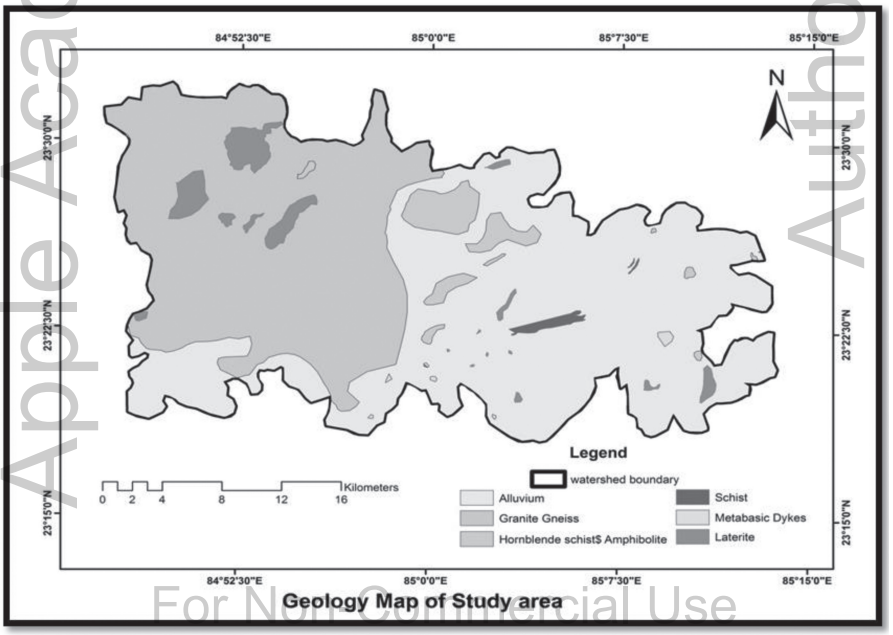

FIGURE 34.5 Map showing geology of study area using LISS III data.

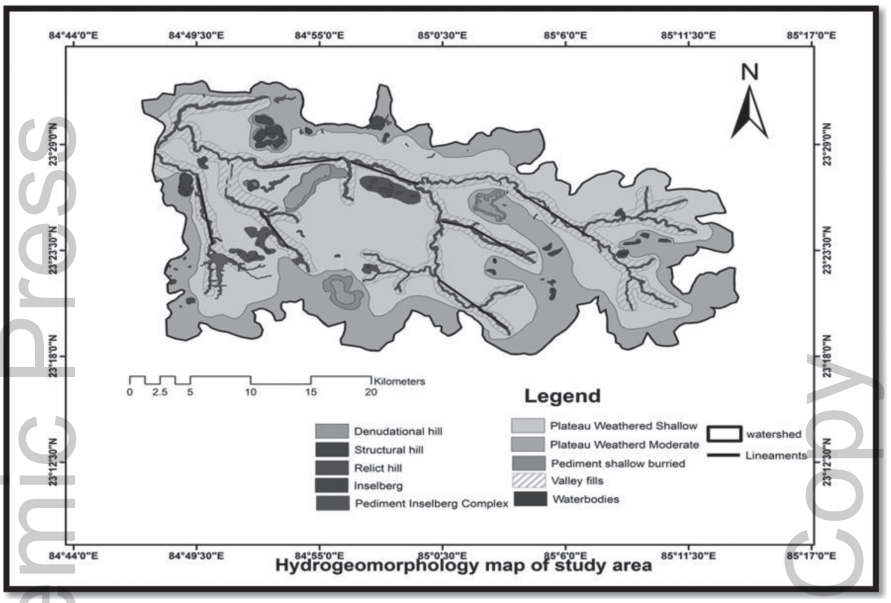

FIGURE 34.6 Map showing hydrogeomorphology of study area using LISS III satellite data.

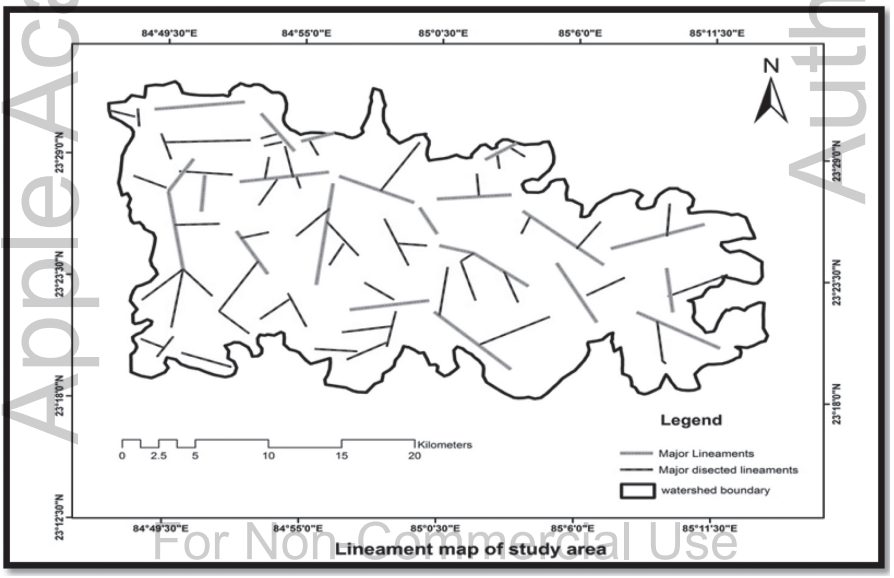

FIGURE 34.7 Map showing lineaments of study area using LISS III satellite data.

TABLE 34.1 Theme and Theme Weight, Unit Weight, Normalized Weight and Total Weight of Different Land Classes

Theme and theme weight	S. No	Class	Unit Weight	Normalized Weight	Total Weight
Landuse Land cover**(5)**	1	Rural-urban areas	5	0.10	0.5
	2	Intense agriculture	6	0.12	0.6
	3	Sparse agriculture	6	0.12	0.6
	4	Fallow land	3	0.06	0.3
	5	Open forest	7	0.14	0.7
	6	Degraded forest	7	0.14	0.7
	7	Barren land	3	0.06	0.3
	8	Barren land rocky	2	0.04	0.2
	9	Reservoir/water bodies	8	0.17	0.85
Hydrogeomorphology **(9)**	1	Denudation hills	2	0.03	0.27
	2	Structural hills	3	0.05	0.45
	3	Relict hills	3	0.05	0.45
	4	Inselberg	4	0.06	0.54
	5	Pediment inselberg complex	5	0.08	0.72
	6	Plateau weathered shallow	6	0.10	0.9
	7	Plateau weathered moderate	6	0.10	0.9
	8	Plateau shallow buried	7	0.11	0.99
	9	Valley fills	7	0.11	0.99
	10	Lineaments	8	0.13	1.17
	11	Waterbodies	8	0.13	1.17
Slope **(7)**	1	0–5	8	0.14	0.98
	2	5–10	7	0.12	0.84
	3	10–15	6	0.10	0.7
	4	15–20	5	0.09	0.63
	5	20–30	5	0.09	0.63
	6	30–40	3	0.05	0.35
	7	40–50	2	0.03	0.21
Stream **(7)**	1	1st order	4	0.03	0.21
	2	2nd order	4	0.06	0.42
	3	3rd order	5	0.12	0.84
	4	4th order	6	0.19	1.33

TABLE 34.1 *(Continued)*

Theme and theme weight	S. No	Class	Unit Weight	Normalized Weight	Total Weight
	5	5th order	7	0.25	1.75
	6	6th order	8	0.32	2.24
Lithology **(6)**	1	Alluvium	4	0.26	1.56
	2	Granite Gneiss	1	0.06	0.36
	3	Hornblende schist	2	0.13	0.78
	4	Amphibolite schist	2	0.13	0.78
	5	Metabasic dykes	3	0.2	1.2
	6	Laterite	3	0.2	1.2
Soil **(7)**	1	Coarser loamy	3	0.75	5.25
	2	Fine loamy	1	0.25	1.75

34.3 RESULT AND DISCUSSION

Different classes of Landuse landcover were digitized with the help of Arc-GIS 10.3 software based on visual interpretation by using image interpretation keys. Each land-use landcover classes having different percolation capacity of water, i.e., because of hard surface and cemented construction total 81.68 km^2 area is mainly covered with built-up areas shows nil infiltration capacity. Area of 143.65 km^2 is mainly covered with intensive agriculture where infiltration capacity is good as compared to built-up areas hence which is one of the prospects to enhance or increase groundwater recharge condition. Different land-use classes and their infiltration capacity based on soil texture of different classes as Intense agriculture (good), sparse agriculture (good), open forest (good), degraded forest (fair), reservoir/water bodies (good), lake (fair), fallow land (poor), barren land rocky (poor), barren land (poor), built up (poor). As per earlier study runoff is high in these plateau terrain areas because of that most of agricultural land is converted into fallow land which is having less infiltration capacity of water. Infiltration capacity mainly depends on soil and geology of areas. Most of the areas are mainly covered by fine loamy soil having less infiltration rate and water transmission rate.

34.3.1 LITHOLOGY

Groundwater prospect of any area is not only controlled by climatic conditions, but also the lithology and geologic structure have great control as they

influence the nature of flow, erosion, and sediment transportation. The basic rocks present in the area is mainly oldest rock as unclassified metamorphic represented by Mica Schist, Hornblende schist, and amphibolites which form the basement rocks in the study area. The overlying Chotanagpur Gneissic Complex comprising Granite gneiss forms the most widespread outcrop in the study area. Laterite, metabasic dykes, and recent alluvial deposits are other rock types found in the area. Lineaments are found mainly along the valley fills and having an excellent source of groundwater. There are mainly two types of lineaments as major lineaments and major dissected lineament. Rainfall in these areas is high still facing water scarcity may be because of undulating topography or presence of basic and meta basic dykes, and quartz reefs in the areas acted as barriers for flows of water (Singh et al., 1997).

Alluvium comprising of sand silt, clay, and gravel has been given higher weightage as compared to sedimentary rocks like sandstone, shale. Among the metamorphic rocks, granitoid gneiss because of its high weathering due to a high fractured condition in the area has been given higher weightage as compared to fractured granite gneiss.

34.3.2 GEOMORPHOLOGY

Landforms observed in the study areas are Structural hill, Denudation hill**,** Relict hill**,** Inselberg**,** Pediment Inselberg complex, Valley fills**,** Plateau dissected shallow, and Plateau dissected moderate. The study area is having varied hydrogeological characteristics due to which groundwater potential differs from one region to another. Lineaments acting as fracture zones generally act as conduits for movement of groundwater in hard rocks. Along these zones, the yield is significantly higher, and wells are likely to be sustainable for a longer duration. There are dykes, quartz which generally act as barriers for groundwater movement. Drainage ordering map has been prepared which shows upper South Koel watershed having 6th order streams. Highest order is mainly along valley fills, and small order streams are mainly dominated along the structural hills and denudational hills areas as shown in Figure 34.8.

The hydrogeomorphology in the hard rock terrain is highly influenced by the lithology and structure of the underlying formations and is one of the most important features in evaluating the groundwater potential and prospect (Kumar et al., 2008). Material associated with river/ waterbodies and active and active floodplain has higher water retention capability and therefore constitutes best landforms for high groundwater potential.

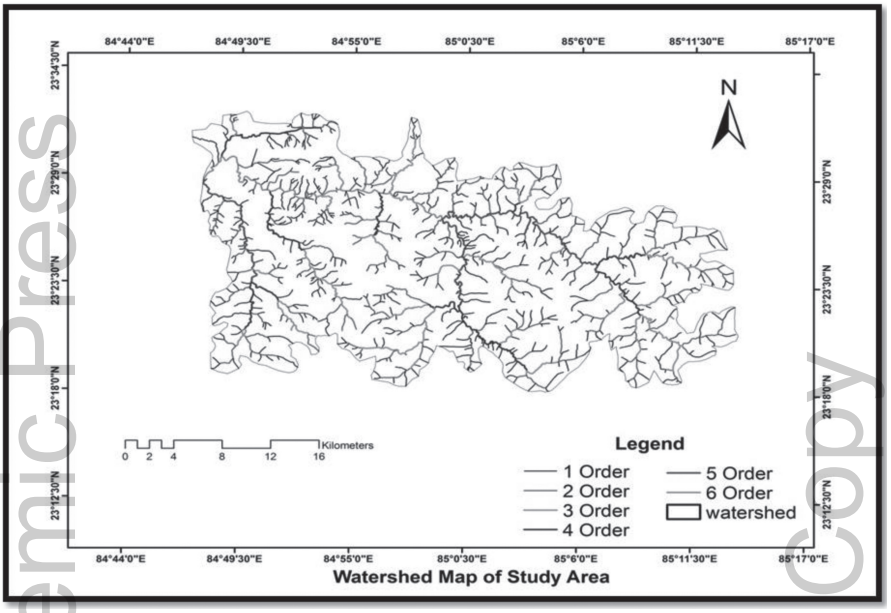

FIGURE 34.8 Map showing streams order of Upper South Koel river basin using toposheet (1:50,000).

34.3.3 SOIL

The soil for the study area is represented by four main soil categories namely fine, fine loamy, loamy, and coarse loamy (Figure 34.9). Rank of soil has been assigned on the basis of their infiltration rate; sandy soil has high infiltration rate. Hence coarse loamy soil dominated by high sand proportion has been given higher priority, whereas the fine soil exhibiting least infiltration rate due to higher clay proportion were assigned a low priority (Figure 34.10).

34.3.4 SLOPE

Slope and relief map is prepared using DEM data shows slope between 0–25 degrees in which 1.92 sq. km. of area covered with slope between (0–5) degrees show very good prospect of groundwater and along 14–92 km^2 of an

area having slope >25 is mainly affected by water scarcity, and groundwater prospect is not too good along these areas.

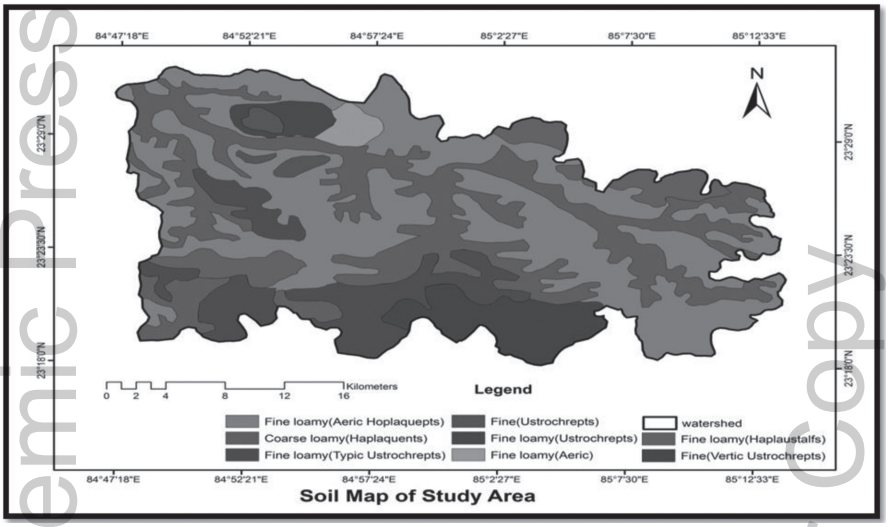

FIGURE 34.9 Soil map of study area using NBSS data source.

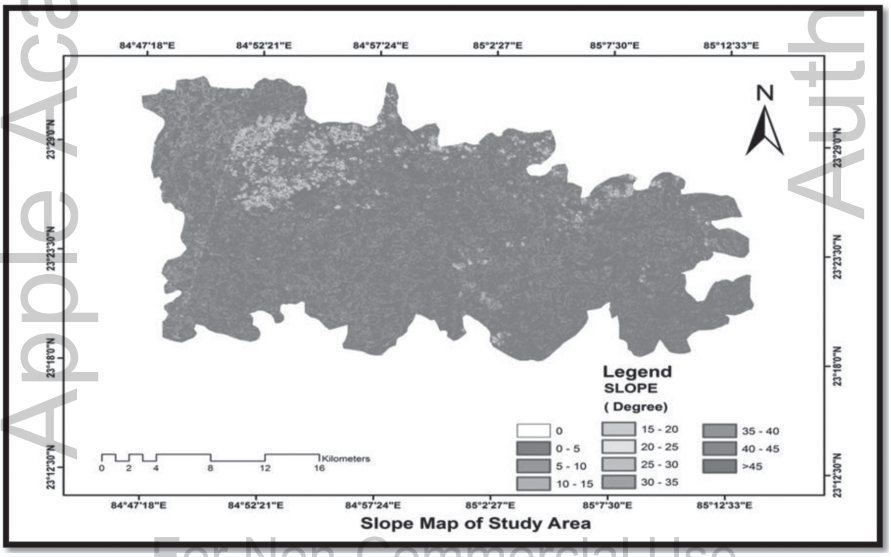

FIGURE 34.10 Slope map of the study area using Cartosat 1 DEM data.

Groundwater prospect with the help of Slope Map		
S.NO	**Slope (Degree)**	**Area (sq km)**
1	0–5	1.92
2	5–10	516.29
3	10–15	197.52
4	15–20	32.61
5	20–25	9.19
6	>25	14.92

34.3.5 WEIGHTED OVERLAY

On the basis of integrating all the above map, i.e., Landuse and cover map, Hydrogeomorphology map, Lineament map, slope, streams, lithology, and soil map on the Arc-GIS platform, the final map of Groundwater prospect is prepared which show groundwater status of the study area as shown in Figure 34.11.

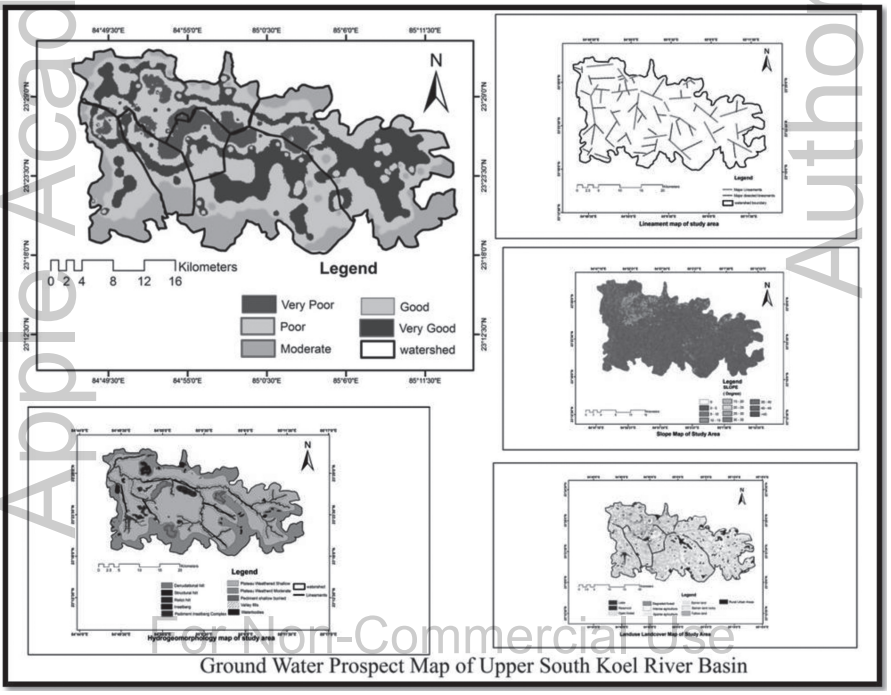

FIGURE 34.11 Groundwater prospect map of the study area using weighted overlay techniques.

34.3.6 FIELD VALIDATION

Various field data has been collected during field checks to validate our work. Number of wells in differentlanduse, i.e., no built-up areas along hills hence no wells and hand pumps were found in landforms as Structural hills, denudation hills, relict hills, and inselbergs. Depth of water level map is mainly prepared with the help of ground surveying data, i.e., the number of wells and their depth lying in the study area and the number of wells observed in different landforms of the study area. Depth of water level mainly in summer and pre-monsoon season is >14 m to 11 m. Maximum 25–35 bore wells found in plateau dissected moderate having depth of 3–6 m shown in Table 34.2. Different wells have different yield range. Yield range in this studyis varies between > 10 to >80 Lpm which shows >10 Lpm in relict hills and maximum water can be yield from valley fills, i.e., >80 Lpm. Depth rangeis mainly varies from 30–80m of the water table. Water quality is portable and having different recharge conditions shown in Table 34.3. Depth of water table and groundwater yield map has been prepared based on these data which shows the depth of water table is from < 3 m to > 14 m and having high water yield range shown in Figures 34.12 and 34.13. Water harvesting structures or recharge conditions must be developed in these areas to enhance the groundwater prospect so that maximum water yield from these tube wells. Map prepared with the help of field data shows an approx similar result with the map prepared by using Arc GIS software in

TABLE 34.2 Showing Depth of Water Level (Summer/Pre-Monsoon/Post-Monsoon) of Different Wells and Dug Wells Locations of Study Area

	Field data			
S. No	**Landforms**	**No of Wells**	**Types of Wells**	**Depth of water level (Summer/Pre-monsoon)**
1	Structural hill	No wells	-	>14 meters
2	Denudational hill	No wells	-	11–14 meters
3	Relict hill	No wells	-	11–14 meters
4	Inselberg	No wells	-	11–14 meters
5	Pediment Inselberg complex	6–7	Borewells	9–11 meters
6	Plateau weathered shallow	20–25	Borewells	6–9 meters
7	Plateau weathered moderate	25–35	Dug wells and Borewells	3–6meters
8	Valley fills	No wells	-	<3 meters

GIS platform by using weighted overlay analysis of various thematic maps which used to validate our work.

34.3.7 GROUND WATER PROSPECT

The final map generated by using overlay analysis in Arc-GIS software mainly shows five zones of groundwater prospect, i.e., very good to very poor.

TABLE 34.3 Yield Range of Wells Depth of Different Wells and Dug Wells of Different Locations of Study Area

		Yield Ranges of wells			
S. No	**Landforms**	**Yield range of wells(Lpm)**	**Depth range of wells(meter)**	**Water Quality**	**Recharge condition**
1	Structural hill	-	-	-	-
2	Denudational hill	-	-	-	-
3	Relict hill	>10	-	-	-
4	Inselberg	10–25	30–80	Portable	Limited
5	PedimentInselberg complex	25–40	30–80	Portable	Limited
6	Plateau weathered shallow	40–65	30–80	Portable	Low priority
7	Plateau weathered Moderate	65–80	30–80	Portable	Moderate
8	Valley fills	>80	30–80	Portable	Good

1) **Very Poor**: These areas are covered with open forest and characterized by hills with a high slope greater than 25 degrees resulting in high runoff and covering an area of 15 sq. km. Soil comprised of gravel- loamy soil and not suitable for groundwater development. Depth of water level is >14 meters not having any recharge condition. Dominated with lower order streams. Therefore, groundwater prospect are nil to very poor mainly along the major cracks and weathered zones.
2) **Poor**: Mainly comprised of steep slope (20–25) degrees and covered with fallow land with very high runoff zone. Covering an area of 10 sq. km. groundwater prospects are very poor to poor in these Inselbergs. Depth of water level is 11–14 meters not having any wells and recharging condition.

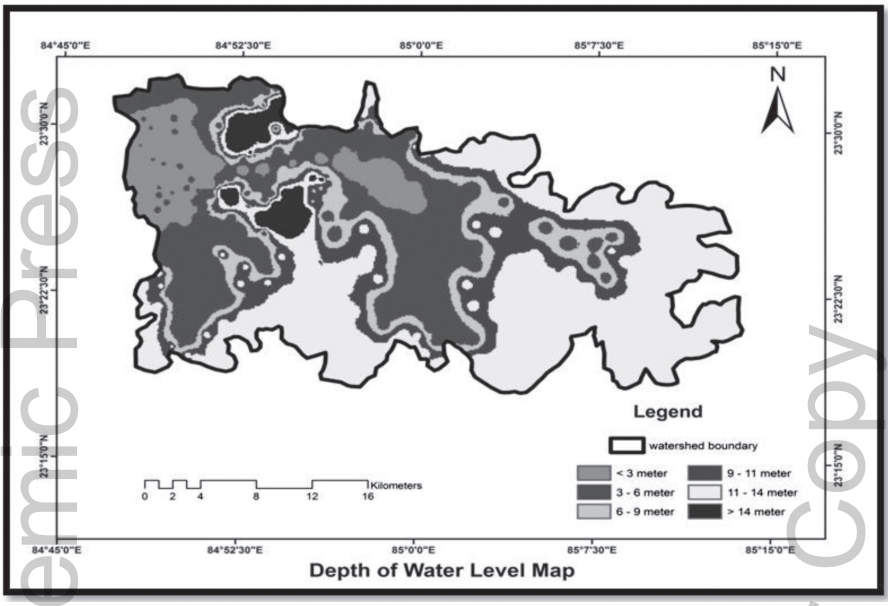

FIGURE 34.12 Map showing the depth of water level of study area using field data.

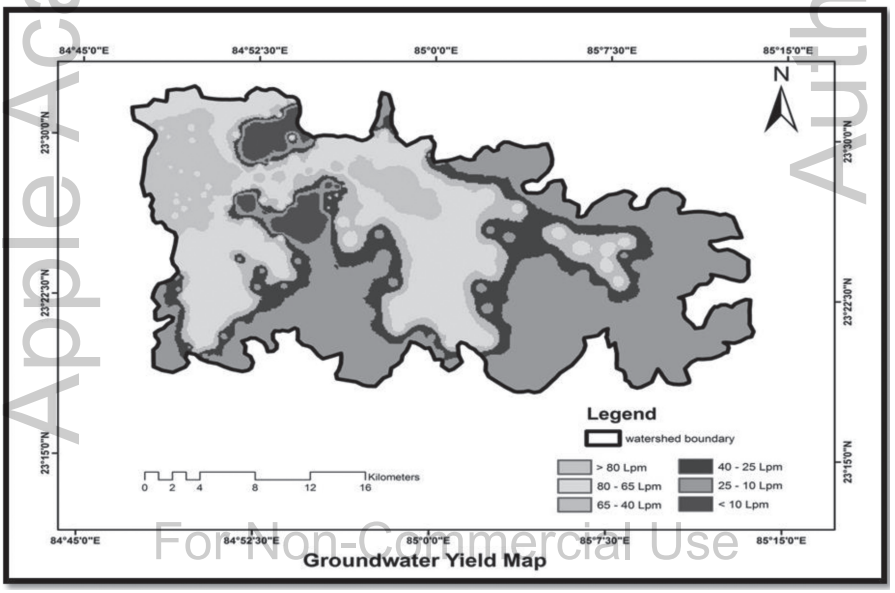

FIGURE 34.13 Map showing a groundwater yield of study area using field data.

3) **Poor – Moderate**: These comprises of isolated hills, knobs, and ridges having slope between 15–20 degrees that rise abruptly from a gently sloping or virtually level surrounding plain. The unit covering an area of 33 sq. km. represents barren land with shallow well-drained gravelly sandy soil on sloping landscape with severe erosion. Groundwater prospect are poor to moderate. Limited yield may be expected from fractured zone in these pediments a weathered and fractured rock comprises the aquifer material having depth of water level as 11–14 meters.
4) **Moderate – Good**: Aquifer material constituted by fractured rock with marginal weathered rock thickness. Because of gentle slope (10–15 degrees) covered with mainly intense agriculture with less erosion in the weathered zones, groundwater prospects are good in these zones covering an area of 197 sq. km. In hard rock's they form very good recharge and storage zones based upon the thickness of weathering/accumulated material, its composition and recharge conditions. 20–25 number of dug wells and bore wells having depth of water level as 6–9 meter of yield 40–60 Lpm.
5) **Good**: Covered by open forest and sparse agricultural land having slopes lying between 5–10 degree with aquifer material largely constituted by weathered rock, clay, and fractured rock. As weathering is comparatively more than in plateau weathered shallow, slightly higher yield may be expected from the deeper fractures under thick weathered zones. Groundwater prospects are moderate to good covering an area of 516 sq km. Depth of water level is 3–6 meters having 25–35 dug wells and bore wells of 65–80 Lpm yield range.
6) **Very Good**: Aquifer material comprises mainly of loose sediments, weathered, and fractured rock fragments mainly along higher order streams, i.e., of 6th order. Covering an area of 1.92 sq. km. valley fills are located along lineaments and in pediment areas having slope between 0–25 degrees. Due to better recharge conditions in the valley from surrounding uplands groundwater prospect are very good. Depth of water level is <3-meter having good source of recharge.

34.4 CONCLUSIONS

The final integrated map as generated by applying weighted overlay analysis in Arc GIS platform which shows five prospect grades in terms of water resources potentiality viz.; very good, good, moderate-poor, poor

to moderate, poor, and very poor. Good water prospect shows very good zones cover only along valley fills (cover 45% of the area), very good zones cover only 12% of the study area. They are located along lineaments and in pediment areas. Moderate prospect zone covers 15% of the area. Features like buried pediplains, peneplains, and denundational hills come under this category, whereas poor regions cover up to 22%. These features are mainly confined to undulating upland and buried pediments with the intermountain valley. Lastly, very poor groundwater prospect zones are approximately 10%. These features include dissected pediments, inselberg complex and residual hill. Geologically it is observed that the groundwater is mainly confined to secondary porosity, i.e., fractured zone, fault, joint, and weathered column. It is observed from field survey and also from various wells located in the region the hard granite gneisses, and Meta basic dykes sometimes act as barriers for the groundwater flow in the region. The geoinformatics based groundwater potential mapping help to enhance the zones required specific watershed management to increase groundwater potential and combat future drought. This will serve as an insurance against future droughts in the study area.

ACKNOWLEDGMENTS

Authors are thankful to Bhuvan for online availability of LISS-III Satellite data and Cartosat 1 DEM data. The first author acknowledges the receipt of financial assistance under the Fellowship (DST INSPIRE) from Ministry of Science and Technology and Department of Science and Technology.

KEYWORDS

- **Arc GIS**
- **field validation**
- **groundwater prospect**
- **overlay analysis**
- **Upper South Koel river**

REFERENCES

Amadi, A. N., Nwawulu, C. D., Unuevho, I., Okoye, N. O., Okunlola, I. A., Egharevba, N, A., Ako, T. A., & Alkali, Y. B., (2011). Evaluation of the groundwater potential in Pompo Village, Gidan Kwano, Minna using vertical electrical resistivity sounding. *British J. Appl. Sci. Technol.*, *1*, 53–66.

Chi, K. H., & Lee, B. J., (1994). Extracting potential groundwater area using remotely sensed data and GIS techniques. In: *Proceedings of the Regional Seminar on Integrated Application of Remote Sensing and GIS for Land and Water Resource Management* (pp. 64–69). Bangkok.

Flug, M., Seitz, H. L. H., & Scott, J. F., (2000). Multicriteria decision analysis applied to Glen Canyon Dam. *J. Water Resour. Plan Manage ASCE., 126*, 270–276.

Ganapuram, S., Kumar, G. T. V., Krishna, I. V. M., Kahya, E., & Demirel, M. C., (2009). Mapping of groundwater potential zones in the Musi basin using remote sensing data and GIS. *Adv. Eng. Softw*., *40*, 506–518.

Hajkowicz, S., & Higgins, A., (2008). A comparison of multiple criteria analysis techniques for water resource management. *Eur. J. Oper. Res*., *184*, 255–265.

Horton, R. E., (1945). Erosional development of streams and their drainage basins, hydrophysical approach to quantitative morphology. *Geol. Soc. Am. Bull*., *56*, 275–370.

Jaiswal, R., Mukherjee, S., Krishnamurthy, J., & Saxena, R., (2003). Role of remote sensing and GIS techniques for generation of groundwater prospect zones towards rural development – an approach. *Int. J. Remote Sens*., *24*, 993–1008.

Jha, M. K., Chowdhury, A., Chowdary, V. M., & Peiffer, S., (2007). Groundwater management and development by integrated remote sensing and geographic information systems: Prospects and constraints. *Water Resour. Manage*., *21*, 427–467.

Joubert, A., Stewart, T. J., & Eberhard, R., (2003). Evaluation of water supply augmentation and water demand management options for the City of Cape Town. *J. Multi-Criteria Decis. Anal*., *12*, 17–25.

Kamaraju, M. V. V., Bhattacharya, A., Reddy, G. S., Rao, G. C., Murthy, G. S., & Rao, T. C. M., (1995). Groundwater potential evaluation of West Godavari District, Andhra Pradesh State, India – a GIS approach. *Ground Water*, *34*, 318–325.

Krishnamurthy, J., Srinivas, G., Jayaram, V., & Chandrasekhar, M. G., (1996). Influence of rock types and structures in the development of drainage networks in typical hard rock terrain. *ITC Journal*, *3/4*, 252–259.

Kumar, A., & Pandey, A. C., (2016). Geoinformatics based groundwater potential assessment in hard rock terrain of Ranchi urban environment, Jharkhand State (India) using MCDM–AHP techniques. *Groundwater for Sustainable Development*, *2/3*, 27–41.

Kumar, A., & Srivastava, S. K., (1991). Geomorphological units, their geohydrological characteristic and vertical electrical sounding response near Munger, Bihar. *J. Indian Soc. Remote Sens*., *19*, 205–215.

Kumar, M. G., Agarwal, A. K., & Bali, R., (2008). Delineation of potential sites for water harvesting structures using remote sensing and GIS. *J. Indian Soc. Remote Sens*., *36*, 323–334.

Machiwal, D., Jha, M. K., & Mal, B. C., (2011). Assessment of groundwater potential in a semi-arid region of India using remote sensing, GIS and MCDM techniques. *Water Resour. Manage*., *25*, 1359–1386.

Machiwal, D., Mishra, A., Jha, M. K., Sharma, A., & Sisodia, S. S., (2012). Modeling short-term spatial and temporal variability of groundwater level using geostatistics and GIS. *Arab J. Geosci.*, *21*(1), 117–136.

Meijerink, A. M. J., (1996). Remote sensing applications to hydrology: Groundwater. *Hydrol. Sci. J.*, *41*, 549–561.

Mondal, M. S., Pandey, A. C., & Garg, R. D., (2007). Groundwater prospects evaluation based on hydrogeomorphological mapping using high-resolution satellite images: A case study in Uttarakhand. *J. Indian Soc. Remote Sens*., *36*, 69–76.

Nour, S., (1996). Groundwater potential for irrigation in the East Oweinat area, Western Desert. *Egypt Environ. Geol.*, *27*, 143–154.

Pandey, A. C., & Stuti, (2017). Geospatial technique for runoff estimation based on SCS-CN method in upper South Koel River Basin of Jharkhand (India). *Int. J. Hydro.*, *1*(7), 00037. doi: 10.15406/ijh.2017.01.00037].

Parveen, R., Kumar, U., & Singh, V. K., (2012). Geomorphometric characterization of upper South Koel Basin, Jharkhand: A remote sensing & GIS approach, *Journal of Water Resource and Protection*, *4*, 1042–1050.

Rajiv Gandhi National Drinking Water Mission Atlas, (2005). *Rajiv Gandhi National drinking water mission Atlas for Jharkhand State* (Vol. I & II). Hyderabad: National Remote Sensing Centre, Department of Space, Govt. of India.

Sharma, D., & Jugran, D. K., (1992). Hydromorphological studies around Pinjaur-Kala Amb area, Ambala district (Haryana), and Sirmour district (Himachal Pradesh). *J. Indian Soc. Remote Sens*., *29*, 281–286.

Shekhar, S., & Pandey, A. C., (2014). Delineation of groundwater potential zone in hard rock terrain of India using remote sensing, geographical information. *Geocarto. International*, doi: 10.1080/10106049.2014.894584.

Shekhar, S., Pandey, A. C., & Nathawat, M. S., (2012). Evaluation of fluoride contamination in groundwater sources in hard rock terrain in Garhwa district, Jharkhand, *India. Int. Journal of Environmental Sciences*, *3*(3). doi:10.6088/ijes.2012030133010.

Srivastava, V. K., Giri, D. N., & Bharadwaj, P., (2012). Study and mapping of groundwater prospect using remote sensing, GIS and geoelectrical resistivity techniques – a case study of Dhanbad district, Jharkhand, India, *J. Ind. Geophys. Union*, *16*(2), 55–63.

Teeuw, R. M., (1995). Groundwater exploration using remote sensing and a low-cost geographical information system. *Hydrol. Sci. J.*, *3*, 21–30.

Tirkey, A. S., Ghosh, M., & Pandey, A. C., (2016). Soil erosion assessment for developing suitable sites for artificial recharge of groundwater in a drought-prone region of Jharkhand state using geospatial technique. *Arab J. Geosci., 9*, 362. doi: 10.1007/s12517-016-2391-0.

Waters, P., Greenbaum, D., Smart, P. L., & Osmaston, H., (1990). Applications of remote sensing to groundwater hydrology. *Remote Sens. Rev*., *4*, 223–264.

CHAPTER 35

GEO-PROCESSING BASED HYDROLOGICAL SENSITIVITY ANALYSIS AND ITS IMPACT ON FOREST AND TERRAIN ATTRIBUTES IN THE HAZARIBAGH WILDLIFE SANCTUARY, JHARKHAND, INDIA

SAURABH KUMAR GUPTA[1], A. C. PANDEY[2], and STUTI[1]

[1]*Research Scholar, Centre for Land Resource Management, School of Natural Resource Management, Central University of Jharkhand, Brambe, Jharkhand, India*

[2]*Professor, School of Natural Resource Management, Centre for Land Resource Management, Central University of Jharkhand, Brambe, Jharkhand, India, E-mail: arvindchandrap@yahoo.com*

ABSTRACT

The health of a watershed is vital to ensure the sustainability of water resources. Understanding and recognizing the spatial changes in the sensitive hydrological zones (HSZs) in a watershed is of prime importance to maintain water sustainability in the forest regions. In the present research satellite data-based spatial technique known as topographic wetness index (TWI) was used to identify HSZs in the forest landscape. This study was conducted in the Hazaribagh Wildlife Sanctuary, Jharkhand, India. Further, the relationship of HSZ with a slope length (LS) factor, flow accumulation, and forest cover were observed. The result shows that the watershed that contains high wetted area is the healthiest watershed and has good forest productivity. The LS factor and flow accumulation negatively related to HSZs. The present study emphasizes the protection of stream corridors

through land use management. Also, the forest cover in the areas of degraded and forest blank (FB) needs to be given the highest priority for decreasing the hydrological sensitivity by improving soil moisture retention capacity and water demand of the landscape.

35.1 INTRODUCTION

The variable source area VSA (Hewlett and Hibbert, 1967) is the hydrology idea to survey commitments of various parts of a watershed to run-off generation (Wu, 2016). The sensitive hydrological zones (HSZs) are characterized as parts of VSAs which are more susceptible to create runoff contrasted with different parts of the watershed (Walter et al., 2000). HSZs assume a basic part in watershed hydrology. The idea of HSZs relates the watershed scale issues to different regions in the watershed that possibly contribute water saturation and soil moisture retention capacity. The extensive research has been utilizing HSZs based way to deal with comprehend watershed hydrology and prioritize the watershed based on water demand of landscape. The spatial variation of HSZs would additionally encourage organizing precise runoff generation areas, and their land uses. Forest degradation by human association changes the land uses in a part of a watershed, which prompts water asset degradation. However, its impacts on water assets shift crosswise over various parts of the watershed. For instance, urbanization, and agriculture that happened near the streams has a more prominent effect than far from the streams (Wu, 2016). The program named Healthy Watersheds Initiative (HWI) presented by the United States Environmental Protection Agency (USEPA, 2009), the dynamic attributes of water their interconnections with the land cover such as in forest region and secures all vital hydrologic, geomorphic, and different procedures all in the interconnected framework. Ensuring healthy watersheds gives various advantages, including adequate water to influence vegetation cover and better human wellbeing. Additionally, it lessens the vulnerability of water assets to future land use and environmental change impacts (USEPA, 2011).

To delineate HSZs topographic indices was used based on Digital Elevation Models (DEM) such as Topographic Wetness Indices (TWI). The TWI values have some predictive power concerning soil and vegetation characteristics, but scatter among the relationships is high, and TWIs usually explain less than 40 % of the variation in soil and vegetation properties (Thompson and Moore, 1996; Florinsky et al., 2002; Sorenson et al., 2006; Seibert et al., 2007). The 20 and 30 m DEMs produced spatial distributions of TWI

values that most closely matched with the distribution of mapped soil types, the relative wetness determined from depth to groundwater maps, and the spatial distribution of forest stands managed partly on the basis of wetted and drainage networks (Wu, 2016). In the present study, we utilized the Topographic Wetness Index (TWI) for calculating HSZs areas. The HSZz was then related to LS factor, flow accumulation, and forest cover.

35.2 MATERIALS AND METHODS

35.2.1 STUDY AREA

This study was performed in the Hazaribagh Wildlife Sanctuary, Jharkhand, India (Figure 35.1). It lies between 24°45’22” N to 24°08′20″N latitude and 85° 30’13” E to 85°21′58″E longitude and also includes bird Sanctuary and other biodiversity parks. The climate of the region is tropical having hot summers and chilly winters. In summer, the greatest temperature rises to up to 41 degrees and low of 19 degrees. In winter, most extreme high and low temperature decreased is 19 degrees and 7 degrees respectively. The sanctuary has Sambhar, Deer, Bison, and various mammalian fauna. The Cheetah, Kakar, Nilgai, Sambar, and Wild Boar are among the most effective and frequently spotted creatures, especially close to the waterholes at the time of the sunset.

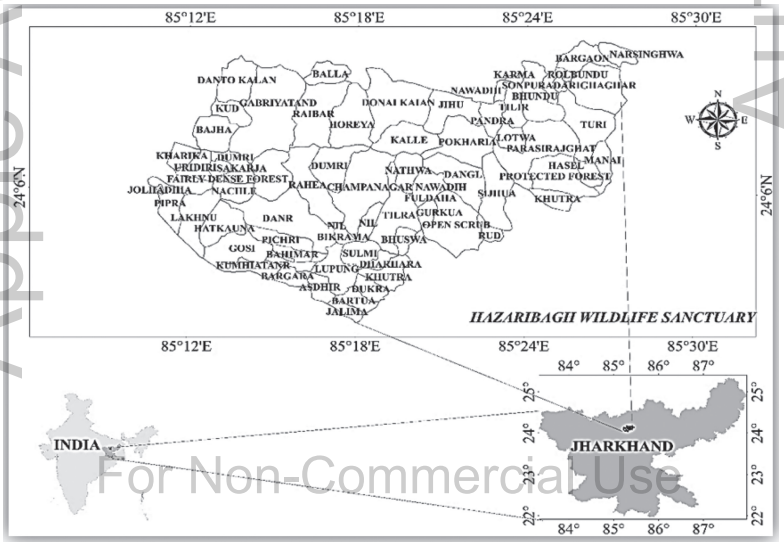

FIGURE 35.1 Study area – Hazaribagh Wildlife Sanctuary.

35.2.2 METHODOLOGY

The flow chart of all processing steps and analysis was given in Figure 35.2 which indicates the methodology adopted in the present study. It includes the preprocessing SRTM DEM 1 arc second resolution (https://earthexplorer.usgs.gov/) for HSZ analysis and estimation of terrain attributes. The Sentinel–2A satellite data was used for finding the forest cover area. Each part of the methodology is illustrated below.

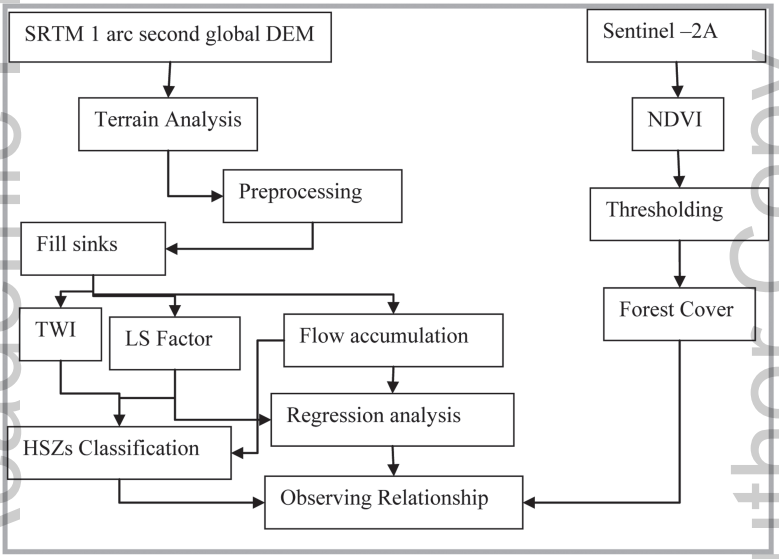

FIGURE 35.2 Methodology adopted.

35.2.3 TOPOGRAPHIC WETNESS INDEX (TWI)

The application of TWIs to explain the spatial distribution of moisture and soil and vegetation characteristics has encountered problems of several types. The Quantum GIS (QGIS) and System for Automated Geoscientific Analyses GIS (SAGA GIS) software were used for the calculation of TWI and its processing. Both GIS software are freely available and user-friendly. TWI used in QGIS was suggested by Beven and Kirk by (1979) as

$$TWI = \ln (A_s / \tan\beta) \quad (1)$$

where, As is the (upslope) flow accumulation area (or drainage area) per unit contour length (Wilson and Gallant, 2000) and β is the angle of the slope.

TWI has found a wide range of application in hydrology (Moore et al., 1991; Quinn et al., 1995; Sorenson et al., 2006).

35.2.4 HYDROLOGICAL SENSITIVE ZONE CLASSIFICATION

The TWI indicates the spatial distribution of surface saturation and soil moisture. The HSZ was classified based on TWI index values, the positive value of TWI represents the high wetted area, and low HSZs and its negative parts represent HSZ. The histogram of TWI shows that TWI is the high number of negatives values and low in positive values. Therefore, all the negative values (–18.55 to 0) were classified as HSZs classes, representing very low to high HSZ and the positive part (7.9 to 0) was separated as high wetted area as given in Figure 35.3. The ARC GIS was used for the classification of HSZs based on the natural breaks method (Jenks) of classification. The statistics of the classified HSZ were calculated by pixel count and DEM resolution.

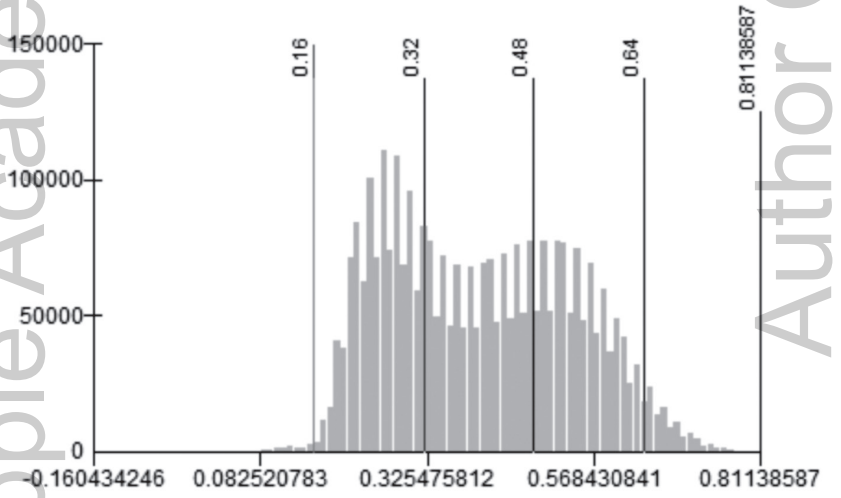

FIGURE 35.3 NDVI threshold for forest classification.

35.2.5 TERRAIN ATTRIBUTES

35.2.5.1 LS FACTOR

Length-Slope (LS) factor (Moore, 1992) implemented in the revised universal soil loss equation (RUSLE) was used in this study. It gives a value

for the water erosion potential (A^s) to a slope of 22.13 m length and a slope angle of 5 degrees. It can be represented as the following equation:

$$LS = (m+1)\left(\frac{As}{22.13}\right)^m \left(\left(\frac{sin\beta}{0.0896}\right)^n\right) \quad (2)$$

where $m = 0.4$ and $n = 1.3$ for a slope length (LS) <100 *m* and a slope angle <14°. LS and slope gradient (sin β) are most often considered topographic factors are influencing soil loss. The SAGA GIS was used for the calculation of the LS Factor.

35.2.5.2 FLOW ACCUMULATION

The flow accumulation operation plays out a collective count of the number of pixels that normally drain into outlets. The process can be used to discover drainage pattern. The flow accumulation is calculated by taking flow direction as input parameters which helps as to demarcate a total number of pixels that will drain into an outlet. The flow direction operation decides the characteristics of drainage direction for all pixels in a digital elevation model (DEM). The output derived as flow accumulation map contains hydrological flow values that indicate the number of input pixels which contribute to a water body and the outlets of the largest water body have the largest value.

35.2.5.3 NDVI BASED FOREST CLASSIFICATION

NDVI: Vegetation cover is possibly the most crucial element in the process of soil erosion study and management. It is the most dynamic factor in a watershed which can be readily altered to control the loss of water and soil. It is a numerical indicator, which uses the visible and near-infrared bands of the remote sensing data for identifying green vegetation in the study site. The NDVI algorithm subtracts the red reflectance values from the near-infrared and divides it by the sum of near-infrared and red bands. Theoretically, NDVI values are represented as a ratio ranging in value from –1 to 1, but in practice, extreme negative values represent water, values around zero represent bare soil and values over 0.5 represent dense green vegetation.

$$NDVI = \frac{NIR - RED}{NIR + RED} \quad (3)$$

Forest Classification: The NDVI values were assessed (0.81 to –0.16) in the forest to gain output of the forest cover distribution in the forest. The NDVI values of 0.64–0.8 named dense forest (DF), very DF having a small area (greater than 0.8) which was not included because of its small size, 0.48–0.64 as moderately dense forest (MDF), 0.32–0.48 as open forest (OF), 0.16 to 0.32 as degraded forest (DeF) and less than these comprises forest blank (FB). The classification threshold of NDVI with its histogram is given in Figure 35.3.

35.3 RESULTS AND DISCUSSION

35.3.1 TOPOGRAPHIC WETNESS INDEX AND HYDROLOGICAL SENSITIVE ZONE

35.3.1.1 TWI

The TWI index used for the measurement of wetness and shows the area of maximum water accumulation potential. The high TWI area represents the highest amount of precipitation, low water demand and the presence of soil type that hold large amounts of water, means less infiltration rate. The figure that represents TWI index is given in Figure 35.4. The figure indicates that the high TWI mainly found in the path of drainage basins.

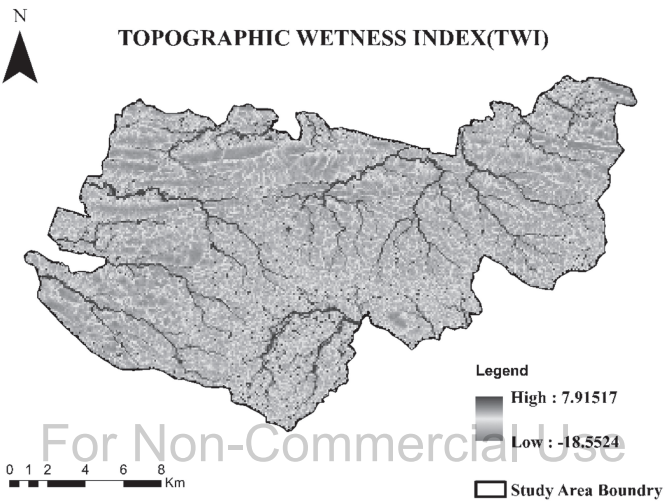

FIGURE 35.4 The topographical wetted index.

35.3.1.2 HSZs CLASSIFICATION AND HIGH WETTED AREA

The previous research on the TWI shows that it is directly proportional to hydrological sensitive zone determination. The HSZ was classified in four zones (high, medium, low, and very low HSZ) given in Figure 35.5. It was found that medium HSZ was in greater magnitude compared to other zones of area equal to 110.39 km^2 (40%). The very low and low HSZs was low in the magnitude of 16.3 km^2 (6%) and 38.8 km^2 (14.29%) respectively. The wetted area that was calculated is very low of about 7 km^2 (2.65%). It means the study area has lacked of clay soil and a large quantity of sandy soil. The High HSZ was 98.89km^2 in the area and has contributed 36.39% of the study area which has larger in magnitude. The statistical part of HSZs classification and the high wetted zone is given (Figure 35.6). The analysis shows that the area encounters the problem of low precipitation and run-off and a large part of the area has a water deficiency (high water demand) for the good forest productivity. These problems have a direct effect on forest vegetation health and their growths.

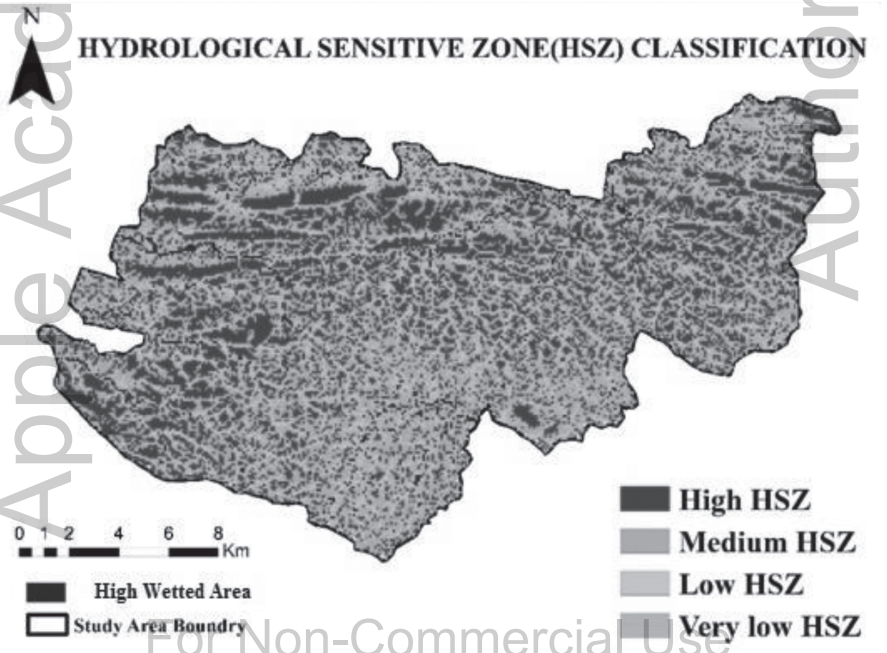

FIGURE 35.5 The hydrological sensitive zones (HSZs) classification based on TWI.

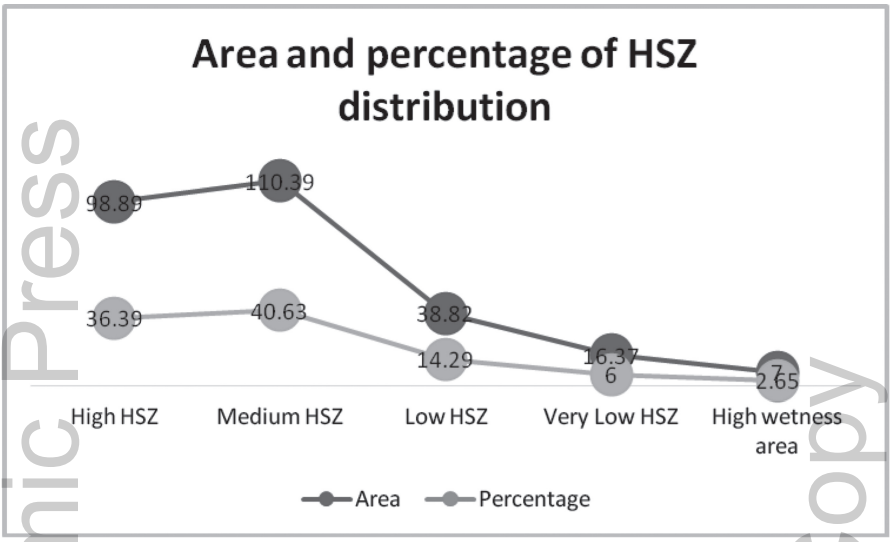

FIGURE 35.6 The statistics of HSZs and high wetted area.

35.3.1.3 THE TERRAIN ATTRIBUTES AND HSZS

LS-Factor: LS factor is used for identifying the net erosion area (Figure 35.7). The high value of LS factor represents the high soil erosion-prone area, and low LS factor shows low soil erosion prone area. The LS-factor is found in the drainage area. The relationship between LS factor and HSZs was observed and concluded that high wetted area has high LS factor and high HSZs mean low LS factor. In Figure 35.8, the scatter plot is given which shows the relationship of LS factor with HSZs and high wetted zone. The negative linear relationship was found between HSZ and LS factor. It shows that here that the HSZ is the area having the low soil erosion, which was found scattered around the drainage boundary.

Flow Accumulation: A sample usage of the flow accumulation tool with an input weighted raster might be to determine how much rain has fallen within a given watershed. In such a case, the weight raster may be a continuous raster representing average rainfall during a given storm. The output from the tool would then represent the amount of rain that would flow through each cell, assuming that all rain became runoff and there was no interception, evapotranspiration, or loss to groundwater. This could also be viewed as the amount of rain that fell on the surface, upslope from each cell. The results of flow accumulation can be used to create a stream network

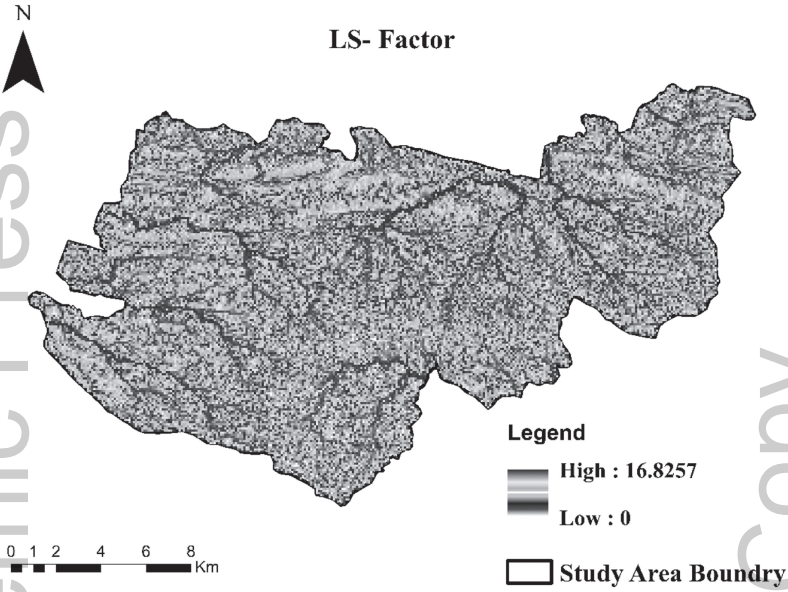

FIGURE 35.7 Figure showing the LS factor.

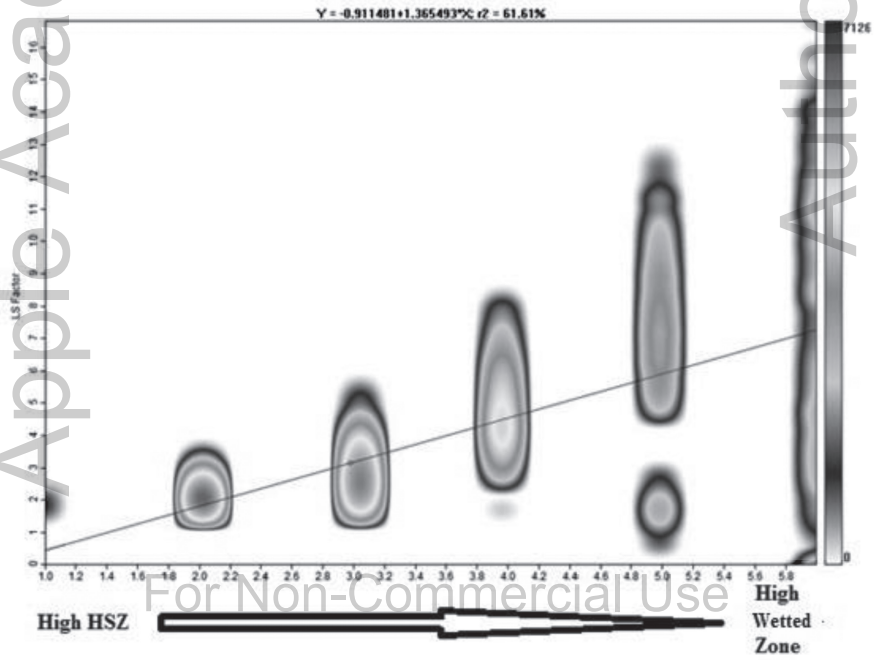

FIGURE 35.8 The relationship between HSZs and high wetted zone area with LS factor.

by applying a threshold value to select cells with a high accumulated flow. The flow accumulation map is given (Figure 35.11). The effort was applied to get information about the relationship between HSZs and Flow accumulation. The observation shows that more the flow accumulation more the TWI index. The result indicated that area having a low flow accumulation has high HSZ and the HSZ decreases with more the flow accumulation. The high wetted area has a high flow accumulation. In Figure 35.9, flow accumulation relationship with the decreasing level of HSZ and increasing level of the wetted area was quite low ($r^2 = 19.48\%$) (Figures 35.10 and 35.11).

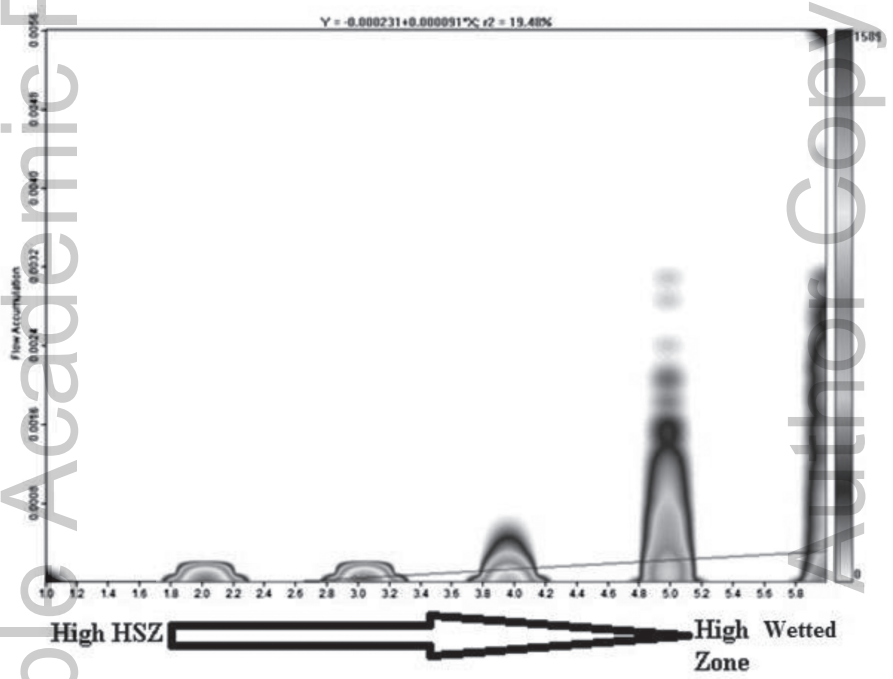

FIGURE 35.9 The relationship between the LS factor and HIGH HSZ and High wetted zone.

Forest Cover and HSZS Distribution: The landscape position and soil moisture exert first-order control on soil properties (e.g., texture, organic matter, and chemistry) and vegetation characteristics, these characteristics correlate with TWI values (e.g., Florinsky et al., 2002, 2004; Sariyildiz et al., 2005; Seibert et al., 2007). The forest cover in the study area is given (Figure 35.12). Forest cover type is a factor that influences watershed hydrology. Forest cover types help in regulation of surface runoff. The Land use changes

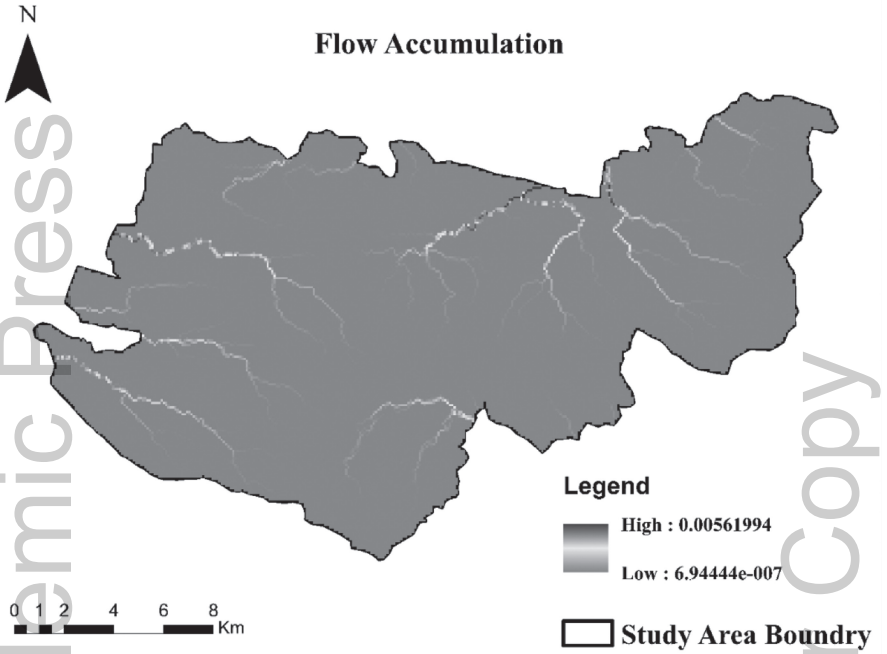

FIGURE 35.10 Showing the flow accumulation.

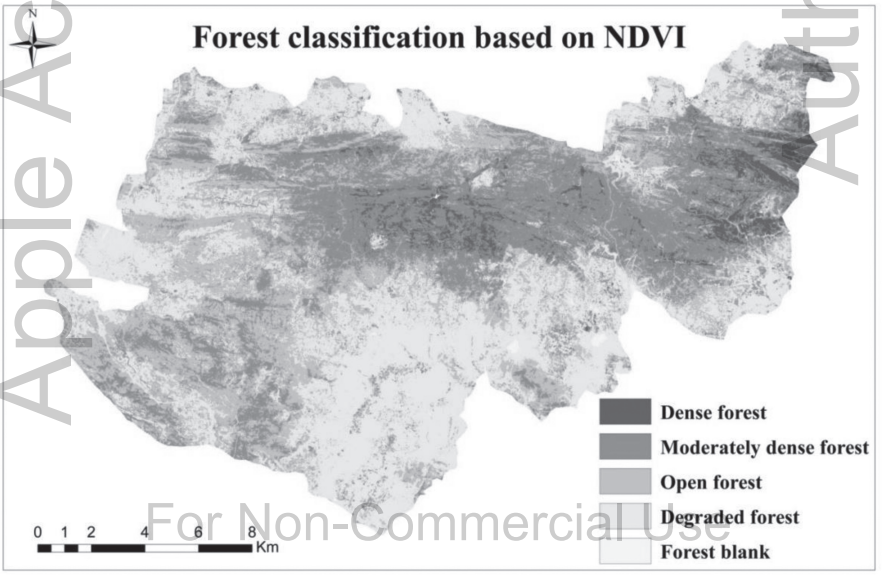

FIGURE 35.11 Forest cover classification in the study area based on NDVI values.

in forest affect water conservation practices in the past several decades. The degraded forest and FB lies on medium HSZ. The OF and some part of MDF lies on high HSZ showing that the forest in the region can tolerate water deficiency condition. They do not depend on the low water presence and need less water for their growth. The DF found scattered around the high wetted zone or drainage basin. The analysis shows that different forest cover lies on different HSZ. The relationship between decreasing wetted and increasing HSZ does not affect forest productivity in some part of the forest cover like MDF and OF. The attention is needed for rebuilding sound watershed and improving soil water retention capacity in degraded and FB part of the forest cover.

Validation: In the Figure 35.12, the false color composite of the Sentinel 2A imagery is given, which indicates the true condition of vegetation and can be taken for validating the obtained results of the classified forest cover. At the FCC, the DF area appears in dark red color. Sometimes, it is misunderstood by the shadow, as the forest canopy cover creates shadows depends upon the sun geometry. The darkness in red color decreases in MDF followed by open and degraded cover area. The degraded forest and FB appears pink and gray-white, respectively. Thus, the above validation of the obtained result is satisfactory.

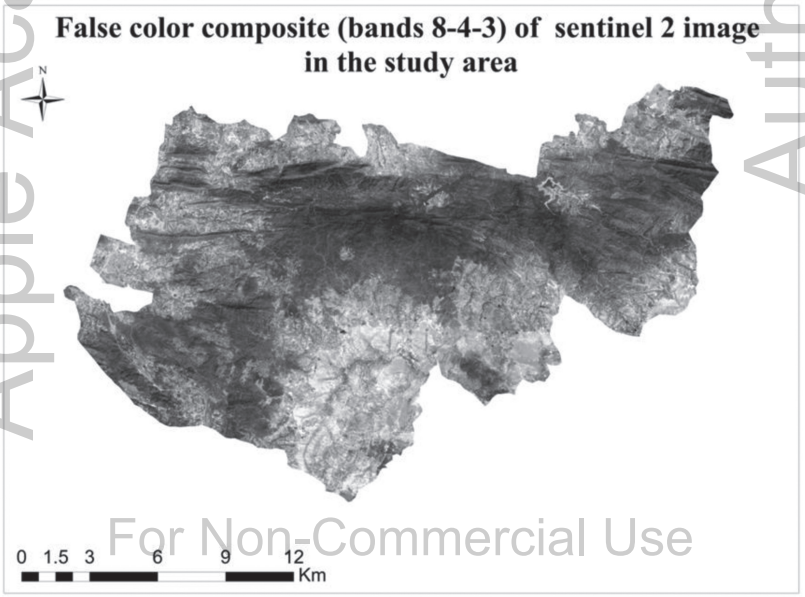

FIGURE 35.12 False color composite of Sentinel imagery.

35.4 CONCLUSIONS

Maintaining healthy watershed is a difficult task due to increased anthropogenic activities in the forest landscape. Different innovative programs such as HWI help to overcome the overall water deficiency. With limited resources, the understanding of the spatial distribution of HSZs in the landscape and their land uses helps prioritize conservation measures and support these programs. In this study, the TWI technique was used to delineate HSZs in the study area. A TWI layer was developed by using SRTM DEM which represents topography. The TWI threshold was used to create different categories of HSZs scenarios for detailed analysis in this study. The whole process was performed using SAGA GIS in R- platform. The relationship between the LS factor and Flow accumulation with HSZ found negative; it is clear that the HZS is the area having the highest water deficiency. Such detailed representation of HSZs would increase the efficacy of land use control measures in protecting water deficiency in the soil and improving the soil moisture retention capacity. The attention is needed for rebuilding sound watershed and improving soil water retention capacity in degraded and FB part of the forest cover. The analysis of land use patterns in HSZs provides insights on how and where to target the management efforts to overcome water deficiency. The significant intrusion of high-intensity land uses into HSZs would signify the deterioration of landscape conditions that would lead to high water demand for vegetation growth. Land planning measures should be taken to protect HSZs from the intrusion of high-intensity land uses.

KEYWORDS

- **forest**
- **forest cover**
- **hydrological sensitive zones**
- **TWI**
- **watershed**

REFERENCES

Beven, K. J., & Kirkby, M. J., (1979). A physically-based, variable contributing area model of basin 25 hydrology, *Hydrological Sciences Bulletin*, *24*, 43–69.

Blyth, E. M., Finch, J., Robinson, M., & Rosier, P., (2004). Can soil moisture be mapped onto the terrain? *Hydrol. Earth Syst. Sci., 8*, 923–930, doi: 10.5194/hess-8-923-2004.

Dunne, T., & Black, R. D., (1970). Partial area contributions to storm runoff in a small New England watershed. *Water Resour. Res*., *6*, 1296–1311.

Dunne, T., Moore, T. R., & Taylor, C. H., (1975). Recognition and prediction of runoff-producing zones 10 in humid regions, *Hydrological Sciences Bulletin*, *20*, 305–327.

Florinsky, I. V., Eilers, R. G., Manning, G. R., & Fuller, L. G., (2002). Prediction of soil properties by digital terrain modeling. *Environ. Model. Softw*., *17*, 295–311.

Florinsky, I. V., McMahon, S., & Burton, D. L., (2004). Topographic control of soil microbial activity: A case study of denitrifiers. *Geoderma*, *119*, 33–53.

Güntner, A., Seibert, J., & Uhlenbrook, S., (2004). Modeling spatial patterns of saturated areas: An evaluation of different terrain indices, *Water Resour. Res*., *40*, W05114, doi:10.1029/2003WR002864.

Hewlett, J. D., & Hibbert, A. R., (1967). Factors affecting the response of small watersheds to precipitation in humid regions, In: Sopper, W. E., & Lull, H. W., (eds.), *Forest Hydrology* (Vol. 20, pp. 275–290). Pergamon Press, Oxford.

Jenson, S. K., & Domingue, J. O., (1988). Extracting topographic structure from digital elevation data for geographic information system analysis. *Photogrammetric Engineering and Remote Sensing*, *54*(11), 1593–1600.

Moore, I. D., Grayson, R. B., & Ladson, A. R., (1991). Digital terrain modeling: A review of hydrological, geomorphological and biological applications. *Hydrol. Process*., *5*, 3–30.

Moore, I. D., & Wilson, J. P., (1992). Length-slope factors for the revised universal soil loss equation: Simplified method of estimation. *Journal of Soil & Water Conservation*, *47*(5), 423–428.

Quinn, P., Beven, K., & Lamb, R., (1995). The ln(αs/tanβ): How to calculate it and how to use it within the TOPMODEL framework, *Hydrol. Process*., *9*, 161–182.

Sariyildiz, T., Anderson, J. M., & Kucuk, M., (2005). Effects of tree species and topography on soil chemistry, litter quality, and decomposition in Northeast Turkey. *Soil Biol. Biochem*., *37*(5), 1695–1706.

Seibert, J., Stendahl, J., & Sorenson, R., (2007). Topographical influences on soil properties in boreal forests. *Geoderma*, *14*, 139–148.

Sørensen, R., Zinko, U., & Seibert, J., (2006). On the calculation of the topographic wetted index: Evaluation of different methods based on field observations, *Hydrol. Earth Syst. Sci*., *10*(10), 101–112. doi:10.5194/hess–10–101–2006.

Thompson, J. C., & Moore, R. D., (1996). Relations between topography and water table depth in a shallow forest soil. *Hydrol. Process., 10,* 1513–1525.

U. S. Department of the Interior | U. S. Geological Survey, URL: http://water.usgs.gov/edu/watershed.html.

USEPA, (2010). *Identifying and Protecting Healthy Watersheds: A Technical Guide. Washington, DC*. Available at: (http://acwi.gov/monitoring/conference/2010/G3/ G3_Gabanski & Godfrey.pdf). Accessed on 14.03.16 USEPA (2011). Healthy watersheds initiative: National framework and action plan. Washington, DC. Available at: (https://www.epa.gov/sites/production/files/2015–10/documents/hwi_action_plan.pdf). Accessed on 14.03.16.

Walter, M. T., Steenhuis, T. S., Mehta, V. K., Thongs, D., Zion, M., & Schneiderman, E., (2002). Refined conceptualization of topmodel for shallow subsurface flows. *Hydrological Process*, *16*, 2041–2046.

Walter, M. T., Walter, M. F., Brooks, E. S., Steenhuis, T. S., Boll, J., & Weiler, K., (2000). Hydrologically sensitive areas: Variable source area hydrologically implications for water quality risk assessment. *Journal of Soil and Water Conservation*, *3*, 277–284.

Wilson, J. P., & Gallant, J. C., (2000). Digital terrain analysis. *Terrain Analysis: Principles and Applications,* 1–27.

INDEX

C

D

E

F

G

H

I

J

K

L

M

N

O

P

S

T

Y

Z

Wastewater Reuse and Watershed Management

Engineering Implications for Agriculture, Industry, and the Environment

Water is a finite resource, and the demand for clean water is constantly growing. Clean freshwater is needed to meet irrigation demands for agriculture, for consumption, and for industrial uses. The world produces billions of tons of wastewater every year. This volume looks at multitude of ways to capture, treat, and reuse wastewater and how to effectively manage watersheds. It presents a selection of new technologies and methods to recycle, reclaim, and reuse water for agricultural, industrial, and environmental purposes.

The editor states that more than 75–80% of the wastewater we produce goes back to nature without being properly treated, leading to pollution and all sorts of negative health and productivity consequences. Topics in this volume cover a wide selection of research, including molluscs as a tool for river health assessment, flood risk modeling, biological removal of toxins from groundwater, saline water intrusion into coastal areas, urban drainage simulations, rainwater harvesting, irrigation topics, and more.

Key features:

- explores the existing methodologies in the field of reuse of wastewater
- looks at different approaches in integrated water resources management
- examines the issues of groundwater management and development
- discusses saline water intrusion in coastal areas
- presents various watershed management approaches
- includes case studies and analyses of various water management efforts

ABOUT THE EDITOR

Ajai Singh, PhD, FIE, is an Associate Professor and Head of the Centre for Water Engineering and Management at the Central University of Jharkhand, Ranchi, India. He has more then 18 years of experience in teaching, research, and extension work. He is a Fellow of the Institution of Engineers (India) and a life member of various societies. He has more than 30 research papers published in national and international journals of repute. Dr. Singh has authored one textbook, *Introduction to Drip Irrigation Systems*, which has proved to be very useful for graduate and postgraduate students of agricultural/civil engineering. He has been awarded the Distinguished Services Certificate (2012) by the Indian Society of Agricultural Engineers, New Delhi. He teaches subjects such as finite element methods, groundwater hydrology, micro irrigation, watershed management, and numerical methods.

ISBN: 978-1-77188-746-5
9 0 0 0 0
9 781771 887465

APP APPLE ACADEMIC PRESS

www.appleacademicpress.com